Distribution Agreement

In presenting this thesis or dissertation as a partial fulfillment of the requirements for an advanced degree from Emory University, I hereby grant to Emory University and its agents the non-exclusive license to archive, make accessible, and display my thesis or dissertation in whole or in part in all forms of media, now or hereafter known, including display on the world wide web. I understand that I may select some access restrictions as part of the online submission of this thesis or dissertation. I retain all ownership rights to the copyright of the thesis or dissertation. I also retain the right to use in future works (such as articles or books) all or part of this thesis or dissertation.

Signature:

_____ _____

Katie L. Strong **Date**

The Design, Synthesis, and Biological Evaluation of Subunit-Selective *N*-Methyl-**D**-Aspartate Receptor Potentiators

By

Katie L. Strong

Doctor of Philosophy

Chemistry

Dennis C. Liotta, PhD

Advisor

David G. Lynn, PhD

Committee Member

Frank E. McDonald, PhD

Committee Member

Stephen F. Traynelis, PhD

Committee Member

Accepted:

Lisa A. Tedesco, PhD

Dean of the James T. Laney School of Graduate Studies

Date

The Design, Synthesis, and Biological Evaluation of Subunit-Selective *N*-Methyl-**D**-Aspartate Receptor Potentiators

By

Katie L. Strong

B.S., University of Mary Washington, 2010

Advisor: Dennis C. Liotta, PhD

An abstract of

A dissertation submitted to the Faculty of the James T. Laney of Graduate Studies of Emory University in partial fulfillment of the requirements for the degree of Doctor of Philosophy in Chemistry

2015

Abstract

The Design, Synthesis, and Biological Evaluation of Subunit-Selective *N*-Methyl-**D**-Aspartate Receptor Potentiators

By: Katie L. Strong

N-methyl-D-aspartate (NMDA) receptors are ionotropic glutamate receptors that mediate a slow, Ca^{2+}-permeable component of excitatory synaptic transmission. These receptors are important for a number of normal neurophysiological processes, and the dysfunction of the NMDA receptor has been indicated in a variety of neurological disorders. For this reason, identification of new pharmacological and therapeutic probes that selectively potentiate specific subunits of this receptor could be of therapeutic relevance. One such subunit-selective potentiator is the tetrahydroisoquinoline compound known as CIQ, which selectivity potentiates GluN2C- and GluN2D-containing NMDA receptors. Chapter One of this thesis discusses the continued structure activity relationship (SAR) around CIQ in an effort to explore important regions of the molecule and to increase potency. The most active analogs tested in Chapter One have EC_{50} values at the GluN2C and GluN2D subunits of 0.26 μM and 0.40 μM, respectively. Chapter Two of this thesis discusses how a specific modification on CIQ yielded a compound, referred to as **1180-55**, that not only potentiated the GluN2C and GluN2D subunits, but also the GluN2B. An SAR around **1180-55** has led to potentiators that have varying degrees of subunit selectivity, including one compound that is selective for the GluN2B subunit. The best-in-class pan-potentiators have EC_{50} values at all three subunits of approximately 0.30 μM. Separation of the enantiomers for a potent potentiator of the GluN2B-, GluN2C-, and GluN2D-containing receptors revealed that the *S*-(-) enantiomer is active at GluN2B, GluN2C, and GluN2D subunits, while the *R*-(+) enantiomer is GluN2C and GluN2D subunit selective. By conducting an SAR and studying the stereoselectivity of this class of **1180-55** compounds, it has been shown that the **1180-55** scaffold can be tuned to target different GluN2 subunits of the NMDA receptor. This tetrahydroisoquinoline class of compounds is no longer limited to the activation of only GluN2C and GluN2D subunits.

The Design, Synthesis, and Biological Evaluation of Subunit-Selective *N*-Methyl-**D**-Aspartate Receptor Potentiators

By

Katie L. Strong

B.S., University of Mary Washington, 2010

Advisor: Dennis C. Liotta, PhD

A dissertation submitted to the Faculty of the James T. Laney of Graduate Studies of Emory University in partial fulfillment of the requirements for the degree of Doctor of Philosophy in Chemistry

2015

The Design, Synthesis, and Biological Evaluation of Subunit-Selective *N*-Methyl-**D**-Aspartate Receptor Potentiators

By

Katie L. Strong

Advisor: Dennis C. Liotta, PhD

A dissertation submitted to the Faculty of the James T. Laney of Graduate Studies of Emory University in partial fulfillment of the requirements for the degree of Doctor of Philosophy in Chemistry

2015

Table of Contents

Chapter 2: The Structure Activity Relationship (SAR) of Tetrahydroisoquinoline Potentiators can be tuned to selectively target GluN2B-containing NMDA Receptors

Chapter 2

List of Illustrations

List of Figures **Page**

List of Tables

List of Schemes

List of Abbreviations

7-C1KY: 7-chlorokynurenate

24(S)-HC: 24-(S)-hydroxycholesterol

25-HC: 25-hydroxycholesterol

ACN: acetonitrile

ADHD: attention deficit hyperactive disorder

AMPA: α-amino-3-hydroxy-5-methyl-4-isoxazolepropionic acid

ATD: amino terminal domain

ATH: asymmetric transfer hydrogenation

BHK: baby hamster kidney

Bn: benzyl

CATIE: Clinical Antipsychotic Trials of Intervention Effectiveness

CBT: cognitive behavioral therapy

CIQ: (3-chlorophenyl)(6,7-dimethoxy-1-((4-methoxyphenoxy)methyl)-3,4-dihydroisoquinolin-2(1*H*)-yl)methanone

*c*Hex: cyclohexyl

*c*Pent: cyclopentyl

CNS: central nervous system

CS: conditioned stimulus

CTD: carboxyl terminal domain

CO_2: carbon dioxide

DAAO: D-amino acid oxidase

D-APV: (2*R*)-amino-5-phosphonovaleric acid

DIPEA: N,N-diisopropylethylamine

DLPFC: dorsolateral prefrontal cortex

DCM: dichloromethane (CH_2Cl_2)

DMF: dimethylformamide

DMAP: 4-dimethylaminopyridine

DSM-5: Diagnostic Statistical Manual of Mental Disorders

DMSO: dimethyl sulfoxide

EC_{50}: half-maximal effective concentration

EDCI: 1-ethyl-3-(3-dimethylaminopropyl)carbodiimide

ee: enantiomeric excess

Et: ethyl

FDA: Federal Drug Administration

GABA: gamma-Aminobutyric acid

GAD: glutamate decarboxylase

GlyT1: glycine transporter I

iGluRs: ionotropic cation-selective ligand-gated channels

HPLC: high pressure liquid chromatography

ICS: intersystem crossing

IP: intraperitoneal

IV: intravenous

*i*Bu: isobutyl

*i*Pr: isopropyl

LBD: ligand binding domain

LCMS: liquid chromatography-mass spectrometry

LTD: long-term depression

LTP: long-term potentiation

KIE: kinetic isotope effect

Me: methyl

mGluRs: second messenger-linked metabotropic glutamate receptors

MW: microwave

NFPS: N[3,(4'-fluorophenyl)-3-(4'-phenylphenoxy)propyl]sarcosine

NMDA: *N*-methyl D-aspartate

NMP: N-methyl-2-pyrrolidone

NRG1: neuregulin-1

OCD: obsessive compulsive disorder

OTC: over-the-counter

PCP: phencyclidine

PBA: pseudobulbar affect

PFC: prefrontal cortex

PTSD: post-traumatic stress disorder

PYD: pyrrolidinone

TEA: triethylamine

THF: tetrahydrofuran

TMD: transmembrane domain

TMS: trimethylsilyl ether

SAR: structure activity relationship

SDS-PAGE: sodium dodecyl sulfate polyacrylamide gel electrophoresis

SNP: single nucleotide polymorphism

SSRI: serotonin reuptake inhibitor

US: unconditional stimulus

Chapter 1: The Continued Design, Synthesis, and Biological Evaluation of a GluN2C/D-Selective NMDA Receptor Class of Tetrahydroisoquinoline Potentiators

1.1 Statement of Purpose

The *N*-methyl-**D** -aspartate (NMDA) receptor is indicated in a number of processes such as learning and memory. The hypofunction of the NMDA receptor has been implicated in schizophrenia[1] and anxiety disorders[2], while hyperactivation of the NMDA receptor has been linked to diseases such as Alzheimer's disease[3] and Parkinson's disease[4]. The NMDA receptor is unique in that is exists as a heterotetrameric structure composed of two GluN1 subunits and two GluN2 subunits, which are further classified into GluN2A, GluN2B, GluN2C, and GluN2D subunits[5]. The GluN2 composition endows the receptors with unique properties, making it therapeutically beneficial to discover and develop subunit-selective allosteric modulators[6]. Despite the importance of these receptors in fundamental neurological processes, a lack of subunit-selective allosteric modulators of the NMDA receptor exist with the potential to become therapeutic probes and drug candidates.

For that reason, in 2007, the Traynelis lab at Emory University conducted a high-throughput screen to identify compounds that acted selectively at one GluN2 subunit over the others. From this Ca^{2+} imaging screen of approximately 60,000 compounds, a GluN2C- and GluN2D-subunit selective potentiator, the tetrahydroisoquinoline compound referred to as **1180**, was discovered.

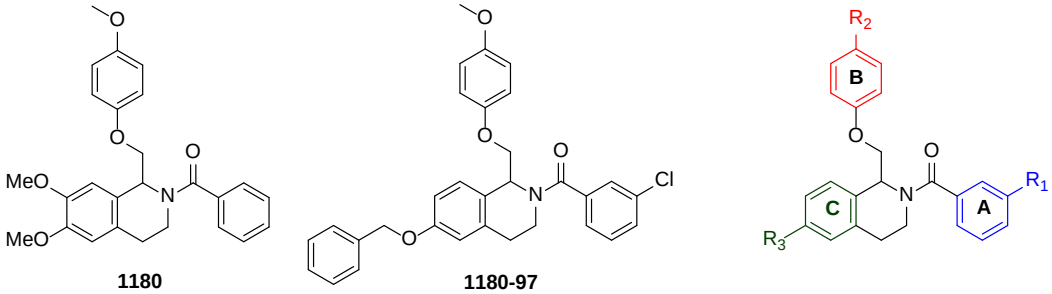

Figure 1. Evolution from compound 1180 to 1180-97, along with generic structure for SAR development.

Compound **1180** underwent extensive structure activity relationship (SAR) studies to drive the potency down from 11 μM and 13 μM at GluN2C- and GluN2D-containing receptors, respectively. One of the most potent compounds of the class after this synthetic work is benzyloxy-containing

1180-97 with approximate EC_{50} values of 0.30 μM at both GluN2C and GluN2D-containing receptors. (**Figure 1**)[7].

The goal of this research was to finish the SAR around rings of the tetrahydroisoquinoline core that were considered to be important and to continue to explore the stereoselectivity of the class since it had previously been established that only the (+)-enantiomer was active at GluN2C and GluN2D-containing NMDA receptors[7,8]. The SAR was continued around portions of the class that had not been explored in previous work including the B-ring, the linker between the B-ring and the core, the C-ring, and the linker between the A-ring and the core (**Figure 1**). The goals of this project were realized with the following strategy:

1) Continue to design an SAR around the tetrahydroisoquinoline class of molecules based on previous work and substituent placement and identity that had not been explored.
2) Synthesize these compounds and test activity in GluN2C- and GluN2D-containing NMDA receptors expressed in *Xenopus laevis* oocytes. The biological evaluation of these compounds was completed in the laboratory of Dr. Steve Traynelis.
3) Separate select CIQ analogs to further study the enantiomeric properties of this class of compounds.

1.2 Introduction and Background

1.2.1 NMDA Structure, function, and localization

Glutamate is the major excitatory neurotransmitter in the mammalian central nervous system (CNS) that acts as an agonist at two types of receptors: second messenger-linked metabotropic glutamate receptors (mGluRs) and ionotropic cation-selective ligand-gated channels (iGluRs). The NMDA (*N*-methyl D-aspartate) receptor, along with AMPA (α-amino-3-hydroxy-5-methyl-4-isoxazolepropionic acid) and kainate receptors, comprise three classes of iGluRs[5]. These receptors have been linked to normal nervous system development and function, and are implicated in a number of diseases, such as Parkinson's disease[4], Alzheimer's disease[3], schizophrenia[1,9,10], and depression[11,12]. The NMDA receptor is distinct from other ionotropic glutamate receptors in terms of its pharmacological

properties. Selective agonists (such as NMDA (**1**)) and antagonists, such as D-APV ((2*R*)-amino-5-phosphonovaleric acid) (**2**), are inactive at AMPA and kainate receptors, but active at the NMDA receptor. The synthetic glutamate mimics AMPA (**3**) and kainic acid (**4**) are active at the AMPA and kainate receptor, respectively, but inactive at NMDA (**Figure 2**).

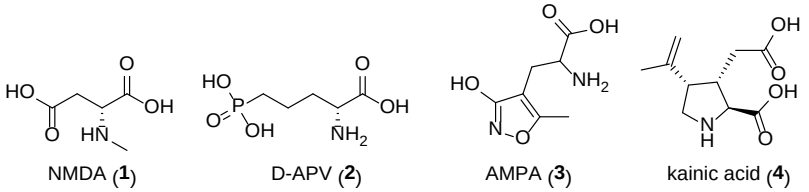

Figure 2. Glutamate mimics that selectively bind to receptors from the iGluR class.

NMDA receptors also show substantial differences from AMPA and kainate receptors in amino acid sequence, and clear differences in terms of their structure[13–15]. The NMDA receptor is unique in that the ion channel shows a high calcium permeability[16], voltage dependent-channel block by physiological concentrations of Mg^{2+}[17], the requirement of the binding of two co-agonists for activation (glycine or D-serine and glutamate), and multimeric subunit composition containing both GluN1 and GluN2 subunits[18]. These features, together with the ability of NMDA receptors to control synaptic plasticity and their involvement in neurological diseases, have created a therapeutic rationale driving the development of NMDA glutamate modulators. Indeed, enhancement or reduction of NMDA receptor function has been suggested as a potential treatment for a variety of neurological disorders (discussed in **Chapter 1.2.2 – 1.2.4**). Due to their relative importance, a great deal is known about NMDA receptors, including the arrangement of different subunits within the tetrameric assembly, functional properties, and binding sites of various agonists, antagonists, and modulators[5,6].

NMDA receptors mediate a slow Ca^{2+}-permeable component of excitatory synaptic transmission[16] that requires the binding of the co-agonist glycine in addition to synaptically-released glutamate. Thus, systems that regulate concentrations of glycine, glutamate, and D-serine can influence NMDA receptor function. In addition to the simultaneous binding of glycine and glutamate[18], the opening of the channel must also be accompanied by a membrane depolarization to relieve channel block by

external magnesium in order to allow current flow[17] (**Figure 3**). The NMDA receptor gating mechanism, which leads to the opening of the ion channel pore, takes on the order of 5-15 milliseconds, which is relatively slow compared to the submillisecond time scale for activation of AMPA receptors[19]. The NMDA receptor is typically composed of two GluN1 subunits and two GluN2 subunits. There is one gene that encodes for GluN1, but four gene product for the GluN2 subunit, labeled GluN2A-GluN2D. Although not as well understood, two GluN3 subunits (GluN3A and GluN3B) can also be incorporated into the NMDA receptor complex, and may alter NMDA receptor properties. NMDA receptors comprised of GluN1, GluN2, and GluN3 subunits have been suggested to exist in the adult brain[20]. Receptors can contain two different GluN2 subunits, such as one GluN2A and one GluN2B subunit, and these so-called triheteromeric NMDA receptors have unique properties[6,21] (**Figure 3**).

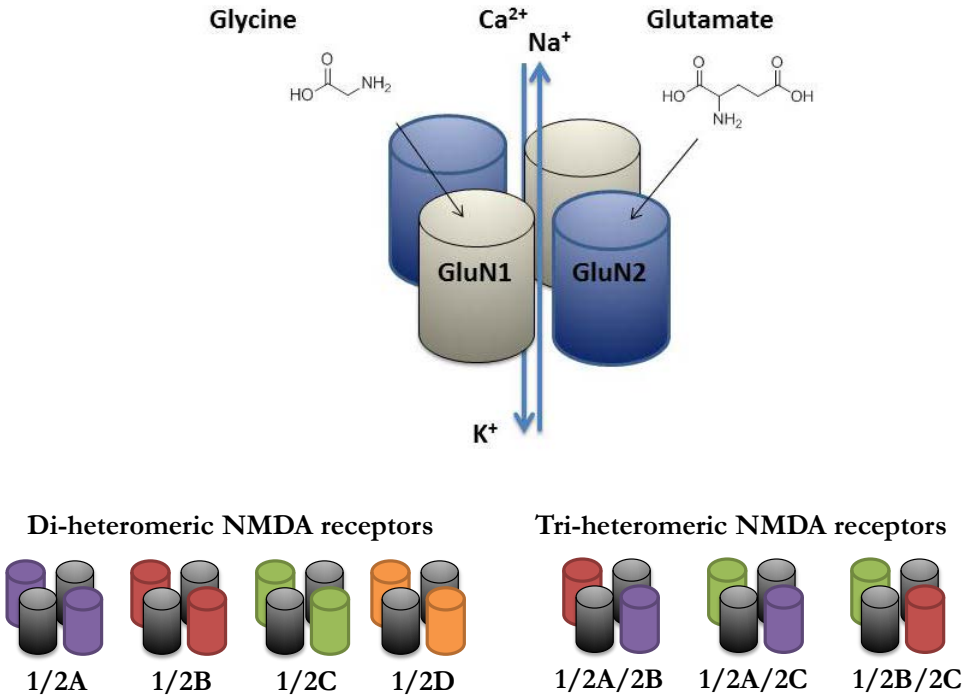

Figure 3. Opening of NMDA receptor and combinations of GluN1/GluN2-containing receptors.

The ionotropic glutamate receptors as a class have a somewhat similar sequence homology, suggesting that the three receptors share a similar architecture. The structure of all ionotropic

glutamate receptor subunits includes four semiautonomous domains: an amino terminal domain (ATD), a ligand binding domain (LBD), a transmembrane domain (TMD), and a carboxyl terminal domain (CTD) (**Figure 4**). The TMD region is the ion pore of the receptor.

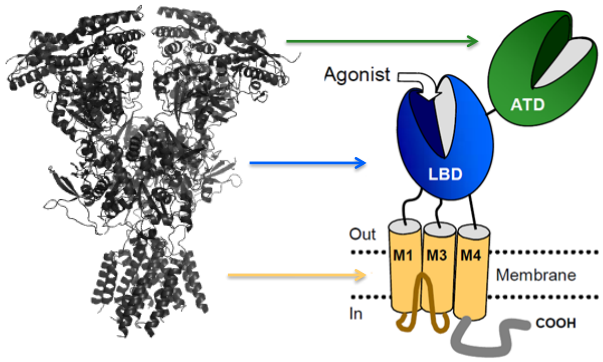

Figure 4. NMDA receptor subunit rearrangement. ATD = Amino terminal domain, LBD = ligand binding domain.

Each of the various NMDA subunits has been studied independently in varying detail. Crystal structures of a GluN1-GluN2B ATD[22,23] revealed a clamshell-like structure divided into two parts, R1 and R2. Although high sequence homology exists between NMDA receptors and non-NMDA receptors in terms of the LBD[24], the ATD of the NMDA receptor shares low sequence homology with non-NMDA receptors. In contrast to non-NMDA receptors, multiple binding sites for allosteric modulators that regulate receptor function have been described in the ATD of NMDA receptor [25]. Zn^{2+} binds to both the GluN2A and GluN2B subunits [26,27] within a pocket in the cleft of the GluN2B ATD clamshell[22], while the GluN2B-selective inhibitor ifenprodil binds at the interface between GluN1 and GluN2B ATD heterodimer, distinct from the zinc binding site[23]. The ATD of the NMDA receptor controls channel opening probability and the deactivation rate following glutamate removal, which is in contrast to the AMPA and kainate receptors, where the ATD does not appear to detectably regulate ion channel activity[28]. This may reflect the closer interaction of ATD with the LBD observed in NMDA receptors (3107 $Å^2$) compared to non-NMDA receptors (1470 $Å^2$)[14].

Crystal structures of the isolated LBD region[18,29,30] of the NMDA receptor reveal a clamshell-like structure composed of two lobes, D1 and D2. The glutamate agonist binding pocket is located in the cleft between D1 and D2, and once glutamate binds, a conformational change takes place whereby the D2 lobe moves to produce a partial closure of the intralobe cleft[18]. Although sequence homology among NMDA and non-NMDA receptor LBD regions are high, evidence suggests that the conformational changes that lead to channel opening differ between NMDA and AMPA[29,30].

The transmembrane domain (TMD) forms the ion channel pore and is comprised of three transmembrane helices and a loop that exits and enters the pore, which resembles an inverted potassium channel[13]. The TMD is connected to the LBD by three short linkers associated with each of the transmembrane helices (M1, M3, and M4). M2 typically refers to a short reentrant loop that lines the inner pore of the channel and controls ion permeation and channel blockage[31]. Voltage dependent blockage of the NMDA receptor by extracellular Mg^{2+} ions occurs within the channel pore and is influenced by residues in the TMD[17], similar to uncompetitive antagonists known as channel blockers[9,30]. The intracellular portion of the glutamate receptors comprises the carboxyl terminal domain (CTD), which influences membrane targeting and provides multiple sites for post-translational modifications that can alter receptor function and trafficking[5].

Recently two crystal structures of the heterotetrameric NMDA receptor ATD-LBD-TMD have been solved (**Figure 4**), revealing the structural details that differentiate the NMDA receptor from the closely related AMPA receptor[14,15]. These crystal structures also allow a view of the inter-subunit and inter-domain interactions of the NMDA receptor, which should be valuable in understanding how molecules interact with the receptor to modulate activity. Both crystal structures were of an intact GluN2B-containing NMDA receptor, and both structures revealed that the ATD is much more tightly packed and in closer contact with the LBD in the NMDA receptor than in the AMPA receptor. The ATD and the LBD appear to be a single unit (**Figure 4**), while in AMPA receptors, a clear divide exists because of flexible linkers connect the LBD and ATD[13]. This spacing may be the reason that NMDA receptors show pronounced regulation of ion channel function by the ATD[28].

Overall 2-fold symmetry of the receptor was observed for the extracellular portion of the glutamate receptor family, with subunits organized in a layered dimer-of-dimer arrangement, where 2-fold symmetry between the ATD and LBD exists, and pseudo-fourfold symmetry within the TMD. While the ATD and LBD portions of the receptor were elucidated in the two crystal structures, more studies in addition to higher resolution structures will be necessary to fully understand the ion-pore and TMD regions.

There are four GluN2 gene products: GluN2A, GluN2B, GluN2C, and GluN2D. Each GluN2 subunit imparts unique properties to the receptors, with differences in the deactivation time course, channel opening probability, channel open duration, and agonist sensitivity [6,18,33,34]. GluN2A-containing receptors have a much faster deactivation time course than the other GluN2 subtypes[35], and are also less sensitive to glycine and glutamate than the other subtypes. In terms of opening probability, recombinant GluN2A receptors have a high open probability, nearly 10-fold higher than GluN2C and GluN2D-containing receptors[36]. Channel properties including Mg^{2+}blockade, Ca^{2+} permeability, and single-channel conductance vary between GluN2A/B and GluN2C/D receptors, and are determined by a single GluN2 residue in the M3 transmembrane region[37]. Not only are pharmacological properties dependent on GluN2 subunit composition, but also developmental expression levels and location in the brain. At the embryonic stage of a rat brain, low levels of GluN1, GluN2B, and GluN2D can be observed, whereas GluN2A and GluN2C are not prominently expressed. By birth, GluN2B is expressed in the cortex and hippocampus, while GluN2D is expressed in the thalamus, hypothalamus, and brain stem. GluN2A is expressed in the hippocampus and cortex and GluN2C is most highly expressed in the cerebellum[38–40]. In the adult rat brain, all NMDA receptor subunits are expressed, with GluN2A being most strongly expressed, while GluN2D is detected in the lowest amounts (**Figure 5**). The high expression of GluN2B and GluN2D at birth and in early childhood suggests that these receptors are important for synaptogenesis and synaptic maturation, while the expression of GluN2B and GluN2A in the adult brain suggests that these two receptors may be important functions crucial to higher learning such as

synaptic function and plasticity[6,38]. Since subunit composition determines pharmacological properties of the receptor and expression location in the brain, a number of disease states could be targeted with subunit-selective modulators, including schizophrenia, cognitive decline, and anxiety (discussed below).

Figure 5. Profile of GluN2 subunit composition in an adult rat brain.

1.2.2 Therapeutic rationale for NMDA receptor positive allosteric modulators as a treatment for schizophrenia

Schizophrenia, reported to affect 1% of the world's population[41], is accompanied by symptoms that are characterized as positive and negative. Positive symptoms are behaviors that were usually not present before, such as hallucinations, delusions, and agitated body movements. Negative symptoms, on the other hand, can be thought of as behavioral deficits and include withdrawal, lack of motivation, and lack of affective response. Schizophrenia is also often accompanied by cognitive impairment, which is typically subtle, but is common and can include problems with working memory, attention, and decision-making.[42] While many people are treated with antipsychotic medication, this treatment only reduces symptomology without being curative. A landmark 18-month study, known as Clinical Antipsychotic Trials of Intervention Effectiveness (CATIE), that enrolled 1,500 patients with schizophrenia compared the effectiveness of a first generation antipsychotic, perphenazine, with the more commonly used second-generation antipsychotics[43]. Researchers expected to find that the second-generation drugs were superior to perphenazine, but instead little difference was found in terms of efficacy, safety, and effectiveness in reducing negative symptoms. Instead, the key difference between the drugs was side effect profile[44]. Based on these results, the

authors of the paper recommended novel treatments for schizophrenia that differ in mechanism of action from the commonly prescribed antipsychotics.

The NMDA receptor is one such pathway that researchers have attempted to target in an effort to reduce the symptomology of schizophrenia, and there are many instances in the literature where the NMDA receptor has been indicated in the disease. Genetic linkage studies have identified genes implicated in schizophrenia that also encode or regulate a number of proteins that influence NMDA receptor activity.[45] One example of this is neuregulin-1 (*NRG1*), which regulates expression of glutamate subtypes and has specifically been linked to GluN2C expression. It has been reported that neuregulin-β regulates GluN2C expression in maturing synapses of cerebellar granule cells,[46] and post-mortem schizophrenia patients and control patients with a specific *NRG1* polymorphism were reported to have lower levels of GluN2C expression in the cerebellum.[47] It was also shown that mice hypomorphic for *nrg1* exhibited behavioral abnormalities that could be reversed with the antipsychotic clozapine and that these hypomorphic mice expressed less functional NMDA receptors than control mice.[48] A second gene related to schizophrenia is *G72*, which interacts with D-amino acid oxidase (DAAO). DAAO is an enzyme that catabolizes through oxidation D-serine, an NMDA receptor agonist, suggesting that schizophrenia is implicated in the NMDA receptor pathway.[49] Other schizophrenia risk genes related to the NMDA receptor activity include *RGS4*,[50] dysbindin,[51] and *PPP3CC*.[52]

Studies have also demonstrated altered NMDA expression levels in the brains of those diagnosed with schizophrenia. In a small study (9 schizophrenia patients and 10 controls) that measured the gene expression of GluN1, GluN2A, GluN2B, GluN2C, and GluN2D subtypes in post-mortem samples of nine elderly schizophrenic patients using *in-situ* hybridization, researchers found increased levels of GluN2D gene expression in the molecular and granular layer of the right cerebellum.[47] A similar study which looked at the alternations in gene expression of GluN2 subunit mRNA in the prefrontal, parieto-temporal, and cerebellar cortex tissue from 15 post-mortem schizophrenia patients found a 53% increase in GluN2D mRNA expression in the prefrontal cortex compared to

controls, but no significant differences for the other subtypes.[53] Researchers suggest that an increase in GluN2D expression is a compensation for hypoactivity of the NMDA receptor in these regions of the brain; the GluN2D subtype has a considerably longer decay rate and lowered threshold for magnesium blockade than other GluN2 subtypes that would help ensure that its overexpression would correct for NMDA receptor activity deficiencies.[47]

In a larger, more recent study that analyzed post-mortem samples from 37 patients diagnosed with schizophrenia, researchers found decreased expression of GluN2C and GluN1 in the dorsolateral prefrontal cortex (DLPFC). Although researchers saw no change compared to controls concerning the GluN2B subtype, in an antemortem testing cohort, schizophrenia patients that carried the minor allele of a GluN2B gene single nucleotide polymorphism (SNP) rs1805502 had significantly decreased levels of reasoning ability compared to schizophrenia patients that did not carry this polymorphism. Interestingly, researchers also found that expression of the SNP rs1805502 correlated to a decrease in GluN1 gene expression in the schizophrenia patients.[54] The decreased expression of GluN2C and GluN1 in the DLPFC was also observed in an additional study utilizing *in situ* hybridization that compared post-mortem samples from 15 schizophrenia patients with 15 controls.[55]

The glutamate hypofunction hypothesis, which links NMDA receptor activity and schizophrenia, originated in the 1950's when it was reported that the effects of using PCP, an NMDA receptor channel blocker, were almost synonymous to schizophrenic symptomology; users of PCP exhibit behaviors that closely mirrored the positive and negative effects of schizophrenia.[56,57] NMDA receptor channel blockers MK-801[58] and ketamine[59–62] also induce these same schizophrenia-like symptoms, and for this reason, the administration of NMDA receptor channel blockers has become a widely used and accepted model of schizophrenia in humans and animals.[63,64] While the majority of antipsychotic medications relay on D2 dopamine antagonists, amphetamine, which induces dopamine release, only induces symptomology that mimics the positive effects of schizophrenia,[65] while NMDA receptor channel blocker induce both the positive and negative effects.

Schizophrenia is most likely a result of dysfunction from a number of neurotransmitter systems, including GABA. Post-mortem analysis of schizophrenia patients revealed a decrease in GABA in the nucleus accumbens and the thalamus.[66] The hypofunction of the GABAergic system secondary to a reduction of GABA and glutamate decarboxylase (GAD) in fast-spiking, parvalbumin-containing interneurons has been proposed to contribute to the disease. In this model, NMDA receptors in GABAergic neurons serve as homeostatic sensors for principle cell activity. Hypofunction of the NMDA receptor system is interpreted as decreased principle cell drive and triggers reduced GABAergic function as the interneuron seeks to increase principle cell activity to restore normal activity.[67]

The NMDA receptor agonist D-serine has shown to improve the positive and negative symptoms of schizophrenia, in addition to the cognitive deficits.[68–70] Additionally, the activity of the NMDA receptor can be indirectly regulated, and recent clinical trials have focused on developing and testing inhibitors of the indirect modulator glycine transporter I (GlyT1) as a means to increase activity of the NMDA receptor [71]. GlyT1 plays an essential role in controlling the level of glycine at the excitatory synapses of the NMDA receptor and prevents high levels of glycine that would lead to saturation of the glycine site. GlyT1 inhibition should increase the concentration of glycine at the NMDA receptor within synapses, but activation of the receptor would still rely on glutamate release. In contrast to agonists that enhance the maximally effective response of NMDA receptors, GlyT1 inhibitors instead increase the open probability of the NMDA receptor only under certain physiological conditions that lead to non-saturating concentrations of glycine or related glycine site agonists [72,73]. This unique mechanism of action of GlyT1 inhibitors may have clinical benefits in disease states that have been proposed to stem from a deficiency of NMDA receptor activity, such as schizophrenia[74–77]. Hoffmann La-Roche developed the GlyT1 inhibitor Bitopertin (also referred to as RO4917838 and RG1678), which had advanced to Phase III clinical trials after the successful completion of two Phase II trials [78]. This compound would have been the first in its class of third generation schizophrenia drugs, but unfortunately, in January of 2014 it was reported that the first

two Phase III clinical trials meant to test the effect of Bitopertin on the negative symptoms of schizophrenia failed to meet their primary endpoints [79]. Despite this information, the interest in GlyT1 inhibitors remains, however there is still a need to study the modulation of the NMDA receptor pathway through novel means, including the use of positive allosteric modulators.

1.2.3 Therapeutic rationale for NMDA receptor positive allosteric modulators as cognitive enhancers

Activation of NMDA receptors leads to long-term potentiation (LTP), a mechanism underlying synaptic strength[80], and changes in synaptic strength are believed to play a role in forming memories and learning[81]. Additionally, the deletion of the GluN1 NMDA gene in the CA1 pyramidal cells in the hippocampus leads to an absence of LTP in the CA1 cells, and hippocampal GluN1 knockout mice show deficiencies in spatial learning [82], object recognition, and contextual fear memory [83]. GluN2B receptor overexpression in the forebrain of mice results in enhanced activation of NMDA receptors in response to stimulation [84], which has been shown to improve learning, long-term memory, and spatial performance. These genetically modified mice also exhibit superior cued and contextual fear conditioning, along with faster fear extinction [85–88]. (A more complete discussion of the role of GluN2B in cognitive enhancement is included in **Chapter 2.2.1**). For these reasons, modulation of the NMDA receptor has become a strategy for enhancing cognitive function, especially for the aging population that are experiencing cognitive decline[89].

While NMDA receptor antagonists inhibit LTP, and certain NMDA antagonists, such as ketamine[90,91] and the competitive antagonist SDZ EAA494[92], have been shown to negatively affect memory and learning in human studies, there are instances where inhibition of the NMDA receptor results in improved cognitive function. One important example of this is memantine, a drug FDA-approved for its ability to slow down the cognitive decline associated with Alzheimer's disease[93]. The reasoning behind memantine's ability to inhibit cognitive decline has been demonstrated in hippocampal slice experiments where Mg^{2+} is reduced[94]. The reduction of Mg^{2+} resulted in inhibition of LTP, but the addition of memantine restored this loss. A similar effect was observed with the

NMDA antagonist D-APV (**2**)[95], and although memantine and D-APV have different mechanism of actions, it is thought that these compounds block the activation brought on by removal of Mg^{2+}, but then sufficient glutamate restores the NMDA receptor to normal channel functioning, which results in LTP[96].

Additionally, the application of exogenous glycine[97–99], as well as the application of GlyT1 inhibitors, such as *N*[3-(4'-fluorophenyl)-3-(4'-phenylphenoxy)propyl]sarcosine (NFPS) (**5**)[98,99] and CP-802,079 (**6**)[100], have been shown to increase glycine levels at the NMDA receptor, which in turn increases activation of the NMDA receptor. Evidence for the improvement in cognitive function with GlyT1 inhibitors include studies where **5**[101] and **6**[100] increased LTP in hippocampal slices, inhibitor **5** enhanced social memory in rats, and inhibitor SSR 504734 (**7**) heightened cognitive ability in rats in a test to measure cognitive flexibility[102] (**Figure 6**).

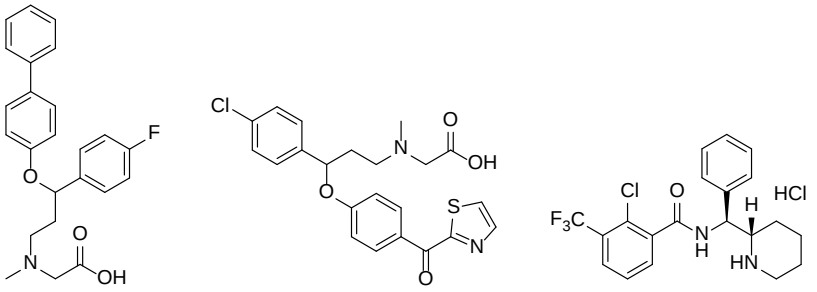

NFPS (**5**) CP-802,079 (**6**) SSR 504734 (**7**)

Figure 6. GlyT1 inhibitors shown to affect cognitive function.

Alternatively, increasing levels of D-serine, a co-agonist for the glycine site, has been shown to rescue LTP potentiation in hippocampal slices where the NMDA agonist 7-chlorokynurenate (7-C1KY) has been applied[103,104]. The enzyme serine racemase converts L-serine and glycine into D-serine in astrocytes, and serine racemace knockout mice exhibited deficits in object recognition tests and odor sequence tests compared to controls, suggesting disruption of memory for order when D-serine is not available[105]. Utilizing HPLC (high pressure liquid chromatography) to measure tissue availability of D-serine, L-serine, and serine racemase in young and old mice hippocampal slices, researchers found that in older samples compared to younger, the levels of D-serine had decreased, while the levels of L-serine were slightly higher. This decline in the ratio of D-serine to L-serine can be

explained by a significant decline in the levels of serine racemase in aged mice. The LTP was weaker in the hippocampal slices from older mice compared to younger as well, but this effect could be rescued by the application of D-serine; age-dependent LTP decline could be reversed when the glycine site of the NMDA receptor was saturated with D-serine[106]. While GlyT-1 inhibitors and D-serine represent continued efforts to enhance cognitive function, an additional possibility for increasing NMDA potentiation is the modulation of the receptor through positive allosteric modulators.

1.2.4 Therapeutic rationale for NMDA positive allosteric modulators as a treatment for anxiety disorders

While fear is a normal human emotion, continued fear when the threat of danger has passed can lead to a number of debilitating anxiety disorders. The most recent Diagnostic and Statistical Manual of Mental Disorder, the DSM-5, places anxiety disorder into one of three categories: 1) anxiety disorders, 2) obsessive-compulsive disorders, and 3) trauma and stress-related disorders, including post-traumatic stress disorder (PTSD)[107]. The main treatments for anxiety disorders include benzodiazepines and anti-depressants, such as serotonin-reuptake inhibitors (SSRIs)[108]. Cognitive behavioral therapy (CBT), a form of psychotherapy has also proven successful in treating many types of anxiety disorders[109], but not in conjunction with medication[110,111]. Ketamine, the NMDA receptor channel blocker, has seen a reemergence in the clinical world as its use has been accompanied with positive effects for the treatment of OCD[112] and PTSD[113], although the mechanism of action is not well understood.

Fear research is typically based on the Pavalovian fear conditioning animal model that relies on the pairing of a conditioned stimulus (CS) and an unconditioned stimulus (US). The neutral CS, such as light or a tone, is given in conjunction with an aversive, startling US, which is usually a foot shock. This model has been successful, in part, because the pairing of these two stimuli elicits behaviors from the animal that can be measured (e.g., freezing, elevated blood pressure, or startle response), and represent a learned fear response. By gradually administering the CS without the US, the fear can

eventually be reduced, and again, a set of behavioral markers represent the extinction of the fear[114]. NMDA receptors play a fundamental role in learning and memory, and it thought that the molecular mechanisms in the amygdala behind the acquisition of fear have much in common with learning and memory[114].

NMDA antagonists that weaken LTP or LTD (long-term depression) in the amygdala have been shown to impair fear acquisition and fear extinction.[115,116] Studies with a number of NMDA antagonists have blocked fear acquisition[117–119] and reduced fear extinction[120–122] in animal models of fear conditioning, while amygdala infusions of the GluN2B-selective inhibitors ifenprodil[123] and traxoprodil[124] impair fear conditioning. Co-agonist for the glycine site, D-serine, is a partial agonist at GluN2A, GluN2B, and Glu2D, but causes greater potentiation at GluN2C than saturating concentration of glycine. Interestingly, D-serine enhanced fear excitation when infused in the amygdala, suggesting that modulation of the GluN2C receptor is a means to heighten fear extinction[125]. GluN2C knockout mice are impaired during tests of fear acquisition[2] and direct amygdala injections of CIQ (**22**), a positive allosteric modulator for GluN2C- and GluN2D-containing receptors, have resulted in mice that have enhanced fear acquisition and improved fear extinction[126]. These studies combined highlight the potential for a positive allosteric modulator in treating anxiety disorders.

1.2.5 Classes of NMDA receptor modulators

The diversity of functions mediated by many possible subunit combinations makes the NMDA receptor a candidate for a therapeutic target for a variety of disease states, including schizophrenia, cognitive enhancement, and anxiety disorders (**Chapters 1.2.2 – 1.2.4**). Moreover, a variety of binding sites for antagonists and modulators with varying degrees of subunit-selectivity have been discovered and exploited.

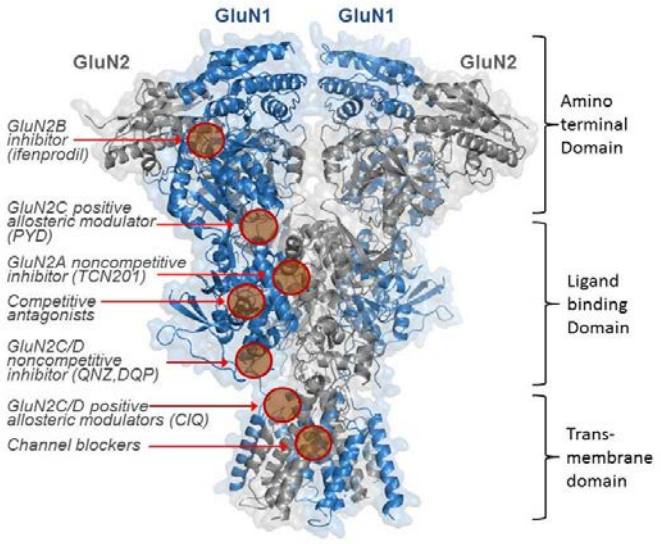

Figure 7. NMDA receptor crystal structure and binding locations of NMDA receptor modulators. Figure was generated using PDB code 4PE5.

Uncompetitive antagonists, also known as channel blockers, bind deep in the ion pore (**Figure 7**) and require activation of the receptor prior to binding[32]. FDA-approved adamantine (**8**) and memantine (**9**) (**Figure 8**), in contrast to high-affinity channel blockers, have been well-tolerated in the clinic. This may reflect their fast unbinding-rates and relatively low affinity, which favors blockade of channels that are opened for prolonged periods of time over transiently activated receptors. Memantine and adamantine have been approved by the FDA for the symptomatic treatment of Alzheimer's [93]. Ketamine (**10**) is an anesthetic that is typically used more often in children than adults[127], and it has also been effective in multiple trials for treatment-resistant depression [128]. Additionally, ketamine has been effective in preliminary clinical trials for obsessive compulsive disorder (OCD)[112] and post-traumatic stress disorder (PTSD)[113]. These initial successful outcomes will most likely lead to the testing of ketamine in additional clinical settings. Other well-studied channel blockers that share a similar binding site within the pore include MK-801 (**11**) and phencyclidine (PCP) (**12**). Dextromethorphan (**13**), the active ingredient in common over-the-counter (OTC) antitussives, and its primary metabolite, dextrorphan (**14**), are also noncompetitive NMDA receptor antagonists that act at a binding site within the pore[129–131]. While the demethylated

metabolite **14** is more potent than dextromethorphan **13** at NMDA receptors[130,132], both compounds have off-target effects at sigma 1 and sigma 2 receptors[133,134]. In 2010, Nuedexta, a combination of dextromethorphan hydrobromide and quinidine sulfate (which surpresses the metabolism of dextromethorphan to dextrorphan[135]) became the first FDA approved drug for the treatment of pseudobulbar affect (PBA), which is a neurological disease characterized by involuntary bursts of emotion, such as laughing or crying[136]. Currently, available channel blockers are unable to differentiate between GluN2 subunits, with less than 10-fold selectivity described[137]. This lack of subunit-selectivity has been suggested to be partially responsible for the associated negative side effects, which include altered cardiovascular function, decreased motor function, hallucinations and delusions[138].

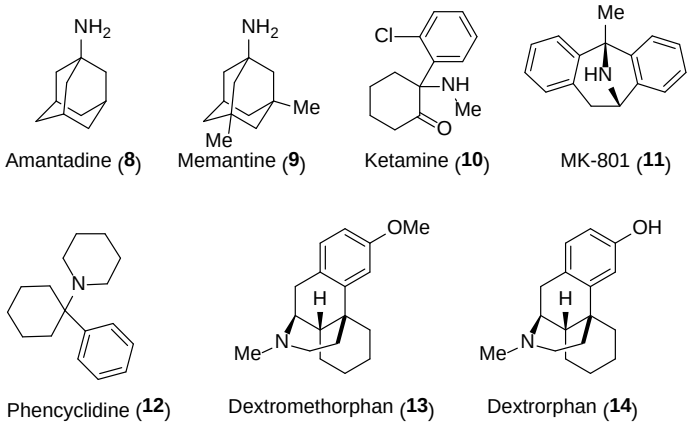

Figure 8. NMDA receptor channel blockers.

A breakthrough in the discovery of NMDA receptor modulators was the identification of the first subunit-selective NMDA receptor modulator, the noncompetitive antagonist ifenprodil (**15**), which is up to 400 times more selective for receptors that contain the GluN2B subunit than GluN2A, GluN2C, or GluN2D subunits [139,140]. Ifenprodil was originally reported to be a neuroprotectant and related compounds, such as traxoprodil (**16**) and Ro 25-6981 (**17**) (**Figure 9**), have been tested in advanced clinical trials for traumatic brain injury, neuropathic pain, and treatment-resistant depression [141–145]. GluN2B-selective inhibitors are typically better tolerated than channel blockers in terms of many unwanted side effects, including motor ataxia[144]. Initial enthusiasm has been

dampened however due to observed side effects that are similar to behaviors observed with PCP use, raising concerns of abuse potential[147]. Further research is required, but the ifenprodil template and the binding mechanism continue to be a resource for finding new scaffolds that selectively modulate GluN2B-containing receptors.

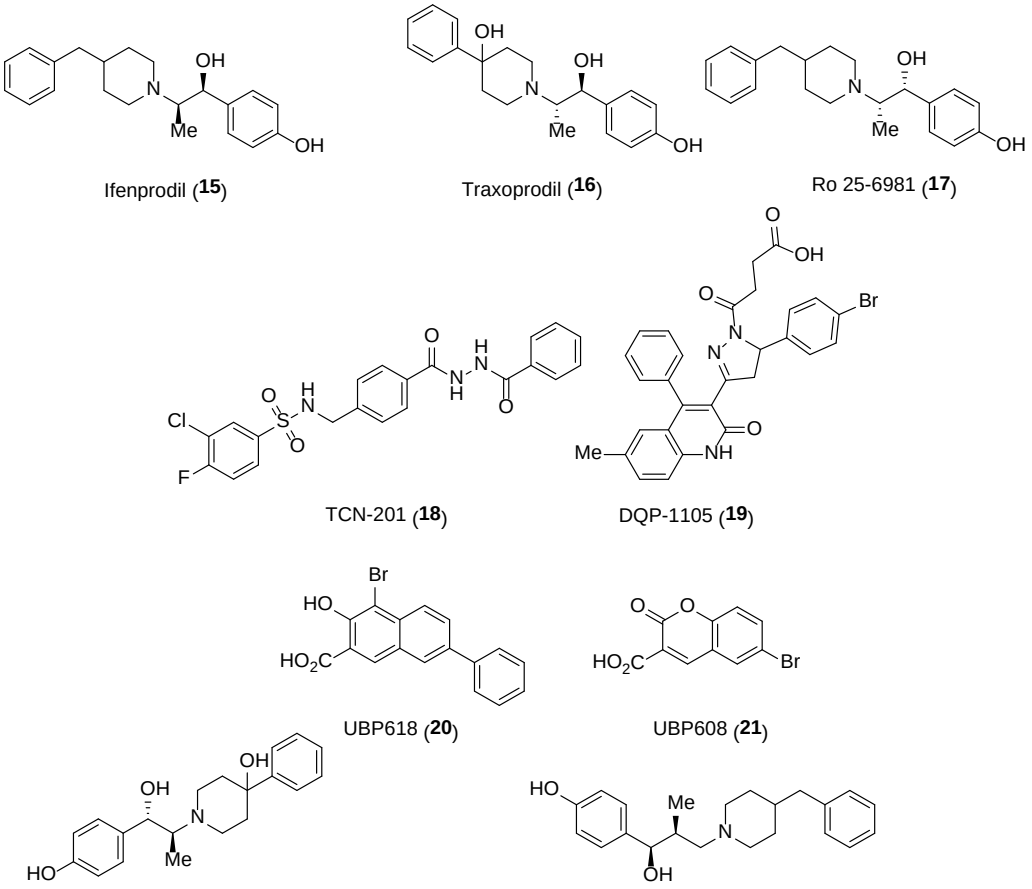

Figure 9. NMDA receptor subunit-selective antagonists.

More recently, an allosteric modulator highly selective for GluN2A-containing receptors, TCN-201 (**18**), was identified [148]. TCN-201 acts as a noncompetitive modulator that depends on glycine; the binding of TCN-201 accelerates the dissociation of glycine, and thus is an allosteric regulator of glycine binding [149,150]. Although more work is necessary to elucidate the exact binding site of the compound, initial studies suggest that TCN-201 binds at the GluN1/GluN2 LBD interface, a novel site of NMDA receptor modulation [151] (**Figure 7**). An additional class of noncompetitive antagonists include the dihydroquinoline-pyrazolines such as DQP-1105 (**19**), compounds that show an IC_{50}

increase following glutamate binding, but not glycine, and based on site-directed mutagenesis have been suggested to bind to the S2 region of the LBD [152] (**Figure 7**). A series of naphthalene and phenanthrene derivatives that act as positive and negative modulators of the NMDA receptor with varying degrees of potencies and selectivity have also been discovered (**Figures 9** and **10**). The naphthalene compound UBP618 (**20**) exhibits non-selective inhibition with approximate IC_{50} values of 2 μM at each of the subunits, while UBP608 (**21**) exclusively inhibits GluN2A-containing receptors [153]. The structurally related compound UBP714 (**22**) no longer exhibits any inhibition, but instead slight potentiation with a modest selectivity for GluN2A and GluN2B-containing receptors over GluN2D-containing receptors [154]. Additional selective potentiators include UBP512 (**23**) for GluN2A-containing receptors and UBP710 (**24**) for GluN2A and GluN2B-containing receptors. Compound **23** also shows inhibition at GluN2C and GluN2D-containing receptors, but no activity at GluN2B-containing receptors [153,155]. The structure activity relationship studies [156] suggest that these compounds bind in the LBD region [153].

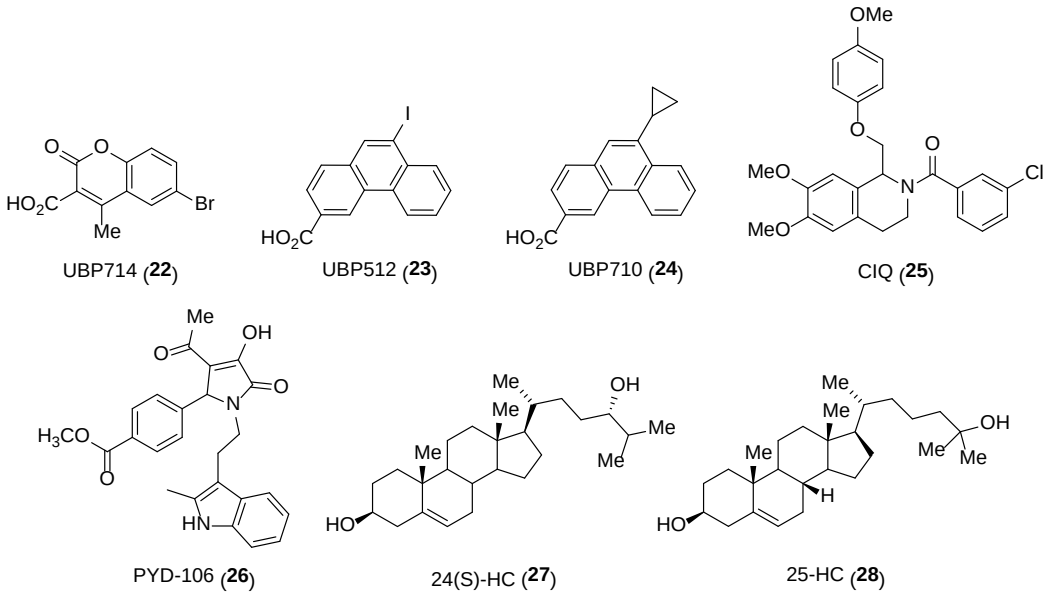

Figure 10. NMDA receptor subunit-selective positive allosteric modulators.

Three other classes, in addition to the naphthalene and phenanthrene (**22**-**24**) compounds, have been reported as small molecule subunit-selective allosteric potentiators. Tetrahydroisoquinoline compounds such as the prototype CIQ (**25**) are selective for GluN2C and GluN2D-containing

receptors with EC_{50} values of 3-6 μM, and SAR studies have revealed that activity resides exclusively in the (+) enantiomer [7,157,8]. Site-directed mutagenesis suggests that the structural determinants of action for these compounds reside within the pre-M1-M1 region [158] (**Figure 7**). Recently, a pyrrolidinone (PYD) class of compounds has been reported that are ~50-fold selective for the GluN2C subunit over GluN2A, GluN2B, or GluN2D[159,160], and a potent member of this class, PYD-106 (**26**), was reported to have an EC_{50} value at GluN2C of 13 μM[160]. These compounds appear to target a new site at the interface between the LBD and ATD [160](**Figure 7**). Additionally, The endogenous oxysterol and major cholesterol metabolite in the brain, 24-(S)-hydroxycholesterol (24(S)-HC) (**27**), has also been identified as a potent positive allosteric modulator selective for the NMDA receptor over AMPA or GABA (gamma-Aminobutyric acid) receptors. Although the binding site of **27** and its synthetic derivatives has not been fully elucidated, it does appear to be distinct from the neurosteroid pregnenolone sulfate [161]. Further studies regarding the mechanism of action behind these oxysterols revealed that a second endogenous oxysterol, 25-hydroxycholesterol (25-HC) (**28**), non-competitively inhibited the potentiation of 24(S)-HC (but did not inhibit pregnenolone sulfate), suggesting two novel binding sites for this class of compounds [162].

1.2.6 Mechanism of action and structural determinants of CIQ

CIQ (**25**) was initially discovered in a Ca^{2+} imaging high-throughput screen using 96-well plates to identify novel GluN2C and GluN2D-containing NMDA receptor modulators. A baby hamster kidney (BHK) cell line expressing either GluN2C or GluN2D was used in the primary screen, which measured an increase or decrease in Ca^{2+} flux, to test approximately 100,000 compounds. Of this initial primary screening library, 839 compounds (hit rate of 1.4%) altered the response by more than 40% of the control response, and 516 compounds were purchased and taken forward in the secondary screen, a two-electrode voltage clamp assay of *Xenopus oocytes* expressing rat recombinant GluN1/GluN2D. At 10 μM, only 54 compounds produced more than 25% inhibition or potentiation and warranted the analysis of full dose-response curves at GluN2A-, GluN2B-, GluN2C-, GluN2D-containing receptors. From the tertiary screen of 54 compounds, 5 potentiators

(less than 0.01% of the compounds tested in the primary screen) were discovered, and one of these potentiators was tetrahydroisoquinoline compound **1180**. Compound **1180** had an EC_{50} value at GluN2C-containing receptors and GluN2D-containing receptors of 11 μM (181%) and 13 μM (162%), respectively, but early SAR led to chloro-derivative CIQ (**25**), which had improved activity at both GluN2C- and GluN2D-containing receptors over the initial screening hit, **1180** (**Figure 11**).

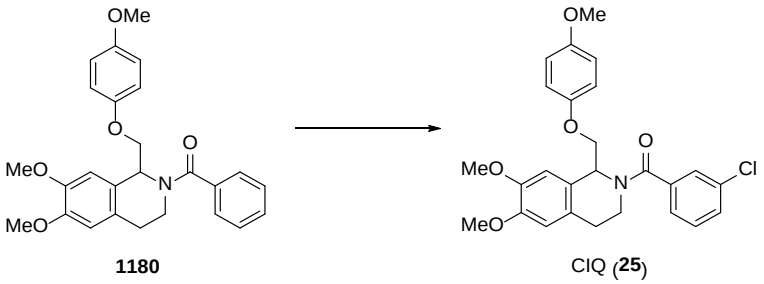

Figure 11. Scaffold of initial screening hit (1180) and CIQ.

The CIQ class of compounds, selective for GluN2C and GluN2D-containing NMDA receptors, provided researchers with a unique tool to study the role of GluN2C and GluN2D subunits in brain function and dysfunction. While there are a number of subunit-selective antagonists for NMDA receptors, there is a lack of subunit-selective potentiators, and for that reason researchers have continued to study and report the mechanism of action and binding site of this class of tetrahydroisoquinoline compounds on GluN2C- and GluN2D-containing receptors[157,158].

In a two-electrode voltage clamp assay in rat recombinant NR2C- and NR2D-containing receptors expressed in *Xenopus laevis* oocytes, CIQ was reported to have an EC_{50} value of 2.7 μM (197%) and 2.8 μM (211%), respectively[157]. Similar EC_{50} values were reported irrespective of the GluN1 splice variant paired with GluN2C and GluN2D, and recombinant human NMDA receptors solicited the same effects. CIQ had no effect on GluN2A- and GluN2B-containing NMDA receptors (**Figure 12**), AMPA, or kainate receptors.[157]

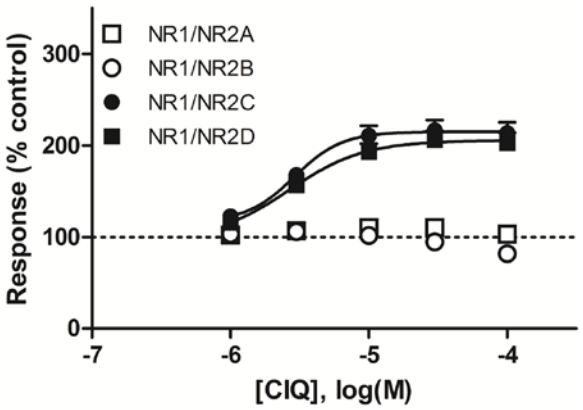

Figure 12. Dose-response curve of CIQ at GluN2A, GluN2B, GluN2C, and GluN2D-containing receptors.

In terms of triheteromeric NMDA receptors, research utilizing oocytes co-injected with GluN1, GluN2C or GluN2D, and a magnesium-insensitive, low-glutamate potency GluN2A mutant (GluN2A*)[163] suggested that CIQ was potentiating triheteromeric receptors, although to a lesser degree than GluN2C and GluN2D-containing diheteromeric receptors. Although CIQ elicits potentiation at GluN2C and GluN2D- containing receptors, potentiation of triheteromeric receptors is suggestive that only one copy in the receptor complex is needed[157].

The binding of CIQ to GluN2C- and GluN2D-containing NMDA receptors had no effect on the glutamate or glycine EC_{50} value, and it did not have an impact on the IC_{50} of Mg^{2+} inhibition. Equal levels of potentiation were observed in the presence of glutamate and NMDA, but no potentiation was recorded when only glutamate or glycine was applied. CIQ potentiation was voltage-independent, and was unaffected by acidic pH, suggesting CIQ plays no role in relieving tonic proton inhibition[157].

To further study the mechanism by which CIQ potentiates the NMDA receptor, a single channel analysis was conducted. At 10 μM, CIQ increased open probability to 190% of the control and decreased the mean shut time to 75%, but had no impact on the mean open time. This suggests that CIQ is binding in a location of the NMDA receptor that impacts channel opening, but has minimal influence on receptor open state stability.

GluN2A-GluN2D chimeric subunits were utilized to determine more exact molecular determinants of CIQ activity since CIQ has no effect on GluN2A-containing receptors. Gain of function studies revealed that the L-S1-M1 region, where L represents the linker between the ATD and LBD, was required for CIQ potentiation. Chimeric receptors with varying and smaller portions of these regions were synthesized and tested, and the regions that elicited activity in the GluN2D-containing GluN2A chimeric receptors in the presence of CIQ were narrowed down to the linker and five residues (residues 590-594) in the M1 transmembrane helix. Although CIQ caused potentiation in the GluN2A chimeric receptor when these two regions were transferred, CIQ did not cause potentiation in the chimeric receptors when only the linker or the five residues were transferred.

Loss of function studies confirmed that the linker region and the M1 region of the transmembrane helix are important structural determinants for activity. Insertion of the GluN2A linker between the ATD and S1 region of the LBD, along with insertion of the GluN2A ATD had no detrimental effects on CIQ activity. However, site-directed mutagenesis of a single residue that is conserved in the M1 region of the TMD in GluN2C- and GluN2D-containing receptors, but not in NR2A- and GluN2B-containing receptors did have an impact on CIQ activity; mutation of this residue in the NR2D chimeric receptors (NR2D T592I) completely abolished CIQ activity. GluN2A-containing GluN2D chimeric receptors containing a 16 amino acid portion of the linker between the ATD and S1 region of the LBD, along with residue T592 in the M1 region were potentiated by CIQ, suggesting that these are the main structural determinants for CIQ activity[157] (**Figure 13**). Although these are important structural determinants for NMDA receptor CIQ-mediated activity, the binding site remains to be determined.

Although these regions together are crucial for potentiation by CIQ, it is unlikely that CIQ is interacting with both the linker of the ATD and LBD and the M1 region simultaneously; according to crystal structures of the NMDA receptor, the sites are too far apart[14,15]. One well-established binding site that has been identified on the NMDA receptor is the ATD interface between GluN1 and GluN2 where ifenprodil binds[23], but even though the linker between the ATD and LBD is a

molecular determinant for CIQ activity, CIQ does not share a binding site with ifenprodil on the ATD interface nor is it binding to the linker region. Potentiation of the NMDA receptor by CIQ was still observed when tested with receptors where both the GluN1 ATD and GluN2 ATD, along with the ATD-LBD linker from both subunits were lacking, suggesting the binding site is elsewhere[158]. Further studies also ruled out other well-established binding sites, including the ion channel pore and the lower portion of the ATD where GluN2C- and GluN2D-selective inhibitors bind.[152] CIQ also does not occupy the exact binding site of GluN2A-selective compound TCN-201[151], but the binding sites could overlap.

To elucidate details behind this novel binding site, an alanine screen of 23 residues in the M1 helix was conducted since mutation of a sole residue (Thr592) on the NR2D subunit abolished activity[157]. From this screen, 6 residues reduced potentiation by CIQ, while 2 residues increased potentiation, and of these 8 residues, the 2 residues (V582 and M586) that caused increased potentiation also modified the glutamate and glycine potencies of the receptor. When V582 was mutated to an alanine, the glutamate and glycine potency increased, but with the M586A mutation, glutamate potency decreased. Although this data suggests that these residues are implicated in agonist potency, the M1 helix region does not constitute part of the agonist binding pocket, and therefore, the M1 helix mutations are most likely involved in the modifying the gating mechanism of the receptor[158]. Additional site-directed mutagenesis of residues 5 Å away from the GluN2 M1 helix revealed that the mutation of 4 residues in the GluN2D S1-M1 region and 2 residues in the GluN1 M4 helix affected CIQ potentiation, and interestingly, the GluN2D S1-M1 region of the receptor is highly implicated in the gating mechanism of the receptor. In the NMDA crystal structure, these amino acids compose a pre M1 cuff helix that make crucial van der Waals contacts with the M3 helix, which acts as the gate for the receptor[13]. CIQ modulates the NMDA receptor by increasing the frequency of the channel opening[157], so it stands to reason that mutations in the pre M1 helix, a region implicated in gating, disrupt any escalations in channel opening caused by CIQ[158].

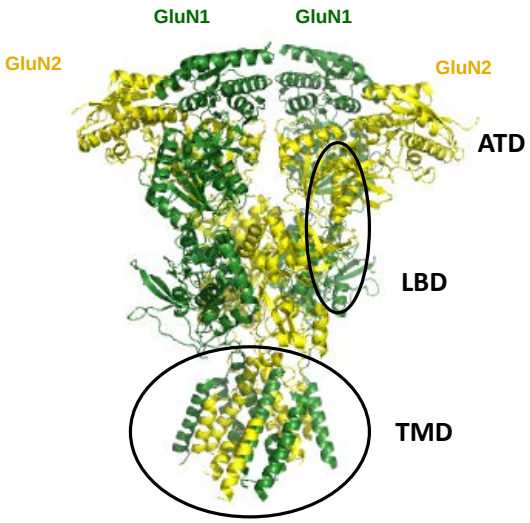

Figure 13. Structural determinants of CIQ potentiation include the GluN2 linker between the ATD and LBD and residues of the GluN2D pre M1 and M1 helix.

1.2.7 Overview of previous SAR for tetrahydroisoquinoline class of compounds

For SAR modification, CIQ was divided into three rings, and previous research had recognized important substituent identity and placement for each of these rings. Extensive work on the A-ring revealed that the R_1 position was most favorable for activity, and a bromo, iodo, trifluromethyl, and phenyl group in the *meta*-position yielded the most potent compounds (**Figure 14**). While electron-withdrawing groups were less potent, these compounds were more efficacious at GluN2C- and GluN2D-containing receptors. Replacement of the aromatic ring with different ring systems, such as pyridine ring systems, napthyl ring systems, furans, and thiophenes completely eliminated activity with the exception of 2-thiophene, which had weak activity exclusively at GluN2C-containing receptors. The amide linker appears to be required for activity as well; replacement of the amide with a urea, thiourea, sulfonamide, and tertiary amine linker led to a complete loss in activity[7].

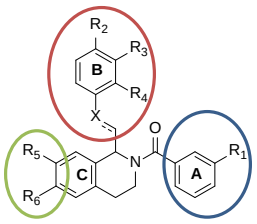

A ring:
- Halogens in R_1 position are most favorable for activity

B ring and linker:
- Only methoxy and thiomethyl in R_2 position lead to activity
- Substituents in the R_3 and R_4 position kill activity
- Ether linker is optimal, but C=C also causes activity

C ring:
- Dimethoxy in R_5 and R_6 position is active
- Substituent in R_5 position is not necessary; single methoxy in R_6 is active
- OBn in R_5 position is more potent than dimethoxy groups

Figure 14. Summary of previous SAR around the CIQ scaffold.

Modifications to the CIQ scaffold on the B-ring suggest that this ring has very specific substituent requirements for potentiation at the GluN2C- and GluN2D-containing receptors. On the CIQ scaffold, only a methoxy and thiomethyl group in the R_2 position caused potentiation, and the thiomethyl group was only active if a chloro-group was in the R_1 position on the A-ring (**Figure 13**). Functionality in the R_3 and R_4 positions eliminated activity, as did ethoxy, benzyloxy, and trifluro substituents in the R_1 position. In terms of the linker between the core and B-ring, the ether linkage was optimal for activity and solubility; a carbon-carbon double bond linker also lead to activity, but these compounds were difficult to work with as they were reported to be less soluble during synthesis and initial oocyte testing[7].

Minimal work was done on the C-ring, but it is notable that a single methoxy in the R_6 position of the ring had comparable activity at GluN2C- and GluN2D-containing receptors, meaning that the methoxy in the R_5 position is not absolutely essential for potentiation. While a methoxy in the R_3 position was active, a benzyloxy group was actually the most potent with EC_{50} values at GluN2C and GluN2C ranging from 0.3 μM to 0.4 μM when the A-ring contained a chloro or bromo group in the R_1 position on the A-ring[7]. Despite this work, SAR efforts were continued around the B-ring, the C-ring, and the linkers attaching the core to the B-rings and A-rings. The work discussed in this thesis begins with the synthesis in the following section.

1.3 Synthesis and Rationale for GluN2C/D-Selective positive modulators

1.3.1 Shortened Linker between Core and B-ring

In previous SAR work, the ether functionality linking the tetrahydroisoquinoline core and the B ring in CIQ had been changed to a thioether and an aliphatic group. While these two changes resulted in compounds with diminished activity compared to CIQ, compounds with a carbon-carbon double bond in place of the ether had comparable activity to CIQ (**Figure 14**). Optimization of the atoms in the linker had been explored, but the length of the linker had not been. The synthesis of compounds with a shortened linker was envisioned to start with the commercially available methoxy-phenyl acetic acids **29** and 2-(3,4-dimethoxyphenyl)ethylamine **30** to give amide **31** from an EDCI coupling reaction (**Scheme 1**). The yields from this reaction were low, however, and the synthesis was modified by converting the methoxy-phenyl acetic acids **29** into more reactive acid chlorides **32** using thionyl chloride (**Scheme 2**).

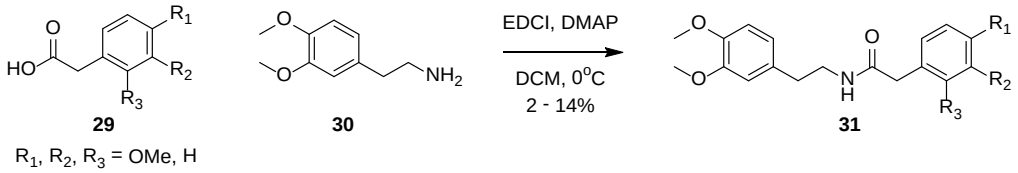

Scheme 1. EDCI coupling of phenethylamines and methoxy-phenyl acetic acids.

The acid chlorides **32** were then reacted with the commercially available 3,4-dimethoxyphenethylamine **30** to afford amides **31**. The acyclic amides were cyclized with phosphorus oxychloride in a Bischler-Napieralski reaction to form the dihydroisoquinolines **33** which were reduced to the tetrahydroisoquinolines **34** with sodium borohydride. Compounds **34** were acylated with a substituted benzoyl chloride to form compounds shown in **Table 1**: **1180-56, 1180-59, 1180-60, 1180-61, 1180-62, 1180-63**, and **1180-164** (**Scheme 2**).

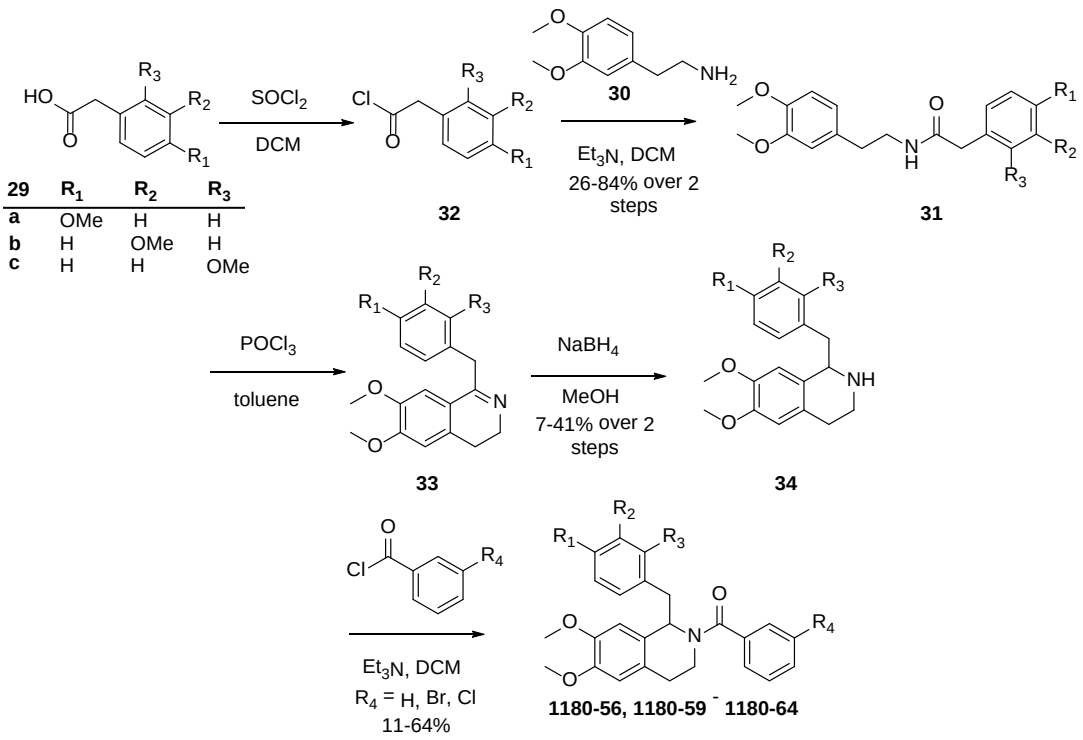

Scheme 2. Synthesis of shortened-linker compounds.

Table 1. Summary of compounds with shortened linker between B-ring and core.

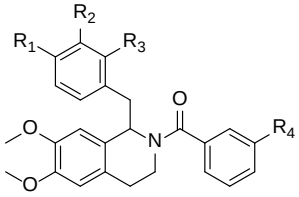

1180-X

1180-X	R_1	R_2	R_3	R_4
56	OMe	H	H	Br
59	H	OMe	H	Br
60	OMe	H	H	Cl
61	OMe	H	H	H
62	H	H	OMe	H
63	H	OMe	H	Cl
64	H	OMe	H	H

1.3.2 Nitrogen functionality on B-ring

Previous SAR had revealed that substituents in the *para*-position of the B-ring were optimal for GluN2C/D potentiation, and that ether and thioether functionalities resulted in activity. Further

exploration of the B-ring included a trifluromethyl group, a benzyl group, and a hydroxyl group, but not any nitrogen-containing moieties. Compounds were synthesized with a nitro group, a methylamino group, and dimethylamino group to study the impact of replacing the oxygen in CIQ with nitrogen functionality. Compounds containing a dimethylamino group in the *para*-position on the B ring were synthesized beginning with commercially available 2-(3,4-dimethoxyphenyl)ethylamine **30.** Phenethylamine **30** underwent an acylation reaction with 2-chloroacetyl chloride to form α-chloroamide **35**, which was followed by an alkylation on the phenol using *p*-nitrophenol and cesium fluoride[164] to afford acyclic amide **36**. The reduction of the nitro group on compound **36** was performed using hydrogenolysis to afford aniline **37**. Compound **37** was then subjected to reductive amination conditions using sodium cyanoborohydride and paraformaldehyde to give dimethylamino **38**[165], which was cyclized using a Bischler-Napieralski reaction to yield dihydroisoquinoline **39**. Reduction with sodium borohydride followed by acylation with a substituted benzoyl chloride afforded the final compounds **1180-77, 1180-78**, and **1180-79** (**Scheme 3).**

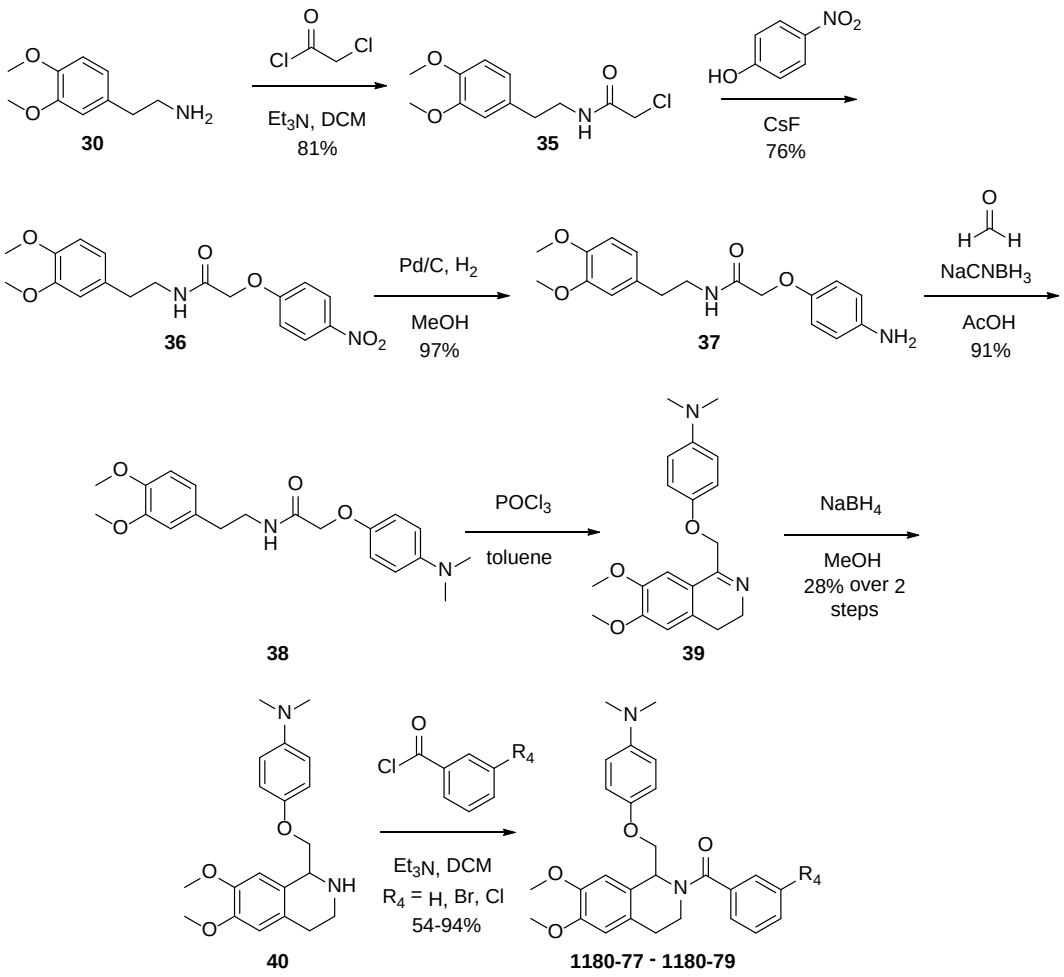

Scheme 3. Synthesis of dimethylamino containing compounds, 1180-77, 1180-78, and 1180-79.

Unfortunately, the synthesis of primary and secondary amines on the B-ring would not be feasible by the above synthesis; a primary or secondary amine would not survive the Bischler-Napieralski cyclization due to the nucleophilic nature of these amines. Synthesis of the compounds containing a nitro group, an aniline group, and a methylamino group on the B ring diverged from the synthesis of compounds **1180-77**, **1180-78**, and **1180-79** after the synthesis of acyclic amide **36**. Under Bischler-Napieralski conditions, amide **36** was cyclized with phosphorus oxychloride and subsequently reduced with sodium borohydride to form the tetrahydroisoquinoline core **42**, with the nitro-substitution on the B ring still intact. Acylation of the tetrahydroisoquinoline **42** with substituted benzoyl chloride reagents afforded the final compounds **1180-72, 1180-73**, and **2029**. The reduction of the nitro group to a primary amine was performed utilizing tin(II) chloride dihydrate[166] which

afforded compounds **1180-74**, **1180-75**, and **1180-76.** Reductive amination on aniline-containing **1180-75** and **1180-76** using parafomaldyde and sodium borohydride[165] afforded the methylamino functionalized compounds **1180-80** and **1180-81** (**Scheme 4**)**.** All compounds with nitrogen functionality on the B-ring as shown in **Table 2**.

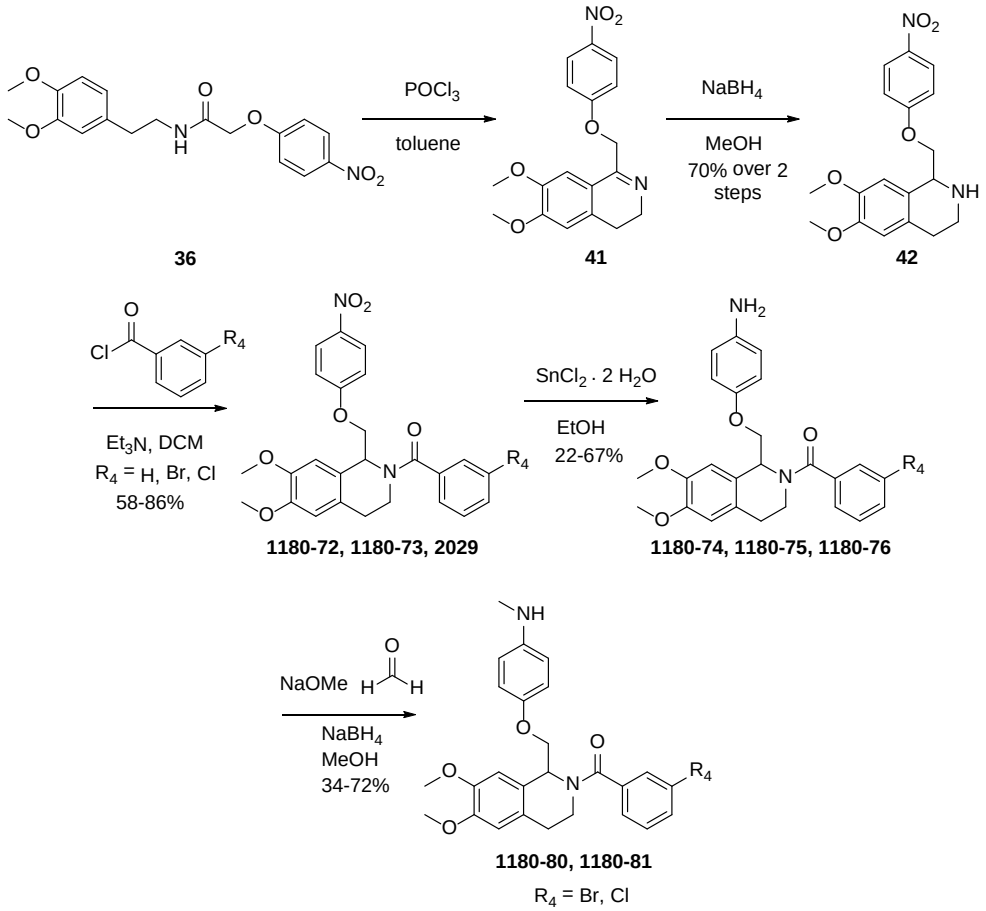

Scheme 4. Synthesis of nitro, aniline, and methylamino-containing compounds.

Table 2. Summary of compounds containing nitrogen functionality on B-ring.

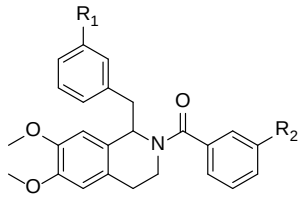

1180-X

	R_1	R_2
2029	NO_2	Cl
1180-72	NO_2	Br
1180-73	NO_2	H
1180-74	NH_2	H
1180-75	NH_2	Br
1180-76	NH_2	Cl
1180-77	NMe_2	Br
1180-78	NMe_2	H
1180-79	NMe_2	Cl
1180-80	NHMe	Cl
1180-81	NHMe	Br

1.3.3 Compounds with thioamide linker between core and A-ring

While CIQ derivatives were synthesized with different linkers between the core and A-ring, a thioamide linker had previously not been explored. The thioamide linker became important as the series diverged from the initial scaffold with dimethoxy functionality on the C-ring (discussed in **Chapter 2**), and select examples of potent, GluN2C/D-selective analogs were converted to thioamide-containing compounds using Lawesson's reagent in refluxing toluene[167] (**Scheme 5**) to give compounds **1180-154, 1180-61, 1180-62,** and **1180-64** (**Table 3**). Compounds **1391**, **1390** (CIQ), **1180-26**, and **1180-98** were either purchased or synthesized by Dr. Rose Santangelo as previously described.[7]

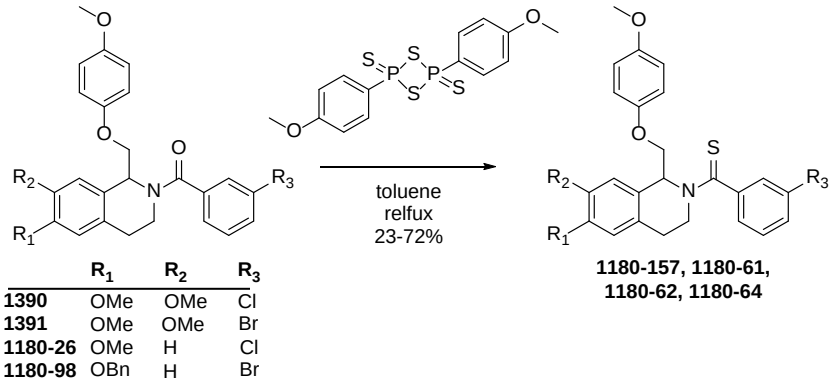

	R_1	R_2	R_3
1390	OMe	OMe	Cl
1391	OMe	OMe	Br
1180-26	OMe	H	Cl
1180-98	OBn	H	Br

Scheme 5. Conversion of select CIQ analogs to thioamide-containing compounds.

Table 3. Summary of thioamide-containing compounds.

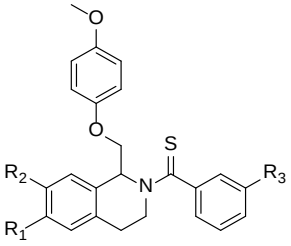

1180-X	R_1	R_2	R_3
157	OMe	OMe	Br
161	OMe	OMe	Cl
160	OMe	H	Cl
164	OBn	H	Br

1.3.4 Modifications to the C-ring to enhance potency

SAR around the three rings of CIQ revealed that benzyl functionality on the C-ring, as in compound **1180-97**, was more optimal for potentiation at GluN2C and GluN2D receptors compared to dimethoxy groups (**Figure 14**). For this reason, phenethyl-containing compounds **1180-121** and **1180-122** were synthesized to explore whether GluN2C/D potentiation of the NMDA receptors would continue in the presence of analogs with extended and lengthy C-ring functionality. Additionally, **1180-138** and **1180-153**, compounds with isosteric replacement of the ether linkage and benzyl group, respectively, were also synthesized (**Table 4**).

Table 4. Summary of compounds with modified functionality on the C-ring.

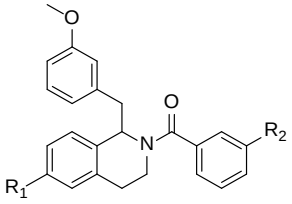

1180-X

1180-X	R_1	R_2
97*	OBn	Cl
122	OCH_2Ph	Br
123	OCH_2Ph	Cl
138	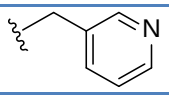	H
151	SBn	Br

*Synthesized by Dr. Rose Santangelo-Freel

Compounds **1180-121**, **1180-122**, **1180-138**, and **1180-153** were synthesized beginning with bromine-substituted phenethylamine **43**, which was subjected to acylation conditions to yield *N*-(3-bromophenethyl)-2-chloroacetamide **44**. The chlorine was then displaced by *para*-methoxyphenol to give linear amide **45**. The bromine in compound **45** was exchanged for an iodine in an aromatic Finkelstein reaction[168] to give compound **46**. Iodo-**46** was reacted with 2-phenylethanol or pyridin-3-ylmethanol in an Ullmann copper-catalyzed coupling reaction[169] to yield oxygen-containing linear amides **47a** and **47b**, respectively. In a similar fashion, compound **48** was synthesized from iodo-**46** in a second Ullmann copper-catalyzed reaction using ethylene glycol as a ligand and benzylthiol[170] (**Scheme 7**). All linear amides, regardless of functionality on the C-ring, were then cyclized using phosphorous oxychloride in a Bischler-Napieralski reaction to afford dihydroisoquinolines **49**, which were reduced with sodium borohydride to yield the corresponding tetrahydroisoquinolines **50**. The final step of the synthesis was an acylation with the appropriate benzoyl chloride to give final compounds **1180-122**, **1180-123**, **1180-138**, and **1180-153** (**Scheme 8**).

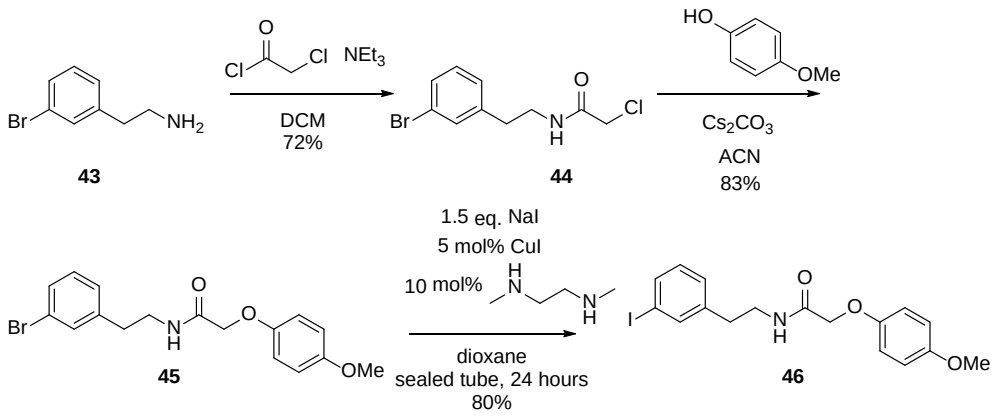

Scheme 6. Synthesis of linear amides with ether and thioether functionality on the future C-ring.

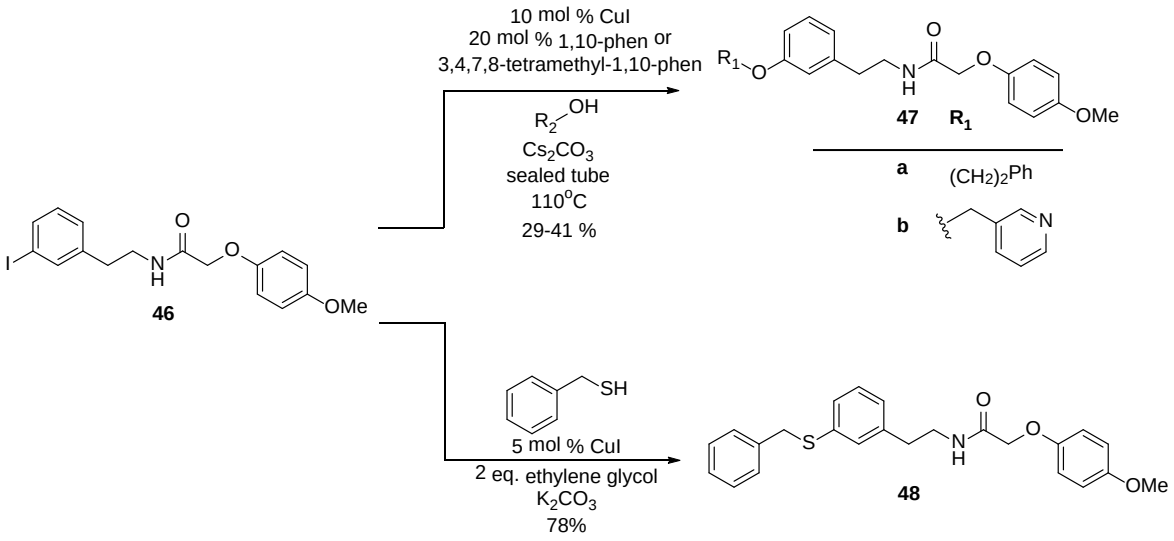

Scheme 7. Installation of oxygen and sulfur functionality on future C-ring.

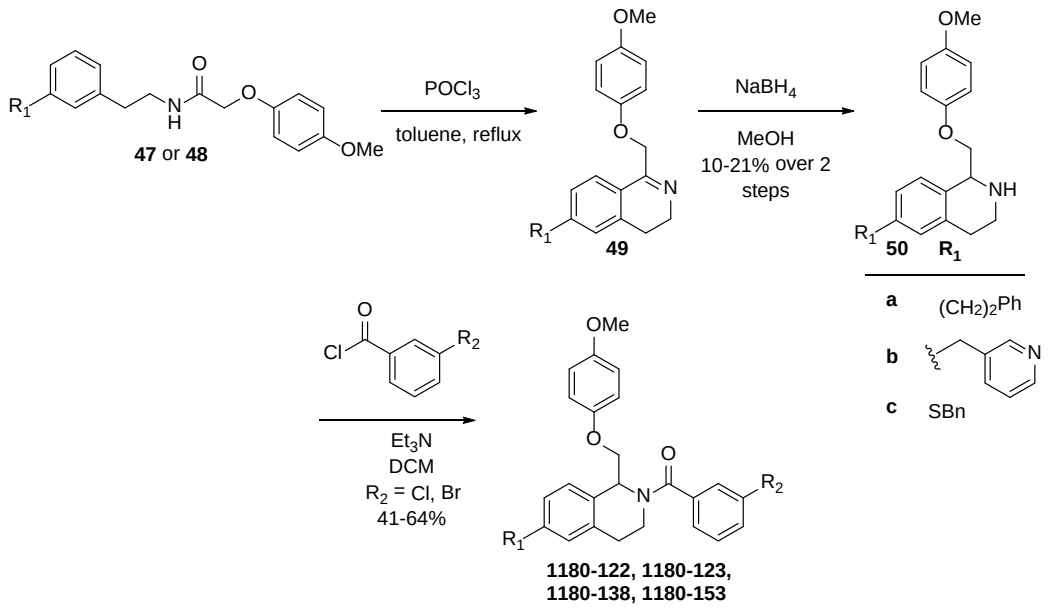

Scheme 8. Cyclization and Reduction to afford final tetrahydroisoquinoline compounds.

1.3.5 Separation of enantiomers for select CIQ analogs

Previous separation of CIQ enantiomers had revealed that only one enantiomer, (+)-CIQ was active *in vitro* at GluN2C/D-containing receptors, while (-)-CIQ was inactive[8]. Additional enantiomers for compounds **1391**, **1369**, and **1180-11** were separated via the OD-RH semi-prep chiral column to ensure that this pattern of activity was consistent throughout the class (**Scheme 9**). Although the active enantiomers from this series have been assigned a (+)-optical rotation value, methods to determine the absolute stereochemistry have thus far not yielded a determination, but efforts toward a crystal structure are ongoing.

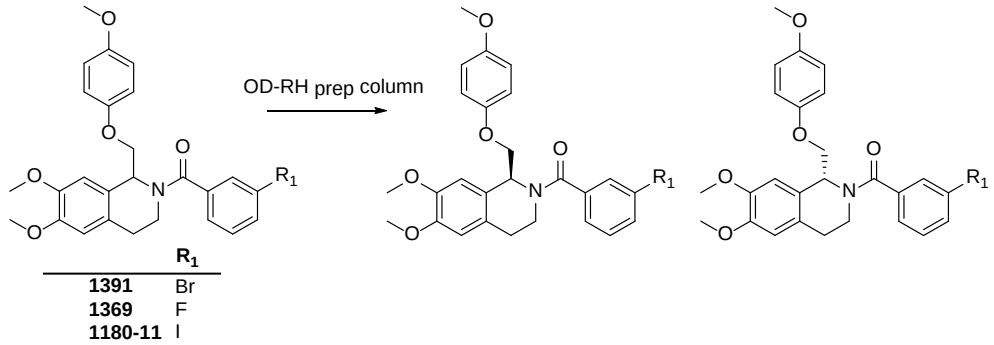

Scheme 9. Separation of select CIQ analogs via the OD-RH prep column.

1.4 Results and Discussion

All compounds were tested in Xenopus laevis expressing recombinant rat GluN1/GluN2A, GluN1/GluN2B, GluN1/GluN2C, and GluN1/GluN2D-containing receptors at saturating agonist concentrations. Under these experimental conditions, all compounds showed no activity at GluN2A and GluN2B subunits, and therefore the following tables only show data at GluN2C and GluN2D subunits.

1.4.1 Shortened Linker between Core and B-ring

Reducing the linker length by one atom between the core and B-ring to a single methylene group resulted in a complete loss in activity regardless of the substituent on the A-ring and the location of the methoxy group on the B-ring (**Table 5**). While the oxygen is not absolutely essential since a carbon-carbon double bond as a linkage leads to activity (**Figure 14**), the results suggest that a linker length of at least 2 atoms is required for activity at GluN2C- and GluN2D-containing receptors.

Table 5. Effect of shortening linker between core and B-ring.

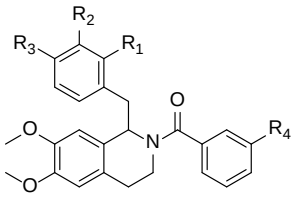

					$I_{30\mu M}$ / $I_{control}$ (mean ± SEM, %)		EC_{50} (max.) (μM %)[a]	
1180	**R_1**	**R_2**	**R_3**	**R_4**	**GluN2C**	**GluN2D**	**GluN2C**	**GluN2D**
60	H	H	OMe	Cl	94 ± 4.0	90 ± 3.6	-	-
61	H	H	OMe	H	100 ± 4.6	97 ± 4.9	-	-
63	H	OMe	H	Cl	91 ± 1.3	91 ± 1.4	-	-
59	H	OMe	H	Br	96 ± 2.5	94 ± 2.6	-	-
64	H	OMe	H	H	90 ± 3.9	91 ± 1.8	-	-
62	OMe	H	H	H	85 ± 2.5	85 ± 1.5	-	-

[a] Fitted EC_{50} values are shown to two significant digits when potentiation at 30 μM exceeded 120%; values in parentheses are the fitted maximum response as a percentage of the initial glutamate (100 μM) and glycine (30 μM) current. Data are from between 3-4 oocytes from 1 frog for each compound and receptor tested.

1.4.2 Nitrogen functionality on B-ring

Although a number of substituents had been placed in the para-position of the B-ring, previous SAR had not included nitrogen-group functionality. The CIQ scaffold had very specific requirements in terms of B-ring substituent placement and identify, and extension of the SAR with nitrogen functionality only confirmed previous results (**Table 6**). The electron-withdrawing nitro-group (**1180-72** and **1180-73**) caused a loss in activity, as did aniline functionality (**1180-74**, **1180-75**, and **1180-76**). While the addition of both of these functionalities on the B-ring eliminated potentiation regardless of the substituent in the R_1 position, this was not the case when substituted amines were present on the B-ring. Mono-substituted compound **1180-81** with a bromo group on the A-ring was weakly active at GluN2C-containing receptors, while **1180-80** with a chloro group was inactive at both receptors. The only compounds with nitrogen functionality on the B-ring that were active were compounds **1180-77** and **1180-79** with dimethylamino functionality, but only when a halogen was present on the A-ring. Despite activity, the nitrogen compounds were less potent and efficacious than when a methoxy group was on the B-ring as in CIQ.

Table 6. Effect of nitrogen-containing substituent identity on the B-ring.

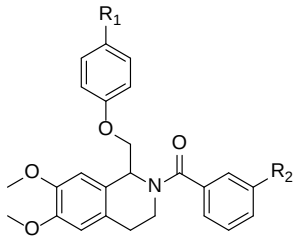

			$I_{30\mu M}$ / $I_{control}$ (mean ± SEM, %)		EC_{50} (max.) (μM %)[a]	
1180	**R_1**	**R_2**	**GluN2C**	**GluN2D**	**GluN2C**	**GluN2D**
72	NO_2	Br	94 ± 3.6	89 ± 3.2	-	-
73	NO_2	H	88 ± 1.7	86 ± 2.2	-	-
76	NH_2	Cl	96 ± 2.4	100 ± 2.3	-	-
75	NH_2	Br	89 ± 1.2	92 ± 0.92	-	-
74	NH_2	H	100 ± 4.1	92 ± 0.92	-	-
80	NHMe	Cl	106 ± 1.6	102 ± 2.1	-	-

81	NHMe	Br	122 ± 4.5	110 ± 1.4	41 (172%)	-
79	NMe_2	Cl	145 ± 5.4	122 ± 2.7	34 (195%)	28 (141%)
77	NMe_2	Br	154 ± 5.6	121 ± 2.2	14 (167%)	14 (125%)
78	NMe_2	H	99 ± 2.8	96 ± 2.1	-	-

[a] Fitted EC_{50} values are shown to two significant digits when potentiation at 30 μM exceeded 120%; values in parentheses are the fitted maximum response as a percentage of the initial glutamate (100 μM) and glycine (30 μM) current. Data are from between 3-10 oocytes from 1-2 frogs for each compound and receptor tested.

1.4.3 Compounds with thioamide linker between core and A-ring

As discussed later in **Chapter 2.4.6**, the thioamide linker leads to significant increases in activity for compounds that potentiate GluN2B-containing receptors. For this reason, potent amide-containing GluN2C- and GluN2D-selective potentiators were converted to thioamide-containing compounds. Unfortunately, from the four examples that were synthesized (**Table 7**), it appears as if a thioamide linker on scaffolds that selectively potentiate GluN2C- and GluN2D containing receptors causes a complete loss in activity. This is in deep contrast to the compounds that are discussed in **Chapter 2**, and the significance of CIQ-like thioamide-containing compounds will be discussed in **Chapter 2.4.8**.

Table 7. Effect of thioamide linker on GluN2C and GluN2D selective CIQ compounds.

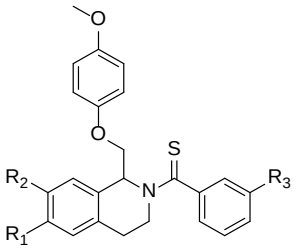

				$I_{30\mu M}$ / $I_{control}$ (mean ± SEM, %)		EC_{50} (max.) (μM %)[a]	
1180	**R_1**	**R_2**	**R_3**	**GluN2C**	**GluN2D**	**GluN2C**	**GluN2D**
157	OMe	OMe	Br	111 ± 2.0	105 ± 3.6	-	-
161	OMe	OMe	Cl	98 ± 2.6	112 ± 1.1	-	-
160	OMe	H	Cl	114 ± 1.4	100 ± 2.5	-	-
164	OBn	H	Br	103 ± 2.7	106 ± 1.8	-	-

[a] Fitted EC_{50} values are shown to two significant digits when potentiation at 30 μM exceeded 120%; values in parentheses are the fitted maximum response as a percentage of the initial glutamate (100 μM) and glycine (30 μM) current. Data are from between 3-10 oocytes from 1-2 frogs for each compound and receptor tested.

1.4.4 Modifications to the C-ring to enhance potency

Replacement of the dimethoxy groups on the C-ring to a single benzyloxy group on the CIQ scaffold, as in **1180-97**, led to significant increases in potency (**Figure 14**), and compounds with phenethyl-containing compounds were equally potent as **1180-97**. Extending the linker between the C-ring and the aromatic functionality of the C-ring were not detrimental to potentiation, suggesting that the binding pocket in the NMDA receptor can accommodate bulk in the C-ring region. When the functionality coming off of the B-ring is extended, all activity was lost, but these results suggest that modifications around the C-ring could serve as a starting place to develop more potent compounds for GluN2C- and GluN2D-containing receptors. Work was not continued on the phenethyl-containing compounds though because adding carbon atoms to the C-ring made the compounds less drug-like. Although potent, these compounds did not offer any advantages compared to the benzyl-containing compounds.

Table 8. Effect of substituent identity on the C-ring.

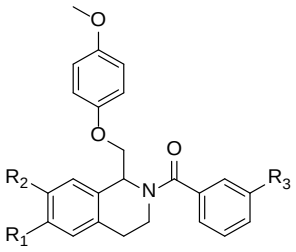

				$I_{30\mu M}$ / $I_{control}$ (mean ± SEM, %)		EC_{50} (max.) (μM %)[a]	
1180	**R_1**	**R_2**	**R_3**	**GluN2C**	**GluN2D**	**GluN2C**	**GluN2D**
CIQ	OMe	OMe		217 ± 11	206 ± 9.5	2.9 (217%)	2.9 (208%)
97[b]	OBn	H	Cl	224 ± 4.2	158 ± 7.8	0.49 (258%)	0.60 (210%)
98[b]	OBn	H	Br	207 ± 22	180 ± 9.7	0.36 (251%	0.44 (235%)
122	$O(CH_2)_2Ph$	H	Br	265 ± 14	251 ± 15	0.51 (257%)	0.21 (267%)
123	$O(CH_2)_2Ph$	H	Cl	264 ± 29	223 ± 14	0.26 (244%)	0.40 (216%)

138	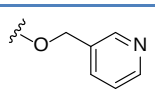	H	Br	175 ± 14	167 ± 15	5.6 (186%)	6.3 (180%)
151	SBn	H	Cl	190 ± 15	206 ± 8.0	0.46 (197%)	0.55 (213%)

[a] Fitted EC_{50} values are shown to two significant digits when potentiation at 30 μM exceeded 120%; values in parentheses are the fitted maximum response as a percentage of the initial glutamate (100 μM) and glycine (30 μM) current. Data are from between 8-10 oocytes from 2-3 frogs for each compound and receptor tested. [b]Synthesized by Dr. Rose Santangelo

Since solubility of the CIQ compounds has proven to be an issue in the past, hindering initial drug testing and limiting future studies, compound **1180-138** with pyridine functionality on the C-ring was synthesized. This compound has a logP of 5.74 compared to isosteric analog **1180-98** with benzyl functionality, which had a logP of 7.08 (**Figure 15**). Although **1180-138** was still GluN2C- and GluN2D-selective and caused activity, the compound was approximately 20-fold less potent than **1180-98**. This suggests that activity at GluN2C- and GluN2D-containing receptors is amenable to bulk at the C-ring, but hydrophobic functionality is optimal. For this reason, the SAR only included 3-pyridine, and efforts were not continued to study the impact of moving the nitrogen around the aromatic ring.

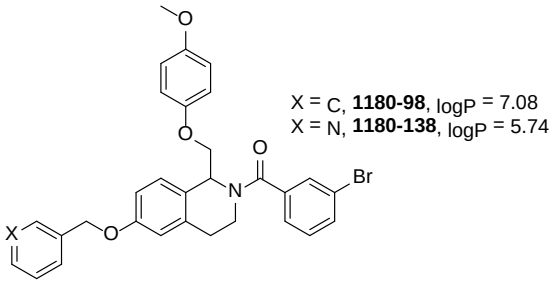

Figure 15. LogP values of 1180-98 and 1180-138, and the diminished activity of 1180-138.

Lastly, compound **1180-151** was synthesized with a thioether linking the C-ring and the C-ring functionality. This compound was comparable in terms of activity to **1180-97**, **98**, **121**, and **122** with an EC_{50} value of 0.46 at GluN2C and 0.55 at GluN2D-containing receptors, but did not offer any advantages over **1180-97**, so efforts were not continued to explore compounds with a thioether linker. This data does suggest though that activity is not limited to only oxygen-containing functionality on the C-ring.

1.4.5 Separation of enantiomers for select CIQ analogs

Three dimethoxy-containing CIQ compounds, **1319**, **1369**, and **1180-11**, were separated via the OD-RH semi-prep column, and in all cases, activity only resided in the (+)-enantiomer. This high level of stereoselectivity suggests that the binding pocket preferentially accommodates one enantiomer, and could provide an opportunity to further enhance selectivity within the class. Multiple attempts were made to obtain a crystal structure of one of these enantiomers, but at this point, all attempts were unsuccessful. Without an absolute confirmation of stereochemistry, (*S*) and (*R*) assignments cannot be made, and the active enantiomer continues to be referred to as the (+)-enantiomer, although a stereoselective model[7] for the reduction of the imine utilized to initially synthesize the enantiomers predicts that the active enantiomer with a (+) optical rotation value is the (*R*)-enantiomer[8].

Table 9. Stereoselectivity of enantiomers of select CIQ analogs.

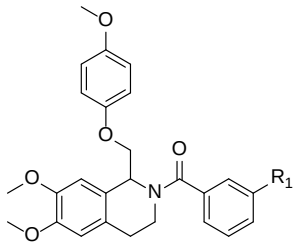

		$I_{30\mu M}$ / $I_{control}$ (mean ± SEM, %)		EC_{50} (max.) (μM %)[a]	
	R_1	**GluN2C**	**GluN2D**	**GluN2C**	**GluN2D**
1391	Br	191 ± 14	190 ± 7.5	1.6 (197%)	1.1 (190%)
(+)-1391	Br	317 ± 28	326 ± 17	4.2 (334%)	5.7 (335%)
(-)-1391	Br	100 ± 5.0	96 ± 3.2	-	-
1369	F	177 ± 11	170 ± 7.4	7.8 (190%)	8.1 (168%)
(+)-1369	F	183 ± 8.8	178 ± 4.4	14 (193%)	23 (220%)
(-)-1369	F	93 ± 4.4	90 ± 0.82	-	-
1180-11[b]	I	233 ± 12	174 ± 16	6.0 (250)	4.1 (181)
(+)-1180-11	I	198 ± 14	274 ± 15	2.0 (204)	3.8 (285)
(-)-1180-11	I	98 ± 5.3	85 ± 3.8	-	-

[a] Fitted EC_{50} values are shown to two significant digits when potentiation at 30 μM exceeded 120%; values in parentheses are the fitted maximum response as a percentage of the initial glutamate (100 μM) and glycine (30

μM) current. Data are from between 9-23 oocytes from 2-4 frogs for each compound and receptor tested. [b] Synthesized by Dr. Rose Santangelo-Freel

1.5 Conclusions

The discovery of compound **1180** represented the first small molecule that could act as a GluN2C- and GluN2D-containing NMDA receptor positive allosteric modulator. Initial, but extensive SAR revealed that to cause potentiation, the CIQ scaffold must meet specific requirements in terms of substituent placement and identity, linker length, and type of aromatic rings around the tetrahydroisoquinoline core. The final pieces of the SAR that were completed in this project were consistent with previous results; drastic modifications to the original CIQ scaffold resulted in a complete loss of activity.

Shortening the linker between the B-ring and the core, as in compounds **1180-59**, **1180-60, 1180-61, 1180-62, 1180-63**, and **1180-64** eliminated activity regardless of the substituent on the A-ring and the location of the methoxy group on the B-ring. While the linker does not necessarily require the ether linkage as in the initial screening hit **1180**, activity does require a linker length of at least 2 atoms. In addition to the B-ring linker, the B-ring itself has stringent requirements for activity at GluN2C and GluN2D-containing NMDA. Previous SAR had not included substituents on the B-ring with nitrogen functionality, but the synthesis of compounds with nitro, aniline, monoamino, and dimethylamino moieties suggests that the methoxy group in the original screening hit is optimal for activity. Only the dimethylamino-containing compounds, **1180-77** and **1180-79**, had activity at both GluN2C and GluN2D, although the potency of these compounds was significantly weak with EC_{50} values at the two subunits ranging between 14 and 34 μM.

Previous research had suggested that the optimal linker between the A-ring and the core was an amide bond, and changing the linker to a sulfonamide, urea, or thiourea resulted in either a complete loss in activity or diminished activity. Converting the amide to a thioamide also led to a loss in activity, and the significance of this resultis discussed in **Chapter 2.4.8**.

The C-ring of the CIQ scaffold is more amenable to changes than the other two rings, and previous research had revealed that a single benzyloxy group (**1180-97** and **1180-98**) as opposed to the

dimethoxy functionality on the CIQ scaffold led to activity. Since this change led to an approximate 10-fold increase in potency (**Table 8**), a number of compounds were synthesized that were similar to the benzyloxy-containing **1180-97**. Compounds with phenethyl functionality, **1180-122** and **1180-123**, were just as active as **1180-97**, but extending the scaffold by one extra carbon led to compounds that were less drug-like than **1180-97**. Replacement of the ether linkage as in **1180-151** maintained the activity of **1180-97**, but replacement of the aromatic ring with a pyridine moiety (**1180-138**) caused a significant decrease in potency. This suggests that while the NMDA receptor binding pocket can accommodate significant bulk coming off of the C-ring, the pocket prefers hydrophobic functionality.

The synthesis of these final compounds helped to complete the SAR of the GluN2C- and GluN2D-subunit selective CIQ, and helped to elucidate important substituents of the B- and C-rings for activity at these two subunits. While the B-ring is very constrained in terms of substituent identity and functionality, activity at GluN2C- and GluN2D-containing receptors is less dependent on specific C-ring functionality. Activity persisted even when the dimethoxy substituents were replaced with a single benzyloxy group, and these results were the first hint that the C-ring plays an important role in dictating potency, efficacy, and subunit-selectivity.

1.6 Experimental details

1.6.1. Chemistry experimental procedures

General Experimental: All reagents were purchased from commercial vendors and used without further purification. Thin layer chromatography (TLC) on precoated aluminum plates (silica gel 60 F254, 0.25 mm) or LCMS (Varian) were used to monitor reaction progress. Purification by flash column chromatography was done on a Teledyne ISCO Combiflash Companion using Teledyne Redisep normal phase columns. Proton and carbon NMR spectra were recorded on an INOVA-400 (400 MHz), VNMRS-400 (400 MHz), Mercury 300 Vx (300 MHz) or INOVA-600 (600 MHz). All chemical shifts were reported in parts per million and coupling constants were reported in Hertz (Hz). The spectra were referenced to the solvent peak. Mass spectra were performed by the Emory

University Mass Spectroscopy Center on either a VG 70-S Nier Johnson or JEOL instrument. Purity was established by HPLC (Varian) in two solvents systems (MeOH:water and ACN:water) unless indicated by combustion analysis. The conditions were determined for each individual compound. Elemental analysis was performed by Atlantic Microlab, Inc (Norcross, GA) for C, H, and N, and agreed with proposed structures within 0.4 $\pm$ of theoretical values. Optical rotation values were obtained using a Perkin-Elmer 314 instrument.

General Procedure for 3,4-dihydroisoquinoline Compounds (Procedure I): The amide (1.0 equiv.) was suspended in dry toluene and the reaction mixture was brought to reflux. Phosphorous trichloride (3.0 equiv.) was added and the reaction was allowed to stir for approximately 3 hours before cooling to room temperature. The excess toluene was decanted and the remaining residue was carried on without further purification.

General Procedure for 3,4-dihydroisoquinoline Compounds (Procedure II): The amide (1.0 equiv.) was suspended in dry toluene and the reaction mixture was brought to reflux. Phosphorous trichloride (3.0 equiv.) was added and allowed to stir for approximately 3 hours before cooling to room temperature. The reaction mixture was made basic (pH 13) with concentrated NH_4OH and the organic layer was extracted into DCM. The organic layer was then washed with water (3x), brine (3x), dried with $MgSO_4$, filtered, and concentrated *in vacuo*. The resulting residue was carried on without further purification.

General Procedure for 1,2,3,4-tetrahydroisoquinoline Compounds (Procedure III): The dihydroisoquinoline (1.0 equiv.) was dissolved in dry MeOH and brought to 0°C using an ice bath. Sodium borohydride (3.0 equiv.) was added slowly and the reaction was allowed to stir overnight and warm to room temperature. The volatiles were concentrated *in vacuo*, and the resulting residue was extracted into DCM. The organic layer was washed with water (3x) and brine (3x), dried with $MgSO_4$, filtered, and concentrated *in vacuo*. The resulting residue was then subjected to column chromatography to afford the title compound.

General Procedure for 3,4-dihydroisoquinolin-2(1H)-yl)methanone) Compounds (Procedure IV): The tetrahydroisoquinoline (1.0 equiv.) was dissolved in dry DCM and brought to 0°C using an ice bath. Triethylamine (3.0 equiv.) was added, followed by the benzoyl chloride (1.2 equiv.). The reaction mixture stirred for approximately 2 hours under an argon atmosphere, at which point TLC indicated complete conversion. The reaction was quenched with 1M HCl and extracted into DCM. The organic layer was washed with water (3x) and brine (3x), dried with $MgSO_4$, filtered, and concentrated *in vacuo*. The resulting residue was then subjected to column chromatography to afford the title compound.

General Procedure for 3,4-dihydroisoquinolin-2(1H)-yl)methanethione Compounds (Procedure V) : Tetrahydroisoquinoline (1 eq.) was dissolved in dry toluene and 2,4-bis(4-methoxyphenyl)-1,3,2,4-dithiadiphosphetane 2,4-disulfide (0.5 – 1 eq.) was added. The reaction was brought to reflux. After 2 - 8 hours, the solvent was removed under reduced pressure and the residue was dissolved in DCM. The solution was washed with a 10% solution of $NaHCO_3$, dried with $MgSO_4$, filtered, and concentrated *in vacuo*. The resulting residue was then subjected to column chromatography to afford the title compound.

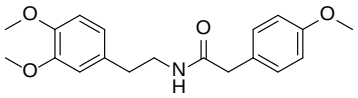

N-(3,4-dimethoxyphenethyl)-2-(4-methoxyphenyl)acetamide (31a): To a solution of 2-(4-methoxyphenyl)acetic acid (3.5 g, 21 mmol) dissolved in DCM (25 mL), sulfurous dichloride (4.5 ml, 63 mmol) was added. The mixture stirred for approximately 15 minutes, and was immediately concentrated *in vacuo*. The resulting solution was then added to a cooled solution of 2-(3,4-dimethoxyphenyl)ethanamine (1.5 ml, 8.6 mmol) and triethylamine (3.6 ml, 25 mmol) in DCM (36 mL). The reaction stirred for 3 hours, at which point TLC indicated complete conversion. The reaction was quenched with 1M HCl and extracted into DCM. The organic layer was washed with water and brine, dried over $MgSO_4$, and excess solvent was removed *in vacuo*. The crude residue was purified by silica gel chromatography (ISCO, Silicycle 80 g column, 10-80% EtOAc/hexanes

gradient) to afford the title compound as a white solid (1.2 g, 26 %); ^{1}H NMR ($CDCl_3$, 400 MHz) δ: 7.09-7.05 (m, 2H), 6.85-6.81 (m, 2H), 6.73-6.71 (d, *J* = 7.9 Hz, 2H), 6.61-6.60 (d, *J* = 1.8 Hz, 1H), 6.56-6.53 (m, 2H), 3.85 (s, 3H), 3.81 (s, 3H), 3.79 (s, 3H), 3.46 (s, 2H), 3.44-3.41 (t, *J* = 6.0 Hz, 2H), 2.69-2.65 (t, *J* = 6.7 Hz, 2H); ^{13}C NMR ($CDCl_3$, 100 MHz) δ: 35.31, 41.02, 43.31, 55.49, 56.10, 111.45, 112.02, 114.57, 120.84, 126.85, 126.9, 130.81, 131.32, 147.81, 149.18, 159.02, 171.77. HRMS calcd. for $C_{19}H_{23}O_4N_1$, 330.16999 $[M + H]^+$; found 330.17031 $[M + H]^+$.

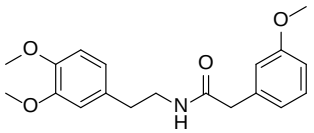

N-(3,4-dimethoxyphenethyl)-2-(3-methoxyphenyl)acetamide (31b). To a solution of 2-(3-methoxyphenyl)acetic acid (3.5 g, 21 mmol) dissolved in DCM (25 mL), sulfurous dichloride (4.5 ml, 63 mmol) was added. The mixture stirred for approximately 15 minutes and was immediately concentrated *in vacuo*. The resulting solution was then added to a cooled solution of 2-(3,4-dimethoxyphenyl)ethanamine (1.5 ml, 8.6 mmol) and triethylamine (3.6 ml, 26 mmol) in DCM (36 mL). The reaction stirred for 3 hours, at which point the TLC indicated complete conversion. The reaction was quenched with 1M HCl and extracted into DCM. The organic layer was washed with water and brine, dried over $MgSO_4$, and excess solvent was removed *in vacuo*. The crude residue was purified by silica gel chromatography (ISCO, Redisep 80 g column, 10-80% EtOAc/hexanes gradient) to afford a white solid (2.4 g, 84 %). ^{1}H NMR ($CDCl_3$, 400 MHz) δ: 7.23-7.19 (t, *J* = 8.2 Hz, 1H), 6.82-6.79 (m, 1H), 6.75-6.70 (m, 3H), 6.59 (d, *J* = 2.0 Hz, 1H), 6.54-6.52 (m, 1H), 3.84 (s, 3H), 3.82 (s, 3H), 3.81 (s, 3H), 3.48 (s, 2H), 3.45-3.40 (t, *J* = 6.7 Hz, 2H), 2.68-2.65 (t, *J* = 6.8 Hz, 2H); ^{13}C NMR ($CDCl_3$, 100 MHz) δ: 170.9, 160.2, 149.2, 147.7, 136.4, 131.3, 130.2, 121.8, 120.8, 115.1, 113.1, 111.9, 111.4, 56.1, 55.9, 55.3, 44.1, 40.1, 35.2. HRMS calcd. for $C_{19}H_{23}O_4N_1$, 330.17024 $[M + H]^+$; found 330.16999 $[M + H]^+$.

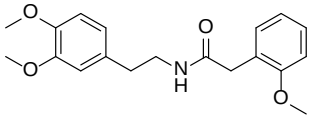

N-(3,4-dimethoxyphenethyl)-2-(2-methoxyphenyl)acetamide (31c): To a solution of 2-(2-methoxyphenyl)acetic acid (3.5 g, 21 mmol) dissolved in DCM (25 mL), sulfurous dichloride (4.5 mL, 63 mmol) was added. The mixture stirred for approximately 15 minutes and was immediately concentrated *in vacuo*. The resulting solution was then added to a cooled solution of 2-(3,4-dimethoxyphenyl)ethanamine (1.5 ml, 8.6 mmol) and triethylamine (3.6 ml, 26 mmol) in DCM (36 mL). The reaction stirred for 3 hours, at which point the TLC indicated complete conversion. The reaction was quenched with 1M HCl and extracted into DCM. The organic layer was washed with water and brine, dried over $MgSO_4$, and excess solvent was removed *in vacuo*. The crude residue was purified by silica gel chromatography (ISCO, Redisep 80 g column, 10-80% EtOAc/hexanes gradient) to afford a white solid (2.2 g, 78 %). ^{1}H NMR ($CDCl_3$, 400 MHz) δ: 7.25 - 7.14 (m, 2H), 6.91 - 6.88 (m, 1H), 6.82-6.80 (m, 1H), 6.70-6.68 (m, 1H), 6.5 (m, 1H), 6.54-6.52 (m, 1H), 5.73 (s, 1H), 3.83 (s, 3H), 3.78 (s, 3H), 3.67 (s, 3H), 3.5 (s, 2H), 3.43-3.38 (q, J = 6.65, J = 12.52, 2H), 2.66-2.62 (t, J = 6.65 Hz, 2H); ^{13}C NMR ($CDCl_3$, 100 MHz) δ: 35.25, 38.96, 40.72, 55.45, 56.97, 56.14, 110.80, 111.41, 111.93, 120.71, 121.19, 123.86, 128.93, 131.42, 131.56, 147.68, 149.10, 157.21 171.45; HRMS calcd. for $C_{19}H_{23}O_4N_1$, 330.17024 $[M + H]^+$; found 330.16969 $[M + H]^+$.

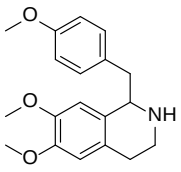

6,7-dimethoxy-1-(4-methoxybenzyl)-1,2,3,4-tetrahydroisoquinoline (34a): Dihydroisoquinoline **33a** was prepared via Procedure I using amide **31a** (1.2 g, 3.7 mmol) and phosphorus trichloride (1.1 mL, 1.1 mmol) in dry toluene (21 mL). The crude solid (0.88 g) was filtered and carried on without further purification. HRMS calcd. for $C_{19}H_{21}O_3N_1$, 312.15942 $[M + H]^+$; found 312.15977 $[M + H]^+$. Tetrahydroisoquinoline **34a** was prepared via Procedure III using dihydroisoquinline **33a** (0.90 g, 2.8 mmol) and sodium borohydride (0.30 g, 8.5 mmol) in dry MeOH (43 mL). The crude residue was purified by silica gel chromatography (ISCO, Redisep 20 g column, 0-20% MeOH/DCM gradient) to afford the title compound as a brown solid (0.36 g, 41 %); ^{1}H NMR ($CDCl_3$, 400 MHz) δ: 7.14-7.12

(d, *J* = 8.8 Hz, 2H), 6.85-6.83 (d, *J* = 8.5 Hz, 2H), 6.58 (s, 1H), 6.06 (s, 1H), 4.66-4.63 (q, *J* = 8.8 Hz, *J* = 4.2 Hz, 1H), 3.85 (s, 3 H), 3.78 (s, 3H), 3.57 (s, 3H), 3.37-3.35 (m, 2H), 3.17-3.12 (m, 2H), 2.98-2.93 (m, 2H); ^{13}C NMR ($CDCl_3$, 100 MHz) δ: 159.0, 148.7, 147.3, 131.4, 138.2, 123.9, 123.6, 114.3, 111.4, 110.1, 56.0, 55.7, 55.5, 40.4, 38.8, 25.5. HRMS calcd. for $C_{19}H_{23}O_3N_1$, 314.17507 $[M + H]^+$; found 314.17543 $[M + H]^+$.

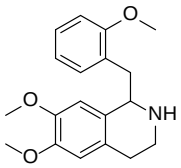

6,7-dimethoxy-1-(2-methoxybenzyl)-1,2,3,4-tetrahydroisoquinoline (34c): Dihydroisoquinoline **33c** was prepared via Procedure I using amide **31c** (2.2 g, 6.7 mmol) and phosphorus trichloride (1.8 mL, 21 mmol) in dry toluene (37 mL). The crude solid (2.2 g) was filtered and carried on without further purification. HRMS calcd. for $C_{19}H_{22}O_3N_1$, 312.15942 $[M + H]^+$; found 312.15915 $[M + H]^+$. Tetrahydroisoquinoline **34c** was prepared via Procedure III using dihydroisoquinoline **33c** (2.2 g, 7.2 mmol) and sodium borohydride (0.82 g, 22 mmol) in dry MeOH (36 mL). The crude residue was purified by silica gel chromatography (ISCO, Redisep 20 g column, 0-20% MeOH/DCM gradient) to afford the title compound as a brown solid (0.19 g, 8.0 %); ^{1}H NMR ($CDCl_3$, 400 MHz) δ: 7.21-7.18 (t, *J* = 7.85, 1H), 7.01-6.99 (m, 3H), 6.83-6.77 (m, 2H), 6.74-6.66 (m, 2H), 6.46 (s, 1H), 6.423 (s, 1H), 5.81 (s, 2H), 4.75-4.68 (q, *J* = 5.2, *J* = 15.2, 1H), 4.53-4.70 (q, *J* = 5.6, *J* = 9.2, 1H); ^{13}C NMR ($CDCl_3$, 100 MHz) δ: 25.68, 28.26, 35.85, 37.46, 37.65, 37.75, 51.67, 53.44, 54.97, 55.45, 55.43, 55.87, 55.98, 110.40, 110.51, 111.11, 111.41, 120.42, 120.78, 124.52, 125.47, 125.75, 126.71, 127.31, 128.57, 128.70, 131.27, 131.936, 132.23, 145.755, 146.65, 146.97, 149.09, 158.01, 158.23; HRMS calcd. for $C_{19}H_{23}O_3N_1$, 314.17507 $[M + H]^+$; found 314.17474 $[M + H]^+$.

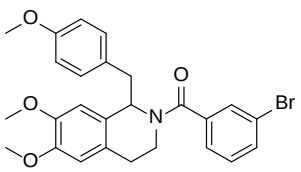

(3-bromophenyl)(6,7-dimethoxy-1-(4-methoxybenzyl)-3,4-dihydroisoquinolin-2(1H)-yl)methanone (1180-56): Tetrahydroisoquinoline **1180-56** was prepared via Procedure IV using tetrahydroisoquinoline **34a** (0.38 g, 1.2 mmol) and 3-bromobenzoyl chloride (0.16 mL, 1.2 mmol) in DCM (10 mL). The crude residue was purified by silica gel chromatography (ISCO, Redisep 12 g column, 10 – 80% EtOAc/hexanes gradient) to afford the title compound as a white foam (0.16 g, 26 %, mixture of two amide rotamers) TLC (EtOAc: hexanes, 1:1, v/v) Rf = 0.62; ^{1}H NMR ($CDCl_3$, 400 MHz) δ: 7.50-7.39 (dd, *J* = Hz, *J* = Hz, 1H), 7.31-7.21 (m, 1H), 7.15-7.05 (m, 2H), 6.87-6.81 (m, 3H), 6.74-6.68 (m, 1H), 6.64 (s, 0.5 H), 6.55 (s, 0.5 H), 6.36 (s, 0.5 H), 6.24 (s, 0.5 H), 5.81 (m, 0.5 H), 4.88-4.83 (dd, *J* = 6.0 Hz, *J* = 13.2 Hz, 0.5H), 4.68-4.65 (dd, *J* = 5.2 Hz, *J* = 9.6 Hz, 0.5H), 3.83-3.69 (m, 9H), 3.61-3.58 (m, 0.5 H), 3.41-3.28 (m, 1H), 3.14-3.13 (m, 1H), 3.10-3.02 (m, 1H), 2.85-2.53 (m, 2H); ^{13}C NMR ($CDCl_3$, 100 MHz) δ: 169.6, 168.9, 158.9, 158.7, 148.4, 148.0, 147.4, 138.7, 138.2, 132.6, 132.4, 131.0, 130.8, 130.4, 129.9, 129.8, 129.7, 129.4, 128.4, 127.9, 126.2, 125.2, 125.1, 124.9, 122.8, 122.6, 114.4, 113.9, 111.8, 111.4, 110.6, 109.9, 60.2, 56.2, 56.1, 55.9, 55.5, 55.4, 53.9, 42.4, 41.9, 41.5, 35.6, 29.1, 28.1; HRMS cald. For $C_{26}H_{27}NO_4Br$, 496.11180 $[M + H]^+$; found, 496.11200 $[M + H]^+$.

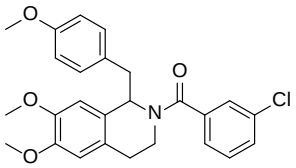

(3-chlorophenyl)(6,7-dimethoxy-1-(4-methoxybenzyl)-3,4-dihydroisoquinolin-2(1H)-yl)methanone (**1180-60**)**:** Tetrahydroisoquinoline **1180-60** was prepared via Procedure IV using tetrahydroisoquinoline **34a** (0.18 g, 0.59 mmol) and 3-chlorobenzoyl chloride (0.90 mL, 0.71 mmol) in DCM (13 mL). The crude residue was purified by silica gel chromatography (ISCO, Redisep 12 g column, 10 – 80% EtOAc/hexanes gradient) to afford the title compound as a white foam (0.38 g, 64 %, mixture of two amide rotamers) TLC (EtOAc: hexanes, 1:1, v/v) Rf = 0.61; ^{1}H NMR ($CDCl_3$, 400 MHz) δ: 7.34-7.08 (m, 4H), 6.86-6.80 (m, 3H), 6.85-6.36 (m, 2H), 6.26 (s, 0.5 H), 5.82-5.79 (m, 0.5 H), 4.88-4.83 (dd, *J* = 6.1 Hz, *J* = 13.1 Hz, 0.5H), 4.68-4.65 (dd, *J* = 4.9 Hz, *J* = 9.5 Hz, 0.5H),

3.84-3.69 (m, 9H), 3.61-3.56 (m, 1H), 3.37-3.28 (m, 1H), 3.14-3.12 (d, *J* = 6.8, 1H), 3.07-3.01 (m, 1H), 2.85-2.52 (m, 2H). ^{13}C NMR ($CDCl_3$, 100 MHz) δ: 168.9, 158.9, 158.7, 148.0, 147.5, 138.5, 138.0, 134.7, 134.5, 131.0, 130.9, 130.2, 129.9, 129.7, 129.6, 129.5, 128.2, 127.9, 126.9, 126.2, 125.2, 124.8, 124.5, 114.4, 113.9, 111.8, 11.4, 110.6, 109.9, 60.2, 56.2, 56.1, 55.9, 55.5, 55.4, 42.4, 41.9, 41.5, 25.6, 29.1, 28.1. HRMS cald. For $C_{26}H_{27}NO_4Cl$, 452.16231 $[M + H]^+$; found, 452.16270 $[M + H]^+$.

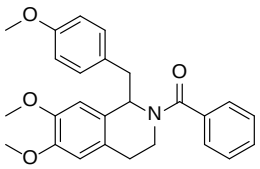

((6,7-dimethoxy-1-(4-methoxybenzyl)-3,4-dihydroisoquinolin-2(1H)-yl)(phenyl)methanone (**1180-61**)**:** Tetrahydroisoquinoline **1180-61** was prepared via Procedure IV using tetrahydroisoquinoline **34a** (0.18 g, 0.59 mmol) and benzoyl chloride (0.080 mL, 0.71 mmol) in DCM (13 mL). The crude residue was purified by silica gel chromatography (ISCO, Redisep 12 g column, 10 – 80% EtOAc/hexanes gradient) to afford the title compound as a white foam (0.13 g, 53 %, mixture of two amide rotamers) TLC (EtOAc: hexanes, 1:1, v/v) Rf = 0.67; ^{1}HNMR ($CDCl_3$, 400 MHz) δ: 7.41-7.34 (m, 2H), 7.29-6.25 (m, 3H) 7.15-7.13 (d, *J* = 8.8 Hz, 1H), 6.88-6.67 (m, 3H), 6.57-6.37 (m, 1H), 6.10 (s, 0.5 H), 5.88-5.85 (m, 0.5 H), 4.87-4.83 (dd, *J* = 5.6 Hz, *J* = 13.2 Hz, 0.5H), 4.77-4.73 (t, *J* = 7.2 Hz, 0.5H), 3.85-3.64 (m, 10H), 3.36-3.25 (m, 1H), 3.16-3.03 (m, 2H), 2.86-2.49 (m, 2H); ^{13}C NMR ($CDCl_3$, 100 MHz) δ: 171.3, 170.6, 158.8, 158.6, 148.3, 147.9, 147.3, 136.9, 131.1, 130.9, 130.2, 129.8, 129.5, 129.3, 128.7, 128.4, 128.1, 126.7, 126.7, 126.3, 125.5, 114.2, 113.9, 111.8, 111.3, 110.7, 110.1, 59.9, 56.1, 56.0, 55.9, 55.6, 55.5, 42.5, 41.9, 41.5, 35.7, 29.2, 28.1 HRMS calcd. For $C_{26}H_{28}NO_4$, 418.20179 $[M + H]^+$; found, 418.20165 $[M + H]^+$.

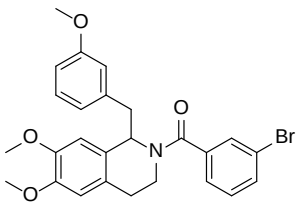

(3-bromophenyl)(6,7-dimethoxy-1-(3-methoxybenzyl)-3,4-dihydroisoquinolin-2(1H)-yl)methanone (**1180-59**)**:** Dihydroisoquinoline **33b** was prepared via Procedure I using amide **31b**

(2.4 g, 7.2 mmol) and phosphorus trichloride (3.0 mL, 22 mmol) in dry toluene (35 mL). The crude solid (2.7 g) was carried on without further purification. HRMS calcd. for $C_{19}H_{21}O_3N_1$, 312.15942 [M + H]$^+$; found 312.15964 [M + H]$^+$. Tetrahydroisoquinoline **34b** was prepared via Procedure III using dihydroisoquinoline **33b** (2.7 g, 8.7 mmol) and sodium borohydride (0.98 g, 26 mmol) in dry MeOH (42 mL). The crude residue was subjected to flash column chromatography (ISCO, Redisep 24 g column, 0-10% MeOH/DCM gradient) to afford tetrahydroisoquinoline **34b** (0.50 g, 18 %) in an impure form. The impurities were inseparable by chromatography. The product was visible by LCMS and was carried on without further purification. HRMS calcd. for $C_{19}H_{23}NO_3$, 314.17507 [M + H]$^+$; found, 314.17484 [M + H]$^+$. Tetrahydroisoquinoline **1180-59** was prepared via Procedure IV using tetrahydroisoquinoline **34b** (0.20 g, 0.62 mmol) and 3-bromobenzoyl chloride (0.10 mL, 0.75 mmol) in DCM (10 mL). The crude residue was purified by silica gel chromatography (ISCO, Redisep12 g column, 10-80% EtOAc/hexanes gradient) to afford the title compound as a white foam (0.094 g, 31 %, mixture of two amide rotamers) TLC (EtOAc: hexanes, 1:1, v/v) Rf = 0.54; ^{1}H NMR ($CDCl_3$, 400 MHz) δ: 7.55-7.08 (m, 4H), 6.88-6.75 (m, 3H), 6.68-6.40 (m, 2H), 6.24 (s, 0.5 H), 5.91-5.87 (m, 0.5 H), 4.91-4.87 (dd, *J* = 6.1 Hz, *J* = 13.4 Hz, 0.5H), 4.79-4.75 (dd, *J* = 5.2, *J* = 9.2, 0.5H), 3.88-3.72 (m, 9H), 3.66-3.62 (m, 1H), 3.45-3.33 (m, 1H), 3.20 (d, *J* = 7.2 Hz, 1H), 3.19-3.08 (m, 1H), 2.91-2.57 (m, 2H). ^{13}C NMR ($CDCl_3$, 100 MHz) δ: 169.5, 168.9, 160.1, 159.8, 148.5, 147.5, 147.5, 139.5, 139.5, 138.9, 138.7, 138.1, 132.7, 132.5, 130.4, 130.0, 129.8, 129.5, 129.3, 128.5, 128.1, 127.8, 126.2, 125.5, 125.2, 125.1, 122.9, 122.7, 122.5, 122.2, 115.5, 115.4, 112.6, 112.5, 111.8, 111.3, 110.5, 109.9, 76.9, 56.1, 55.9, 55.5, 43.4, 42.5, 41.9, 35.7, 29.1, 28.01. HRMS calcd. For $C_{26}H_{27}NO_4Br$, 496.11180 [M + H]$^+$; found, 496.11228 [M + H]$^+$.

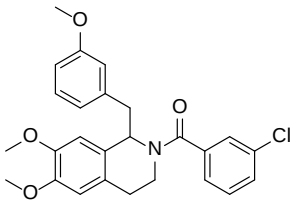

(3-chlorophenyl)(6,7-dimethoxy-1-(3-methoxybenzyl)-3,4-dihydroisoquinolin-2(1H)-yl)methanone (**1180-63**)**:** Dihydroisoquinoline **33b** was prepared via Procedure I using amide **31b**

(2.0 g, 6.2 mmol) and phosphorus trichloride (1.7 mL, 19 mmol) in dry toluene (35 mL). The crude solid (2.6 g) was carried on without further purification. HRMS calcd. for $C_{19}H_{21}O_3N_1$, 312.15942 [M + H]$^+$; found 312.15907 [M + H]$^+$. Tetrahydroisoquinoline **34b** was prepared via Procedure III using dihydroisoquinoline **33b** (2.6 g, 8.4 mmol) and sodium borohydride (0.95 g, 25 mmol) in dry MeOH (42 mL). The crude residue was subjected to flash column chromatography (ISCO, Redisep 24 g column, 0-10% MeOH/DCM gradient) to afford tetrahydroisoquinoline **34b** (0.5 g, 18 %) in an impure form. The impurities were inseparable by chromatography. The product was visible by LCMS and was carried on without further purification. HRMS calcd. for $C_{19}H_{23}NO_3$, 314.17507 [M + H]$^+$; found, 314.17484 [M + H]$^+$. Tetrahydroisoquinoline **1180-63** was prepared via Procedure IV using tetrahydroisoquinoline **34b** (0.23 g, 0.74 mmol) and 3-chlorobenzoyl chloride (0.11 mL, 0.89 mmol) in DCM (16 mL). The crude residue was purified by silica gel chromatography (ISCO, Redisep 12 g column, 10-80% EtOAc/hexanes gradient) to afford the title compound as a white foam (0.095 g, 31 %, mixture of two amide rotamers) TLC (EtOAc: hexanes, 1:1, v/v) Rf = 0.59; ^{1}H NMR ($CDCl_3$, 400 MHz) δ: 7.36 – 7.09 (m, 4H), 6.84 – 6.77 (m, 2H), 6.70 – 6.62 (m, 1H), 6.55 – 6.37 (m, 2H), 6.23 (s, 0.5 H) 5.88-5.85 (m, 0.5 H), 4.89-4.85 (dd, *J* = 6.0 Hz, *J* = 12.8 Hz, 0.5H), 4.74-4.72 (dd, *J* = 5.2 Hz, *J* = 8.8 Hz, 0.5H), 3.86–3.69 (m, 9H), 3.64–3.59 (m, 1H), 3.42–3.30 (m, 1H), 3.17 (d, *J* = 6.8 Hz, 1H), 3.13–3.04 (m, 1 H), 2.81–2.53 (m, 2H). ^{13}C NMR ($CDCl_3$, 100 MHz) δ: 169.6, 169.1, 160.1, 159.8, 148.4, 148.1, 147.5, 139.0,138.5, 137.9,134.8, 134.5, 130.2, 129.9, 129.7, 129.6, 129.5, 128.1, 127.8, 126.9, 126.2, 125.1, 124.7, 124.6, 122.5, 122.3, 115.5, 115.4, 112.6, 112.5, 111.8, 111.3, 110.5, 109.8, 60.1, 56.1, 55.9, 55.4, 55.4, 43.4, 42.5, 41.9, 35.7, 29.1, 28.1. HRMS calcd. For $C_{26}H_{27}NO_4Cl$, 452.16165 [M + H]$^+$; found, 452.16148 [M + H]$^+$.

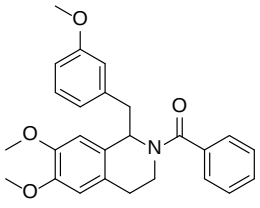

(6,7-dimethoxy-1-(3-methoxybenzyl)-3,4-dihydroisoquinolin-2(1H)-yl)(phenyl)methanone (**1180-64**)**:** Dihydroisoquinoline **33b** was prepared via Procedure I using amide **31b** (2.0 g, 6.2 mmol) and phosphorus trichloride (1.7 mL, 19 mmol) in dry toluene (35 mL). The crude solid (2.6 g) was carried on without further purification. HRMS calcd. for $C_{19}H_{21}O_3N_1$, 312.15942 $[M + H]^+$; found 312.15907 $[M + H]^+$. Tetrahydroisoquinoline **34b** was prepared via Procedure III using dihydroisoquinoline **33b** (2.6 g, 8.4 mmol) and sodium borohydride (0.95 g, 25 mmol) in dry MeOH (42 mL). The crude residue was subjected to flash column chromatography (ISCO, Redisep 24 g column, 0-10% MeOH/DCM gradient) to afford tetrahydroisoquinoline **34b** (0.50 g, 18 %) in an impure form. The impurities were inseparable by chromatography. The product was visible by LCMS and was carried on without further purification. HRMS calcd. for $C_{19}H_{23}NO_3$, 314.17507 $[M + H]^+$; found, 314.17484 $[M + H]^+$. Tetrahydroisoquinoline **1180-64** was prepared via Procedure IV using tetrahydroisoquinoline **34b** (0.23 g, 0.74 mmol) and benzoyl chloride (0.10 mL, 0.89 mmol) in DCM (16 mL). The crude residue was purified by silica gel chromatography (ISCO, Silicycle 12 g column, 10-80% EtOAc/hexanes gradient) to afford the title compound as a white foam (0.12 g, 32 %, mixture of two amide rotamers) TLC (EtOAc: hexanes, 1:1, v/v) Rf = 0.63; ^{1}HNMR ($CDCl_3$, 400 MHz) δ: 7.38 -7.32 (m, 2H), 7.26-7.24 (m, 3H), 7.21-7.12 (m, 1H), 6.88-6.76 (m, 2H), 6.64-6.34 (m, 2H), 6.06 (s, 0.5 H) 5.91-5.87 (m, 0.5 H), 4.89-4.79 (m, 1H), 3.86-3.63 (m, 9H), 3.37-3.29 (m, 2H), 3.21-3.07 (m, 2H), 2.89-2.76 (m, 2H); ^{13}C NMR ($CDCl_3$, 100 MHz) δ: 171.2, 170.6, 160.0, 159.8, 148.3, 147.9, 147.4, 139.7, 139.2, 136.8, 136.5, 129.8, 129.6, 129.5, 129.3, 128.7, 128.4, 128.3, 127.9, 126.3, 125.3, 122.5, 122.3, 115.4, 115.1, 112.7, 112.6, 111.7, 111.3, 110.6, 110.0, 59.8, 56.1, 56.0, 55.9, 55.4, 43.5, 42.5, 41.9, 35.8, 29.1, 28.1. HRMS calcd. For $C_{26}H_{28}NO_4$, 418.20072 $[M + H]^+$; found, 418.20045 $[M + H]^+$.

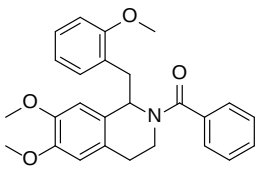

(6,7-dimethoxy-1-(2-methoxybenzyl)-3,4-dihydroisoquinolin-2(1H)-yl)(phenyl)methanone (1180-62): Tetrahydroisoquinoline **1180-62** was prepared via Procedure IV using tetrahydroisoquinoline **34c** (0.19 g, 1.9 mmol) and benzoyl chloride (0.072 mL, 0.63 mmol) in DCM (14 mL). The crude residue was purified by silica gel chromatography (ISCO, Redisep 12 g column, 10 – 80% EtOAc/hexanes gradient) to afford the title compound as a white foam (0.26 g, 38 %, mixture of two amide rotamers) TLC (EtOAc: hexanes, 1:1, v/v) Rf = 0.67; ^{1}H NMR ($CDCl_3$, 400 MHz) δ: 7.34-7.25 (m, 1H), 7.24-7.21 (m, 3H), 7.21-7.10 (m, 2H), 6.91-6.83 (m, 2H), 6.69-6.65(m, 2H), 6.54-6.50 (d, *J* = 16.8 Hz, 0.5H), 6.33 (s, 0.5 H), 6.09-6.06 (m, 0.5 H), 5.04-5.00 (dd, *J* = 4.8 Hz, *J* = 9.2 Hz, 0.5H), 4.91-4.87 (dd, *J* = 2.8 Hz, *J* = 10.0 Hz, 0.5H), 3.86-3.83 (m, 4H), 3.77-3.65 (m, 3H), 3.57-3.47 (m, 3H), 3.45-3.29 (m, 1H), 3.12-3.04 (m, 1H), 3.02-2.92 (m, 1H), 2.81-2.75 (m, 1H), 2.59-2.55 (m, 1H); ^{13}C NMR ($CDCl_3$, 100 MHz) δ: 170.2, 170.5, 158.4, 157.9, 148.2, 147.8, 147.5, 147.4, 137.0, 136.4, 131.7, 131.3, 129.9, 129.3, 128.9, 128.8, 128.6, 128.5, 128.3, 128.11, 126.8, 126.6, 126.2, 125.1, 120.8, 120.4, 111.6, 111.3, 110.6, 110.4, 110.0, 57.6, 56.1, 55.7, 55.0, 51.6, 41.2, 38.4, 37.0, 35.3, 29.3, 28.3; HRMS cald. For $C_{26}H_{28}NO_4$, 418.20045 $[M + H]^+$; found, 418.20068 $[M + H]^+$.

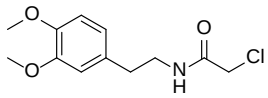

2-chloro-N-(3,4-dimethoxyphenethyl)acetamide (35): 2-(3,4-dimethoxyphenyl)ethanamine (5.0 g mL, 28 mmol) was dissolved in dry DCM (100 mL) and brought to 0°C using an ice bath. Triethylamine (12 mL, 83 mmol), followed by 2-chloroacetyl chloride (3.7 g, 33 mmol), was added. The reaction stirred for 3 hours, at which point TLC indicated complete conversion. The reaction was quenched with 1M HCl and extracted into DCM. The organic layer was then washed with water and brine, dried with $MgSO_4$, filtered, and concentrated *in vacuo*. The crude product was purified by silica gel chromatography (ISCO, Redisep 80 g column, 10-80% EtOAc/hexanes gradient) to afford the title compound as a white solid (4.7 g, 66 %). TLC (EtOAc/hexanes, 1:1, v/v) Rf: 0.42; ^{1}H NMR ($CDCl_3$, 400 MHz) δ: 6.79-6.77 (m, 1H), 6.72-6.67 (m, 2H), 6.61 (s, 1H), 3.98 (s, 2H), 3.84 (s,

3H), 3.82 (s, 3H), 3.54-3.47 (q, *J* = 7.0 Hz, *J* = 12.9 Hz, 2H), 2.77-2.73 (t, *J* = 7.0 Hz, 2H); ^{13}C NMR ($CDCl_3$, 100 MHz) δ: 165.9, 149.2, 147.9, 131.0, 120.9, 111.9, 111.6, 56.1, 56.0, 42.9, 41.3, 35.3. HRMS calcd. for $C_{12}H_{16}ClO_3N_1$, 258.08915 $[M + H]^+$; found 258.08895 $[M + H]^+$.

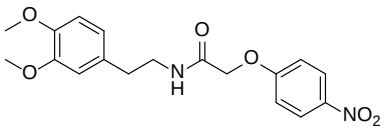

N-(4-methoxyphenethyl)-2-(4-methoxyphenoxy)acetamide (36): To a solution of *p*-nitrophenol (1.5 g, 11 mmol) in dry DMF (27 mL) was added CsF (5.5 g, 36 mmol) and the reaction mixture was allowed to stir for 2 hours. A solution of amide **35** (2.3 g, 9.0 mmol) dissolved in dry DMF (10. mL) was added and the resulting reaction mixture stirred for 96 hours at 50 °C. After TLC indicated complete conversion, water was added and the reaction mixture was extracted into DCM (3x). The organic layer was washed with water and brine, dried over $MgSO_4$, and concentrated *in vacuo*. The crude residue was purified by silica gel chromatography (ISCO, Redisep 80 g column, 10-80% EtOAc/hexanes gradient) to afford the title compound as a yellow solid (2.5 g, 76 %). TLC (EtOAc/hexanes, 1:1, v/v) Rf: 0.25; ^{1}H NMR ($CDCl_3$, 400 MHz) δ: 7.09 - 7.07 (m, 2H), 6.85 - 6.83 (m, 4H), 6.82 - 6.78 (m, 2H), 7.65 (s, 1H), 4.42 (s, 2H), 3.80 (s, 3H), 3.78 (s, 3H), 3.59 (q, *J* = 6.4 Hz, *J* = 12.8 Hz, 2H), 2.79 (t, *J* = 12.8 Hz, 2H); ^{13}C NMR ($CDCl_3$, 100 MHz) δ: 168.6, 158.5, 154.9, 151.4 ,130.7, 129.9, 115.8, 115.0, 114.3, 68.3, 55.9, 55.5, 40.5, 34.9. HRMS calcd. for $C_{18}H_{20}O_6N_2$, 361.13941 $[M + H]^+$; found 361.13950 $[M + H]^+$.

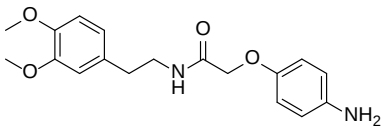

2-(4-aminophenoxy)-N-(3,4-dimethoxyphenethyl)acetamide (37): Amide **36** (2.5 g, 6.9 mmol) in EtOH (15 ml) was subjected to hydrogenation conditions with 10% Pd/C (0.25 g) under a hydrogen atmosphere (1 atm) for 14 hours. The reaction mixture was filtered over celite and the filtrate was concentrated *in vacuo* to afford a white solid (2.9 g, 97 %). TLC (MeOH:DCM, 1:10, v/v) Rf: 0.71; ^{1}H NMR ($CDCl_3$, 400 MHz) δ: 6.76-6.75 (d, *J* = 16 Hz, 1H), 6.68-6.62 (m, 5H), 6.60-6.57

(m, 2H), 4.36 (s, 2H), 3.83 (s, 3H), 3.81 (s, 3H), 3.57-3.53 (q, J = 6.8 Hz, J = 13.2 Hz, 2H), 3.48 (s, 2H), 2.77-2.74 (s, 2H); ^{13}C NMR ($CDCl_3$, 100 MHz) δ: 168.9, 150.5, 149.2, 147.9, 141.5, 131.3, 120.9, 116.5, 116.0, 112.1, 111.6, 68.5, 56.1, 56.0, 40.4, 35.5; HRMS calcd. for $C_{18}H_{22}O_4N_2$, 331.16523 [M + H]$^+$; found 331.16467 [M + H]$^+$.

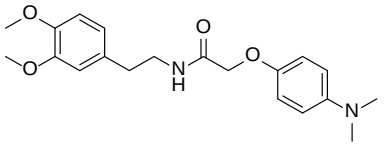

N-(3,4-dimethoxyphenethyl)-2-(4-(dimethylamino)phenoxy)acetamide (38): Amide **37** (1.6 g, 4.9 mmol) and paraformaldehyde (1.5 g, 49 mmol) were dissolved in AcOH (33 ml). Sodium cyanoborohydride (1.5 g, 25 mmol) was added to this solution and the reaction stirred for 18 hours. Upon completion, the reaction was made pH 13 with 1N NaOH, and extracted into DCM. The organic layer was washed with water and brine, dried with $MgSO_4$, and concentrated *in vacuo*. The crude residue was purified by silica gel chromatography (ISCO, Redisep 20 g column, 0-20% MeOH/DCM gradient) to afford the title compound as a white solid (1.56 g, 89 %). TLC (MeOH/DCM, 1:10, v/v) Rf: 0.76; ^{1}H NMR ($CDCl_3$, 400 MHz): 6.78-6.74 (m, 3H), 6.70-6.66 (m, 4H), 4.39 (s, 2H), 3.84 (s, 3H), 3.82 (s, 3H), 3.57 (m, J = 6.4 Hz, 2H), 2.86 (s, 6H), 2.79-2.75 (t, J = 7.2 Hz, 2H); ^{13}C NMR ($CDCl_3$, 100 MHz) δ: 168.9, 149.5, 149.2, 147.9, 146.8, 131.3, 120.9, 115.8, 114.6, 112.0, 111.5, 68.5, 56.1, 56.0, 41.7, 40.4, 35.5; HRMS calcd. for $C_{20}H_{26}O_4N_2$, 359.19653 [M + H]$^+$; found 359.19603 [M + H]$^+$.

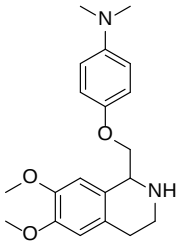

4-((6,7-dimethoxy-1,2,3,4-tetrahydroisoquinolin-1-yl)methoxy)-N,N-dimethylaniline (40): Dihydroisoquinoline **39** was prepared via procedure I using amide **38** (2.0 g, 4.4 mmol) and phosphorus trichloride (1.2 mL, 13 mmol) in dry toluene (24 mL). The crude solid (2.1 g) was carried

on without further purification. HRMS calcd. for $C_{20}H_{24}O_3N_2$, 341.18597 $[M + H]^+$; found 341.18555 $[M + H]^+$. Tetrahydroisoquinoline **40** was prepared via procedure III using dihydroisoquinoline **39** (2.7 g, 7.9 mmol) and sodium borohydride (0.97 g, 24 mmol) in dry MeOH (39 mL). The crude residue was purified by silica gel chromatography (ISCO, Redisep 20 g column, 0-20% MeOH:DCM gradient) to afford the title compound as a white solid (0.73 g, 27 %) TLC (MeOH/DCM, 1:10, v/v) Rf: 0.69; ^{1}H NMR ($CDCl_3$, 400 MHz) δ: 6.88-6.86 (m, 2H), 6.73-6.71 (m, 2H), 6.66 (s, 1H), 6.60 (s, 1H), 4.33- 4.30 (t, J = 6.0 Hz, 1H), 4.09-4.08 (d, J = 6.0 Hz, 2H), 3.84 (s, 3H), 3.82 (s, 3H), 3.22-3.17 (m, 1H), 3.04-2.98 (m, 1H), 2.82 (s, 6H), 2.79-2.74 (m, 2H); ^{13}C NMR ($CDCl_3$, 100 MHz) δ: 151.2, 148.0, 147.4, 146.3, 128.2, 126.7, 115.8, 114.9, 112.1, 109.7, 71.5, 56.2, 56.0, 55.0, 41.9, 39.8, 29.4; HRMS calcd. for $C_{20}H_{26}O_3N_2$, 343.20162 $[M + H]^+$; found 343.20124 $[M + H]^+$.

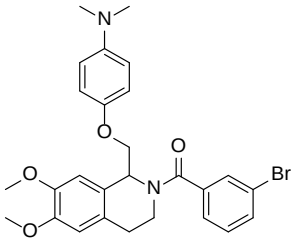

((3-bromophenyl)(1-((4-(dimethylamino)phenoxy)methyl)-6,7-dimethoxy-3,4-dihydroisoquinolin-2(1H)-yl)methanone) (**1180-77**)**:** Tetrahydroisoquinoline **1180-77** was prepared via Procedure IV using tetrahydroisoquinoline **40** (0.25 g, 0.73 mmol) and 3-bromobenzoyl chloride (0.12 mL, 0.88 mmol) in DCM (12 mL). The crude residue was purified by silica gel chromatography (ISCO, Redisep 25 g column, 10-80% EtOAc/hexanes gradient) to afford the title compound as a white foam (0.25 g, 64 %, mixture of two amide rotamers) TLC (EtOAc: hexanes, 1:1, v/v) Rf = 0.25; ^{1}H NMR ($CDCl_3$, 400 MHz) δ 7.78-7.43 (m, 2H), 7.31-7.23 (m, 2H), 6.87-6.79 (m, 2H), 6.71-6.69 (m, 2H), 6.65 (s, 0.5H), 6.61 (s, 0.5H), 6.48 (s, 0.5H), 5.95-5.92 (m, 0.5H), 5.08-5.05 (dd, J = 3.6 Hz, J = 9.2 Hz, 0.5H), 4.87-4.82 (dd, J = 5.6 Hz, J = 13.2 Hz, 0.5H), 4.37-4.30 (m, 1H), 4.18-3.92 (m, 1H), 3.86-3.78 (m, 7H), 3.74-3.62 (m, 1H), 3.27-3.01 (m, 1H), 2.85 (s, 6H), 2.83-2.64 (m, 2H). ^{13}C NMR ($CDCl_3$,100 MHz) δ: 170.2, 169.4, 151.1, 150.7, 148.9, 148.4, 147.9, 147.8,

146.4, 146.2, 138.6, 132.8, 132.7, 131.1, 1330.4, 130.2, 129.9, 127.3, 126.3, 126.2, 125.4, 125.3, 124.2, 122.9, 122.6, 115.9, 115.5, 114.9, 111.9,111.5, 110.4, 109.9, 71.2, 70.4, 57.6, 56.3, 56.2, 51.9, 42.9, 41.9, 41.8, 35.7, 29.2, 27.8. HRMS calcd. for $C_{27}H_{30}N_2O_4Br$, 252.13835 $[M + H]^+$; 525.13783 found, $[M + H]^+$; Anal. ($C_{27}H_{29}N_2O_4Br$): C, H, N.

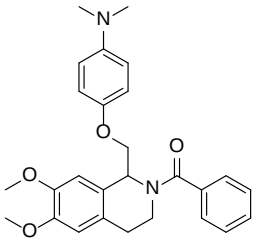

((1-((4-(dimethylamino)phenoxy)methyl)-6,7-dimethoxy-3,4-dihydroisoquinolin-2(1H)-yl)(phenyl)methanone) (**1180-78**)**:** Tetrahydroisoquinoline **1180-78** was prepared via Procedure IV using tetrahydroisoquinoline **40** (0.25 g, 0.73 mmol) and benzoyl chloride (0.10 mL, 0.88 mmol) in DCM (12 mL). The crude residue was purified by silica gel chromatography (ISCO, Redisep 25 g column, 10-80% EtOAc/hexanes gradient) to afford the title compound as a white foam (0.17 g, 54 %, mixture of two amide rotamers) TLC (EtOAc: hexanes, 1:1, v/v) Rf = 0.14; ^{1}H NMR ($CDCl_3$, 400 MHz) δ: 7.53-7.51 (m, 1H), 7.39 (s, 4H), 6.88-6.81 (m, 1H), 6.76-6.60 (m, 4H), 6.47 (s, 1H), 5.98-5.95 (m, 0.5H), 5.14-5.10 (dd, *J* = 4.4 Hz, *J* = 9.2 Hz, 0.5H), 4.90-4.86 (dd, *J* = 5.6 Hz, *J* = 12.8 Hz, 0.5H), 4.39-4.31 (m, 1H), 4.15-3.94 (m, 1H), 3.85-3.77 (m, 7H), 3.68-3.61 (m, 1H), 3.33-3.08 (m, 1H), 2.84 (s, 6H), 2.83-2.64 (m, 2H). ^{13}C NMR ($CDCl_3$, 100 MHz) δ:171.9, 171.2, 151.2, 150.8, 148.7, 148.3, 147.9, 147.6, 146.2, 136.7, 129.8, 128.6, 127.7, 127.4, 126.9, 126.4, 125.6, 124.6, 115.9, 115.6, 115.0, 114.9, 111.9, 111.5, 110.4, 110.0, 71.3, 70.6, 57.4, 56.2, 56.1, 51.7, 42.9, 41.9, 41.8, 35.7, 29.3, 27.9; HRMS calcd. for $C_{27}H_{31}N_2O_4$, 447.22783 $[M + H]^+$; found, 447.22759 $[M + H]^+$.

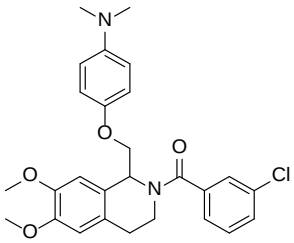

((3-chlorophenyl)(1-((4-(dimethylamino)phenoxy)methyl)-6,7-dimethoxy-3,4-dihydroisoquinolin-2(1H)-yl)methanone) (**1180-79**)**:** Tetrahydroisoquinoline **1180-79** was prepared via Procedure IV using tetrahydroisoquinoline **40** (0.25 g, 0.73 mmol) and 3-chlorobenzoyl chloride (0.11 mL, 0.88 mmol) in DCM (12 mL). The crude residue was purified by silica gel chromatography (ISCO, Redisep 25 g column, 10-80% EtOAc/hexanes gradient) to afford the title compound as a white foam (0.33 g, 94 %, mixture of two amide rotamers) TLC (EtOAc: hexanes, 1:1, v/v) Rf = 0.25; ^{1}H NMR ($CDCl_3$, 400 MHz) δ: 7.61-7.25 (m, 4H), 6.87-6.84 (m, 1H), 6.80-6.78 (m, 1H), 6.72-6.68 (m, 2H), 6.63 (s, 0,5H), 6.60 (s, 0.5H), 6.47 (s, 0.5H), 5.95-5.93 (m, 0.5H), 5.08-5.05 (dd, *J* = 4.0 Hz, *J* = 9.2 Hz, 0.5H), 4.87-4.82 (dd *J* = 5.6 Hz, *J* = 12.8 Hz, 0.5H), 4.37-4.33 (m, 1H), 4.17-3.92 (m, 1H), 3.86-3.62 (m, 7H), 3.74-3.62 (m, 1H), 3.27-3.02 (m, 1H), 2.85 (s, 6H), 2.83-2.64 (m, 1H). ^{13}C NMR ($CDCl_3$, 100 MHz) δ: 179.3, 169.6, 151.1, 148.8, 148.4, 147.9, 147.7, 146.4, 146.3, 138.3, 134.8, 134.5, 130.2, 129.9, 129.8, 128.2, 127.3, 127.1, 126.3, 125.9, 125.3, 124.9, 124.2, 115.9, 115.5, 114.8, 111.9, 111.5, 110.4, 109.9, 71.2, 70.4, 57.6, 56.2, 56.2, 51.9, 42.8, 41.9, 41.8, 35.6, 29.3, 27.8. HRMS calcd. for $C_{27}H_{29}N_2O_4Cl$, 481.18886 $[M + H]^+$; found, 481.18843 $[M + H]^+$; Anal. ($C_{27}H_{29}N_2O_4Cl$): C, H, N.

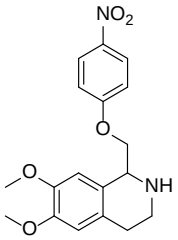

6,7-dimethoxy-1-((4-nitrophenoxy)methyl)-1,2,3,4-tetrahydroisoquinoline (**42**):

Dihydroisoquinoline **41** was prepared via Procedure I using amide **36** (2.5 g, 6.8 mmol) and phosphorus trichloride (1.9 mL, 20. mmol) in dry toluene (38 mL). The crude yellow solid (3.0 g) was carried on without further purification. HRMS calcd. for $C_{18}H_{18}O_5N_2$, 343.12885 $[M + H]^+$; found 343.12898 $[M + H]^+$. Tetrahydroisoquinoline **42** was prepared via Procedure III using dihydroisoquinoline **41** (3.0 g, 8.8 mmol) and sodium borohydride (1.3 g, 33.4 mmol) in dry MeOH (44 mL). The crude residue was purified by silica gel chromatography (ISCO, Redisep 20 g column,

0-20% MeOH/DCM gradient) to afford the title compound as a yellow solid (2.1 g, 70 %) TLC (MeOH/DCM, 1:10, v/v) Rf: 0.66; ^{1}H NMR ($CDCl_3$, 400 MHz) δ: 8.21-8.18 (m, 2H), 7.01-6.98 (m, 2H), 6.67 (s, 1H), 6.64 (s, 1H), 4.42 (m, 1H), 4.23 (m, 2H), 3.87 (s, 3H), 3.85 (s, 3H), 3.09 (m, 1H), 3. 076 (m, 3H), 2.78 (m, 2H); ^{13}C NMR ($CDCl_3$, 100 MHz) δ: 163.9, 148.3, 147.5, 141.8, 128.5, 126.2, 125.7, 114.7, 112.3, 109.6, 76.8, 71.8, 56.3, 56.1, 54.6, 39.9, 29.3. HRMS calcd. for $C_{18}H_{20}O_5N_2$, 345.14450 $[M + H]^+$; found 345.14450 $[M + H]^+$.

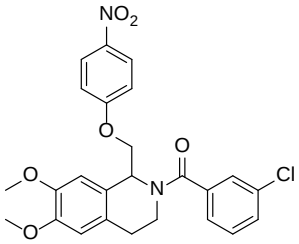

(3-chlorophenyl)(6,7-dimethoxy-1-((4-nitrophenoxy)methyl)-3,4-dihydroisoquinolin-2(1H)-yl)methanone (2029): Tetrahydroisoquinoline **2029** was prepared via Procedure IV using tetrahydroisoquinoline **42** (0.70 g, 2.0 mmol) and 3-chlorobenzoyl chloride (0.30 mL, 2.5 mmol) in DCM (33 mL). The crude residue was purified by silica gel chromatography (ISCO, Redisep 25 g column, gradient 10-80% EtOAc/hexanes gradient) to afford the title compound as a yellow foam (0.86 g, 86.2 %, mixture of two amide rotamers) TLC (EtOAc: hexanes, 1:1, v/v) Rf = 0.50; ^{1}H NMR ($CDCl_3$, 400 MHz) δ: 8.17-8.15 (m, 2H), 7.55-7.33 (m, 2H), 7.26-7.24 (m, 1H), 7.00-6.98 (m, 1H), 6.92-6.76 (m, 1H), 6.67-6.63 (m, 1H), 6.47 (s, 1H), 5.98-5.96 (m, 0.5H), 5.18-5.16 (d, J = 6.8 Hz, 0.5H), 4.89-4.86 (d, J = 7.6 Hz, 0.5H), 4.47-4.27 (m, 2H), 4.09-4.06 (m, 1H), 3.85-3.79 (m, 6H), 3.65-3.58 (m, 1H), 3.22-3.10 (m, 1H), 2.92-2.70 (m, 2H); ^{13}C NMR ($CDCl_3$,100 MHz) δ: 170.3, 169.8, 163.7, 163.1, 149.2, 148.7, 147.9, 142.0, 137.9, 134.9, 130.3, 130.2, 128.0, 127.5, 127.0, 126.4, 126.3, 125.6, 124.8, 124.3, 122.9, 114.9, 114.5, 112.1, 111.6, 110.3, 109.7, 70.8, 70.0, 60.6, 57.1, 56.3, 56.2, 53.7, 51.6, 49.6, 43.1, 35.7, 29.1, 27.7, 21.3. HRMS calcd. For $C_{25}H_{24}N_2O_6Cl$, 483.13174 $[M + H]^+$; found, 483.13178 $[M + H]^+$.

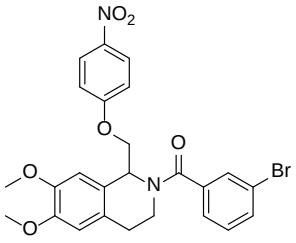

(3-bromophenyl)(6,7-dimethoxy-1-((4-nitrophenoxy)methyl)-3,4-dihydroisoquinolin-2(1H)-yl)methanone (1180-72): Tetrahydroisoquinoline **1180-72** was prepared via Procedure IV using tetrahydroisoquinoline **42** (0.70 g, 2.1 mmol) and 3-bromobenzoyl chloride (0.30 mL, 2.5 mmol) in DCM (33 mL). The crude residue was purified by silica gel chromatography (ISCO, Redisep 25 g column, 10-80% EtOAc/hexanes gradient) to afford the title compound as a yellow foam (0.86 g, 68 %, mixture of two amide rotamers) TLC (EtOAc: hexanes, 1:1, v/v) Rf = 0.43; ^{1}H NMR ($CDCl_3$, 400 MHz) δ: 8.18-8.14 (m, 2H), 7.71-7.49 (m, 2H), 7.38-7.24 (m, 2H), 7.00-6.98 (m, 1H), 6.93-6.76 (m, 1H), 6.67-6.63 (m, 1H), 6.48 (s, 0.5H), 5.97-5.96 (m, 0.5H), 5.18-5.16 (d, *J* = 6.8 Hz, 0.5H), 4.89-4.86 (dd, *J* = 4.8 Hz, J = 12.8 Hz, 0.5H), 4.50-4.42 (m, 1H), 4.32-4.00 (m, 1H), 3.84-3.79 (m, 6H), 3.65-3.57 (m, 1H), 3.22-3.09 (m, 1H), 2.92-2.69 (m, 2H);^{13}C NMR ($CDCl_3$, 100 MHz) δ: 170.1, 169.7, 163.6, 163,1, 149.2, 148.7, 148.2, 147.9, 142.2, 142.1, 138.1, 133.1, 132.9, 130.9, 130.5, 130.3, 129.8, 127.5, 126.5, 125.3, 124.3, 123,0, 114.8, 114.6, 112.1, 111.6, 110.3, 109.7, 70.8, 69.9, 65.3, 64.2, 60.6, 57.1, 56.3, 56.2, 51.6, 43.1, 35.7, 29.1, 27.7, 21.3. HRMS calcd. For $C_{25}H_{24}N_2O_6Br$, 527.08122 $[M + H]^+$; found, 527.08124 $[M + H]^+$.

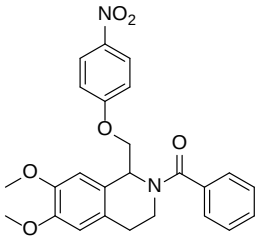

(6,7-dimethoxy-1-((4-nitrophenoxy)methyl)-3,4-dihydroisoquinolin-2(1H)-yl)(phenyl)methanone (**1180-73**): Tetrahydroisoquinoline **1180-73** was prepared via Procedure IV using tetrahydroisoquinoline **42** (0.70 g, 2.1 mmol) and benzoyl chloride (0.30 mL, 2.5 mmol) in DCM (33 mL). The crude residue was purified by silica gel chromatography (ISCO, Redisep 25 g

column, 10-80% EtOAc/hexanes gradient) to afford the title compound as a yellow foam (0.86 g, 68 %, mixture of two amide rotamers). TLC (EtOAc: hexanes, 1:1, v/v) Rf = 0.44; ^{1}HNMR ($CDCl_3$, 400 MHz) δ: 8.19-8.17 (m, 2H), 7.46-7.39 (m, 5H), 7.02-7.00 (m, 1H), 6.87-6.77 (m, 1H), 6.71-6.63 (m, 1H), 6.46 (s, 0.5H), 6.00-5.98 (m, 0.5H), 5.25-5.23 (d, *J* = 5.2 Hz, 0.5H), 4.91-4.89 (d, *J* = 7.6, 0.5H), 4.52-4.44 (m, 2H), 4.29-4.05 (m, 1H), 3.91-3.78 (m, 6H), 3.63-3.56 (m, 1H), 3.22-3.11 (m, 1H), 2.94-2.67 (m, 2H) ^{13}C NMR ($CDCl_3$, 100 MHz) δ:171.8, 171.4, 163.8, 163.5, 149.1, 148.6, 148.1, 141.9, 136.2, 130.1, 128.9, 128.8, 127.6, 126.8, 126.6, 126.2, 124.6, 123.3, 114.9, 114.6, 112.1, 111.6, 110.4, 109.8, 106.5, 70.9, 70.2, 56.9, 56.3, 56.2, 53,7m 51.4, 43.1, 35.6, 29.2, 27.8 HRMS calcd. For $C_{25}H_{25}N_2O_6$, 449.17071 $[M + H]^+$; found, 449.17080 $[M + H]^+$; Anal. ($C_{25}H_{25}N_2O_6$): C, H, N.

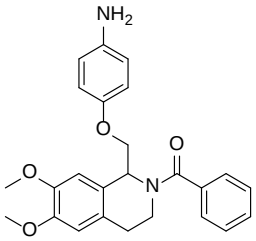

((1-((4-aminophenoxy)methyl)-6,7-dimethoxy-3,4-dihydroisoquinolin-2(1H)-yl)(phenyl)methanone) (**1180-74**): Tetrahydroisoquinoline **1180-73** (0.30 g, 0.70 mmol) and tin(II) chloride dihydrate (0.70 g, 3.3 mmol) were suspended in EtOH (2.7 ml) and heated to 70 °C. The reaction mixture was allowed to stir for three hours. Upon completion, the reaction was basified to pH 9 with saturated $NaHCO_3$. DCM was added and the mixture was filtered through a silica plug eluting with 10% MeOH/DCM. The organics were separated and washed with water and brine, dried over $MgSO_4$, and concentrated *in vacuo*. The crude residue was purified by silica gel chromatography (ISCO, Redisep 25 g column, 10-80% EtOAc/hexanes gradient) to yield the title compound as an off-white foam (0.090 g, 33 %, mixture of two amide rotamers) TLC (MeOH/DCM, 1:10, v/v) Rf = 0.73; ^{1}H NMR ($CDCl_3$, 400 MHz) δ: 7.52-7.50 (m, 1H), 7.39 (s, 4H), 6.98-6.76 (m, 2H), 6.65-6.57 (m, 3H), 6.46 (s, 0.5H), 5.96-5.94 (m, 0.5H), 5.13-5.10 (dd, *J* = 4.4 Hz, *J* = 8.8 Hz, 0.5H), 4.89-4.85 (dd, *J* = 5.6 Hz, J = 12.8 Hz, 0.5H), 4.36-4.07 (m, 2H), 3.94-3.76 (d, 6 H), 3.67-3.59 (m, 1H), 3.43 (s, 2H), 3.23-3.09 (m, 1H), 2.86-2.63 (m, 2H). ^{13}C NMR ($CDCl_3$, 100 MHz) δ:

171.9, 171.2, 152.1, 151.7, 148.7, 148.3, 147.9, 147.7, 140.6, 136.7, 129.8, 129.7, 128.7, 128.6, 127.8, 127.4, 126.9, 126.5, 125.7, 124.6, 116.5, 116.2, 115.8, 114.2, 112.0, 111.6, 110.1, 71.3, 70.6, 57.4, 56.2, 56.1, 53.7, 51.7, 42.9, 35.7, 29.9, 29.3, 27.9, 22.9. HRMS calcd. For $C_{25}H_{27}N_2O_4$, 419.19653 $[M + H]^+$; found, 419.19721 $[M + H]^+$.

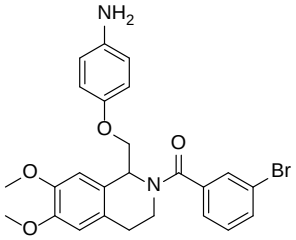

(3-bromophenyl)(6,7-dimethoxy-1-((4-(methylamino)phenoxy)methyl)-3,4-dihydroisoquinolin-2(1H)-yl)methanone (**1180-75**): Tetrahydroisoquinolone **1180-72** (.22 g, 0.44 mmol) and paraformaldehyde (0.066 g, 2.2 mmol) were suspended in dry methanol (5.5 mL) and sodium methoxide (0.10 ml, 0.44 mmol) was added dropwise at 0°C. The reaction was brought to reflux and stirred for one hour. The reaction was then brought to room temperature and after the addition of sodium borohydride (0.083 g, 2.2 mmol), the reaction was allowed to reflux for one additional hour. The reaction was allowed to cool to room temperature and 1 M NaOH was added. The reaction mixture was extracted into DCM, washed with water and brine, dried with $MgSO_4$, filtered, and concentrated *in vacuo*. The crude residue was purified by silica gel chromatography (ISCO, Redisep 20 g column, 0-80 % EtOAc:hexanes gradient) to afford the title compound as a white foam (0.15 g, 68 %, mixture of two amide rotamers). TLC (MeOH:DCM, 1:10, v/v) Rf = 0.85; ^{1}HNMR ($CDCl_3$, 400 mHz) δ: 7.77-7.51 (m, 2H), 7.45-7.25 (m, 2H), 6.83-6.65 (m, 3H), 6.60-6.58 (m, 2H), 6.47 (s, 0.5H), 5.94-5.92 (m, 0.5H), 5.06-5.05 (d, J = 5.2 Hz, 0.5H), 4.87-4.82 (dd, J = 5.6 Hz, J = 12.8 Hz, 0.5H), 4.33-4.32 (m, 1H), 4.16-3.92 (m, 2H), 3.86-3.85 (m, 6H), 3.74-3.65 (m, 1H), 3.24-3.08 (m, 1H), 2.85-2.83 (m, 1H), 2.79 (s, 3H), 2.77-2.65 (m, 1H); ^{13}CNMR (100 MHz, $CDCl_3$) δ: 170.2, 169.4, 151.3, 150.8, 148.8, 148.4, 147.9, 147.7, 144.4, 138.5, 132.8, 131.7, 131.1, 130.4, 130.2, 129.9, 127.3, 126.3, 126.2, 125.4, 125.4, 124.2, 122.9, 233.6, 116.2, 115.8, 113.8, 111.9, 111.5, 110.4,

109.9, 71.3, 70.5, 57.6, 56.2, 56.2, 51.9, 42.9, 35.7, 32.1, 31.8, 30.8, 29.8, 29.6, 29.2, 27.8, 22.9. 14.4,13.9; HRMS calcd. For $C_{26}H_{27}N_2O_4Cl$, 467.1732 $[M + H]^+$; found, 467.17265 $[M + H]^+$.

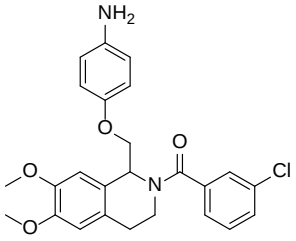

((1-((4-aminophenoxy)methyl)-6,7-dimethoxy-3,4-dihydroisoquinolin-2(1H)-yl)(3-chlorophenyl)methanone) (**1180-76**): Tetrahydroisoquinoline **2029** (0.56 g, 1.1 mmol) and tin (II) chloride dihydrate (1.2 g, 5.7 mmol) were suspended in EtOH (5.8 ml) and heated to 70 °C. The reaction mixture was allowed to stir for three hours. Upon completion, the reaction was basified to pH 9 with saturated $NaHCO_3$. DCM was added and the mixture was filtered through a silica plug eluting with 10% MeOH/DCM. The organics were separated and washed with water and brine, dried over $MgSO_4$, and concentrated *in vacuo*. The crude residue was purified by silica gel chromatography (ISCO, Redisep 40 g column, 10-80% EtOAc/hexanes gradient) to afford the title compound as a white foam (0.21 g, 42 %, mixture of two amide rotamers) TLC (MeOH:DCM, 1:10, v/v) Rf = 0.64; ^{1}H NMR ($CDCl_3$, 400 MHz) δ: 7.60-7.31 (m, 3H), 7.29-7.24 (m, 1H), 6.74-6.75 (m, 1H), 6.70-6.60 (m, 4H), 6.46 (s, 0.5H), 5.93-5.90 (m, 0.5H), 5.07-5.04 (dd, J = 3.6 Hz, J = 9.2 Hz, 0.5H), 4.86-4.82 (dd, J = 5.6 Hz, J = 13.2 Hz, 0.5H), 4.32-4.29 (m, 1H), 4.14-3.91 (m, 2H), 3.85-3.77 (d, 6H), 3.74-3.64 (m, 1H), 3.44 (s, 2H), 3.23-3.07 (m, 1H), 2.85-2.64 (m, 2H). ^{13}C NMR ($CDCl_3$, 100 MHz) δ: 170.3, 169.6, 151.9, 151.5, 148.8, 148.4, 147.9, 147.7, 140.8, 138.3, 138.1, 134.8, 134.5, 130.2, 129.9, 129.8, 128.2, 127.3, 127.1, 126.2, 125.9,125..3, 124.9, 124.1, 116.5, 116.1, 115.6, 111.9, 111.5, 110.8, 110.4, 109.9, 104.4, 87.2 81.2, 76.9, 71.2, 70.3, 65.6, 60.6, 57.5, 56.2, 56.1, 54.8, 51.9, 42.8, 35.7, 29.2, 27.8, 21.3. HRMS calcd. for $C_{25}H_{26}N_2O_4Cl$, 453.15756 $[M + H]^+$; found, 453.15723 $[M + H]^+$. Anal. ($C_{25}H_{26}N_2O_4Cl$): C, H, N.

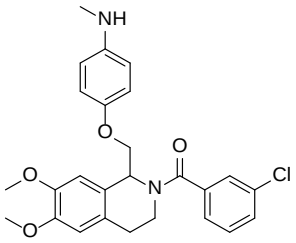

(3-chlorophenyl)(6,7-dimethoxy-1-((4-(methylamino)phenoxy)methyl)-3,4-dihydroisoquinolin-2(1H)-yl)methanone (**1180-80**): Tetrahydroisoquinolone **1180-76** (.10 g, 0.22 mmol) and paraformaldehyde (0.033 g, 1.1 mmol) were suspended in dry methanol (2.8 ml) and sodium methoxide (0.050 ml, 0.22 mmol) was added dropwise at 0°C. The reaction was brought to reflux and stirred for one hour. The reaction was then brought to room temperature, and after the addition of sodium borohydride (0.042 g, 1.1 mmol), the reaction was allowed to reflux for one additional hour. The reaction was allowed to cool to room temperature and 1 M NaOH was added. The reaction mixture was extracted into DCM, washed with water and brine, dried with $MgSO_4$, filtered, and concentrated *in vacuo*. The crude residue was purified by silica gel chromatography (ISCO, Redisep 20 g column, 0-80 % EtOAc:hexanes gradient) to afford the title compound as a white foam (0.074 g, 72 %, mixture of two amide rotamers). TLC (EtOAc: hexanes, 1:1, v/v) Rf = 0.17; ^{1}HNMR ($CDCl_3$, 400 mHz) δ: 7.61 -7.27 (m, 4H), 6.82-7.78 (m, 1H), 6.76-6.73 (d, J = 8.4 Hz, 1H), 6.65-6.60 (d, J = 20 Hz, 1H), 6.56-6.54 (m, 2H), 6.47 (m, 0.5H), 5.95-5.92 (m, 0.5H), 5.07-5.04 (dd, J = 3.6 Hz, J = 9.2 Hz, 0.5H), 4.87-4.83 (dd, J = 5.6 Hz, J = 12.8 Hz, 0.5H), 4.33-4.31 (m, 1H), 4.16-3.93 (m, 1H), 3.86-3.78 (m, 6H), 3.73-3.65 (m, 1H), 3.24-3.08 (m, 1H), 2.85-2.81 (m, 1H), 2.78 (s, 3H), 2.77-2.65 (m, 1H). 13C NMR ($CDCl_3$, 100 MHz) δ: 170.3, 169.7, 151.4, 150.9, 148.8, 148.4, 147.9, 147.7, 144.3, 114.1, 138.3, 134.9, 134.5, 130.2, 129.9, 129.8, 128.2, 127.3, 127.1, 126.2, 125.9, 125.3, 124.9, 1214.2, 116.2, 115.8, 113.9, 111.9, 111.5, 110.4, 109.9,71.3, 70.5, 66.1, 57.7, 56.3, 56.1, 52.5, 51.9, 42.8, 35.6, 31.9, 29.2, 27.8, 15.5. HRMS calcd. For $C_{26}H_{27}N_2O_4Cl$, 467.1732 $[M + H]^+$; found, 467.17265 $[M + H]^+$. Analysis (calcd., found for $C_{26}H_{27}N_2O_4Cl$) C: (66.88, 66.73), H (5.83, 5.95), N (6.00, 5.82).

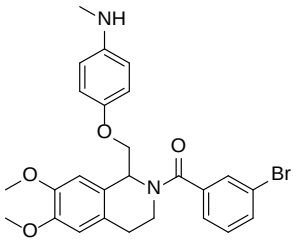

(3-bromophenyl)(6,7-dimethoxy-1-((4-(methylamino)phenoxy)methyl)-3,4-dihydroisoquinolin-2(1H)-yl)methanone (**1180-81**): Tetrahydroisoquinolone **1180-75** (.22 g, 0.44 mmol) and paraformaldehyde (0.066 g, 2.2 mmol) were suspended in dry methanol (5.5 mL) and sodium methoxide (0.10 ml, 0.44 mmol) was added dropwise at 0°C. The reaction was brought to reflux and stirred for one hour. The reaction was then brought to room temperature and after the addition of sodium borohydride (0.083 g, 2.2 mmol), the reaction was allowed to reflux for one additional hour. The reaction was allowed to cool to room temperature and 1 M NaOH was added. The reaction mixture was extracted into DCM, washed with water and brine, dried with $MgSO_4$, filtered, and concentrated *in vacuo*. The crude residue was purified by silica gel chromatography (ISCO, Redisep 20 g column, 0-80 % EtOAc:hexanes gradient) to afford the title compound as a white foam (0.15 g, 68 %, mixture of two amide rotamers). TLC (MeOH:DCM, 1:10, v/v) Rf = 0.85; ^{1}HNMR ($CDCl_3$, 400 mHz) δ: 7.77-7.51 (m, 2H), 7.45-7.25 (m, 2H), 6.83-6.65 (m, 3H), 6.60-6.58 (m, 2H), 6.47 (s, 0.5H), 5.94-5.92 (m, 0.5H), 5.06-5.05 (d, *J* = 5.2 Hz, 0.5H), 4.87-4.82 (dd, *J* = 5.6 Hz, *J* = 12.8 Hz, 0.5H), 4.33-4.32 (m, 1H), 4.16-3.92 (m, 2H), 3.86-3.85 (m, 6H), 3.74-3.65 (m, 1H), 3.24-3.08 (m, 1H), 2.85-2.83 (m, 1H), 2.79 (s, 3H), 2.77-2.65 (m, 1H). ^{13}CNMR (100 MHz, $CDCl_3$) δ: 170.2, 169.4, 151.3, 150.8, 148.8, 148.4, 147.9, 147.7, 144.4, 138.5, 132.8, 131.7, 131.1, 130.4, 130.2, 129.9, 127.3, 126.3, 126.2, 125.4, 125.4, 124.2, 122.9, 233.6, 116.2, 115.8, 113.8, 111.9, 111.5, 110.4, 109.9, 71.3, 70.5, 57.6, 56.2, 56.2, 51.9, 42.9, 35.7, 32.1, 31.8, 30.8, 29.8, 29.6, 29.2, 27.8, 22.9. 14.4,13.9; HRMS calcd. For $C_{26}H_{27}N_2O_4Cl$, 467.1732 $[M + H]^+$; found, 467.17265 $[M + H]^+$.

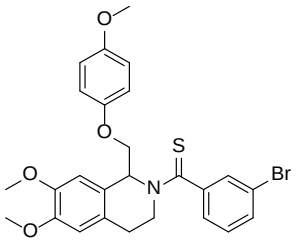

(3-bromophenyl)(6,7-dimethoxy-1-((4-methoxyphenoxy)methyl)-3,4-dihydroisoquinolin-2(1H)-yl)methanethione (1180-157): Tetrahydroisoquinoline **1180-157** was prepared via General Procedure V using tetrahydroisoquinoline **1391** (0.060 g, 0.15 mmol) and 2,4-bis(4-methoxyphenyl)-1,3,2,4-dithiadiphosphetane 2,4-disulfide (0.077 g, 0.15 mmol) in toluene (7.0 mL). The crude residue was purified by silica gel chromatography (ISCO, Redisep 12 g column, 0-80% EtOAc/hexanes gradient) to afford the title compound as a yellow foam (0.035 g, 45%); TLC (EtOAc:hexanes, 1:1, v/v) Rf = 0.62; ^{1}H NMR ($CDCl_3$, 400 MHz) δ: 7.46-7.37 (m, 2H), 7.24-7.15 (m, 2H), 6.85-6.79 (m, 5H), 6.69-6.41 (m, 1H), 5.74-5.73 (m, 0.5H), 5.35-5.32 (m, *J* = 4.0 Hz, *J* = 4.0 Hz, 0.5H), 4.63-4.60 (dd, 4.8 Hz, *J* = 4.4 Hz,0.5H), 4.50-4.47 (m, *J* = 4.4 Hz, *J* = 4.8 Hz, 0.5H), 4.03-3.99 (m, 1H), 3.86-3.69 (m, 10H), 3.66-3.59 (m, 0.5H), 3.13-3.23 (m, 0.5H), 2.94-2.72 (m, 2H); ^{13}C NMR (100 MHz, $CDCl_3$) δ: 200.2, 198.8, 154.6, 154.5, 152.8, 152.3, 149.1, 148.6, 148.3, 145.1, 144.9, 131.8, 131.6, 130.4, 129.9, 127.0, 125.7, 124.9, 123.4, 1122.8, 115.9, 115.6, 114.9, 114.8, 111.8, 111.3, 110.0, 109.6, 70.6, 61.6, 58.4, 56.3, 56.2, 56.1, 55.9, 48.2, 29.4, 27.4; HRMS calcd. for $C_{26}H_{26}BrNO_4S$, 550.06581 $[M + H]^+$; 550.06618$[M + H]^+$ found.

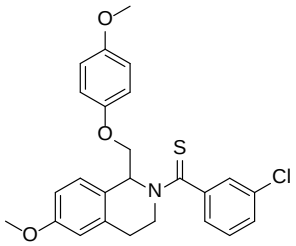

(3-chlorophenyl)(6-methoxy-1-((4-methoxyphenoxy)methyl)-3,4-dihydroisoquinolin-2(1H)-yl)methanethione (1180-160): Tetrahydroisoquinoline **1180-160** was prepared via General Procedure V using tetrahydroisoquinoline **1180-26** (0.17 g, 0.39 mmol) and 2,4-bis(4-methoxyphenyl)-1,3,2,4-dithiadiphosphetane 2,4-disulfide (0.17 g, 0.39 mmol) in toluene (15 mL).

The crude residue was purified by silica gel chromatography (ISCO, Redisep 12 g column, 0-80% EtOAc/hexanes gradient) to afford the title compound as a yellow foam (0.073 g, 41%); TLC (EtOAc:hexanes, 1:1, v/v) Rf = 0.75; ^{1}H NMR ($CDCl_3$, 400 MHz) δ: 7.30-7.23 (m, 3H), 7.12-7.10 (m, 1H), 6.89-6.69 (m, 7H), 5.73-5.69 (m, *J* = 4.8 Hz, *J* = 4.8 Hz, 0.5H), 5.40-5.37 (m, *J* = 4.0 Hz, *J* = 4.0 Hz, 0.5H), 4.69-4.65 (dd, *J* = 4.0 Hz, *J* = 4.4 Hz, 0.5H), 4.48-4.45 (dd, *J* = 4.8 Hz, J = 4.0 Hz, 0.5H), 4.21-4.08 (m, 0.5H), 4.03-3.86 (m, 2H), 3.29-3.75 (m, 6H), 3.70-3.61 (m, 0.5H), 3.35-3.27 (m, 0.5H), 2.98-2.89 (m, 1H), 2.83-2.79 (m, 0.5H); ^{13}C NMR (100 MHz, $CDCl_3$) δ: 200.4, 199.0, 159.5, 158.8, 154.6, 154.4, 152.9, 152.3, 145.0, 144.7, 136.2, 134.9, 134.7, 130.2, 128.8, 128.7, 128.5, 128.1, 125.2, 123.8, 115.9, 115.6, 114.9, 114.8, 114.1, 113.6, 113.2, 70.9, 61.5, 58.4, 55.9, 55.6, 55.5, 48.1, 42.7, 30.1, 28.1; HRMS calcd. for $C_{25}H_{25}ClNO_3S$, 454.12382 $[M + H]^+$; 454.12388 $[M + H]^+$ found.

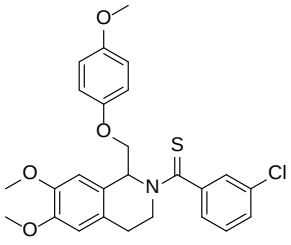

(3-chlorophenyl)(6,7-dimethoxy-1-((4-methoxyphenoxy)methyl)-3,4-dihydroisoquinolin-2(1H)-yl)methanethione (1180-161): Tetrahydroisoquinoline **1180-161** was prepared via General Procedure V using tetrahydroisoquinoline **1390** (0.10 g, 0.21 mmol) and 2,4-bis(4-methoxyphenyl)-1,3,2,4-dithiadiphosphetane 2,4-disulfide (0.086 g, 0.21 mmol) in toluene (11 mL). The crude residue was purified by silica gel chromatography (ISCO, Redisep 12 g column, 0-80% EtOAc/hexanes gradient) to afford the title compound as a yellow foam (0.074 g, 72%); TLC (EtOAc:hexanes, 1:1, v/v) Rf = 0.60; ^{1}H NMR ($CDCl_3$, 400 MHz) δ: 7.34-7.25 (m, 2.5H), 7.15-7.12 (m, 1H), 6.88-6.81 (m, 5H), 6.72-6.44 (m, 1.5H), 5.79-5.75 (m, *J* = 5.2 Hz, *J* = 5.2 Hz, 0.5H), 5.38-5.35 (m, *J* = 4.0 Hz, *J* = 4.4 Hz, 0.5H), 4.66-4.62 (dd, *J* = 4.8 Hz, *J* = 4.4 Hz, 0.5H), 4.53-4.50 (dd, *J* = 4.4 Hz, *J* = 4.4 Hz, 0.5H), 4.26-4.15 (m, 0.5H), 4.05-3.98 (m, 1H), 3.92-3.77 (m, 10H), 3.71-3.61 (m, 0.5H), 3.34-3.26 (m, 0.5H), 2.97-2.75 (m, 1.5H); ^{13}C NMR (100 MHz, $CDCl_3$) δ: 200.3, 198.9, 154.6, 154.5, 152.8, 152.3, 149.1, 148.6, 148.3, 144.8, 134.7, 130.2, 128.8, 128.6, 127.0, 125.7, 124.9, 123.4, 115.9, 115.6, 115.0,

114.9, 111.9, 111.3, 110.0, 109.6, 70.6, 61.6, 58.3, 56.3, 56.2, 55.9, 48.2, 29.5, 27.4; HRMS calcd. for $C_{26}H_{27}ClNO_4S$, 484.13438 $[M + H]^+$; 484. 13503 $[M + H]^+$ found. Anal. ($C_{26}H_{26}N_1O_4SCl$): C, H, N.

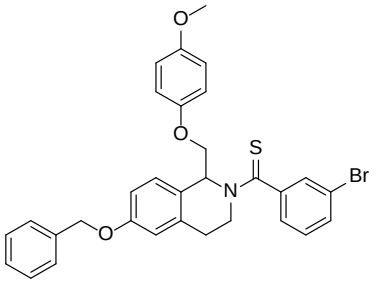

(6-(benzyloxy)-1-((4-methoxyphenoxy)methyl)-3,4-dihydroisoquinolin-2(1H)-yl)(3-bromophenyl)methanethione (1180-164): Tetrahydroisoquinoline **1180-164** was prepared via General Procedure V using tetrahydroisoquinoline **1180-98** (0.10 g, 0.18 mmol) and 2,4-bis(4-methoxyphenyl)-1,3,2,4-dithiadiphosphetane 2,4-disulfide (0.072 g, 0.18 mmol) in toluene (6.7 mL). The crude residue was purified by silica gel chromatography (ISCO, Redisep 12 g column, 0-80% EtOAc/hexanes gradient) to afford the title compound as a yellow foam (0.024 g, 23%); TLC (EtOAc:hexanes, 1:1, v/v) Rf = 0.89; ^{1}H NMR ($CDCl_3$, 400 MHz) δ: 7.49-7.33 (m, 7H), 7.32-7.24 (m, 1H), 7.19-7.16 (m, 1H), 6.95-6.76 (m, 7H), 5.75-5.70 (m, *J* = 5.6 Hz, *J* = 4.8 Hz, 0.5H), 5.42-5.39 (m, *J* = 4.0 Hz, *J* = 4.0 Hz, 0.5H), 5.08 (s, 2H), 4.71-4.67 (m, *J* = 4.4 Hz, *J* = 4.0 Hz, 0.5H), 4.50-4.46 (m, *J* = 4.0 Hz, *J* = 4.4 Hz, 0.5H), 4.20-4.13 (m, 0.5H), 4.05-3.87 (m, 1.5H), 3.83-3.64 (m, 4H), 3.73-3.29 (m, 0.5H), 2.99-2.92 (m, 1H), 2.85-2.81 (m, 0.5H); ^{13}C NMR (100 MHz, $CDCl_3$) δ: 200.3, 198.9, 158.7, 158.0, 154.6, 254.4, 152.9, 152.3, 145.2, 144.9, 136.9, 136.8, 136.3, 135.0, 131.7, 130.4, 128.9, 128.9, 128.5, 128.4, 128.3, 128.2, 127.7, 125.6, 124.1, 122.9, 115.9, 115.6, 115.2, 114.9, 114.8, 114.6, 114.3, 113.9, 70.7, 70.3, 70.3, 61.5, 58.4, 55.9, 48.1, 42.6, 30.1, 28.1; HRMS calcd. for $C_{31}H_{29}BrNO_3S$, 574.10679 $[M + H]^+$; 574.10460 $[M + H]^+$ found. Anal. ($C_{31}H_{28}N_1O_3SBr$): C, H, N.

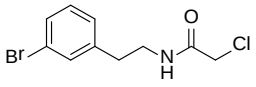

N-(3-bromophenethyl)-2-chloroacetamide (43): 2-(3-bromophenyl)ethanamine (2.8 g, 20. mmol) was dissolved in dry DCM (72 mL) and triethylamine (5.6 mL, 40. mmol) was added followed by 2-chloroacetyl chloride (1.9 ml, 24 mmol). After stirring for 3 hours the reaction was quenched with

1M HCl and extracted into DCM. The organic layer was washed with water and brine, dried with $MgSO_4$, filtered, and concentrated *in vacuo*. The crude product was purified by silica gel chromatography (10-90 % EtOAc/hexanes) to afford the title compound as a yellow solid (3.6 g, 65 %). TLC (EtOAc:hexanes, 1:1, v/v) Rf = 0.46; ^{1}HNMR ($CDCl_3$, 400 MHz) δ: 7.38-7.35 (m, 2H), 7.18 (t, *J* = 7.6 Hz, 1H), 7.13-7.11 (m, 1H), 6.59 (bs, 1H), 4.02 (s, 2H), 3.53 (q, J = 6.8 Hz, 2H), 2.81 (t, *J* = 6.8 Hz, 2H); ^{13}CNMR ($CDCl_3$, 100 MHz) δ: 166.1, 140.8, 132.0, 130.5, 130.1, 127.6, 122.9, 42.8, 40.9, 35.4; HRMS calcd. for $C_{10}H_{12}ON^{35}Cl^{79}Br$, 275.97853 $[M + H]^+$; 275.97861 found, $[M + H]^+$.

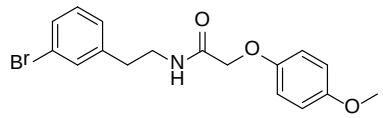

N-(3-bromophenethyl)-2-(4-methoxyphenoxy)acetamide (44): 4-methoxyphenol (1.9 g, 16 mmol) was dissolved in dry ACN (39 mL) and Cs_2CO_3 (17 g, 52 mmol) was added. The reaction was allowed to stir for 2 hours before amide **43** (3.6 g, 13 mmol) dissolved in dry ACN (15 mL) was added and the reaction was allowed to stir at room temperature overnight. The reaction was quenched with saturated aqueous ammonium chloride and extracted into EtOAc. The organic layer was washed with water (3x) and brine (3x), dried with $MgSO_4$, filtered, and concentrated *in vacuo*. The crude residue was purified by silica gel chromatography (ISCO, Redisep 40 g column, 10-80 % EtOAc/hexanes gradient) to afford the title compound as a white solid (3.9 g, 83 %). TLC (EtOAc:hexanes, 1:1, v/v) Rf = 0.45; ^{1}H NMR ($CDCl_3$, 400 MHz) δ: 7.36-7.33 (m, 2H), 7.14 (t, *J* = 8.0 Hz, 1H), 7.08-7.06 (m, 1H), 6.83-6.76 (m, 4H), 6.63 (bs, 1H), 4.4 (s, 2H), 3.76 (s, 3H), 3.56 (q, *J* = 6.8 Hz, 2H), 2.80 (t, *J* = 6.8 Hz, 2H). ^{13}C NMR ($CDCl_3$, 100 MHz) δ: 1.68.7, 154.9, 151.5, 132.0, 130.4, 129.9, 127.6, 122.9, 115.8, 115.0, 68.3, 55.9, 40.1, 35.6; HRMS calcd. for $C_{17}H_{19}O_3N^{79}Br$, 364.05428 $[M + H]^+$; 364.05494 found, $[M + H]^+$.

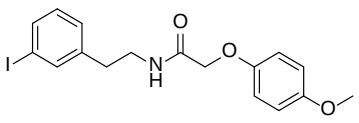

N-(3-iodophenethyl)-2-(4-methoxyphenoxy)acetamide (46): A 10 mL sealed vial was charged with amide **46** (2.0 g, 5.5 mmol), copper(I) iodide (0.052 g, 0.28 mmol), and sodium iodide (1.2 g, 8.2 mmol). The vial was sealed, evacuated, and backfilled with argon. *N*1, *N*2-dimethylethane-1,2-diamine (0.062 ml, 0.55 mmol) and dioxane (5.5 ml) were added, and the reaction was stirred at 110 °C for 24 hours. The reaction was then allowed to cool to room temperature, quenched with a 30 % ammonium hydroxide solution, and diluted with water. The reaction was extracted into EtOAc, washed with water (3x) and brine (3x), dried with $MgSO_4$, filtered, and concentrated *in vacuo*. The crude residue was purified by silica gel chromatography (ISCO, Redisep 40 g column, 10-90 % EtOAc/hexanes gradient) to afford the title compound as a white solid (1.8 g, 80 %). TLC (EtOAc:hexanes, 1:1, v/v) Rf = 0.48; ^{1}H NMR ($CDCl_3$, 400 MHz) δ: 7.56-7.55 (m, 1H), 7.12-7.10 (m, 1H), 7.00 (t, *J* = 8.0 Hz, 1H), 6.84-6.77 (m, 4H), 6.62 (bs, 1H), 4.41 (s, 2H), 3.76 (s, 3H), 3.58 (q, *J* = 6.8 Hz, 2H), 2.77 (t, *J* = 7.2 Hz, 2H); ^{13}C NMR ($CDCl_3$, 100 MHz) δ: 168.7, 154.9, 151.5, 141.2, 137.9, 135.9, 130.6, 128.3, 115.9, 115.0, 94.9, 68.3, 55.9, 40.1, 35.5; HRMS calcd. for $C_{17}H_{19}O_3N^{127}I$, 412.04042 $[M + H]^+$; 412.04049 found, $[M + H]^+$

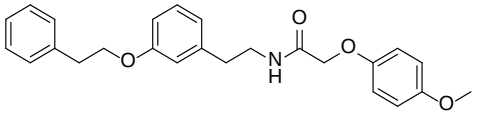

2-(4-methoxyphenoxy)-N-(3-phenethoxyphenethyl)acetamide (47a): A 5.0 mL sealed vial was charged with amide **46** (0.25 g, 0.59 mmol), copper(I) iodide (0.011 g, 0.059 mmol), 3,4,7,8-tetramethyl-1,10-phenanthroline (0.028 g, 0.12 mmol), and cesium carbonate (0.38 g, 1.2 mmol). The vial was sealed, evacuated, and back-filled with argon. 2-phenylethanol (0.66 ml, 5.5 mmol) was added, and the vial was submerged in an oil bath heated to 110 °C. After stirring for 24 hours, TLC indicated complete conversion. The reaction was allowed to cool to room temperature, diluted with EtOAc, and filtered thru a plug of celite rinsing with EtOAc. The organic layer was washed with water (3x) and brine (3x), dried with $MgSO_4$, filtered, and concentrated *in vacuo*. The crude residue was purified by silica gel chromatography (ISCO, Redisep 40 g column, 10-90 % EtOAc/hexanes gradient) to afford the title compound as a white solid (1.2 g, 47 %). TLC (EtOAc:hexanes, 1:1, v/v)

Rf = 0.67; ^{1}H NMR ($CDCl_3$, 400 MHz) δ: 7.32-7.16 (m, 6H), 6.82-6.72 (m, 7H), 6.65 (bs, 1H), 4.39 (s, 2H), 4.13 (t, *J* = 6.8 Hz, 2H), 3.76 (s, 3H), 3.57 (q, *J* = 6.8 Hz, 2H), 3.07 (t, *J* = 7.2 Hz, 2H), 2.79 (t, *J* = 6.8 Hz, 2H); ^{13}C NMR ($CDCl_3$, 100 MHz) δ: 168.6, 159.3, 154.9, 151.5, 140.4, 138.4, 129.9, 129.2, 128.7, 126.7, 121.3, 115.8, 115.2, 115.0, 112.8, 68.8, 68.3, 55.9, 40.2, 36.0, 35.9; HRMS calcd. for $C_{25}H_{28}O_4N$, 406.21209 $[M + H]^+$; 406.21214 found, $[M + H]^+$.

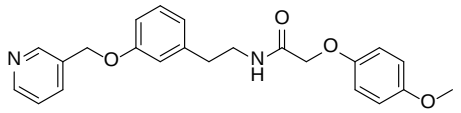

2-(4-methoxyphenoxy)-N-(3-(pyridin-3-ylmethoxy)phenethyl)acetamide (47b): A 10 mL sealed vial was charged with amide **46** (2.1 g, 5.1 mmol), copper(I) iodide (0.097 g, 0.51 mmol), 3,4,7,8-tetramethyl-1,10-phenanthroline (0.24 g, 1.0 mmol), and cesium carbonate (3.3 g, 10. mmol). The vial was sealed, evacuated, and back-filled with argon. pyridin-3-ylmethanol (4.6 ml, 48 mmol) was added, and the vial was submerged in an oil bath heated to 110 °C. After stirring for 24 hours, the reaction was allowed to cool to room temperature, diluted with EtOAc, and filtered thru a plug of celite rinsing with EtOAc. The organic layer was washed with water (3x) and brine (3x), dried with $MgSO_4$, filtered, and concentrated *in vacuo*. The crude residue was purified by silica gel chromatography (ISCO, Redisep 40 g column, 10-90 % EtOAc/hexanes gradient) to afford the title compound as a white solid (0.58 g, 30 %). TLC (EtOAc:hexanes, 1:1, v/v) Rf = 0.20; ^{1}H NMR ($CDCl_3$, 400 MHz) δ: 8.68 (s, 1H), 8.60 (d, *J* = 4.8 Hz, 1H), 7.78-7.76 (m, 1H), 7.34-7.31 (m, 1H), 7.22 (t, *J* = 7.6 Hz, 1H), 6.87-6.77 (m, 7H), 6.70 (bs, 1H), 5.05 (s, 2H), 4.42 (s, 2H), 3.76 (s, 3H), 3.60 (q, *J* = 6.4 Hz, 2H), 2.83 (t, *J* = 6.4 Hz, 2H); ^{13}C NMR ($CDCl_3$, 100 MHz) δ: 168.6, 158.9, 154.9, 151.5, 149.6, 149.2, 140.6, 135.6, 132.7, 130.1, 123.8, 122.0, 115.9, 115.5, 115.0, 113.0, 68.4, 67.6, 55.9, 40.1, 35.9; HRMS calcd. for $C_{23}H_{25}O_4N_2$, 393.18088 $[M + H]^+$; 393.18108 found, $[M + H]^+$.

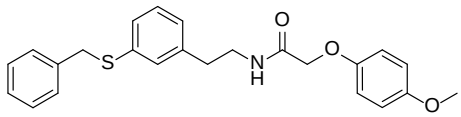

N-(3-(benzylthio)phenethyl)-2-(4-methoxyphenoxy)acetamide (48): A 10 mL sealed vial was charged with amide **46** (1.5 g, 3.7 mmol), copper(I) iodide (0.035 g, 0.18 mmol), ethane-1,2-diol (0.41

g, 7.3 mmol), and potassium carbonate (1.0 g, 7.3 mmol). The vial was sealed, evacuated, and back-filled with argon. Phenylmethanethiol (0.42 ml, 4.7 mmol) and 2-propanol (3.7 mL) were added, and the vial was submerged in an oil bath heated to 80 °C. After stirring for 24 hours, the reaction was allowed to cool to room temperature, diluted with EtOAc, and filtered thru a plug of celite rinsing with EtOAc. The organic layer was washed with water (3x) and brine (3x), dried with $MgSO_4$, filtered, and concentrated *in vacuo*. The crude residue was purified by silica gel chromatography (ISCO, Redisep 40 g column, 10-90 % EtOAc/hexanes gradient) to afford the title compound as a white solid (1.2 g, 78 %). TLC (EtOAc:hexanes, 1:1, v/v) Rf = 0.49; ^{1}H NMR ($CDCl_3$, 400 MHz) δ: 7.30-7.18 (m, 6H), 7.12 (s, 1H), 6.98-6.96 (m, 1H), 6.86-6.79 (m, 4H), 6.62 (s, 1H), 4.42 (s, 1H), 4.10 (s, 1H), 3.77 (s, 3H), 3.55 (q, *J* = 6.8 Hz, 2H), 2.78 (t, *J* = 7.2 Hz, 2H); ^{13}C NMR ($CDCl_3$,100 MHz) δ: 168.6, 154.9, 151.5, 139.5, 137.4, 137.0, 130.1, 129.3, 129.1, 128.7, 128.0, 127.4, 127.1, 115.8, 115.1, 68.3, 55.9, 40.1, 39.1, 35.7; HRMS calcd. for $C_{24}H_{25}O_4N_1S$, 408.16279 $[M + H]^+$; 408.16164 found, $[M + H]^+$.

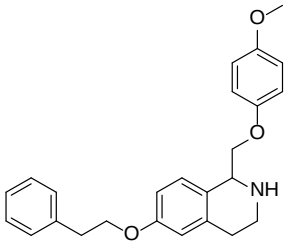

1-((4-methoxyphenoxy)methyl)-6-phenethoxy-1,2,3,4-tetrahydroisoquinoline (50a):
Dihydroisoquinoline **49a** was prepared via Procedure I using **47a** (0.74 g, 1.8 mmol) and phosphorous trichloride (1.1 mL, 5.4 mmol) in dry toluene (10. mL). The crude residue (0.79 g) was carried on without further purification. HRMS calcd. for $C_{25}H_{26}O_3N$, 388.19702 $[M + H]^+$; found 388.19095 $[M + H]^+$. Tetrahydroisoquinoline **50a** was prepared via Procedure III using dihydroisoquinoline **49a** (0.72 g, 1.9 mmol) and sodium borohydride (0.21 g, 5.6 mmol) in dry MeOH (9.3 mL). The crude residue was purified by silica gel chromatography (ISCO, Redisep 20 g column, 0-20% MeOH/DCM gradient) to afford the title compound as a green foam (0.30 g, 42 %). TLC (MeOH/DCM, 1:10, v/v) Rf: 0.47 ^{1}H NMR ($CDCl_3$, 400 MHz) δ: 7.32-7.13 (m, 5H), 7.03 (d, *J*

= 8.4 Hz, 1H), 6.97-6.94 (m, 1H), 6.81-6.67 (m, 4H), 6.63-6.62 (m, 1H), 4.62-4.59 (m, 1H), 4.42-4.39 (m, 1H), 4.34-4.29 (m, 1H), 4.12 (t, *J* = 7.2 Hz, 2H), 3.72 (s, 3H), 3.54-3.48 (m, 1H), 3.25-3.19 (m, 1H), 3.17-2.94 (m, 4H); ^{13}C NMR ($CDCl_3$, 100 MHz) δ: 158.6, 154.7, 152.1, 138.2, 134.4, 129.2, 128.7, 127.5, 126.8, 120.8, 116.5, 114.7, 114.6, 114.3, 69.2, 68.9, 55.9, 54.2, 39.7, 35.9, 26.3; HRMS calcd. for $C_{25}H_{28}O_3N$, 390.20637 $[M + H]^+$; found 390.20631 $[M + H]^+$.

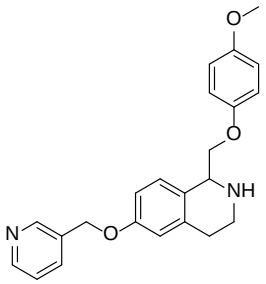

1-(((4-methoxybenzyl)oxy)methyl)-6-(pyridin-3-ylmethoxy)-1,2,3,4-tetrahydroisoquinoline (50b): Dihydroisoquinoline **49b** was prepared via Procedure I using **147b** (0.58 g, 1.5 mmol) and phosphorous trichloride (0.92 mL, 4.5 mmol) in dry toluene (7.5 mL). The crude residue (0.99 g) was carried on without further purification. HRMS calcd. for $C_{24}H_{25}O_3N$, 389.18597 $[M + H]^+$; found 389.18638 $[M + H]^+$ .Tetrahydroisoquinoline **50b** was prepared via Procedure III using dihydroisoquinoline **49b** (0.99 g, 2.6 mmol) and sodium borohydride (0.85 g, 2.2 mmol) in dry MeOH (7.5 mL). The volatiles were concentrated *in vacuo*, and the resulting residue was made basic (pH 13) with 1M NaOH. The organic layer was washed with water (3x) and brine (3x), dried with $MgSO_4$, filtered, and concentrated *in vacuo*. The resulting residue was then subjected to column chromatography to afford the title compound. The crude residue was purified by silica gel chromatography (ISCO, Redisep 20 g column, 0-20% MeOH/DCM gradient) to afford the title compound as a yellow solid (0.12 g, 23 %). TLC (MeOH/DCM, 1:10, v/v) Rf: 0.57; ^{1}H NMR ($CDCl_3$, 400 MHz) δ: 8.66-8.65 (m, 1H), 8.58-8.56 (dd, *J* = 1.6 Hz, *J* = 4.8 Hz, 1H), 7.77-7.75 (m, 1H), 7.32-7.29 (m, 1H), 7.10 (d, *J* = 8.8 Hz, 1H), 6.88-6.77 (m, 5H), 6.74-6.73 (m, 1H), 4.37-4.34 (dd, *J* = 3.6 Hz, *J* = 9.2 Hz, 1H), 4.13-4.03 (m, 2H), 3.74 (s, 3H), 3.25-3.18 (m, 1H), 3.05-2.99 (m, 1H), 2.84-2.81 (m, 2H); ^{13}C NMR ($CDCl_3$, 100 MHz) δ: 157.2, 154.3, 153.1, 149.6, 149.2, 137.6, 135.5,

132.8, 127.9, 127.6, 123.8, 115.8, 115.2, 114.9, 113.2, 71.4, 67.7, 55.9, 54.8, 39.8, 30.1; HRMS calcd. for $C_{24}H_{27}O_3N_2$, 391.20162 $[M + H]^+$; found 391.20201 $[M + H]^+$.

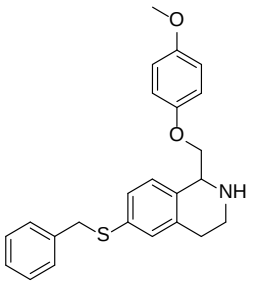

6-(benzylthio)-1-((4-methoxyphenoxy)methyl)-1,2,3,4-tetrahydroisoquinoline (50c): Dihydroisoquinoline **49c** was prepared via Procedure I using amide **48** (1.6 g, 3.8 mmol) and phosphorous trichloride (2.4 mL, 11 mmol) in dry toluene (19 mL). The crude residue (0.75 g) was carried on without further purification. HRMS calcd. for $C_{24}H_{23}O_2N_1S$, 390.15223 $[M + H]^+$; found 390.15084 $[M + H]^+$. Tetrahydroisoquinoline **50c** was prepared via Procedure III using dihydroisoquinoline **49c** (0.75 g, 1.9 mmol) and sodium borohydride (0.22 g, 5.8 mmol) in dry MeOH (9.6 mL). The crude residue was purified by silica gel chromatography (ISCO, Redisep 20 g column, 0-20% MeOH/DCM gradient) to afford the title compound as a yellow solid (0.15 g, 20 %). TLC (MeOH/DCM, 1:10, v/v) Rf: 0.70; ^{1}H NMR ($CDCl_3$, 400 MHz) δ: 7.31-7.24 (m, 5H), 7.13-7.06 (m, 3H), 6.89-6.82 (m, 4H), 4.39-4.36 (dd, J = 3.6 Hz, J = 9.2 Hz, 1H), 4.19-4.05 (m, 4H), 3.78 (s, 3H), 3.25-3.19 (m, 1H), 3.06-2.99 (m, 1H), 2.81-2.78 (m, 2H); ^{13}C NMR ($CDCl_3$, 100 MHz) δ: 154.3, 153.0, 137.6, 136.8, 134.7, 132.9, 130.9, 129.2, 129.1, 128.8, 127.5, 127.2, 115.8, 114.8, 71.2, 55.9, 55.0, 39.8, 39.2, 29.7; HRMS calcd. for $C_{24}H_{25}O_2N_1S$, 390.15139 $[M + H]^+$; found 390.15177 $[M + H]^+$.

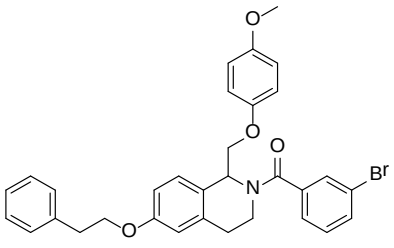

(3-bromophenyl)(1-((4-methoxyphenoxy)methyl)-6-phenethoxy-3,4-dihydroisoquinolin-2(1H)-yl)methanone (1180-122): Tetrahydroisoquinoline **1180-122** was prepared via Procedure IV using tetrahydroisoquinoline **50a** (0.15 g, 0.38 mmol) and 3-bromobenzoyl chloride (0.061 mL, 0.47 mmol) in DCM (6.0 mL). The crude residue was purified by silica gel chromatography (ISCO, Redisep 12 g column, 10 – 80% EtOAc/hexanes gradient) to afford the title compound as an off-white foam (0.14 g, 64 % yield, mixture of two amide rotamers) TLC (EtOAc: hexanes, 1:1, v/v) Rf = 0.88; ^{1}HNMR ($CDCl_3$, 400 MHz) δ: 7.73 (s, 0.5H), 7.53-7.50 (m, 1.5H), 7.42-7.39 (m, 0.5H), 7.33-7.17 (m, 6.5H), 6.92-6.67 (m, 7H), 5.96 (t, *J* = 4.8 Hz, 0.5H), 5.12-5.09 (m, *J* = 9.2 Hz, *J* = 2.8 Hz, 0.5 H), 4.85-4.81 (m, *J* = 5.2 Hz, *J* = 12.8 Hz, 0.5H), 4.27-4.29 (m, 1H), 4.16 (t, *J* = 7.2 Hz, 2H), 3.92-3.89 (m, 0.5H), 3.75 (s, 3H), 3.72-3.57 (m, 0.5H), 3.27-3.20 (m, 1H), 3.09 (t, *J* = 6.8 Hz, 2H), 2.92-2.70 (m, 2H); ^{13}C NMR ($CDCl_3$, 100 MHz) δ: 170.3, 169.5, 158.5, 158.0, 154.4, 154.3, 153.1, 142.6, 138.6, 138.5, 138.4, 136.6, 135.7, 132.9, 132.8, 131.1, 130.5, 130.2, 129.9, 129.3, 128.8, 128.4, 126.8, 126.3, 125.5, 125.3, 124.5, 122.9, 122.7, 115.9, 115.5, 114.9, 114.8, 114.5, 113.7, 113.5, 71.3, 70.2, 68.9, 57.3, 55.9, 52.0, 42.8, 36.0, 35.5, 29.9, 28.6; HRMS calcd. for $C_{32}H_{31}NO_4{}^{79}Br$, 572.14310 $[M + H]^+$; found, 572.14341 $[M + H]^+$.

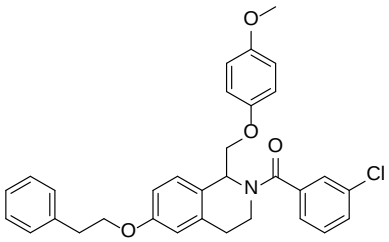

(3-chlorophenyl)(1-((4-methoxyphenoxy)methyl)-6-phenethoxy-3,4-dihydroisoquinolin-2(1H)-yl)methanone (1180-123): Tetrahydroisoquinoline **180-123** was prepared via Procedure IV using tetrahydroisoquinoline **50a** (0.15 g, 0.38 mmol) and 3-chlorobenzoyl chloride (0.060 mL, 0.47 mmol) in DCM (6.0 mL). The crude residue was purified by silica gel chromatography (ISCO, Redisep 12 g column, 10 – 80% EtOAc/hexanes gradient) to afford the title compound as an off-white foam (0.13 g, 64 % yield, mixture of two amide rotamers) TLC (EtOAc: hexanes, 1:1, v/v) Rf = 0.86; ^{1}HNMR ($CDCl_3$, 400 MHz) δ: 7.57 (s, 0.5H), 7.40-7.16 (m, 8H), 7.07-6.99 (m, 0.5H), 6.92-

6.66 (m, 7H), 5.96 (t, *J* = 4.8 Hz, 0.5H), 5.13-5.10 (m, *J* = 3.2 Hz, *J* = 9.6 Hz, 0.5H), 4.86-4.81 (m, *J* = 6.0 Hz, *J* = 13.2 Hz, 0.5H), 4.37-4.25 (m, 1H), 4.15 (t, *J* = 7.2 Hz, 2H), 4.12-4.09 (m, 0.5H), 3.92-3.88 (m, 0.5H), 3.75 (s, 3H), 3.73-3.62 (m, 0.5H), 3.27-3.20 (m, 1H), 3.08 (t, *J* = 6.0 Hz, 2H), 2.92-2.70 (m, 2H); ^{13}C NMR ($CDCl_3$, 100 MHz) δ: 170/5, 169/7, 158.5, 158.0, 154.4, 154.3, 153.1, 152.6, 138.4, 138.2, 136.7, 135.6, 134.9, 134.6, 130.3, 129.9, 129.2, 128.9, 128.8, 128.4, 128.2, 127.1, 126.8, 125.9, 125.5, 124.9, 124.5, 115.9, 115.5, 115.0, 114.9, 114.5, 113.7, 113.5, 71.3, 70.2, 69.0, 57.3, 56.0, 52.0, 42.9, 36.0, 35.5, 30.0, 28.6; HRMS calcd. for $C_{32}H_{31}NO_4{}^{35}Cl$, 528.19361 $[M + H]^+$; found, 528.19379 $[M + H]^+$. Anal. ($C_{32}H_{31}NO_4Cl$): C, H, N.

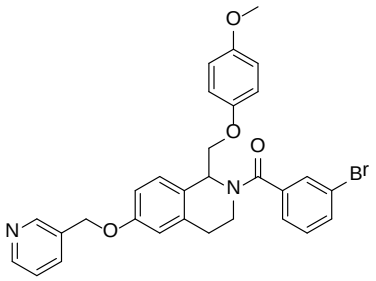

(3-bromophenyl)(1-(((4-methoxybenzyl)oxy)methyl)-6-(pyridin-3-ylmethoxy)-3,4-dihydroisoquinolin-2(1H)-yl)methanone (1180-138): Tetrahydroisoquinoline **1180-138** was prepared via Procedure IV using tetrahydroisoquinoline **50b** (0.12 g, 0.31 mmol) and 3-bromobenzoyl chloride (0.050 mL, 0.38 mmol) in DCM (5.0 mL). The crude residue was purified by silica gel chromatography (ISCO, Redisep 12 g column, 10 – 80% EtOAc/hexanes gradient) to afford the title compound as an off-white foam (0.096 g, 53 % yield, mixture of two amide rotamers) TLC (EtOAc: hexanes, 1:1, v/v) Rf = 0.22; ^{1}HNMR ($CDCl_3$, 400 MHz) δ: 8.70-8.61 (m, 2H), 7.81-7.75 (m, 1H), 7.57-7.42 (m, 2H), 7.38-7.25 (m, 3H), 6.98-6.78 (m, 7H), 5.99 (t, *J* = 4.4 Hz, 0.5H), 5.15-5.13 (m, *J* = 8.8 Hz, *J* = 2.8 Hz, 0.5 H), 5.09 (s, 2H), 4.89-4.84 (m, *J* = 5.2 Hz, *J* = 12.4 Hz, 0.5H), 4.36-4.33 (m, 1H), 4.17-4.12 (t, *J* = 10.4 Hz, 0.5H), 3.95-3.92 (dd, *J* = 2.8 Hz, *J* = 9.6 Hz, 0.5H), 3.73 (s, 3H), 3.72-3.66 (m, 1.5H), 3.31-3.12 (m, 1H), 2.95-2.75 (m, 2H). ^{13}C NMR ($CDCl_3$, 100 MHz) δ: 170.3, 169.5, 157.9, 157.5, 154.4, 154.3, 152.9, 152.5, 149.4, 148.8, 138.5, 138.5, 138.4, 136.9, 135.8, 132.9, 132.8, 131.5, 130.2, 129.9, 128.9, 128.5, 126.3, 125.3, 125.2, 123.9, 122.9, 112.7, 115.9,

115.5, 115.3, 114.9, 114.8, 114.7, 113.8, 113.7, 71.3, 70.1, 67.7, 57.3, 55.9, 51.9, 42.8, 35.4, 29.9, 28.5, 21.4; HRMS calcd. for $C_{31}H_{30}N_2O_4{}^{79}Br$, 573.13968 $[M + H]^+$; found, 573.13957 $[M + H]^+$.

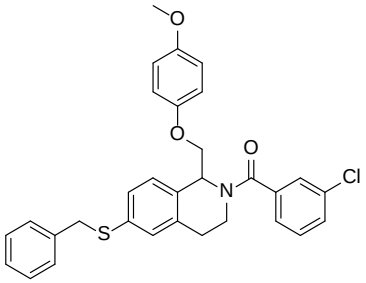

(6-(benzylthio)-1-((4-methoxyphenoxy)methyl)-3,4-dihydroisoquinolin-2(1H)-yl)(3-chlorophenyl)methanone (1180-153): Tetrahydroisoquinoline **1180-153** was prepared via Procedure IV using tetrahydroisoquinoline **50c** (0.15 g, 0.39 mmol) and 3-chlorobenzoyl chloride (0.075 mL, 0.59 mmol) in DCM (6.1 mL). The crude residue was purified by silica gel chromatography (ISCO, Redisep 12 g column, 10 – 80% EtOAc/hexanes gradient) to afford the title compound as an yellow foam (0.087 g, 41 % yield, mixture of two amide rotamers). TLC (EtOAc: hexanes, 1:1, v/v) Rf = 0.83; ^{1}HNMR ($CDCl_3$, 400 MHz) δ: 7.43-7.10 (m, 12H), 6.93-6.79 (m, 4H), 6.00 (t, J = 4.0 Hz, 0.5H), 5.17-5.15 (m, 0.5H), 4.90-4.85 (m, J = 5.6 Hz, J = 12.8 Hz, 0.5H), 4.42-4.34 (m, 1H), 4.14 (d, J = 8.0 Hz, 2H), 3.96-3.93 (m, 0.5H), 3.77 (s, 3H), 3.73-3.59 (m, 1H), 3.29-3.08 (m, 1H), 2.91-2.71 (m, 2H); ^{13}C NMR ($CDCl_3$, 100 MHz) δ: 170.4, 169.7, 154.4, 152.9, 152.4, 138.1, 138.0, 137.5, 137.2, 136.7, 135.9, 135.5, 135.0, 134.9, 134.6, 131.5, 130.3, 129.9, 129.1, 128.8, 128.4, 128.1, 127.7, 127.5, 127.1, 125.8, 124.9, 115.9, 115.5, 114.9, 114.9, 71.3, 70.0, 57.5, 55.9, 52.2, 42.9, 39.1, 38.6, 35.5, 29.6, 28.2; HRMS calcd. for $C_{31}H_{29}N_1O_3ClS$, 530.15512 $[M + H]^+$; found, 530.15447 $[M + H]^+$.

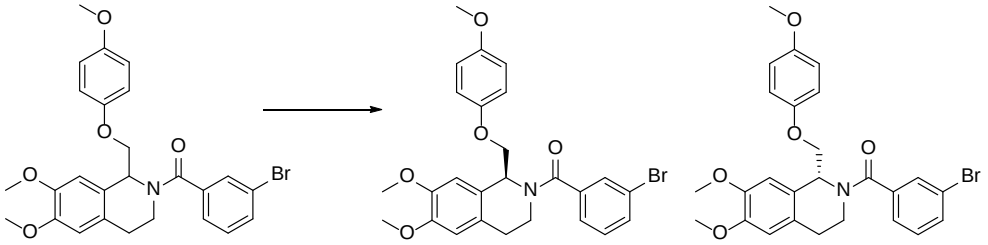

Separation of 1391: 1391 was purchased from Life Chemicals and the racemic mixture (0.10 g) was separated via a ChiralPak OD-RH 30 mm x 250 mm, 5 μM column utilizing the following

conditions: 75% ACN (0.1% formic acid) / 25% water (0.1% formic acid), flow rate of 10 mL/min for 30 minutes to afford peak one (0.030 g): t_R = 25.62 minutes; peak two (0.033 g): 27.56 min. The enantiomeric excess was calculated using an Agilent 1200 HPLC pump on a Chiral OD-RH column (4.6 mm x 150 mm, 5 μm) utilizing the following conditions: 75% ACN (0.1% formic acid) / 25% water (0.1% formic acid), flow rate of 0.5 mL/min for 20 minutes; peak one: t_R = 8.61 minutes, $[\alpha]D_{20}$ = +104 (c 0.1, dry $CHCl_3$); peak 2: t_R = 9.79 minutes, $[\alpha]D_{20}$ = -128 (c 0.1, dry $CHCl_3$), 100% ee. The proton spectrum for each enantiomer was identical to that of the racemic mixture.

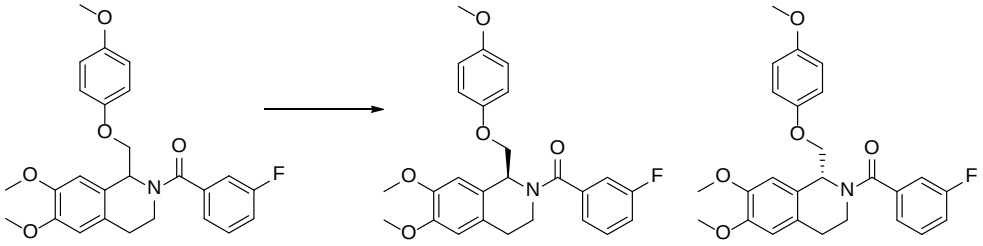

Separation of 1369: 1369 was purchased from Life Chemicals and the racemic mixture (0.032 g) was separated via a ChiralPak OD-RH 30 mm x 250 mm, 5 μM column utilizing the following conditions: 60% ACN (0.1% formic acid) / 40% water (0.1% formic acid), flow rate of 10 mL/min for 40 minutes to afford peak one (0.013 g): t_R = 24.28 minutes; peak two (0.016 g): t_R = 27.36 min. The enantiomeric excess was calculated using an Agilent 1200 HPLC pump on a Chiral OD-RH column (4.6 mm x 150 mm, 5 μm) utilizing the following conditions: 60% ACN (0.1% formic acid) / 40% water (0.1% formic acid), flow rate of 0.5 mL/min for 30 minutes; peak one: t_R = 13.47 minutes, $[\alpha]D^{20}$ = +89.4 (c 1.0, dry $CHCl_3$); peak 2: t_R = 15.53 minutes, $[\alpha]D^{20}$ = -102 (c 1.0, dry $CHCl_3$), 100% ee. The proton spectrum for each enantiomer was identical to that of the racemic mixture.

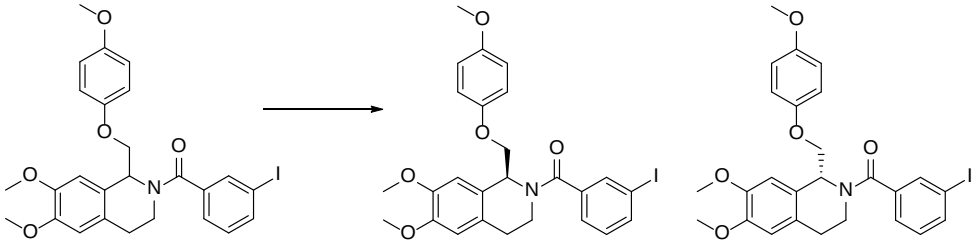

Separation of 1180-11: 1180-11 was synthesized as previously described[7] and the racemic mixture (0.12 g) was separated via a ChiralPak OD-RH 30 mm x 250 mm, 5 μM column utilizing the following conditions: 65% ACN (0.1% formic acid) / 35% water (0.1% formic acid), flow rate of 10 mL/min for 40 minutes to afford peak one (0.029 g): t_R = 30.06 minutes; peak two (0.044 g): 35.27 min. The enantiomeric excess was calculated using an Agilent 1200 HPLC pump on a Chiral OD-RH column (4.6 mm x 150 mm, 5 μm) utilizing the following conditions: 65% ACN (0.1% formic acid) / 35% water (0.1% formic acid), flow rate of 0.5 mL/min for 30 minutes; peak one: t_R = 17.33 minutes, $[\alpha]D^{20}$ = +106 (c 0.1, dry $CHCl_3$); peak 2: t_R = 19.89 minutes, $[\alpha]D^{20}$ = -93 (c 0.1, dry $CHCl_3$), 100% ee. The proton spectrum for each enantiomer was identical to that of the racemic mixture.

1.6.2 In vitro analysis of 1180 series analogs

All protocols utilizing *Xenopus laevis* were approved by Emory University Institutional Animal Care and Use Committee. Two-electrode voltage-clamp recordings were performed on *Xenopus laevis* oocytes were injected with mRNA to express recombinant rat GluN1/GluN2A-, GluN1/GluN2B-, GluN1/GluN2C-, GluN1/GluN2D-, GluA1-, or GluK2-containing receptors. cDNAs for rat GluN1-1a (GenBank accession numbers U11418 and U08261; hereafter GluN1), GluN2A (D13211), GluN2B (U11419), GluN2C (M91563), GluN2D (L31611), GluA1 (X17184), GluK (Z11548) were provided by D. S. Heinermann from the Salk Institute, S. Nakanishi from Kyoto University, and P. Seeburg from University of Heidelberg. Oocyte isolation, cRNA synthesis and cRNA were performed as previously described[137]. For the two-electrode voltage clamp recordings, oocytes were situated in a perfusion chamber and continually washed with the recording solution that contained 90 mM NaCl, 1.0 mM KCl, 0.5 mM BaCl2, 0.005 mM EDTA, and 10 mM HEPES at a

pH of 7.4 and a temperature of 23°C. The glass electrodes with a tip resistance of 0.5 – 2.5 MΩ were pulled from thin-walled glass capillary tubes and filled with 0.3-3.0 M KCl. The membrane potential of the oocytes was held at -40 mV by an OC-725C amplifier (Warner Instrument Co). All compounds were made as 20 mM stock solutions in DMSO and diluted to reach the desired final concentration in recording solution containing 100 μM glutamate and 30 μM glycine; final DMSO content was 0.05-0.5% (vol/vol). Oocytes expressing GluK2 receptors were pretreated with concanavalin A (10 μM) for 10 minutes. Recombinant GluNA1 and GluK2 receptors were activated by 100 μM glutamate. A gradual increase in current response over the course of the experiment is common with oocytes expressing GluN1/GluNA, but to prevent this, oocytes expressing GluN1/GluN2A were either pretreated with 50 μM BAPTA-AM (1,2-bis(oaminophenoxy)ethane-N,N,N',N'-tetraacetic acid tetraacetoxymethyl ester) for 10 min or injected with 50 nl of 2 mM K-BAPTA (potassium 1,2-bis(o-aminophenoxy)ethane-N,N,N',N'-tetraacetic acid). All compounds that had a modest effect on GluN1/GluN2A expressing oocytes were not studied further.

Every test compound was recorded at 5-7 concentrations in a least 4 oocytes from at least 2 different frogs. The potentiation of the test compounds at a concentration of 30 μM was averaged and reported as $I_{30\mu M} / I_{control}$ (mean $\pm$ SEM, %), where I equals current. For test compounds with potentiation that exceeded 120% at 30 μM, an EC_{50} value (the half-maximal effective concentration of potentiator) was determined by fitting the following equation

$$Response = (100 - maximum) / (1 + ([concentration] / EC_{50})^{N}) + maximum$$

to the mean composite composition-response data normalized to the current in the absence of the potentiator (100%) where N equals the Hill slope and maximum is the maximal response predicted for saturating concentration of potentiator.

To compare the EC_{50} value and maximum effect of two compounds at the same subunit, an unpaired t-test was run. Compounds were only denoted as being significantly stastically different if the p value was less than 0.05.

References:

(1) Coyle, J. T. NMDA Receptor and Schizophrenia: A Brief History. *Schizophr. Bull.* **2012**, *38* (5), 920–926.

(2) Hillman, B. G.; Gupta, S. C.; Stairs, D. J.; Buonanno, A.; Dravid, S. M. Behavioral Analysis of NR2C Knockout Mouse Reveals Deficit in Acquisition of Conditioned Fear and Working Memory. *Neurobiol. Learn. Mem.* **2011**, *95* (4), 404–414.

(3) Reisberg, B.; Doody, R.; Stöffler, A.; Schmitt, F.; Ferris, S.; Möbius, H. J. Memantine in Moderate-to-Severe Alzheimer's Disease. *N. Engl. J. Med.* **2003**, *348* (14), 1333–1341.

(4) Hallett, P. J.; Standaert, D. G. Rationale for and Use of NMDA Receptor Antagonists in Parkinson's Disease. *Pharmacol. Ther.* **2004**, *102* (2), 155–174.

(5) Traynelis, S. F.; Wollmuth, L. P.; McBain, C. J.; Menniti, F. S.; Vance, K. M.; Ogden, K. K.; Hansen, K. B.; Yuan, H.; Myers, S. J.; Dingledine, R. Glutamate Receptor Ion Channels: Structure, Regulation, and Function. *Pharmacol. Rev.* **2010**, *62* (3), 405–496.

(6) Paoletti, P.; Bellone, C.; Zhou, Q. NMDA Receptor Subunit Diversity: Impact on Receptor Properties, Synaptic Plasticity and Disease. *Nat. Rev. Neurosci.* **2013**, *14* (6), 383–400.

(7) Santangelo Freel, R. M.; Ogden, K. K.; Strong, K. L.; Khatri, A.; Chepiga, K. M.; Jensen, H. S.; Traynelis, S. F.; Liotta, D. C. Synthesis and Structure Activity Relationship of Tetrahydroisoquinoline-Based Potentiators of GluN2C and GluN2D Containing N-Methyl-D-Aspartate Receptors. *J. Med. Chem.* **2013**, *56* (13), 5351–5381.

(8) Balu, D. T.; Li, Y.; Puhl, M. D.; Benneyworth, M. A.; Basu, A. C.; Takagi, S.; Bolshakov, V. Y.; Coyle, J. T. Multiple Risk Pathways for Schizophrenia Converge in Serine Racemase Knockout Mice, a Mouse Model of NMDA Receptor Hypofunction. *Proc. Natl. Acad. Sci.* **2013**, *110* (26), E2400–E2409.

(9) Olney, J. W.; Newcomer, J. W.; Farber, N. B. NMDA Receptor Hypofunction Model of Schizophrenia. *J. Psychiatr. Res.* **1999**, *33* (6), 523–533.

(10) Murrough, J. W. Ketamine as a Novel Antidepressant: From Synapse to Behavior. *Clin. Pharmacol. Ther.* **2012**, *91* (2), 303–309.

(11) Skolnick, P.; Popik, P.; Trullas, R. Glutamate-Based Antidepressants: 20 Years on. *Trends Pharmacol. Sci.* **2009**, *30* (11), 563–569.

(12) Sobolevsky, A. I.; Rosconi, M. P.; Gouaux, E. X-Ray Structure, Symmetry and Mechanism of an AMPA-Subtype Glutamate Receptor. *Nature* **2009**, *462* (7274), 745–756.

(13) Karakas, E.; Furukawa, H. Crystal Structure of a Heterotetrameric NMDA Receptor Ion Channel. *Science* **2014**, *344* (6187), 992–997.

(14) Lee, C.-H.; Lü, W.; Michel, J. C.; Goehring, A.; Du, J.; Song, X.; Gouaux, E. NMDA Receptor Structures Reveal Subunit Arrangement and Pore Architecture. *Nature* **2014**, *advance online publication*.

(15) MacDermott, A. B.; Mayer, M. L.; Westbrook, G. L.; Smith, S. J.; Barker, J. L. NMDA-Receptor Activation Increases Cytoplasmic Calcium Concentration in Cultured Spinal Cord Neurones. *Nature* **1986**, *321* (6069), 519–522.

(16) Mayer, M. L.; Westbrook, G. L.; Guthrie, P. B. Voltage-Dependent Block by Mg2+ of NMDA Responses in Spinal Cord Neurones. *Nature* **1984**, *309* (5965), 261–263.

(17) Furukawa, H.; Singh, S. K.; Mancusso, R.; Gouaux, E. Subunit Arrangement and Function in NMDA Receptors. *Nature* **2005**, *438* (7065), 185–192.

(18) Forsythe, I. D.; Westbrook, G. L. Slow Excitatory Postsynaptic Currents Mediated by N-Methyl-D-Aspartate Receptors on Cultured Mouse Central Neurones. *J. Physiol.* **1988**, *396*, 515–533.

(19) Rauner, C.; Köhr, G. Triheteromeric NR1/NR2A/NR2B Receptors Constitute the Major N-Methyl-D-Aspartate Receptor Population in Adult Hippocampal Synapses. *J. Biol. Chem.* **2011**, *286* (9), 7558–7566.

(20) Hansen, K. B.; Ogden, K. K.; Yuan, H.; Traynelis, S. F. Distinct Functional and Pharmacological Properties of Triheteromeric GluN1/GluN2A/GluN2B NMDA Receptors. *Neuron* **2014**, *81* (5), 1084–1096.
(21) Karakas, E.; Simorowski, N.; Furukawa, H. Structure of the Zinc-Bound Amino-Terminal Domain of the NMDA Receptor NR2B Subunit. *EMBO J.* **2009**, *28* (24), 3910–3920.
(22) Karakas, E.; Simorowski, N.; Furukawa, H. Subunit Arrangement and Phenylethanolamine Binding in GluN1/GluN2B NMDA Receptors. *Nature* **2011**, *475* (7355), 249–253.
(23) Furukawa, H.; Gouaux, E. Mechanisms of Activation, Inhibition and Specificity: Crystal Structures of the NMDA Receptor NR1 Ligand-binding Core. *EMBO J.* **2003**, *22* (12), 2873–2885.
(24) Paoletti, P.; Neyton, J. NMDA Receptor Subunits: Function and Pharmacology. *Curr. Opin. Pharmacol.* **2007**, *7* (1), 39–47.
(25) Paoletti, P.; Ascher, P.; Neyton, J. High-Affinity Zinc Inhibition of NMDA NR1–NR2A Receptors. *J. Neurosci.* **1997**, *17* (15), 5711–5725.
(26) Rachline, J.; Perin-Dureau, F.; Goff, A. L.; Neyton, J.; Paoletti, P. The Micromolar Zinc-Binding Domain on the NMDA Receptor Subunit NR2B. *J. Neurosci.* **2005**, *25* (2), 308–317.
(27) Hansen, K. B.; Furukawa, H.; Traynelis, S. F. Control of Assembly and Function of Glutamate Receptors by the Amino-Terminal Domain. *Mol. Pharmacol.* **2010**, *78* (4), 535–549.
(28) Yao, Y.; Harrison, C. B.; Freddolino, P. L.; Schulten, K.; Mayer, M. L. Molecular Mechanism of Ligand Recognition by NR3 Subtype Glutamate Receptors. *EMBO J.* **2008**, *27* (15), 2158–2170.
(29) Vance, K. M.; Simorowski, N.; Traynelis, S. F.; Furukawa, H. Ligand-Specific Deactivation Time Course of GluN1/GluN2D NMDA Receptors. *Nat. Commun.* **2011**, *2*, 294.
(30) Hansen, K. B.; Ogden, K. K.; Traynelis, S. F. Subunit-Selective Allosteric Inhibition of Glycine Binding to NMDA Receptors. *J. Neurosci. Off. J. Soc. Neurosci.* **2012**, *32* (18), 6197–6208.
(31) Talukder, I.; Borker, P.; Wollmuth, L. P. Specific Sites within the Ligand-Binding Domain and Ion Channel Linkers Modulate NMDA Receptor Gating. *J. Neurosci. Off. J. Soc. Neurosci.* **2010**, *30* (35), 11792–11804.
(32) Huettner, J. E.; Bean, B. P. Block of N-Methyl-D-Aspartate-Activated Current by the Anticonvulsant MK-801: Selective Binding to Open Channels. *Proc. Natl. Acad. Sci.* **1988**, *85* (4), 1307–1311.
(33) Cull-Candy, S. G.; Leszkiewicz, D. N. Role of Distinct NMDA Receptor Subtypes at Central Synapses. *Sci. Signal.* **2004**, *2004* (255), re16–re16.
(34) Paoletti, P. Molecular Basis of NMDA Receptor Functional Diversity. *Eur. J. Neurosci.* **2011**, *33* (8), 1351–1365.
(35) Vicini, S.; Wang, J. F.; Li, J. H.; Zhu, W. J.; Wang, Y. H.; Luo, J. H.; Wolfe, B. B.; Grayson, D. R. Functional and Pharmacological Differences Between RecombinantN-Methyl-D-Aspartate Receptors. *J. Neurophysiol.* **1998**, *79* (2), 555–566.
(36) Erreger, K.; Dravid, S. M.; Banke, T. G.; Wyllie, D. J. A.; Traynelis, S. F. Subunit-Specific Gating Controls Rat NR1/NR2A and NR1/NR2B NMDA Channel Kinetics and Synaptic Signalling Profiles. *J. Physiol.* **2005**, *563* (2), 345–358.
(37) Siegler Retchless, B.; Gao, W.; Johnson, J. W. A Single GluN2 Subunit Residue Controls NMDA Receptor Channel Properties via Intersubunit Interaction. *Nat. Neurosci.* **2012**, *15* (3), 406–413, S1–S2.
(38) Monyer, H.; Burnashev, N.; Laurie, D. J.; Sakmann, B.; Seeburg, P. H. Developmental and Regional Expression in the Rat Brain and Functional Properties of Four NMDA Receptors. *Neuron* **1994**, *12* (3), 529–540.
(39) Akazawa, C.; Shigemoto, R.; Bessho, Y.; Nakanishi, S.; Mizuno, N. Differential Expression of Five N-Methyl-D-Aspartate Receptor Subunit mRNAs in the Cerebellum of Developing and Adult Rats. *J. Comp. Neurol.* **1994**, *347* (1), 150–160.

(40) Watanabe, M.; Inoue, Y.; Sakimura, K.; Mishina, M. Developmental Changes in Distribution of NMDA Receptor Channel Subunit mRNAs: *NeuroReport* **1992**, *3* (12), 1138–1140.
(41) Perälä, J.; Suvisaari, J.; Saarni, S. I.; Kuoppasalmi, K.; Isometsä, E.; Pirkola, S.; Partonen, T.; Tuulio-Henriksson, A.; Hintikka, J.; Kieseppä, T.; Härkänen, T.; Koskinen, S.; Lönnqvist, J. Lifetime Prevalence of Psychotic and Bipolar I Disorders in a General Population. *Arch. Gen. Psychiatry* **2007**, *64* (1), 19–28.
(42) Schizophrenia http://www.nimh.nih.gov/health/topics/schizophrenia/index.shtml (accessed Oct 1, 2015).
(43) Effectiveness of Antipsychotic Drugs in Patients with Chronic Schizophrenia — NEJM http://www.nejm.org.proxy.library.emory.edu/doi/full/10.1056/NEJMoa051688 (accessed Sep 30, 2015).
(44) Lieberman, J. A.; Stroup, T. S. The NIMH-CATIE Schizophrenia Study: What Did We Learn? *Am. J. Psychiatry* **2011**, *168* (8), 770–775.
(45) Moghaddam, B. Bringing Order to the Glutamate Chaos in Schizophrenia. *Neuron* **2003**, *40* (5), 881–884.
(46) Ozaki, M.; Sasner, M.; Yano, R.; Lu, H. S.; Buonanno, A. Neuregulin-Beta Induces Expression of an NMDA-Receptor Subunit. *Nature* **1997**, *390* (6661), 691–694.
(47) Schmitt, A.; Koschel, J.; Zink, M.; Bauer, M.; Sommer, C.; Frank, J.; Treutlein, J.; Schulze, T.; Schneider-Axmann, T.; Parlapani, E.; Rietschel, M.; Falkai, P.; Henn, F. A. Gene Expression of NMDA Receptor Subunits in the Cerebellum of Elderly Patients with Schizophrenia. *Eur. Arch. Psychiatry Clin. Neurosci.* **2010**, *260* (2), 101–111.
(48) Stefansson, H.; Petursson, H.; Sigurdsson, E.; Steinthorsdottir, V.; Bjornsdottir, S.; Sigmundsson, T.; Ghosh, S.; Brynjolfsson, J.; Gunnarsdottir, S.; Ivarsson, O.; Chou, T. T.; Hjaltason, O.; Birgisdottir, B.; Jonsson, H.; Gudnadottir, V. G.; Gudmundsdottir, E.; Bjornsson, A.; Ingvarsson, B.; Ingason, A.; Sigfusson, S.; Hardardottir, H.; Harvey, R. P.; Lai, D.; Zhou, M.; Brunner, D.; Mutel, V.; Gonzalo, A.; Lemke, G.; Sainz, J.; Johannesson, G.; Andresson, T.; Gudbjartsson, D.; Manolescu, A.; Frigge, M. L.; Gurney, M. E.; Kong, A.; Gulcher, J. R.; Stefansson, K. Neuregulin 1 and Susceptibility to Schizophrenia. *Am. J. Hum. Genet.* **2002**, *71* (4), 877–892.
(49) Chumakov, I.; Blumenfeld, M.; Guerassimenko, O.; Cavarec, L.; Palicio, M.; Abderrahim, H.; Bougueleret, L.; Barry, C.; Tanaka, H.; Rosa, P. L.; Puech, A.; Tahri, N.; Cohen-Akenine, A.; Delabrosse, S.; Lissarrague, S.; Picard, F.-P.; Maurice, K.; Essioux, L.; Millasseau, P.; Grel, P.; Debailleul, V.; Simon, A.-M.; Caterina, D.; Dufaure, I.; Malekzadeh, K.; Belova, M.; Luan, J.-J.; Bouillot, M.; Sambucy, J.-L.; Primas, G.; Saumier, M.; Boubkiri, N.; Martin-Saumier, S.; Nasroune, M.; Peixoto, H.; Delaye, A.; Pinchot, V.; Bastucci, M.; Guillou, S.; Chevillon, M.; Sainz-Fuertes, R.; Meguenni, S.; Aurich-Costa, J.; Cherif, D.; Gimalac, A.; Duijn, C. V.; Gauvreau, D.; Ouelette, G.; Fortier, I.; Realson, J.; Sherbatich, T.; Riazanskaia, N.; Rogaev, E.; Raeymaekers, P.; Aerssens, J.; Konings, F.; Luyten, W.; Macciardi, F.; Sham, P. C.; Straub, R. E.; Weinberger, D. R.; Cohen, N.; Cohen, D. Genetic and Physiological Data Implicating the New Human Gene G72 and the Gene for D-Amino Acid Oxidase in Schizophrenia. *Proc. Natl. Acad. Sci.* **2002**, *99* (21), 13675–13680.
(50) Morris, D. W.; Rodgers, A.; McGhee, K. A.; Schwaiger, S.; Scully, P.; Quinn, J.; Meagher, D.; Waddington, J. L.; Gill, M.; Corvin, A. P. Confirming RGS4 as a Susceptibility Gene for Schizophrenia. *Am. J. Med. Genet. Part B Neuropsychiatr. Genet. Off. Publ. Int. Soc. Psychiatr. Genet.* **2004**, *125B* (1), 50–53.
(51) Straub, R. E.; Jiang, Y.; MacLean, C. J.; Ma, Y.; Webb, B. T.; Myakishev, M. V.; Harris-Kerr, C.; Wormley, B.; Sadek, H.; Kadambi, B.; Cesare, A. J.; Gibberman, A.; Wang, X.; O'Neill, F. A.; Walsh, D.; Kendler, K. S. Genetic Variation in the 6p22.3 Gene DTNBP1, the Human Ortholog of the Mouse Dysbindin Gene, Is Associated with Schizophrenia. *Am. J. Hum. Genet.* **2002**, *71* (2), 337–348.
(52) Evidence for association of schizophrenia with genetic variation in the 8p21.3 gene, PPP3CC, encoding the calcineurin gamma subunit

http://www.pnas.org.proxy.library.emory.edu/content/100/15/8993.full (accessed Sep 30, 2015).

(53) Akbarian, S.; Sucher, N. J.; Bradley, D.; Tafazzoli, A.; Trinh, D.; Hetrick, W. P.; Potkin, S. G.; Sandman, C. A.; Bunney, W. E.; Jones, E. G. Selective Alterations in Gene Expression for NMDA Receptor Subunits in Prefrontal Cortex of Schizophrenics. *J. Neurosci. Off. J. Soc. Neurosci.* **1996**, *16* (1), 19–30.

(54) Weickert, C. S.; Fung, S. J.; Catts, V. S.; Schofield, P. R.; Allen, K. M.; Moore, L. T.; Newell, K. A.; Pellen, D.; Huang, X.-F.; Catts, S. V.; Weickert, T. W. Molecular Evidence of N-Methyl-D-Aspartate Receptor Hypofunction in Schizophrenia. *Mol. Psychiatry* **2013**, *18* (11), 1185–1192.

(55) Beneyto, M.; Meador-Woodruff, J. H. Lamina-Specific Abnormalities of NMDA Receptor-Associated Postsynaptic Protein Transcripts in the Prefrontal Cortex in Schizophrenia and Bipolar Disorder. *Neuropsychopharmacology* **2007**, *33* (9), 2175–2186.

(56) LUBY ED; COHEN BD; ROSENBAUM G; GOTTLIEB JS; KELLEY R. STudy of a New Schizophrenomimetic Drug—sernyl. *AMA Arch. Neurol. Psychiatry* **1959**, *81* (3), 363–369.

(57) Domino, E. F. NEUROBIOLOGY OF PHENCYCLIDINE (SERNYL), A DRUG WITH AN UNUSUAL SPECTRUM OF PHARMACOLOGICAL ACTIVITY. *Int. Rev. Neurobiol.* **1964**, *6*, 303–347.

(58) Wu, J.-H.; Zou, H.; Yu, J.; Zhou, X.-D.; Xie, Q.-L.; Jin, M.-L. [Animal models of schizophrenia using different laboratory mouse strains]. *Sheng Li Xue Bao* **2003**, *55* (4), 381–387.

(59) Krystal, J. H.; Karper, L. P.; Seibyl, J. P.; Freeman, G. K.; Delaney, R.; Bremner, J. D.; Heninger, G. R.; Bowers, M. B.; Charney, D. S. Subanesthetic Effects of the Noncompetitive NMDA Antagonist, Ketamine, in Humans. Psychotomimetic, Perceptual, Cognitive, and Neuroendocrine Responses. *Arch. Gen. Psychiatry* **1994**, *51* (3), 199–214.

(60) Umbricht, D.; Schmid, L.; Koller, R.; Vollenweider, F. X.; Hell, D.; Javitt, D. C. Ketamine-Induced Deficits in Auditory and Visual Context-Dependent Processing in Healthy Volunteers: Implications for Models of Cognitive Deficits in Schizophrenia. *Arch. Gen. Psychiatry* **2000**, *57* (12), 1139–1147.

(61) Parwani, A.; Weiler, M. A.; Blaxton, T. A.; Warfel, D.; Hardin, M.; Frey, K.; Lahti, A. C. The Effects of a Subanesthetic Dose of Ketamine on Verbal Memory in Normal Volunteers. *Psychopharmacology (Berl.)* **2005**, *183* (3), 265–274.

(62) Saykin, A. J.; Gur, R. C.; Gur, R. E.; Mozley, P. D.; Mozley, L. H.; Resnick, S. M.; Kester, D. B.; Stafiniak, P. Neuropsychological Function in Schizophrenia. Selective Impairment in Memory and Learning. *Arch. Gen. Psychiatry* **1991**, *48* (7), 618–624.

(63) Lodge, D.; Mercier, M. S. Ketamine and Phencyclidine: The Good, the Bad and the Unexpected. *Br. J. Pharmacol.* **2015**, *172* (17), 4254–4276.

(64) Jentsch, J. D.; Roth, R. H. The Neuropsychopharmacology of Phencyclidine: From NMDA Receptor Hypofunction to the Dopamine Hypothesis of Schizophrenia. *Neuropsychopharmacol. Off. Publ. Am. Coll. Neuropsychopharmacol.* **1999**, *20* (3), 201–225.

(65) Sams-Dodd, F. Effects of Continuous D-Amphetamine and Phencyclidine Administration on Social Behaviour, Stereotyped Behaviour, and Locomotor Activity in Rats. *Neuropsychopharmacology* **1998**, *19* (1), 18–25.

(66) Perry, T. L.; Kish, S. J.; Buchanan, J.; Hansen, S. Gamma-Aminobutyric-Acid Deficiency in Brain of Schizophrenic Patients. *Lancet Lond. Engl.* **1979**, *1* (8110), 237–239.

(67) Lisman, J. E.; Coyle, J. T.; Green, R. W.; Javitt, D. C.; Benes, F. M.; Heckers, S.; Grace, A. A. Circuit-Based Framework for Understanding Neurotransmitter and Risk Gene Interactions in Schizophrenia. *Trends Neurosci.* **2008**, *31* (5), 234–242.

(68) Tsai, G.; Yang, P.; Chung, L. C.; Lange, N.; Coyle, J. T. D-Serine Added to Antipsychotics for the Treatment of Schizophrenia. *Biol. Psychiatry* **1998**, *44* (11), 1081–1089.

(69) Heresco-Levy, U.; Javitt, D. C.; Ebstein, R.; Vass, A.; Lichtenberg, P.; Bar, G.; Catinari, S.; Ermilov, M. D-Serine Efficacy as Add-on Pharmacotherapy to Risperidone and Olanzapine for Treatment-Refractory Schizophrenia. *Biol. Psychiatry* **2005**, *57* (6), 577–585.

(70) Cain, C. K.; McCue, M.; Bello, I.; Creedon, T.; Tang, D.; Laska, E.; Goff, D. C. D-Cycloserine Augmentation of Cognitive Remediation in Schizophrenia. *Schizophr. Res.* **2014**, *153* (1–3), 177–183.

(71) Harvey, R. J.; Yee, B. K. Glycine Transporters as Novel Therapeutic Targets in Schizophrenia, Alcohol Dependence and Pain. *Nat. Rev. Drug Discov.* **2013**, *12* (11), 866–885.

(72) Eulenburg, V.; Armsen, W.; Betz, H.; Gomeza, J. Glycine Transporters: Essential Regulators of Neurotransmission. *Trends Biochem. Sci.* **2005**, *30* (6), 325–333.

(73) Cubelos, B.; Giménez, C.; Zafra, F. Localization of the GLYT1 Glycine Transporter at Glutamatergic Synapses in the Rat Brain. *Cereb. Cortex* **2005**, *15* (4), 448–459.

(74) Heresco-Levy, U.; Javitt, D. C.; Ermilov, M.; Mordel, C.; Horowitz, A.; Kelly, D. Double-Blind, Placebo-Controlled, Crossover Trial of Glycine Adjuvant Therapy for Treatment-Resistant Schizophrenia. *Br. J. Psychiatry J. Ment. Sci.* **1996**, *169* (5), 610–617.

(75) Heresco-Levy U; Javitt DC; Ermilov M; Mordel C; Silipo G; Lichtenstein M. EFficacy of High-Dose Glycine in the Treatment of Enduring Negative Symptoms of Schizophrenia. *Arch. Gen. Psychiatry* **1999**, *56* (1), 29–36.

(76) Tsai, G.; Lane, H.-Y.; Yang, P.; Chong, M.-Y.; Lange, N. Glycine Transporter I Inhibitor, N-Methylglycine (sarcosine), Added to Antipsychotics for the Treatment of Schizophrenia. *Biol. Psychiatry* **2004**, *55* (5), 452–456.

(77) Lane, H.-Y.; Chang, Y.-C.; Liu, Y.-C.; Chiu, C.-C.; Tsai, G. E. Sarcosine or D-Serine Add-on Treatment for Acute Exacerbation of Schizophrenia: A Randomized, Double-Blind, Placebo-Controlled Study. *Arch. Gen. Psychiatry* **2005**, *62* (11), 1196–1204.

(78) Umbricht, D.; Alberati, D.; Martin-Facklam, M.; Borroni, E.; Youssef, E. A.; Ostland, M.; Wallace, T. L.; Knoflach, F.; Dorflinger, E.; Wettstein, J. G.; Bausch, A.; Garibaldi, G.; Santarelli, L. Effect of Bitopertin, a Glycine Reuptake Inhibitor, on Negative Symptoms of Schizophrenia: A Randomized, Double-Blind, Proof-of-Concept Study. *JAMA Psychiatry* **2014**, *71* (6), 637–646.

(79) Media Release http://www.roche.com/media/media_releases/med-cor-2014-01-21.htm (accessed Jun 19, 2014).

(80) Collingridge, G. L.; Kehl, S. J.; McLennan, H. Excitatory Amino Acids in Synaptic Transmission in the Schaffer Collateral-Commissural Pathway of the Rat Hippocampus. *J. Physiol.* **1983**, *334*, 33–46.

(81) Lisman, J. Long-Term Potentiation: Outstanding Questions and Attempted Synthesis. *Philos. Trans. R. Soc. B Biol. Sci.* **2003**, *358* (1432), 829–842.

(82) Tsien, J. Z.; Huerta, P. T.; Tonegawa, S. The Essential Role of Hippocampal CA1 NMDA Receptor–Dependent Synaptic Plasticity in Spatial Memory. *Cell* **1996**, *87* (7), 1327–1338.

(83) Rampon, C.; Tang, Y.-P.; Goodhouse, J.; Shimizu, E.; Kyin, M.; Tsien, J. Z. Enrichment Induces Structural Changes and Recovery from Nonspatial Memory Deficits in CA1 NMDAR1-Knockout Mice. *Nat. Neurosci.* **2000**, *3* (3), 238–244.

(84) Tang, Y.-P.; Shimizu, E.; Dube, G. R.; Rampon, C.; Kerchner, G. A.; Zhuo, M.; Liu, G.; Tsien, J. Z. Genetic Enhancement of Learning and Memory in Mice. *Nature* **1999**, *401* (6748), 63–69.

(85) Cao, X.; Cui, Z.; Feng, R.; Tang, Y.-P.; Qin, Z.; Mei, B.; Tsien, J. Z. Maintenance of Superior Learning and Memory Function in NR2B Transgenic Mice during Ageing. *Eur. J. Neurosci.* **2007**, *25* (6), 1815–1822.

(86) Jacobs, S. A.; Tsien, J. Z. Genetic Overexpression of NR2B Subunit Enhances Social Recognition Memory for Different Strains and Species. *PLoS ONE* **2012**, *7* (4), e36387.

(87) Yihui Cui; Jing Jin; Xuliang Zhang; Hao Xu; Liguo Yang; Dan Du; Qingwen Zeng; Joe Z. Tsien; Huiting Yu; Xiaohua Cao. Forebrain NR2B Overexpression Facilitating the Prefrontal

Cortex Long-Term Potentiation and Enhancing Working Memory Function in Mice. *PLoS ONE* **2011**, *6* (5), 1–10.

(88) White, T. L.; Youngentob, S. L. The Effect of NMDA-NR2B Receptor Subunit over-Expression on Olfactory Memory Task Performance in the Mouse. *Brain Res.* **2004**, *1021* (1), 1–7.

(89) Collingridge, G. L.; Volianskis, A.; Bannister, N.; France, G.; Hanna, L.; Mercier, M.; Tidball, P.; Fang, G.; Irvine, M. W.; Costa, B. M.; Monaghan, D. T.; Bortolotto, Z. A.; Molnár, E.; Lodge, D.; Jane, D. E. The NMDA Receptor as a Target for Cognitive Enhancement. *Neuropharmacology* **2013**, *64*, 13–26.

(90) Morgan, C. J. A.; Mofeez, A.; Brandner, B.; Bromley, L.; Curran, H. V. Acute Effects of Ketamine on Memory Systems and Psychotic Symptoms in Healthy Volunteers. *Neuropsychopharmacol. Off. Publ. Am. Coll. Neuropsychopharmacol.* **2004**, *29* (1), 208–218.

(91) Rowland, L. M. Subanesthetic Ketamine: How It Alters Physiology and Behavior in Humans. *Aviat. Space Environ. Med.* **2005**, *76* (7), C52–C58.

(92) Rockstroh, S.; Emre, M.; Tarral, A.; Pokorny, R. Effects of the Novel NMDA-Receptor Antagonist SDZ EAA 494 on Memory and Attention in Humans. *Psychopharmacology (Berl.)* **1996**, *124* (3), 261–266.

(93) Chen, H.-S. V.; Lipton, S. A. The Chemical Biology of Clinically Tolerated NMDA Receptor Antagonists. *J. Neurochem.* **2006**, *97* (6), 1611–1626.

(94) Frankiewicz, T.; Parsons, C. G. Memantine Restores Long Term Potentiation Impaired by Tonic N-Methyl-D-Aspartate (NMDA) Receptor Activation Following Reduction of Mg2+ In Hippocampal Slices. *Neuropharmacology* **1999**, *38* (9), 1253–1259.

(95) Coan, E. J.; Irving, A. J.; Collingridge, G. L. Low-Frequency Activation of the NMDA Receptor System Can Prevent the Induction of LTP. *Neurosci. Lett.* **1989**, *105* (1-2), 205–210.

(96) Fitzjohn, S. M.; Doherty, A. J.; Collingridge, G. L. The Use of the Hippocampal Slice Preparation in the Study of Alzheimer's Disease. *Eur. J. Pharmacol.* **2008**, *585* (1), 50–59.

(97) Berger, A. J.; Dieudonné, S.; Ascher, P. Glycine Uptake Governs Glycine Site Occupancy at NMDA Receptors of Excitatory Synapses. *J. Neurophysiol.* **1998**, *80* (6), 3336–3340.

(98) Bergeron, R.; Meyer, T. M.; Coyle, J. T.; Greene, R. W. Modulation of N-Methyl-D-Aspartate Receptor Function by Glycine Transport. *Proc. Natl. Acad. Sci.* **1998**, *95* (26), 15730–15734.

(99) Chen, L.; Muhlhauser, M.; Yang, C. R. Glycine Tranporter-1 Blockade Potentiates NMDA-Mediated Responses in Rat Prefrontal Cortical Neurons in Vitro and in Vivo. *J. Neurophysiol.* **2003**, *89* (2), 691–703.

(100) Martina, M.; Gorfinkel, Y.; Halman, S.; Lowe, J. A.; Periyalwar, P.; Schmidt, C. J.; Bergeron, R. Glycine Transporter Type 1 Blockade Changes NMDA Receptor-Mediated Responses and LTP in Hippocampal CA1 Pyramidal Cells by Altering Extracellular Glycine Levels. *J. Physiol.* **2004**, *557* (Pt 2), 489–500.

(101) Manahan-Vaughan, D.; Wildförster, V.; Thomsen, C. Rescue of Hippocampal LTP and Learning Deficits in a Rat Model of Psychosis by Inhibition of Glycine Transporter-1 (GlyT1). *Eur. J. Neurosci.* **2008**, *28* (7), 1342–1350.

(102) Nikiforuk, A.; Kos, T.; Rafa, D.; Behl, B.; Bespalov, A.; Popik, P. Blockade of Glycine Transporter 1 by SSR-504734 Promotes Cognitive Flexibility in glycine/NMDA Receptor-Dependent Manner. *Neuropharmacology* **2011**, *61* (1–2), 262–267.

(103) Oliver, M. W.; Larson, J.; Lynch, G. Activation of the Glycine Site Associated with the NMDA Receptor Is Required for Induction of LTP in Neonatal Hippocampus. *Int. J. Dev. Neurosci.* **1990**, *8* (4), 417–424.

(104) Bashir, Z. I.; Tam, B.; Collingridge, G. L. Activation of the Glycine Site in the NMDA Receptor Is Necessary for the Induction of LTP. *Neurosci. Lett.* **1990**, *108* (3), 261–266.

(105) DeVito, L. M.; Balu, D. T.; Kanter, B. R.; Lykken, C.; Basu, A. C.; Coyle, J. T.; Eichenbaum, H. Serine Racemase Deletion Disrupts Memory for Order and Alters Cortical Dendritic Morphology. *Genes Brain Behav.* **2011**, *10* (2), 210–222.

(106) Mothet, J. P.; Rouaud, E.; Sinet, P.-M.; Potier, B.; Jouvenceau, A.; Dutar, P.; Videau, C.; Epelbaum, J.; Billard, J.-M. A Critical Role for the Glial-Derived Neuromodulator D-Serine in the Age-Related Deficits of Cellular Mechanisms of Learning and Memory. *Aging Cell* **2006**, *5* (3), 267–274.

(107) Bukalo, O.; Pinard, C. R.; Holmes, A. Mechanisms to Medicines: Elucidating Neural and Molecular Substrates of Fear Extinction to Identify Novel Treatments for Anxiety Disorders. *Br. J. Pharmacol.* **2014**, *171* (20), 4690–4718.

(108) Allgulander, C.; Bandelow, B.; Hollander, E.; Montgomery, S. A.; Nutt, D. J.; Okasha, A.; Pollack, M. H.; Stein, D. J.; Swinson, R. P.; World Council of Anxiety. WCA Recommendations for the Long-Term Treatment of Generalized Anxiety Disorder. *CNS Spectr.* **2003**, *8* (8 Suppl 1), 53–61.

(109) Stewart, R. E.; Chambless, D. L. Cognitive-Behavioral Therapy for Adult Anxiety Disorders in Clinical Practice: A Meta-Analysis of Effectiveness Studies. *J. Consult. Clin. Psychol.* **2009**, *77* (4), 595–606.

(110) Rodrigues, H.; Figueira, I.; Gonçalves, R.; Mendlowicz, M.; Macedo, T.; Ventura, P. CBT for Pharmacotherapy Non-Remitters--a Systematic Review of a next-Step Strategy. *J. Affect. Disord.* **2011**, *129* (1-3), 219–228.

(111) Barlow, D. H.; Gorman, J. M.; Shear, M. K.; Woods, S. W. Cognitive-Behavioral Therapy, Imipramine, or Their Combination for Panic Disorder: A Randomized Controlled Trial. *JAMA* **2000**, *283* (19), 2529–2536.

(112) Rodriguez, C. I.; Kegeles, L. S.; Levinson, A.; Feng, T.; Marcus, S. M.; Vermes, D.; Flood, P.; Simpson, H. B. Randomized Controlled Crossover Trial of Ketamine in Obsessive-Compulsive Disorder: Proof-of-Concept. *Neuropsychopharmacology* **2013**, *38* (12), 2475–2483.

(113) Feder A; Parides MK; Murrough JW; et al. Efficacy of Intravenous Ketamine for Treatment of Chronic Posttraumatic Stress Disorder: A Randomized Clinical Trial. *JAMA Psychiatry* **2014**, *71* (6), 681–688.

(114) Johansen, J. P.; Cain, C. K.; Ostroff, L. E.; LeDoux, J. E. Molecular Mechanisms of Fear Learning and Memory. *Cell* **2011**, *147* (3), 509–524.

(115) Dalton, G. L.; Wu, D. C.; Wang, Y. T.; Floresco, S. B.; Phillips, A. G. NMDA GluN2A and GluN2B Receptors Play Separate Roles in the Induction of LTP and LTD in the Amygdala and in the Acquisition and Extinction of Conditioned Fear. *Neuropharmacology* **2012**, *62* (2), 797–806.

(116) Bauer, E. P.; Schafe, G. E.; LeDoux, J. E. NMDA Receptors and L-Type Voltage-Gated Calcium Channels Contribute to Long-Term Potentiation and Different Components of Fear Memory Formation in the Lateral Amygdala. *J. Neurosci. Off. J. Soc. Neurosci.* **2002**, *22* (12), 5239–5249.

(117) Miserendino, M. J.; Sananes, C. B.; Melia, K. R.; Davis, M. Blocking of Acquisition but Not Expression of Conditioned Fear-Potentiated Startle by NMDA Antagonists in the Amygdala. *Nature* **1990**, *345* (6277), 716–718.

(118) Lee, H.; Kim, J. J. Amygdalar NMDA Receptors Are Critical for New Fear Learning in Previously Fear-Conditioned Rats. *J. Neurosci. Off. J. Soc. Neurosci.* **1998**, *18* (20), 8444–8454.

(119) Lin, C.-H.; Yeh, S.-H.; Lu, H.-Y.; Gean, P.-W. The Similarities and Diversities of Signal Pathways Leading to Consolidation of Conditioning and Consolidation of Extinction of Fear Memory. *J. Neurosci.* **2003**, *23* (23), 8310–8317.

(120) Baker, J. D.; Azorlosa, J. L. The NMDA Antagonist MK-801 Blocks the Extinction of Pavlovian Fear Conditioning. *Behav. Neurosci.* **1996**, *110* (3), 618–620.

(121) Falls, W. A.; Miserendino, M. J.; Davis, M. Extinction of Fear-Potentiated Startle: Blockade by Infusion of an NMDA Antagonist into the Amygdala. *J. Neurosci. Off. J. Soc. Neurosci.* **1992**, *12* (3), 854–863.

(122) Santini, E.; Muller, R. U.; Quirk, G. J. Consolidation of Extinction Learning Involves Transfer from NMDA-Independent to NMDA-Dependent Memory. *J. Neurosci. Off. J. Soc. Neurosci.* **2001**, *21* (22), 9009–9017.

(123) Rodrigues, S. M.; Schafe, G. E.; LeDoux, J. E. Intra-Amygdala Blockade of the NR2B Subunit of the NMDA Receptor Disrupts the Acquisition but Not the Expression of Fear Conditioning. *J. Neurosci. Off. J. Soc. Neurosci.* **2001**, *21* (17), 6889–6896.
(124) Walker, D. L.; Davis, M. Amygdala Infusions of an NR2B-Selective or an NR2A-Preferring NMDA Receptor Antagonist Differentially Influence Fear Conditioning and Expression in the Fear-Potentiated Startle Test. *Learn. Mem. Cold Spring Harb. N* **2008**, *15* (2), 67–74.
(125) Walker, D. L.; Ressler, K. J.; Lu, K.-T.; Davis, M. Facilitation of Conditioned Fear Extinction by Systemic Administration or Intra-Amygdala Infusions of D-Cycloserine as Assessed with Fear-Potentiated Startle in Rats. *J. Neurosci. Off. J. Soc. Neurosci.* **2002**, *22* (6), 2343–2351.
(126) Ogden, K. K.; Khatri, A.; Traynelis, S. F.; Heldt, S. A. Potentiation of GluN2C/D NMDA Receptor Subtypes in the Amygdala Facilitates the Retention of Fear and Extinction Learning in Mice. *Neuropsychopharmacology* **2014**, *39* (3), 625–637.
(127) Mellon, R. D.; Simone, A. F.; Rappaport, B. A. Use of Anesthetic Agents in Neonates and Young Children: *Anesth. Analg.* **2007**, *104* (3), 509–520.
(128) Hasselmann, H. Ketamine as Antidepressant? Current State and Future Perspectives. *Curr. Neuropharmacol.* **2014**, *12* (1), 57–70.
(129) Church, J.; Lodge, D.; Berry, S. C. Differential Effects of Dextrorphan and Levorphanol on the Excitation of Rat Spinal Neurons by Amino Acids. *Eur. J. Pharmacol.* **1985**, *111* (2), 185–190.
(130) Church, J.; Jones, M. G.; Davies, S. N.; Lodge, D. Antitussive Agents as N-Methylaspartate Antagonists: Further Studies. *Can. J. Physiol. Pharmacol.* **1989**, *67* (6), 561–567.
(131) Franklin, P. H.; Murray, T. F. High Affinity [3H]dextrorphan Binding in Rat Brain Is Localized to a Noncompetitive Antagonist Site of the Activated N-Methyl-D-Aspartate Receptor-Cation Channel. *Mol. Pharmacol.* **1992**, *41* (1), 134–146.
(132) Pechnick, R. N.; Poland, R. E. Comparison of the Effects of Dextromethorphan, Dextrorphan, and Levorphanol on the Hypothalamo-Pituitary-Adrenal Axis. *J. Pharmacol. Exp. Ther.* **2004**, *309* (2), 515–522.
(133) Shin, E.-J.; Nah, S.-Y.; Chae, J. S.; Bing, G.; Shin, S. W.; Yen, T. P. H.; Baek, I.-H.; Kim, W.-K.; Maurice, T.; Nabeshima, T.; Kim, H.-C. Dextromethorphan Attenuates Trimethyltin-Induced Neurotoxicity via σ1 Receptor Activation in Rats. *Neurochem. Int.* **2007**, *50* (6), 791–799.
(134) Musacchio, J.; Klein, M.; Canoll, P. D. Dextromethorphan and Sigma Ligands: Common Sites but Diverse Effects. *Life Sci.* **1989**, *45* (19), 1721–1732.
(135) M Schadel, D. W. Pharmacokinetics of Dextromethorphan and Metabolites in Humans: Influence of the CYP2D6 Phenotype and Quinidine Inhibition. *J. Clin. Psychopharmacol.* **1995**, *15* (4), 263–269.
(136) Pseudobulbar Affect | NUEDEXTA https://www.nuedexta.com/ (accessed Aug 12, 2014).
(137) Dravid, S. M.; Erreger, K.; Yuan, H.; Nicholson, K.; Le, P.; Lyuboslavsky, P.; Almonte, A.; Murray, E.; Mosley, C.; Barber, J.; French, A.; Balster, R.; Murray, T. F.; Traynelis, S. F. Subunit-Specific Mechanisms and Proton Sensitivity of NMDA Receptor Channel Block. *J. Physiol.* **2007**, *581* (1), 107–128.
(138) Lipton, S. A. Failures and Successes of NMDA Receptor Antagonists: Molecular Basis for the Use of Open-Channel Blockers like Memantine in the Treatment of Acute and Chronic Neurologic Insults. *NeuroRx* **2004**, *1* (1), 101–110.
(139) Williams, K. Ifenprodil Discriminates Subtypes of the N-Methyl-D-Aspartate Receptor: Selectivity and Mechanisms at Recombinant Heteromeric Receptors. *Mol. Pharmacol.* **1993**, *44* (4), 851–859.
(140) Chenard, B. L.; Bordner, J.; Butler, T. W.; Chambers, L. K.; Collins, M. A.; De Costa, D. L.; Ducat, M. F.; Dumont, M. L.; Fox, C. B. (1S,2S)-1-(4-Hydroxyphenyl)-2-(4-Hydroxy-4-Phenylpiperidino)-1-Propanol: A Potent New Neuroprotectant Which Blocks N-Methyl-D-Aspartate Responses. *J. Med. Chem.* **1995**, *38* (16), 3138–3145.

(141) Gotti, B.; Duverger, D.; Bertin, J.; Carter, C.; Dupont, R.; Frost, J.; Gaudilliere, B.; MacKenzie, E. T.; Rousseau, J.; Scatton, B. Ifenprodil and SL 82.0715 as Cerebral Anti-Ischemic Agents. I. Evidence for Efficacy in Models of Focal Cerebral Ischemia. *J. Pharmacol. Exp. Ther.* **1988**, *247* (3), 1211–1221.

(142) Taniguchi, K.; Shinjo, K.; Mizutani, M.; Shimada, K.; Ishikawa, T.; Menniti, F. S.; Nagahisa, A. Antinociceptive Activity of CP-101,606, an NMDA Receptor NR2B Subunit Antagonist. *Br. J. Pharmacol.* **1997**, *122* (5), 809–812.

(143) Chizh, B. A.; Headley, P. M.; Tzschentke, T. M. NMDA Receptor Antagonists as Analgesics: Focus on the NR2B Subtype. *Trends Pharmacol. Sci.* **2001**, *22* (12), 636–642.

(144) Yurkewicz, L.; Weaver, J.; Bullock, M. R.; Marshall, L. F. The Effect of the Selective NMDA Receptor Antagonist Traxoprodil in the Treatment of Traumatic Brain Injury. *J. Neurotrauma* **2005**, *22* (12), 1428–1443.

(145) Preskorn, S. H.; Baker, B.; Kolluri, S.; Menniti, F. S.; Krams, M.; Landen, J. W. An Innovative Design to Establish Proof of Concept of the Antidepressant Effects of the NR2B Subunit Selective N-Methyl-D-Aspartate Antagonist, CP-101,606, in Patients with Treatment-Refractory Major Depressive Disorder. *J. Clin. Psychopharmacol.* **2008**, *28* (6), 631–637.

(146) Boyce, S.; Wyatt, A.; Webb, J. K.; O'Donnell, R.; Mason, G.; Rigby, M.; Sirinathsinghji, D.; Hill, R. G.; Rupniak, N. M. J. Selective NMDA NR2B Antagonists Induce Antinociception without Motor Dysfunction: Correlation with Restricted Localisation of NR2B Subunit in Dorsal Horn. *Neuropharmacology* **1999**, *38* (5), 611–623.

(147) Nicholson, K. L.; Mansbach, R. S.; Menniti, F. S.; Balster, R. L. The Phencyclidine-like Discriminative Stimulus Effects and Reinforcing Properties of the NR2B-Selective N-Methyl-D-Aspartate Antagonist CP-101 606 in Rats and Rhesus Monkeys. *Behav. Pharmacol.* **2007**, *18* (8), 731–743.

(148) Bettini, E.; Sava, A.; Griffante, C.; Carignani, C.; Buson, A.; Capelli, A. M.; Negri, M.; Andreetta, F.; Senar-Sancho, S. A.; Guiral, L.; Cardullo, F. Identification and Characterization of Novel NMDA Receptor Antagonists Selective for NR2A- over NR2B-Containing Receptors. *J. Pharmacol. Exp. Ther.* **2010**, *335* (3), 636–644.

(149) Edman, S.; McKay, S.; MacDonald, L. J.; Samadi, M.; Livesey, M. R.; Hardingham, G. E.; Wyllie, D. J. A. TCN 201 Selectively Blocks GluN2A-Containing NMDARs in a GluN1 Co-Agonist Dependent but Non-Competitive Manner. *Neuropharmacology* **2012**, *63* (3), 441–449.

(150) McKay, S.; Griffiths, N.; Butters, P.; Thubron, E.; Hardingham, G.; Wyllie, D. Direct Pharmacological Monitoring of the Developmental Switch in NMDA Receptor Subunit Composition Using TCN 213, a GluN2A-Selective, Glycine-Dependent Antagonist. *Br. J. Pharmacol.* **2012**, *166* (3), 924–937.

(151) Hansen, K. B.; Traynelis, S. F. Structural and Mechanistic Determinants of a Novel Site for Noncompetitive Inhibition of GluN2D-Containing NMDA Receptors. *J. Neurosci.* **2011**, *31* (10), 3650–3661.

(152) Costa, B. M.; Irvine, M. W.; Fang, G.; Eaves, R. J.; Mayo-Martin, M. B.; Skifter, D. A.; Jane, D. E.; Monaghan, D. T. A Novel Family of Negative and Positive Allosteric Modulators of NMDA Receptors. *J. Pharmacol. Exp. Ther.* **2010**, *335* (3), 614–621.

(153) Irvine, M. W.; Costa, B. M.; Volianskis, A.; Fang, G.; Ceolin, L.; Collingridge, G. L.; Monaghan, D. T.; Jane, D. E. Coumarin-3-Carboxylic Acid Derivatives as Potentiators and Inhibitors of Recombinant and Native N-Methyl-D-Aspartate Receptors. *Neurochem. Int.* **2012**, *61* (4), 593–600.

(154) Monaghan, D. T.; Irvine, M. W.; Costa, B. M.; Fang, G.; Jane, D. E. Pharmacological Modulation of NMDA Receptor Activity and the Advent of Negative and Positive Allosteric Modulators. *Neurochem. Int.* **2012**, *61* (4), 581–592.

(155) Costa, B. M.; Irvine, M. W.; Fang, G.; Eaves, R. J.; Mayo-Martin, M. B.; Laube, B.; Jane, D. E.; Monaghan, D. T. Structure-Activity Relationships for Allosteric NMDA Receptor Inhibitors Based on 2-Naphthoic Acid. *Neuropharmacology* **2012**, *62* (4), 1730–1736.

(156) Mullasseril, P.; Hansen, K. B.; Vance, K. M.; Ogden, K. K.; Yuan, H.; Kurtkaya, N. L.; Santangelo, R.; Orr, A. G.; Le, P.; Vellano, K. M.; Liotta, D. C.; Traynelis, S. F. A Subunit-Selective Potentiator of NR2C- and NR2D-Containing NMDA Receptors. *Nat. Commun.* **2010**, *1*, 90.

(157) Santangelo Freel, R. M.; Ogden, K. K.; Strong, K. L.; Khatri, A.; Chepiga, K. M.; Jensen, H. S.; Traynelis, S. F.; Liotta, D. C. Correction to Synthesis and Structure Activity Relationship of Tetrahydroisoquinoline-Based Potentiators of GluN2C and GluN2D Containing N-Methyl-D-Aspartate Receptors. *J. Med. Chem.* **2014**, *57* (11), 4975–4975.

(158) Ogden, K. K.; Traynelis, S. F. Contribution of the M1 Transmembrane Helix and Pre-M1 Region to Positive Allosteric Modulation and Gating of N-Methyl-D-Aspartate Receptors. *Mol. Pharmacol.* **2013**, *83* (5), 1045–1056.

(159) Zimmerman, S. S.; Khatri, A.; Garnier-Amblard, E. C.; Mullasseril, P.; Kurtkaya, N. L.; Gyoneva, S.; Hansen, K. B.; Traynelis, S. F.; Liotta, D. C. Design, Synthesis, and Structure–Activity Relationship of a Novel Series of GluN2C-Selective Potentiators. *J. Med. Chem.* **2014**, *57* (6), 2334–2356.

(160) Khatri, A.; Burger, P. B.; Swanger, S. A.; Hansen, K. B.; Zimmerman, S.; Karakas, E.; Liotta, D. C.; Furukawa, H.; Snyder, J. P.; Traynelis, S. F. Structural Determinants and Mechanism of Action of a GluN2C-Selective NMDA Receptor Positive Allosteric Modulator. *Mol. Pharmacol.* **2014**, *86* (5), 548–560.

(161) Paul, S. M.; Doherty, J. J.; Robichaud, A. J.; Belfort, G. M.; Chow, B. Y.; Hammond, R. S.; Crawford, D. C.; Linsenbardt, A. J.; Shu, H.-J.; Izumi, Y.; Mennerick, S. J.; Zorumski, C. F. The Major Brain Cholesterol Metabolite 24(S)-Hydroxycholesterol Is a Potent Allosteric Modulator of N-Methyl-D-Aspartate Receptors. *J. Neurosci. Off. J. Soc. Neurosci.* **2013**, *33* (44), 17290–17300.

(162) Linsenbardt, A. J.; Taylor, A.; Emnett, C. M.; Doherty, J. J.; Krishnan, K.; Covey, D. F.; Paul, S. M.; Zorumski, C. F.; Mennerick, S. Different Oxysterols Have Opposing Actions at N-Methyl-D-Aspartate Receptors. *Neuropharmacology* **2014**, *85*, 232–242.

(163) Hatton, C. J.; Paoletti, P. Modulation of Triheteromeric NMDA Receptors by N-Terminal Domain Ligands. *Neuron* **2005**, *46* (2), 261–274.

(164) Tahirovic, Y. A.; Geballe, M.; Gruszecka-Kowalik, E.; Myers, S. J.; Lyuboslavsky, P.; Le, P.; French, A.; Irier, H.; Choi, W.; Easterling, K.; Yuan, H.; Wilson, L. J.; Kotloski, R.; McNamara, J. O.; Dingledine, R.; Liotta, D. C.; Traynelis, S. F.; Snyder, J. P. Enantiomeric Propanolamines as Selective N-Methyl-D-Aspartate 2B Receptor Antagonists†. *J. Med. Chem.* **2008**, *51* (18), 5506–5521.

(165) Ono, M.; Watanabe, R.; Kawashima, H.; Kawai, T.; Watanabe, H.; Haratake, M.; Saji, H.; Nakayama, M. 18F-Labeled Flavones for in Vivo Imaging of β-Amyloid Plaques in Alzheimer's Brains. *Bioorg. Med. Chem.* **2009**, *17* (5), 2069–2076.

(166) Bellamy, F. D.; Ou, K. Selective Reduction of Aromatic Nitro Compounds with Stannous Chloride in Non Acidic and Non Aqueous Medium. *Tetrahedron Lett.* **1984**, *25* (8), 839–842.

(167) Coppola, G. M.; Kukkola, P. J.; Stanton, J. L.; Neubert, A. D.; Marcopulos, N.; Bilci, N. A.; Wang, H.; Tomaselli, H. C.; Tan, J.; Aicher, T. D.; Knorr, D. C.; Jeng, A. Y.; Dardik, B.; Chatelain, R. E. Perhydroquinolylbenzamides as Novel Inhibitors of 11β-Hydroxysteroid Dehydrogenase Type 1. *J. Med. Chem.* **2005**, *48* (21), 6696–6712.

(168) Klapars, A.; Buchwald, S. L. Copper-Catalyzed Halogen Exchange in Aryl Halides: An Aromatic Finkelstein Reaction. *J. Am. Chem. Soc.* **2002**, *124* (50), 14844–14845.

(169) Wolter, M.; Nordmann, G.; Job, G. E.; Buchwald, S. L. Copper-Catalyzed Coupling of Aryl Iodides with Aliphatic Alcohols. *Org. Lett.* **2002**, *4* (6), 973–976.

(170) Kwong, F. Y.; Buchwald, S. L. A General, Efficient, and Inexpensive Catalyst System for the Coupling of Aryl Iodides and Thiols. *Org. Lett.* **2002**, *4* (20), 3517–3520.

Chapter 2: The Structure Activity Relationship (SAR) of Tetrahydroisoquinoline Potentiators can be tuned to selectively target GluN2B-containing NMDA Receptors

2.1 Statement of Purpose

Our lab had previously reported the discovery of a tetrahydroisoquinoline compound known as CIQ (**Chapter 1**), which is a GluN2C- and GluN2D-containing NMDA receptor positive allosteric modulator. To date, CIQ represents the only small, drug-like molecule selective for potentiation at GluN2C- and GluN2D-containing receptors. While a number of subunit-selective inhibitors have been identified (**Chapter 1.2.2**), the literature is lacking in terms of small molecules that potentiate selectivity at one GluN2 subunit over another. For this reason, an extensive SAR was built around the CIQ scaffold in attempt to increase potency and efficacy at GluN2C and GluN2D-containing receptors[1]. In the process of modifying the C-ring of the CIQ scaffold, one compound was discovered, **1180-55**, that not only potentiated GluN2C- and GluN2D-containing receptors, but also GluN2B-containing receptors. Compound **1180-55** has isopropoxy functionality where CIQ has dimethoxy functionality (**Figure 1**), and this change led to a compound with a different pattern of subunit-selectivity than CIQ.

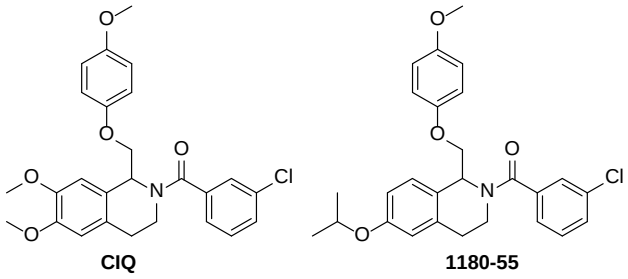

Figure 1. Structure of CIQ and isopropoxy-containing 1180-55.

Potentiation at the GluN2B-containing NMDA receptor was novel for the series and provided our group with the unique opportunity to develop a positive allosteric modulator selective for GluN2B-containing NMDA receptors. Through continued modifications to the CIQ scaffold, we attempted to tune out the GluN2C and GluN2D potentiation and home in on the GluN2B potentiation of this class of compounds. Although a number of endogenous molecules selective for GluN2B-containing

NMDA receptors exist (**Chapter 2.2.2**), there is a still a need for small, drug-like molecules with GluN2B-containing NMDA receptor potentiation and selectivity.

Additionally, the structural determinants of CIQ were identified as the GluN2 pre-M1 and M1 helices[2,3] (**Chapter 1.2.6**), but the structural determinants of **1180-55** were not assumed to be identical. In addition to the development of an SAR around the isopropoxy containing-**1180-55**, a second aim of this project, in collaboration with the Traynelis lab, was to begin to identify the structural determinants of GluN2B potentiation and to elucidate details surrounding the mechanism of action of **1180-55**. The goals of this project were realized with the following strategy:

1) Design analogues based on **1180-55** with an emphasis on potency and GluN2B-containing NMDA receptor selectivity.
2) Synthesize these compounds and test activity in GluN2C- and GluN2D-containing NMDA receptors expressed in *Xenopus laevis* oocytes. The biological evaluation of these compounds was completed in the laboratory of Dr. Steve Traynelis.
3) Begin to identify the structural determinants within the GluN1/GluN2B-containing and GluN1/GluN2D-containing NMDA receptors of **1180-55** *in vitro*, and begin to determine the level of divergence between the **1180-55** class of molecules and the GluN2C- and GluN2D-selective CIQ class of molecules.

2.2 Introduction and Background

2.2.1 Therapeutic rationale for GluN2B-selective NMDA positive modulators

Higher cognitive functions, such as planning ahead, comprehension, and intelligence rely on working memory[4]. Working memory is the process of encountering a stimulus, transiently holding the information, and responding appropriately[5], and much of working memory depends on the prefrontal cortex (PFC)[6,7]. Inhibiting NMDA receptor activity in rat PFC with channel blockers ketamine and MK-801 reduced performance in tests of working memory in an animal model of attention deficit hyperactivity disorder (ADHD)[8], and GluN2A- and GluN2B-containing receptors

are heavily expressed in the forebrain regions, which include the PFC[9], suggesting that activity from these NMDA receptor subunits are critical for many cognitive processes[10].

Several lines of evidence suggest enhancement of the function of GluN2B-containing NMDA receptors could improve memory formation. Overexpression of GluN2B in the PFC of rats resulted in enhanced LTP, but not LTD, and the GluN2B-selective antagonist Ro25-6981 abolished this improvement, suggesting that overexpression of GluN2B was responsible for the effect[11]. Similarly, GluN2B receptor overexpression in the forebrain of mice resulted in enhanced activation of NMDA receptor responses in response to stimulation,[12] which was shown to improve learning and long-term memory, spatial performance, and cued and contextual fear conditioning of the transgenic mice compared to wild-type. Additionally, mice with this enhanced activation exhibit faster fear extinction.[11,13–15] Both GluN2A- and GluN2B-containing receptors are heavily expressed in the PFC, but compared to GluN2A subunits the GluN2B has a slower deactivation time course[16], which allows for the longer depolarization times that are required for working memory[10,17,18]. This is one hypothesis behind the integral role of GluN2B-containing receptors in the process of higher cognitive thought.

During the aging process, the expression of NMDA GluN2B receptors decreases, which may play a role in a reduced ability to retain information and learn new material as one ages.[9,19] Additional studies have suggested that age-dependent cognitive decline could be linked to decreased levels of synaptic plasticity and GluN2B expression.[20–23] Therefore, the development of positive allosteric modulators that selectively enhance GluN2B function not only have potential uses as pharmacological tools, but also may be of therapeutic interest by providing a means to improve memory performance in the aging poulation.[24]

2.2.2 Endogenous compounds for the GluN2B NMDA receptor

Multiple endogenous compounds have been characterized as being selective for the GluN2B subunits compared to other GluN2 subunits (**Figure 2**). Polyamines such as spermine (**1**), which has an approximate EC_{50} value of 150 μM,[25] selectively potentiate the response of GluN1/GluN2B

receptors by both enhancing the binding of glutamate as well as reducing tonic proton inhibition present at physiological pH.[25,26] The neurosteroid pregnenolone sulfate (**2**) potentiates GluN2A and GluN2B-containing receptors by enhancing the open probability.[27] Additionally, a number of aminoglycoside antibiotics, including neomycin B (**3**), kanamycin A (**4**), and streptomycin (**5**), selectivity potentiate GluN2B-containg receptors with EC_{50} values typically between 38 and 134 μM.[28] Despite this, there is still a need for potent, drug-like positive GluN2B-selective positive allosteric modulators of NMDA receptor function because all three classes of compounds have physicochemical properties that complicate their use as tool compounds. In addition, polyamines and amino glycosides show low potency.

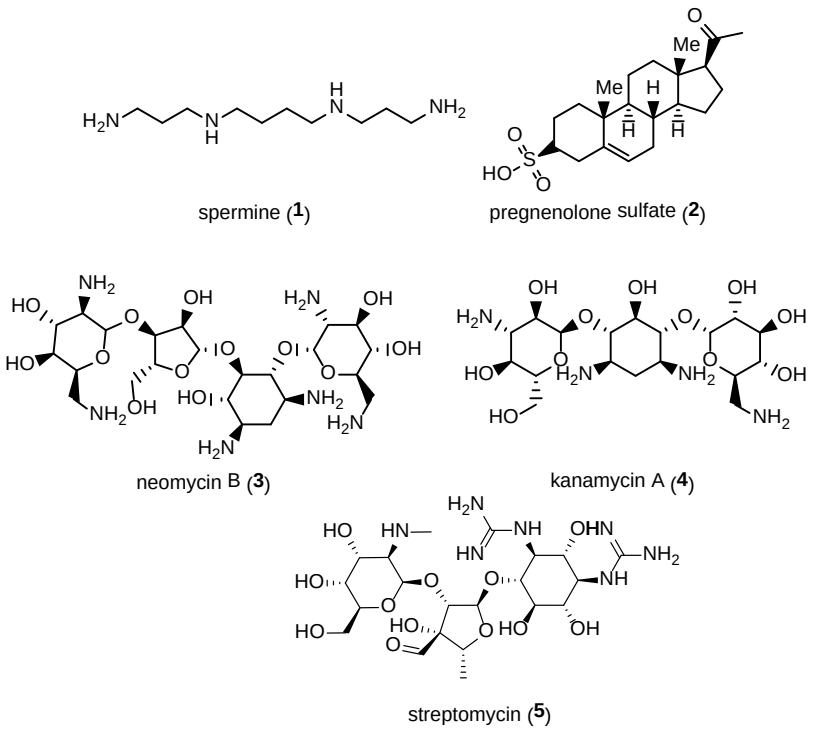

Figure 2. Endogenous compounds selective for potentiation at GluN2B-containing receptors.

2.2.3 Photocrosslinking

Through extensive point mutations utilizing NR2A-NR2D chimeric subunits, the structural determinants of CIQ (**22**) activity were identified as the GluN2 ATD-LBD linker and one residue in the TMD[2]. Further research suggested that CIQ was interacting with the TMD region of GluN2D,

and that the pre M1 and M1 helix were crucial for CIQ-mediated potentiation[3] (**Chapter 1.2.6**). Preliminary site-directed mutagenesis, discussed in **Chapter 2.2.4**, revealed that the structural determinants of **1180-55** differ from CIQ, and for this reason, photoaffinity labeling was explored. Photoaffinity labeling, which utilizes light and a photoactivatable moiety, is one method with the potential to shed light on receptor-ligand interactions, including binding sites. The process of photoaffinity labeling is depicted in **Figure 3**. Ligand receptor interactions are typically reversible and are not strong enough to withstand harsh conditions associated with purification and proteolysis, but photoaffinity labeling enables the formation of a nonreversible receptor-ligand bond. Photoaffinity labeling requires a ligand with a photoactivatable moiety that in the presence of light forms an irreversible covalent bond with the receptor. After a receptor and activated ligand have been exposed to light, the covalently modified receptor can be purified by SDS-page, proteolyzed by typsin, and subjected to protein mass spectroscopy. In theory, the peptide that the ligand is bound to should have the mass signature of the covalently attached ligand[29,30].

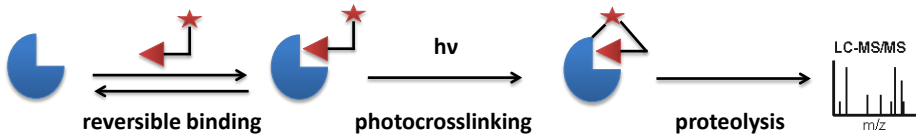

Figure 3. Basic principle behind photoaffinity labeling.

Three major types of photoaffinity labels are used: benzophenones, aryl azides, and diazrines (**Figure 4**). Benzophenones are irradiated at wavelengths around 350 nm, a higher wavelength that typically does not damage the biological sample. In the presence of UV light, initially a triplet diradical is formed and if the benzophenone is not in the presence of a reaction partner, it will return back to the ground state. If the benzophenone in the diradical state is in the presence of a reactive species, it will first abstract a hydrogen from a reactive species of the target and the remaining radical on the benzophenone will combine with the radical of the reactive species to form the benzhydrol. Drawbacks of benzophenone use include their bulk, which can potentially impact ligand activity, and their requirement of a longer period of irradiation which comes with the risk of non-specific

labeling[31]. Azides and diazirines, on the other hand, are smaller and require a shorter period of irradiation, limiting the nonspecific labeling. Azides require shorter wavelengths (less than 300nm), which can potentially damage the biological samples, while diazrines absorb at the most optimal wavelengths for biological samples – between 350 and 380 nm[29]. Once exposed to light, an azide will initially form a singlet nitrene and a diazrine will form a singlet carbene. These intermediates, with lifespans of approximately 1 ms, are very reactive and will insert into a carbon-hydrogen bond or a heteroatom-hydrogen bond[30]. The singlet carbene or nitrene can also undergo intersystem crossing (ISC) to form the corresponding triplet states, which are more stable than the singlet states (e.g., the triplet carbene is approximately 20 kcal/mol lower in energy than the singlet carbene)[32]. Triplet states behave more like diradicals; the radical will first abstract a hydrogen from the reactive species and then the two species will recombine to form the product.

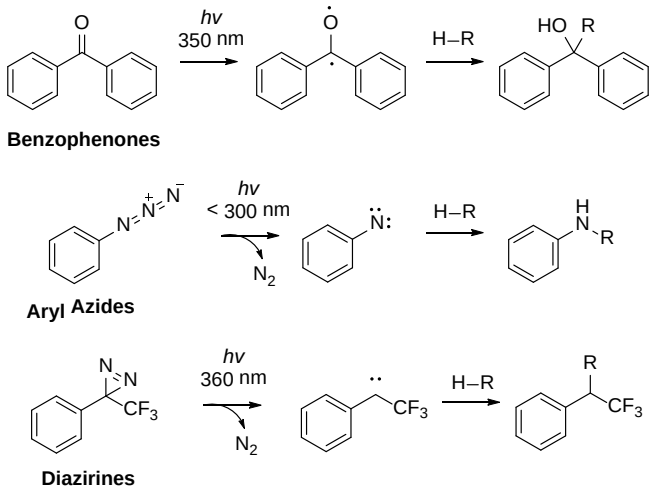

Figure 4. Reactivity of photoaffinity labels.

In addition to a photoactivatable moiety, a probe used for photoaffinity labeling processes also typically requires a second tag, such a biotin group that facilitates protein purification; the biotin tag can act as a pull-down handle during SDS-page purification[29]. The biotin tag is typically installed via a ligation reaction between an azide functionalized biotin (**6**) and a terminal alkyne on the ligand (**7**),

and a popular ligation reaction for biotin tagging is the copper (I) catalyzed azide alkyne [3 +2] cycloaddition[33–35], a click chemistry reaction, to afford 1,4-substituted triazole product **8** (**Figure 5**)

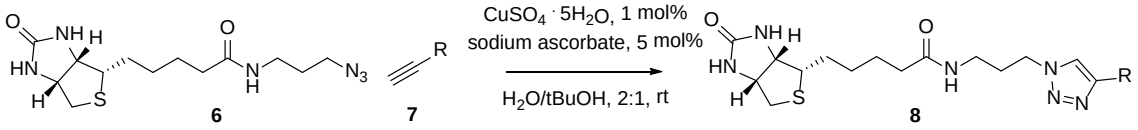

Figure 5. Azide alkyne [3 +2] cycloaddition to install biotin tag on photoaffinity ligand.

As discussed in **Chapter 2.3.7**, benzophenone, azide, and alkyne functionalities were attached to the **1180-55** core for initial experiments to test the viability of photocrosslinking. It was envisioned that a compound would be synthesized that contained both a photoaffinity label and an alkyne for biotin tagging, and this compound would be utilized in a photoaffinity labeling experiment. The photoaffinity labeled ligand would be incubated with transfected HEK (human embryonic kidney) cells and irradiated with the appropriate wavelength. The cells would then be pelleted by centrifugation and biotinylated, and following purification and Western blot, the NMDA receptor protein would be digested by trypsin and analyzed via mass spectrometry[36] (**Figure 6**).

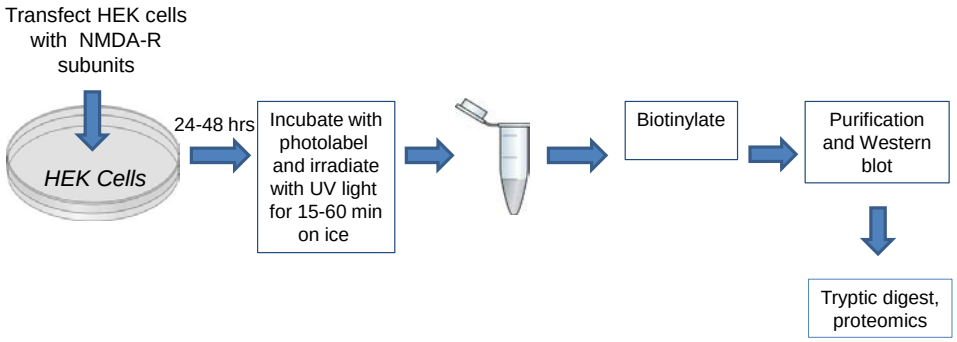

Figure 6. Flowchart depicting steps of photoaffinity labeling.

2.2.4 The identification of 1180-55 and its emergence as a distinct class from CIQ-like compounds

Isopropoxy-containing compound **1180-55** was discovered when conducting an SAR around the CIQ class of compounds, a series selective for GluN2C- and GluN2D-containing receptors. After extensive work on CIQ, it was discovered that the addition of an isopropoxy group in place of

dimethoxy functionality on the C-ring led to GluN2B potentiation. While this difference in the two compounds was startling, and provided a unique opportunity to develop at GluN2B-selective potentiator, further research revealed additional dissimilarities. At saturating concentrations of glutamate and glycine, CIQ potentiates GluN2C- and GluN2D-containing NMDA receptors, while **1180-55** potentiates GluN2B-, GluN2C-, and GluN2D-containing receptors (**Figure 7**). At low agonist concentrations (EC_{30} of glutamate and glycine), CIQ shows enhanced efficacy, potentiating the receptor almost 5-fold at GluN2C- and GluN2D-subunits, but at the same low agonist concentrations, **1180-55** potentiates GluN2A-GluN2B-, GluN2C-, and GluN2D-containing receptors. Compound **1180-55** not only potentiates GluN2A- and GluN2B- containing receptors at these low concentrations, but the compound is also more efficacious than CIQ at GluN2C- and GluN2D-containing receptors, enhancing the response over 10-fold at the GluN2C-subunit (**Figure 8**).

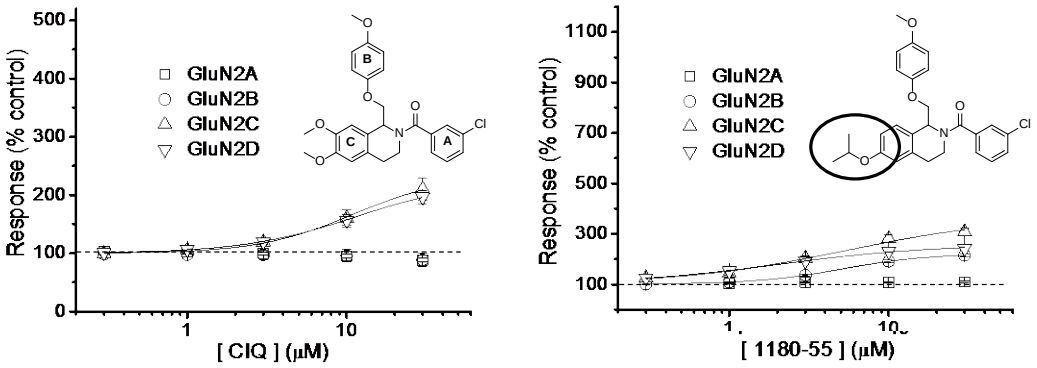

Figure 7. Dose-response curves of CIQ and 1180-55 at GluN2A-, GluN2B-, GluN2C-, and GluN2D-containing NMDA receptors at saturating concentrations of agonist.

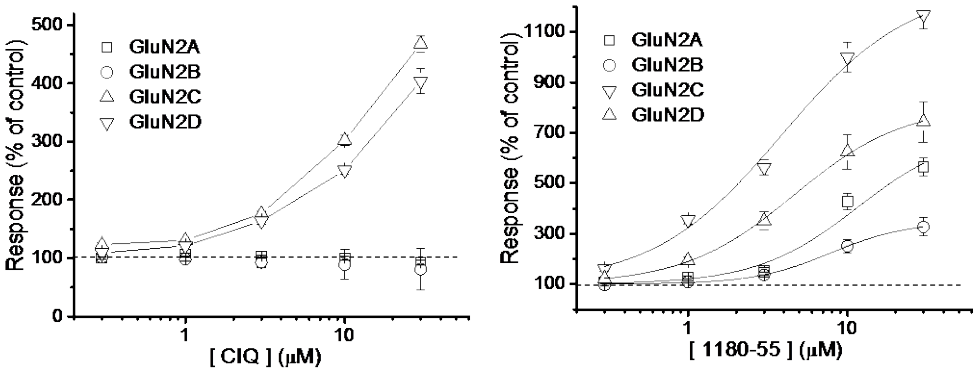

Figure 8. Dose-response curves of CIQ and 1180-55 at GluN2A-, GluN2B-, GluN2C-, and GluN2D-containing NMDA receptors at low concentrations of agonist.

Previous research had shown that CIQ has virtually no effect on glutamate and glycine potency at any subunits[2], but **1180-55** enhances glutamate and glycine EC_{50} values at all subunits. The effect of **1180-55** on glutamate and glycine EC_{50} values at the GluN2C-containing receptor is shown in **Figure 9**.

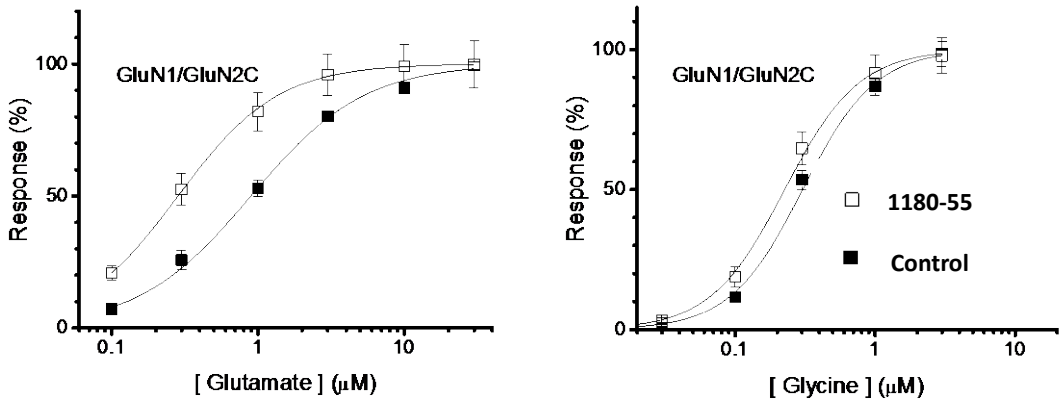

Figure 9. Glycine and glutamate potency shifts at the GluN1/GluN2C NMDA receptor in the absence and presence of 1180-55.

CIQ also has no impact on deactivation time course of the receptor, but **1180-55** slows down the deactivation of the receptor at all subunits. This is depicted in **Figure 10**, which highlights the compound's effect on the GluN2C and GluN2D subunits. A slowing of deactivation time course represents enhanced potency and slower dissociation from the binding pocket, which is consistent

with the enhanced effect of **1180-55** on the receptor at low concentrations and saturating concentrations of glutamate and glycine (**Figure 8**).

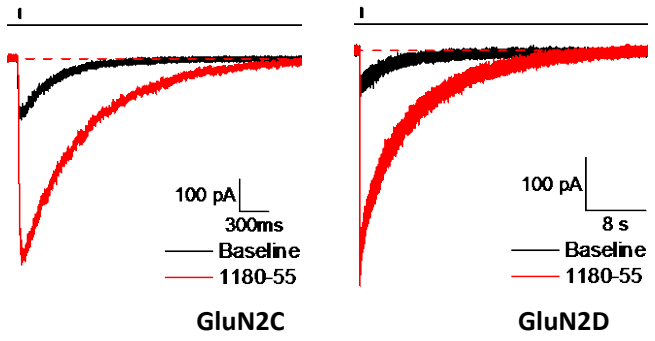

Figure 10. Effect of 1180-55 on the deactivation time course of GluN2C- and GluN2D-containing NMDA receptors.

In addition to these pharmacological differences, site-directed mutagenesis revealed different structural determinants for CIQ and **1180-55** activity. Extensive prior work (discussed in **Chapter 1.2.6**) revealed that the pre M1 helix and the M1 helix of the GluN2 subunit were important structural determinants for CIQ potentiation, and research has shown that some residues of the GluN2 pre M1 and M1 helix are structural determinants for **1180-55** activity (**Figure 11**). However, point mutations made to the pre M1 helix of the GluN1 subunit had very minimal effect on CIQ potentiation, while these same changes did affect **1180-55** activity on the NMDA receptor (**Figure 12**). This suggests that racemic **1180-55** is interacting with the GluN1 subunit in addition to the GluN2 subunit, while CIQ is interacting with the GluN2 subunit, and these novel structural determinants within the GluN1 subunit may be responsible for the potentiation at the GluN2B subunit from **1180-55**.

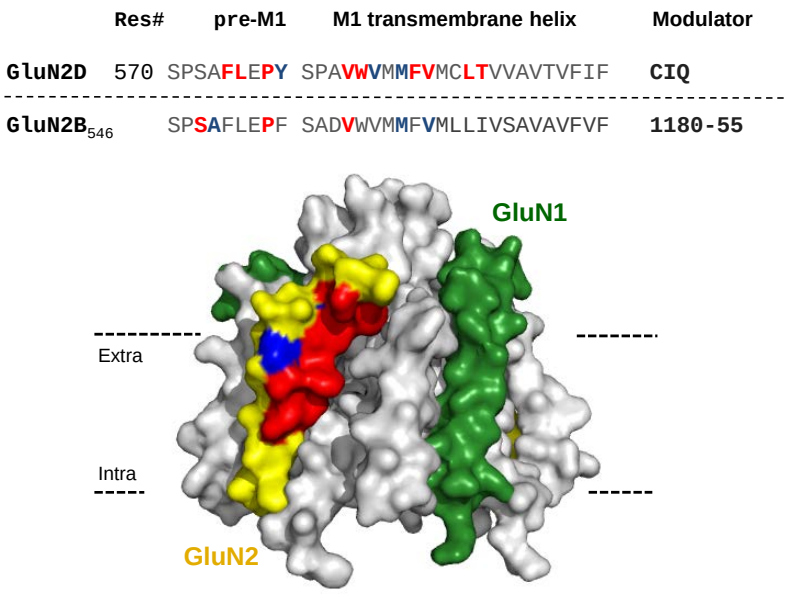

Figure 11. Comparison of point mutations on the GluN2 subunit that enhanced (blue) or inhibited (red) potentiation by CIQ and 1180-55. Sites on the space-filled model highlight the effect on CIQ potentiation.

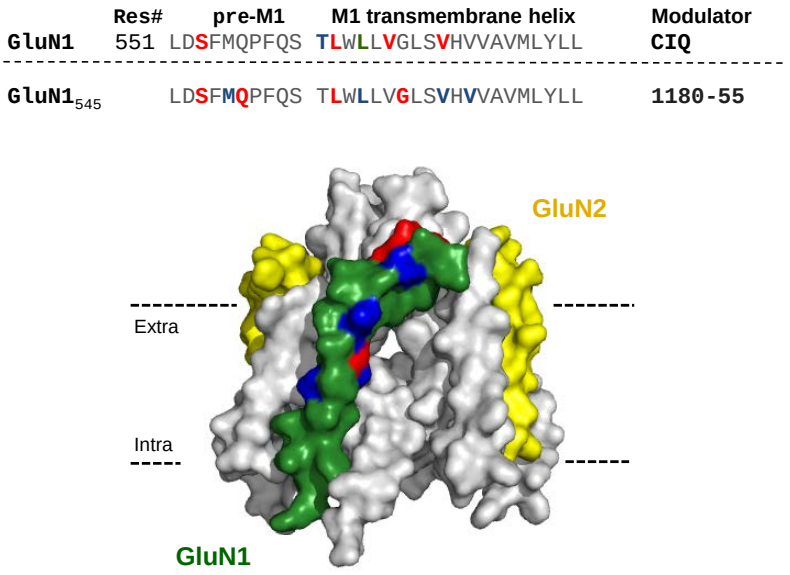

Figure 12. Comparison of point mutations on the GluN1 subunit that enhanced (blue) or inhibited (red) 1180-55 or CIQ potentiation. Sites on the space-filled model highlight the effect on **1180-55** potentiation.

These mutagenesis studies, in combination with the pharmacological work on agonist potency and deactivation time course, showed that **1180-55** was distinct from CIQ. With this in mind, an SAR

around the A-, B-, and C-rings of the **1180-55** scaffold (**Figure 13**) was initiated with the goal of increasing potency and selectivity for the GluN2B-subunit.

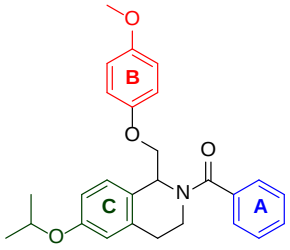

Figure 13. Generic structure of 1180-55 for SAR development.

2.3 Synthesis of tetrahydroisoquinoline-containing compounds with GluN2B potentiator activity.

2.3.1 Synthetic routes towards oxygen-containing racemic tetrahydroisoquinoline-containing compounds

The nonselective potentiation of **1180-55** appeared to stem from modifications to the C-ring, and all functionality to the C-ring was installed via one of four methods. Compounds with an ether linkage in the R_1 position were synthesized beginning with commercially available 2-(3-methoxyphenyl)ethylamine **9**, which was demethylated using HBr and acetic acid to afford 3-(2-aminoethyl)phenol hydrobromide **10**. The amine was Boc-protected using di-*tert*-butyl dicarbonate to give phenol **11**[37], which underwent an alkylation to deliver the corresponding *i*Bu, *i*Pr, and *c*Pent ethers as in compounds **12**. Under acidic conditions, the Boc group was removed to yield the functionalized phenethylamine compounds **13**, which were acylated with chloroacetyl chloride to give α-chloroamide-containing compounds **14.** *Ortho*, *meta*, and *para*-substituted phenols were then alkylated to yield linear amides **15** (**Scheme 1**).

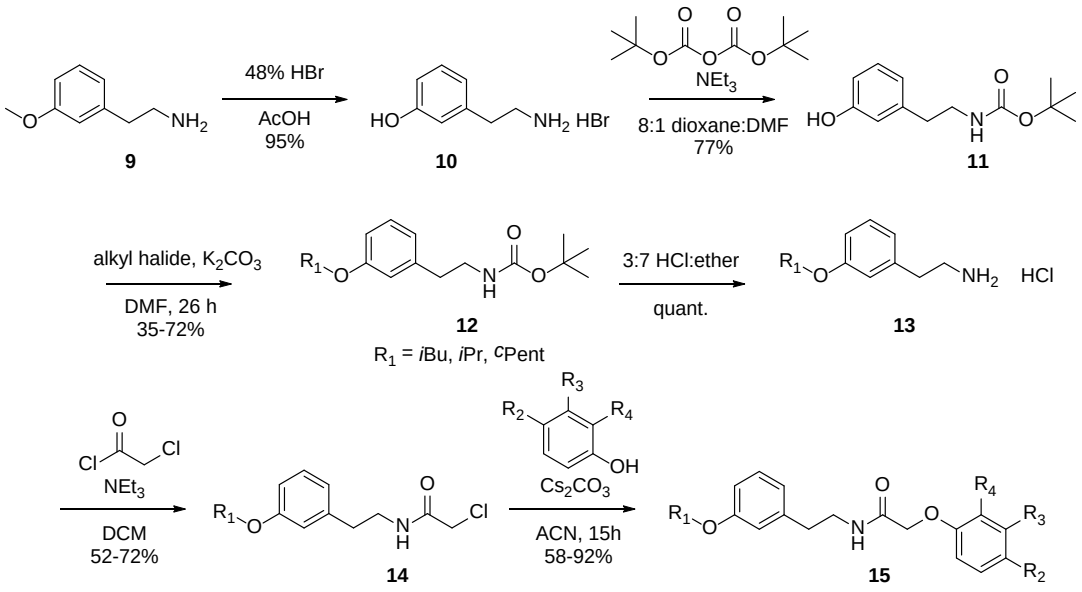

Scheme 1. Installation of oxygen-containing functionality on future C-ring via an alkylation.

Conversion of phenol **11** to the corresponding ethers could also be afforded via a base-catalyzed Mitsunobu reaction[38] (**Scheme 2**).

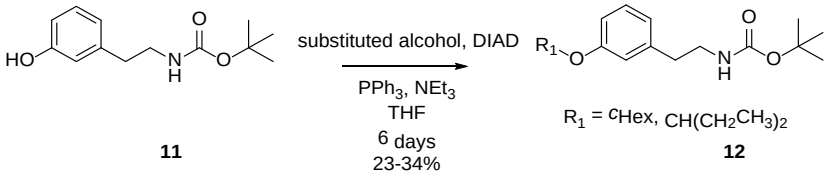

Scheme 2. Installation of oxygen-containing functionality on future C-ring via a Mitsunobu reaction.

The Mitsunobu reaction was explored as an alternative to the alkylation since often the nucleophilic attack by the phenol on the secondary alkyl halides were low yielding, but the Mitsunobu reaction was sluggish; often even after stirring for 6 days or longer, the starting materials had failed to completely react, and the yields were low. Nonetheless, final compounds with cyclohexyloxy and pentan-3-yloxy substituents were synthesized by installing the ether functionality with this methodology (**Table 1**). A summary of compounds subjected to acylation conditions with chloroacetyl chloride and alkylation conditions are shown in **Table 2** and **Table 3**, respectively.

Table 1. Summary of phenolic compounds subjected to alkylation or Mitsunobu conditions.

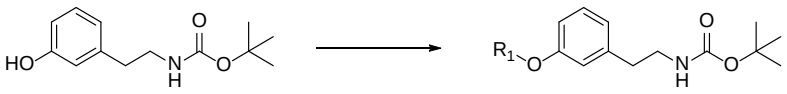

Starting Material ID	Reaction Conditions	R_1	Product ID
11	Alkylation	*i*Pr	**12a**
11	Alkylation	*i*Bu	**12b**
11	Mitsunobu	$CH(CH_2CH_3)_2$	**12c**
11	Mitsunobu	*c*Hex	**12d**
11	Alkylation	*c*Pent	**12e**

Table 2. Summary of compounds subjected to acylation with 2-chloroacetyl chloride.

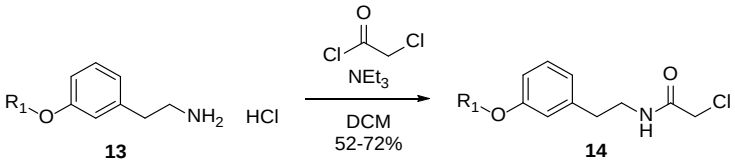

Starting Material ID	R_1	Product ID
13a	*i*Pr	**14a**
13b	*i*Bu	**14b**
13c	$CH(CH_2CH_3)_2$	**14c**
13d	*c*Hex	**14d**
13e	*c*Pent	**14e**
13f	Me	**14f**
13g	Et	**14g**

Table 3. Summary of α-chloroamides subjected to alkylation conditions.

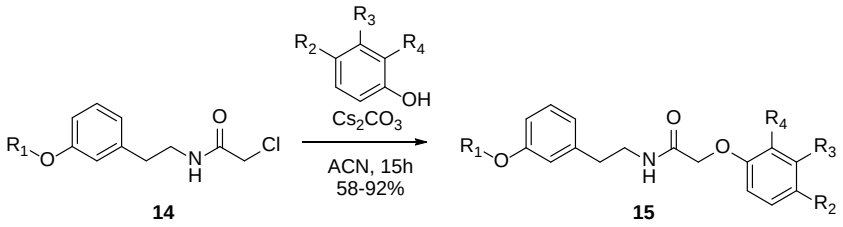

Starting Material ID	R_1	R_2	R_3	R_4	Product ID
14a	*i*Pr	OMe	H	H	**15a**
14a	*i*Pr	H	OMe	H	**15b**
14a	*i*Pr	H	H	OMe	**15c**
14a	*i*Pr	OEt	H	H	**15d**
14a	*i*Pr	O*i*Pr	H	H	**15e**
14b	*i*Bu	OMe	H	H	**15f**
14c	$CH(CH_2CH_3)_2$	OMe	H	H	**15g**
14d	*c*Hex	OMe	H	H	**15h**
14e	*c*Pent	OMe	H	H	**15i**
14e	*c*Pent	OEt	H	H	**15j**
14f	OMe	OMe	H	H	**15k**
14g	OEt	OEt	H	H	**15l**

Alternatively, C-rings containing oxygen functionality could also be installed using an Ullmann coupling sequence (**Scheme 3**). Bromide-substituted phenethylamine **16** was subjected to acylation conditions to yield amide **17**, and the chloride was then displaced by *para*-substituted phenols to give amides **18**. The bromide in compounds **18** were then exchanged for an iodide in an aromatic Finkelstein reaction[39] to give compounds **19**.

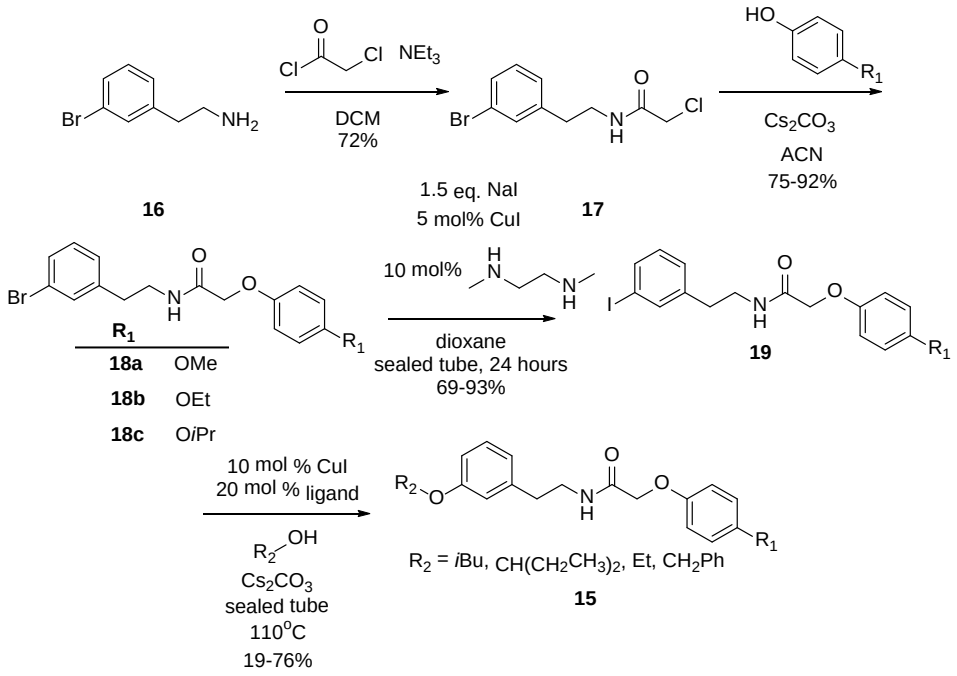

Scheme 3. Installation of oxygen-containing functionality on future C-ring via an Ullmann coupling.

The aryl iodide intermediate **19** was then reacted with a variety of alcohols (**Table 5**) in a copper-catalyzed coupling reaction[40] to yield amide **15** in an alternative fashion to that shown in **Scheme 1**. A number of ligands and conditions were screened to optimize the Ullmann copper coupling (**Table 4**).

Table 4. Screening conditions to optimize Ullmann copper coupling.

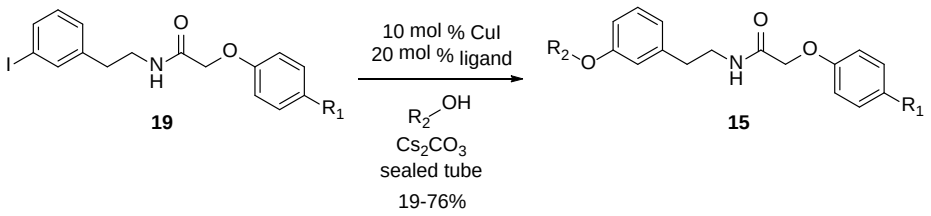

	Alcohol	Ligand	Temp	Time	Yield
1	Isobutanol	1,10-phen	110°C	48 hrs	39%
2	Isobutanol	1,10-phen	110°C	24 hrs	36%
3	3-Pentanol	1,10-phen	110°C	24 hrs	19%
4	2-Phenylethanol	1,10-phen	110°C	24 hrs	50%
5	2-Phenylethanol	3,4,7,8-tetramethyl-1,10-phen	110°C	24 hrs	47%
6	Benzyl alcohol	3,4,7,8-tetramethyl-1,10-phen	110°C	24 hrs	32%
7	Benzyl alcohol	3,4,7,8-tetramethyl-1,10-phen	80°C	24 hrs	76%
8	Benzyl alcohol	1,10-phen	80°C	24 hrs	68%
9	3-Pyridinylmethanol	3,4,7,8-tetramethyl-1,10-phen	80 to 110°C	48 hrs	30%
10	2-Phenylethanol	*N,N*-dimethylethylenediamine	110°C	24 hrs	-
11	2-Phenylethanol	tetramethylethylenediamine	110°C	24 hrs	23%
12	2-Phenylethanol	*N,N*-dimethylglycine	110°C	24 hrs	40%

It has been reported that bidentate nitrogen ligands are most effective for achieving high yields in Ullmann copper couplings[41], and initial conditions (reactions 1 - 4) utilized a catalytic system composed of 1,10-phenanthroline, CuI, and Cs_2CO_3 at 110°C[40]. Under these conditions, the yield appears to be substrate dependent as the primary alcohol gave higher yields than secondary linear and cyclic alcohols. It did not appear as if reaction time impacted the yield significantly; at 24 hours and at 48 hours, the coupling with isobutanol gave similar yields.

Since 1,10-phenanthroline was only giving modest yields, other ligands were explored for the reaction. It has been reported that the electron-donating methyl groups on the pyridine ring of 3,4,7,8-tetramethyl-1,10-phenanthroline make the ligand more efficient in these copper couplings[42]. The alkyl substituents most likely help to solubilize the active copper catalyst, but also the electron donation of the methyl groups increases the electron density of the carbon center, which in turn increases the sigma donating ability of the nitrogen to accelerate the oxidative addition step of the reaction[42]. Comparing reactions 4 and 5, the alcohol was kept constant as phenylethanol, but the

tetramethyl-substituted phenanthroline was used as an alternative to the unsubstituted 1,10-phentanthroline ligand. This however, made no significant difference in the yield of the reaction. It was expected that reaction 6 with benzyl alcohol would be the highest yielding coupling reaction since the alcohol is deprotonated prior to coordination to the copper, and benzyl alcohol is the most acidic alcohol in the optimization process. The reaction with benzyl alcohol only afforded 32% when the temperature was 110°C, but once the temperature was lowered to 80°C as in reaction 7, a significant increase in yield (76%) was observed.

Unfortunately, lowering the temperature when different alcohols were used, such as 3-pyridinylmethanol, did not result in higher yields like with benzyl alcohol. The lowered temperature combined with the use of the primary alcohol benzyl alcohol were the conditions most suitable for the conversion of aryl iodide **19** to compound **15**.

N,N-dimethylethylenediamine, which was the ligand for the aromatic Finkelstein reaction, resulted in product, but it was unfortunately too reactive; a prominent side product was a compound where the ligand had actually coupled instead of the alcohol. The product yield was not measured when it became apparent by LCMS that both were forming during the reaction. Tetramethylethylenediamine (reaction 11) was also tested as a ligand since it would be unable to couple to the aryl iodide, but the yield was only 23%. *N,N*-dimethylglycine (reaction 12) as a ligand[43] did not appear to offer any advantages over the phenanthroline based ligands either as the yield was only 40%.

Table 5. Compounds subjected to Ullmann copper-catalyzed coupling to attach oxygen functionality.

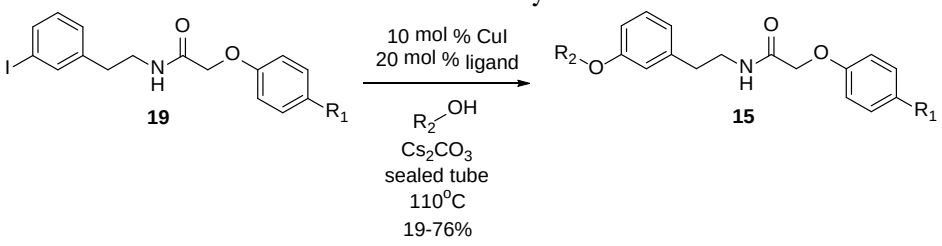

Starting Material ID	R_1	R_2	Product ID
19a	OMe	OEt	**15m**
19b	OEt	O*i*Bu	**15n**
19b	OEt	$OCH(CH_2CH_3)_2$	**15o**
19c	O*i*Pr	O*i*Bu	**15p**
19a	OMe	OBn	**15q**
19b	OEt	OBn	**15r**

It was not expected that isopropanol as an alcohol in the coupling reactions would result in high yields since secondary alcohol 3-pentanol resulted in only 19% yield. To circumvent the coupling of isopropanol and to take advantage of the success of phenylmethanol in the Ullmann coupling, a three step-reaction pathway was utilized to install the isopropoxy functionality on the linear amides (**Scheme 4**). Once the benzyloxy linear amides **15** were synthesized using the previously described conditions, the benzyl group could be removed in a palladium-catalyzed hydrogenation to give compounds **20**, which could be alkylated with 2-iodopropane to afford isopropoxy containing compounds **15a** and **15e**. Although this method was only used to make isopropoxy compounds (because the isopropyl group is so fundamental to this project that large quantities were needed), by this method any oxygen-containing functionality could be installed regardless of how amenable its alcohol counterpart performs in the Ullmann copper coupling or the Mitsunobu reaction as in **Scheme 2**. The alkylation reactions on compounds **20** using alkyl halides was also more successful than the alkylation reactions on compounds **11** in **Scheme 1** because compounds **11** have an electron-withdrawing Boc-group, which makes compounds **11** poor nucleophiles for attack on the alkyl halide.

The phenols on compounds **20** do not have this group, which makes these intermediates better-suited nucleophiles for an alkylation with primary and secondary alkyl halides.

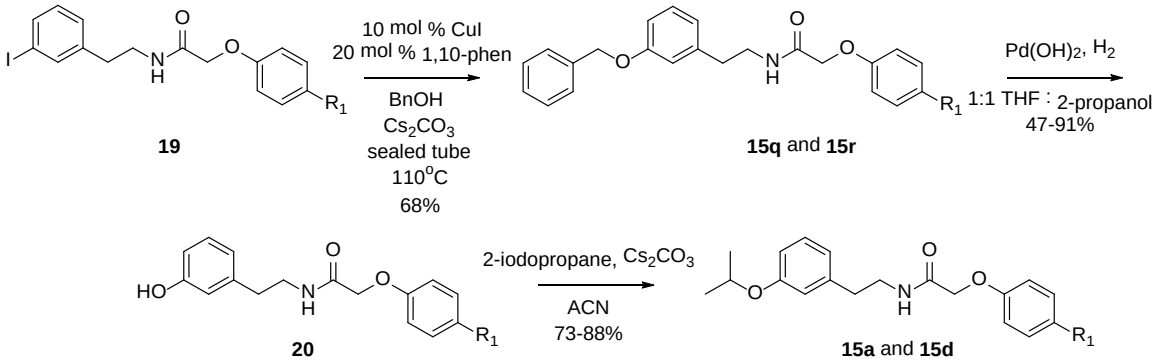

Scheme 4. Installation of isopropoxy functionaliy on future C-ring.

2.3.2 Synthetic routes towards nitrogen-containing racemic tetrahydroisoquinoline-containing compounds

In addition to installing oxygen-containing moieties on the C-ring, nitrogen-containing compounds were also synthesized by more than one route. The first route began with commercially available nitro-substituted phenethylamine hydrochloride salt **21,** which involved an acylation and subsequent alkylation of *para*-methoxyphenol to afford amide **23**. Utilizing hydrogenolysis the nitro functionality was then reduced to aniline **24,** which was subjected to reductive amination conditions[44] to yield the dimethylamino-containing amide **25a** (**Scheme 5**).

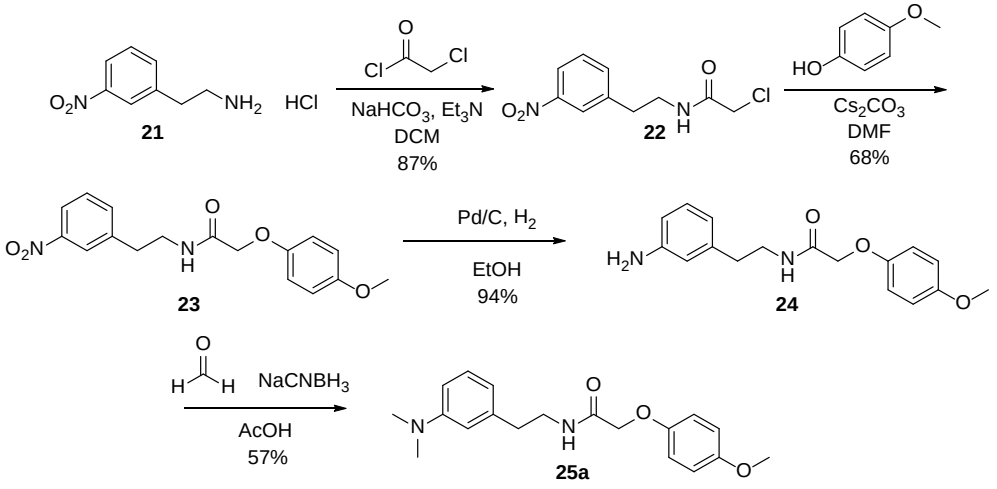

Scheme 5. Synthesis of dimethylamino functionality on future C-ring.

Although this synthetic route can be utilized to synthesize a number of compounds since many different amines could be installed via reductive amination of intermediate **24**, the aryl iodide **19** also provided an opportunity for a divergent synthesis.

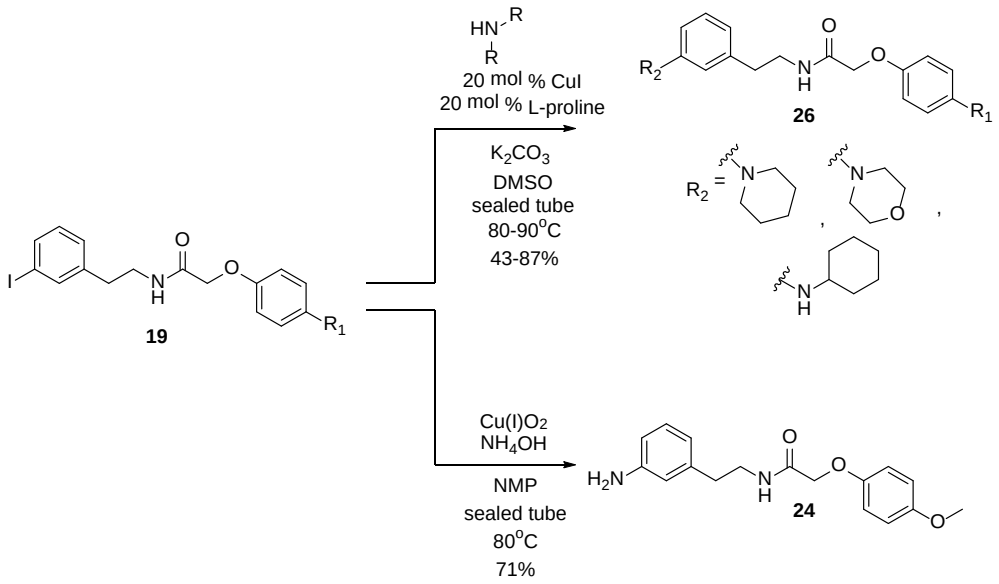

Scheme 6. Installation of nitrogen-containing functionality on future C-ring.

The aryl iodide in intermediate **19** can also be directly converted to nitrogen functionality by one of two methods shown in **Scheme 6**. Compound **19** was subjected to Ullmann copper-catalyzed coupling[45] with cyclohexylamine or a variety of cyclic amines to afford the mono- or disubstituted anilines **26** (**Table 6**). An alternate copper-catalyzed reaction[46] of aryl halide **19** and aqueous ammonia afforded aniline **24**, which following two separate reductive amination steps also afforded isopropylamino-containing amide **25b** and isopropyl(methyl)amino-containing amide **25c** (**Scheme 7**).

Table 6. Compounds subjected to Ullmann copper-catalyzed coupling to attach nitrogen functionality.

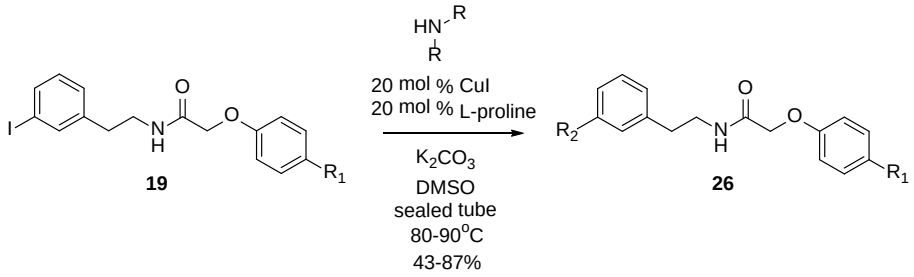

Starting Material ID	R_1	R_2	Product ID
19a	OMe	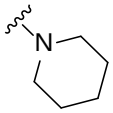	**26a**
19a	OMe	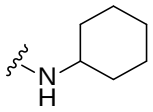	**26b**
19a	OMe	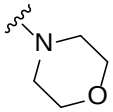	**26c**
19b	OEt	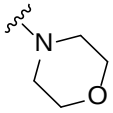	**26d**

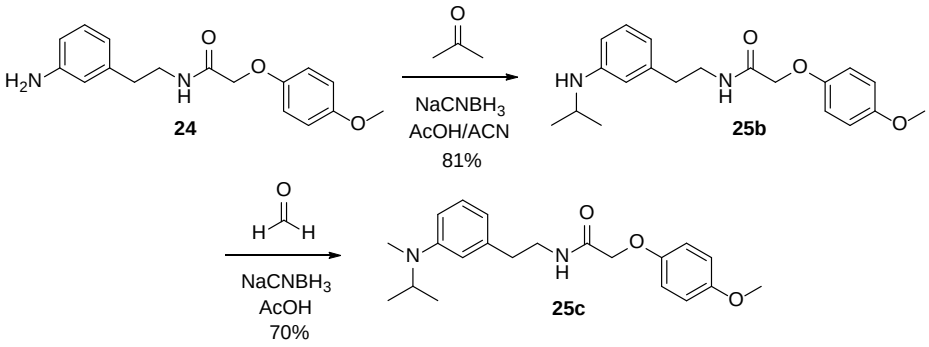

Scheme 7. Reductive animation to afford substituted amines on future C-ring.

2.3.3. Steps to cyclize tetrahydoisoquinoline compounds and installation of the A-ring

Oxygen or nitrogen-containing intermediates **15, 25,** and **26** were then cyclized using Bischler-Napieralski conditions to form the dihydroisoquinolines **27**, which were reduced with sodium

borohydride to afford tetrahydroisoquinolines **28**[47] (**Scheme 8**). All linear amides subjected to these conditions are listed in **Table 7**.

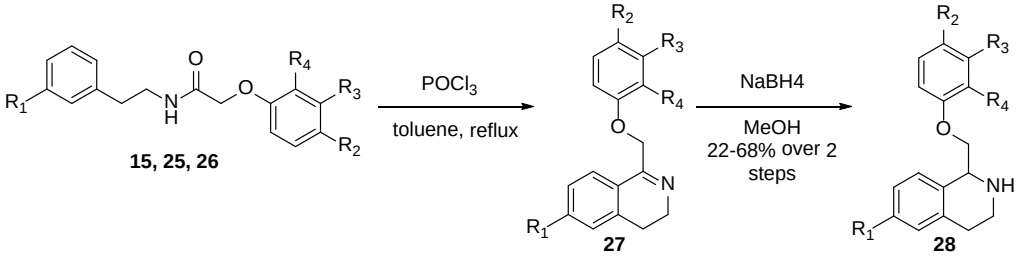

Scheme 8. Cyclization and reduction to afford tetrahydroisoquinoline scaffold.

Table 7. Compounds subjected to cyclization and reduction.

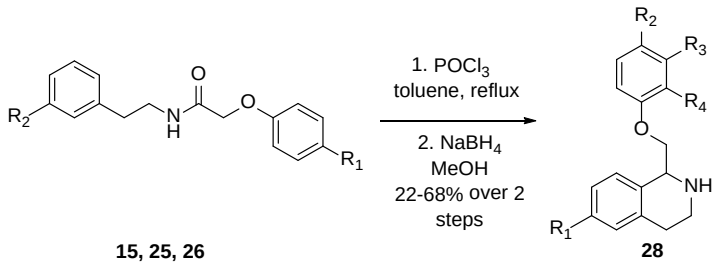

15, 25, 26 **28**

Starting Material ID	R_1	R_2	R_3	R_4	Product ID
15a	O*i*Pr	OMe	H	H	**28a**
15b	O*i*Pr	H	OMe	H	**28b**
15c	O*i*Pr	H	H	OMe	**28c**
15d	O*i*Pr	OEt	H	H	**28d**
15e	O*i*Pr	O*i*Pr	H	H	**28e**
15f	O*i*Bu	OMe	H	H	**28f**
15n	O*i*Bu	OEt	H	H	**28g**
15p	O*i*Bu	O*i*Pr	H	H	**28h**
15g	$OCH(CH_2CH_3)_2$	OMe	H	H	**28i**
15o	$OCH(CH_2CH_3)_2$	OEt	H	H	**28j**
15i	O*c*Pent	OMe	H	H	**28k**
15j	O*c*Pent	OEt	H	H	**28l**
15h	O*c*Hex	OMe	H	H	**28m**
15m	OMe	OEt	H	H	**28n**
15l	OEt	OEt	H	H	**28o**
25a	NMe_2	OMe	H	H	**28p**
26a	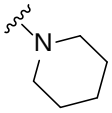	OMe	H	H	**28q**
26b	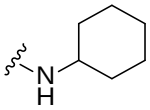	OMe	H	H	**28r**
26c	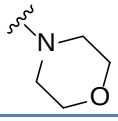	OMe	H	H	**28s**
26d	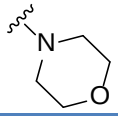	OEt	H	H	**28t**
25b	NH*i*Pr	OMe	H	H	**28u**
25c	N*i*PrMe	OMe	H	H	**28v**

Tetrahydroisoquinolines **28** were then either acylated with a variety of benzoyl chlorides or were subjected to EDCI coupling to afford final compounds. Compound **1180-141** was synthesized via a reduction of the nitro-containing compound **1180-142**. Compound **1180-89** required removal of the TBDMS protecting group on compound **30** and compound **1180-321** required the removal of the benzyl protecting group on compound **1180-320** (**Scheme 9**). All final compounds are listed in **Table 8** and **Table 9**.

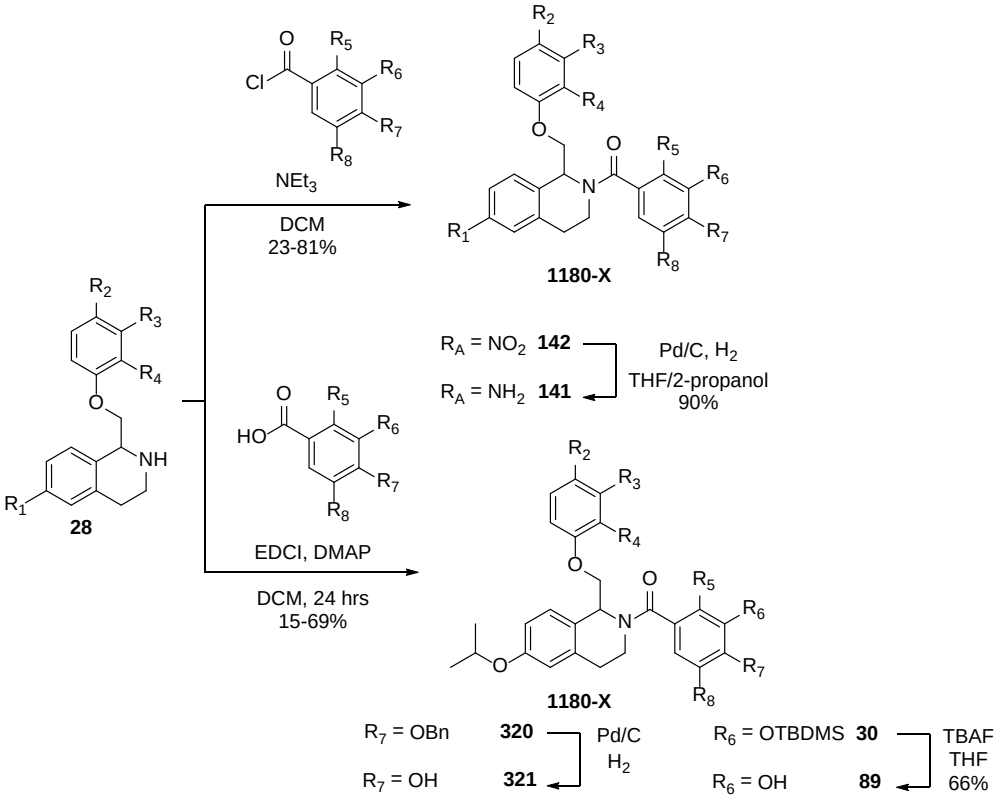

Scheme 9. Installation of A-ring via an acylation or EDCI coupling.

Table 8. Summary of compounds with isopropoxy functionality on C-ring.

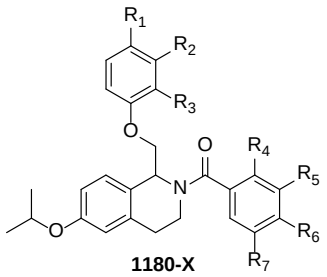

1180-X

1180-X	R_1	R_2	R_3	R_4	R_5	R_6	R_7
55	OMe	H	H	H	Cl	H	H
82	H	OMe	H	H	Cl	H	H
84	H	H	OMe	H	Cl	H	H
88	OMe	H	H	H	Br	H	H
140	OMe	H	H	H	F	H	H
153	OMe	H	H	H	I	H	H
89	OMe	H	H	H	OH	H	H
91	OMe	H	H	H	CF_3	H	H
142	OMe	H	H	H	NO_2	H	H
141	OMe	H	H	H	NH_2	H	H
90	OMe	H	H	H	H	Cl	H
85	OMe	H	H	H	H	OMe	H
319	OMe	H	H	H	H	OCF_3	H
320	OMe	H	H	H	H	OBn	H
321	OMe	H	H	H	H	OH	H
83	OEt	H	H	H	Cl	H	H
86	OEt	H	H	H	Br	H	H
87	OEt	H	H	H	F	H	H
92	OEt	H	H	H	CF_3	H	H
100	OEt	H	H	H	H	H	H
102	OEt	H	H	H	Ph	H	H
129	OEt	H	H	H	Me	H	H
130	OEt	H	H	H	OMe	H	H
132	OEt	H	H	H	H	Cl	H
133	OEt	H	H	H	H	F	H
148	OEt	H	H	Cl	H	H	H
147	OEt	H	H	F	H	H	H
131	OEt	H	H	H	H	Me	H
103	OEt	H	H	H	Cl	Cl	H
134	OEt	H	H	H	F	F	H
144	OEt	H	H	H	Cl	F	H
101	OEt	H	H	H	Cl	H	Cl
264	O*i*Pr	H	H	H	Cl	H	H
270	O*i*Pr	H	H	H	F	H	H
271	O*i*Pr	H	H	H	CF_3	H	H

Table 9. Summary of final compounds with modified C-ring functionality.

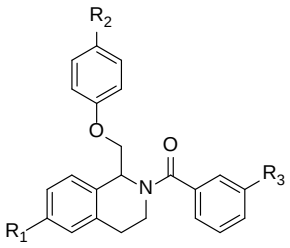

1180-X

1180-X	R_1	R_2	R_3
106	O*c*Pent	OMe	Br
110	O*c*Pent	OEt	Cl
111	O*c*Pent	OEt	Br
112	O*c*Pent	OEt	F
107	O*c*Hex	OMe	Cl
108	O*c*Hex	OMe	Br
109	$OCH(CH_2CH_3)_2$	OMe	Cl
125	$OCH(CH_2CH_3)_2$	OEt	F
114	O*i*Bu	OMe	Cl
115	O*i*Bu	OMe	Br
124	O*i*Bu	OEt	Cl
126	O*i*Bu	OEt	F
139	O*i*Bu	O*i*Pr	Cl
152	OEt	OMe	Cl
268	OEt	OEt	Cl
269	OEt	OEt	F
104	NMe_2	OMe	Cl
105	NMe_2	OMe	Br
146	NMe*i*Pr	OMe	Cl
145	NMe*i*Pr	OMe	Br
150	NH*i*Pr	OMe	Cl
116	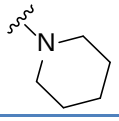	OMe	Cl
119	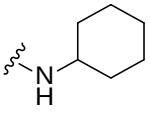	OMe	Cl
120	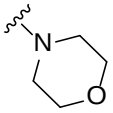	OMe	Cl
121	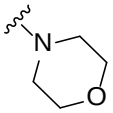	OMe	Br

127	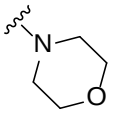	OEt	Cl
128	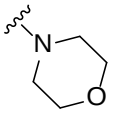	OEt	F

A number of compounds were then converted from amides to thioamides using Lawesson's reagent[48]. This reaction was completed either by refluxing in toluene or by microwave convection (**Table 10**).

Table 10. Summary of final compounds converted from amides to thioamides.

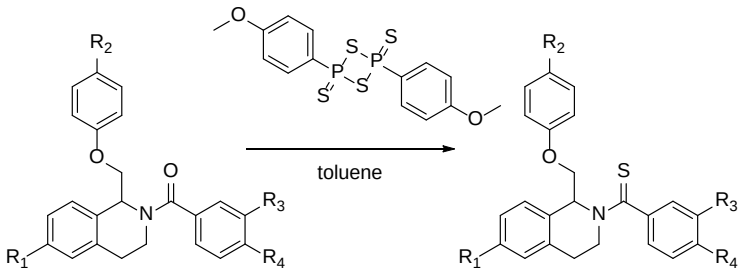

Starting Material ID	Reaction Conditions	Yield	R_1	R_2	R_3	R_4	Product ID
1180-55	Reflux (4 hrs)	68%	O*i*Pr	OMe	Cl	H	**1180-163**
1180-140	Reflux (4 hrs)	65%	O*i*Pr	OMe	F	H	**1180-166**
1180-83	Reflux (2 hrs)	34%	O*i*Pr	OEt	Cl	H	**1180-149**
1180-86	Reflux (2 hrs)	35%	O*i*Pr	OEt	Br	H	**1180-156**
1180-87	Reflux (4 hrs)	68%	O*i*Pr	OEt	F	H	**1180-154**
1180-92	Reflux (4 hrs)	56%	O*i*Pr	OEt	CF_3	H	**1180-168**
1180-103	Reflux (2 hrs)	43%	O*i*Pr	OEt	Cl	Cl	**1180-155**
1180-144	Reflux (4 hrs)	35%	O*i*Pr	OEt	Cl	F	**1180-165**
1180-131	MW: 150°C for 35 min	50%	O*i*Pr	OEt	H	Me	**1180-304**
1180-132	MW: 150°C for 35 min	70%	O*i*Pr	OEt	H	Cl	**1180-305**
1180-264	MW: 150°C for 30 min	51%	O*i*Pr	O*i*Pr	Cl	H	**1180-265**
1180-270	MW: 150°C for 35 min	67%	O*i*Pr	O*i*Pr	F	H	**1180-272**
1180-271	MW: 150°C for 35 min	69%	O*i*Pr	O*i*Pr	CF_3	H	**1180-273**
1180-112	Reflux (4 hrs)	41%	*c*Pent	OEt	F	H	**1180-162**
1180-126	Reflux (4 hrs)	59%	O*i*Bu	OEt	F	H	**1180-169**
1180-268	Reflux (4 hrs)	12%	OEt	OMe	Cl	H	**1180-170**
1180-104	Reflux (4 hrs)	48%	NMe_2	OMe	Cl	H	**1180-167**

Finally, linkers from the core to the A-ring alternative to amides and thioamides were explored. The sulfonamide-containing **1180-199** was synthesized by reacting tetrahydroisoquinoline **28d** with 3-chlorobenzene-1-sulfonyl chloride, and the thiourea and urea linkers were synthesized via a reaction with tetrahydroisoquinoline **28d** and 1-chloro-3-isothiocyanatobenzene or 1-chloro-3-isocyanatobenzene, respectively (**Scheme 10**).

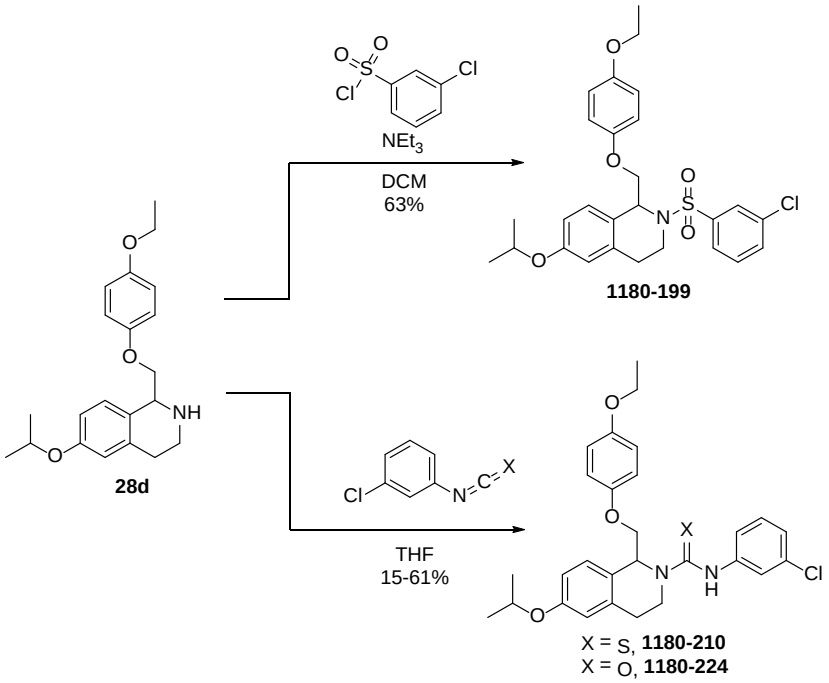

Scheme 10. Synthesis of sulfonamide, thiourea, and urea-containing compounds.

2.3.4. Synthesis of 1180-55 and 1180-163 enantiomers

All compounds with GluN2B activity had been synthesized as racemic mixtures and therefore synthesizing or separating the enantiomers was pursued to explore the stereospecificity of the NMDA receptor activity. When the enantiomers of CIQ were separated, only the (+)-enantiomer was active at GluN2C and GluN2D-containing NMDA receptors, while the (-)-enantiomer was inactive[49], but it was unknown in which enantiomer the GluN2B-activity would reside.

The initial plan for the synthesis of the **1180-55** enantiomers was to install a second chiral center, which would allow for the separation via a diastereomeric mixture (**Scheme 11**). This chiral center could be removed following separation of the diastereomers, and then the resulting amine could be acylated with 3-chlorobenzoyl chloride to give both the (*S*)- and (*R*)-enantiomer.

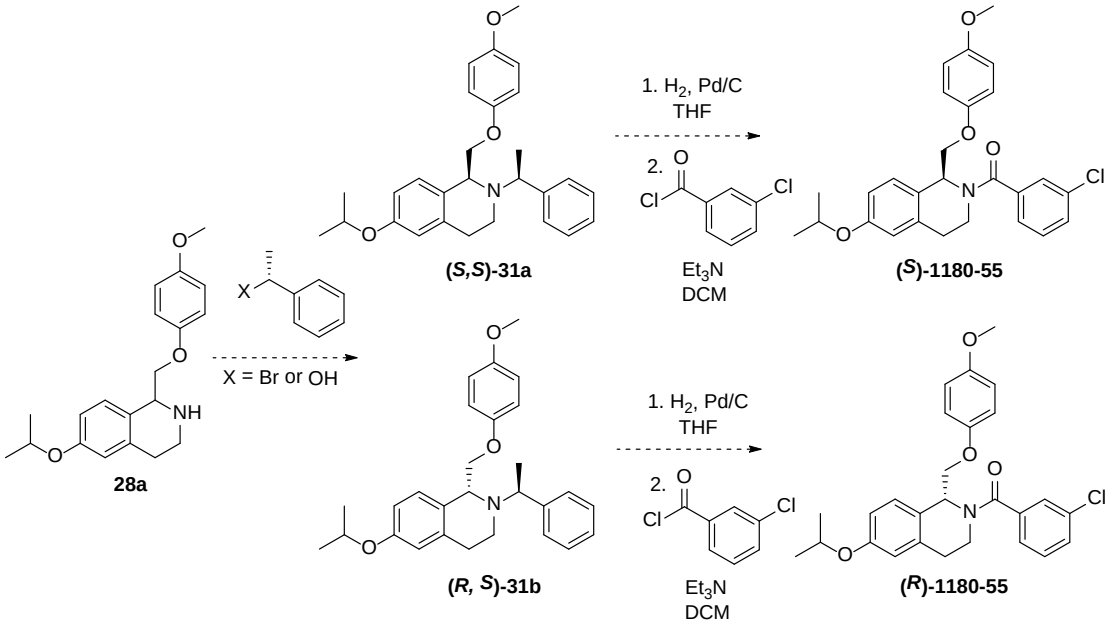

Scheme 11. Proposed route for separation of 1180-55 enantiomers via a diastereomeric mixture.

To ensure that the diastereomers could be synthesized, first a diastereomeric mixture was synthesized from racemic starting materials by an alkyation reaction[50] with tetrahydroisoquinoline **28a** and racemic (1-bromoethyl)benzene **32** (**Scheme 12**). This racemic mixture of diastereomers was separated via column chromatography using a 7:1 hexanes:EtOAc mixture spiked with 2.8% NEt_3.

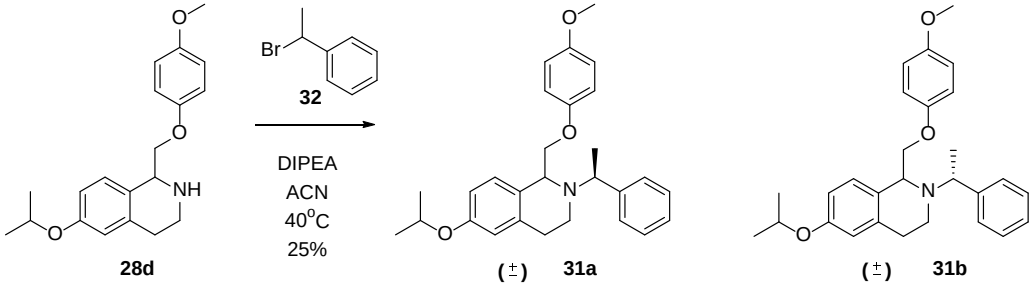

Scheme 12. Synthesis of racemic diastereomeric mixture for separation of 1180-55 enantiomers.

Although this alkylation yielded separable products, the conditions would not be suitable for the synthesis of non-racemic diastereomers because (1-bromoethyl)benzene **32** is not sold in enantiomerically pure form. The synthesis of (*S*)-(1-bromoethyl)benzene **32** was envisioned to come from an Appel reaction with (*R*)-1-phenylethanol **33**, however when this reaction was conducted,

chirality of the bromo-compound was lost (**Scheme 13**). Most likely a different solvent choice would have resulted in a product with a preference for the (*S*)-configuration.

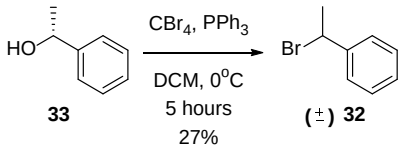

Scheme 13. Attempted synthesis of chiral (1-bromoethyl)benzene via an Appel reaction.

The importance of the solvent in the above Appel reaction can be explained by the mechanism. During the third step of the reaction shown with carbon tetrachloride (**Scheme 14**), the chloride ion attacks the carbon alpha to the alcohol to form the alkyl halide and triphenphosphine oxide as the byproduct, and this decomposition most likely takes places via a tight ion-pair (**Scheme 14**)[51–53].

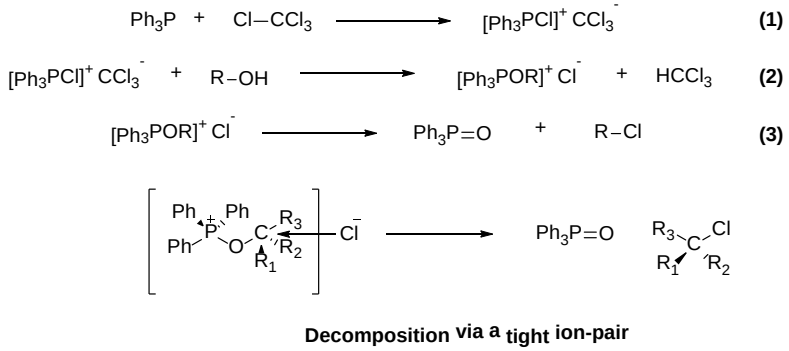

Scheme 14. Appel reaction mechanism.

In this S_N2 displacement from a tight ion pair, the solvent choice is critical. A polar aprotic solvent, such as DMF or ACN, would help to promote the S_N2 reaction, and a solvent with a small dielectric constant, ε, (cyclohexane, hexane, toluene, or carbon tetrachloride) generally confers high ion-pairing. DCM has a dielectric constant of 8.9, meaning it is not an optimal solvent for a reaction that requires a tight-ion pair to successfully invert the stereochemistry. While polar aprotic solvents are well suited for S_N2 reactions, it has been shown that ACN as a solvent causes a loss in stereochemistry with tertiary alcohols[54]. This suggests that dielectric constant is probably more important, although PPh_3 tends to be insoluble in nonpolar solvents that have the appropriate dielectric constant.

For these reasons, an alternative method for the synthesis of the diastereomers was sought where the chiral center would be installed prior to the Bischler-Naperielski cyclization (**Scheme 15**). Previous research had demonstrated that the chiral methylbenzyl group can act direct the stereochemistry of nearby or adjacent reaction centers[55–57]. However, this chiral reduction was reported to require a temperature of -78°C, so when conducted at only 0°C, it was anticipated that the reaction would result in a mixture of diastereomers, even if one conformation was preferred.

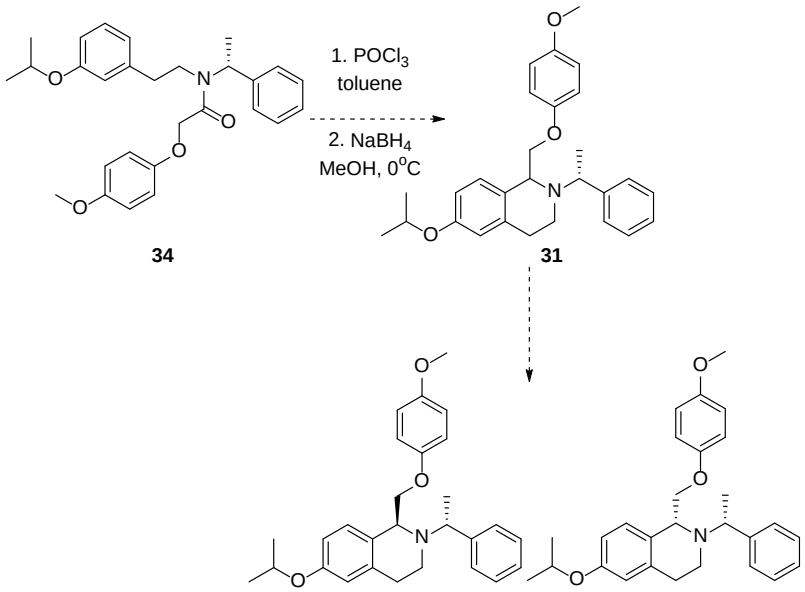

Scheme 15. Installation of chiral center to result in a diastereomeric mixture following reduction.

Even though the literature suggested that the reduction required a temperature of -78°C to be stereoselective, at 0°C the diastereomeric ratio of **31** was 95:5 and only one diastereomer was isolated (**Scheme 16**). For reduction of this particular tetrahydroisoquinoline such stringent temperature requirements do not need to be met for a stereoselective reduction.

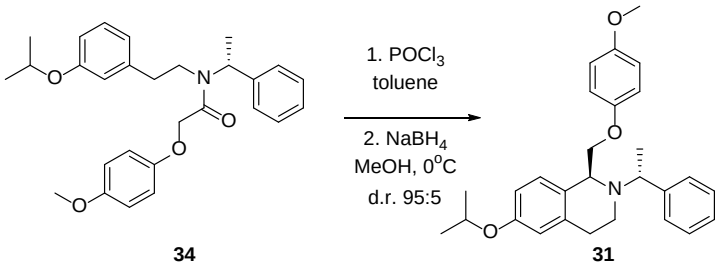

Scheme 16. Isolation of only one diastereomer following the reduction at 0°C.

Based on the rationale shown in **Scheme 17**, the (*R*)-imine is proposed to give an amine product with (*S*, *R*) stereochemistry. The iminium exists as a flat portion of the molecule, and $A^{1,3}$ strain would exist if the methyl group of the chiral directing group were in the plane, making it much more likely that the hydrogen would exist in the plane of the iminium[55]. In this conformation, the hydride would then attack from the *Si* face that is opposite to the large phenyl group, resulting in (*S*, *R*) stereochemistry (**Scheme 17**).

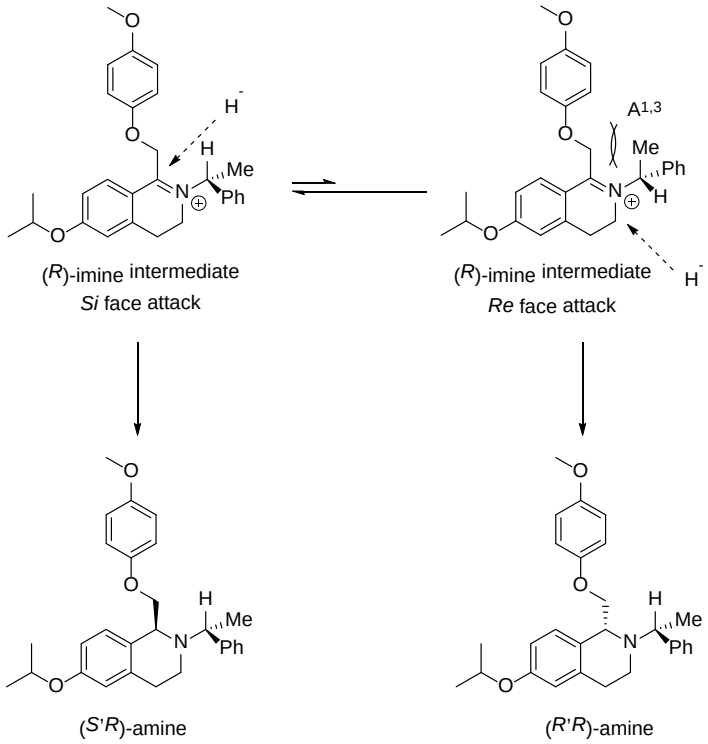

Scheme 17. Proposed rationale to explain the stereoselectivity of the sodium borohydride reduction.

Since the cyclization and reduction of (*R*)-amide **34** (**Scheme 16**) resulted in the isolation of only the (*S*, *R*)-diastereomer, the (*R*, *S*)-diastereomer needed to be synthesized. The synthesis of both diastereomers began with the reduction of 2-(3-hydroxyphenyl)acetic acid **35** to give phenol **36**, which was then alkylated to yield alcohol **37**. Using an Appel reaction, compound **37** was converted to compound **38**, which was then subjected to Finkelstein reaction conditions to yield compound **39**. Either enantiomer of chiral amine **40** was then alkylated with compound **39** to give (*S*) and (*R*)-**41**, which following an acylation, could be alkylated to yield (*S*) and (*R*)-**34**. Utilizing Bischler-Napieralski conditions, (*S*) and (*R*)-**34** were cyclized to give imines **43**, which were reduced with sodium borohydride to yield chiral tetrahydroisoquinolines **31**. The chiral-directing group was then removed by hydrogenolysis to give amine (*S*) and (*R*)-**28**, which were acylated to separately yield both enantiomers of compound **1180-55.** Amide-containing compounds were then converted to thioamide-containing compounds **1180-163** by refluxing with Lawesson's reagent in toluene (**Scheme 18**).

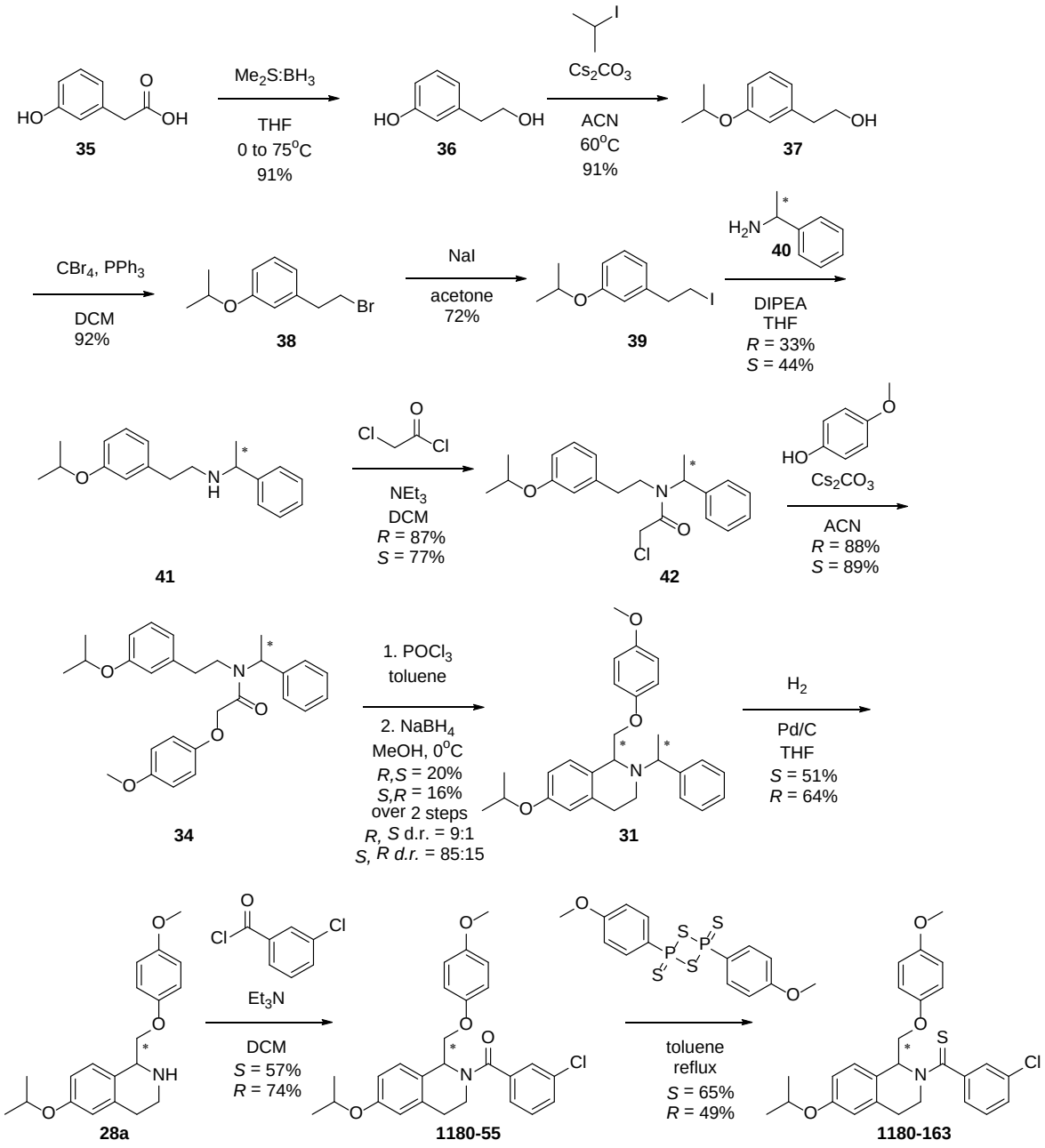

Scheme 18. Synthesis of 1180-55 and 1180-163 enantiomers.

It proved difficult to obtain a crystal structure of either of the amide-containing **1180-55** enantiomers, but once the amide of each enantiomer was converted to thioamide compound **1180-163**, the addition of a heavy sulfur atom allowed for easier crystallization, and a crystal structure of *S*-(-) enantiomer **1180-163** using X-ray crystallography was obtained (**Figure 14**). This confirmed that the

model proposed in the literature[1,49,55] (**Scheme 17**) for the stereoselective reduction of the imine is correct.

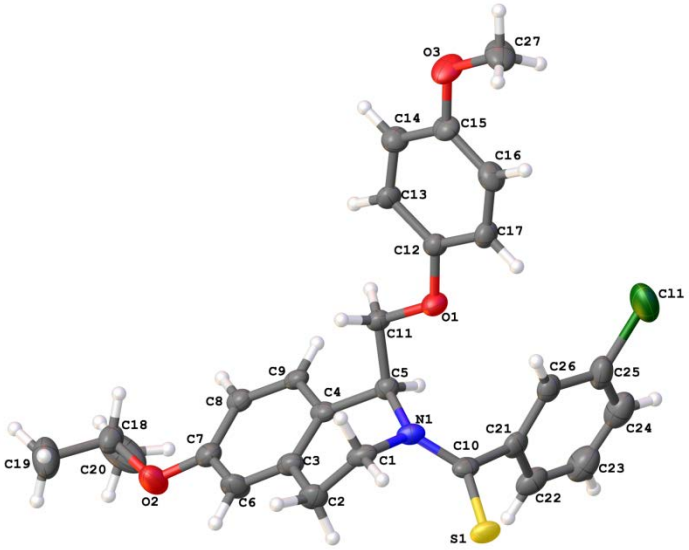

Figure 14. Crystal structure of (*S*)-(-)-1180-163.

2.3.5. Separation of 1180-87, 1180-103, and 1180-92 via chiral prep chromatography

Although the synthesis of **1180-55** and **1180-163** enantiomers was successful, the synthesis was resource and time intensive in that it lacked divergence and required two separate syntheses, one synthesis for each enantiomer. For this reason, separation via semi-prep chiral chromatography was explored for the separation of enantiomers of interest, and enantiomers **1180-87**, **1180-103**, and **1180-92** were separated using an AD-H semi-prep column (**Scheme 19**). This provides a method to separate any compound of the **1180-55** series. Both enantiomers of compound **1180-87** and **1180-92** were then converted to thioamide-containing enantiomers **1180-154** and **1180-168**, respectively, with Lawesson's reagent (**Table 11**).

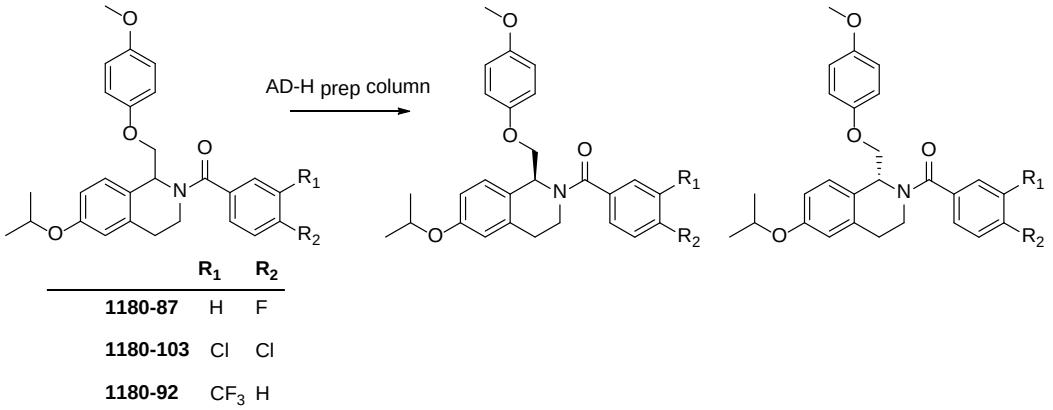

Scheme 19. Separation of 1180-87, 1180-103, and 1180-92 enantiomers via AD-H semi-prep column chromatography.

Table 11. Summary of separated enantiomers converted from amides to thioamides.

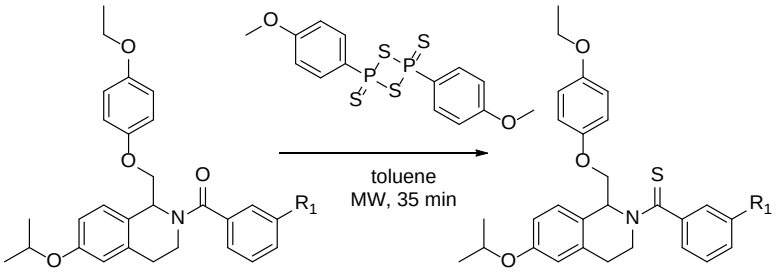

Starting Material ID	Yield	R_1	Product ID
(*S*)-(-)-1180-87	56%	F	**(*S*)-(-)-1180-154**
(*R*)-(+)-1180-87	65%	F	**(*R*)-(+)-1180-154**
(-)-1180-92	50%	CF_3	**(*S*)-(-)-1180-168**
(+)-1180-92	48%	CF_3	**(*R*)-(+)-1180-168**

The stereochemistry of **1180-87** and **118-154** enantiomers were assigned by comparing optical rotation values and retention times on the analytical HPLC to the **1180-163** enantiomers since the stereochemistry of this pair could be defined based on the (*S*)-(-)-**1180-63** crystal structure (**Figure 14**). To determine the stereochemistry of **1180-92** and **1180-168**, crystals were grown of **1180-168** enantiomers. At the time of this publication, the crystal structure is being resolved.

2.3.6. Synthesis of compounds for initial photoaffinity labeling experiments.

To test the viability of photoaffinity labeling experiments, first compounds needed to be synthesized with photoaffinity labels to ensure that scaffolds with this functionality did not eliminate activity at the NMDA receptor. Originally, the benzophenone functionality was installed on tetrahydroisoquinoline **23s** via an EDCI coupling to yield compound **1180-135** (**Scheme 20**).

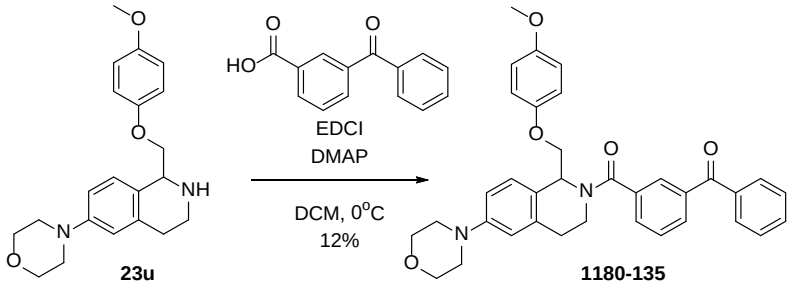

Scheme 20. Synthesis of 1180-135.

There was also interest in installing an azide, and this was originally attempted with a copper coupling[58] to convert **1180-105** into azide-containing tetrahydroisoquinoline **1180-143** (**Scheme 21**). No product was isolated, and instead the azide was installed via a diazotization of the aniline on **1180-141** with sodium nitrite under acidic conditions followed by the addition of sodium azide to produce **1180-143**[59] (**Scheme 22**).

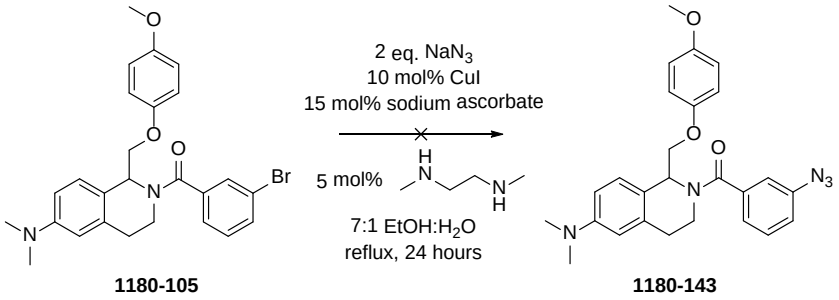

Scheme 21. Attempted conversion from 1180-105 to 1180-143.

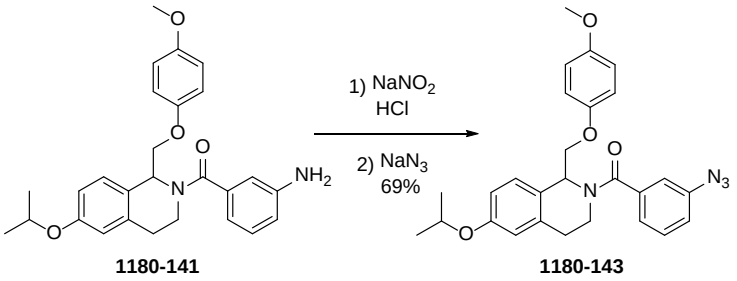

Scheme 22. Synthesis of azide-containing 1180-143 from 1180-141.

In addition to installing functionalities with the ability to photocrosslink, it would also be necessary to determine if the tetrahydroisoquinoline scaffold was amenable to an alkyne since it was imagined that an alkyne would participate in a [3 + 2] cycloaddition reaction with azide functionalized biotin (**8**) to install the biotin tag. The transformation from **1180-153** to final product **1180-282** (**Scheme 23**) was done in two steps: a Sonogashira coupling to install the protected alkyne and removal of the TMS-group under mild basic conditions[60].

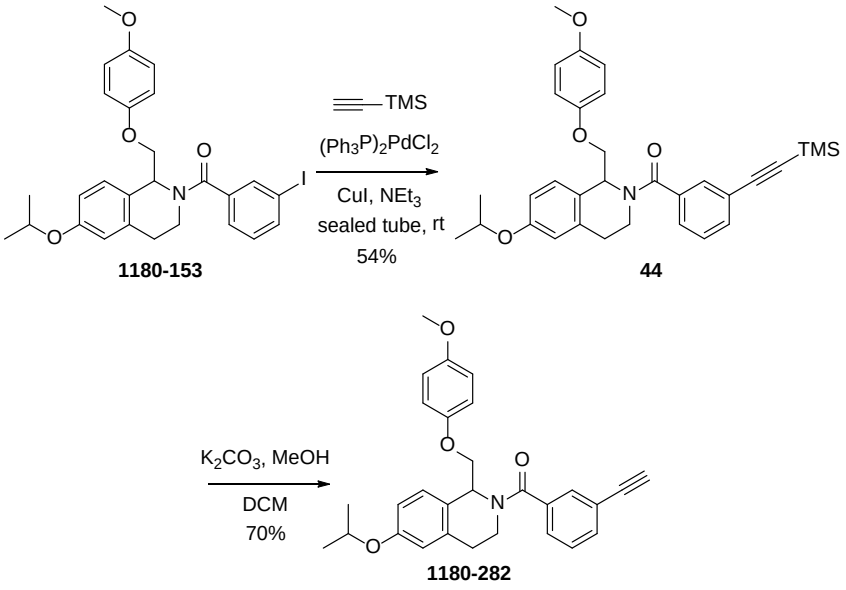

Scheme 23. Conversion of 1180-153 to alkyne-containing 1180-282.

2.4 Results and Discussion

All compounds were tested in Xenopus laevis expressing recombinant rat GluN1/GluN2A, GluN1/GluN2B, GluN1/GluN2C, and GluN1/GluN2D-containing receptors at saturating agonist

concentrations. Under these experimental conditions, the majority of compounds showed virtually no activity at GluN2A subunits, so the following tables only show data at GluN2B, GluN2C, and GluN2D subunits.

2.4.1 The effect of oxygen-containing functionality on the C-ring

A modification to the C-ring of the CIQ scaffold was responsible for the potentiation at the GluN2B-containing NMDA receptor, and for that reason a number of compounds were synthesized where the isopropoxy of **1180-55** was replaced with different ether-containing functionality. A number of compounds with branched, cyclic, and linear ethers were synthesized and tested against GluN2A-, GluN2B-, GluN2C-, and GluN2D-containing NMDA receptors. In order to evaluate whether other modifications to the C-ring would compare to **1180-55**, a variety of ether linked moieties were installed on compounds that contained the *para*-methoxy on the B-ring and a halogen in the *meta*-position on the A-ring (**Table 12**). Previously published compound **1180-26** with a methoxy in the R_1 position,[1] was selective for GluN2C and GluN2D subunits, but when the methoxy on the C-ring was replaced with an ethoxy group as in compound **1180-152**, potentiation occurred at the GluN2B subunit in addition to GluN2C and GluN2D. While **1180-152** was active at GluN2B, the branched and cyclic-containing compounds were more potent at the GluN2B subunit with lower EC_{50} values ranging from 1.1 μM to 5.0 μM compared to 7.5 μM and maximum percentage values in the 200 to 300% range compared to only 167%. Moving from an isopropoxy as in compounds **1180-55** and **1180-88** to a slightly larger isobutyl group as in **1180-114** and **1180-115** caused noticeable increases in terms of maximum percent as all three subunits. Compound **1180-114** potentiated GluN2C and GluN2D subunits with a maximum effect of 408% and 475%, respectively, and GluN2B at 335%, while isopropxy compounds typically only induced a maximum effect in the upper 200's at the three subunits. Notably, both compounds **1180-114** and **1180-115** also potentiate the GluN2A subunit, while isoproxy-containing compounds do not. Extending the length of the C-ring functionality from an isopropoxy to a pentan-3-yloxy retained the activity at GluN2B, and **1180-109** caused a maximum potentiation at this subunit of 339%, similar to isobutyl-containing compounds.

Extending functionality on the C-ring to either a cyclopentyl or cyclohexyl group, however, caused a loss in both EC_{50} value and maximum percentage compared to the isobutyl and pentan-3-yloxy-containing compounds. Based on this information, the trend for activity in terms of maximum effect at GluN2B is as follows: OMe < OEt < O*i*Pr ~ *c*Hex ~ *c*Pent < *i*Bu ~ pentan-3-yloxy. The effect is size dependent in that smaller groups (OMe and OEt) are inactive or weak potentiators, and larger groups, such as cyclopentyl and cylohexyl are weaker compared to isobutyl and pentan-3-yloxy-containing compounds. Despite this semblance of a trend, all the compounds were active at GluN2B, GluN2C, and GluN2D-containing receptors, and none of the compounds showed a selectivity profile that favored GluN2B.

Table 12. The effect of oxygen-containing functionality on the C-ring when the B-ring contains a *para*-methoxy group.

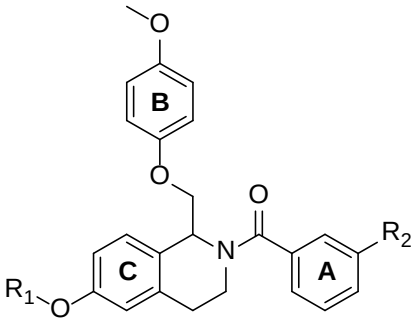

			$I_{30\mu M}$ / $I_{control}$ (mean ± SEM, %)			EC_{50} (max.) (μM %)[a]		
	R_1	**R_2**	**GluN2B**	**GluN2C**	**GluN2D**	**GluN2B**	**GluN2C**	**GluN2D**
26[c]	Me	Cl	90 ± 5.4	274 ± 20	215 ± 19	-	1.5 (204%)	1.9 (206%)
152	Et	Cl	158 ± 8.9	285 ± 23	329 ± 15	7.5 (167%)	2.9 (286%)	3.4 (332%)
55	*i*Pr	Cl	214 ± 7.3	243 ± 13	308 ± 17	5.0 (215%)	2.6 (250%)	4.3 (323%)
88	*i*Pr	Br	205 ± 14	290 ± 14	362 ± 18	3.6 (210%)	1.6 (299%)	2.2 (366%)
114[b]	*i*Bu	Cl	332 ± 19	393 ± 62	472 ± 70	1.4 (335%)[d]	1.2 (408%)	1.5 (475%)
115[b]	*i*Bu	Br	311 ± 13	300 ± 18	440 ± 4.8	1.1 (321%)	6.2 (309%)	1.5 (438%)
109[b]	$CH(CH_2CH_3)_2$	Cl	331 ± 17	286 ± 26	381 ± 40	1.8 (339%)	2.2 (300%)	2.3 (390%)
107	*c*Hex	Cl	259 ± 8.7	222 ± 19	309 ± 37	2.7 (261%)	2.0 (223%)	3.3 (304%)
108[b]	*c*Hex	Br	241 ± 29	210 ± 18	253 ± 4.1	3.8 (251%)	1.9 (213%)	3.2 (218%)
106[b]	*c*Pent	Br	225 ± 69	227 ± 29	276 ± 3.3	2.0 (224%)	2.0 (235%)	2.9 (277%)

[a]Fitted EC_{50} values are shown to two significant digits when potentiation at 30 μM exceeded 120%; values in parentheses are the fitted maximum response as a percentage of the initial glutamate (100 μM) and glycine (30 μM) current. Data are from between 7-27 oocytes from 2-5 frogs for each compound and receptor tested. [b]Potentiation at GluN2A was equal to or greater than 120% at 30 μM with BAPTA from between 4-14 oocytes from 1-3 frogs. This effect was not studied further. [c]Synthesized by Dr. Rose Santangelo-Freel. [d]p value <0.05 when comparing **1180-114** and **1180-55** EC_{50} value and max. response; p value <0.05 when comparing **1180-114** and **1180-107** max. response.

When the methoxy in the R_2 position was exchanged for an ethoxy (**Table 13**), selectivity did begin to emerge. Compound **1180-268** was inactive at all subunits, but once the ethoxy in the R_1 position on the C-ring was replaced with branched functionality, activity at the GluN2B subunit returned. Compounds **1180-83** and **1180-186** with an isopropoxy on the C-ring were only active at GluN2B and GluN2C subunits, while **1180-124** and **1180-110** were active at all three subunits. Compound **1180-111** was only slightly active at GluN2D with potentiation at 120% at 30 μM of compound though. With these examples, a clear trend is not immediately evident, but it would appear as if the combination of a *para*-ethoxy on the B-ring and an isopropxy on the C-ring leads to compounds that do not potentiate at GluN2D. Although **1180-124** with an isobutyl on the C-ring is not as selective as **1180-83** and **1180-86**, it is more efficacious at all three subunits with maximum effect values in the upper 200's and 300's; **1180-83** and **1180-86** do not have values that reach 200%. From this data set, isobutyl-containing compounds **1180-124**, **1180-114**, **1180-115** (from **Table 12**) emerge as the most potent and efficacious nonselective potentiators with activity at all four GluN2 subunits.

Table 13. The effect of oxygen-containing functionality on the C-ring when the B-ring contains a *para*-ethoxy group.

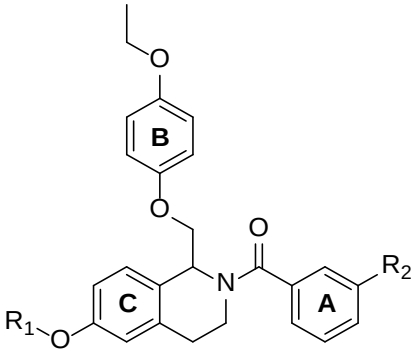

			$I_{30\mu M}$ / $I_{control}$ (mean ± SEM, %)			EC_{50} (max.) (μM %)[a]		
	R_1	**R_2**	**GluN2B**	**GluN2C**	**GluN2D**	**GluN2B**	**GluN2C**	**GluN2D**
268	Et	Cl	104 ± 2.7	91 ± 3.9	75 ± 2.7	-	-	-
83	*i*Pr	Cl	156 ± 8.4	126 ± 2.9	100 ± 1.8	5.7 (159%)	2.9 (121%)	-
86[b]	*i*Pr	Br	136 ± 7.9	133 ± 5.1	98 ± 1.9	3.9 (140%)	3.3 (132%)	-
124[b]	*i*Bu	Cl	294 ± 33	238 ± 11	342 ± 21	1.0 (305%)[c]	1.3 (240%)	1.7 (345%)
110	*c*Pent	Cl	213 ± 25	204 ± 13	193 ± 6.6	4.0 (210%)	4.4 (204%)	4.3 (188%)
111	*c*Pent	Br	224 ± 16	193 ± 15	120 ± 15	3.3 (227%)	4.0 (191%)	4.0 (132%)

[a]Fitted EC_{50} values are shown to two significant digits when potentiation at 30 μM exceeded 120%; values in parentheses are the fitted maximum response as a percentage of the initial glutamate (100 μM) and glycine (30 μM) current. Data are from between 7-13 oocytes from 2-3 frogs for each compound and receptor tested. [b]Potentiation at GluN2A was equal to or greater than 120% at 30 μM with BAPTA from between 4 oocytes from 1 frog. This effect was not studied further. [c] p value <0.05 when comparing **1180-124** and **1180-183** EC_{50} value and max. response; p value <0.05 when comparing **1180-124** and **1180-110** EC_{50}.

2.4.2 The effect of nitrogen-containing functionality on the C-ring

In addition to studying the effect of ether linked moieties on the C-ring, nitrogen-containing functional groups were also installed (**Table 14**). A number of mono- and di-substituted nitrogen-containing compounds were synthesized that were active at GluN2B, GluN2C, and GluN2D subunits. Compounds **1180-104** and **1180-105** with dimethyl functionality were GluN2C and GluN2D-selective, but when one of the methyl groups was replaced with an isopropyl group (**1180-145** and **1180-146**), GluN2B activity returned. Isopropylamino-containing compound **1180-150** was active at GluN2B, GluN2C, and GluND, but was much less potent at GluN2B compared to

isopropyl(methyl)amino-containing **1180-145** and **1180-146** with an EC_{50} value of 15 μM. Compound **1180-150** represents one of the only compounds synthesized with functionality on the C-ring that could act as a hydrogen bond donor, and it is one of the least potent compounds in the series at GluN2B. This could partially help to explain why **1180-150** is much less potent at GluN2B than its oxygen-containing counterpart **1180-55**.

Compounds **1180-116** and **1180-119** with bulky, nitrogen-containing functionality (a piperidine and a cyclohexane, respectively) on the C-ring have modest EC_{50} values at all three subunits, but a significant decrease was observed when the C-ring contained a morpholine group. This result confirms earlier observations (discussed in **Chapter 1.3.4**) that the binding pocket of the NMDA receptors is more amenable to **1180** compounds with hydrophobic functionality on the C-ring; heteroatoms placed anywhere on C-ring functionality other than alpha to the C-ring results in a significant loss in activity.

Overall, compounds with nitrogen-containing functionality were not selective for GluN2B, and were often not as potent at oxygen-containing compounds. Nitrogen-containing compounds do consistently give very robust potentiation at GluN2C and GluN2D though with maximum effect values often in the upper 300's and 400's; compound **1180-146** has a maximum effect of 536% at GluN2D. This effect was not studied further, but could act as a starting point to develop more efficacious GluN2C and GluN2D potentiators if nitrogen-containing compounds that do not potentiate GluN2B could be identified.

Table 14. The effect of nitrogen-containing functionality on C-ring.

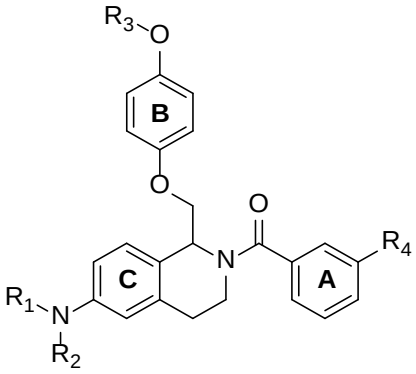

					$I_{30\mu M}$ / $I_{control}$ (mean ± SEM, %)			EC_{50} (max.) (μM %)[a]		
	R_1	R_2	R_3	R_4	GluN2B	GluN2C	GluN2D	GluN2B	GluN2C	GluN2D
104	Me	Me	Me	Cl	127 ± 4.1	288 ± 18	322 ± 20	6.5 (111%)	4.4 (310%)	4.7 (345%)
105	Me	Me	Me	Br	99 ± 3.6	285 ± 11	307 ± 18	_	2.5 (294%)	3.8 (319%)
146	Me	*i*Pr	Me	Cl	228 ± 12	404 ± 30	500 ± 56	6.0 (235%)	2.2 (428%)	4.3 (536%)
145[b]	Me	*i*Pr	Me	Br	216 ± 15	391 ± 49	456 ± 26	5.0 (218%)	2.7 (468%)	3.1 (474%)
150	H	*i*Pr	Me	Cl	138 ± 5.2	239 ± 14	333 ± 30	15 (151%)[c]	4.8 (252%)	5.9 (348%)
116	piperidine		Me	Cl	213 ± 20	289 ± 14	418 ± 42	6.8 (219%)[d]	2.8 (300%)	5.2 (451%)
119	cyclohexane		Me	Cl	156 ± 7.2	274 ± 29	285 ± 24	3.2 (157%)	2.8 (297%)	3.9 (302%)
120	morpholine		Me	Cl	146 ± 4.3	273 ± 16	231 ± 40	27 (186%)	15 (330%)	22 (400%)
121	morpholine		Me	Br	152 ± 4.4	279 ± 18	284 ± 50	15 (164%)	10 (309%)	14 (414%)
127	morpholine		Et	Cl	127 ± 4.7	133 ± 4.4	104 ± 2.4	16 (143%)	42 (146%)	_

[a] Fitted EC_{50} values are shown to two significant digits when potentiation at 30 μM exceeded 120%; values in parentheses are the fitted maximum response as a percentage of the initial glutamate (100 μM) and glycine (30 μM) current. Data are from between 7-12 oocytes from 2 frogs for each compound and receptor tested. [b]Potentiation at GluN2A was equal to or greater than 120% at 30 μM with BAPTA from 4 oocytes from 1 frog. This effect was not studied further. [c] p value <0.05 when comparing **1180-150** and **1180-146** EC_{50} value and max. response. [d]p value <0.05 when comparing **1180-116** and **1180-120** EC_{50}.

After exploring a variety of changes to the C-ring, Compounds **1180-83** and **1180-86 (Table 13)** were the most selective compounds with activity at only the GluN2B and GluN2C subunits. For this reason, in moving forward with the SAR, the isoproxy on the C-ring were initially held constant while the A- and B-rings were explored.

2.4.3 The effect of A-ring modifications

For clarity, all modifications to the A-ring have been divided into three tables, and the first (**Table 15**) depicts compounds where the B-ring contains a *para*-methoxy group. Modifications to the CIQ scaffold had revealed that the *meta*-position of the A-ring was optimal for activity, so all substituents on the isopropoxy-containing scaffold were originally placed in the *meta*-position as well. A trend is observed moving from a fluoride (**1180-140**) to an iodine (**1180-153**). Interestingly, the EC_{50} value at all three subunits decreases with decreasing electronegativity and increasing atomic radius, but the maximum effect is actually larger, especially at GluN2B, for the least potent fluorine-containing **1180-104**. This suggests that the A-ring is tolerable of a variety of substituents in the *meta*-position, and activity is not strictly determined by size or electronegativity. A clear trend was also observed when comparing electron withdrawing groups and electron donating groups. The electron withdrawing group compounds, the CF_3-containing **1180-91** and the nitro-containing **1180-142**, were active at all three subunits, while the compounds with electron donating groups (**1180-89** and **1180-141**) showed no activity at any subunits. This suggests that while the A-ring is not highly sensitive to size, it is sensitive to electronics.

Moving substituents from the *meta*-position to the *para*-position did not absolutely result in a loss of activity. Compound **1180-90** with a chloro-group in the *para*-position of the A-ring continued to be active at all three subunits, although it was less potent than **1180-55** with the chlorine in the meta-position. Methyl-containing **1180-85** was active at only GluN2C, although with an EC_{50} value of 22 μM. Despite the low potency, this compound could be used as a starting point to develop GluN2C-selective isopropoxy-containing compounds. For this reason, **1180-319** and **1180-320**, were synthesized. The trifluoromethyl group and the hydroxyl group are isosteres of the methoxy group,

but neither of these was selective for the GluN2C subunit. Compound **1180-319** was active at GluN2B, GluN2C, and GluN2D subunits, while hydroxyl compound **1180-320** was inactive all three subunits.

Table 15. The effect of A-ring modifications when the B-ring contains a *para*-methoxy group.

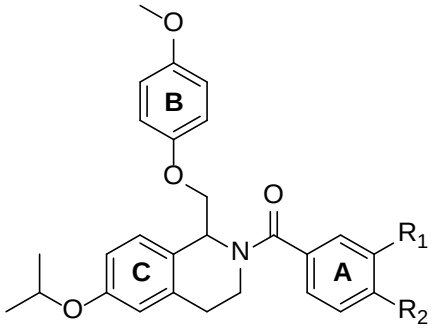

			$I_{30\mu M}$ / $I_{control}$ (mean ± SEM, %)			EC_{50} (max.) (μM %)[a]		
	R_1	**R_2**	**GluN2B**	**GluN2C**	**GluN2D**	**GluN2B**	**GluN2C**	**GluN2D**
140[b]	F	H	249 ± 7.6	343 ± 28	289 ± 19	21 (340%)	6.1 (377%)	12 (490%)
55	Cl	H	214 ± 7.3	243 ± 13	308 ± 17	5.0 (215%)	2.6 (250%)	4.3 (323%)
88	Br	H	205 ± 14	290 ± 14	362 ± 18	3.6 (210%)	1.6 (299%)	2.2 (266%)
153	I	H	159 ± 8.7	215 ± 15	408 ± 27	1.9 (173%)[c]	0.78 (296%)	1.3 (372%)
91[b]	CF_3	H	196 ± 13	363 ± 25	334 ± 16	5.6 (208%)	2.9 (385%)	3.2 (349%)
142[b]	NO_2	H	198 ± 7.7	337 ± 21	335 ± 52	5.7 (210%)	3.0 (352%)	4.3 (363%)
89	OH	H	98 ± 3.4	117 ± 8.4	105 ± 6.2	–	–	–
141	NH_2	H	105 ± 3.4	105 ± 8.9	106 ± 9.1	–	–	–
90	H	Cl	163 ± 9.6	251 ± 9.5	244 ± 13	9.4 (171%)[d]	7.9 (259%)	8.6 (249%)
85	H	OMe	96 ± 1.8	138 ± 4.0	114 ± 3.0	–	22 (158%)	-
319	H	OCF_3	130 ± 5.9	137 ± 4.1	147 ± 3.1	3.5 (139%)	1.9 (144%)	2.0 (148%)
321	H	OH	84 ± 3.1	93 ± 2.5	83 ± 0.79	-	-	-
320	H	OBn	89 ± 4.3	109 ± 1.8	98 ± 1.5	-	-	-

[a] Fitted EC_{50} values are shown to two significant digits when potentiation at 30 μM exceeded 120%; values in parentheses are the fitted maximum response as a percentage of the initial glutamate (100 μM) and glycine (30 μM) current. Data are from between 4-14 oocytes from 2-3 frogs for each compound and receptor tested. [b]Potentiation at GluN2A was equal to or greater than 120% at 30 μM with BAPTA from 4 oocytes from 1 frog. This effect was not studied further. [c] p value <0.05 when comparing **1180-153** and **1180-140** EC_{50} value and max. response; p value <0.05 when comparing **1180-153** and **1180-88** EC_{50}. [d] p value <0.05 when comparing **1180-90** and **1180-55** EC_{50} value. Compounds **1180-55** and **1180-88** were shown in previous tables and were included here for comparison.

Since selectivity for GluN2B and GluN2C had begun to emerge when the methoxy on the B-ring was exchanged for an ethoxy (**Table 13**), A-ring modifications were also made to a scaffold that contained an ethoxy group on the B-ring (**Table 16**). Substitution on the A-ring was required for activity as compound **1180-100** was inactive at all subunits. Similarly to when a methoxy group was on the B-ring, compounds with electron-donating groups, such as **1180-129** with a methyl group and **1180-130** with a methoxy group, were inactive. Activity was observed, however when the electron-withdrawing CF_3 group (**1180-92**) was placed in the *meta*-position of the ring. **1180-92**, along with halogen-containing compounds **1180-83** and **1180-86**, showed selectivity towards GluN2B and GluN2C. Notably, compound **1180-87** with fluorine substitution was active at only GluN2B with a potency of 2.8 μM.

The bulky phenyl-containing compound (**1180-102**) and **1180-131** with a methyl group in the *para*-position on the ring were inactive. Inactivity when substituents were placed in the *para*-position on the A-ring when the B-ring contains an ethoxy group is in contrast to the results observed for *para*-substituents on the A-ring for B-ring methoxy-containing compounds (**Table 15**); **1180-90** and **1180-85** were active in some capacity. **1180-90** was active at GluN2B, GluN2C, and GluN2D subunits, while **1180-85** was weakly active exclusively at GluN2C. These results reveal that slight modifications made to both the A-rings and the B-rings simultaneously can drastically change the subunit-selectivity of the series, and this series can be manipulated, with only small changes, to target different subunits.

Table 16. The effect of A-ring modifications when the B-ring contains a *para*-ethoxy group.

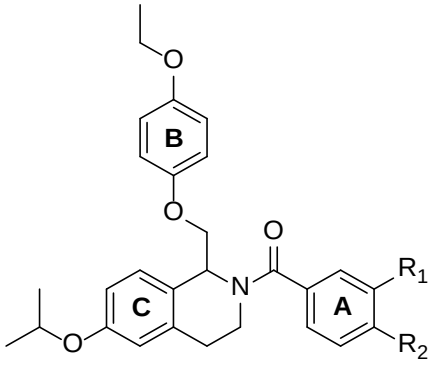

			$I_{30\mu M}$ / $I_{control}$ (mean ± SEM, %)			EC_{50} (max.) (μM %)[a]		
	R_1	**R_2**	**GluN2B**	**GluN2C**	**GluN2D**	**GluN2B**	**GluN2C**	**GluN2D**
100	H	H	88 ± 1.1	83 ± 2.5	69 ± 2.3	-	-	-
83	Cl	H	156 ± 8.4	126 ± 2.9	100 ± 1.8	5.7 (159%)	2.9 (121%)	-
86[b]	Br	H	136 ± 7.9	133 ± 5.1	98 ± 1.9	3.9 (140%)	3.3 (132%)	-
87	F	H	151 ± 4.2	103 ± 2.2	91 ± 1.7	2.8 (152%)	-	-
92	CF_3	H	124 ± 7.0	129 ± 3.8	95 ± 8.6	2.5 (122%)	1.4 (124%)	-
102	Ph	H	105 ± 3.3	95 ± 3.7	94 ± 2.3	-	-	-
129	Me	H	78 ± 1.2	66 ± 2.1	43 ± 2.3	-	-	-
130	OMe	H	89 ± 5.1	65 ± 4.1	44 ± 4.5	-	-	-
131	H	Me	74 ± 2.8	61 ± 8.4	39 ± 8.9	-	-	-

[a] Fitted EC_{50} values are shown to two significant digits when potentiation at 30 μM exceeded 120%; values in parentheses are the fitted maximum response as a percentage of the initial glutamate (100 μM) and glycine (30 μM) current. Data are from between 6-17 oocytes from 2-3 frogs for each compound and receptor tested. [b]Potentiation at GluN2A was equal to or greater than 120% at 30 μM with BAPTA from 4 oocytes from 1 frog. This effect was not studied further. Compound **1180-83** and **1180-86** was shown in a previous table and included here for comparison.

Since **1180-87** was selective for GluN2B, the fluorine and the chlorine were then moved around the ring to probe ideal substituent placement (**Table 17**). A chlorine or fluorine in the *ortho*-position (**1180-147** and **1180-148**) or the *para*-position (**1180-132** and **1180-133**) caused a complete loss of activity, suggesting that *meta*-position substitution is required for activity. Although *para*-substitution completely eliminated activity, disubstitution in the *meta*- and *para*-position revived activity at the GluN2B, GluN2C, and GluN2D subunits in compounds **1180-134** and **1180-144** and at the GluN2B

and GluN2C subunits in **1180-103**. Even though disubstituted compounds **1180-134** and **1180-144** were active at GluN2D, the maximum effect was only 136% and 135%, while the maximum effect at GluN2B and GluN2C were in the ranges of 175% to 143%. Interesting, **1180-132** and **1180-144** also showed potentiation at GluN2A, although this effect was not studied further. Compound **1180-101** with 2,4-dichloro substitution was inactive at all subunits.

Table 17. The effect of substituent location on the A-ring

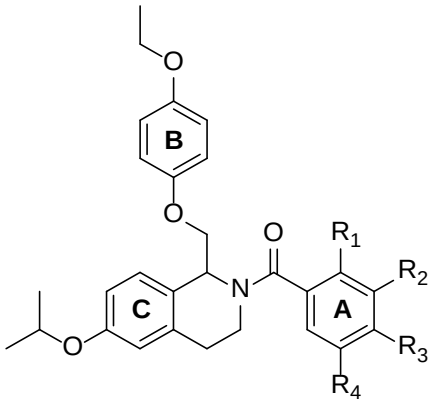

					$I_{30\mu M}$ / $I_{control}$ (mean ± SEM, %)			EC_{50} (max.) (μM %)[a]		
	R_1	**R_2**	**R_3**	**R_4**	**GluN2B**	**GluN2C**	**GluN2D**	**GluN2B**	**GluN2C**	**GluN2D**
147	F	H	H	H	61 ± 2.4	68 ± 4.1	55 ± 4.5	-	-	-
148	Cl	H	H	H	67 ± 4.1	93 ± 6.3	79 ± 3.4	-	-	-
133	H	H	F	H	118 ± 5.8	107 ± 6.7	90 ± 3.7	-	-	-
132[b]	H	H	Cl	H	111 ± 2.1	101 ± 7.8	88 ± 7.7	-	-	-
134[b]	H	F	F	H	172 ± 6.0	145 ± 6.6	133 ± 3.7	5.1 (175%)	2.4 (143%)	2.0 (136%)
103	H	Cl	Cl	H	120 ± 4.4	134 ± 5.1	101 ± 4.2	1.4 (134%)	0.65 (139%)	-
144	H	Cl	F	H	169 ± 7.8	159 ± 6.3	133 ± 4.8	2.2 (171%)	1.5 (162%)	2.4 (135%)
101	H	Cl	H	Cl	107 ± 3.1	93 ± 3.9	79 ± 4.2	-	-	-

[a] Fitted EC_{50} values are shown to two significant digits when potentiation at 30 μM exceeded 120%; values in parentheses are the fitted maximum response as a percentage of the initial glutamate (100 μM) and glycine (30 μM) current. Data are from between 6-17 oocytes from 2-3 frogs for each compound and receptor tested. [b] Potentiation at GluN2A was equal to or greater than 120% at 30 μM with BAPTA from between 4-8 oocytes from 1-2 frogs. This effect was not studied further.

2.4.4 Optimization of C-ring when A- and B-rings are held constant

After probing the A-ring in addition to the C-ring, it appeared as if **1180-87** with a fluorine in the *meta*-position of the A-ring in combination with an ethoxy group on the B-ring was optimal in terms of GluN2B selectivity. For this reason, a number of compounds were synthesized that maintained the fluorine on the A-ring and *para*-ethoxy functionality on the B-ring, but had modified C-ring ether moieties (**Table 18**). Unfortunately, none of these compounds compared to **1180-87** in terms of GluN2B selectivity, but were either completely inactive or equally potent at GluN2B, GluN2C, and GluN2D. All the compounds were similar in potency, efficacy, and subunit-selectivity to their chloro- or bromo-containing counterparts. Compound **1180-269** was completely inactive just like the chloro-containing **1180-268** was, and **1180-126**, **1180-125**, and **1180-112** were active at GluN2B, GluN2C, and GluN2D like the compounds shown in **Table 13**.

Table 18. Effect of combining optimal A-ring and B-ring modifications

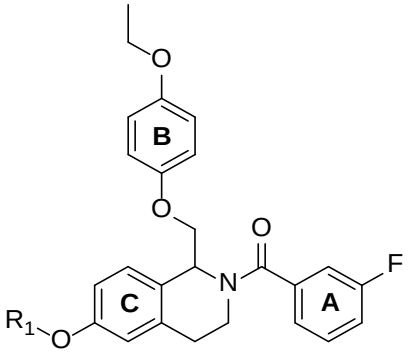

		$I_{30\mu M}$ / $I_{control}$ (mean ± SEM, %)			EC_{50} (max.) (μM %)[a]		
	R_1	**GluN2B**	**GluN2C**	**GluN2D**	**GluN2B**	**GluN2C**	**GluN2D**
87	*i*Pr	151 ± 4.2	103 ± 2.2	91 ± 1.7	2.8 (152%)[c]	-	-
269	Et	94 ± 1.3	77 ± 3.2	67 ± 2.0	-	-	-
126[b]	*t*Bu	332 ± 13	309 ± 15	351 ± 17	2.7 (340%)	3.3 (317%)	3.7 (357%)
125	$CH(CH_2CH_3)_2$	297 ± 12	194 ± 7.7	196 ± 15	2.6 (304%)	3.1 (198%)	3.4 (198%)
112	*c*Pent	202 ± 13	169 ± 2.7	161 ± 4.4	4.9 (200%)	4.3 (170%)	5.1 (157%)
128[b]	morpholine	107 ± 8.9	113 ± 3.8	101 ± 3.7	-	-	-

[a] Fitted EC_{50} values are shown to two significant digits when potentiation at 30 μM exceeded 120%; values in parentheses are the fitted maximum response as a percentage of the initial glutamate (100 μM) and glycine (30 μM) current. Data are from between 8-17 oocytes from 2-3 frogs for each compound and receptor tested. [b] Potentiation at GluN2A was equal to or greater than 120% at 30 μM with BAPTA from 3 oocytes from 1 frog. This effect was not studied further. [c] p value <0.05 when comparing **1180-87** and **1180-126** EC_{50} value. Compound **1180-87** was shown in previous tables and was included here for comparison.

2.4.4 Optimization of B-ring modifications

The final ring to be explored in greater detail was the B-ring, and initially the methoxy group was moved around the ring to discern optimal B-ring location (**Table 19**). Compound **1180-82** was weakly active at GluN2C and GluN2D, and this compound could serve as a starting point for finding additional GluN2C- and GluN2D-subunit selective potentiators that veer from the CIQ scaffold.

Compound **1180-82** represents one of the ways that the series of isopropoxy-containing compounds has diverged from the CIQ series; CIQ-like compounds with dimethoxy functionality on the C-ring are only active when substituents on the B-ring are in the *para*-position, but this is clearly not the case for the compounds that resemble **1180-55** since **1180-82** shows activity. A more extensive discussion of how the two series have diverged through the course of this project is discussed in **Chapter 2.4.8**. The two series are similar though in that B-ring functionality in the ortho-position (**1180-84**) eliminates activity at all subunits.

Table 19. Effect of B-ring substituent location.

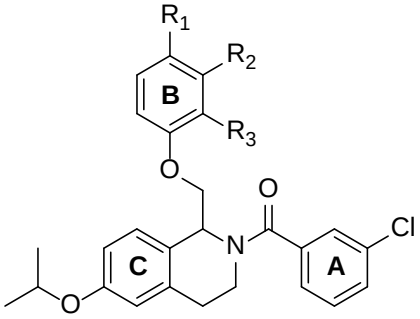

				$I_{30\mu M}$ / $I_{control}$ (mean ± SEM, %)			EC_{50} (max.) (μM %)[a]		
	R_1	**R_2**	**R_3**	**GluN2B**	**GluN2C**	**GluN2D**	**GluN2B**	**GluN2C**	**GluN2D**
55	OMe	H	H	214 ± 7.3	243 ± 13	308 ± 17	5.0 (215%)	2.6 (250%)	4.3 (323%)
82	H	OMe	H	99 ± 5.6	132 ± 3.8	124 ± 2.9	_	6.9 (132%)	6.1 (126%)
84	H	H	OMe	116 ± 2.2	114 ± 2.9	104 ± 2.4	_	_	_

[a] Fitted EC_{50} values are shown to two significant digits when potentiation at 30 μM exceeded 120%; values in parentheses are the fitted maximum response as a percentage of the initial glutamate (100 μM) and glycine (30 μM) current. Data are from between 7-27 oocytes from 2-5 frogs for each compound and receptor tested. Compound **1180-55** was shown in previous tables and were included here for comparison.

Since the *para*-position was optimal for GluN2B activity, functionality other than a methyl group was installed (**Table 20**), and from this data a trend for GluN2B selectivity that is dependent on size emerged. When the B-ring functionality is a methoxy group (**1180-55**), activity was observed at GluN2B, GluN2C, and GluN2D, but when the methoxy was exchanged for an ethoxy group (**1180-83**), the compound became more selective by no longer hitting GluN2D. The isopropoxy on the B-

ring (**1180-264**) led to a compound that was also more selective than **1180-55** with activity at GluN2B and minimal activity at GluN2C. Since the isopropoxy on the B-ring appeared to give a compound that leaned towards GluN2B-selectivity and fluoro-containing **1180-87** also had GluN2B selectivity, it was anticipated that compound **1180-270**, which combined the two, would be GluN2B-selective. Unfortunately, **1180-270** and **1180-127** with a CF_3 group showed activity at GluN2B and GluN2C. Despite activity at both GluN2B and GluN2C, compounds **1180-270** and **1180-271** do lean towards GluN2B as the maximum effects at GluN2C for **1180-270** and **1180-271** are only 136% and 129%, respectively.

Table 20. Effect of B-ring substituent identity

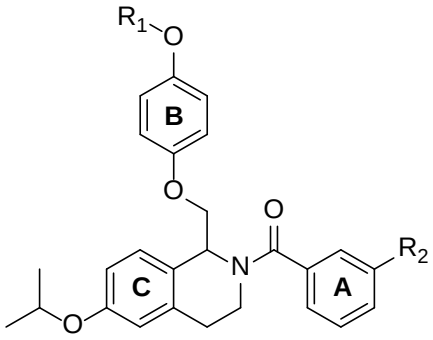

			$I_{30\mu M}$ / $I_{control}$ (mean ± SEM, %)			EC_{50} (max.) (μM %)[a]		
	R_1	**R_2**	**GluN2B**	**GluN2C**	**GluN2D**	**GluN2B**	**GluN2C**	**GluN2D**
55	Me	Cl	214 ± 7.3	243 ± 13	308 ± 17	5.0 (215%)	2.6 (250%)	4.3 (323%)
83	Et	Cl	156 ± 8.4	126 ± 2.9	100 ± 1.8	5.7 (159%)	2.9 (121%)	-
264	*i*Pr	Cl	158 ± 7.5	134 ± 8.0	111 ± 3.8	3.8 (144%)	2.4 (138%)	_
140[b]	Me	F	249 ± 7.6	343 ± 28	289 ± 19	21 (340%)	6.1 (377%)	12 (490%)
87	Et	F	151 ± 4.2	103 ± 2.2	91 ± 1.7	2.8 (152%)	-	-
270	*i*Pr	F	179 ± 4.1	133 ± 4.5	103 ± 2.2	7.5 (186%)	3.3 (136%)	_
271	*i*Pr	CF_3	156 ± 7.6	122 ± 4.0	107 ± 4.8	1.3 (141%)	1.0 (129%)	-

[a] Fitted EC_{50} values are shown to two significant digits when potentiation at 30 μM exceeded 120%; values in parentheses are the fitted maximum response as a percentage of the initial glutamate (100 μM) and glycine (30 μM) current. Data are from between 7-27 oocytes from 2-5 frogs for each compound and receptor tested. [b] Potentiation at GluN2A was equal to or greater than 120% at 30 μM with BAPTA from 4 oocytes from 1 frog. This effect was not studied further. Compounds **1180-55, 1180-87, 1180-83**, and **1180-140** were shown in previous tables and were included here for comparison.

Analyzing the data from all three rings shows that selectivity for GluN2B over the other subunits or even GluN2B/GluN2C selectivity is not strictly dictated by the substituent identification of one particular ring. The method of systematically modifying one ring and then holding these findings constant while another ring is modified has only been semi-successful in driving down potency and developing a GluN2B-subunit selective potentiator. It has been difficult to find overall patterns in activity because identified trends pertaining to one ring do not always apply once a second part of the molecule or a different ring is changed. For example, one observed trend for the A-ring is that the fluoro substituent (**1180-87**) is best for GluN2B selectivity, but this is only the case when the B-ring

contains an ethoxy-group. When the B-ring contains a methoxy-group or an isopropoxy group, these fluoro-containing compounds, **1180-140** and **1180-270,** are no longer superior to other A-ring modifications. The same holds true when the C-ring contains anything other than an isopropoxy group as almost all the compounds in **Table 18** are active in a similar fashion to chloro- or bromo-containing compounds in **Table 13**. The two compounds in **Table 21** are another example of this disconnect in previously observed trends. Based on the results from **Table 20**, it would be expected that **1180-139** would be more selective than **1180-124** based on the exchange of an ethoxy group for an isopropoxy on the B-ring, but instead all three compounds, regardless of the B-ring substituent, exhibit robust potentiation at all three subunits.

Despite this, one trend that does hold true is one made when discussing **Table 12**: compounds with an isobutyl on the C-ring as shown in **Table 21** are the most efficacious and potent potentiators of all four subunits, including GluN2A. These compounds have EC_{50} values around 1.0 μM at the GluN2B, GluN2C, and GluN2D subunits and the maximum effect values are typically in the 300 – 400% range. While the goal of the project has been to develop GluN2B potentiators, a number of pan-potentiators that do not discriminate against any subunits have emerged. These compounds could represent a new therapeutic tool to study the effects of NMDA potentiation.

Table 21. Effect of isopropoxy functionality on B-ring

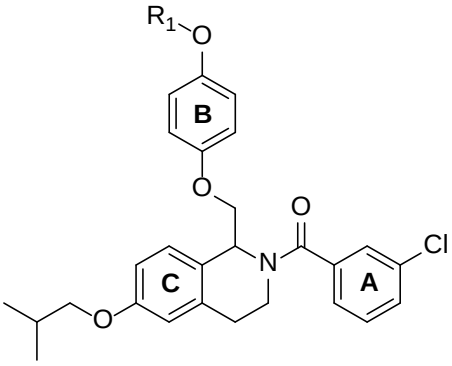

		$I_{30\mu M}$ / $I_{control}$ (mean ± SEM, %)			EC_{50} (max.) (μM %)[a]		
	R_1	**GluN2B**	**GluN2C**	**GluN2D**	**GluN2B**	**GluN2C**	**GluN2D**
114[b]	Me	332 ± 19	393 ± 62	472 ± 70	1.4 (335%)	1.2 (408%)	1.5 (475%)
124[b]	Et	294 ± 33	238 ± 11	342 ± 21	1.0 (305%)	1.3 (240%)	1.7 (345%)
139[b]	*i*Pr	283 ± 16	316 ± 16	329 ± 70	0.91 (262%)	0.71 (315%)	0.88 (331%)

[a] Fitted EC_{50} values are shown to two significant digits when potentiation at 30 μM exceeded 120%; values in parentheses are the fitted maximum response as a percentage of the initial glutamate (100 μM) and glycine (30 μM) current. Data are from between 7-27 oocytes from 2-5 frogs for each compound and receptor tested. [b] Potentiation at GluN2A was equal to or greater than 120% at 30 μM with BAPTA from 4 oocytes from 1 frog. This effect was not studied further. Compounds **1180-114** and **1180-124** were shown in previous tables and were included here for comparison.

2.4.6 Optimization of linker between core and A-ring

Although obvious patterns have been rare while developing the SAR for these isopropoxy-based compounds, a constant trend was observed when modifying the linker between the A-ring and the core. When converting the amide to a thioamide linker, potency at all three subunits increased significantly; certain thioamide-containing compounds were up to 50-fold more potent than their amide-containing counterparts as exemplified in **Table 22**. For clarity, all thioamide compounds have been divided into **Tables 22** through **26**.

Table 22. Effect of thioamide A-ring linker on potency and efficacy when B-ring contains a *para*-methoxy group

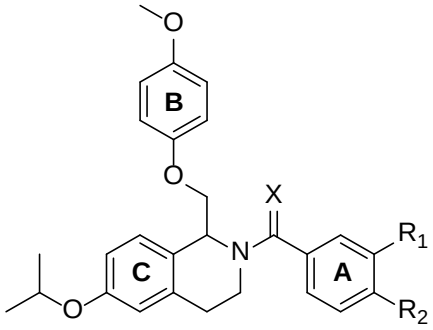

				$I_{30\mu M}$ / $I_{control}$ (mean ± SEM, %)			EC_{50} (max.) (μM %)[a]		
	R_1	R_2	X	GluN2B	GluN2C	GluN2D	GluN2B	GluN2C	GluN2D
55	Cl	H	O	214 ± 7.3	243 ± 13	308 ± 17	5.0 (215%)[c]	2.6 (250%)	4.3 (323%)
163[b]	Cl	H	S	228 ± 14	252 ± 11	247 ± 12	0.11 (228%)	0.32 (273%)	0.14 (260%)
140[b]	F	H	O	249 ± 7.6	343 ± 28	289 ± 19	21 (340%)[d]	6.1 (377%)	12 (490%)
166[b]	F	H	S	270 ± 34	216 ± 5.5	200 ± 9.1	1.3 (280%)	1.2 (219%)	1.3 (203%)

[a] Fitted EC_{50} values are shown to two significant digits when potentiation at 30 μM exceeded 120%; values in parentheses are the fitted maximum response as a percentage of the initial glutamate (100 μM) and glycine (30 μM) current. Data are from between 3-27 oocytes from 2-5 frogs for each compound and receptor tested. [b]Potentiation at GluN2A was equal to or greater than 120% at 30 μM with BAPTA from 4-6 oocytes from 1 frog. This effect was not studied further. [c]p value <0.05 when comparing **1180-55** and **1180-163** EC_{50} value. [d]p value <0.05 when comparing **1180-140** and **1180-166** EC_{50} values. Compounds **1180-55** and **140** were shown in previous tables and were included here for comparison.

Compound **1180-163** with a thioamide is significantly more potent at GluN2B than amide-containing compound **1180-55**, and EC_{50} values at GluN2C and GluN2D subunits are also in the nanomolar region. Although most compounds synthesized in the class and discussed in **Chapter 2** are active to some degree towards at least one subunit, until modifications to the A-ring linker were made, EC_{50} values had remained in the micromolar region and rarely dipped in the nanomolar region. When applied to compounds discussed in **Chapter 2**, the thioamide switch consistently, regardless of substituent identity on the B-ring or A-ring, caused an increase in potency at all the subunits, and one

example of this is **1180-166**. While the amide-containing compound **1180-140** had an EC_{50} value of 21 μM at GluN2B, thioamide compound **1180-166** had an EC_{50} value of only 1.3 μM, which represents a 16-fold increase in potency. Potency also increased at the GluN2C and Glu2ND-containing receptors, although not to the same degree as GluN2B; GluN2C increased only 5-fold, while GluN2D increased 9-fold. While compound **1180-140** was significantly more potent at GluN2C and GluN2D, the thioamide in **1180-166** caused the compound to be equally potent at all subunits. In terms of maximum effect values, **1180-163** has similar maximum effects at all three subunits compared to **1180-55**, but **1180-166** actually has a decreased maximum effect value at all subunits compared to **1180-140**. Interestingly, GluN2D is impacted the most, with the maximum effect dropping from a robust 490% to a more modest 203%, which represents over a 50% decrease in maximum effect value. The GluN2C maximum effect drops from 377% to 219%, but the GluN2B subunit is affected the least, dropping from 340% to only 280%. Although the effect is subtle, this is one of the first examples where the thioamide not only plays a role in increasing potency at all subunits, but also appears to slightly push activity towards GluN2B and away from GluN2C and GluN2D.

Table 23. Effect of thioamide A-ring linker on potency and efficacy when B-ring contains a *para*-ethoxy group.

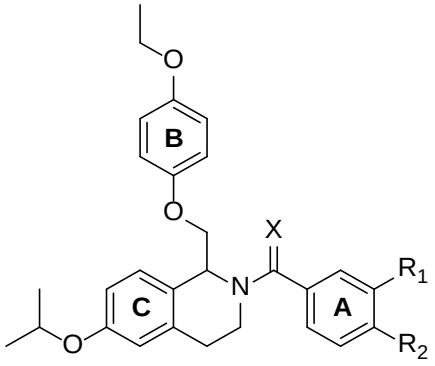

				$I_{30\mu M}$ / $I_{control}$ (mean ± SEM, %)			EC_{50} (max.) (μM %)[a]		
	R_1	**R_2**	**X**	**GluN2B**	**GluN2C**	**GluN2D**	**GluN2B**	**GluN2C**	**GluN2D**
83	Cl	H	O	156 ± 8.4	126 ± 2.9	100 ± 1.8	5.7 (159%)[c]	2.9 (121%)	-
149[b]	Cl	H	S	169 ± 11	229 ± 22	170 ± 17	0.97 (177%)	5.3 (268%)	1.5 (219%)
86[b]	Br	H	O	136 ± 7.9	133 ± 5.1	98 ± 1.9	3.9 (140%)[c]	3.3 (132%)	-
156	Br	H	S	166 ± 8.7	152 ± 10	131 ± 3.5	0.55 (118%)	0.79 (131%)	0.13 (131%)
87	F	H	O	151 ± 4.2	103 ± 2.2	91 ± 1.7	2.8 (152%)[d]	-	-
154	F	H	S	184 ± 5.6	166 ± 10	154 ± 5.4	0.70 (190%)	1.4 (145%)	1.2 (153%)
92	CF_3	H	O	124 ± 7.0	129 ± 3.8	95 ± 8.6	2.5 (122%)[d]	1.4 (124%)	-
168	CF_3	H	S	185 ± 14	139 ± 7.3	126 ± 4.8	1.0 (179%)	0.33 (141%)	0.45 (128%)
103	Cl	Cl	O	120 ± 4.4	134 ± 5.1	101 ± 4.2	1.4 (134%)[c]	0.65 (139%)	-
155	Cl	Cl	S	146 ± 5.6	146 ± 10	133 ± 5.1	0.15 (146%)	0.60 (154%)	0.37 (133%)
144	Cl	F	O	169 ± 7.8	159 ± 6.3	133 ± 4.8	1.4 (134%)[c]	0.65 (139%)	2.4 (135%)
165	Cl	F	S	203 ± 11	161 ± 7.5	142 ± 4.1	1.3 (221%)	0.75 (161%)	0.73 (134%)
131	H	Me	O	74 ± 2.8	61 ± 8.4	39 ± 8.9	-	-	-
304	H	Me	S	95 ± 5.3	84 ± 2.4	78 ± 1.9	-	-	-

132[b]	H	Cl	O	111 ± 2.1	101 ± 7.8	88 ± 7.7	-	-	-
305	H	Cl	S	104 ± 3.7	99 ± 4.1	99 ± 2.6	-	-	-

[a] Fitted EC_{50} values are shown to two significant digits when potentiation at 30 μM exceeded 120%; values in parentheses are the fitted maximum response as a percentage of the initial glutamate (100 μM) and glycine (30 μM) current. Data are from between 3-26 oocytes from 2-5 frogs for each compound and receptor tested. *Potentiation at GluN2A was equal to or greater than 120% at 30 μM with BAPTA from 4 oocytes from 1 frog. This effect was not studied further. [c]p value <0.05 when comparing thioamide and amide pair EC_{50} values. [d]p value <0.05 when comparing thioamide and amide pair EC_{50} values and max. responses. Compounds **1180-83, 1180-86, 1180-87, 1180-92, 1180-103, 1180-131, 1180-132,** and **1180-144** were shown in previous tables and were included here for comparison.

Table 23 displays all thioamide-containing compounds with an ethoxy in the *para*-position of the B-ring. While it was anticipated the converting the amide to a thioamide would increase potency, but maintain subunit-selectivity, especially in the case of **1180-87**, that unfortunately did not happen. All of these thioamide-containing compounds are less selective that their amide-containing counterparts, hitting GluN2B, GluN2C, and GluN2D-containing receptors. However, many of the compounds scarcely potentiate GluN2D; **1180-156**, **1180-168**, **1180-155**, and **1180-165** have maximum effect values of only 131%, 126%, 133%, and 142% at 30 μM compared to 166%, 185%, 146%, and 203% at GluN2B at 30 μM, respectively. These four compounds lean towards GluN2B and GluN2C-subunits, which may provide a starting point (discussed in **Chapter 2.4.9**) to develop GluN2B- and GluN2C-selective compounds. Four of the six thioamide-containing compounds (**1180-154**, **1180-168**, **1180-155**, and **1180-165**) were more efficacious at GluN2B- than either GluN2C- or GluN2D-containing receptors.

Converting the amide of the compounds shown in **Table 23** to a thioamide tended to make the biggest difference in terms of EC_{50} value at the GluN2B subunit when comparing the amide- and thioamide-compounds. For example, thioamide-containing **1180-149** is 6-fold more potent at GluN2B than amide-containing **1180-183**, while the potency actually decreased at the GluN2C subunit when moving from an amide to a thioamide. A similar trend was seen with thioamide-containing **1180-155**, which was 9-fold more potent at GluN2B than amide-containing **1180-103**, but the EC_{50} at GluN2C is approximately the same at both the thioamide and amide-containing

compounds. This data again suggests that the thioamide-containing compounds may be more amenable to the GluN2B-containing NMDA receptor than the GluN2C- or GluN2D-containing receptors. With only one exception (**1180-156**), moving from the amide to the thioamide also increased the maximum effect at the GluN2B subunit, and this was most obvious with disubstituted compounds **1180-144** and **1180-165**; the maximum effect at GluN2B for the amide-containing compound **1180-144** was only 134%, but the thioamide-containing maximum effect was a considerably more robust 221%.

Compounds **1180-304** and **1180-305** were synthesized from **1180-131** and **1180-132**, respectively, to determine whether the thioamide effect is strong enough to revive a compound with no activity at any subunits. These thioamide-containing compounds were inactive at all subunits. For thioamide-containing compounds, functionality in the *meta*-position of the A-ring is preferred to the *para*-position. Similarily to amide-containing compounds though, disubstitution on the A-ring leads to activity.

Table 24. Effect of thioamide A-ring linker on potency and efficacy when B-ring contains a *para*-isopropoxy group.

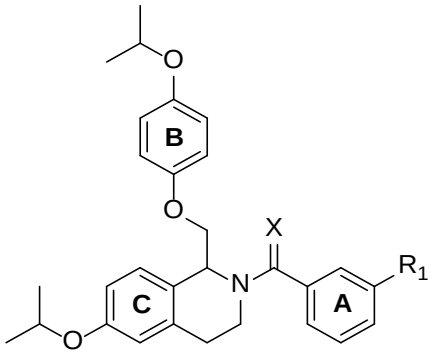

			$I_{30\mu M}$ / $I_{control}$ (mean ± SEM, %)			EC_{50} (max.) (μM %)[a]		
	R_1	**X**	**GluN2B**	**GluN2C**	**GluN2D**	**GluN2B**	**GluN2C**	**GluN2D**
264	Cl	O	159 ± 7.5	134 ± 8.0	111 ± 3.8	3.8 (144%)[c]	2.4 (138%)	_
265	Cl	S	207 ± 5.7	137 ± 7.0	147 ± 7.6	0.38 (185%)	0.63 (140%)	0.42 (137%)
270	F	O	179 ± 4.1	133 ± 4.5	103 ± 2.2	7.5 (186%)[c]	3.3 (136%)	_
272	F	S	168 ± 7.9	140 ± 5.8	141 ± 11	0.46 (202%)	0.48 (160%)	0.44 (148%)

271	CF_3	O	156 ± 7.6	122 ± 4.0	107 ± 4.8	1.3 (141%)[d]	1.0 (129%)	-
273[b]	CF_3	S	185 ± 4.6	169 ± 10	134 ± 5.6	0.27 (193%)	0.31 (180%)	0.34 (134%)

[a] Fitted EC_{50} values are shown to two significant digits when potentiation at 30 μM exceeded 120%; values in parentheses are the fitted maximum response as a percentage of the initial glutamate (100 μM) and glycine (30 μM) current. Data are from between 3-26 oocytes from 2-5 frogs for each compound and receptor tested. [b]$I_{3\mu M}$ / $I_{control}$. [c]p value <0.05 when comparing thioamide and amide pair EC_{50} values. [d]p value <0.05 when comparing thioamide and amide pair EC_{50} values and max. responses. Compounds **1180-264, 1180-270,** and **1180-271** were shown in previous tables and were included here for comparison.

Many of the most potent compounds with activity at GluN2B, GluN2C, and GluN2D subunits are those shown in **Table 24** with an isopropoxy on the B-ring and a thioamide linker. Compounds **1180-265**, **1180-272**, and **1180-273** have EC_{50} values that range from 0.27 μM – 0.68 μM at the three subunits. While activity was observed at all three subunits for the B-ring isopropoxy compounds, maximum effect values are consistently higher at GluN2B than GluN2C and GluN2D; maximum effect values at GluN2D are only in the range of 130% to 140%, while GluN2B maximum effect values are closer to a value of 200%. These compounds add to an earlier observation that the B-ring is tolerable, and in fact, may prefer the bulky isopropoxy group to a methoxy or ethoxy group. In **Table 20**, the results suggested that the B-ring had a significant role in driving selectivity for GluN2B. Although the thioamide-containing compounds shown in **Table 24** picked up activity at GluN2D that was not seen with the amide-containing counterparts, these isopropoxy B-ring compounds are more potent across all three subunits compared to thioamide compounds with an ethoxy or methoxy on the B-ring (**Tables 22** and **23**).

Although maximum effect leans towards GluN2B activity, the three compounds shown in **Table 24** are equally potent at GluN2B, GluN2C, and GluN2D-containing receptors. These three compounds represent scaffolds that could be used to study the impact of GluN2B, GluN2C, and GluN2D potentiation. Pan-potentiators for the NMDA receptor are not common, and these three compounds exhibit pan-potentiation with activity in the nanomolar region.

Table 25. Effect of thioamide A-ring linker on fluro-containing compounds

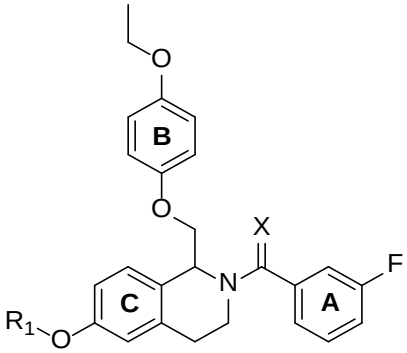

			$I_{30\mu M}$ / $I_{control}$ (mean ± SEM, %)			EC_{50} (max.) (μM %)[a]		
	R_1	**X**	**GluN2B**	**GluN2C**	**GluN2D**	**GluN2B**	**GluN2C**	**GluN2D**
126[b]	*i*Bu	O	332 ± 13	309 ± 15	351 ± 17	2.7 (340%)	3.3 (317%)	3.7 (357%)
169	*i*Bu	S	394 ± 3.3	394 ± 50	651 ± 68	0.40 (398%)[c]	0.40 (305%)	0.20 (564%)
112	*c*Pent	O	202 ± 13	169 ± 2.7	161 ± 4.4	4.9 (200%)	4.3 (170%)	5.1 (157%)
162	*c*Pent	S	211 ± 6.0	248 ± 26	281 ± 23	0.17 (217%)[c]	0.15 (249%)	0.11 (286%)

[a] Fitted EC_{50} values are shown to two significant digits when potentiation at 30 μM exceeded 120%; values in parentheses are the fitted maximum response as a percentage of the initial glutamate (100 μM) and glycine (30 μM) current. Data are from between 3-26 oocytes from 2-5 frogs for each compound and receptor tested. *Potentiation at GluN2A was equal to or greater than 120% at 30 μM with BAPTA from 3 oocytes from 1 frog. This effect was not studied further. [c]p value <0.05 when comparing thioamide and amide pair EC_{50} values. Compounds **1180-126** and **1180-112** were shown in previous tables and were included here for comparison.

When it appeared as if the thioamide-containing compounds had the potential to push activity towards GluN2B and away from GluN2C and GluN2D, two compounds with a fluoride on the A-ring and an ethoxy on the B-ring were converted from amides to thioamides. Based on the results of **Table 22 –Table 24**, potentiation at all subunits from the thioamide-containing compounds was not a surprise. The two compounds in **Table 25**, **1180-169** with isobutyl functionality and **1180-162** with cyclopentyl functionality, show that the thioamide switch works on C-ring functionality other than the isopropoxy group.

When converting the fluoro-containing compounds in **Table 25** from amide to thioamide compounds, a trend is observed that is consistent with what was seen in **Tables 22, 23** and **24**. The potency at all three subunits increases significantly, often more than 10-fold, and the maximum effect remains approximately the same at all three subunits. Compound **1180-169** has maximum effect values ranging from 305 to 564%, which is the most potentiation observed from a thioamide-containing compound. While the compounds in **Table 22** and **Table 23** with an isopropoxy group on the C-ring leaned slightly towards GluN2B in terms of EC_{50} value and/or maximum effect, the compounds shown in **Table 25** are equally active and potent at all three subunits.

Table 26. Effect of thioamide A-ring linker on potency and efficacy

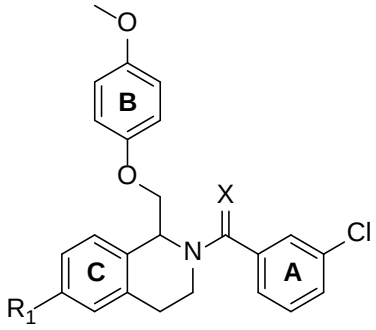

			$I_{30\mu M}$ / $I_{control}$ (mean ± SEM, %)			EC_{50} (max.) (μM %)[a]		
	R_1	**X**	**GluN2B**	**GluN2C**	**GluN2D**	**GluN2B**	**GluN2C**	**GluN2D**
152	OEt	O	158 ± 8.9	285 ± 23	329 ± 15	7.5 (167%)	2.9 (286%)	3.4 (332%)
170	OEt	S	139 ± 4.9	126 ± 13	111 ± 6.1	0.23 (144%)	0.58 (138%)	-
104	NMe_2	O	127 ± 4.1	288 ± 18	322 ± 20	6.5 (111%)	4.4 (310%)	4.7 (345%)
167	NMe_2	S	108 ± 2.1	136 ± 4.1	131 ± 2.1	-	1.1 (138%)	0.87 (130%)

[a] Fitted EC_{50} values are shown to two significant digits when potentiation at 30 μM exceeded 120%; values in parentheses are the fitted maximum response as a percentage of the initial glutamate (100 μM) and glycine (30 μM) current. Data are from between 3-26 oocytes from 2-5 frogs for each compound and receptor tested. [b]Potentiation at GluN2A was equal to or greater than 120% at 30 μM with BAPTA from 4-8 oocytes from 1-2 frogs. This effect was not studied further. Compounds **1180-152** and **1180-104** were shown in previous tables and were included here for comparison.

Lastly, two final compounds, **1180-152** and **1180-104**, were converted from an amide to a thioamide, and the results (**Table 26**) from this synthesis are unique from those shown previously. Compound

1180-170 with an ethoxy group on the C-ring was GluN2B- and GluN2C-selective, although the activity at these two subunits is minimal with maximum effect values of 144% and 138%, respectively. Compound **1180-170** is more potent at GluN2B and GluN2C than amide-containing compound **1180-152**, but the maximum effect at GluN2C actually decreased significantly from 286% to 138% when moving from an amide to a thioamide. The maximum effect at GluN2B, however, remained approximately the same with a value of 167% for **1180-152** and 144% for **1180-170**. This is one of the only examples where converting the amide to a thioamide actually led to a decrease in maximum potentiation at any subunits.

While **1180-170** is the only thioamide-containing compound synthesized with no activity at GluN2D, **1180-167** is the only thioamide-containing compound with no activity at GluN2B. **1180-167** has an EC_{50} value at GluN2C of 1.1 μM and 0.87 μM at GluN2D, and a maximum effect value of 138% and 130%, respectively. Although the maximum effect is modest, this nitrogen-containing compound is the only thioamide compound synthesized thus far that is selective for GluN2C- and GluN2D-containing receptors. As discussed in **Chapter 1.4.3**, all the GluN2C/GluN2D-selective amide-containing compounds were inactive as the thioamide-containing compounds, and although **1180-104** has activity at GluN2B, the potentiation at 30 μM was only 127% and the maximum effect was only 111%. This was an amide-containing compound that heavily leaned towards GluN2C- and GluN2D, and still had activity as the thioamide version, which is in deep contrast to the effects observed for CIQ-like compounds discussed in **Chapter 1.4.3**. The nitrogen-containing compounds as thioamides could provide a means to develop potent, drug-like GluN2C- and GluN2D-selective potentiators to be used as therapeutic probes in addition to the prototypical CIQ scaffold. The different effects of the thioamide conversion on compounds from **Chapter 1** and **Chapter 2** will be discussed more thoroughly in **Chapter 2.4.8**.

Table 27. Effect of sulfonamide A-ring linker on potency and efficacy

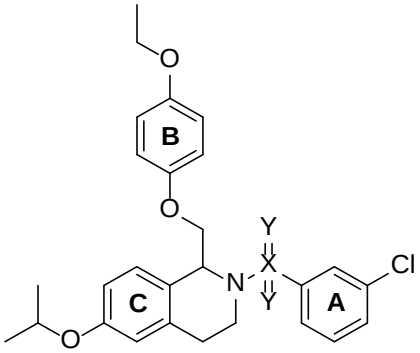

				$I_{30\mu M}$ / $I_{control}$ (mean ± SEM, %)			EC_{50} (max.) (μM %)[a]		
	X	**Y**	**Y**	**GluN2B**	**GluN2C**	**GluN2D**	**GluN2B**	**GluN2C**	**GluN2D**
83	C	O	-	156 ± 8.4	126 ± 2.9	100 ± 1.8	5.7 (159%)	2.9 (121%)	-
149[b]	C	S	-	169 ± 11	229 ± 22	170 ± 17	0.97 (177%)	5.3 (268%)	1.5 (219%)
199	S	O	O	97.5 ± 2.5	111 ± 2.6	97.0 ± 3.2	-	-	-

[a] Fitted EC_{50} values are shown to two significant digits; values in parentheses are the fitted maximum response as a percentage of the initial glutamate (100 μM) and glycine (30 μM) current. NE indicates less than 10% potentiation. Data are from between 6-17 oocytes from 2-4 frogs for each compound and receptor tested. [b]Potentiation at GluN2A was equal to or greater than 120% at 30 μM with BAPTA from 4 oocytes from 1 frog. Compound **1180-83** and **1180-149** was shown in previous tables and was included here for comparison.

After it became apparent that the thioamide significantly increased potency at all subunits, other A-ring linkerswere explored, including a sulfonamide (**Table 27**). Compound **1180-199**, which mimics compounds **1180-83** and **1180-199** on the A- B- and C-rings, displayed no detectable activity at any subunits. For this reason, no other compounds with a sulfonamide linker were synthesized. Compounds **1180-224** and **1180-210** with a urea and thiourea linker, respectively, were also synthesized (**Table 28**). These two compounds were GluN2C- and GluN2D-selective, although urea-containing compound **1180-224** displayed minimal activity at these two subunits. Compound **1180-210** with a thiourea linker could be used as a GluN2C- and GluN2D-selective therapeutic probe, as the maximum effect demonstrates potentiation and the EC_{50} value at both subunits is below 1.0 μM.

Table 28. Effect of urea and thiourea A-ring linkers on potency and efficacy

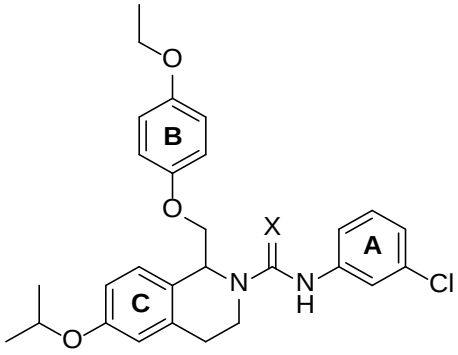

		$I_{30\mu M}$ / $I_{control}$ (mean ± SEM, %)			EC_{50} (max.) (μM %)[a]		
	X	**GluN2B**	**GluN2C**	**GluN2D**	**GluN2B**	**GluN2C**	**GluN2D**
224	O	113 ± 1.3	133 ± 3.8	128 ± 1.8	-	7.8 (127%)	2.1 (128%)
210	S	116 ± 1.1	199 ± 13	173 ± 17	-	0.54 (180%)	0.70 (146%)

[a] Fitted EC_{50} values are shown to two significant digits; values in parentheses are the fitted maximum response as a percentage of the initial glutamate (100 μM) and glycine (30 μM) current. NE indicates less than 10% potentiation. Data are from between 6-17 oocytes from 2-4 frogs for each compound and receptor tested.

2.4.7 Modeling the lowest energy conformations of thioamide- and amide-containing compounds

Compared to amide bonds, thioamide bonds have a larger rotational barrier[61,62]. The higher barrier to rotation could help to explain why the thioamide-containing compounds are more potent than the amide-containing compounds, and modeling of the lowest energy conformations of thioamide **1180-163** and amide **1180-55** were completed to compare the two linkers.

All the compounds (with the exception of urea and thiourea compounds **1180-210** and **1180-224**, respectively) exist as rotamers (**Figure 15**). This is evident in the NMR solutions, where a 1:1 mixture was always observed.

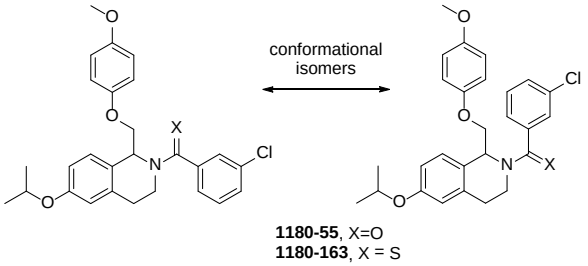

Figure 15. Conformational isomers of prototypical 1180-55 and 1180-163.

Using Macromolecule, the lowest energy conformations within 5 kcal/mol of the ground state (global minimum) were modeled for both **(*S*)-1180-55** and **(*S*)-1180-163**. While most ligands do not bind in the lowest global minimum, over 60% bind within 5 kcal/mol of the global minimum[63], therefore a 5 kcal / mol energy barrier was chosen as the energy cut-off for the study. As shown in **Figure 16**, within 5 kcal/mol of the global minimum, the amide bond is predicted to exist in both conformations, while the thioamide is predicted to exist in only one: the conformation where the A-ring is positioned upwards. This modeling could help to explain the increased potency associated with the thioamide-containing compounds.

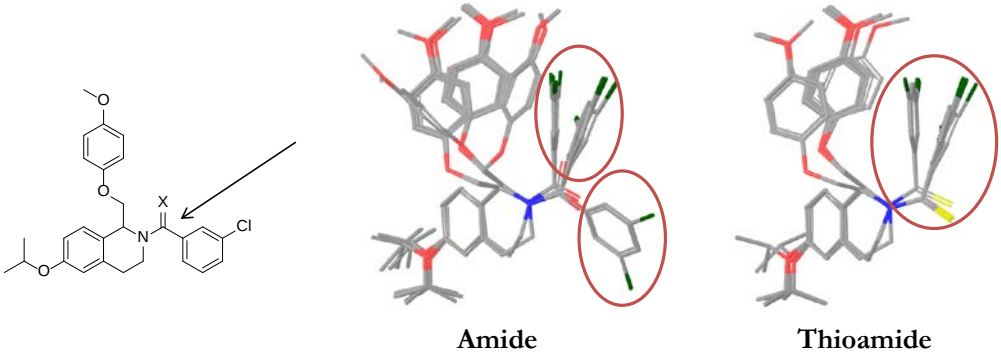

Figure 16. Modeling to compare the amide- and thioamide-containing compounds.

To lend credence to the modeling work, the lowest energy conformations of the thioamide-containing **(*S*)-1180-163** overlay well (RMSD 0.8Å) with the crystal structure of **(*S*)-(-)-1180-163** (introduced in **Chapter 2.4.8)**, which in theory should exist in the lowest energy conformation (**Figure 17**).

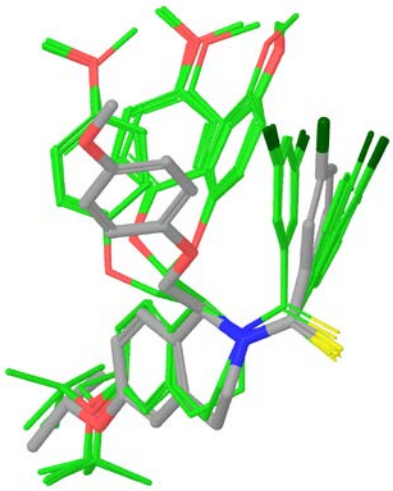

Figure 17. Crystal structure (grey) of (*S*)-(-)-1180-163 overlaid with the lowest energy conformations of (*S*)-1180-163 (green)

Additionally, models of the lowest energy conformations of **1180-199**, the sulfonamide-containing compound, reveal that the sulfonamide linker forces the A-ring to be a position that is opposite that of the A-ring of thioamide-**1180-163**. The A-ring is mostly pointed "downwards" resembling the conformation that the thioamide modeling would suggest is not favored for activity. This is shown in **Figure 18**, where the lowest energy conformations are overlaid with the **(*S*)-(-)-1180-163** crystal structure.

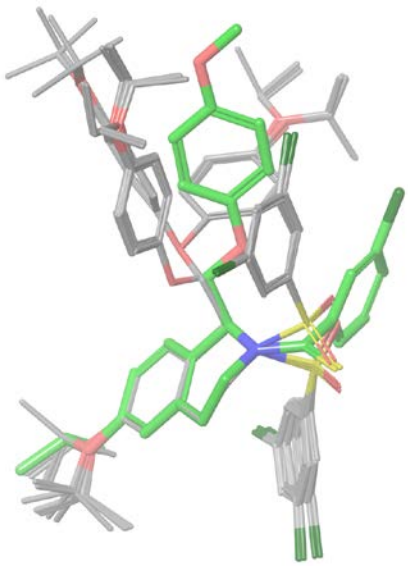

Figure 18. Crystal structure (green) of (*S*)-(-)-1180-163 overlaid with the lowest energy conformations of (*S*)-1180-199 (gray)

Sulfonamide **1180-199** has no activity at any subunits (**Table 27**), which is what the modeling would also predict if the conformation of the A-ring had any impact on activity. This suggests that the increased rigidity of the thioamide may be forcing the A-ring to remain in only one conformation, and this conformation may be better suited to exert the desired effect on the NMDA receptor binding pocket.

2.4.8 Evaluation of 1180-55 and 1180-163 enantiomers to discern stereoselectivity of isopropoxy-containing compounds

Although over 100 compounds had been synthesized, these compounds were all tested in ooyctes as the racemic mixture, and therefore the enantiomers of **1180-55** and **1180-163** were synthesized to study whether the GluN2B activity was contained in exclusively one enantiomer.

Table 29. Stereoselectivity of 1180-55 and 1180-163 enantiomers.

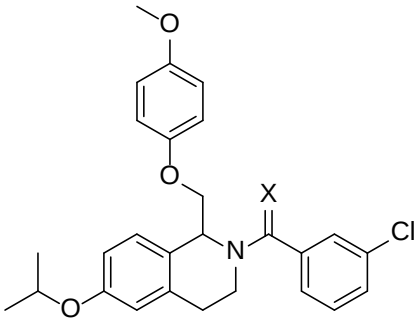

		$I_{10\mu M}$ / $I_{control}$ (mean ± SEM, %)			EC_{50} (max.) (μM %)[a]		
	X	**GluN2B**	**GluN2C**	**GluN2D**	**GluN2B**	**GluN2C**	**GluN2D**
1180-55	O	191 ± 6.5	231 ± 12	281 ± 3.1	5.0 (215%)	2.6 (250%)	4.3 (323%)
(*R*)-(+)-1180-55	O	150 ± 5.6	323 ± 17	345 ± 19	5.0 (167%)	1.0 (342%)	1.3 (384%)
(*S*)-(-)-1180-55	O	269 ± 21	361 ± 20	336 ± 19	5.2 (307%)	3.9 (360%)	4.5 (350%)
1180-163	S	212 ± 2.2	272 ± 2.5	231 ± 2.5	0.11 (228%)	0.32 (273%)	0.14 (260%)
(*R*)-(+)-1180-163	S	121 ± 5.9	252 ± 8.4	215 ± 9.5	-	1.7 (252%)	2.3 (255%)
(*S*)-(-)-1180-163	S	203 ± 11	302 ± 14	299 ± 12	0.28 (202%)	0.50 (316%)	0.50 (313%)

[a] Fitted EC_{50} values are shown to two significant digits when potentiation at 30 μM exceeded 120%; values in parentheses are the fitted maximum response as a percentage of the initial glutamate (100 μM) and glycine (30

μM) current. Data are from between 3-26 oocytes from 2-5 frogs for each compound and receptor tested. Compound **1180-55** and **1180-163** were shown in previous tables and was included here for comparison.

The enantiomers of **1180-55** and **1180-163** were separated via a chiral synthesis, and the stereochemistry of one of the thioamide-containing enantiomers was determined to be the *S*-(-) enantiomer using X-ray crystallography. In contrast to the CIQ scaffold, where only one enantiomer exhibited activity (discussed in **Chapter 1.4.5**),[1] evaluation of the **1180-55** and **1180-163** enantiomers revealed that both enantiomers were active (**Table 29**). The *(R)*-(+)-**1180-55** enantiomer was active at all three subunits, but the maximum potentiation at GluN2B was only 167%, while at GluN2C and GluN2D the maximum effect was between 342 and 384%; this enantiomer, although active at the GluN2B subunit, does lean towards GluN2C- and GluN2D activity. The *S*-(-)-**1180-55** enantiomer was also active at the GluN2B, GluN2C, and GluN2D subunit, but the efficacy at each subunit was comparable. When both amide-containing enantiomers were converted to the thioamide version, the (R)-(+)-enantiomer no longer exhibited any activity at the GluN2B subunit. *S-(-)*-**1180-163** was active at GluN2B, GluN2C, and GluN2D subunits, while *R-(+)*-**1180-163** was selective for GluN2C and GluN2D. This suggests that the GluN2B activity lies in the *S*-(-) enantiomer, while the *R*-(+) enantiomer is selective for GluN2C and GluN2D-containing NMDA receptors. The stereoselectivity of the series provides a unique opportunity to try to further enhance the selectivity of these compounds for GluN2B- containing receptors. Additionally, the (*R*)-(+)-enantiomer of **1180-163** may also provide a means to develop potent GluN2C- and GluN2D-containing compounds.

2.4.9 Evaluation of 1180-87 and 1180-154 enantiomers with the goal of developing GluN2B-selective potentiator

Since the separation of **1180-55** and **1180-163** enantiomers revealed that the GluN2B activity was residing in the (*S*)-(-)-enantiomer, this suggested that separation of GluN2B-selective **1180-87** would result in a one enantiomer with activity exclusively at GluN2B.

Table 30. Stereoselectivity of 1180-87 and 1180-154 enantiomers.

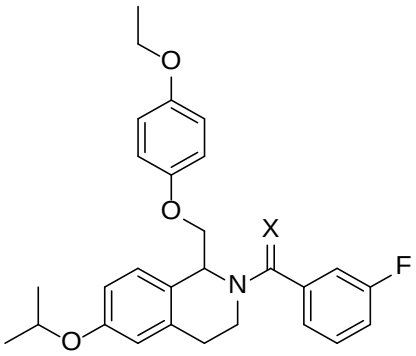

		$I_{30\mu M}$ / $I_{control}$ (mean ± SEM, %)			EC_{50} (max.) (μM %)[a]		
	X	**GluN2B**	**GluN2C**	**GluN2D**	**GluN2B**	**GluN2C**	**GluN2D**
1180-87	O	151 ± 4.2	103 ± 2.2	91 ± 1.7	2.8 (152%)	-	-
(*R*)-(+)-1180-87	O	103 ± 1.2	103 ± 2.8	86 ± 2.1	-	-	-
(*S*)-(-)-1180-87[b]	O	195 ±10	131 + 5.4	119 ± 4.9	6.7 (206%)	7.6 (132%)	-
1180-154	S	184 ± 5.6	166 ± 10	154 ± 5.4	0.70 (190%)	1.4 (145%)	1.2 (153%)
(*R*)-(+)-1180-154	S	95 ± 1.6	58 ± 0.5	74 ± 3.2	-	-	-
(*S*)-(-)-1180-154	S	206 ± 13	153 ± 11	185 ± 9.4	0.49 (213%)	0.46 (163%)	0.47 (190%)

[a] Fitted EC_{50} values are shown to two significant digits when potentiation at 30 μM exceeded 120%; values in parentheses are the fitted maximum response as a percentage of the initial glutamate (100 μM) and glycine (30 μM) current. Data are from between 3-26 oocytes from 2-5 frogs for each compound and receptor tested. Compound **1180-87** and **1180-154** were shown in previous tables and included here for comparison.

The potentiation of (*S*)-(-)-**1180-87** does lean towards GluN2B (**Table 30**); potentiation at 30 μM at GluN2B was almost 200%, while potentiation at GluN2C and GluN2D was only 131% and 119%, respectively. No activity at any subunits was recorded for the (*R*)-(+)-enantiomer, further suggesting that GluN2B activity resides in the (*S*)-(-)-enantiomer. When **1180-154** was separated, the results were different than the **1180-163** separated enantiomers. Racemic thioamide compound **1180-163** was active at GluN2B, GluN2C, and GluN2D-containing subunits, and both enantiomers were active; the (*S*)-(-)-enantiomer was active at all three subunits, while the (*R*)-(+)-enantiomer was GluN2C- and GluN2D-selective. It was expected that the separation of **1180-154** would give similar results, but instead only (*S*)-(-)-**1180-154** was active, while (*R*)-(+)-**1180-154** was completely inactive at all

subunits. This most likely means that (*R*)-(+)-**1180-163** and (*R*)-(+)-**1180-154** are interacting with the NMDA receptor differently, and this will be discussed in greater detail in Chapter 2.4.11.

2.4.10 Evaluation of 1180-92, 1180-168, 1180-103, enantiomers with the goal of developing a GluN2B/GluN2C-selective potentiator

Racemic compounds **1180-92** and **1180-103** were selective for GluN2B- and GluN2C-containing receptors over GluN2D-containing receptors, and based on the results from the separation of **1180-163**, it was anticipated that the separation of these two compounds would result in one enantiomer (hypothesized to be the (*S*)-(-)-enantiomer) that would be active at GluN2B- and GluN2C-containing receptors, while the other enantiomer (hypothesized to be the (*R*)-(-)-enantiomer) would be selective for GluN2C-containing receptors. When compound **1180-92** was separated (**Table 31**), activity at GluN2B and GluN2C subunits resided exclusively in the (*S*)-(-)-enantiomer, while the (*R*)-(+)-enantiomer was completely inactive. This is in contrast to the separation of the **1180-55** enantiomers where both enantiomers were active, but similar to the separation of **1180-154** where all activity resided in the (*S*)-(-)-enantiomer. The (*S*)-(-)-enantiomer of **1180-92**, which was GluN2B- and GluN2C-selective, could be used as a probe to study the selective enhancement of these two subunits. Additionally, CIQ was GluN2C/GluN2D-selective, but the activity at these two receptors was never separated; a GluN2C-selective or GluN2D-selective compound was never identified. A GluN2B/GluN2C-selective compound suggests that the GluN2C/GluN2D activity of the tetrahydroisoquinoline compounds could eventually be separated with more work.

Table 31. Stereoselectivity of 1180-92 and 1180-168 enantiomers.

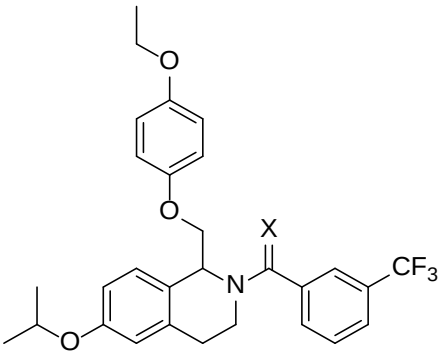

		$I_{30\mu M}$ / $I_{control}$ (mean ± SEM, %)			EC_{50} (max.) (μM %)[a]		
	X	**GluN2B**	**GluN2C**	**GluN2D**	**GluN2B**	**GluN2C**	**GluN2D**
1180-92	O	124 ± 7.0	129 ± 3.8	95 ± 8.6	2.5 (122%)	1.4 (124%)	-
(*S*)-(+)-1180-92	O	75 ± 3.2	73 ± 4.1	75 ± 2.4	-	-	-
(*R*)-(-)-1180-92	O	207 ± 7.8	132 ± 7.3	116 ± 5.2	1.9 (210%)	1.2 (141%)	
1180-168	S	185 ± 14	139 ± 7.3	126 ± 4.8	1.0 (179%)	0.33 (141%)	0.45 (128%)
(*R*)-(+)-1180-168	S	156 ±8.6	146 ± 8.1	157 ± 15	0.21 (173%)	0.24 (182%)	0.30 (160%)
(*S*)-(-)-1180-168	S	95 ± 1.8	87 ± 7.7	87 ± 1.5	-	-	-

[a] Fitted EC_{50} values are shown to two significant digits when potentiation at 30 μM exceeded 120%; values in parentheses are the fitted maximum response as a percentage of the initial glutamate (100 μM) and glycine (30 μM) current. Data are from between 3-26 oocytes from 2-5 frogs for each compound and receptor tested. Compound **1180-92** and **1180-168** were shown in previous tables and was included here for comparison.

For the five pairs of enantiomers that have previously been discussed, the GluN2B-activity resided in the (-)-enantiomer. The stereochemistry of these enantiomers was assigned by comparing optical rotation values and retention times on the analytical HPLC to the **1180-163** enantiomers since the stereochemistry of this pair could be defined based on the (*S*)-(-)-**1180-63** crystal structure (**Table 32**). In the previously discussed cases, biological activity has been reported in the enantiomer with a negative optical rotation value, and this enantiomer was given the (*S*)-assignment. The (-)-enantiomer was consistently the enantiomer with activity at GluN2B, while the (+)-enantiomer was always inactive (or selective for GluN2C/D). For the separation of the **1180-168** enantiomers though, the

(+)-enantiomer exhibited activity at all subunits, while the (-)-enantiomer was completely inactive (**Tables 31**). This could mean that assigning stereochemistry based on optical rotation values and HPLC retention time is not appropriate for this compound as the (+)-enantiomer may have an (*S)*-configuration and the (-)-enantiomer may have an (*R)*-configuration. However, this data could also mean that for the **1180-168** pair of enantiomers, the (*R*)-enantiomer is active and the (*S*)-enantiomer is not, which is in contrast to the separation of **1180-154** and **1180-103** (discussed below). It is also in deep contrast to the enantiomers of its amide-containing counterparts **1180-92** where the (-)-enantiomer holds all the activity and the (+)-enantiomer is inactive. For this reason, crystal structures of both **1180-168** enantiomers were grown, allowing for the definition of absolute stereochemistry for this pair. The two enantiomers were assigned as (*R*)-(+)-**1180-168** and (*S*)-(-)-**1180-168** based on the crystal structures (**Figure 19**). Activity at the (*R*)-(+)-enantiomer and inactivity at the (*S*)-(-)-enantiomer is unique for the **1180-168** enantiomer, and thus far represents the only active (*R*)-(+)-enantiomer. All biological data and characterization of separated enantiomers is summarized in **Table 32.**

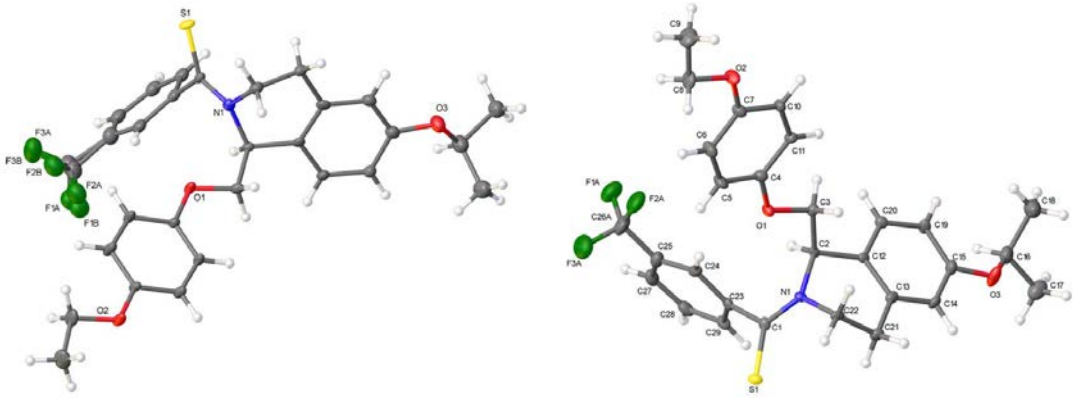

Figure 19. Crystal structure of (*S*)-(-)-1180-168 (left) and (*R*)-(+)-1180-168 (right).

Table 32. Summary of characterization and biological activity for separated enantiomers.

1180-	Analytical column retention time (min)	Optical rotation value	Assigned stereochemistry	GluN2 subunit activity
55	61.5 (OD-RH)	-92	S	GluN2B/GluN2C/GluN2D
	59.2 (OD-RH)	+91	R	GluN2B/GluN2C/GluN2D
163	32.2 (AD-H)	-142	**S**[a]	GluN2B/GluN2C/GluN2D
	24.2 (AD-H)	+114	R	GluN2C/GluN2D
87	18.1 (AD-H)	-102	S	GluN2B
	33.4 (AD-H)	+103	R	-
154	78.7 (AD-H)	-121	S	GluN2B/GluN2C/GluN2D
	73.9 (AD-H)	+129	R	-
103	27.3 (AD-H)	-88	S	GluN2B/GluN2C
	40.0 (AD-H)	+107	R	-
92	11.7 (AD-H)	-103	S	GluN2B/GluN2C
	17.5 (AD-H)	+100	R	-
168	13.2 (AD-H)	-162	S[a]	-
	11.6 (AD-H)	+136	R[a]	GluN2B/GluN2C

[a]Assigned based on crystal structure (**Figure 12** and **Figure 19**).

Compound **1180-103** (**Table 33**), also GluN2B/GluN2C-selective, was separated with a similar hypothesis in mind when approaching the separation of **1180-92**. It was anticipated that the (*S*)-(-)-enantiomer would be active at GluN2B- and GluN2C-containing receptors, while the (*R*)-(+)-enantiomer would be inactive, and the results supported this hypothesis. The (*S*)-(-)-enantiomer was active, while the (*R*)-(+)-enantiomer was not. However, (*S*)-(-)-**1180-103** was only active at 30 μM at GluN2B-containing receptors, while the racemic mixture was active at GluN2B- and GluN2C-containing receptors at this same concentration. The biological data does not suggest that (*S*)-(-)-**1180-103** is completely GluN2B selective though because while potentiation at 30 μM did not exceed 120%, at only 3.0 μM, potentiation at GluN2C- and GluN2D-containing did exceed 120%. This suggests that (*S*)-(-)-**1180-163** is interacting with the receptor in a complex manner, which is discussed in **Chapter 2.4.11.**

Evaluation of these seven pairs of enantiomers has revealed that the GluN2B-activity can be isolated and only resides in one enantiomer. Based on a crystal structure of (*S*)-(-)-**1180-163**, the enantiomer active at GluN2B has been assigned as the (*S*)-(-)-enantiomer in all cases except for **1180-168**, where the (*R*)-(+)-enantiomer is active over the (*S*)-(-)-enantiomer. While the separation of these

enantiomers has only led to one compound that leans toward GluN2B ((*S*)-(-)-**1180-87**), many potent compounds that exhibit activity at GluN2B, GluN2C, and GluN2D subunits have been synthesized with EC_{50} values in the nanomolar region, including (*S*)-(-)-**1180-154**, (*S*)-(-)-**1180-163**, and (*R*)-(+)-**1180-168**, which show dramatic improvement in potentiation and selectivity compared to the original GluN2B potentiator, racemic **1180-55**.

Table 33. Stereoselectivity of 1180-103 enantiomers.

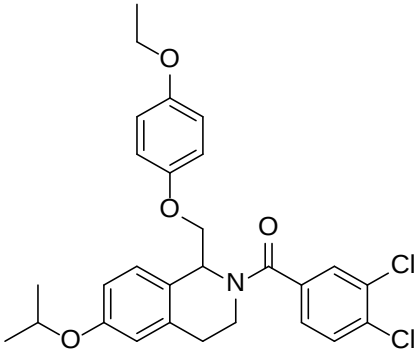

		$I_{30\mu M}$ / $I_{control}$ (mean ± SEM, %)			EC_{50} (max.) (μM %)[a]		
	X	**GluN2B**	**GluN2C**	**GluN2D**	**GluN2B**	**GluN2C**	**GluN2D**
1180-103	O	120 ± 4.4	134 ± 5.1	101 ± 4.2	1.4 (134%)	0.65 (139%)	-
(*R*)-(+)-1180-103	O	83 ±4.9	92 ± 6.7	93 ± 8.0	-	-	-
(*S*)-(-)-1180-103	O	153 ± 9.7	114 ± 6.8[c]	102 ± 6.0[c]	0.94 (163%)	-	-

[a] Fitted EC_{50} values are shown to two significant digits when potentiation at 30 μM exceeded 120%; values in parentheses are the fitted maximum response as a percentage of the initial glutamate (100 μM) and glycine (30 μM) current. Data are from between 3-26 oocytes from 2-5 frogs for each compound and receptor tested. Compound **1180-103** was shown in previous tables and was included here for comparison. [c]Potentiation did not exceed 120% at 30 μM, but at 3μM, the potentiation was greater than 120%.

2.4.11 Relating the evaluation of the enantiomers to the structural determinants of the 1180-55 and CIQ tetrahydroisoquinoline classes

Previous work on racemic CIQ revealed that the main structural determinants of activity for this compound resided in the pre M1 and M1 helix of the TMD GluN2D subunit with only minimal structural determinants on the pre M1 and M1 helix of the GluN1 subunit[3] (discussed in **Chapter 1.2.6** and **Chapter 2.2.4**). This is depicted in **Figure 20,** where point mutations made to the

GluN2D subunit are shown to alter CIQ activity (shown in blue and red) to a much larger degree than point mutations made to the GluN1 subunit. This suggests that either the binding site or downstream structural determiants for CQ action reside in the GluN2D M1 and pre M1 helix. In contrast to these results, numerous point mutations made to the pre M1 and M1 helix of the GluN2 subunit ***and*** the GluN1 subunit did affect **1180-55**-mediated potentiation (**Figure 21**), raising the possibility that **1180-55** engages a different binding site or different downstream strucutural deterimants than CIQ.

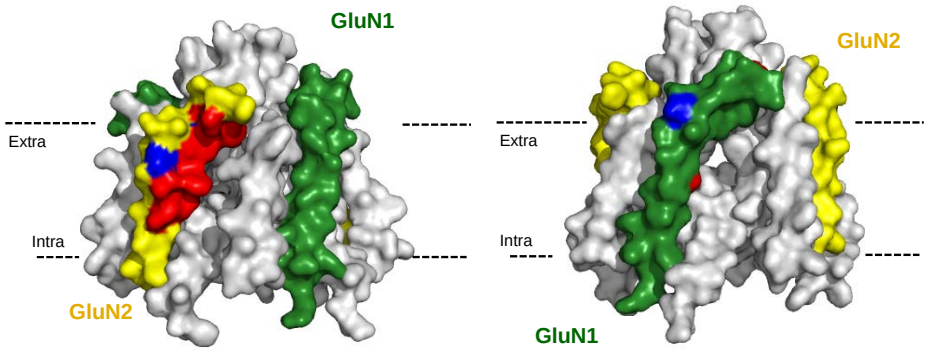

Figure 20. Point mutations that enhanced (blue) or inhibited (red) activity by CIQ on the GluN2 subunit (left) and GluN1 (right).

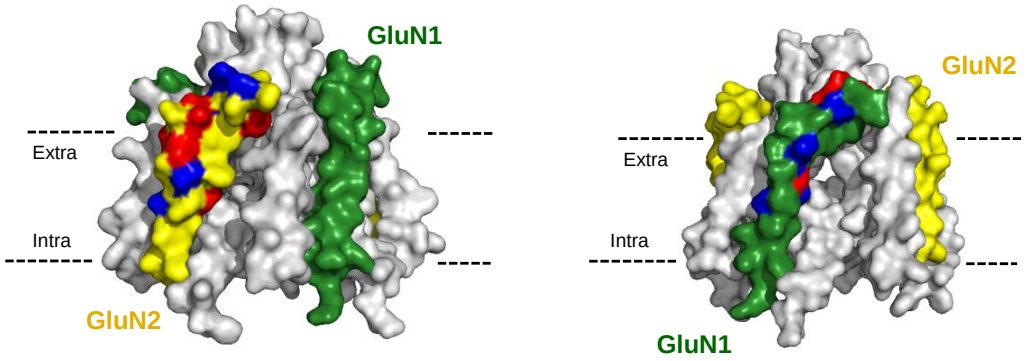

Figure 21. Point mutations that enhanced (blue) or inhibited (red) activity by 1180-55 on the GluN2 subunit (left) and GluN1 (right).

Based on these site-directed mutagenesis results, it was hypothesized that when the enantiomers of **1180-55** and **1180-163** were separated, one enantiomer would interact with the GluN2 subunit and

one would interact with the GluN1 subunit. Since CIQ interacted with the M1 helix of GluN2D, one enantiomer was hypothesized to interact with the GluN2 subunit and exhibit activity at GluN2C and GluN2D subunits, while the other enantiomer was hypothesized to interact with GluN1 and be GluN2B-selective. When the **1180-55** and **1180-163** enantiomers were evaluated (**Table 30**) however, (*R*)-(+)-**1180-163** was GluN2C and GluN2D-selective, while (*S*)-(-)-**1180-163** was active at GluN2B, GluN2C, and GluN2D subunits. This would imply that the (*R*)-(+)-enantiomer is interacting with the GluN2 subunit as predicted. If the (*S*)-(-)-enantiomer is interacting with residues on the GluN1 subunit, this pan-potentiation seems reasonable in hindsight since the GluN1 subunit is an obligatory subunit in the NMDA receptor and will exist in every receptor regardless of GluN2 subunit composition. Even though (*S*)-(-)-**1180-168** appears to be no more selective than the racemic mixture in terms of activity, this enantiomer could be more selective in the sense that the compound is no longer interacting with the CIQ structural determinants – the GluN2C and GluN2D pre M1 and M1 helices

Separation of **1180-154** and **1180-103** resulted in different results than the separation of **1180-55** and **1180-163**; in these cases, only one enantiomer was active, while one was completely inactive. If the hypothesis is correct that racemic **1180-163** is interacting with both the GluN1 and GluN2 subunits, but the (R)-(+)-enantiomer is interacting with the GluN2D subunit and the (S)-(-)-enantiomer is interacting with the GluN1 subunit, then the inactivity of the (*R*)-(+)-enantiomers of **1180-154** and **1180-103** would suggest that these compounds in the racemic form do not interact with the GluN2D subunit. With the synthesis of these racemic compounds, the interactions with the CIQ structural determinants have been altered so that this series is now completely distinct from the CIQ class in that these compounds only interact with the GluN1 subunit.

Preliminary site-directed mutagenesis work (not shown) with racemic **1180-87** has shown that the actions of **1180-87** is influenced by residues in the GluN2B pre M1 helix, and mutations in this region influences **1180-87** activity more than **1180-55**. This could help to explain why **1180-87** is more selective than **1180-55** for GluN2B potentiation. That is, the compound may be minimally interacting

with the GluN1 pre M1 and M1 helix and not interacting with the GluN2C or GluN2D M1 helices. Instead, **1180-87** could be mainly interacting with the GluN2B pre M1 helices, but more work is needed to confirm this. The site-directed mutagenesis work in combination with the biological activity suggests that there could potentially be three main structural determinants for this tetrahydroisoquinoline class. The GluN2 M1 helices (site 1) where point mutations most heavily influence CIQ activity, the GluN2 pre M1 helix (site 2) that influence GluN2B activity, and the GluN1 pre M1 and M1 helix (site 3). In this scenario, CIQ and (*R*)-(+)-**1180-55** would interact with site 1, **1180-87** would interact with site 2, and pan-potentiators would interact with site 3 (**Figure 22**). To confirm this, extensive mutagenesis studies would need to be conducted on the **1180-55**, **1180-87**, and **1180-154** enantiomers.

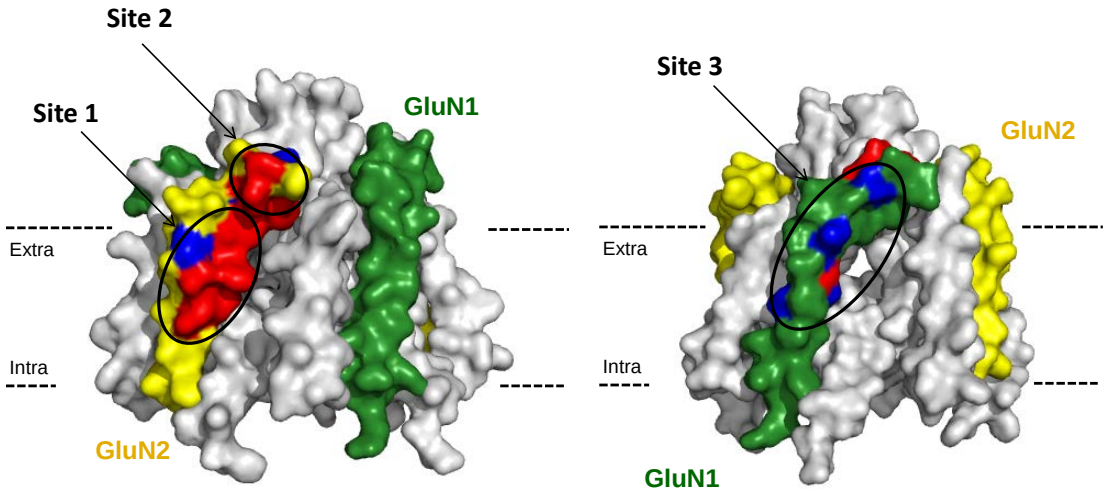

Figure 22. Depiction of the three sites on the GluN2 (left) and GluN1 (right) subunits that influence activity of the receptor by the prototypical compounds discussed.

2.4.12 Evaluation of initial testing for photocrosslinking experiments

Although site-directed mutagenesis would be one way to test the important structural determinants for activity from the compounds discussed, photoaffinity labeling could be also help reveal which residues these compounds interact with. Initial work done on the photoaffinity labeling experiments was the testing of compounds with azide, benzophenone, and alkyne functionality to ensure that these functional groups did not eliminate activity.

The benzophenone functionality was placed on morpholine-containing tetrahydroisoquinoline **28d**, and despite the bulkiness of this compound, **1180-135** was active at GluN2C- and GluN2D-containing receptors with modest EC_{50} values of 2.6 μM and 3.3 μM (**Table 34**). Compound **1180-135** with benzophenone functionality actually exhibited increased potency at GluN2 and GluN2D subunits compared to morpholine-containing compound **1180-120** with a chlorine on the A-ring, that had EC_{50} values of 15 μM and 22 μM. Although these resulted suggested that a compound with benzophenone functionality would be active and could eventually be used in photocrosslinking experiments, the compound was not potentiating the GluN2B subunit. The lack of activity at GluN2B could be due to the morpholine group on the C-ring, but regardless, the smaller azide functionality was also investigated as a possible photoaffinity label. Compound **1180-143** with isopropoxy functionality on the C-ring and an azide on the A-ring was active at GluN2B-, GluN2C-, and GluN2D-contaning receptors (**Table 35**). Although more efficacious at GluN2C and GluN2D than GluN2B, these result suggests that an azide could be used a photoaffinity label. The azide functionality is preferred to the benzophenone functionality due to its smaller size and because it induced potentiation at GluN2B-containing receptors.

Table 34. Effect of benzophenone functionality on potency and efficacy.

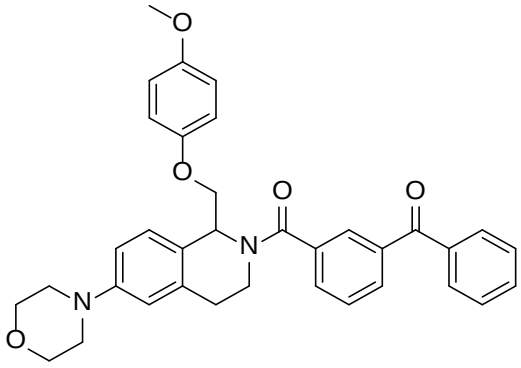

	$I_{30\mu M}$ / $I_{control}$ (mean ± SEM, %)			EC_{50} (max.) (μM %)[a]		
1180-	**GluN2B**	**GluN2C**	**GluN2D**	**GluN2B**	**GluN2C**	**GluN2D**
135	103 ± 6.4	206 ± 9.2	172 ± 4.3	-	2.6 (243%)	3.3 (181%)

[a] Fitted EC_{50} values are shown to two significant digits when potentiation at 30 μM exceeded 120%; values in parentheses are the fitted maximum response as a percentage of the initial glutamate (100 μM) and glycine (30 μM) current. Data are from between 7-9 oocytes from 2 frogs for each compound and receptor tested.

Table 35. Effect of azide and alkyne functionality on potency and efficacy.

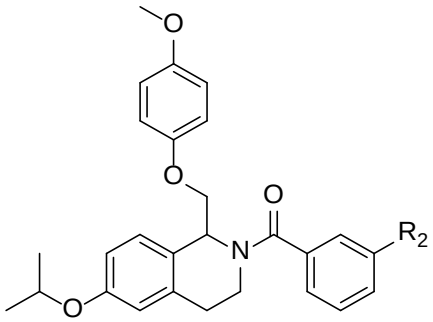

		$I_{30\mu M}$ / $I_{control}$ (mean ± SEM, %)			EC_{50} (max.) (μM %)[a]		
1180-	**R_1**	**GluN2B**	**GluN2C**	**GluN2D**	**GluN2B**	**GluN2C**	**GluN2D**
143	N_3	173 ± 19	270 ± 25	373 ± 36	13 (187%)	1.2 (279%)	1.1 (420%)
282	CCH	165 ± 5.4	254 ± 19	356 ± 14	5.4 (170%)	1.4 (262%)	2.3 (275%)

[a] Fitted EC_{50} values are shown to two significant digits when potentiation at 30 μM exceeded 120%; values in parentheses are the fitted maximum response as a percentage of the initial glutamate (100 μM) and glycine (30 μM) current. Data are from between 4-10 oocytes from 1-2 frogs for each compound and receptor tested.

Additionally, alkyne functionality was explored to ensure that an alkyne would not eliminate activity at the NMDA receptors. Compound **1180-282** with an alkyne on the A-ring was active at GluN2B-,

GluN2C-, and GluN2D-containing receptors. This suggests that the [3 +2] cycloaddition to attach the azide functionalized biotin (**8**) would be a possibility for the photoaffinity experiments. Since both the azide and alkyne were active on the A-ring, either functionality could be place on that ring, but the final compound for the photoaffinity experiments would need to have both an azide and an alkyne. One of these functionalities would need to be moved to the B-ring. The synthesis of compounds with an azide or alkyne on the B-ring would need to be completed, but this work suggests that the A-ring would be amenable to either a photoaffinity label or a tag for the attachment of biotin.

2.5 Conclusion

While the previously published compound known as CIQ[1] was selective for GluN2C and GluN2D-containing receptors over GluN2A and GluN2B-containing receptors, the replacement of dimethoxy groups on the C-ring with single isopropoxy functionality led to a tetrahydroisoquinoline compound that potentiated the GluN2B-subunit. The **1180-55** compound proved distinct from CIQ in tests that studied the effect on agonist potency and deactivation as well; CIQ has no impact on agonist potency or deactivation time course at any subunits, but **1180-55** does. A thorough SAR around **1180-55** has resulted in a number of compounds with increased potency and efficacy at GluN2B-, GluN2C-, and GluN2D-containing receptors compared to **1180-55**, and the best-in-class compound is **1180-169** with EC_{50} values at each subunit that range from 0.20 – 0.40 μM with maximum effect values in the 400-500% range. Even though this compound is active at GluN2B in addition to GluN2C and GluN2D subunits, this represents a drastic improvement on potency and efficacy at the GluN2C and GluN2D subunits compared to CIQ and the initial screening hit (**Figure 23**).

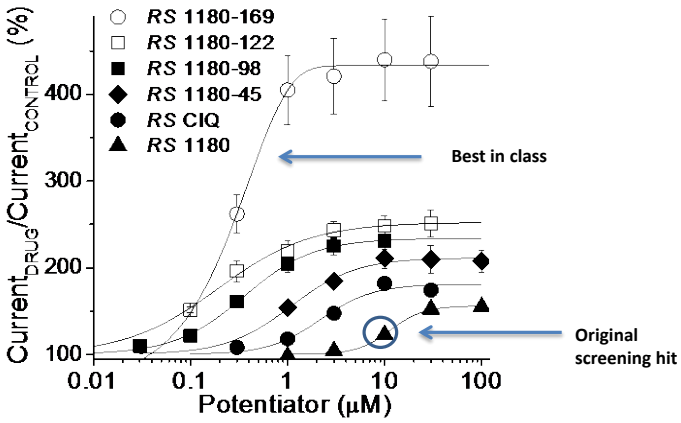

Figure 23. Improved potency from the original screening hit to 1180-169, the best-in-class compound, at the GluN2D subunit.

The SAR has also led to a number of compounds with varying degrees of subunit selectivity that include GluN2B/GluN2C selectivity, GluN2C/GluN2D selectivity, and GluN2B selectivity. While branched or cyclic moieties on the C-ring are essential for GluN2B-activity, a second important component for GluN2B-selectivity over the other subunits is the B-ring, as ethoxy-containing B-rings led to compounds that were consistently selective for GluN2B/GluN2C-subunits over GluN2D. When an ethoxy group was placed on the B-ring of the **1180-55** scaffold, the isopropoxy functionality was able to revive a compound that was inactive at all subunits; **1180-53**, which resembles CIQ, had no activity, but **1180-83** was selective for GluN2B- and GluN2C-containing receptors, while **1180-55** is active at GluN2B-, GluN2C-, and GluN2D-containing receptors (**Figure 24**). Even compounds with isopropoxy functionality on the B-rings were active and selective for GluN2B/GluN2C subunits over GluN2D, but based on the inactivity of **1180-53**, isopropoxy functionality would most likely not be active on the CIQ scaffold. This preference for larger, bulkier substituents on the B-ring is a key difference between the CIQ scaffold and the **1180-55** scaffold, and by exploiting this difference, we were able to push the tetrahydroisoquinoline scaffold towards GluN2B. Further SAR led to one compound, **1180-87**, that was completely selective for GluN2B over the other subunits.

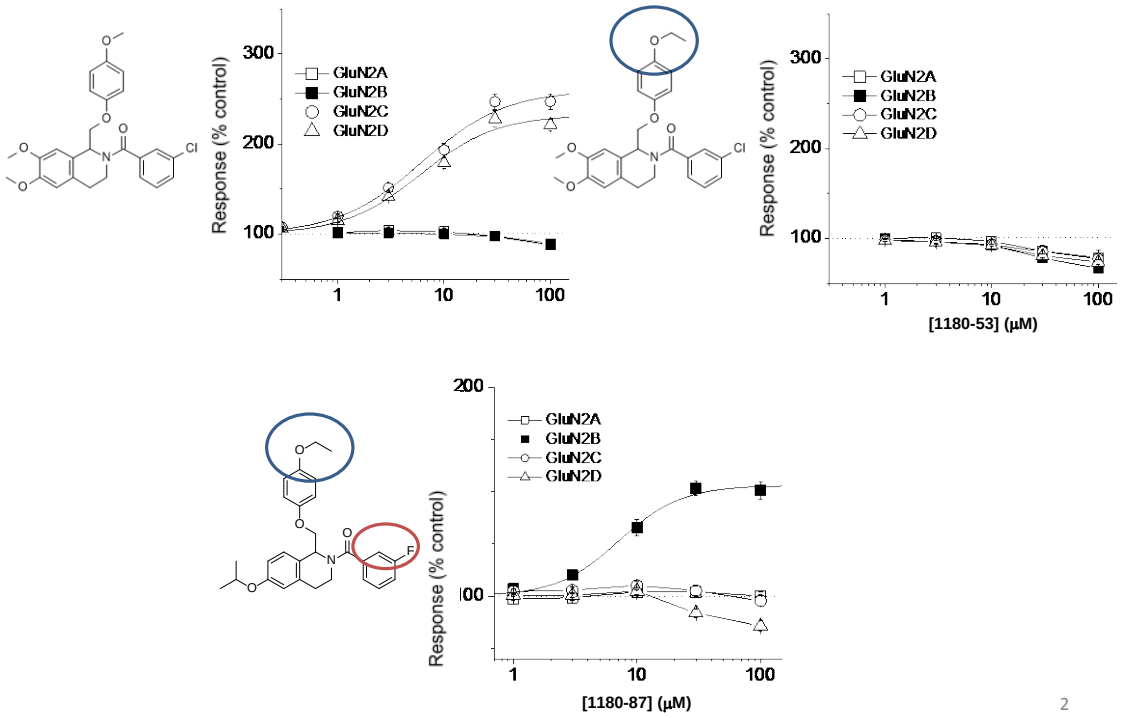

Figure 24. The isopropoxy functionality on the C-ring (1180-83) revives activity at the GluN2B-, GluN2C-, and GluN2D-containing receptors that had been eliminated by the ethoxy functionality on the CIQ scaffold (1180-53). A-ring modifications led to a GluN2B selective compound (1180-87).

While the isopropoxy functionality on the C-ring and an ethoxy group on the B-ring led to the most selective compounds, the most significant shifts in potency arise from modifications to the A-ring linker. While the majority of compounds have EC_{50} values in the micromolar range, thioamide-containing compounds are consistently more potent at all active subunits with EC_{50} values in the nanomolar region. The thioamide A-ring linker is not only important for potency, but it is also a key pharmacophore of the tetrahydroisoquinoline compounds active at the GluN2B subunit. All compounds that were GluN2C- and GluN2D-selective as the amide were inactive as the thioamide, but all compounds active at GluN2B as the amide were active as the thioamide at GluN2B-, GluN2C-, and/or GluN2D-containing receptors.

An extensive SAR around all three rings of the **1180-55** scaffold has revelaed that the C-ring is important for pan potentiation at GluN2B, GluN2C, and GluN2D subunits, and a variety of ether and amine functionality can be tolerated in the R_1 position as labeled in Figure X. While the amine functionality is active at all three subunits, the oxygen-containing C-ring compounds are typically more efficacious. In terms of selectivity, an isopropyl is the optimal functionality, but the isobutyl functionality is superior in terms of efficacy and potentiation at all three subunits as shown when comparing **1180-55** and **1180-114** in **Table 12** and **1180-83** and **1180-124** in **Table 13**. In terms of the B-ring, the *para*-position is the only location tht leds to GluN2B activity, and a trend in evident in terms of size; the ethoxy and isopropoxy are more selective than the smaller methoxy. The A-ring is amenable to a variety of functionality in the meta-position, although halogen groups were explored most extensively and installed when studying other ring of the tetrahydroisoquinoline. Moving a halogen group from the meta-position to the ortho- or para-position generally led to a loss in activity, while disubstitution in the meta- and para-positions led to active compounds. Finally, the A-ring linker, as discussed above, is important for driving the potentcy at all three subunits into the nanomolar region. The most potent compounds throughout the entire series are those with a thioamide linker, and this may be a result of the ability of the thioamide to hold the rotamer in a preferred conformation. While the thioamide linker was important for activity, other linkers such as the sulfonamide and the urea were inactive at all three subunits, while the thiourea linker-containing compound was selective for GluN2C- and GluN2D-containing NMDA receptors.

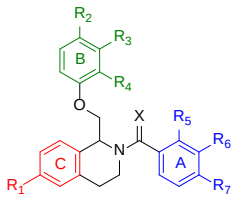

C-ring

- Small alkyl chains and cyclic ethers lead to potent nonselective potentiators and occasionally selective potentiators
- Nitrogen containing heterocycles or alkyl chains in R_1 position lead to loss in activity overall , but still potentiate GluN2B

B-ring

- OEt in R_2 position as opposed to OMe leads to a gain in selectivity and/or potency depending on C-ring substituents
- OMe in the R_3 position leads to GluN2C/GluN2D-selective compound, while OMe in the R_4 position eliminates activity.

A-ring

- Halogens in the R_6 position cause potentiation, while R_7 halogens are inactive when OEt is on B-ring. Halogens in the R_5 position are inactive as well.
- R_6 and R_7 disubsitituted compounds are active

A-ring Linker

- Converting the amide to a thioamide leads to increases in potencies
- Sulfonamide and urea linker are inactive, while thiourea is GluN2C/D selective

Figure 25. Summary of SAR around 1180-55 series of comopounds.

With the separation of the **1180-55** and **1180-163** enantiomers via a chiral synthesis and the resolution of the *S*-(-) enantiomer by X-ray crystallography, we have determined that the GluN2B activity resides exclusively in the *S*-(-) enantiomer. While both enantiomers are active, the *R*-(+) enantiomer is selective for GluN2C and GluN2D-containing receptors and the *S*-(-) enantiomer causes potentiation at GluN2B, GluN2C, and GluN2D-containing receptors. Separation of GluN2B-selective compound **1180-87** and GluN2B/GluN2C selective compounds **1180-103**, **1180-92**, and **1180-168** further highlighted that the GluN2B activity is exclusive for the (-)-enantiomer.

While CIQ has structural determinants that reside almost exclusively on the GluN2 subunit, site-directed mutagenesis has shown that **1180-55** has structural determinants on both the GluN1 and GluN2 subunits. Based on the activity of the **1180-55** and **1180-163** enantiomers, it stands to reason that the (*R*)-(+)-enantiomers, which are CIQ-like, are most likely interacting with the GluN2 subunit, while the (S)-(-)-enantiomers are interacting with the GluN1 subunit. With the separation of these enantiomers, we have separated these two structural determinant sites. When **1180-154** was separated the (*R*)-(+)-enantiomer was inactive, suggesting that with the synthesis of **1180-154**, we have completely eliminated interaction with the GluN2 site, or the CIQ-like site, and have begun to develop compounds for a completely distinct site from the site for CIQ.

By expanding on the CIQ scaffold we have developed potentiators that are able to target the GluN2B subunit. Potentiation of the GluN2B subunit has been observed with certain endogenous molecules, such as polyamines, neurosteroids, and aminoglycoside antibiotics, but is still rare with small, drug-like molecules. There is a need for potent compounds that can be utilized as therapeutic probes for the study of GluN2B potentiation, and with the synthesis of many of these compounds, namely **1180-87**, **1180-154**, **1180-271**, **1180-272**, and **1180-169**, we have shown that the CIQ series could provide these therapeutic tools.

2.6. Experimental Details

2.6.1 Chemistry experimental procedures

General Experimental: All reagents were purchased from commercial vendors and used without further purification. Thin layer chromatography (TLC) on precoated aluminum plates (silica gel 60 F254, 0.25 mm) or LCMS (Varian) were used to monitor reaction progress. Purification by flash column chromatography was done on a Teledyne ISCO Combiflash Companion using Teledyne Redisep normal phase columns. Proton and carbon NMR spectra were recorded on an INOVA-400 (400 MHz), VNMRS-400 (400 MHz), Mercury 300 Vx (300 MHz) or INOVA-600 (600 MHz). All chemical shifts were reported in parts per million and coupling constants were reported in Hertz (Hz). The spectra were referenced to the solvent peak. Mass spectra were performed by the Emory University Mass Spectroscopy Center on either a VG 70-S Nier Johnson or JEOL instrument. Purity was established by HPLC (Varian) in two solvents systems (MeOH:water and ACN:water) unless indicated by combustion analysis. The conditions were determined for each individual compound. Elemental analysis was performed by Atlantic Microlab, Inc (Norcross, GA) for C, H, and N, and agreed with proposed structures within 0.4 + of theoretical values. Optical rotation values were obtained using a Perkin-Elmer 314 instrument.

General Preparation for phenethylcarbamate compounds (Procedure I). Potassium carbonate (4.0 equiv) was added to a solution of tert-butyl 3-hydroxyphenethylcarbamate 3 (1.0 equiv) in dry DMF (44.4 ml) and the reaction was allowed to stir for 2 hours before the alkyl halogen (1.5 – 2.0

equiv) was added and the reaction was heated to 60°C. After stirring for 24 hours, the reaction was quenched with saturated NH_4Cl and extracted into EtOAc. The organic layer was washed with water and brine, dried with $MgSO_4$, filtered, and concentrated in vacuo. The resulting residue was subjected to flash column chromatography to afford the title compound.

General Preparation for phenethylcarbamate compounds (Procedure II). Triphenylphosphine (1.0 equiv), the substituted alcohol (1.2 equiv), and triethylamine (1.0 equiv) were added to a solution of tert-butyl 3-hydroxyphenethylcarbamate (1.0 equiv) dissolved in dry THF. The reaction was brought to 0 °C with an ice bath and (Z)-diisopropyl diazene-1,2-dicarboxylate (1.0 equiv) was added dropwise. After stirring for 6 days, the reaction was quenched with 1M HCl and extracted into EtOAc. The organic layer was washed with water and brine, dried with $MgSO_4$, filtered, and concentrated *in vacuo*. The resulting residue was subjected to flash column chromatography to afford the title compound.

General Preparation for phenylethanamine hydrochloride compounds (Procedure III): The phenethylcarbamate compound was dissolved in a solution of ether and 12 N HCl (2:1 mixture) and allowed to stir at room temperature for 40 minutes. The volatiles were removed *in vacuo* to afford the title compound, which was carried forward without any further purification.

General Preparation for 2-chloro-*N*-phenethylacetamide compounds (Procedure IV): A solution of the phenethylamine (1 equiv.) in dry DCM was brought to 0°C using an ice bath. Triethylamine (2 equiv.) was added followed by the dropwise addition of 2-chloroacetyl chloride (1.2 equiv.) The reaction was allowed to cool to room temperature and stir for 3 hours. Upon completion by TLC, the reaction was quenched with 1M HCl, extracted into DCM, washed with water and brine, dried with $MgSO_4$, filtered, and concentrated *in vacuo*. The resulting residue was then subjected to column chromatography to afford the title compound.

General Procedure for *N*-(phenethyl)-2-(phenoxy)acetamide compounds (Procedure V): To a solution of phenol (1.2 equiv.) dissolved in dry ACN was added Cs_2CO_3 (4 equiv.). The solution was

allowed to stir for 2 hours before the 2-chloro-*N*-phenethylacetamide compound (1.0 equiv.) dissolved in dry ACN was added and the reaction was allowed to stir for 15 hours. Once TLC indicated complete conversion, the reaction was quenched with saturated NH_4Cl and extracted into EtOAc. The organic layer was washed with water and brine, dried with $MgSO_4$, filtered, and concentrated *in vacuo*. The resulting residue was then subjected to column chromatography to afford the title compound.

General Procedure for *N*-(3-iodophenethyl)-2-(phenoxy)acetamide compounds (Procedure VI): A 10 mL sealed vial was charged with the *N*-(3-bromophenethyl)-2-phenoxyacetamide compound (1.0 equiv), copper(I) iodide (0.5 equiv), and sodium iodide (1.5 equiv). The vial was sealed, evacuated, and backfilled with argon. This was repeated twice more before *N*1,*N*2-dimethylethane-1,2-diamine (0.1 equiv) and dry dioxane were added and the reaction was stirred at 110 °C for 24 hours. The reaction was then allowed to cool to room temperature, quenched with a 30 % ammonium hydroxide solution, and diluted with water. The reaction was extracted into EtOAc, washed with water and brine, dried with $MgSO_4$, filtered, and concentrated in vacuo. The resulting residue was then subjected to column chromatography to afford the title compound.

General Procedure for N-(phenethyl)-2-(phenoxy)-acetamide compounds (Procedure VII): A 10 mL sealed vial was charged with the *N*-(3-iodophenethyl)-2-(phenoxy)acetamide compounds (1.0 equiv), copper(I) iodide (0.1 equiv), 1,10-phenanthroline (0.2 equiv), and cesium carbonate (2.0 equiv). The vial was sealed, evacuated, and back-filled with argon. This was repeated twice more before the alcohol 3-pentanol (9.3 equiv) was added, and the vial was submerged in an oil bath heated to 110 °C. After stirring for 24 – 48 hours, the reaction was allowed to cool to room temperature, diluted with EtOAc, and filtered thru a plug of celite rinsing with EtOAc. The organic layer was washed with water and brine, dried with $MgSO_4$, filtered, and concentrated in vacuo. The resulting residue was then subjected to column chromatography to afford the title compound.

General Procedure for 2-(4-methoxyphenoxy)-N-(3-(piperidin-1-yl)phenethyl)acetamide, N-(3-(cyclohexylamino)phenethyl)-2-(4-methoxyphenoxy)acetamide, and 2-(phenoxy)-N-(3-morpholinophenethyl)acetamide compounds (Procedure VIII): A 10 mL sealed vial was charged with the *N*-(3-iodophenethyl)-2-(phenoxy)acetamide compounds (1.0 equiv), copper(I) iodide (0.2 equiv), potassium carbonate (2.0 equiv), and L-proline (0.2 equiv). The vial was sealed, evacuated, and back-filled with argon. This was repeated twice more before DMSO was added followed by cyclic amines or cyclohexanes (1.5 equiv) and the reaction was submerged in an oil bath heated to 80 °C. After stirring for 48 hours, the reaction appeared to be complete by LCMS and TLC. The reaction was allowed to cool to room temperature, diluted with EtOAc, and washed with water (3x), brine (6x), and 5.0 % LiCl solution (8x). The organic layer was dried with $MgSO_4$, filtered, and concentrated in vacuo. The resulting residue was then subjected to column chromatography to afford the title compound.

General Procedure for N-(3-(amino)phenethyl)-2-(4-methoxyphenoxy)acetamide compounds (Procedure IX): The N-(3-(amino)phenethyl)-2-(4-methoxyphenoxy)acetamide compound (1.0 equiv) and paraformaldehyde (10 equiv) were dissolved in AcOH and sodium cyanoborohydride (5.0 equiv) was added in one portion at room temperature. After stirring for 4 - 20 hours the reaction was brought to 0^oC was made basic using concentrated NH_4OH. The reaction was extracted into EtOAc, washed with water and brine, dried with $MgSO_4$, filtered, and concentrated in vacuo. The resulting residue was then subjected to column chromatography to afford the title compound.

General Procedure for 3,4-dihydroisoquinoline Compounds (Procedure X): The amide (1.0 equiv) was suspended in dry toluene and the reaction mixture was brought to reflux. Phosphorous trichloride (3.0 equiv) was added and the reaction was allowed to stir until TLC indicated complete conversion. The reaction was allowed to cool to room temperature, the excess toluene was decanted, and the remaining residue was carried on without further purification.

General Procedure for 3,4-dihydroisoquinoline Compounds (Procedure XI): The amide (1.0 equiv) was suspended in dry toluene and the reaction mixture was brought to reflux. Phosphorous trichloride (3.0 equiv) was added and allowed to stir until TLC indicated complete conversion. The reaction was allowed to cool to room temperature, made basic (pH 13) with concentrated NH_4OH, and the organic layer was extracted into DCM. The organic layer was then washed with water, brine, dried with $MgSO_4$, filtered, and concentrated in vacuo. The resulting residue was carried on without further purification.

General Procedure for 1,2,3,4-tetrahydroisoquinoline Compounds (Procedure XII): The dihydroisoquinoline (1.0 equiv) was dissolved in dry MeOH and brought to 0°C using an ice bath. Sodium borohydride (3.0 equiv) was added slowly and the reaction was allowed to stir overnight and warm to room temperature. The volatiles were concentrated in vacuo, and the resulting residue was extracted into DCM. The organic layer was washed with water and brine, dried with $MgSO_4$, filtered, and concentrated *in vacuo*. The resulting residue was then subjected to column chromatography to afford the title compound.

General Procedure for 3,4-dihydroisoquinolin-2(1H)-yl)methanone) Compounds (Procedure XIII): The tetrahydroisoquinoline (1.0 equiv) was dissolved in dry DCM and brought to 0°C using an ice bath. Triethylamine (2.0 equiv) was added followed by the benzoyl chloride (1.2 equiv). The reaction mixture stirred for approximately 3 hours under an argon atmosphere, at which point TLC indicated complete conversion. The reaction was quenched with 1M HCl and extracted into DCM. The organic layer was washed with water and brine, dried with $MgSO_4$, filtered, and concentrated in vacuo. The resulting residue was then subjected to column chromatography to afford the title compound.

General Procedure for 3,4-dihydroisoquinolin-2(1H)-yl)methanone) Compounds (Procedure XIV): Benzoic acid (1.0 equiv) was dissolved in dry DCM and brought to 0 °C using an ice bath. N1-((ethylimino)methylene)-N3,N3-dimethylpropane-1,3-diamine (1.2 equiv) and N,N-dimethylpyridin-4-amine (1.2 equiv) were added and the reaction was allowed to stir for 2 hours before

tetrahydroisoquinoline (1.0 equiv) dissolved in dry DCM was added. The reaction was allowed to stir overnight and warm to room temperature. The reaction was quenched with DI water, extracted into DCM, washed with water and brine, dried with $MgSO_4$, filtered, and concentrated in vacuo. The resulting residue was then subjected to column chromatography to afford the title compound.

General Procedure for 3,4-dihydroisoquinolin-2(1H)-yl)methanethione) Compounds (Procedure XV): The dihydroisoquinoline (1 equiv) was dissolved in dry toluene and 2,4-bis(4-methoxyphenyl)-1,3,2,4-dithiadiphosphetane 2,4-disulfide (0.5 – 1 equiv) was added. The reaction was brought to reflux. After 2 - 8 hours, the solvent was removed under reduced pressure and the residue was dissolved in DCM. The solution was washed with a 10% solution of $NaHCO_3$, dried with $MgSO_4$, filtered, and concentrated in vacuo. The resulting residue was then subjected to column chromatography to afford the title compound.

General Procedure for 3,4-dihydroisoquinolin-2(1H)-yl)methanethione) Compounds (Procedure XVI): The dihydroisoquinoline (1 equiv) was dissolved in dry toluene and 2,4-bis(4-methoxyphenyl)-1,3,2,4-dithiadiphosphetane 2,4-disulfide (0.5 – 1 equiv) were dissolved in toluene in a sealed tube. The material was heated to 150°C for 35 minutes in the microwave. The reaction was diluted with DCM, quenched with saturated sodium bicarbonate. The organic layer was washed with water and brine, dried with MgSO4, filtered, and concentrated in vacuo. The resulting residue was then subjected to column chromatography to afford the title compound.

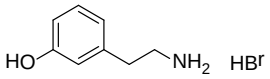

3-(2-aminoethyl)phenol hydrobromide (10): 2-(3-methoxyphenyl)ethanamine (8.0 g, 53 mmol) was dissolved in AcOH (80. mL). 48% HBr (86 mL) was added and the reaction was brought to reflux for 4 hours before cooling to room temperature. Excess solvent was removed *in vacuo* using EtOH as an azetrope to afford a green solid (11 g, 95 %). ^{1}H NMR (CD_3OD, 400 MHz) δ: 7.14 (t, *J* = 8.0 Hz, 1H), 6.73-6.66 (m, 3H), 3.14 (t, *J* = 7.6 Hz, 2H), 2.88 (t, *J* = 8.4 Hz, 2H); ^{13}C NMR

(CD_3OD, 100 MHz) δ: 157.8, 138.1, 129.8, 119.6, 115.4, 113.9, 48.5, 47.2, 40.7, 33.3; HRMS calcd. for $C_8H_{12}O_1N_1$, 138.09134 $[M + H]^+$; 138.09105 found, $[M + H]^+$.

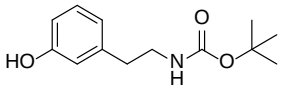

tert-butyl 3-hydroxyphenethylcarbamate (11): Amine 1 (7.2 g, 33 mmol) was dissolved in dioxane (98 mL) and dry DMF (12 mL). Triethylamine (4.6 mL, 33 mmol) was added and the mixture was allowed to stir for 15 minutes before di-tert-butyl dicarbonate (7.2 g, 33 mmol) was added. The resulting mixture stirred overnight at room temperature. The volatiles were concentrated *in vacuo* and the resulting residue was extracted into EtOAc. The organic layer was then washed with water and brine, dried with $MgSO_4$, filtered, and concentrated *in vacuo*. The crude residue was purified by silica gel chromatography (ISCO, Redisep 80 g column, 10-80% EtOAc/hexanes gradient) to afford the title compound as a white solid (6.0 g, 77 %) TLC (MeOH:DCM, 1:10, v/v) Rf = 0.73; ^{1}H NMR ($CDCl_3$, 400 MHz) δ: 7.14 (t, *J* = 8.0 Hz, 1H), 6.73-6.56 (m, 4H), 4.65 (s, 1H), 3.35 (q, *J* = 6.4 Hz, *J* = 12.8 Hz, 2H), 2.70 (t, *J* = 6.8, 2H), 1.42 (s, 9H); ^{13}C NMR ($CDCl_3$, 100 MHz) δ: 156.6, 156.5, 140.8, 129.9, 120.9, 115.9, 113.8, 79.9, 41.8, 36.2, 28.6; HRMS calcd. for $C_{13}H_{19}O_3N_1{}^{23}Na_1$, 260.12571[M + H]$^+$; 260.12550 found, $[M + H]^+$.

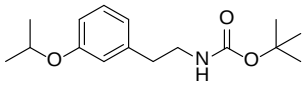

tert-butyl 3-isopropoxyphenethylcarbamate (12a): Compound **12a** was prepared via procedure I using compound **11** (2.6 g, 11 mmol), potassium carbonate (5.0 g, 36 mmol) and 2-iodopropane (1.4 ml, 9.1 mmol) in dry DMF (28mL). The crude residue was purified by silica gel chromatography (ISCO, Redisep 80 g column, 10-80% EtOAc/hexanes gradient) to afford the title compound as a clear oil (1.8 g, 72 %) TLC (MeOH:DCM, 1:10, v/v) Rf = 0.86; ^{1}HNMR ($CDCl_3$, 400 MHz) δ: 7.17 (t, *J* = 8.0 Hz, 1H), 6.75-6.70 (m, 3H), 4.55-4.51 (m, 1H), 3.36-3.35 (m, 2H), 2.73 (t, *J* = 7.2, 2H), 1.41 (s, 9H), 1.32 (s, 3H), 1.30 (s, 3H); ^{13}C NMR ($CDCl_3$, 100 MHz) δ: 158.3, 156.1, 140.9, 129.8, 121.2,

116.6, 113.9, 79.4, 69.9, 41.9, 36.4, 28.6, 22.3; HRMS calcd. for $C_{16}H_{25}O_3N_1{}^{23}Na_1$, 280.19072 $[M + H]^+$; 280.19035 found, $[M + H]^+$.

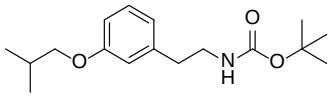

tert-butyl 3-isobutoxyphenethylcarbamate (12b): Compound **12b** was prepared via procedure I using compound **11** (3.5 g, 15 mmol), potassium carbonate (8.2 g, 59 mmol) and 1-iodo-2-methylpropane (2.6 ml, 22 mmol) in dry DMF (44 mL). The crude residue was purified by silica gel chromatography (ISCO, Redisep 80 g column, 10-80% EtOAc/hexanes gradient) to afford the title compound as a clear oil (1.5 g, 35 %) TLC (EtOAc/hexanes, 1:3, v/v) Rf = 0.58; ^{1}HNMR ($CDCl_3$, 400 MHz) δ: 7.19 (t, *J* = 8.0 Hz, 1H), 6.76-6.72 (m, 3H), 4.53 (bs, 1H), 3.69 (d, *J* = 6.4 Hz, 2H), 3.38-3.33 (m, 2H), 2.76-2.73 (m, 2H), 2.09-2.02 (m, 1H), 1.41 (s, 9H), 1.00 (d, *J* = 6.8 Hz, 6H); HRMS calcd. for $C_{12}H_{20}ON$, 194.15394 $[M + H]^+$; 194.15390 found, $[M + H]^+$.

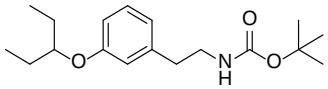

tert-butyl 3-(pentan-3-yloxy)phenethylcarbamate (12c): Compound **12c** was prepared via procedure II using compound **11** (3.0 g, 13 mmol), triphenylphosphine (3.3 g, 13mmol), triethylamine (1.8 ml, 13 mmol), 3-pentanol (1.6 ml, 15 mmol), and (Z)-diisopropyl diazene-1,2-dicarboxylate (2.1 ml, 13 mmol) in dry THF (13 ml). The crude residue was purified by silica gel chromatography (ISCO, Redisep 40 g column, 10-90% EtOAc/hexanes gradient) to afford the title compound as a clear oil (1.3 g, 34 %). TLC (EtOAc:hexanes, 1:1, v/v) Rf = 0.86; ^{1}H NMR ($CDCl_3$, 400 MHz) δ: 7.17 (t, *J* = 8.0 Hz, 1H), 6.75-6.72 (m, 3H), 4.55 (bs, 1H), 4.12-4.06 (m, 1H), 3.38-3.33 (m, 2H), 2.73 (t, *J* = 6.8 Hz, 2H), 1.69-1.62 (m, 4H), 1.42 (s, 9H), 0.93 (t, *J* = 7.6 Hz, 6H); ^{13}C NMR ($CDCl_3$, 100 MHz) δ: 159.1, 156.1, 129.7, 121.1, 116.8, 113.9, 80.3, 79.3, 41.8, 36.4, 28.6, 22.3, 9.83; HRMS calcd. for $C_{13}H_{22}ON$, 208.16959 $[M + H]^+$; 208.16956 found, $[M + H]^+$.

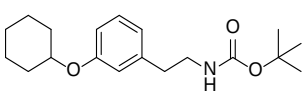

tert-butyl 3-(cyclohexyloxy)phenethylcarbamate (12d): Compound **12d** was prepared via procedure II using compound **11** (2.0 g, 8.4 mmol), triphenylphosphine (2.2 g, 8.4 mmol), triethylamine (1.2 ml, 8.4 mmol), cyclohexanol (0.88 ml, 8.4 mmol) and (Z)-diisopropyl diazene-1,2-dicarboxylate (1.4 ml, 8.4 mmol) in dry THF (8.4 ml). The crude residue was purified by silica gel chromatography (ISCO, Redisep 40 g column, 10-90% EtOAc/hexanes gradient) to afford the title compound as a white solid (0.63 g, 23%). TLC (EtOAc:hexanes, 1:1, v/v) Rf = 0.92; ^{1}H NMR ($CDCl_3$, 400 MHz) δ: 7.17 (t, 1H, *J* = 15.6 Hz), 6.78-6.71 (m, 3H), 4.52 (bs, 1H), 4.24-4.18 (m, 1H), 3.36-3.35 (m, 2H), 2.75-2.72 (m, 2H), 1.98-1.94 (m, 2H), 1.82-1.78 (m, 2H) 1.54-1.26 (m, 15H); ^{13}C NMR ($CDCl_3$, 100 MHz) δ: 158.1, 156.1, 140.7, 129.7, 121.1, 116.8, 114.0, 75.4, 63.3, 41.9, 36.4, 32.0, 28.6, 25.8, 24.0; HRMS calcd. for $C_{14}H_{22}ON$, 220.16959 $[M + H]^+$; 220.16960 found, $[M + H]^+$.

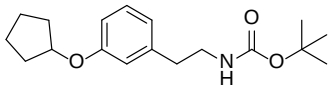

tert-butyl 3-(cyclopentyloxy)phenethylcarbamate (12e): Compound **12e** was prepared via procedure I using compound **11** (1.2 g, 5.1 mmol), cesium carbonate (6.9 g, 21.2 mmol) and iodocyclopentane (0.83 ml, 4.3 mmol) in dry DMF (13 mL). The crude residue was purified by silica gel chromatography (ISCO, Redisep 80 g column, 10-80% EtOAc/hexanes gradient) to afford the title compound as a white solid (0.61 g, 47 %) TLC (MeOH:DCM, 1:10, v/v) Rf = 0.83; ^{1}HNMR ($CDCl_3$, 400 MHz) δ: 7.17 (t, *J* = 8.0 Hz, t), 6.73-6.69 (m, 3H), 4.75-4.71 (m, 1H), 4.53 (s, 1H), 3.78-3.33 (m, 2H), 2.73 (t, *J* = 7.2 Hz, 2H), 1.92-1.74 (m, 6H), 1.73-1.56 (m, 2H), 1.42 (s, 9H); ^{13}C NMR ($CDCl_3$, 100 MHz) δ: 158.5, 156.1, 140.7, 129.7, 120.9, 116.3, 113.5, 79.2, 41.8, 36.4, 33.1, 28.6, 24.2; HRMS calcd. for $C_{18}H_{27}O_3N^{23}Na$, 382.18832 $[M + H]^+$; 382.18798 found, $[M + H]^+$.

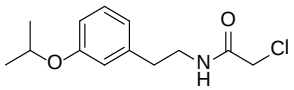

2-chloro-N-(3-isopropoxyphenethyl)acetamide (14a): Compound **13a** was prepared via procedure III using Compound **12a** (2.9 g, 11 mmol). The compound was carried forward without further purification. HRMS calcd. for $C_{11}H_{18}O_1N_1$, 180.13829 $[M + H]^+$; 180.13808 found, [M +

H]$^+$. Compound **14a** was prepared via procedure IV amine **13a** (2.2 g, 10 mmol), triethylamine (2.8 ml, 20 mmol) and 2-chloroacetyl chloride (0.97 ml, 12 mmol) in dry DCM (43 mL) and saturated $NaHCO_3$ (10. mL). The crude product was purified by silica gel chromatography (10-90 EtOAc/hexanes) to afford the title compound as a clear oil (1.8 g, 71 %). TLC (EtOAc:hexanes, 1:1, v/v) Rf = 0.58; ^{1}HNMR ($CDCl_3$, 400 MHz) δ: 7.20 (t, *J* = 7.6 Hz, 1H), 6.77-6.71 (m, 3H), 6.61 (bs, 1H), 4.56-4.49 (m, 1H), 4.00 (s, 2H), 3.54 (q, *J* = 7.2 Hz, *J* = 12.8 Hz, 2H), 2.79 (t, *J* = 7.2 Hz, 2H), 1.32 (s, 3H), 1.30 (s, 3H); ^{13}CNMR ($CDCl_3$, 100 MHz) δ: 166.1, 158.4, 140.1, 129.9, 121.1, 116.7, 114.2, 69.9, 42.9, 41.1, 35.7, 22.3; HRMS calcd. for $C_{13}H_{19}O_2N_1{}^{35}Cl_1$, 256.10988 $[M + H]^+$; 256.10950 found, $[M + H]^+$.

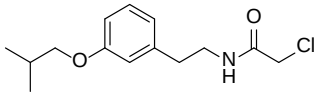

2-chloro-N-(3-isobutoxyphenethyl)acetamide (14b): Compound **13b** was prepared via procedure III using compound **12b** (1.7 g, 5.8 mmol). The compound was carried forward without further purification. HRMS calcd. for $C_{12}H_{20}ON$, 194.15394 $[M + H]^+$; 194.15384 found, $[M + H]^+$. Compound **14b** was prepared via procedure IV using amine **13b** (1.3 g, 5.5 mmol), triethylamine (1.5 ml, 11 mmol) and 2-chloroacetyl chloride (0.52 ml, 6.6 mmol) in DCM (20 mL) and saturated $NaHCO_3$ (10. mL). The crude product was purified by silica gel chromatography (10-90% EtOAc/hexanes) to afford the title compound as a clear oil (0.91 g, 62 %). TLC (EtOAc:hexanes, 1:1, v/v) Rf = 074; ^{1}HNMR ($CDCl_3$, 400 MHz) δ: 7.24-7.19 (m, 2H), 6.78-6.73 (m, 3H), 6.60 (bs, 1H), 4.01 (s, 2H), 3.69 (d, *J* = 8.0 Hz, 2H), 3.55 (q, *J* = 6.8 Hz, 2H), 2.80 (t, *J* = 6.8 Hz, 2H), 2.09-2.03 (m, 1H), 1.00 (d, *J* = 6.0 Hz, 6H); ^{13}CNMR ($CDCl_3$, 100 MHz) δ: 165.9, 159.8, 140.0, 129.9, 121.0, 115.2, 112.9, 74.5, 42.9, 41.1, 35.7, 28.5, 19.5; HRMS calcd. for $C_{14}H_{21}O_2N_1{}^{35}Cl_1$, 270.12553 $[M + H]^+$; 270.12551 found, $[M + H]^+$.

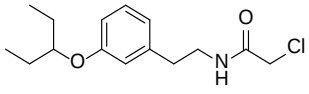

2-chloro-N-(3-(pentan-3-yloxy)phenethyl)acetamide (14c): Compound **13c** was prepared via procedure III using compound **12c** (1.3 g, 4.3 mmol). The compound was carried forward without further purification. HRMS calcd. for $C_{13}H_{22}ON$, 208.16959 $[M + H]^+$; 208.16952 found, $[M + H]^+$. Compound **14c** was prepared via procedure III using by amine **13c** (1.1 g, 4.6 mmol), triethylamine (1.3 ml, 8.1 mmol) and 2-chloroacetyl chloride (0.44 ml, 5.5 mmol) in DCM (18 mL) and saturated $NaHCO_3$ (10. mL). The crude product was purified by silica gel chromatography (10-90 % EtOAc/hexanes) to afford the title compound as a clear oil (0.74 g, 58 %). TLC (EtOAc:hexanes, 1:1, v/v) Rf = 0.71; ^{1}HNMR ($CDCl_3$, 400 MHz) δ: 7.20 (t, *J* = 15.6 Hz, 1H), 6.77-6.72 (m, 3H), 6.62 (bs, 1H), 4.13-4.07 (m, 1H), 4.02 (s, 2H), 3.55 (q, *J* = 7.2 Hz, 2H), 2.79 (t, *J* = 6.8 Hz, 2H), 1.69-1.62 (m, 4H), 0.93 (t, *J* = 7.6 Hz, 6H); ^{13}CNMR ($CDCl_3$, 100 MHz) δ: 116.0, 159.3, 140.1, 129.9, 120.9, 116.7, 114.2, 80.3, 42.9, 41.0, 35.7, 26.2, 9.8; HRMS calcd. for $C_{15}H_{23}O_2N^{35}Cl$, 284.14118 $[M + H]^+$; 284.14120 found, $[M + H]^+$.

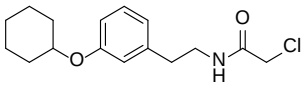

2-chloro-N-(3-(cyclohexyloxy)phenethyl)acetamide (14d): Compound **13d** was prepared via procedure III using compound **12d** (1.1 g, 3.5 mmol). The compound was carried forward without further purification. HRMS calcd. for $C_{14}H_{22}ON$, 220.16960 $[M + H]^+$; 220.16955 found, $[M + H]^+$. Compound **14d** was prepared via Procedure IV using amine **13d** (0.86 g, 8.4 mmol), triethylamine (0.94 ml, 6.8 mmol) and 2-chloroacetyl chloride (0.33 ml, 4.1 mmol) in DCM (13 mL) and saturated $NaHCO_3$ (10. mL). The crude product was purified by silica gel chromatography (10-90% EtOAc/hexanes) to afford the title compound as a white solid (0.70 g, 70 %). TLC (EtOAc:hexanes, 1:1, v/v) Rf = 0.50; ^{1}HNMR ($CDCl_3$, 400 MHz) δ: 7.19 (t, *J* = 7.6 Hz, 1H), 6.78-6.73 (m, 3H), 6.60 (bs, 1H), 4.25-4.19 (m, 1H), 4.00 (s, 2H), 3.54 (q, *J* = 7.2 Hz, 2H), 2.79 (t, *J* = 7.2 Hz, 2H), 1.98-1.94 (m, 2H), 1.80-1.77 (m, 2H), 1.58-1.45 (m, 3H), 1.39-1.26 (m, 3H); ^{13}CNMR ($CDCl_3$, 100 MHz) δ: 165.9, 158.3, 140.0, 129.9, 121.1, 116.7, 114.3, 75.6, 42.9, 41.1, 35.7, 32.1, 25.8, 24.0; HRMS calcd. for $C_{16}H_{23}O_2N^{35}Cl$, 296.14418 $[M + H]^+$; 296.14129 found, $[M + H]^+$.

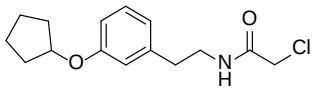

2-chloro-N-(3-(cyclopentyloxy)phenethyl)acetamide (14e): Compound **13e** was prepared via procedure III using compound **12e** (1.3 g, 4.5 mmol). The compound was carried forward without further purification. HRMS calcd. for $C_{13}H_{20}ON$, 206.15449 $[M + H]^+$; 206.15376 found, $[M + H]^+$. Compound **14e** was prepared via procedure IV using amine **13e** (1.0 g, 4.1 mmol), triethylamine (1.2 mL, 8.3 mmol) and 2-chloroacetyl chloride (0.40 ml, 5.0 mmol) in DCM (15 mL) and saturated $NaHCO_3$ (10. mL). The crude product was purified by silica gel chromatography (10-90 % EtOAc/hexanes) to afford the title compound as a clear oil (0.61 g, 52 %). TLC (EtOAc:hexanes, 1:1, v/v) Rf = 0.48; ^{1}HNMR ($CDCl_3$, 400 MHz) δ: 7.19 (t, *J* = 7.6 Hz, 1H), 6.75-6.73 (m, 2H), 6.70-6.69 (m, 1H), 6.59 (bs, 1H), 4.76-4.72 (m, 1H), 4.01 (s, 2H), 3.55 (q, *J* = 7.6 Hz, 2H), 2.79 (t, *J* = 7.2 Hz, 2H), 1.91-1.73 (m, 6H), 1.65-1.55 (m, 2H); ^{13}CNMR ($CDCl_3$, 100 MHz) δ: 166.0, 158.6, 139.9, 129.8, 120.8, 116.3, 113.8, 79.3, 42.9, 41.1, 35.7, 33.1, 24.2; HRMS calcd. for $C_{15}H_{20}O_2N^{35}Cl^{23}Na$, 304.10748 $[M + H]^+$; 304.10734 found, $[M + H]^+$.

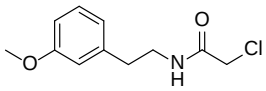

2-chloro-N-(3-methoxyphenethyl)acetamide (14f): Compound **14f** was prepared via procedure IV using commercially available 2-(3-methoxyphenyl)ethanamine (5.0 g, 33 mmol), triethylamine (9.2 mL, 66 mmol) and 2-chloroacetyl chloride (3,2 ml, 39 mmol) in DCM (120 mL). The crude product was purified by silica gel chromatography (10-90 % EtOAc/hexanes) to afford the title compound as a clear oil (5.4 g, 72 %). TLC (EtOAc:hexanes, 1:1, v/v) Rf = 0.67; ^{1}HNMR ($CDCl_3$, 400 MHz) δ: 7.28 (d, *J* = 8.4 Hz, 1H), 6.84-6.81 (m, 2H), 6.78-6.77 (m, 1H), 6.67 (bs, 1H), 4.06 (s, 2H), 3.83 (s, 3H), 3.58 (q, *J* = 7.2 Hz, 2H), 2.85 (t, *J* = 7.2 Hz, 2H); ^{13}CNMR ($CDCl_3$, 100 MHz) δ: 166.0, 160.1, 140.1, 129.9, 121.3, 114.5, 112.4, 55.4, 42.9, 41.1, 35.7; HRMS calcd. for $C_{11}H_{14}O_2N^{35}Cl^{23}$, 228.07858 $[M + H]^+$; 228.07848 found, $[M + H]^+$.

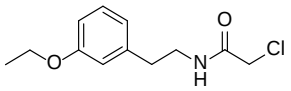

2-chloro-N-(3-ethoxyphenethyl)acetamide (14g): Compound **14g** was prepared via procedure IV using commercially available 2-(3-ethoxyphenyl)ethanamine (3.0 g, 18 mol), triethylamine (5.1, 33 mol), and 2-chloroacetyl chloride (1.7 ml, 22 mmol) in DCM (69 mL). The crude product was purified by silica gel chromatography (10-90 EtOAc/hexanes) to afford the title compound as a white solid (3.1 g, 71 %). TLC (EtOAc:hexanes, 1:1, v/v) Rf = 0.48; ^{1}HNMR ($CDCl_3$, 400 MHz) δ: 7.26-7.22 (m, 1H), 6.80-6.75 (m, 3H), 6.63 (bs, 1H), 4.07-4.00 (m, 4H), 3.57 (q, *J* = 6.4 Hz, 2H), 2.83 (t, *J* = 6.8 Hz, 2H), 1.44-1.41 (m, 3H); ^{13}CNMR ($CDCl_3$, 100 MHz) δ: 159.2, 139.8, 129.7, 120.9, 114.9, 112.6, 63.3, 42.6, 40.8, 35.5, 14.8;

HRMS calcd. for $C_{12}H_{17}O_2N^{35}Cl^{23}$, 242.09423 $[M + H]^+$; 242.09395 found, $[M + H]^+$.

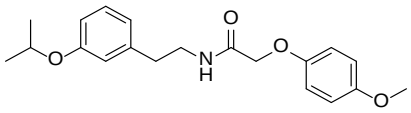

N-(3-isopropoxyphenethyl)-2-(4-methoxyphenoxy)acetamide (15a): Compound **15a** was prepared via procedure V using 4-methoxyphenol (1.1 g, 8.6 mmol) and Cs_2CO_3 (12 g, 36 mmol) in dry ACN (22 ml) and amide **14a** (1.8 g, 7.2 mmol) in dry ACN (10. mL). The crude residue was purified by silica gel chromatography (ISCO, Redisep 40 g column, 10-80% EtOAc/hexanes gradient) to afford the title compound as a clear oil (2.0 g, 82 %). TLC (EtOAc:hexanes, 1:1, v/v) Rf = 0.30; ^{1}HNMR ($CDCl_3$, 400 MHz) δ: 7.19-7.15 (m, 1H), 6.82-6.66 (m, 7H), 4.54-4.49 (m, 1H), 4.39 (s, 2H), 3.75 (s, 3H), 3.59-3.53 (m, 2H), 2.79 (t, *J* = 6.8 Hz, 2H), 1.32-1.29 (m, 6H); ^{13}CNMR (100 MHz, $CDCl_3$) δ: 168.6, 158.4, 154.9, 151.5, 140.3, 129.9, 121.1, 116.6, 115.9, 115.0, 113.9, 69.9, 68.4, 55.9, 40.2, 35.9, 22.3; HRMS calcd. for $C_{20}H_{25}O_4N_1$, 344.18564 $[M + H]^+$; 344.18515 found, $[M + H]^+$.

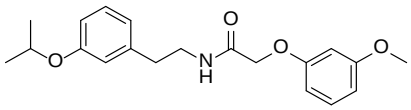

N-(3-isopropoxyphenethyl)-2-(3-methoxyphenoxy)acetamide (15b): Compound **15b** was prepared via procedure V using 3-methoxyphenol (0.76 g, 6.1 mmol) and Cs_2CO_3 (6.6 g, 20. mmol) in dry ACN (15 mL) and amide **14a** (1.3 g, 5.1 mmol) dry ACN (10 mL). The crude residue was purified by silica gel chromatography (ISCO, Redisep 40 g column, 10-80% EtOAc/hexanes gradient) to afford the title compound as a yellow oil (1.5 g, 84 %). TLC (EtOAc:hexanes, 1:1, v/v) Rf = 0.68; ^{1}HNMR ($CDCl_3$, 400 MHz) δ: 7.20-7.15 (m, 2H), 6.75-6.69 (m, 3H), 6.62 (bs, 1H), 6.57-6.54 (m, 1H), 6.45-6.39 (m, 2H), 4.53-4.49 (m, 1H), 4.43 (s, 2H), 3.77 (s, 3H), 3.60-3.54 (m, 2H), 2.81-2.77 (t, *J* = 7.2 Hz, 2H) 1.31 (s, 3H), 1.29 (s, 3H);^{13}CNMR ($CDCl_3$, 100 MHz) δ: 168.2, 161.2, 158.5, 158.3, 140.3, 130.5, 129.9, 121.1, 116.6, 114.0, 107.8, 106.8, 101.5, 69.9, 67.5, 55.6, 40.3, 35.9, 22.3; HRMS calcd. for $C_{20}H_{25}O_4N_1$, 344.18564 $[M + H]^+$; 344.18527 found, $[M + H]^+$.

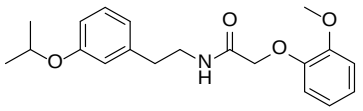

N-(3-isopropoxyphenethyl)-2-(2-methoxyphenoxy)acetamide (15c): Compound **15c** was prepared via procedure V using 2-methoxyphenol (0.68 ml, 6.1 mmol) and Cs_2CO_3 (8.3 g, 25 mmol) in dry ACN (15mL) and amide **14a** (1.3 g, 5.1 mmol) dry ACN (10 mL). The crude residue was purified by silica gel chromatography (ISCO, Redisep 40 g column, 10-80% EtOAc/hexanes gradient) to afford the title compound as a yellow solid (1.4 g, 82%). TLC (EtOAc:hexanes, 1:1, v/v) Rf = 0.65; ^{1}HNMR (400 MHz, $CDCl_3$) δ: 7.17-7.13 (t, *J* = 8.0 Hz, 1H), 7.03 (bs, 1H), 7.01-6.79 (m, 1H), 6.90-6.83 (m, 3H), 6.74-6.69 (m, 3H), 4.51-4.48 (m, 3H), 3.78 (s, 3H), 3.60-3.55 (q, *J* = 6.8 Hz, *J* = 13.2 Hz, 2H), 2.80-2.77 (t, *J* = 7.2 Hz, 2H), 1.30 (s, 3H), 1.28 (s, 3H); ^{13}C NMR ($CDCl_3$, 100 MHz) δ: 168.8, 158.3, 149.8, 147.3, 140.5, 129.8, 123.3, 121.3, 121.1, 116.5, 115.7, 113.9, 112.2, 69.8, 69.8,

55.9, 40.3, 35.9, 22.3; HRMS calcd. for $C_{20}H_{25}O_4N_1$, 344.18564 $[M + H]^+$; 344.18551 found, $[M + H]^+$.

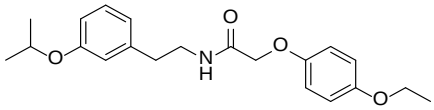

2-(4-ethoxyphenoxy)-N-(3-isopropoxyphenethyl)acetamide (15d): Compound **15d** was prepared via Procedure V using 4-ethoxyphenol (0.84 g, 6.1 mmol) and Cs_2CO_3 (6.6 g, 21 mmol) in dry ACN (15 ml) and amide **14a** (1.3 g, 5.1 mmol) in dry ACN (10. mL). The crude residue was purified by silica gel chromatography (ISCO, Redisep 40 g column, 10-80% EtOAc/hexanes gradient) to afford the title compound as a yellow oil (1.6 g, 86%). TLC (EtOAc:hexanes, 1:1, v/v) Rf = 0.67; ^{1}H NMR ($CDCl_3$, 400 MHz) δ: 7.20-7.15 (m, 1H), 6.83-6.70 (m, 7H), 6.65 (bs, 1H), 4.54-4.48 (m, 1H), 4.39 (s, 2H), 3.96 (q, J = 7.2 Hz, J = 14.0 Hz, 2H), 3.59-3.53 (m, 2H), 2.81-2.77 (m, 2H), 1.24 (t, J = 7.2 Hz, 3H), 1.31 (s, 3H), 1.29 (s, 3H); ^{13}C NMR ($CDCl_3$,100 MHz) δ: 168.6, 158.4, 154.3, 151.4, 140.4, 129.9, 121.1, 116.6, 115.8, 115.6, 113.9, 69.8, 68.3, 64.2, 40.2, 35.9, 22.3, 15.1; HRMS calcd. for $C_{21}H_{27}O_4N_1$, 358.20129 $[M + H]^+$; 358.20121 found, $[M + H]^+$.

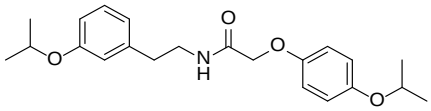

N-(3-isopropoxyphenethyl)-2-(4-isopropoxyphenoxy)acetamide (15e): Compound **15e** was prepared via procedure V using 4-isopropoxyphenol (1.3 ml, 8.2 mmol) and Cs_2CO_3 (8.9 g, 27 mmol) in dry ACN (21 mL) and amide **14a** (1.8 g, 6.8 mmol) dry ACN (10 mL). The crude residue was purified by silica gel chromatography (ISCO, Redisep 40 g column, 10-80% EtOAc/hexanes gradient) to afford the title compound as a yellow solid (1.8 g, 70%). TLC (EtOAc:hexanes, 1:1, v/v) Rf = 0.65; ^{1}HNMR (400 MHz, $CDCl_3$) δ: 7.20 (t, J = 7.5 Hz, 1H), 6.85-6.69 (m, 8H), 4.58-4.40 (m, 4H), 3.59 (q, J = 6.9 Hz, 2H), 2.81 (t, J = 6.9 Hz, 2H), 1.34-1.31 (12H) ; ^{13}C NMR ($CDCl_3$, 100 MHz) δ: 168.4, 158.1, 152.8, 151.3, 140.2, 129.7, 120.9, 117.4, 116.4, 115.6, 113.8, 70.7, 69.7, 68.1, 39.9, 35.7, 22.1; HRMS calcd. for $C_{22}H_{29}O_4N_1Na$, 394.19888 $[M + H]^+$; 394.19901 found, $[M + H]^+$.

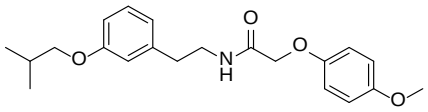

N-(3-isobutoxyphenethyl)-2-(4-methoxyphenoxy)acetamide (15f): Compound **15f** was prepared via procedure V using 4-methoxyphenol (0.50 g, 4.0 mmol) and Cs_2CO_3 (4.4 g, 14 mmol) in dry ACN (5.1 ml) and amide **14b** (0.91 g, 3.4 mmol) in dry ACN (5.1 mL). The crude residue was purified by silica gel chromatography (ISCO, Redisep 40 g column, 10-80% EtOAc/hexanes gradient) to afford the title compound as a white solid (1.1 g, 92%). TLC (EtOAc:hexanes, 1:1, v/v) Rf = 0.69; ^{1}H NMR ($CDCl_3$, 400 MHz) δ: 7.18 (t, *J* = 7.6 Hz, 1H), 6.82-6.71 (m, 7H), 6.66 (bs, 1H), 4.39 (s, 2H), 3.75 (s, 3H), 3.67 (d, *J* = 6.8 Hz, 2H), 3.57 (q, *J* = 6.4 Hz, 2H), 2.79 (t, *J* = 6.8 Hz, 2H), 2.08-2.01 (m, 1H), 0.99 (d, *J* = 6.8 Hz, 6H); ^{13}C NMR ($CDCl_3$, 100 MHz) δ: 168.6, 159.7, 154.9, 151.5, 140.3, 129.9, 121.1, 115.8, 115.2, 115.0, 112.8, 74.5, 68.3, 55.9, 40.2, 35.9, 28.5, 19.5; HRMS calcd. for $C_{21}H_{28}O_4N_1$, 358.20129 $[M + H]^+$; 358.20125 found, $[M + H]^+$.

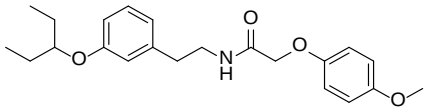

2-(4-methoxyphenoxy)-N-(3-(pentan-3-yloxy)phenethyl)acetamide (15g): Compound **15g** was prepared via procedure V using 4-methoxyphenol (0.39 g, 3.2 mmol) and Cs_2CO_3 (2.6 g, 7.9 mmol) in dry ACN (4.0 ml) and amide **14c** (0.74 g, 2.6 mmol) in dry ACN (4.0 mL). The crude residue was purified by silica gel chromatography (ISCO, Redisep 40 g column, 10-80% EtOAc/hexanes gradient) to afford the title compound as a white solid (0.61 g, 63 %). TLC (EtOAc:hexanes, 1:1, v/v) Rf = 0.57; ^{1}H NMR ($CDCl_3$, 400 MHz) δ: 7.17 (t, *J* = 8.0 Hz, 1H), 6,83-6.69 (m, 7H), 6.67 (bs, 1H), 4.10-4.07 (m, 1H), 3.76 (s, 1H), 3.58 (q, *J* = 6,4 Hz, 2H), 2.79 (t, *J* = 7.2 Hz, 2H), 1.68-1.61 (m, 4H), 0.92 (t, *J* = 7.2 Hz, 6H); ^{13}C NMR ($CDCl_3$, 100 MHz) δ: 168.6, 159.2, 154.9, 151.5, 140.4, 129.9, 120.9, 116.7, 115.8, 115.0, 114.0, 80.2, 68.3, 55.9, 40.2, 35.9, 26.2, 9.8; HRMS calcd. for $C_{22}H_{30}O_4N$, 372.21694 $[M + H]^+$; 372.21711 found, $[M + H]^+$.

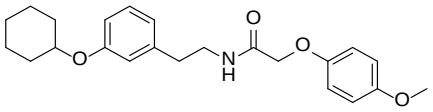

N-(3-(cyclohexyloxy)phenethyl)-2-(4-methoxyphenoxy)acetamide (15h): Compound **15h** was prepared via procedure V using 4-methoxyphenol (0.35 g, 2.8 mmol) and Cs_2CO_3 (3.1 g, 9.5 mmol) in dry ACN (7.1 ml) and amide **14d** (0.70 g, 2.3 mmol) in dry ACN (7.1 mL). The crude residue was purified by silica gel chromatography (ISCO, Redisep 40 g column, 10-80% EtOAc/hexanes gradient) to afford the title compound as a white solid (0.52 g, 58 %). TLC (EtOAc:hexanes, 1:1, v/v) Rf = 0.58; ^{1}H NMR ($CDCl_3$, 400 MHz) δ: 7.17 (t, *J* = 8.0 Hz, 1H), 6.83-6.69 (m, 7H), 6.66 (bs, 1H), 4.39 (s, 1H), 4.24-4.18 (m, 1H), 3.76 (s, 3H), 3.58 (q, *J* = 6.8 Hz, 2H), 2.79 (t, *J* = 7.2 Hz, 2H), 1.97-1.94 (m, 2H), 1.78-1.76 (m, 2H), 1.57-1.24 (m, 6H); ^{13}C NMR ($CDCl_3$, 100 MHz) δ: 168.6, 158.3, 154.8, 151.5, 140.3, 129.8, 121.1, 116.8, 115.8, 115.0, 114.1, 75.5, 68.3, 55.9, 40.2, 35.9, 32.0, 25.8, 24.0; HRMS calcd. for $C_{23}H_{40}O_4N$, 384.21694 $[M + H]^+$; 384.21715 found, $[M + H]^+$.

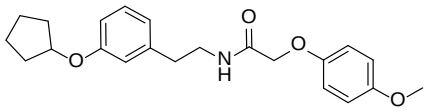

N-(3-(cyclopentyloxy)phenethyl)-2-(4-methoxyphenoxy)acetamide (15i): Compound **15i** was prepared via Procedure V using 4-methoxyphenol (0.32 g, 2.6 mmol) and Cs_2CO_3 (2.8 g, 8.7 mmol) in dry ACN (6.5 ml) and amide **14e** (0.91 g, 3.4 mmol) in dry ACN (6.5 mL). The crude residue was purified by silica gel chromatography (ISCO, Redisep 40 g column, 10-80% EtOAc/hexanes gradient) to afford the title compound as a white solid (1.1 g, 92%). TLC (EtOAc:hexanes, 1:1, v/v) Rf = 44; ^{1}H NMR ($CDCl_3$, 400 MHz) δ: 7.17 (t, *J* = 8.4 Hz, 1H), 6.83-6.69 (m, 7H), 6.65 (bs, 1H), 4.71 (q, 1H), 4.39 (s, 2H), 3.76 (s, 3H), 3.58 (q, *J* = 6.8 Hz, 2H), 2.79 (t, *J* = 7.2 Hz, 2H), 1.88-1.74 (m, 6H), 1.61-1.56 (m, 2H); ^{13}C NMR ($CDCl_3$, 100 MHz) δ: 168.6, 158.6, 154.9, 151.5, 140.2, 129.8, 120.8, 116.3, 115.8, 115.0, 113.7, 79.3, 68.3, 55.9, 40.2, 35.9, 33.1, 24.2; HRMS calcd. for $C_{22}H_{28}O_4N$, 370.20129 $[M + H]^+$; 370.20139 found, $[M + H]^+$.

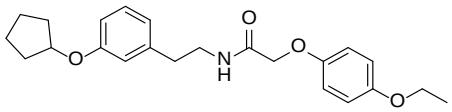

N-(3-(cyclopentyloxy)phenethyl)-2-(4-ethoxyphenoxy)acetamide (15j): Compound **15j** was prepared via Procedure V using 4-ethoxyphenol (0.73 g, 5.3 mmol) and Cs_2CO_3 (5.7 g, 14 mmol) in dry ACN (6.6 ml) and amide **14e** (1.2 g, 4.4 mmol) in dry ACN (6.6 mL). The crude residue was purified by silica gel chromatography (ISCO, Redisep 40 g column, 10-80% EtOAc/hexanes gradient) to afford the title compound as a white solid (1.4 g, 86%). TLC (EtOAc:hexanes, 1:1, v/v) Rf = 0.81; ^{1}H NMR ($CDCl_3$, 400 MHz) δ: 7.19-7.15 (m, 1H), 6.82-6.69 (m, 7H), 6.65 (bs, 1H), 4.73-4.71 (m, 1H), 4.39 (s, 3H), 3.97 (q, *J* = 7.2 Hz, 2H), 3.58 (q, *J* = 6.4 Hz, 2H), 2.79 (t, *J* = 6.8 Hz, 2H), 1.92-1.72 (m, 6H), 1.96-1.56 (m, 2H), 1.38 (t, *J* = 6.8 Hz, 3H); ^{13}C NMR ($CDCl_3$, 100 MHz) δ: 168.6, 158.6, 154.2, 151.4, 140.3, 129.8, 120.9, 116.2, 115.8, 115.7, 113.7, 79.2, 68.3, 64.1, 40.2, 35.9, 33.1, 24.3, 15.1; HRMS calcd. for $C_{23}H_{30}O_4N$, 384.21694 $[M + H]^+$; 384.21704 found, $[M + H]^+$

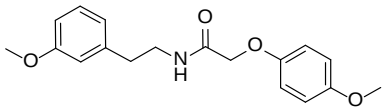

N-(3-methoxyphenethyl)-2-(4-methoxyphenoxy)acetamide (15k): Compound **15k** was prepared via Procedure V using 4-methoxyphenol (3.6 g, 29 mmol) and Cs_2CO_3 (23 g, 72 mmol) in dry ACN (36 ml) and amide **14f** (1.2 g, 4.4 mmol) in dry ACN (6.6 mL). The crude residue was purified by silica gel chromatography (ISCO, Redisep 40 g column, 10-80% EtOAc/hexanes gradient) to afford the title compound as a white solid (1.4 g, 86%). TLC (EtOAc:hexanes, 1:1, v/v) Rf = 0.49; ^{1}H NMR ($CDCl_3$, 400 MHz) δ: 7.22 (t, *J* = 8.0 Hz, 1H), 6.85-6.75 (m, 7H), 6.68 (bs, 1H), 4.43 (s, 2H), 3.80 (s, 3H), 3.79 (s, 3H), 3.61 (q, *J* = 6.4 Hz, 2H), 2.83 (t, *J* = 6.8 Hz, 2H) ; ^{13}C NMR ($CDCl_3$, 100 MHz) δ: 168.6, 160.0, 154.9, 151.5, 140.4, 129.9, 121.3, 115.8, 115.0, 114.6, 112.2, 68.3, 55.9, 55.4, 40.7, 35.9; HRMS calcd. for $C_{18}H_{24}O_4N$, 316.15433 $[M + H]^+$; 316.119 found, $[M + H]^+$

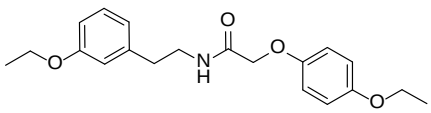

N-(3-ethoxyphenethyl)-2-(4-ethoxyphenoxy)acetamide (15l): Compound **15l** was prepared via procedure V using 4-ethoxyphenol (2.1 g, 15 mmol) and Cs_2CO_3 (12 g, 38 mmol) in dry ACN (19 ml) and amide **14g** (3.1 g, 12 mmol) in dry ACN (19 mL). The crude residue was purified by silica gel chromatography (ISCO, Redisep 80 g column, 10-80% EtOAc/hexanes gradient) to afford the title compound as a white solid (2.7 g, 62 %). TLC (EtOAc:hexanes, 1:1, v/v) Rf = 0.27; ^{1}H NMR ($CDCl_3$, 400 MHz) δ: 7.21 (t, *J* = 10 Hz, 1H), 6.85-6.74 (m, 7H), 6,69 (bs, 1H), 4.41 (s, 2H), 4.04-3.95 (m, 4H), 3.63-3.55 (m, 2H), 2.82 (t, *J* = 8.4 Hz), 1.44-1.38 (m 6H); ^{13}C NMR ($CDCl_3$, 100 MHz) δ: 168.4, 159.2, 154.0, 151.3, 140.1, 129.7, 120.9, 115.6, 115.5, 114.9, 112.5, 68.1, 63.9, 63.3, 39.9, 35.7, 14.8; HRMS calcd. for $C_{20}H_{26}O_4N$, 344.18563 $[M + H]^+$; 344.18564 found, $[M + H]^+$

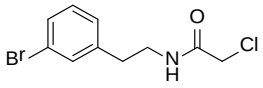

N-(3-bromophenethyl)-2-chloroacetamide (17): Compound **17** was prepared via procedure IV using 2-(3-bromophenyl)ethanamine (2.8 g, 20. mmol), triethylamine (5.6 mL, 40. mmol) and 2-chloroacetyl chloride (1.9 ml, 24 mmol). The crude product was purified by silica gel chromatography (10-90 % EtOAc/hexanes) to afford the title compound as a yellow solid (3.6 g, 65 %). TLC (EtOAc:hexanes, 1:1, v/v) Rf = 0.46; ^{1}HNMR ($CDCl_3$, 400 MHz) δ: 7.38-7.35 (m, 2H), 7.18 (t, *J* = 7.6 Hz, 1H), 7.13-7.11 (m, 1H), 6.59 (bs, 1H), 4.02 (s, 2H), 3.53 (q, *J* = 6.8 Hz, 2H), 2.81 (t, *J* = 6.8 Hz, 2H); ^{13}CNMR ($CDCl_3$, 100 MHz) δ: 166.1, 140.8, 132.0, 130.5, 130.1, 127.6, 122.9, 42.8, 40.9, 35.4; HRMS calcd. for $C_{10}H_{12}ON^{35}Cl^{79}Br$, 275.97853 $[M + H]^+$; 275.97861 found, $[M + H]^+$.

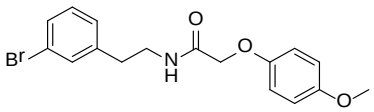

N-(3-bromophenethyl)-2-(4-methoxyphenoxy)acetamide (18a): Compound **18a** was prepared via procedure V using 4-methoxyphenol (1.9 g, 16 mmol) and Cs_2CO_3 (17 g, 52 mmol) in dry ACN (39 ml) and amide **17** (3.6 g, 13 mmol) in dry ACN (15 mL). The crude residue was purified by silica gel chromatography (ISCO, Redisep 40 g column, 10-80 % EtOAc/hexanes gradient) to afford the

title compound as a white solid (3.9 g, 83 %). TLC (EtOAc:hexanes, 1:1, v/v) Rf = 0.45; ^{1}H NMR ($CDCl_3$, 400 MHz) δ: 7.36-7.33 (m, 2H), 7.14 (t, *J* = 8.0 Hz, 1H), 7.08-7.06 (m, 1H), 6.83-6.76 (m, 4H), 6.63 (bs, 1H), 4.4 (s, 2H), 3.76 (s, 3H), 3.56 (q, *J* = 6.8 Hz, 2H), 2.80 (t, *J* = 6.8 Hz, 2H). ^{13}C NMR ($CDCl_3$, 100 MHz) δ: 1.68.7, 154.9, 151.5, 132.0, 130.4, 129.9, 127.6, 122.9, 115.8, 115.0, 68.3, 55.9, 40.1, 35.6; HRMS calcd. for $C_{17}H_{19}O_3N^{79}Br$, 364.05428 $[M + H]^+$; 364.05494 found, $[M + H]^+$.

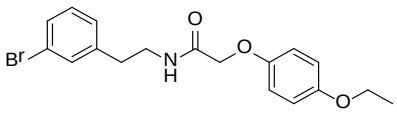

N-(3-bromophenethyl)-2-(4-ethoxyphenoxy)acetamide (18b): Compound **18b** was prepared via procedure V using 4-ethoxyphenol (1.8 g, 13 mmol) in and Cs_2CO_3 (14 g, 43 mmol) dry ACN (33 ml) and amide **17** (3.0 g, 11 mmol) in dry ACN (10 mL). The crude residue was purified by silica gel chromatography (ISCO, Redisep 40 g column, 10-80 % EtOAc/hexanes gradient) to afford the title compound as a white solid (3.8 g, 92 %). TLC (EtOAc:hexanes, 1:1, v/v) Rf = 0.47; ^{1}H NMR ($CDCl_3$, 400 MHz) δ: 7.35-7.33 (m, 2H), 7.15 (t, *J* = 8.0 Hz, 1H), 7.08-7.06 (m, 1H), 6.83-6.75 (m, 4H), 6.63 (bs, 1H), 4.39 (s, 2H), 3.97 (q, *J* = 7.2 Hz, 2H), 3.57 (q, *J* = 6.4 Hz, 2H), 2.80 (t, *J* = 6.8, 2H), 1.38 (t, *J* = 6.8 Hz, 3H); ^{13}C NMR ($CDCl_3$, 100 MHz) δ: 168.7, 154.3, 151.4, 141.1, 132.0, 130.4, 129.9, 127.6, 122.9, 115.9, 115.7, 68.3, 64.2, 40.1, 35.6, 15.1; HRMS calcd. for $C_{18}H_{21}O_3N^{79}Br$, 378.06993 $[M + H]^+$; 378.07060 found, $[M + H]^+$.

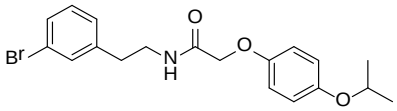

N-(3-bromophenethyl)-2-(4-isopropoxyphenoxy)acetamide (18c): Compound **18c** was prepared via Procedure V using 4-isopropoxyphenol (1.0 mL, 6.6 mmol) and Cs_2CO_3 (6.4 g, 20. mmol) in dry ACN (9.8 ml) and amide **17** (1.8 g, 6.6 mmol) dry ACN (9.8 mL). The crude residue was purified by silica gel chromatography (ISCO, Redisep 40 g column, 10-80 % EtOAc/hexanes gradient) to afford the title compound as an off-white solid (1.9 g, 75 %). TLC (EtOAc:hexanes, 1:1, v/v) Rf = 0.58; ^{1}H NMR ($CDCl_3$, 400 MHz) δ: 7.36-7.34 (m, 2H), 7.19 (t, *J* = 8.0 Hz, 1H), 7.08-7.06 (m, 1H), 6.81-6.75

(m, 4H), 6.62 (bs, 1H), 4.46-4.39 (m, 3H), 3.54 (q, *J* = 6.4 Hz, 2H), 2.80 (t, *J* = 6.8 Hz, 2H), 1.30 (d, *J* = 6.0 Hz, 6H); ^{13}C NMR ($CDCl_3$, 100 MHz) δ: 168.8, 153.1, 151.4, 141.1, 132.0, 130.5, 130.0, 127.7, 122.9, 117.6, 115.8, 70.9, 68.3, 40.1, 35.6, 22.3; HRMS calcd. for $C_{19}H_{23}O_3N^{79}Br$, 392.08558 $[M + H]^+$; 392.08586 found, $[M + H]^+$.

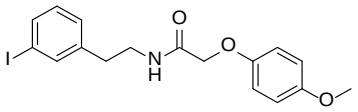

N-(3-iodophenethyl)-2-(4-methoxyphenoxy)acetamide (19a): Compound **19a** was prepared via procedure VI using amide **18a** (2.0 g, 5.5 mmol), copper(I) iodide (0.052 g, 0.28 mmol), sodium iodide (1.2 g, 8.2 mmol), and *N*1,*N*2-dimethylethane-1,2-diamine (0.062 ml, 0.55 mmol) in dry dioxane (5.5 ml). The crude residue was purified by silica gel chromatography (ISCO, Redisep 40 g column, 10-90 % EtOAc/hexanes gradient) to afford the title compound as a white solid (1.8 g, 80 %). TLC (EtOAc:hexanes, 1:1, v/v) Rf = 0.48; ^{1}H NMR ($CDCl_3$, 400 MHz) δ: 7.56-7.55 (m, 1H), 7.12-7.10 (m, 1H), 7.00 (t, *J* = 8.0 Hz, 1H), 6.84-6.77 (m, 4H), 6.62 (bs, 1H), 4.41 (s, 2H), 3.76 (s, 3H), 3.58 (q, *J* = 6.8 Hz, 2H), 2.77 (t, *J* = 7.2 Hz, 2H); ^{13}C NMR ($CDCl_3$, 100 MHz) δ: 168.7, 154.9, 151.5, 141.2, 137.9, 135.9, 130.6, 128.3, 115.9, 115.0, 94.9, 68.3, 55.9, 40.1, 35.5; HRMS calcd. for $C_{17}H_{19}O_3N^{127}I$, 412.04042 $[M + H]^+$; 412.04049 found, $[M + H]^+$.

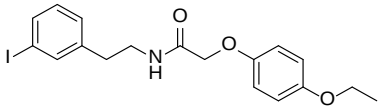

2-(4-ethoxyphenoxy)-N-(3-iodophenethyl)acetamide (19b): Compound **19b** was prepared via procedure VI using amide **18b** (2.2 g, 5.8 mmol), copper(I) iodide (0.056 g, 0.29 mmol), sodium iodide (1.3 g, 8.8 mmol), *N1*,*N2*-dimethylethane-1,2-diamine (0.066 ml, 0.59 mmol) in dry dioxane (5.8 ml). The crude residue was purified by silica gel chromatography (ISCO, Redisep 40 g column, 10-90 % EtOAc/hexanes gradient) to afford the title compound as a white solid (1.7 g, 69 %). TLC (EtOAc:hexanes, 1:1, v/v) Rf = 0.27; ^{1}H NMR ($CDCl_3$, 400 MHz) δ: 7.58-7.56 (m, 2H), 7.13 (d, *J* = 8.0 Hz, 1H), 7.04-7.00 (m, 1H), 6.85-6.77 (m, 4H), 6.65 (bs, 1H), 4.42 (s, 2H), 4.01 (q, *J* = 7.2 Hz,

2H), 3.57 (q, *J* = 7.2 Hz, 2H), 2.79 (t, *J* = 6.8 Hz, 2H), 1.40 (t, *J* = 6.8 Hz, 3H); ^{13}C NMR ($CDCl_3$, 100 MHz) δ: 168.7, 154.3, 151.3, 141.2, 137.9, 135.9, 130.6, 128.3, 115.8, 115.7, 94.9, 68.3, 64.2, 40.0, 35.5, 15.1; HRMS calcd. for $C_{18}H_{21}O_3N^{127}I$, 426.05067 $[M + H]^+$; 426.050613 found, $[M + H]^+$.

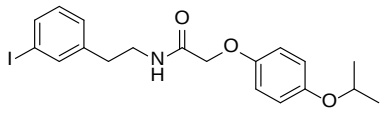

N-(3-iodophenethyl)-2-(4-isopropoxyphenoxy)acetamide (19c): Compound **19c** was prepared via procedure VI using amide **18c** (1.4 g, 3.5 mmol), copper(I) iodide (0.066 g, 0.35 mmol), sodium iodide (0.78 g, 5.2 mmol), N1,N2-dimethylethane-1,2-diamine (0.078 ml, 0.69 mmol) in dry dioxane (3.5 ml). The crude residue was purified by silica gel chromatography (ISCO, Redisep 40 g column, 10-90 % EtOAc/hexanes gradient) to afford the title compound as a white solid (0.95 g, 62 %). TLC (EtOAc:hexanes, 1:1, v/v) Rf = 0.47; ^{1}H NMR ($CDCl_3$, 400 MHz) δ: 7.59 (m, 2H), 7.14 (d, *J* = 7.6 Hz, 1H), 7.03 (t, *J* = 8.4 Hz, 1H), 6.86-6.78 (m, 4H), 6.65 (bs, 1H), 4.48-4.43 (m, 3H), 3.61 (q, *J* = 6.8 Hz, 2H), 2.80 (t, *J* = 6.8 Hz, 2H), 1.32 (d, *J* = 6.4 Hz, 6H); ^{13}C NMR ($CDCl_3$, 100 MHz) δ: 168.7, 153.2, 151.4, 141.3, 137.9, 135.9, 130.6, 128.3, 117.6, 115.8, 94.9, 70.9, 68.3, 40.1, 35.5, 22.3; HRMS calcd. for $C_{19}H_{23}O_2N^{127}I$, 440.07171 $[M + H]^+$; 440.07209 found, $[M + H]^+$.

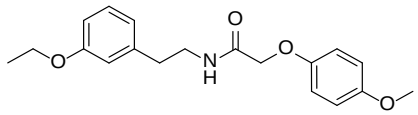

N-(3-ethoxyphenethyl)-2-(4-methoxyphenoxy)acetamide (15m): Compound **15m** was prepared via procedure VII using amide **19a** (2.0 g, 4.8 mmol), copper(I) iodide (0.093 g, 0.48 mmol), 1,10-phenanthroline (0.18 g, 0.97 mmol), and cesium carbonate (3.2 g, 9.7 mmol) in ethanol (2.4 ml, 41 mmol). The crude residue was purified by silica gel chromatography (ISCO, Redisep 40 g column, 10-90 % EtOAc/hexanes gradient) to afford the title compound as a yellow oil (0.67 g, 42 %). TLC (EtOAc:hexanes, 1:1, v/v) Rf = 1.1; ^{1}H NMR ($CDCl_3$, 400 MHz) δ: 7.23-7.19 (m, 1H), 6.86-6.74 (m, 7H), 6.69 (bs, 1H), 4.42 (s, 2H), 4.00 (q, *J* = 6.8 Hz, 2H), 3.78 (s, 3H), 3.6 (q, *J* = 6.4 Hz, 2H), 2.82 (t, *J* = 6.8 Hz, 2H), 1.41 (t, *J* = 7.2 Hz, 3H); ^{13}C NMR ($CDCl_3$, 100 MHz) δ: 168.6, 159.4, 154.9, 151.5,

140.3, 129.9, 121.2, 115.8, 115.2, 115.0, 112.7, 68.3, 63.5, 55.9, 40.2, 35.9, 15.1; HRMS calcd. for $C_{19}H_{24}O_4N$, 330.16998 $[M + H]^+$; 330.16922 found, $[M + H]^+$.

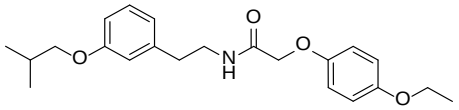

2-(4-ethoxyphenoxy)-N-(3-isobutoxyphenethyl)acetamide (15n): Compound **15n** was prepared via procedure VII using amide **19b** (1.7 g, 4.0 mmol), copper(I) iodide (0.15 g, 0.81 mmol), 1,10-phenanthroline (0.15 g, 0.81 mmol), and cesium carbonate (2.6 g, 8.1 mmol) in 2-methylpropan-1-ol (4.0 ml, 44 mmol). The crude residue was purified by silica gel chromatography (ISCO, Redisep 40 g column, 10-90 % EtOAc/hexanes gradient) to afford the title compound as a white solid (0.54 g, 36 %). TLC (EtOAc:hexanes, 1:1, v/v) Rf = 0.63; ^{1}H NMR ($CDCl_3$, 400 MHz) δ: 7.20 (t, *J* = 8.0 Hz, 1H), 6.84-6.73 (m, 7H), 6.68 (bs, 1H), 4.42 (s, 2H), 4.00 (q, *J* = 7.2 Hz, 2H), 3.70 (d, *J* = 6.8 Hz, 2H), 3.60 (q, *J* = 6.4 Hz, 2H), 2.82 (t, *J* = 7.2 Hz, 2H), 2.10-2.04 (m, 1H), 1.42 (t, *J* = 7.2 Hz, 3H), 1.02 (d, *J* = 6.4 Hz, 6H); ^{13}C NMR ($CDCl_3$, 100 MHz) δ: 168.6, 159.7, 154.2, 151.4, 140.3, 129.8, 121.1, 115.8, 115.7, 115.2, 112.8, 74.5, 68.3, 64.2, 40.2, 35.9, 28.5, 19.5, 15.2; HRMS calcd. for $C_{23}H_{30}O_4N$, 372.21694 $[M + H]^+$; 372.21685 found, $[M + H]^+$.

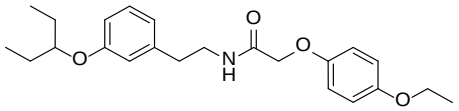

2-(4-ethoxyphenoxy)-N-(3-(pentan-3-yloxy)phenethyl)acetamide (15o): Compound **15o** was prepared via procedure VII using amide **19b** (1.3 g, 3.1 mmol), copper(I) iodide (0.011 g, 0.059 mmol), 1,10-phenanthroline (0.20 g, 1.1 mmol), and cesium carbonate (2.0 g, 6.2 mmol) in 3-pentanol (3.1 ml, 29 mmol). The crude residue was purified by silica gel chromatography (ISCO, Redisep 40 g column, 10-90 % EtOAc/hexanes gradient) to afford the title compound as a white solid (0.23 g, 19 %). ^{1}H NMR ($CDCl_3$, 400 MHz) δ: 7.19 (t, *J* = 7.6 Hz, 1H), 6.84-6.66 (m, 7H), 4.42 (s, 2H), 4.14-4.08 (m ,1H), 4.98 (q, *J* = 7.2 H, 2H), 3.62 (q, *J* = 6.8 Hz, 2H), 2.81 (t, *J* = 6.8 Hz, 2H), 1.71-1.63 (m, 4H), 1.40 (t, *J* = 7.2 Hz, 3H), 0.95 (t, *J* = 7.2 Hz, 6H); ^{13}C NMR ($CDCl_3$, 100 MHz) δ:

168.6, 159.2, 154.2, 151.5, 140.3, 129.8, 120.9, 116.8, 115.8, 115.7, 114.0, 80.2, 68.3, 64.2, 40.2, 35.9, 26.2, 15.1, 9.8; HRMS calcd. for $C_{23}H_{32}O_4N$, 386.23259 $[M + H]^+$; 386.23279 found, $[M + H]^+$.

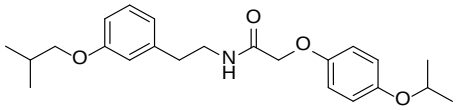

N-(3-isobutoxyphenethyl)-2-(4-isopropoxyphenoxy)acetamide (15p): Compound **15p** was prepared via Procedure VII using amide **19c** (0.95 g, 2.2 mmol), copper(I) iodide (0.082 g, 0.43 mmol), 1,10-phenanthroline (0.39 g, 0.22 mmol), and cesium carbonate (1.4 g, 4.3 mmol) in 2-methylpropan-1-ol (1.8 ml, 20. mmol). The crude residue was purified by silica gel chromatography (ISCO, Redisep 40 g column, 10-90 % EtOAc/hexanes gradient) to afford the title compound as a yellow solid (0.26 g, 32 %). TLC (EtOAc:hexanes, 1:1, v/v) Rf = 0.60; ^{1}H NMR ($CDCl_3$, 600 MHz) δ: 7.18 (t, *J* = 7.2 Hz, 1H), 6.83-6.79 (m, 2H), 6.76-6.70 (m, 5H), 6.66 (bs, 1H), 4.43-4.38 (m, 3H), 3.68 (d, *J* = 6.6 Hz, 2H), 3.57 (q, *J* = 7.2 Hz, 2H), 2.79 (t, *J* = 7.2 Hz, 2H), 2.07-2.02 (m, 1H), 1.29-1.28 (dd, *J* = 2.4 Hz, 6.0 Hz, 6H), 0.99 (d, *J* = 7.2 Hz, 6H); ^{13}C NMR ($CDCl_3$, 150 MHz) δ: 186.3, 168.6, 159.7, 153.1, 151.1, 140.3, 129.8, 121.1, 117.6, 115.8, 115.2, 112.8, 74.5, 70.9, 68.3, 40.2, 35.9, 28.5, 22.7, 19.5; HRMS calcd. for $C_{23}H_{32}O_4N$, 386.23258 $[M + H]^+$; 386.23273 found, $[M + H]^+$.

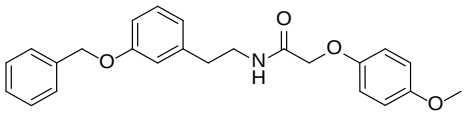

N-(3-(benzyloxy)phenethyl)-2-(4-ethoxyphenoxy)acetamide (15q): Compound **15q** was prepared via Procedure VII using amide **19a** (5.0 g, 12 mmol), copper(I) iodide (0.23 g, 1.2 mmol), 3,4,7,8-tetramethyl-1,10-phenanthroline (0.58 g, 2.4 mmol), and cesium carbonate (7.9 g, 24 mmol) in phenylmethanol (15 ml, 110 mmol). The crude residue was purified by silica gel chromatography (ISCO, Redisep 40 g column, 10-90 % EtOAc/hexanes gradient) to afford the title compound as a white solid (3.2 g, 69 %). TLC (EtOAc:hexanes, 1:1, v/v) Rf = 0.50; ^{1}H NMR ($CDCl_3$, 400 MHz) δ: 7.45-7.31 (m, 5H), 7.23 (t, *J* = 7.8 Hz, 1H), 6.89-6.77 (m, 7H), 6.68 (bs, 1H), 5.05 (s, 2H), 4.24 (s, 2H), 3.76 (s, 3H), 3.60 (q, *J* = 6.6 Hz, 2H), 2.85 (t, *J* = 6.6 Hz, 2H); ^{13}C NMR ($CDCl_3$, 100 MHz) δ:

168.6, 159.3, 154.9, 151.5, 140.4, 137.1, 129.9, 128.8, 128.2, 127.8, 121.6, 115.9, 115.6, 115.0, 113.1, 70.1, 68.4, 55.9, 40.2, 35.9; HRMS calcd. for $C_{24}H_{26}O_4N$, 392.18563 $[M + H]^+$; 392.18572 found, $[M + H]^+$.

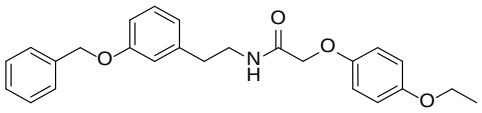

N-(3-(benzyloxy)phenethyl)-2-(4-ethoxyphenoxy)acetamide (15r): Compound **15r** was prepared via procedure VII using amide **19b** (2.5 g, 5.9 mmol), copper(I) iodide (0.11 g, 0.59 mmol), 3,4,7,8-tetramethyl-1,10-phenanthroline (0.28 g, 1.2 mmol), and cesium carbonate (3.8 g, 12 mmol) in phenylmethanol (7.4 ml, 55 mmol). The crude residue was purified by silica gel chromatography (ISCO, Redisep 40 g column, 10-90 % EtOAc/hexanes gradient) to afford the title compound as a white solid (1.8 g, 76 %). TLC (EtOAc:hexanes, 1:1, v/v) Rf = 0.50; ^{1}H NMR ($CDCl_3$, 400 MHz) δ: 7.44-7.33 (m, 5H), 7.22 (t, *J* = 7.6 Hz, 1H), 6.88-6.76 (m, 7H), 6.67 (s, 1H), 5.04 (s, 2H), 4.42 (s, 2H), 3.96 (q, *J* = 7.2 Hz, 2H), 3.60 (q, *J* = 6.4 Hz, 2H), 2.83 (t, *J* = 6.8 Hz, 2H), 1.39 (t, *J* = 7.2 Hz, 3H); ^{13}C NMR ($CDCl_3$, 100 MHz) δ: 168.7, 159.3, 154.3, 151.5, 140.5, 137.1, 129.9, 128.8, 128.2, 127.7, 121.6, 115.8, 115.7, 115.6, 113.1, 70.1, 68.3, 64.1, 40.1, 35.9, 15.1; HRMS calcd. for $C_{25}H_{28}O_4N$, 406.20128 $[M + H]^+$; 406.20141 found, $[M + H]^+$.

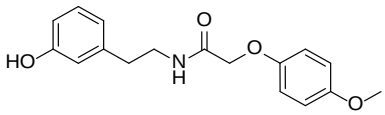

N-(3-hydroxyphenethyl)-2-(4-methoxyphenoxy)acetamide (20a): Amide **15q** (3.3 g, 8.4 mmol) was dissolved in MeOH (26 ml) and THF (26 ml). Dihydroxypalladium (0.64 g, 0.91 mmol) was added. The reaction was hydrogenated at room temperature overnight using a balloon. After stirring overnight the reaction was filtered through a pad of celite washing with MeOH and EtOAc. The organic layer was concentrated *in vacuo*. The crude residue was purified by silica gel chromatography (ISCO, Redisep 40 g column, 10-90 % EtOAc/hexanes gradient) to afford the title compound as a white solid (1.2 g, 47 %). TLC (EtOAc:hexanes, 1:1, v/v) Rf = 0.29; ^{1}H NMR ($CDCl_3$, 400 MHz) δ:

7.16 (t, *J* = 7.6 Hz, 1H), 6.85-6.79 (m, 4H), 6.76-6.68 (m, 3H), 6.29 (bs, 1H), 4.43 (s, 2H), 3.78 (s, 3H), 3.60 (q, *J* = 6.4 Hz, 2H), 2.80 (t, *J* = 6.4 Hz, 2H); HRMS calcd. for $C_{17}H_{19}O_4N$, 302.13868 $[M + H]^+$; 302.13838 found, $[M + H]^+$.

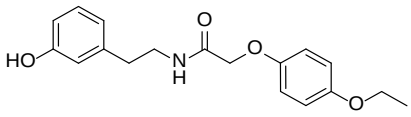

2-(4-ethoxypehnoxy)-N-(3-hydroxyphenethyl)acetamide (20b): Compound **20b** was prepared by dissolving amide **15r** (1.3 g, 3.2 mmol) in MeOH (25 ml) and THF (10 ml) and adding dihydroxypalladium (0.26 g, 0.37 mmol). The reaction was hydrogenated at room temperature overnight using a balloon. After stirring overnight the reaction was filtered through a pad of celite washing with MeOH and EtOAc and the organic layer was concentrated *in vacuo.* The crude residue was purified by silica gel chromatography (ISCO, Redisep 40 g column, 10-90 % EtOAc/hexanes gradient) to afford the title compound as a white solid (0.94 g, 91 %). TLC (EtOAc:hexanes, 1:1, v/v) Rf = 0.44; ^{1}H NMR ($CDCl_3$, 400 MHz) δ: 7.16 (t, *J* = 8.0 Hz, 1H), 6.86-6.78 (m, 4H), 6.77-6.72 (m, 3H), 6.66-6.65 (m, 1H), 6.03 (bs, 1H), 4.43 (s, 2H), 3.98 (q, *J* = 7.2 Hz, 2H), 3.60 (q, *J* = 6.4 Hz, 2H), 2.80 (t, *J* = 6.8 Hz, 2H), 1.40 (t, *J* = 7.2 Hz, 3H); ^{13}C NMR ($CDCl_3$, 100 MHz) δ: 169.1, 156.5, 151.4, 140.4, 130.1, 121.0, 115.8, 115.7, 113.9, 68.2, 64.2, 40.2, 35.8, 15.1; HRMS calcd. for $C_{18}H_{22}O_4N$, 316.15433 $[M + H]^+$; 316.15497 found, $[M + H]^+$.

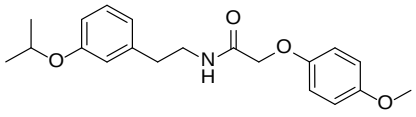

N-(3-isopropoxyphenethyl)-2-(4-methoxyphenoxy)acetamide (15a): Amide **20a** (1.2 g, 3.9 mmol) was dissolved in dry ACN (7.8 mL) and dry DMF (1.5 mL) and cesium carbonate (3.8 g, 12 mmol) was added. The reaction was allowed to stir for 2 hours before 2-iodopropane (0.47 mL, 4.7 mmol) was added. The reaction was heated to 60°C and allowed to stir overnight. The reaction was quenched with saturated aqueous ammonium chloride and extracted into EtOAc. The organic layer was washed with water (3x) and brine (3x), dried with $MgSO_4$, filtered, and concentrated *in vacuo*..

The crude residue was purified by silica gel chromatography The crude residue was purified by silica gel chromatography (ISCO, Redisep 40 g column, 10-80% EtOAc/hexanes gradient) to afford the title compound as a yellow oil (0.98 g, 73%). TLC (EtOAc:hexanes, 1:1, v/v) Rf = 0.30; ^{1}HNMR ($CDCl_3$, 400 MHz) δ: 7.19-7.15 (m, 1H), 6.82-6.66 (m, 7H), 4.54-4.49 (m, 1H), 4.39 (s, 2H), 3.75 (s, 3H), 3.59-3.53 (m, 2H), 2.79 (t, *J* = 6.8 Hz, 2H), 1.32-1.29 (m, 6H); ^{13}CNMR (100 MHz, $CDCl_3$) δ: 168.6, 158.4, 154.9, 151.5, 140.3, 129.9, 121.1, 116.6, 115.9, 115.0, 113.9, 69.9, 68.4, 55.9, 40.2, 35.9, 22.3; HRMS calcd. for $C_{20}H_{25}O_4N_1$, 344.18564 $[M + H]^+$; 344.18515 found, $[M + H]^+$.

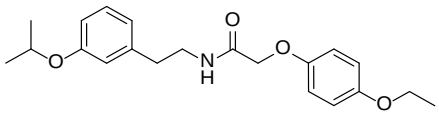

2-(4-ethoxyphenoxy)-N-(3-isopropoxyphenethyl)acetamide (15d): To a solution of amide **20b** (0.94 g, 2.9 mmol) in dry ACN (8.0 mL) and dry DMF (5.0 mL) was added cesium carbonate (2.9 g, 8.9 mmol). The reaction was allowed to stir for 2 hours before 2-iodopropane (0.36 mL, 3.6 mmol) was added and the reaction was heated to 60°C and allowed to stir for 22 hours. The reaction was quenched with saturated aqueous ammonium chloride and extracted into EtOAc. The organic layer was washed with water (3x) and brine (3x), dried with $MgSO_4$, filtered, and concentrated *in vacuo*. The crude residue was purified by silica gel chromatography The crude residue was purified by silica gel chromatography (ISCO, Redisep 40 g column, 10-80% EtOAc/hexanes gradient) to afford the title compound as a yellow oil (0.93 g, 88%). TLC (EtOAc:hexanes, 1:1, v/v) Rf = 0.67; ^{1}H NMR ($CDCl_3$, 400 MHz) δ: 7.20-7.15 (m, 1H), 6.83-6.70 (m, 7H), 6.65 (bs, 1H), 4.54-4.48 (m, 1H), 4.39 (s, 2H), 3.96 (q, *J* = 7.2 Hz, *J* = 14.0 Hz, 2H), 3.59-3.53 (m, 2H), 2.81-2.77 (m, 2H), 1.24 (t, *J* = 7.2 Hz, 3H), 1.31 (s, 3H), 1.29 (s, 3H); ^{13}C NMR ($CDCl_3$,100 MHz) δ: 168.6, 158.4, 154.3, 151.4, 140.4, 129.9, 121.1, 116.6, 115.8, 115.6, 113.9, 69.8, 68.3, 64.2, 40.2, 35.9, 22.3, 15.1; HRMS calcd. for $C_{21}H_{27}O_4N_1$, 358.20129 $[M + H]^+$; 358.20121 found, $[M + H]^+$.

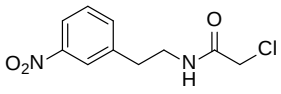

2-chloro-N-(3-nitrophenethyl)acetamide (22): Compound **22** was prepared via Procedure IV using 2-(3-nitrophenyl)ethanamine hydrochloride (1.9 g, 9.4 mmol) was dissolved in dry DCM (34 mL) and saturated $NaHCO_3$ (10. mL) was added. The reaction was brought to 0ºC and triethylamine (2.6 ml, 19 mmol) was added, followed by 2-chloroacetyl chloride (0.83 ml, 11 mmol). The reaction was allowed to stir for 2 hours, at which point TLC indicated complete conversion. The reaction was quenched with 1M HCl and extracted into DCM. The organic layer was then washed with water and brine, dried with $MgSO_4$, filtered, and concentrated *in vacuo* to afford a white solid (1.9 g, 87 %). TLC (EtOAc:hexanes, 1:1, v/v) Rf = 0.52; ^{1}HNMR ($CDCl_3$, 400 MHz): δ 8.08-8.05 (m, 2H), 7.54-7.52 (m, 1H), 7.49-7.45 (t, J = 7.8 Hz, 1H), 6.71 (s, 1H), 3.99 (s, 2H), 3.61-3.56 (q, J = 7.0 Hz, J = 14.1 Hz, 2H), 2.97-2.94 (t, J = 7.4 Hz, 2H); ^{13}CNMR ($CDCl_3$, 100 MHz): δ 166.3, 140.6, 135.3, 129.9, 123.8, 122.1, 42.8, 40.8, 35.4; HRMS calcd. for $C_{12}H_{12}O_3N_2{}^{35}Cl_1$, 243.05130 $[M + H]^+$; 243.05354 found, $[M + H]^+$.

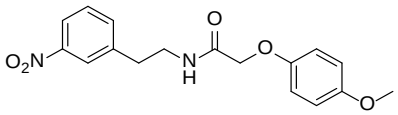

2-(4-methoxyphenoxy)-N-(3-nitrophenethyl)acetamide (23): To a solution of 4-methoxyphenol (1.2 g, 9.8 mmol) dissolved in dry ACN (24 mL) was added potassium carbonate (5.6 g, 41 mmol). The reaction was allowed to stir for 2 hours before amide **22** (1.9 g, 8.1 mmol) dissolved in ACN (10. mL) was added and the reaction was heated to 50 °C. After stirring for 25 hours, the reaction was quenched with saturated NH_4Cl and extracted in EtOAc. The organic layer was then washed with water (3x), brine (3x), dried with $MgSO_4$, filtered, and concentrated *in vacuo*. The crude residue was purified by silica gel chromatography (ISCO, Redisep 40 g column, 10-80% EtOAc/hexanes gradient) to afford the title compound as a yellow oil (1.8 g, 68 %). TLC (EtOAc:hexanes, 1:1, v/v) Rf = 0.34; ^{1}HNMR ($CDCl_3$, 400 MHz): δ 8.09-8.04 (m, 2H), 7.53-7.42 (m, 2H), 6.82-6.75 (m, 4H), 6.66 (s, 1H), 4.40 (s, 2H), 3.75 (s, 3H), 3.66-3.61 (q, J = 7.2 Hz, J = 13.6 Hz, 2H), 2.98-2.94 (m, 2H); ^{13}CNMR (100 MHz, $CDCl_3$): δ 168.9, 154.9, 151.4, 140.8, 135.2, 129.8, 123.8, 122.2, 122.0, 115.8,

115.1, 68.3, 55.9, 39.9, 35.6; HRMS calcd. for $C_{18}H_{19}O_5N_2$, 331.12885 $[M + H]^+$; 331.12936 found, $[M + H]^+$.

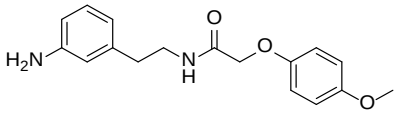

N-(3-aminophenethyl)-2-(4-methoxyphenoxy)acetamide (24): Amide **23** (1.7 g, 5.1 mmol) in EtOH (11 mL) was subjected to hydrogenation conditions with 5 % Pd/C (0.16 g) for 1 hour at 36 psi using the Parr hydrogenator. The reaction mixture was filtered over celite and the filtrate was concentrated *in vacuo* to afford a yellow oil (1.4 g, 94 %). TLC (MeOH:DCM, 1:10, v/v) Rf: 0.78; ^{1}H NMR ($CDCl_3$, 400 MHz) δ: 7.08-7.04 (t, *J* = 7.2 Hz, 1H), 6.84-6.77 (m, 4H), 6.65 (s, 1H), 6.60-6.53 (m, 2H), 6.45-6.47 (m, 1H), 4.40 (s, 2H), 3.76 (s, 3H), 3.58-3.53 (q, *J* = 7.2 Hz, *J* = 13.6 Hz, 2H), 2.74-2.70 (m, 2H); ^{13}C NMR ($CDCl_3$, 100 MHz) δ: 168.6, 154.8, 151.6, 146.7, 140.0, 129.8, 119.3, 115.8, 115.7, 115.0, 113.7, 68.4, 55.9, 41.2, 35.9; HRMS calcd. for $C_{17}H_{21}O_3N_2$, 301.15467 $[M + H]^+$; found 301.15523 $[M + H]^+$.

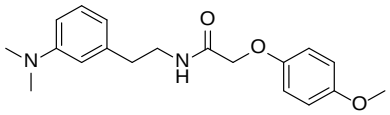

N-(3-(dimethylamino)phenethyl)-2-(4-methoxyphenoxy)acetamide (25a): Amide **24** (1.4 g, 4.7 mmol) and paraformaldehyde (1.4 g, 47 mmol) were suspended in AcOH (32 ml). Sodium cyanoborohydride (1.5 g, 24 mmol) was added and the reaction was allowed to stir for 20 hours. Upon completion, the reaction was made pH 13 with 1M NaOH, and extracted into DCM. The organic layer was washed with water and brine, dried with $MgSO_4$, and concentrated *in vacuo*. The crude residue was purified by silica gel chromatography (ISCO, Redisep 20 g column, 0-20% MeOH/DCM gradient) to afford the title compound as a yellow oil (0.88 g, 57 %). TLC (MeOH/DCM, 1:10, v/v) Rf: 0.76; ^{1}H NMR ($CDCl_3$, 400 MHz): δ 7.18-7.13 (t, *J* = 7.6 Hz, 1H), 6.83-6.75 (m, 4H), 6.68 (s, 1H), 6.62-6.59 (dd, *J* = 2.0 Hz, *J* = 8.0 Hz, 1H), 6.53-6.50 (m, 2H), 4.40 (s, 2H), 3.76 (s, 3H), 3.61-3.56 (q, *J* = 6.8 Hz, *J* = 12.8 Hz, 2H), 2.91 (s, 6H), 2.80-2.77 (t, *J* = 7.2 Hz, *J* =

14.4 Hz, 2H); ^{13}C NMR ($CDCl_3$, 100 MHz) δ: 168.6, 154.9, 151.6, 151.1, 129.7, 129.6, 117.1, 115.9, 115.0, 113.1, 111.1, 68.4, 55.9, 40.9, 40.3, 36.3; HRMS calcd. for $C_{19}H_{25}O_3N_2$, 329.18597 [M + H]$^+$; found 329.18659 [M + H]$^+$.

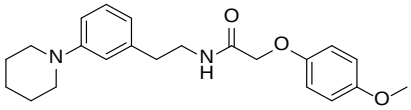

2-(4-methoxyphenoxy)-N-(3-(piperidin-1-yl)phenethyl)acetamide (26a): Compound **26a** was prepared via procedure VIII using amide **19a** (2.0 g, 4.9 mmol), copper(I) iodide (0.19 g, 0.97 mmol), potassium carbonate (1.3 g, 9.7 mmol), L-proline (0.11 g, 0.97 mmol), and piperidine (0.72 ml, 7.3 mmol) in dry DMSO (15 ml). The crude residue was purified by silica gel chromatography (ISCO, Redisep 40 g column, 0-15 % MeOH:DCM gradient) to afford the title compound as a brown solid (1.5 g, 87 %) TLC (MeOH:DCM, 1:10, v/v) Rf = 0.84; ^{1}HNMR ($CDCl_3$, 400 MHz) δ: 7.15 (t, *J* = 7.6 Hz, 1H), 6.82-6.75 (m, 6H), 6.61-6.60 (m, 1H), 4.39 (s, 2H), 3.75 (s, 3H), 3.57 (q, *J* = 6.0 Hz, 2H), 3.10 (t, *J* = 5.6 Hz, 4H), 2.77 (t, *J* = 6.8 Hz, 2H), 1.69-1.64 (m, 4H), 1.56-1.51 (m, 2H); ^{13}CNMR ($CDCl_3$, 100 MHz) δ: 168.6, 154.8, 152.8, 151.5, 139.5, 129.5, 119.8, 117.1, 115.9, 115.0, 114.9, 68.3, 55.9, 50.8, 40.3, 36.2, 26.0, 24.5; HRMS calcd. for $C_{26}H_{29}N_2O_3$, 469.21727 [M + H]$^+$; found 469.21723 [M + H]$^+$.

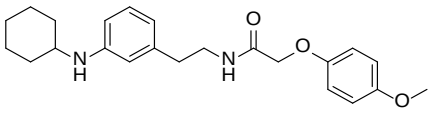

N-(3-(cyclohexylamino)phenethyl)-2-(4-methoxyphenoxy)acetamide (26b): A 10 mL sealed vial was charged with amide **19a** (2.0 g, 4.9 mmol), copper(I) iodide (0.19 g, 0.97 mmol), potassium carbonate (1.3 g, 9.7 mmol), and L-proline (0.11 g, 0.97 mmol). The vial was sealed, evacuated, and back-filled with argon. DMSO (15 ml) was added followed by piperidine (0.84 ml, 7.3 mmol) and the reaction was submerged in an oil bath heated to 80 °C. After stirring for 48 hours, the reaction appeared to be complete by LCMS and TLC. The reaction was allowed to cool to room temperature, diluted with EtOAc, and washed with water (3x), brine (6x), and 5.0 % LiCl solution (8x). The

organic layer was dried with $MgSO_4$, filtered, and concentrated *in vacuo*. The crude residue was purified by silica gel chromatography (ISCO, Redisep 40 g column, 0-15 % MeOH:DCM gradient) to afford the title compound as a red oil (1.6 g, 84 %) TLC (MeOH:DCM, 1:10, v/v) Rf = 0.60; ^{1}HNMR ($CDCl_3$, 400 MHz) δ: 7.06 (t, *J* = 7.6 Hz, 1H), 6.83-6.76 (m, 4H), 6.69 (bs, 1H), 6.46-6.43 (m, 2H), 6.37-6.36 (m, 1H), 4.39 (s, 2H), 3.76 (s, 3H), 3.55 (q, *J* = 6.8 Hz, 2H), 3.24-3.18 (m, 1H), 2.72 (t, *J* = 6.8 Hz, 2H), 2.04-1.99 (m, 2H), 1.75-1.70 (m, 2H), 1.65-1.60 (m, 1H), 1.38-1.28 (m, 2H), 1.24-1.06 (m, 3H); ^{13}CNMR ($CDCl_3$, 100 MHz) δ: 168.5, 154.8, 151.6, 147.9, 139.9, 129.8, 117.4, 115.8, 115.0, 113.9, 111.5, 68.3, 55.9, 51.7, 40.3, 36.1, 33.7, 26.1, 25.3; HRMS calcd. for $C_{23}H_{31}N_2O_3$, 383.23292 $[M + H]^+$; found 383.23288 $[M + H]^+$.

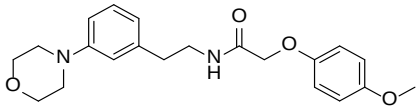

2-(4-methoxyphenoxy)-N-(3-morpholinophenethyl)acetamide (26c): Compound **26c** was prepared via procedure VIII using amide **19a** (0.20 g, 0.49 mmol), copper(I) iodide (0.020 g, 0.097 mmol), potassium carbonate (0.13 g, 0.97 mmol), L-proline (0.011 g, 0.097 mmol), and morpholine (0.063 ml, 0.73 mmol) in dry DMSO (1.5 ml). The crude residue was purified by silica gel chromatography (ISCO, Redisep 40 g column, 0-15 % MeOH:DCM gradient) to afford the title compound as a red oil (0.18 g, 67 %) TLC (MeOH:DCM, 1:10, v/v) Rf = 0.60; ^{1}HNMR ($CDCl_3$, 400 MHz) δ: 7.19 (t, *J* = 8.0 Hz, 1H), 6.83-6.75 (m, 1H), 6.74-6.72 (m, 1H), 6.68-6.66 (m, 2H), 4.39 (s, 2H), 3.81 (t, *J* = 9.6 Hz, 4H), 3.75 (s, 3H), 3.57 (q, *J* = 6.4 Hz, 2H), 3.12 (t, *J* = 5.2 Hz, 4H), 2.79 (t, *J* = 7.2 Hz, 2H); ^{13}CNMR ($CDCl_3$, 100 MHz) δ: 168.6, 154.9, 151.8, 139.8, 129.7, 120.7, 116.3, 115.8, 115.0, 114.1, 68.4, 67.1, 55.9, 49.5, 40.3, 36.2; HRMS calcd. for $C_{21}H_{27}N_2O_4$, 371.19653 $[M + H]^+$; found 371.19655 $[M + H]^+$.

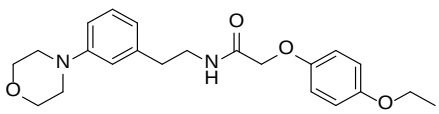

2-(4-ethoxyphenoxy)-N-(3-morpholinophenethyl)acetamide (26d): Compound **26d** was prepared via procedure VIII using amide **19b** (2.0 g, 4.7 mmol), copper(I) iodide (0.18 g, 0.94 mmol), potassium carbonate (1.3 g, 9.4 mmol), L-proline (0.11 g, 0.94 mmol), morpholine (0.61 ml, 7.1 mmol) in dry DMSO (14 ml). The crude residue was purified by silica gel chromatography (ISCO, Redisep 40 g column, 0-15 % MeOH:DCM gradient) to afford the title compound as a brown oil (0.77 g, 43 %) TLC (MeOH:DCM, 1:10, v/v) Rf = 0.90; ^{1}HNMR ($CDCl_3$, 400 MHz) δ: 7.22 (t, *J* = 8.0 Hz, 1H), 6.84-6.76 (m, 5H), 6.71-6.60 (m, 2H), 4.41 (s, 2H), 4.97 (q, *J* = 7.2 Hz, 2H), 3.84 (t, *J* = 4.8 Hz, 4H), 3.60 (q, *J* = 6.4 Hz, 2H), 3.14 (t, *J* = 5.2 Hz, 4H), 2.81 (t, *J* = 7.2 Hz, 2H), 1.40 (t, *J* = 7.2 Hz, 3H); ^{13}CNMR ($CDCl_3$, 100 MHz) δ: 168.6, 154.3, 151.9, 151.5, 139.9, 129.7, 120.6, 116.3, 115.9, 115.7, 114.1, 68.4, 67.1, 64.2, 49.5, 40.3, 36.2, 15.1; HRMS calcd. for $C_{22}H_{29}N_2O_4$, 385.21218 $[M + H]^+$; found 385.21238 $[M + H]^+$.

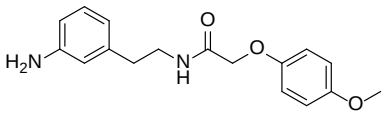

N-(3-aminophenethyl)-2-(4-methoxyphenoxy)acetamide (24): A 10 mL sealed vial was charged with Cu(I) oxide (0.23 g, 1.6 mmol) and amide **19a** (3.3 g, 7.9 mmol). The vial was sealed, evacuated, and purged with argon. Concentrated ammonium hydoxide (5.2 ml, 9.7 mmol) was added followed by NMP (5.2 ml) and the vial was submerged in an oil bath heated to 85 °C. After stirring for 48 hours, the reaction was allowed to cool to room temperature, quenched with water, and extracted into EtOAc. The organic layer was washed with water and brine, dried with $MgSO_4$, filtered, and concentrated *in vacuo*. The crude residue was purified by silica gel chromatography (ISCO, Redisep 40 g column, 0-18 % MeOH:DCM gradient) to afford the title compound as a clear oil (1.7 g, 72 %) TLC (MeOH:DCM, 1:10, v/v) Rf = 0.90; ^{1}H NMR ($CDCl_3$, 400 MHz) δ: 7.09 (t, *J* = 7.8 Hz, 1H), 6.87-6.79 (m, 4H), 6.69 (bs, 1H), 6.55 (d, *J* = 7.8 Hz, 2H), 6.48 (s, 1H), 4.43 (s, 2H), 3.78 (s, 3H), 3.69 (bs, 2H), 3.58 (q, *J* = 6.6 Hz, 2H), 2.74 (t, *J* = 6.6 Hz, 2H); ^{13}C NMR ($CDCl_3$,100 MHz) δ: 168.6,

154.9, 151.6, 146.9, 140.0, 129.8, 119.1, 115.9, 115.6, 115.0, 113.6, 68.4, 55.9, 40.2, 35.9; HRMS calcd. for $C_{17}H_{20}O_3N_2$, 301.15467 $[M + H]^+$; 301.15441 found, $[M + H]^+$.

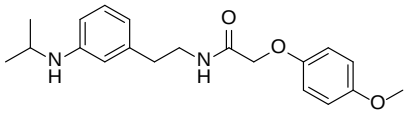

N-(3-(isopropylamino)phenethyl)-2-(4-methoxyphenoxy)acetamide (25b): To a solution of amide **24** (1.7 g, 5.7 mmol) in dry ACN (11 ml), propan-2-one (1.3 ml, 17 mmol) was added followed by sodium cyanoborohydride (1.1 g, 17 mmol). AcOH (11 ml) was added over a period of 10 minutes and the reaction was allowed to stir for 2 hours. AcOH (11 ml) was added again and after stirring for 10 additional minutes, the reaction was brought to 0°C using an ice bath. The reaction was made basic using concentrated NH_4OH, extracted into EtOAc, washed with water and brine, dried with $MgSO_4$, filtered, and concentrated *in vacuo*. The crude residue was purified by silica gel chromatography (ISCO, Redisep 40 g column, 0-90 % EtOAc:hexanes gradient) to afford the title compound as a clear oil (0.74 g, 32 %) TLC (EtOAc:hexanes, 1:1, v/v) Rf = 0.71; ^{1}H NMR ($CDCl_3$, 400 MHz) δ: 7.12-7.09 (m, 1H), 6.85-6.75 (m, 6H), 6.49-6.47 (m, 2H), 6.40 (s, 1H), 4.41 (s, 2H), 3.78 (s, 3H), 3.64-3.57 (m, 3H), 2.75 (t, J = 6.8 Hz, 2H), 1.20 (d, J = 6.0 Hz, 6H); ^{13}C NMR ($CDCl_3$,100 MHz) δ: 168.9, 154.9, 151.5, 147.9, 139.9, 129.9, 117.6, 116.2, 115.1, 113.9, 111.7, 68.3, 55.9, 44.5, 40.3, 35.9, 23.2; HRMS calcd. for $C_{20}H_{27}O_3N_2$, 343.20162 $[M + H]^+$; 343.20120 found, $[M + H]^+$.

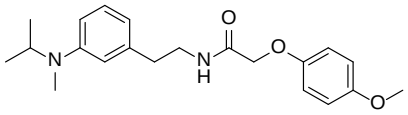

N-(3-(isopropyl(methyl)amino)phenethyl)-2-(4-methoxyphenoxy)acetamide (25c):

Compound **25c** was prepared via procedure IX using amide **25b** (0.79 g, 2.3 mmol), paraformaldehyde (0.69 g, 23 mmol), and sodium cyanoborohydride (0.73 g, 12 mmol) in AcOH (15 mL). After stirring for 4 hours the TLC indicated complete conversion. The crude residue was purified by silica gel chromatography (ISCO, Redisep 40 g column, 0-20 % MeOH:DCM gradient) to afford the title compound as a clear oil (0.58 g, 70%) TLC (MeOH:DCM, 1:10, v/v) Rf = 0.65; ^{1}H

NMR ($CDCl_3$, 400 MHz) δ: 7.14 (t, *J* = 8.0 Hz, 1H), 6.84-6.73 (m, 6H), 6.67-6.65 (m, 1H), 6.60 (s, 1H), 4.40 (s, 2H), 3.76 (s, 3H), 5.58 (q, *J* = 6.8 Hz, 3H), 2.78 (t, *J* = 7.2 Hz, 2H), 2.70 (s, 3H), 1.13 (d, *J* = 6.8 Hz, 6H); ^{13}C NMR ($CDCl_3$,100 MHz) δ: 168.6, 154.9, 151.7, 150.7, 139.7, 129.7, 116.9, 115.9, 115.0, 113.7, 111.7, 68.4, 55.9, 49.1, 40.4, 36.4, 30.1, 23.2, 19.6; HRMS calcd. for $C_{21}H_{28}O_3N_2$, 357.21727 $[M + H]^+$; 357.21763 found, $[M + H]^+$.

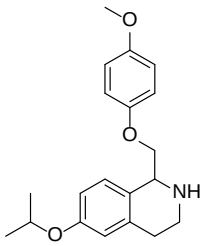

6-isopropoxy-1-((4-methoxyphenoxy)methyl)-1,2,3,4-tetrahydroisoquinoline (28a): Dihydroisoquinoline **27a** was prepared via procedure XI using amide **15a** (2.0 g, 5.8 mmol) and phosphorus trichloride (1.6 mL, 18 mmol) in dry toluene (32 mL). The crude solid (4.5 g) was carried on without further purification. HRMS calcd. for $C_{20}H_{23}O_3N_1$, 326.17507 $[M + H]^+$; found 326.17461 $[M + H]^+$. Tetrahydroisoquinoline **28a** was prepared via procedure XII using dihydroisoquinoline **27a** (4.5 g, 14 mmol) and sodium borohydride (1.9 g, 50. mmol) in dry MeOH (70 mL). The crude residue was purified by silica gel chromatography (ISCO, Redisep 20 g column, 0-20% MeOH/DCM gradient) to afford the title compound as a green solid (0.52 g, 12 % over 2 steps). TLC (MeOH/DCM, 1:10, v/v) Rf: 0.59; ^1H NMR ($CDCl_3$, 400 MHz) δ: 7.02-6.99 (d, *J* = 8.8 Hz, 1H), 6.98-6.94 (m, 2H), 6.77-6.71 (m, 3H), 6.62-6.61 (d, *J* = 2.4 Hz, 1H), 4.62-4.59 (q, *J* = 4.0 Hz, *J* = 6.8 Hz, 1H), 4.52-4.46 (m, 1H), 4.43-4.39 (m, 1H), 4.36-4.32 (m, 1H), 3.72 (s, 3H), 3.53 (m 1H), 3.24-3.13 (m, 2H), 2.99-2.93 (m, 1H), 1.30 (s, 3H), 1.28 (s, 3H); ^{13}C NMR ($CDCl_3$, 100 MHz) δ: 157.8, 154.7, 152.1, 134.3, 127.5, 120.2, 116.6, 115.9, 115.4, 114.8, 70.2, 69.2, 55.9, 54.2, 39.8, 26.1, 22.3, 22.2; HRMS calcd. for $C_{20}H_{25}O_3N_1$, 328.19072 $[M + H]^+$; found 328.19109 $[M + H]^+$.

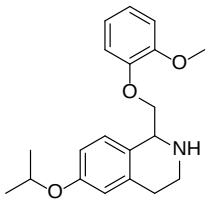

6-isopropoxy-1-((2-methoxyphenoxy)methyl)-1,2,3,4-tetrahydroisoquinoline (28b):

Dihydroisoquinoline **27b** was prepared via procedure X using amide **15b** (1.4 g, 4.2 mmol) and phosphorus trichloride (1.9 mL, 13 mmol) in dry toluene (24 mL). The crude solid (1.5 g) was carried on without further purification. HRMS calcd. for $C_{20}H_{23}O_3N_1$, 326.17507 $[M + H]^+$; found 326.17524 $[M + H]^+$. Tetrahydroisoquinoline **28b** was prepared via procedure XII using dihydroisoquinoline **27b** (1.5 g, 4.7 mmol) and sodium borohydride (0.50 g, 14 mmol) in dry MeOH (23 mL). The crude residue was purified by silica gel chromatography (ISCO, Redisep 20 g column, 0-20% MeOH/DCM gradient) to afford the title compound as a green solid (1.5 g, 36 % over 2 steps). TLC (MeOH/DCM, 1:10, v/v) Rf: 0.55; ^{1}H NMR ($CDCl_3$, 400 MHz) δ: 7.05-7.02 (m, 2H), 6.69-6.93 (m, 1H), 6.84-6.81 (m, 1H), 6.72-6.69 (q, J = 2.4 Hz, J = 8.8 Hz, 1H), 6.62-6.61 (d, J = 1.6 Hz, 1H), 4.77-4.73 (m, 1H), 4.50-4.39 (m, 2H), 3.78 (s, 3H), 3.69-3.66 (m, 1H), 3.45-3.43 (m, 1H), 3.14-3.10 (m, 2H), 1.29 (s, 3H), 1.27 (s, 3H); ^{13}C NMR ($CDCl_3$, 100 MHz) δ: 147.8, 147.4, 134.2, 127.9, 123.8, 121.6, 120.1, 117.8, 115.9, 115.4, 112.7, 71.4, 70.2, 56.3, 53.9, 39.6, 26.1, 22.2; HRMS calcd. for $C_{20}H_{25}O_3N_1$, 328.19072 $[M + H]^+$; found 328.19032 $[M + H]^+$.

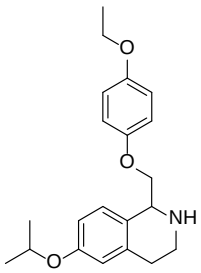

1-((4-ethoxyphenoxy)methyl)-6-isopropoxy-1,2,3,4-tetrahydroisoquinoline (28d):

Dihydroisoquinoline **27d** was prepared via Procedure XI using **15d** (1.6 g, 4.4 mmol) and phosphorous trichloride (1.2 mL, 13 mmol) in dry toluene (24 mL). The crude residue (4.9 g) was

carried on without further purification. HRMS calcd. for $C_{21}H_{25}O_3N_1$, 340.19072 $[M + H]^+$; found 340.19116 $[M + H]^+$. Tetrahydroisoquinoline **27d** was prepared via Procedure XII using dihydroisoquinoline **27d** (4.9 g, 14 mmol) and sodium borohydride (1.6 g, 43 mmol) in dry MeOH (71 mL). The crude residue was purified by silica gel chromatography (ISCO, Redisep 20 g column, 0-20% MeOH/DCM gradient) to afford the title compound as a yellow solid (0.70 g, 14 %). TLC (MeOH/DCM, 1:10, v/v) Rf: 0.58; ^{1}H NMR ($CDCl_3$, 400 MHz) δ: 7.00 (d, *J* = 8.4 Hz, 1H), 6.94-6.89 (m, 2H), 6.77-6.70 (m, 3H), 6.60 (d, *J* = 2.4 Hz, 1H), 4.59-5.58 (m, 1H), 4.51-4.45 (m, 1H), 4.43-4.38 (m, 1H), 4.34-4.29 (m, 1H), 3.91 (q, *J* = 6.8 Hz, *J* = 13.6 Hz, 2H), 3.51-3.47 (m, 1H), 3.24-3.09 (m, 2H), 2.97-2.92 (m, 1H), 1.35 (t, *J* = 6.8 Hz, 3H), 1.29 (s, 3H), 1.28 (s, 3H); ^{13}C NMR ($CDCl_3$, 100 MHz) δ: 157.7, 154.0, 152.1, 134.4, 127.5, 120.6, 116.6, 115.9, 115.5, 113.3, 70.1, 69.4, 64.1, 54.0, 39.8, 26.2, 22.3, 22.2, 15.1; HRMS calcd. for $C_{21}H_{27}O_3N_1$, 342.20637 $[M + H]^+$; found 342.20595 $[M + H]^+$.

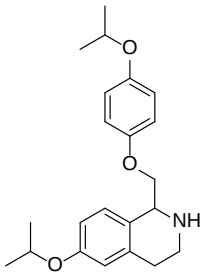

6-isopropoxy-1-((4-isopropoxyphenoxy)methyl)-1,2,3,4-tetrahydroisoquinoline (28e): Dihydroisoquinoline **27e** was prepared via procedure XI using amide **15e** (1.5 g, 4.1 mmol) and phosphorus trichloride (1.2 mL, 12 mmol) in dry toluene (21 mL). The crude solid (1.4 g) was carried on without further purification. HRMS calcd. for $C_{22}H_{28}O_3N_1$, 354.20637 $[M + H]^+$; found 354.20665 $[M + H]^+$. Tetrahydroisoquinoline **28e** was prepared via procedure XII using dihydroisoquinoline **27e** (1.4 g, 3.8 mmol) and sodium borohydride (0.38 g, 12 mmol) in dry MeOH (13 mL). The crude residue was purified by silica gel chromatography (ISCO, Redisep 20 g column, 0-15% MeOH/DCM gradient) to afford the title compound as an off-white solid (0.24 g, 18 % over 2 steps). TLC (MeOH/DCM, 1:10, v/v) Rf: 0.81; ^{1}H NMR ($CDCl_3$, 400 MHz) δ: 7.62 (bs, 1H), 7.04

(d, *J* = 8.1 Hz, 1H), 6.95-6.89 (m, 2H), 6.82-6.77 (m, 2H), 6.74-6.71 (dd, *J* = 2.4 Hz, *J* = 8.4 Hz, 1H), 6.64-6.63 (m, 1H), 4.55-4.47 (m, 2H), 4.44-4.36 (m, 1H), 4.33-4.20 (m, 2H), 3.44-3.36 (m, 1H), 3.19-3.10 (m, 1H), 3.00-2.88 (m, 2H), 1.32-1.27 (m, 12H); ^{13}C NMR ($CDCl_3$, 100 MHz) δ: 157.1, 152.4, 152.3, 135.3, 127.3, 122.6, 117.3, 115.9, 115.8, 114.6, 70.7, 69.8, 54.2, 39.5, 27.5, 22.1, 22.0; HRMS calcd. for $C_{22}H_{30}O_3N_1$, 356.22202 $[M + H]^+$; found 356.22255 $[M + H]^+$.

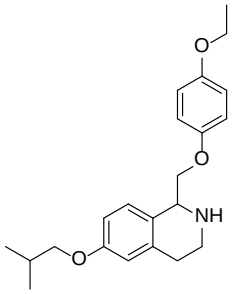

1-((4-ethoxyphenoxy)methyl)-6-isobutoxy-1,2,3,4-tetrahydroisoquinoline (28g):

Dihydroisoquinoline **27g** was prepared via Procedure XI using **15n** (0.54 g, 1.5 mmol) and phosphorous trichloride (0.90 mL, 4.4 mmol) in dry toluene (7.3 mL). The crude residue (0.68 g) was carried on without further purification. HRMS calcd. for $C_{22}H_{28}O_3N$, 354.20637 $[M + H]^+$; found 354.206654 $[M + H]^+$. Tetrahydroisoquinoline **28g** was prepared via Procedure XII using dihydroisoquinoline **27g** (0.68 g, 1.9 mmol) and sodium borohydride (0.22 g, 5.8 mmol) in dry MeOH (9.7 mL). The crude residue was purified by silica gel chromatography (ISCO, Redisep 20 g column, 0-20% MeOH/DCM gradient) to afford the title compound as a green foam (0.35 g, 52 %). TLC (MeOH/DCM, 1:10, v/v) ^{1}H NMR ($CDCl_3$, 400 MHz) δ: 7.04-7.03 (m, 1H), 6.96-6.89 (m, 1H), 6.79-6.74 (m, 4H), 6.66-6.63 (m, 1H), 4.54-5.53 (m, 1H), 4.34-4.08 (m, 2H), 3.97-3.88 (m, 2H), 3.68 (d, *J* = 6.8 Hz, 2H), 3.49-3.39 (m, 1H), 3.28-3.26 (m, 1H), 3.21-2.91 (m, 2H), 2.10-2.02 (m, 1H), 1.40 (t, *J* = 7.2 Hz, 3H), 1.02 (d, *J* = 6.4). ^{13}C NMR ($CDCl_3$, 100 MHz) δ: 158.8, 153.8, 152.3, 134.8, 127.6, 121.8, 116.3, 115.6, 115.4, 114.4, 114.0, 74.6, 69.8, 64.1, 53.7, 39.6, 28.5, 28.4, 26.5, 19.4, 15.1. HRMS calcd. for $C_{22}H_{30}O_3N$, 356.22202 $[M + H]^+$; found 356.22235 $[M + H]^+$.

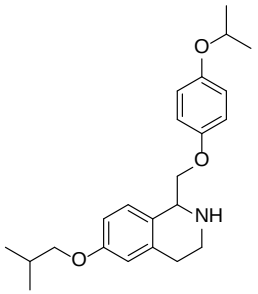

6-isobutoxy-1-((4-isopropoxyphenoxy)methyl)-1,2,3,4-tetrahydroisoquinoline (28h):

Dihydroisoquinoline **27h** was prepared via Procedure X using **15p** (0.24 g, 0.63 mmol) and phosphorous trichloride (0.39 mL, 1.9 mmol) in dry toluene (3.2 mL). The crude residue (0.23 g) was carried on without further purification. HRMS calcd. for $C_{22}H_{30}O_3N$, 368.22202 $[M + H]^+$; found 368.22189 $[M + H]^+$. Tetrahydroisoquinoline **28h** was prepared via Procedure XII using dihydroisoquinoline **27h** (0.23 g, 0.63 mmol) and sodium borohydride (0.071 g, 1.9 mmol) in dry MeOH (3.5 mL). The crude residue was purified by silica gel chromatography (ISCO, Redisep 20 g column, 0-20% MeOH/DCM gradient) to afford the title compound as a brown oil (0.12 g, 51 %). TLC (MeOH/DCM, 1:10, v/v) Rf: 0.65; ^{1}H NMR ($CDCl_3$, 400 MHz) δ: 7.06 (d, J = 8.4 Hz, 1H), 6.88-6.75 (m, 4H), 6.73-6.70 (m, 1H), 6.66-6.65 (m, 1H), 4.43-4.37 (m, 1H), 4.35-4.32 (m, 1H), 4.15-4.09 (m, 1H), 4.06-4.02 (m, 1H), 3.77-3.66 (m, 3H), 3.21-3.17 (m, 1H), 3.03-2.98 (m, 1H), 2.83-2.79 (m, 2H), 1.29 (d, J = 6.0 Hz, 6H), 1.00 (d, J = 7.2 Hz, 6H); ^{13}C NMR ($CDCl_3$, 100 MHz) δ: 158.1, 153.2, 152.3, 137.4, 127.7, 126.5, 117.6, 115.7, 114.8, 112.9, 74.6, 71.3, 71.0, 54.7, 39.9, 30.1, 28.5, 22.3, 19.5; HRMS calcd. for $C_{23}H_{32}O_3N$, 370.23767 $[M + H]^+$; found 370.23767 $[M + H]^+$.

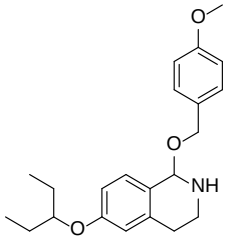

1-((4-methoxybenzyl)oxy)-6-(pentan-3-yloxy)-1,2,3,4-tetrahydroisoquinoline (28i):

Dihydroisoquinoline **27i** was prepared via procedure X using amide **15g** (0.61 g, 1.6 mmol) and

phosphorus trichloride (1.0 mL, 5.0 mmol) in dry toluene (9.0 mL). The crude solid was carried on without further purification. HRMS calcd. for $C_{22}H_{28}O_3N$, 354.20637 $[M + H]^+$; found 354.20640 $[M + H]^+$. Tetrahydroisoquinoline **28i** was prepared via procedure XII using **27i** (0.35 g, 1.0 mmol) and sodium borohydride (0.11 g, 3.0 mmol) in dry MeOH (5.0 mL). The crude residue was subjected to flash column chromatography (ISCO, Redisep 24 g column, 0-10% MeOH/DCM gradient) to afford the title compound as a yellow foam (0.15 g, 43 % over 2 steps). ^{1}H NMR ($CDCl_3$, 400 MHz) δ: 6.98-6.95 (m, 1H), 6.89-6.86 (m, 1H), 6.82-6.69 (m, 3.5H), 6.65-6.62 (m, 0.5H), 6.58-6.56 (m, 1H), 4.84 (m, 0.5H), 4.56-4.54 (m, 0.5H), 4.33-4.19 (m, 1H), 4.14-3.90 (m, 2H), 3.70 (s, 3H), 3.54-3.48 (m, 0.5H), 3.19-3.09 (m, 1H), 2.99-2.83 (m, 1.5H)1.67-1.60 (m, 4H), 0.92 (t, J = 7.2 Hz, 6H); ^{13}C NMR ($CDCl_3$, 100 MHz) δ: 158.3, 154.5, 152.4, 134.9, 127.7, 116.3, 115.9, 115.6, 115.0, 114.7, 80.3, 69.9, 55.9, 53.6, 39.4, 26.2, 9.8; HRMS calcd. for $C_{22}H_{30}NO_3$, 356.22202 $[M + H]^+$; found, 356.22192 $[M + H]^+$.

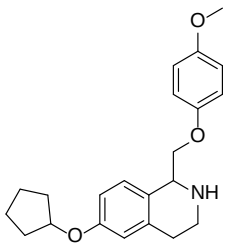

6-(cyclopentyloxy)-1-((4-methoxyphenoxy)methyl)-1,2,3,4-tetrahydroisoquinoline (28k): Dihydroisoquinoline **27k** was prepared via Procedure X using amide **15i** (0.74 g, 2.0 mmol) and phosphorus trichloride (0.75 mL, 8.0 mmol) in dry toluene (11 mL). The crude solid was carried on without further purification. HRMS calcd. for $C_{22}H_{26}O_3N$, 352.19072 $[M + H]^+$; found 352.19037 $[M + H]^+$. Tetrahydroisoquinoline **28k** was prepared via Procedure XII using **27k** (0.44 g, 1.2 mmol) and sodium borohydride (0.14 g, 3.7 mmol) in dry MeOH (6.2 mL). The crude residue was subjected to flash column chromatography (ISCO, Redisep 24 g column, 0-10% MeOH/DCM gradient) to afford the title compound as a green foam (0.21 g, 48 %). ^{1}H NMR ($CDCl_3$, 400 MHz) δ: 7.03-6.96 (m, 3H), 6.79-6.71 (m, 3H), 6.62-6.61 (m, 1H), 4.72-4.69 (m, 1H), 4.63-4.60 (m, 1H), 4.43-4.40 (m, 1H), 4.36-4.31 (m, 1H), 3.73 (s, 3H), 3.54-3.48 (m, 1H), 3.26-3.10 (m, 2H), 3.01-2.94 (m, 1H), 1.92-1.72 (m,

6H), 1.66-1.57 (m, 2H); ^{13}C NMR ($CDCl_3$, 100 MHz) δ: 157.94, 154.65, 152.1, 134.3, 127.4, 120.3, 116.5, 115.7, 115.1, 114.7, 79.5, 69.3, 55.9, 54.3, 39.8, 30.0, 26.4, 24.2; HRMS calcd. for $C_{22}H_{28}NO_3$, 354.20367 $[M + H]^+$; found, 354.20649 $[M + H]^+$

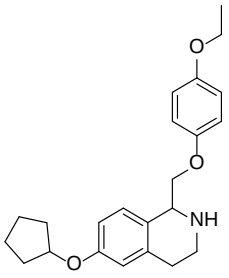

6-(cyclopentyloxy)-1-((4-ethoxyphenoxy)methyl)-1,2,3,4-tetrahydroisoquinoline (28l): Dihydroisoquinoline **27l** was prepared via procedure XI using amide **15j** (1.4 g, 3.8 mmol) and phosphorous trichloride (2.3 mL, 11 mmol) in dry toluene (21 mL). The crude residue (1.1 g) was carried on without further purification. HRMS calcd. for $C_{23}H_{30}O_3N_1$, 368.22202 $[M + H]^+$; found 368.22225 $[M + H]^+$. Tetrahydroisoquinoline **28l** was prepared via procedure XII using dihydroisoquinoline **27l** (1.1 g, 3.0 mmol) and sodium borohydride (0.34 g, 8.9 mmol) in dry MeOH (15 mL). The crude residue was purified by silica gel chromatography (ISCO, Redisep 20 g column, 0-20% MeOH/DCM gradient) to afford the title compound as an off-white solid (0.55 g, 51 %). TLC (MeOH/DCM, 1:10, v/v) Rf: 0.83; ^{1}H NMR ($CDCl_3$, 400 MHz) δ: 7.02-6.94 (m, 3H), 6.78-6.71 (m, 3H), 6.62-6.61 (m, 1H), 4.72-4.68 (m, 1H), 4.61-4.59 (m, 1H), 4.42-4.31 (m, 2H), 3.94 (q, J = 6.8 Hz, 2H), 3.53-3.43 (m, 1H), 3.26-3.11 (m, 2H), 3.01-2.97 (m, 1H), 1.92-1.72 (m, 6H), 1.65-1.56 (m, 2H), 1.37 (t, J = 7.2 Hz, 3H); ^{13}C NMR ($CDCl_3$, 100 MHz) δ: 157.9, 154.0, 152.0, 134.3, 127.3, 120.1, 116.4, 115.6, 115.4, 115.2, 79.5, 69.2, 64.1, 54.3, 39.8, 34.6, 33.0, 26.4, 24.2, 15.1; HRMS calcd. for $C_{23}H_{30}O_3N$, 368.22202 $[M + H]^+$; found 368.22227 $[M + H]^+$.

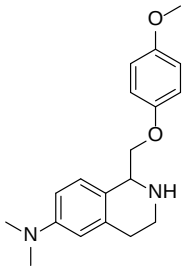

1-((4-methoxyphenoxy)methyl)-N,N-dimethyl-1,2,3,4-tetrahydroisoquinolin-6-amine (28p): Dihydroisoquinoline **27p** was prepared via procedure X using amide **25a** (0.78 g, 2.4 mmol) and phosphoris trichloride (0.67 mL, 7.2 mmol) in dry toluene (13 mL). The crude solid (1.4 g) was carried on without further purification. HRMS calcd. for $C_{19}H_{23}O_2N_2$, 311.17540 $[M + H]^+$; found 311.17594 $[M + H]^+$. Tetrahydroisoquinoline **28p** was prepared via procedure XII using dihydroisoquinoline **27p** (1.4 g, 4.4 mmol) in dry MeOH (22 mL). The crude residue was purified by silica gel chromatography (ISCO, Redisep 20 g column, 0-20% MeOH:DCM gradient) to afford the title compound as a yellow solid (0.53 g, 39 %) TLC (MeOH/DCM, 1:10, v/v) Rf: 0.44; ^{1}H NMR ($CDCl_3$, 400 MHz) δ: 7.05-7.03 (d, *J* = 8.4 Hz, 1H), 6.88-6.79 (m, 4H), 6.61-6.58 (dd, *J* = 2.8 Hz, *J* = 4.8 Hz, 1H), 6.48-6.47 (d, *J* = 2.4 Hz, 1H), 4.35-4.32 (dd, *J* = 2.8 Hz, *J* = 9.2 Hz, 1H), 4.13-4.10 (dd, *J* = 3.2 Hz, *J* = 9.2 Hz, 1H), 4.06-4.02 (m, 1H), 3.75 (s, 3H), 3.23-3.18 (m, 1H), 3.04-2.98 (m, 1H), 2.91 (s, 6H), 2.83-2.79 (m, 2H); ^{13}C NMR ($CDCl_3$, 100 MHz): δ 154.1, 153.2, 149.7, 136.6, 127.3, 115.7, 114.8, 113.1, 111.3, 71.4, 55.9, 54.7, 40.8, 40.0, 30.1; HRMS calcd. for $C_{19}H_{25}O_2N_2$, 313.19105 $[M + H]^+$; found 313.19164 $[M + H]^+$.

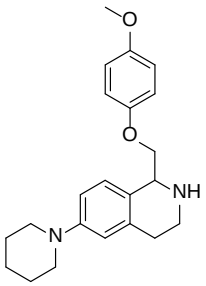

1-((4-methoxyphenoxy)methyl)-6-(piperidin-1-yl)-1,2,3,4-tetrahydroisoquinoline (28q): Dihydroisoquinoline **27q** was prepared via procedure X using amide **26a** (0.16 g, 0.45 mmol) and

phosphorous trichloride (0.28 mL, 1.4 mmol) in dry toluene (2.2 mL). The crude residue (0.23 g) was carried on without further purification. HRMS calcd. for $C_{22}H_{27}O_2N_2$, 351.20670 $[M + H]^+$; found 351.20660 $[M + H]^+$. Tetrahydroisoquinoline **28q** was prepared via procedure XII using dihydroisoquinoline **27q** (0.23 g, 1.9 mmol) and sodium borohydride (0.073 g, 1.9 mmol) in dry MeOH (3.3 mL). The crude residue was purified by silica gel chromatography (ISCO, Redisep 20 g column, 0-20% MeOH/DCM gradient) to afford the title compound as a green foam (0.097 g, 43 % over 2 steps). TLC (MeOH/DCM, 1:10, v/v) Rf: 0.43 ^{1}H NMR ($CDCl_3$, 400 MHz) δ: 7.04 (d, J = 8.4 Hz, 1H), 6.89-6.75 (m, 5H), 6.68-6.67 (m, 1H), 4.35-4.32 (dd, J = 2.8 Hz, J = 9.2 Hz, 1H), 4.14-4.11 (m, 1H), 4.07-4.02 (m, 1H), 3.72 (s, 3H), 3.23-3.18 (m, 1H), 3.10 (t, J = 5.6 Hz, 4H), 3.06-2.99 (m, 1H), 2.81-2.79 (m, 2H), 1.71-1.65 (m, 4H), 1.58-1.53 (m, 2H); ^{13}C NMR ($CDCl_3$, 100 MHz) δ: 154.2, 152.9, 151.2, 136.0, 127.2, 123.9, 116.8, 115.9, 115.0, 114.8, 71.0, 55.92, 54.6, 50.7, 40.1, 29.5, 26.0, 24.5; HRMS calcd. for $C_{22}H_{29}O_2N_2$, 353.22235 $[M + H]^+$; found 353.22243 $[M + H]^+$.

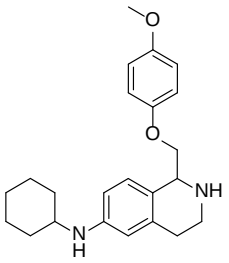

N-cyclohexyl-1-((4-methoxyphenoxy)methyl)-1,2,3,4-tetrahydroisoquinolin-6-amine (28r): Dihydroisoquinoline **27r** was prepared via Procedure XI using amide **27a** (1.6 g, 4.1 mmol) and phosphorus trichloride (2.5 mL, 12 mmol) in dry toluene (23 mL). The crude solid (2.1 g) was carried on without further purification. HRMS calcd. for $C_{23}H_{29}O_3N_2$, 365.22235 $[M + H]^+$; found 365.22244 $[M + H]^+$. Tetrahydroisoquinoline **28r** was prepared via Procedure XII using dihydroisoquinoline **27r** (2.1 g, 5.6 mmol) and sodium borohydride (0.64 g, 17 mmol) in dry MeOH (31 mL). The crude residue was purified by silica gel chromatography (ISCO, Redisep 20 g column, 0-20% MeOH/DCM gradient) to afford the title compound as a green foam (0.17 g, 8.0 %). TLC (MeOH/DCM, 1:10, v/v) Rf: 0.78; ^{1}H NMR ($CDCl_3$, 400 MHz) δ: 6.93 (d, J = 8.4 Hz, 1H), 6.88-

6.84 (m, 2H), 6.82-6.78 (m, 2H), 6.42-6.39 (dd, J = 2.4 Hz, J = 8.4 Hz, 1H), 6.32-6.31 (m, 1H), 4.34-4.31 (m, 1H), 4.13-4.03 (m, 2H), 3.74 (s, 3H), 3.24-3.18 (m, 2H), 3.04-2.97 (m, 1H), 2.76 (t, J = 6.0 Hz, 2H), 2.04-2.00 (m, 2H), 1.77-1.72 (m, 2H), 1.65-1.61 (m, 1H), 1.41-1.30 (m, 2H), 1.26-1.07 (m, 4H); ^{13}C NMR ($CDCl_3$, 100 MHz) δ: 154.1, 153.1, 136.7, 127.5, 122.2, 115.8, 114.8, 113.2, 111.8, 71.3, 55.9, 54.5, 52.4, 51.8, 39.9, 33.7, 29.6, 26.1, 25.2; HRMS calcd. for $C_{23}H_{31}O_2N_2$, 367.23801 [M + H]$^+$; found 367.23808 [M + H]$^+$.

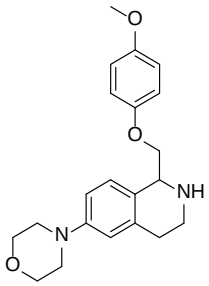

4-(1-((4-methoxyphenoxy)methyl)-1,2,3,4-tetrahydroisoquinolin-6-yl)morpholine (28s): Dihydroisoquinoline **27s** was prepared via procedure X using amide **26c** (1.5 g, 3.9 mmol) and phosphorous trichloride (2.4 mL, 12 mmol) in dry toluene (19 mL). The crude residue (1.6 g) was carried on without further purification. HRMS calcd. for $C_{21}H_{25}O_3N_2$, 353.18597 [M + H]$^+$; found 353.18608 [M + H]$^+$. Tetrahydroisoquinoline **28s** was prepared via procedure XII using dihydroisoquinoline **27s** (1.6 g, 4.6 mmol) and sodium borohydride (0.52 g, 14 mmol) in dry MeOH (23 mL). The crude residue was purified by silica gel chromatography (ISCO, Redisep 40 g column, 0-20% MeOH/DCM gradient) to afford the title compound as a brown foam (0.47 g, 29 % over 2 steps). TLC (MeOH/DCM, 1:10, v/v) Rf: 0.64; ^{1}H NMR ($CDCl_3$, 400 MHz) δ: 7.07 (d, J = 8.4 Hz, 1H), 6.87-6.79 (m, 4H), 6.76-6.74 (m, 1H), 6.71-6.65 (m, 1H), 4.36-4.33 (m, 1H), 4.14-4.03 (m, 2H), 3.85-3.83 (m, 4H), 3.76 (m, 3H), 3.25-3.19 (m, 1H), 3.13-3.11 (m, 4H), 3.05-2.99 (m, 1H), 2.83-2.80 (m, 2H); ^{13}C NMR ($CDCl_3$, 100 MHz) δ: 154.2, 154.1, 150.1, 136.9, 127.4, 126.2, 116.2, 115.7, 114.8, 114.1, 71.4, 67.2, 55.9, 54.7, 49.5, 40.0, 30.3; HRMS calcd. for $C_{21}H_{30}O_2N_3$, 355.20162 [M + H]$^+$; found 355.20169 [M + H]$^+$.

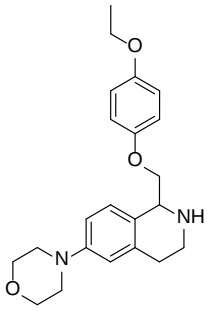

4-(1-((4-ethoxyphenoxy)methyl)-1,2,3,4-tetrahydroisoquinolin-6-yl)morpholine (28t): Dihydroisoquinoline **27t** was prepared via procedure X using amide **26d** (0.77 g, 2.0 mmol) and phosphorous trichloride (1.2 mL, 6.0 mmol) in dry toluene (10. mL). The crude residue (0.78 g) was carried on without further purification. HRMS calcd. for $C_{22}H_{27}O_2N_2$, 367.20162 $[M + H]^+$; found 367.20183 $[M + H]^+$. Tetrahydroisoquinoline **28t** was prepared via procedure XII using dihydroisoquinoline **27t** (0.78 g, 2.1 mmol) and sodium borohydride (0.24 g, 6.4 mmol) in dry MeOH (11 mL). The crude residue was purified by silica gel chromatography (ISCO, Redisep 40 g column, 0-20% MeOH/DCM gradient) to afford the title compound as a brown foam (0.41 g, 52 % over 2 steps). TLC (MeOH/DCM, 1:10, v/v) Rf: 0.47; ^{1}H NMR ($CDCl_3$, 400 MHz) δ: 7.10 (d, J = 8.4 Hz, 1 H), 6.88-6.82 (m, 4H), 6.79-6.76 (dd, J = 2.4 Hz, J = 8.8 Hz, 1H), 6.69-6.68 (m, 1H), 4.37-4.34 (dd, J = 3.2 Hz, J = 8.8 Hz, 1H), 4.15-4.12 (m, 1H), 4.08-4.04 (m, 1H), 4.98 (q, J = 7.2 Hz, 2H), 3.87 (t, J = 4.4 Hz, 4H), 3.26-3.19 (m, 1H), 3.15 (t, J = 5.2 Hz, 4H), 3.06-3.00 (m, 1H), 2.84-2.82 (m, 2H), 1.39 (t, J = 7.2 Hz, 3H); ^{13}C NMR ($CDCl_3$, 100 MHz) δ: 153.5, 153.1, 137.1, 127.4, 126.5, 116.2, 115.7, 115.6, 114.0, 71.5, 67.2, 64.2, 54.8, 49.5, 40.0, 30.4, 15.2; HRMS calcd. for $C_{22}H_{29}O_2N_3$, 369.21727 $[M + H]^+$; found 369.21725 $[M + H]^+$.

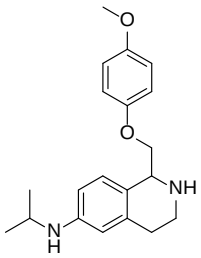

N-isopropyl-1-((4-methoxyphenoxy)methyl)-1,2,3,4-tetrahydroisoquinolin-6-amine (28u): Dihydroisoquinoline **27u** was prepared via procedure X using amide **25b** (0.60 g, 1.8 mmol) and phosphorous trichloride (0.72 mL, 3.5 mmol) in dry toluene (8.7 mL). The crude residue (1.0 g) was carried on without further purification. HRMS calcd. for $C_{20}H_{25}O_2N_2$, 325.19105 $[M + H]^+$; found 325.19081 $[M + H]^+$. Tetrahydroisoquinoline **28u** was prepared via procedure XII using dihydroisoquinoline **27u** (1.0 g, 3.1 mmol) and sodium borohydride (0.23 g, 6.3 mmol) in dry MeOH (16 mL). The crude residue was purified by silica gel chromatography (ISCO, Redisep 20 g column, 0-20% MeOH/DCM gradient) to afford the title compound as a yellow solid (0.039 g, 3.8 % over 2 steps). TLC (MeOH/DCM, 1:10, v/v) Rf: 0.64; ^{1}H NMR ($CDCl_3$, 400 MHz) δ: 6.98-6.96 (d, J = 8.4 Hz, 1H), 6.91-6.79 (m, 4H), 6.46-6.43 (dd, J = 2.4 Hz, J = 8.8 Hz, 1H), 6.36-6.36 (m, 1H), 4.38-4.35 (m, 1H), 4.17-4.13 (m, 1H), 4.10-4.06 (m, 1H), 3.77 (s, 3H), 3.66-3.58 (m, 1H), 3.28-3.21 (m, 1H), 3.07-3.02 (m, 1H), 2.83-2.80 (m, 2H), 1.20 (d, J = 6.4 Hz, 6H); ^{13}C NMR ($CDCl_3$, 100 MHz) δ: 154.2, 153.1, 146.5, 136.7, 127.5, 122.2, 115.8, 114.8, 113.3, 111.9, 71.3, 55.9, 54.6, 44.4, 39.9, 29.7, 23.3; HRMS calcd. for $C_{20}H_{27}O_2N_2$, 327.20670 $[M + H]^+$; found 327.20623 $[M + H]^+$.

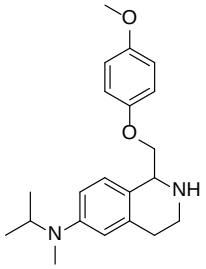

N-isopropyl-1-((4-methoxyphenoxy)methyl)-N-methyl-1,2,3,4-tetrahydroisoquinolin-6-amine (28v): Dihydroisoquinoline **27v** was prepared via procedure X using amide **25c** (0.58 g, 1.6 mmol) and phosphorous trichloride (0.75 mL, 4.9 mmol) in dry toluene (8.2 mL). The crude residue (0.92 g) was carried on without further purification. HRMS calcd. for $C_{21}H_{26}O_2N_2$, 339.20670 $[M + H]^+$; found 339.20656 $[M + H]^+$. Tetrahydroisoquinoline **28v** was prepared via procedure XII using dihydroisoquinoline **27v** (0.53 g, 1.6 mmol) and sodium borohydride (0.19 g, 4.9 mmol) in dry MeOH (8.2 mL). The crude residue was purified by silica gel chromatography (ISCO, Redisep 20 g

column, 0-20% MeOH/DCM gradient) to afford the title compound as a yellow solid (0.27 g, 48 % over 2 steps). TLC (MeOH/DCM, 1:10, v/v) Rf: 0.49; ^{1}H NMR ($CDCl_3$, 400 MHz) δ: 7.06 (d, *J* = 8.4 Hz, 1H), 6.92-6.83 (m, 4H), 6.68-6.66 (m, 1H), 6.60-6.55 (m, 1H), 4.38-4.35 (m, 1H), 4.17-4.04 (m, 3H), 3.78 (s, 3H), 3.27-3.21 (m, 1H), 3.07-3.21 (m, 1H), 2.85-2.78 (m, 2H), 2.73 (s, 3H), 1.23-1.17 (m, 6H); ^{13}C NMR ($CDCl_3$, 100 MHz) δ: 154.1, 153.3, 149.1, 136.8, 127.3, 122.5, 115.7, 114.8, 113.6, 111.6, 71.7, 55.9, 54.7, 49.0, 40.2, 30.6, 30.0, 19.6; HRMS calcd. for $C_{21}H_{28}O_2N_2$, 341.22235 [M + H]$^+$; found 341.22213 [M + H]$^+$.

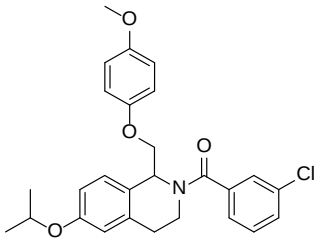

(3-chlorophenyl)(6-isopropoxy-1-((4-methoxyphenoxy)methyl)-3,4-dihydroisoquinolin-2(1H)-yl)methanone (1180-55): Tetrahydroisoquinoline **1180-55** was prepared via Procedure XIII using tetrahydroisoquinoline **28a** (0.15 g, 0.48 mmol) and 3-chlorobenzoyl chloride (0.061 mL, 0.45 mmol) in DCM (7.0 mL). The crude residue was purified by silica gel chromatography (ISCO, Redisep 12 g column, 10 – 80% EtOAc/hexanes gradient) to afford the title compound as an off-white foam (0.15 g, 70% mixture of two amide rotamers). ^{1}HNMR ($CDCl_3$, 400 MHz) δ: 8.04-7.93 (m, 0.5H), 7.56-7.52 (m, 0.5H),7.39-7.19 (m, 4H), 6.91-6.66 (m, 6H), 5.98 (t, *J* = 4.8 Hz, 0.5H), 5.14-5.10 (m, *J* = 3.6 Hz, *J* = 6.0 Hz, 0.5H), 4.87-4.82 (m, *J* = 4.8 Hz, *J* = 5.2 Hz, 0.5H), 4.55-4.49 (m, 1H), 4.37-4.29 (m, 1H), 4.12 (t, *J* = 10 Hz, 0.5H), 3.93-3.90 (m, 0.5H), 3.74 (s, 3H), 3.72-3.64 (m, 1H), 3.29-3.01 (m, 1H), 2.92-2.71 (m, 1.5H), 1.32 (d, *J* = 6.0 Hz, 6H); ^{13}CNMR ($CDCl_3$, 100 MHz) δ: 170.6, 169.8, 157.6, 157.0, 154.4, 154.3, 153.1, 152.6, 138.3, 138.1, 136.6, 135.5, 134.9, 134.8, 134.6, 133.6, 130.4, 130.2, 129.9, 129.8, 128.7, 128.4, 128.3, 127.0, 125.9, 125.1, 124.9, 124.0, 116.2, 115.9, 115.5, 114.9, 114.8, 114.7, 114.5, 76.9, 71.2, 70.1, 57.3, 55.9, 52.0, 42.8, 35.5, 29.9, 28.5, 22.3, 22.2; HRMS calcd. for $C_{27}H_{29}ClN_1O_4$, 466.17784 [M + H]$^+$; found 466.17796 [M + H]$^+$, mp: 72°C.

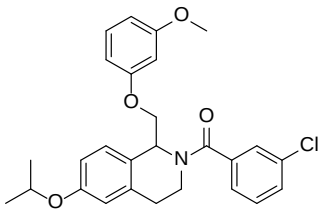

(3-chlorophenyl)(6-isopropoxy-1-((3-methoxyphenoxy)methyl)-3,4-dihydroisoquinolin-2(1H)-yl)methanone) (1180-82): Dihydroisoquinoline **27b** was prepared via Procedure X using amide **15b** (1.4 g, 4.3 mmol) and phosphorus trichloride (1.2 mL, 13 mmol) in dry toluene (24 mL). The crude solid was carried on without further purification. HRMS calcd. for $C_{20}H_{23}O_3N_1$, 326.17507 $[M + H]^+$; found 326.17588 $[M + H]^+$. Tetrahydroisoquinoline **28b** was prepared via Procedure XII using **27b** (4.9 g, 15 mmol) and sodium borohydride (1.7 g, 45 mmol) in dry MeOH (75 mL). The crude residue was subjected to flash column chromatography (ISCO, Redisep 24 g column, 0-10% MeOH/DCM gradient) to afford tetrahydroisoquinoline 38b (0.26 g, 5.0 %) in an impure form. The impurities were inseparable by chromatography. The product was visible by LCMS and was carried on without further purification. HRMS calcd. for $C_{19}H_{23}NO_3$, 314.17507 $[M + H]^+$; found, 314.17484 $[M + H]^+$. Tetrahydroisoquinoline **1180-82** was prepared via Procedure XIII using tetrahydroisoquinoline **28b** (0.26 g, 0.81 mmol) and 3-chlorobenzoyl chloride (0.12 mL, 0.89 mmol) in DCM (13 mL). The crude residue was purified by silica gel chromatography (ISCO, Redisep12 g column, 10-80% EtOAc/hexanes gradient) to afford the title compound as a white foam (0.094 g, 31%, mixture of two amide rotamers) TLC (EtOAc: hexanes, 1:1, v/v) Rf = 0.88 ; ^{1}HNMR ($CDCl_3$, 400 MHz) δ: 7.60-7.13 (m, 5H), 6.92-6.75 (m, 1H), 6.71-6.66 (m, 2H), 6.52-6.42 (m, 3H), 6.00-5.98 (t, *J* = 5.2 Hz, 0.5H), 5.15-5.12 (dd, *J* = 2.8 Hz, *J* = 9.2 Hz, 0.5H), 4.87-4.82 (dd, *J* = 5.2 Hz, *J* = 12.8 Hz, 0.5H), 4.55-4.49 (m, 1H), 4.40-4.33 (m, 1H), 4.19-4.09 (m, 0.5 H), 3.95-3.91 (dd, *J* = 3.6 Hz, *J* = 10.4 Hz, 0.5H), 3.78-3.62 (m, 4H), 3.28-3.09 (m, 1H), 2.92-2.71 (m, 1.5 H), 1.33-1.32 (d, 6H); ^{13}CNMR ($CDCl_3$, 100 MHz) δ: 170.4, 169.6, 168.6, 161.1, 160.9, 160.1, 159.6, 157.9, 157.6, 157.1, 138.4, 138.2, 136.6, 135.6, 134.9, 134.6, 131.9, 130.2, 130.1, 129.9, 129.4, 128.8, 128.4, 127.1, 125.7, 125.1, 124.9, 123.9, 123.5, 122.7, 116.2, 115.9, 115.1, 114.5, 109.3, 108.2, 107.3, 107.1, 106.4, 102.3,

101.3, 100.9, 70.5, 70.1, 69.5, 57.2, 55.6, 51.8, 42.8, 42.3, 35.4, 29.9, 29.6, 28.5, 22.3; HRMS calcd. for $C_{27}H_{29}ClN_1O_4$, 466.17796 $[M + H]^+$; found 466.17733 $[M + H]^+$. Anal. ($C_{27}H_{28}ClN_1O_4$): C, H, N.

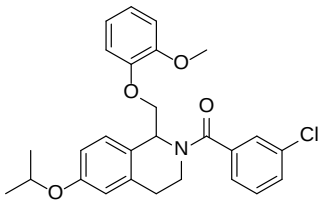

(3-chlorophenyl)(6-isopropoxy-1-((2-methoxyphenoxy)methyl)-3,4-dihydroisoquinolin-2(1H)-yl)methanone (1180-84): Tetrahydroisoquinoline **1180-84** was prepared via Procedure XIII using tetrahydroisoquinoline **28c** (0.20 g, 0.61 mmol) and 3-chlorobenzoyl chloride (0.090 mL, 0.67 mmol) in DCM (9.0 mL). The crude residue was purified by silica gel chromatography (ISCO, Redisep 12 g column, 10 – 80% EtOAc/hexanes gradient) to afford the title compound as an off-white foam (0.15 g, 53 % mixture of two amide rotamers) TLC (EtOAc: hexanes, 1:1, v/v) Rf = 0.72 ^{1}HNMR ($CDCl_3$, 400 MHz) δ: 7.75-7.52 (m, 1H), 7.42-7.19 (m, 3.5 H), 6.96-6.66 (m, 6.5 H), 6.05-6.02 (t, J = 5.6 Hz, 0.5H), 5.19-5.15 (dd, J = 4.0 Hz, J = 10.4 Hz, 0.5H), 4.87-4.83 (dd, J = 5.6 Hz, J = 12.8 Hz, 0.5H), 4.54-4.48 (m, 1H), 4.45-4.35 (m, 1H), 4.24-4.19 (m, 0.5 H), 4.02-3.98 (dd, J = 4.0 Hz, J = 10.4 Hz, 0.5H), 3.90-3.74 (m, 4H), 3.29-3.09 (m, 1H), 2.88-2.73 (m, 1.5 H), 1.34-1.31 (d, 6H); ^{13}CNMR ($CDCl_3$, 100 MHz) δ: 170.6, 169.9, 157.6, 157.1, 149.8, 148.1, 138.2, 136.6, 135.7, 134.5, 130.2, 129.8, 129.7, 128.7, 128.4, 128.3, 127.2, 126.2, 125.3, 124.9, 124.2, 122.1, 122.0, 121.2, 120.8, 116.3, 115.9, 114.7, 114.4, 113.4, 112.7, 111.9, 71.6, 70.2, 70.1, 57.3, 56.2, 55.8, 51.8, 42.7, 35.3, 29.9, 28.4, 22.3, 22.2; HRMS calcd. for $C_{27}H_{29}ClN_1O_4$, 466.17796 $[M + H]^+$; found 466.17790 $[M + H]^+$. Anal. ($C_{27}H_{28}ClN_1O_4$): C, H, N.

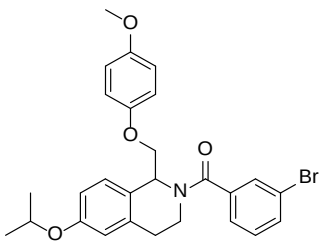

(3-bromophenyl)(6-isopropoxy-1-((4-methoxyphenoxy)methyl)-3,4-dihydroisoquinolin-2(1H)-yl)methanone (1180-88): Tetrahydroisoquinoline **1180-88** was prepared via procedure XIII using tetrahydroisoquinoline **28a** (0.15 g, 0.46 mmol) and 3-bromobenzoyl chloride (0.070 mL, 0.51 mmol) in DCM (8.0 mL). The crude residue was purified by silica gel chromatography (ISCO, Redisep 12 g column, 10 – 80% EtOAc/hexanes gradient) to afford the title compound as a white foam (0.13 g, 56 % mixture of two amide rotamers) TLC (EtOAc: hexanes, 1:1, v/v) Rf = 0.73; ^{1}HNMR ($CDCl_3$, 400 MHz) δ: 7.74-7.50 (m, 2H), 7.42-7.18 (m, 2H), 6.91-6.66 (m, 6H), 5.97-5.95 (t, *J* = 5.2 Hz, 0.5H), 5.13-5.10 (dd, *J* = 3.2 Hz, *J* = 9.6 Hz, 0.5H), 4.86-4.81 (dd, 5.2 Hz, *J* = 12.4 Hz, 0.5H), 4.55-4.49 (m, 1H), 4.37-4.29 (m, 1H), 4.15-4.08 (m, 0.5 H), 3.92-3.89 (dd, *J* = 3.6 Hz, *J* = 9.6, 0.5H), 3.75 (s, 3H), 3.73-3.62 (m, 1H), 3.27-3.08 (m, 1H), 2.29-2.70 (m, 1.5 H), 1.33-1.31 (d, 6H); ^{13}CNMR ($CDCl_3$, 100 MHz) δ: 170.3, 169.6, 157.7, 157.1, 154.4, 154.3, 153.1, 152.8, 138.6, 138.4, 136.6, 135.6, 133.2, 132.8, 131.1, 130.4, 130.1, 129.9, 128.8, 128.3, 126.3, 125.3, 124.1, 122.9, 122.6, 116.2, 115.9, 115.5, 114.9, 114.8, 114.7, 114.5, 71.3, 70.1, 57.3, 55.9, 51.9, 42.8, 35.5, 29.9, 28.5, 22.3, 22.2; HRMS calcd. for $C_{21}H_{27}BrO_3N_1$, 510.12745 $[M + H]^+$; found 510.12750 $[M + H]^+$.

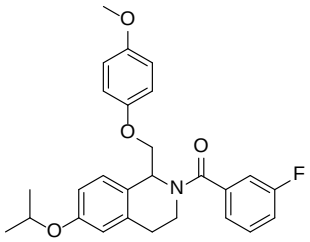

(3-fluorophenyl)(6-isopropoxy-1-((4-methoxyphenoxy)methyl)-3,4-dihydroisoquinolin-2(1H)-yl)methanone (1180-87): Tetrahydroisoquinoline **1180-87** was prepared via procedure XIII using tetrahydroisoquinoline **28a** (0.10 g, 0.32 mmol) and 3-fluorobenzoyl chloride (0.044 mL, 0.38 mmol) in DCM (5.0 mL). The crude residue was purified by silica gel chromatography (ISCO, Redisep 12 g column, 10 – 80% EtOAc/hexanes gradient) to afford the title compound as an off-white foam (0.17 g, 53 % yield, mixture of two amide rotamers). TLC (EtOAc: hexanes, 1:1, v/v) Rf = 0.53; ^{1}HNMR ($CDCl_3$, 400 MHz) δ: 7.41-7.08 (m, 5H), 6.91-6.66 (m, 6H), 5.98-5.96 (m, 0.5H), 5.14-5.13 (m, 0.5H),

4.86-4.82 (m, *J* = 5.2 Hz, *J* = 12.8 Hz, 0.5H), 4.56-4.49 (m, 1H), 4.34-4.30 (m, 1H), 4.12 (t, *J* = 9.6 Hz, 0.5H), 3.94-3.91 (m, 0.5H), 3.74 (s, 3H), 3.69-3.63 (m, 1H), 3.27-3.08 (m, 1H), 2.91-2.70 (m, 1.5H), 1.32 (d, *J* = 6.0 Hz, 6H); ^{13}C NMR ($CDCl_3$, 100 MHz) δ: 170.6, 169.7, 164.0, 161.4, 157.6, 157.5, 154.4, 154.3, 153.1, 152.6, 138.5, 136.6, 135.6, 130.7, 130.6, 130.3, 130.2, 128.7, 128.3, 125.2, 124.1, 123.4, 122.5, 116.9, 116.8, 116.7, 116.6, 116.1, 115.9, 115.5, 115.2, 114.9, 114.8, 114.7, 114.4, 114.2, 114.0, 71.3, 70.2, 70.1, 57.3, 55.9, 51.9, 42.7, 35.5, 29.9, 28.6, 22.3, 22.2; HRMS calcd. for $C_{28}H_{29}NO_4F$, 450.20751 $[M + H]^+$; found, 450.20722 $[M + H]^+$.

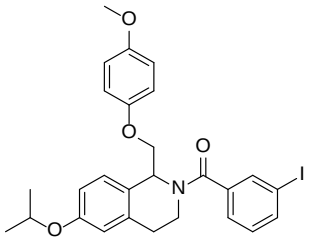

(3-iodophenyl)(6-isopropoxy-1-((4-methoxyphenoxy)methyl)-3,4-dihydroisoquinolin-2(1H)-yl)methanone (1180-153): Tetrahydroisoquinoline **1180-153** was prepared via procedure XIV using 3-iodobenzoic acid (0.18 g, 0.71 mmol) dissolved in dry DCM (2.3 ml) and THF (1.7 ml), N1-((ethylimino)methylene)-N3,N3-dimethylpropane-1,3-diamine hydrochloride (0.16 g, 0.85 mmol), N,N-dimethylpyridin-4-amine (0.096 g, 0.78 mmol), and tetrahydroisoquinoline **28a** (0.23 g, 0.71 mmol). The crude residue was purified by silica gel chromatography (ISCO, Redisep 12 g column, 10 – 80% EtOAc/hexanes gradient) to afford the title compound as an off-white foam (0.15 g, 38 % yield, mixture of two amide rotamers). TLC (EtOAc: hexanes, 1:1, v/v) Rf = 0.64; ^{1}HNMR ($CDCl_3$, 400 MHz) δ: 7.96-7.73 (m, 1.5H), 7.48 (d, *J* = 7.2 Hz, 0.5H), 7.36 (d, *J* = 7.6 Hz, 0.5H), 7.23-7.12 (m, 1.5H), 6.94-6.69 (m, 7H), 5.98 (t, *J* = 5.2 Hz, 0.5H), 5.16-5.13 (m, *J* = 3.6 Hz, *J* = 9.2 Hz, 0.5H), 4.88-4.84 (m, *J* = 5.6 Hz, *J* = 12.8 Hz, 0.5H), 4.59-4.52 (m, 1H), 4.39-4.32 (m, 1H), 4.17-4.12 (m, 0.5H), 3.95-3.92 (dd, *J* = 3.2 Hz, *J* = 9.6Hz, 0.5H), 3.77 (s, 3H), 3.75-3.64 (m, 1H), 3.30-3.11 (m, 1H), 2.94-2.73 (m, 1.5H), 1.35 (d, J = 6.0 Hz, 6H); ^{13}C NMR ($CDCl_3$, 100 MHz) δ: 170.2, 169.4, 157.6, 157.0, 154.4, 154.3, 153.1, 152.6, 142.2, 139.1, 138.8, 138.6, 138.5, 136.7, 136.6, 135.6, 130.5, 130.2, 129.4,

128.7, 128.4, 126.8, 125.8, 125.2, 124.1, 116.2, 115.9, 115.5, 114.9, 114.8, 114.7, 115.5, 71.2, 70.1, 57.3, 55.9, 51.9, 42.8, 35.4, 29.9, 28.5, 22.3, 22.2; HRMS calcd. for $C_{27}H_{28}N_1O_4I$, 558.11358 $[M + H]^+$; found, 558.11362 $[M + H]^+$.

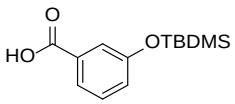

3-(tert-butyldimethylsilyloxy)benzoic acid (29): 3-hydroxybenzoic acid (1.0 g, 7.2 mmol), tert-butylchlorodimethylsilane (4.4 g, 29 mmol), and 1H-imidazole (2.9 g, 43 mmol) were dissolved in dry DMF (36 ml). The reaction was allowed to stir at room temperature overnight. The reaction was quenched with DI water and extracted into hexane, washed with water (3x) and brine (3x), dried with $MgSO_4$, filtered, and concentrated *in vacuo*. THF (3.9 ml), AcOH (12 ml), and aater (3.9 ml) were added sequentially to the resulting white solid (2.0 g) and the reaction was stirred at room temperature for 2 hours. The reaction was quenched with water and concentrated *in vacuo*. The crude residue was purified by silica gel chromatography (ISCO, Redisep 12 g column, 10 – 80% EtOAc/hexanes gradient) to afford the title compound as a white solid (0.65 g, 95%). TLC (EtOAc: hexanes, 1:1, v/v) Rf = 0.83; ^{1}HNMR ($CDCl_3$, 400 MHz) δ: 7.71-7.69 (m, 1H), 7.53-7.54 (m, 1H), 7.34-7.30 (t, J = 8.4 Hz, 1H), 7.09-7.06 (m, 1H), 0.98 (s, 9H), 0.21 (s, 6H); ^{13}CNMR ($CDCl_3$, 100 MHz) δ: 172.2, 156.0, 130.8, 129.8, 126.0, 123.4, 121.7, 25.9, 18.4, -4.2; HRMS calcd. for $C_{13}H_{21}O_3Si$, 353.12545 $[M + H]^+$; found 353.12532 $[M + H]^+$.

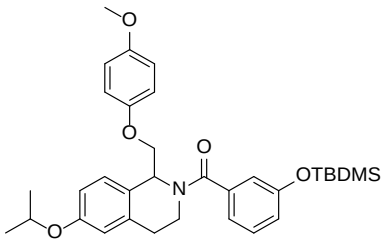

(3-(tert-butyldimethylsilyloxy)phenyl)(6-isopropoxy-1-((4-methoxyphenoxy)methyl)-3,4-dihydroisoquinolin-2(1H)-yl)methanone (30): Tetrahydroisoquinoline **30** was prepared via procedure XIV using benzoic acid 130 (0.21 g, 0.84 mmol), N1-((ethylimino)methylene)-N3,N3-

dimethylpropane-1,3-diamine (0.14 g, 0.92 mmol), N,N-dimethylpyridin-4-amine (0.11 g, 0.92 mmol), and tetrahydroisoquinoline **28a** (.25 g, 0.76 mmol). The crude residue was purified by silica gel chromatography (ISCO, Redisep 12 g column, 10 – 80% EtOAc/hexanes gradient) to afford the title compound as a white foam (0.43 g, 59 % mixture of two amide rotamers) TLC (EtOAc: hexanes, 1:1, v/v) Rf = 0.74; ^{1}HNMR ($CDCl_3$, 400 MHz) δ: 7.29-7.19 (m, 2H), 7.07-6.94 (m, 1H), 6.88-6.66 (m, 8H), 5.97-5.94 (t, *J* = 4.8 Hz, 0.5H), 5.18-5.15 (dd, *J* = 4.0 Hz, *J* = 9.2 Hz, 0.5H), 4.86-4.81 (dd, *J* = 5.2 Hz, *J* = 12.8 Hz, 0.5H), 5.54-4.48 (m, 1H), 4.36-4.29 (m, 1H), 4.11-4.06 (m, 0.5 H), 3.93-3.89 (t, *J* = 4.8 Hz, 0.5H), 3.80-3.56 (m, 1H), 3.74 (s, 3H), 3.26-3.09 (m, 1H), 2.91-2.67 (m, 1.5H), 1.33-1.31 (d, 6H), 0.97-0.92 (m, 9H), 0.18 (s, 6H); ^{13}CNMR ($CDCl_3$, 100 MHz) δ: 171.6, 170.9, 157.4, 156.9, 155.9, 155.7, 154.3, 154.2, 153.2, 152.8, 138.1, 137.9, 136.6, 135.7, 130.0, 129.7, 128.8, 25.5, 124.6, 121.5, 121.3, 120.6, 119.7, 119.6, 118.4, 116.2, 115.9, 115.8, 115.7, 114.8, 114.6, 114.3, 71.4, 70.1, 57.1, 55.9, 51.7, 42.8, 35.5, 30.0, 28.6, 25.9, 22.3, 18.3, -4.2; HRMS calcd. for $C_{33}H_{44}O_5N_1Si$, 562.29833[M + H]$^+$; found 562.29760 [M + H]$^+$.

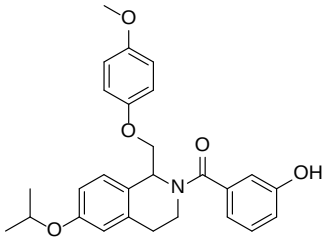

(3-hydroxyphenyl)(6-isopropoxy-1-((4-methoxyphenoxy)methyl)-3,4-dihydroisoquinolin-2(1H)-yl)methanone (89): Tetrahydroisoquinoline **30** (.15 g, 0.27 mmol) was dissolved in THF (1.59 ml) and brought to 0 °C using an ice bath. Tetrabutylammonium fluoride (0.14 g, 0.53 mmol) was added and the reaction was allowed to stir for 5 minutes before the reaction was warmed to room temperature. The reaction stirred for 1 hour, at which point it was complete by TLC. The reaction was quenched with 1M HCl, extracted into EtOAc, washed with water and brine, dried with $MgSO_4$, filtered, and concentrated *in vacuo*. The crude residue was purified by silica gel chromatography (ISCO, Redisep 12 g column, 10 – 80% EtOAc/hexanes gradient) to afford the title

compound as a white foam (0.11 g, 66 % mixture of two amide rotamers) TLC (EtOAc: hexanes, 1:1, v/v) Rf = 0.42; ^{1}HNMR ($CDCl_3$, 400 MHz) δ: 7.19-7.03 (m, 2H), 6.93-6.64 (m, 9H), 5.97-5.94 (t, *J* = 5.2 Hz, *0.5H*), 5.23-5.19 (dd, *J* = 4.4 Hz, *J* = 9.2 Hz, 0.5H), 4.83-4.78 (dd, *J* = 5.6 Hz, *J* = 13.2 Hz, 0.5H), 4.54-4.48 (m, 1H), 4.33-4.26 (m, 1H), 4.14-4.04 (m, 0.5 H), 3.92-3.88 (dd, *J* = 4.0 Hz, *J* = 10.0 Hz, 0.5H), 3.83-3.79 (m, 0.5 H), 3.71 (s, 3H), 3.63-3.55 (m, 0.5 H), 3.51-3.05 (m, 1H), 2.89-2.64 (m, 1.5 H), 1.32-1.30 (d, 3H, *J* = 2.4 Hz), 1.31-1.30 (d, 3H, *J* = 2.4 Hz); ^{13}CNMR ($CDCl_3$, 100 MHz) δ: 172.7, 171.9, 157.5, 157.2, 157.0, 154.3, 154.2, 153.1, 152.6, 136.8, 136.7, 136.4, 135.7, 129.9, 129.6, 128.8, 128.4, 125.2, 124.4, 118.6, 117.6, 116.2, 116.1, 115.9, 115.8, 115.6, 115.5, 114.9, 114.7, 114.4, 114.3, 71.3, 70.3, 70.1, 60.7, 57.2, 55.9, 52.0, 42.9, 35.9, 29.9, 28.6, 22.3, 22.3; HRMS calcd. for $C_{27}H_{30}N_1O_5$, 448.21185[M + H]$^+$; found 448.21131 [M + H]$^+$.

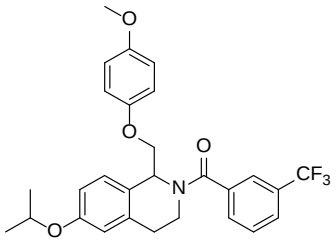

(1-((4-ethoxyphenoxy)methyl)-6-isopropoxy-3,4-dihydroisoquinolin-2(1H)-yl)(3-(trifluoromethyl)phenyl)methanone (91): Tetrahydroisoquinoline **91** was prepared via procedure XIII using tetrahydroisoquinoline **28a** (0.17 g, 0.49 mmol) and 3-(trifluoromethyl)benzoyl chloride (0.080 mL, 0.54 mmol) in DCM (8.0 mL). The crude residue was purified by silica gel chromatography (ISCO, Redisep 12 g column, 10 – 80% EtOAc/hexanes gradient) to afford the title compound as an off-white foam (0.13 g, 54 % mixture of two amide rotamers) TLC (EtOAc: hexanes, 1:1, v/v) Rf = 0.66 ^{1}HNMR ($CDCl_3$, 400 MHz) δ: 7.88-7.48 (m, 4H), 7.22-7.20 (m, 0.5 H), 6.89-6.66 (m, 6.5 H), 5.99-5.96 (m, 0.5 H), 5.09-5.06 (dd, *J* = 3.2 Hz, *J* = 6.4 Hz, 0.5H), 4.89-4.84 (dd, *J* = 5.6 Hz, *J* = 12.8 Hz, 0.5H), 4.55-4.49 (m, 1H), 4.37-4.34 (m, 1H), 4.15-4.10 (m, 0.5 H), 3.98-3.89 (m, 2.5H), 3.70-3.69 (m, 1H), 3.27-3.12 (m, 1H), 2.91-2.72 (m, 1.5H), 1.39-1.35 (t, *J* = 7.2 Hz, 3H), 1.33-1.32 (d, *J* = 1.6 Hz, 3H), 1.31-1.30 (d, *J* = 1.6 Hz, 3H); ^{13}CNMR (100 MHz, $CDCl_3$) δ: 170.5,

169.7, 168.4, 157.6, 157.1, 153.8, 153.6, 152.9, 152.4, 137.4, 137.3, 136.5, 135.4, 133.5, 131.5, 131.1, 130.8, 130.2, 129.4, 129.3, 129.1, 128.7, 127.2, 126.5, 125.2, 123.9, 116.2, 115.9, 115.6, 115.5, 115.4, 115.3, 114.8, 114.5, 76.9, 71.2, 70.1, 64.2, 57.4, 52.1, 42.9, 35.5, 29.8, 28.5, 22.3, 22.2, 15.1; HRMS calcd. for $C_{29}H_{31}F_3N_1O_4$, 514.21914 $[M + H]^+$; found 514.21949 $[M + H]^+$.

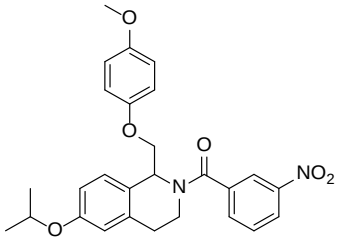

(6-isopropoxy-1-((4-methoxyphenoxy)methyl)-3,4-dihydroisoquinolin-2(1H)-yl)(3-nitrophenyl)methanone (142): Tetrahydroisoquinoline **142** was prepared via procedure XIII using tetrahydroisoquinoline **28a** (0.33 g, 0.99 mmol) and 3-nitrobenzoyl chloride (0.22 mL, 1.2 mmol) in DCM (16 mL). The crude residue was purified by silica gel chromatography (ISCO, Redisep 12 g column, 10 – 80% EtOAc/hexanes gradient) to afford the title compound as an yellow foam (0.26 g, 53 % yield, mixture of two amide rotamers). TLC (EtOAc: hexanes, 1:1, v/v) Rf = 0.45; ^{1}HNMR ($CDCl_3$, 400 MHz) δ: 8.53-8.27 (m, 1.5H), 7.85-7.22 (m, 2.5H), 6.92-6.70 (m, 7H), 5.99-6.01 (m, 0.5H), 5.09-5.07 (m, 0.5H), 4.91-4.86 (m, J = 5.2 Hz, J = 12.4 Hz, 0.5H), 4.59-4.52 (m, 1H), 4.40-4.37 (m, 1H), 4.18 (t, J = 10.4 Hz, 0.5H), 3.96-3.93 (m, J = 3.6 Hz, J = 9.2 Hz, 0.5H), 3.77 (s, 3H), 3.75-3.73 (m, 1H), 3.34-3.14 (m, 1H), 2.98-2.77 (m, 1.5H), 1.35 (d, J = 6.0 Hz, 6H); ^{13}C NMR ($CDCl_3$, 100 MHz) δ: 169.4, 168.6, 157.7, 157.2, 154.5, 153.0, 152.4, 148.4, 148.2, 138.2, 136.5, 135.3, 133.8, 132.9, 130.2, 129.7, 128.7, 128.3, 124.9, 124.6, 124.5, 123.6, 123.4, 122.1, 116.3, 115.9, 115.4, 114.9, 114.6, 71.3, 70.1, 69.9, 57.5, 55.9, 52.3, 42.9, 35.5, 29.8, 28.5, 22.3; HRMS calcd. for $C_{27}H_{29}N_2O_6$, 477.20201 $[M + H]^+$; found, 477.20169 $[M + H]^+$. Anal. ($C_{27}H_{28}N_2O_6$): C, H, N.

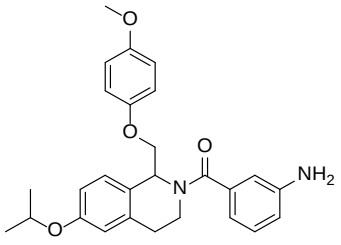

(3-aminophenyl)(6-isopropoxy-1-((4-methoxyphenoxy)methyl)-3,4-dihydroisoquinolin-2(1H)-yl)methanone (141): To a suspension of tetrahydroisoquinoline **142** (0.24 g, 0.49 mmol) in THF (0.82 ml) and 2-propanol (0.82 ml) was added palladium on carbon (0.024 g, 0.015 mmol). The reaction was hydrogenated at room temperature using a balloon. After stirring overnight the reaction was filtered through a pad of celite washing with MeOH and DCM and the volatiles were removed *in vacuo*. The crude residue was purified by silica gel chromatography (ISCO, Redisep 12 g column, 10 – 80% EtOAc/hexanes gradient) to afford the title compound as an off-white foam (0.20 g, 90 % yield, mixture of two amide rotamers). TLC (EtOAc: hexanes, 1:1, v/v) Rf = 0.20; ^{1}HNMR ($CDCl_3$, 400 MHz) δ: 7.23-7.14 (m, 2H), 6.93-6.78 (m, 5.5H), 6.74-6.63 (m, 3.5H), 5.98 (t, *J* = 5.2 Hz, 0.5H), 5.26-5.23 (m, *J* = 4.4 Hz, *J* = 8.8 Hz, 0.5H), 4.87-4.83 (m, *J* = 5.2 Hz, *J* = 12.8 Hz, 0.5H), 4.57-4.51 (m, 1H), 4.37 (d, *J* = 5.6 Hz, 1H), 4.16-3.94 (m, 0.5H), 3.97-3.83 (m, 2H), 3.76 (s, 3H), 3.67-3.60 (m, 0.5), 3.26-3.11 (m, 0.5H), 2.92-2.68 (m, 1H), 1.34 (d, J = 1.6 Hz, 3H), 1.33 (d, *J* = 1.6 Hz, 3H); ^{13}C NMR ($CDCl_3$, 100 MHz) δ: 172.1, 171.4, 157.4, 156.9, 154.2, 153.2, 152.9, 147.0, 146.8, 137.8, 137.6, 136.6, 135.9, 129.7, 129.5, 128.8, 128.4, 125.6, 124.8, 117.5, 116.4, 116.2, 115.9, 115.8, 115.7, 114.9, 114.6, 114.3, 114.2, 113.2, 71.4, 70.6, 70.1, 57.0, 55.9, 51.7, 42.7, 35.5, 30.1, 28.7, 22.3, 22.2; HRMS calcd. for $C_{27}H_{31}N_2O_4$, 447.22783 $[M + H]^+$; found, 447.22712 $[M + H]^+$. Anal. ($C_{27}H_{30}N_2O_4$): C, H, N.

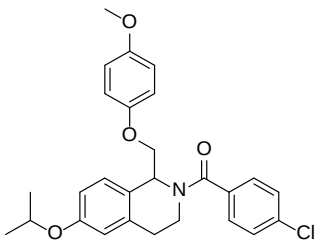

(4-chlorophenyl)(6-isopropoxy-1-((4-methoxyphenoxy)methyl)-3,4-dihydroisoquinolin-2(1H)-yl)methanone (1180-90): Tetrahyddoisoquinoline **1180-90** was prepared via procedure XIII using tetrahydroisoquinoline **28a** (0.15 g, 0.46 mmol) and 4-chlorobenzoyl chloride (0.06 mL, 0.55 mmol) in DCM (8.0 mL). The crude residue was purified by silica gel chromatography (ISCO, Redisep 12 g column, 10 – 80% EtOAc/hexanes gradient) to afford the title compound as an off-white foam (0.07 g, 31 % mixture of two amide rotamers) TLC (EtOAc: hexanes, 1:1, v/v) Rf = 0.79 ^{1}HNMR ($CDCl_3$, 400 MHz) δ: 7.47-7.30 (m, 4H), 7.23-7.16 (m, 0.5 H), 6.91-6.65 (m, 6.5 H), 5.61-5.95 (m, 0.5 H), 5.13-5.11 (dd, 0.5 H, *J* = 8.8 Hz, *J* = 2.8 Hz), 4.85-4.81 (dd, 0.5 H, *J* = 5.2 Hz, *J* = 12.4 Hz), 4.54-4.48 (m, 1H), 4.33-4.32 (m, 1H), 4.12-4.07 (m, 0.5 H), 3.93-3.89 (dd, 0.5 H, *J* = 4.0 Hz, *J* = 9.6 Hz), 3.74 (s, 3H), 3.69-3.66 (m, 1H), 3.26-3.07 (m, 1H), 2.89-2.69 (m, 1.5 H), 1.33-1.31 (d, 6H); ^{13}CNMR (100 MHz, $CDCl_3$) δ: 171.0, 170.2, 157.6, 157.0, 154.4, 154.2, 153.1, 152.6, 136.6, 135.9, 135.7, 135.6, 134.9, 134.8, 131.7, 129.3, 129.1, 128.9, 129.0, 128.9, 128.8, 128.4, 128.3, 128.1, 125.2, 124.1, 116.2, 115.9, 115.6, 115.4, 114.9, 114.8, 114.7, 114.4, 71.3, 70.2, 70.1, 57.3, 55.9, 51.9, 42.8, 35.4, 29.9, 28.6, 22.3, 22.2; HRMS calcd. for $C_{27}H_{29}ClN_1O_4$, 466.17796 $[M + H]^+$; found 466.17812 $[M + H]^+$. Anal. ($C_{27}H_{28}ClN_1O_4$): C, H, N.

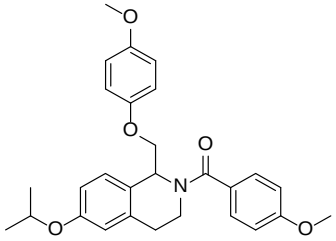

(6-isopropoxy-1-((4-methoxyphenoxy)methyl)-3,4-dihydroisoquinolin-2(1H)-yl)(4-methoxyphenyl)methanone (1180-85): Tetrahydroisoquinoline **1180-85** was prepared via procedure XIII using tetrahydroisoquinoline **28a** (0.10 g, 0.31 mmol) and 4-methoxybenzoyl chloride (0.06 mL, 0.33 mmol) in DCM (10. mL). The crude residue was purified by silica gel chromatography (ISCO, Redisep 12 g column, 10 – 80% EtOAc/hexanes gradient) to afford the title compound as a white foam (0.08 g, 56 % mixture of two amide rotamers) TLC (EtOAc: hexanes, 1:1, v/v) Rf = 0.88

^{1}HNMR ($CDCl_3$, 400 MHz) δ: 7.50-7.48 (m, 1H), 7.37-7.35 (m, 1H), 7.21-7.19 (m, 0.5 H), 6.89-6.66 (m, 8.5 H), 5.95 (m, 0.5 H), 5.28-5.23 (m, 0.5 H), 4.82-4.79 (d, *J* = 7.6 Hz, 0.5H), 4.55-4.47 (m, 1H), 4.35-4.33 (m, 1H), 4.13-4.08 (m, 0.5 H), 3.94-3.84 (m, 1H), 3.82 (s, 3H), 3.74 (m, 3H), 3.69-3.63 (m, 0.5 H), 3.22-3.12 (m, 1H), 2.89-2.69 (m, 1.5 H), 1.32-1.30 (d, 6H); ^{13}CNMR (100 MHz, $CDCl_3$) δ: 171.9, 171.2, 160.8, 157.5, 156.9, 154.2, 153.2, 152.8, 136.8, 135.8, 129.7, 128.9, 128.3, 125.9, 124.8, 116.1, 115.9, 115.6, 114.9, 114.6, 114.3, 114.0, 113.8, 71.5, 70.5, 70.1, 66.1, 57.4, 56.0, 55.9, 55.6, 51.9, 43.0, 35.6, 30.1, 29.9, 28.6, 22.3, 22.2; HRMS calcd. for $C_{28}H_{32}N_1O_5$, 462.22750 $[M + H]^+$; found 462.22672 $[M + H]^+$. Anal. ($C_{28}H_{32}N_1O_5$): C, H, N.

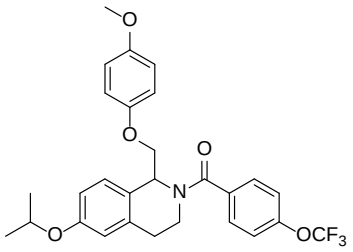

(6-isopropoxy-1-((4-methoxyphenoxy)methyl)-3,4-dihydroisoquinolin-2(1H)-yl)(4-(trifluoromethoxy)phenyl)methanone (1180-319): Tetrahydroisoquinoline **1180-319** was prepared via procedure XIV using 4-(trifluoromethoxy)benzoic acid (0.063 g, 0.31 mmol) dissolved in dry DMF (1.5 ml), N1-((ethylimino)methylene)-N3,N3-dimethylpropane-1,3-diamine hydrochloride (0.070 g, 0.35 mmol), N,N-dimethylpyridin-4-amine (0.041 g, 0.34 mmol), and tetrahydroisoquinoline **28a** (0.10 g, 0.31 mmol). The crude residue was purified by silica gel chromatography (ISCO, Redisep 12 g column, 10 – 80% EtOAc/hexanes gradient) to afford the title compound as an off-white foam (0.050 g, 32% yield, mixture of two amide rotamers). TLC (EtOAc: hexanes, 1:1, v/v) Rf = 0.56; ^{1}HNMR ($CDCl_3$, 400 MHz) δ: 7.58 (d, J =8.0 Hz, 1H), 7.45 (d, J = 8.0 Hz, 1H), 7.29-7.22 (m, 2.5H), 6.95-6.69 (m, 6.5H), 6.00 (t, *J* = 10.8 Hz, 0.5H), 5.16-5.14 (m, *J* = 6.4 Hz, 0.5H), 4.88-4.84 (m, *J* =6.0 Hz, 0.5H), 4.58-4.52 (m, 1H), 4.36-4.35 (m, 1H), 4.14 (t, *J* = 10.4 Hz, 0.5H), 3.98-3.95 (m, 0.5H), 3.77 (s, 3H), 3.74-3.68 (m, 1H), 3.29-3.11 (m, 1H), 2.91-2.74 (m, 1.5H), 1.35 (d, *J* = 6.0 Hz, 6H); ^{13}CNMR (100 MHz, $CDCl_3$) δ: 169.7, 157.4, 156.8, 152.9, 149.9, 136.4, 135.3, 135.1, 134.9, 129.4, 128.4, 128.0,

124.9, 123.8, 122.1, 121.0, 120.6, 118.7, 116.0, 115.6, 115.3, 114.6, 114.5, 114.2, 71.1, 70.0, 69.8, 57.1, 55.7, 51.7, 42.6, 35.2, 29.7, 28.3, 22.1, 22.0; HRMS calcd. for $C_{28}H_{28}N_1O_5F_3$, 516.20057 $[M + H]^+$; found 516.19994 $[M + H]^+$.

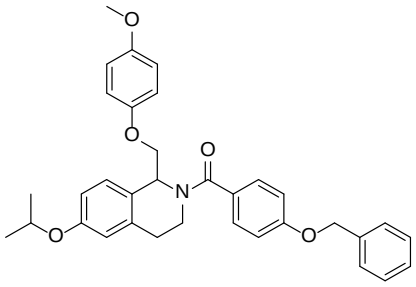

(4-(benzyloxy)phenyl)(6-isopropoxy-1-((4-methoxyphenoxy)methyl)-3,4-dihydroisoquinolin-2(1H)-yl)methanone (1180-320): Tetrahydroisoquinoline **1180-320** was prepared via procedure XIV using 4-(benzyloxy)benzoic acid (0.070 g, 0.31 mmol) dissolved in dry DMF (1.5 ml), N1-((ethylimino)methylene)-N3,N3-dimethylpropane-1,3-diamine hydrochloride (0.070 g, 0.35 mmol), N,N-dimethylpyridin-4-amine (0.041 g, 0.34 mmol), and tetrahydroisoquinoline **28a** (0.10 g, 0.31 mmol). The crude residue was purified by silica gel chromatography (ISCO, Redisep 12 g column, 10 – 80% EtOAc/hexanes gradient) to afford the title compound as an off-white foam (0.050 g, 32% yield, mixture of two amide rotamers). TLC (EtOAc: hexanes, 1:1, v/v) Rf = 0.75; ^{1}HNMR ($CDCl_3$, 400 MHz) δ: 7.54-7.52 (m, 1H), 7.47-7.34 (m, 5.5H), 7.25-7.23 (m, 0.5H), 7.00-6.70 (m, 9H), 5.99 (bs, 0.5H), 5.39 (bs, 0.5H), 5.11 (s, 2H), 4.85 (m, 0.5H), 4.58-4.52 (m, 1H), 4.39 (bs, 1H), 4.17-4.12 (m, 0.5H), 3.98-3.91 (m, 1H), 3.77 (s, 3H), 3.76-3.71 (m, 0.5H), 3.26-3.16 (m, 1H), 2.93-2.73 (m, 1.5H), 1.36-1.34 (dd, J = 2.0 Hz, J = 6.4 Hz, 6H); ^{13}CNMR (100 MHz, $CDCl_3$) δ: 159.8, 156.8, 154.1, 136.6, 135.6, 129.5, 128.9, 128.6, 128.1, 127.4, 125.5, 115.7, 114.7, 77.4, 77.1, 76.7, 71.3, 70.3, 70.0, 69.9, 57.1, 55.7, 51.7, 42.8, 35.4, 29.9, 28.3, 22.1, 22.0; HRMS calcd. for $C_{34}H_{35}N_1O_5$, 538.25880 $[M + H]^+$; found 538.25996 $[M + H]^+$.

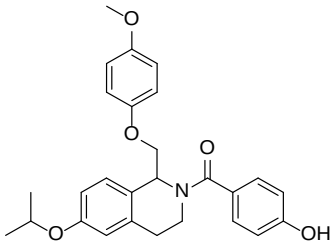

(4-hydroxyphenyl)(6-isopropoxy-1-((4-methoxyphenoxy)methyl)-3,4-dihydroisoquinolin-2(1H)-yl)methanone (1180-321): To a suspension of tetrahydroisoquinoline **1180-320** (0.051 g, 0.095 mmol) in THF (1.9 ml) was added palladium on carbon (0.05 g, 0.095 mmol). The reaction was hydrogenated at room temperature using a balloon. After stirring overnight the reaction was filtered through a pad of celite washing with MeOH and DCM and the volatiles were removed *in vacuo*. The crude residue was purified by silica gel chromatography (ISCO, Redisep 12 g column, 10 – 80% EtOAc/hexanes gradient) to afford the title compound as an off-white foam (0.020 g, 47% yield, mixture of two amide rotamers). TLC (EtOAc: hexanes, 1:1, v/v) Rf = 0.27; ^{1}HNMR ($CDCl_3$, 400 MHz) δ: 7.35 (d, J = 8.0 Hz, 1H), 7.21 (d, J = 8.4 Hz, 1.5H), 6.93-6.91 (m, 0.5H), 6.87-6.68 (m, 8H), 5.99 (bs, 0.5H), 5.31-5.29 (m, 0.5H), 4.83-4.81 (m, 0.5H), 4.58-4.49 (m, 1H), 4.35-4.37 (m, 1H), 4.16-4.10 (m, 0.5H), 3.95-3.93 (m, 1H), 3.75 (s, 3H), 3.73-3.65 (m, 0.5H), 3.31-3.14 (m, 1H), 2.96-2.71 (m, 1.5H), 1.34 (d, J = 2.4 Hz, 3H), 1.33 (d, J = 2.0 Hz, 6H); ^{13}CNMR (100 MHz, $CDCl_3$) δ: 173.1, 172.4, 158.7, 158.5, 157.5, 157.0, 154.2, 153.1, 152.7, 136.6, 135.7, 129.7, 128.8, 128.4, 127.1, 126.9, 125.4, 124.5, 116.2, 115.9, 115.8, 11.6, 114.9, 114.7, 114.4, 71.4, 70.4, 70.1, 57.6, 55.9, 52.2, 43.0, 35.9, 31.8, 30.0, 28.6, 22.9, 22.4, 22.3; HRMS calcd. for $C_{27}H_{29}N_1O_5$, 448.21185 $[M + H]^+$; found 448.21198 $[M + H]^+$.

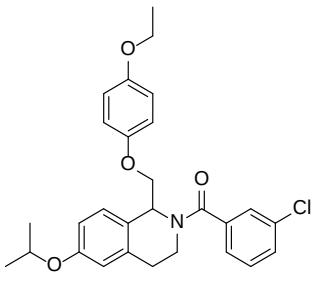

(3-chlorophenyl)(1-((4-ethoxyphenoxy)methyl)-6-isopropoxy-3,4-dihydroisoquinolin-2(1H)-yl)methanone (1180-83): Tetrahydroisoquinoline **1180-83** was prepared via procedure XIII using tetrahydroisoquinoline **28d** (0.15 g, 0.44 mmol) and 3-chlorobenzoyl chloride (0.070 mL, 0.48 mmol) in dry DCM (7.0 mL). The crude residue was purified by silica gel chromatography (ISCO, Redisep 12 g column, 10 – 80% EtOAc/hexanes gradient) to afford the title compound as an off-white foam (0.11 g, 56 % mixture of two amide rotamers) TLC (EtOAc: hexanes, 1:1, v/v) Rf = 0.78 ^{1}HNMR ($CDCl_3$, 400 MHz) δ: 7.37-7.18 (m, 4H), 6.91-6.74 (m, 5H), 6.74-6.66 (m, 2H) 5.97-5.85 (t, *J* = 5.2 Hz, 0.5H), 5.12-5.09 (dd, *J* = 3.6 Hz, *J* = 9.6 Hz, 0.5H), 4.86-4.81 (dd, *J* = 5.2 Hz, *J* = 12.4 Hz, 0.5H), 4.55-4.49 (m, 1H), 4.35-4.32 (m, 1H), 4.14-4.09 (m, 0.5 H), 3.98-3.89 (m, 2.5 H), 3.75-3.66 (m, 1H), 3.25-3.09 (m, 1H), 2.88-2.70 (m, 1.5 H), 1.39-1.35 (t, *J* = 7.2 Hz, 3H), 1.33-1.31 (d, 6H); ^{13}CNMR (100 MHz, $CDCl_3$) δ: 170.2, 169.6, 157.6, 157.1, 153.8, 152.5, 148.3, 138.4, 136.7, 135.6, 134.9, 134.6, 130.2, 129.9, 129.8, 128.8, 128.3, 128.2, 127.1, 125.9, 125.7, 124.9, 124.1, 116.2, 115.9, 115.7, 115.6, 115.5, 114.7, 114.5, 71.3, 70.3, 64.2, 57.3, 52.0, 42.9, 35.5, 29.9, 28.5, 22.3, 22.2, 15.2; HRMS calcd. for $C_{28}H_{31}ClN_1O_4$, 480.19361 $[M + H]^+$; found 480.19337 $[M + H]^+$. Anal. ($C_{28}H_{30}ClN_1O_4$): C, H, N.

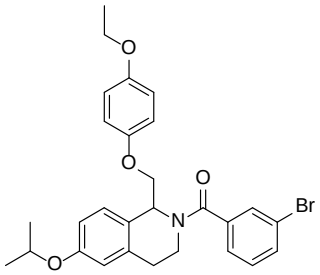

(3-bromophenyl)(1-((4-ethoxyphenoxy)methyl)-6-isopropoxy-3,4-dihydroisoquinolin-2(1H)-yl)methanone (1180-86): Tetrahydroisoquinoline **1180-86** was prepared via procedure XIII using tetrahydroisoquinoline **28d** (0.15 g, 0.44 mmol) and 3-bromobenzoyl chloride (0.070 mL, 0.48 mmol). The crude residue was purified by silica gel chromatography (ISCO, Redisep 12 g column, 10 – 80% EtOAc/hexanes gradient) to afford the title compound as an off-white foam (0.12 g, 51 % mixture of two amide rotamers) TLC (EtOAc: hexanes, 1:1, v/v) Rf = 0.80 ^{1}HNMR ($CDCl_3$, 400

MHz) δ: 7.55-7.41 (m, 2H), 7.29-7.18 (m, 2H), 6.91-6.66 (m, 7H), 5.94-5.93 (m, 0.5 H), 5.12-5.09 (dd, *J* = 3.2 Hz, *J* = 9.2 Hz, 0.5H), 4.85-4.81 (dd, *J* = 5.2 Hz, *J* = 12.8 Hz, 0.5H), 4.55-4.49 (m, 1H), 4.33-4.30 (m, 1H), 4.14-4.09 (m, 0.5 H), 3.98-3.89 (m, 2.5 H), 3.74-3.66 (m, 1H), 3.27-3.09 (m, 1H), 2.9-2.71 (m, 1.5H), 1.39-1.35 (t, *J* = 7.2 Hz, 3H), 1.33-1.31 (d, 6H); ^{13}CNMR (100 MHz, $CDCl_3$) δ: 170.3, 169.5, 157.6, 157.1, 153.7, 153.6, 153.0, 152.5, 138.6, 136.6, 132.9, 132.8, 132.7, 131.0, 130.5, 130.1, 129.9, 128.8, 128.3, 126.3, 125.3, 125.2, 124.1, 122.9, 122.7, 116.2, 115.9, 115.6, 115.5, 115.3, 114.8, 114.5, 71.3, 70.2, 70.1, 64.2, 57.3, 51.9, 42.8, 35.8, 29.9, 28.5, 22.3, 22.2, 15.2; HRMS calcd. for $C_{28}H_{31}BrN_1O_4$, 524.14310 $[M + H]^+$; found 524.14327 $[M + H]^+$. Anal. ($C_{28}H_{30}BrN_1O_4$): C, H, N.

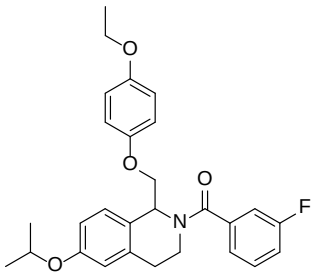

(1-((4-ethoxyphenoxy)methyl)-6-isopropoxy-3,4-dihydroisoquinolin-2(1H)-yl)(3-fluorophenyl)methanone (1180-87): Tetrahydroisoquinoline **1180-87** was prepared via procedure XIII using tetrahydroisoquinoline **28d** (0.15 g, 0.44 mmol) and 3-fluorobenzoyl chloride (0.060 mL, 0.48 mmol) in DCM (7.0 mL). The crude residue was purified by silica gel chromatography (ISCO, Redisep 12 g column, 10 – 80% EtOAc/hexanes gradient) to afford the title compound as an off-white foam (0.090 g, 46 % mixture of two amide rotamers) TLC (EtOAc: hexanes, 1:1, v/v) Rf = 0.80 ^{1}HNMR ($CDCl_3$, 400 MHz) δ: 7.42-7.29 (m, 2H), 7.21-7.06 (m, 2H), 6.90-6.66 (m, 7H), 5.97-5.95 (t, *J* = 4.4 Hz, 0.5H), 5.14-5.11 (dd, *J* = 4.0 Hz, *J* = 10.0 Hz, 0.5H), 4.86-4.81 (dd, *J* = 5.2 Hz, *J* = 12.8 Hz, 0.5H), 4.55-4.48 (m, 1H), 4.37-4.29 (m, 1H), 4.13-4.08 (m, 0.5 H), 3.98-3.89 (2.5 H), 3.76-3.66 (m, 1H), 3.28-3.08 (m, 1H), 2.90-2.69 (m, 1.5 H), 1.39-1.35 (t, *J* = 7.2 Hz, 3H), 1.33-1.31 (d, 6H); ^{13}CNMR (100 MHz, $CDCl_3$) δ: 170.5, 169.8, 163.9, 161.4, 157.6, 157.0, 153.7, 153.6, 153.0, 152.5, 138.6, 136.6, 135.6, 130.7, 130.6, 130.2, 128.7, 128.3, 125.2, 124.2, 123.5, 122.5, 116.9, 116.8, 116.7, 116.6, 116.2, 115.9, 115.7, 115.6, 115.5, 114.7, 114.4, 114.0, 71.3, 70.2, 64.2, 57.3, 51.9, 42.9, 35.5,

29.9, 28.5, 22.3, 22.2, 15.1; HRMS calcd. for $C_{28}H_{31}FN_1O_4$, 464.22316 $[M + H]^+$; found 464.22293 $[M + H]^+$; mp: 75°C.

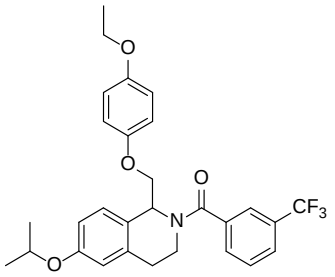

(6-isopropoxy-1-((4-methoxyphenoxy)methyl)-3,4-dihydroisoquinolin-2(1H)-yl)(3-(trifluoromethyl)phenyl)methanone (1180-92): Tetrahydroisoquinoline **1180-92** was prepared via procedure XIII using tetrahydroisoquinoline **28d** (0.13 g, 0.40 mmol) and 3-(trifluoromethyl)benzoyl chloride (0.070 mL, 0.43 mmol) in DCM (7.0 mL). The crude residue was purified by silica gel chromatography (ISCO, Redisep 12 g column, 10 – 80% EtOAc/hexanes gradient) to afford the title compound as an off-white foam (0.19 g, 55 % mixture of two amide rotamers) TLC (EtOAc: hexanes, 1:1, v/v) Rf = 0.66 ^{1}HNMR ($CDCl_3$, 400 MHz) δ: 7.70-7.48 (m, 3.5 H), 7.22-7.19 (m, 0.5 H), 6.89-6.66 (m, 6.5 H), 6.00-5.98 (t, *J* = 5.2 Hz, 0.5H), 5.09-5.07 (dd, *J* = 3.2 Hz, *J* = 9.6 Hz, 0.5H), 4.89-4.84 (dd, *J* = 5.6 Hz, *J* = 12.8 Hz, 0.5H), 4.55-4.49 (m, 1H), 4.36-4.34 (m, 0.5 H), 4.15-4.09 (m, 1H), 3.93-3.89 (m, 0.5 H), 3.74 (s, 3H), 3.69-3.68 (m, 1H), 3.29-3.12 (m, 1H), 2.91-2.72 (m, 1.5 H), 1.33-1.12 (dd, *J* = 1.6 Hz, *J* = 6.4 Hz, 6H); ^{13}CNMR (100 MHz, $CDCl_3$) δ: 170.5, 169.7, 168.2, 157.6, 157.1, 154.4, 154.3, 153.0, 152.5, 137.4, 137.2, 136.6, 135.4, 133.5, 131.1, 130.9, 130.2, 129.4, 129.3, 129.1, 128.7, 128.3, 126.5, 123.9, 116.2, 115.9, 115.4, 115.3, 114.9, 114.8, 114.5, 71.3, 70.1, 57.4, 55.9, 52.1, 42.9, 35.5, 29.9, 28.5, 22.3, 22.2; HRMS calcd. for $C_{29}H_{29}F_3N_1O_4$, 500.20432 $[M + H]^+$; found 500.20415 $[M + H]^+$; mp: 85°C.

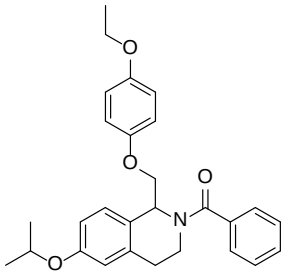

(1-((4-ethoxyphenoxy)methyl)-6-isopropoxy-3,4-dihydroisoquinolin-2(1H)-yl)(phenyl)methanone (1180-100): Tetrahydroisoquinoline **1180-100** was prepared via procedure XIII using tetrahydroisoquinoline **28d** (0.20 g, 0.59 mmol) and benzoyl chloride (0.080 mL, 0.70 mmol) in DCM (9.0 mL). The crude residue was purified by silica gel chromatography (ISCO, Redisep 12 g column, 10 – 80% EtOAc/hexanes gradient) to afford the title compound as an off-white foam (0.06 g, 24 % mixture of two rotamers) TLC (EtOAc: hexanes, 1:1, v/v) Rf = 0.54 ^{1}HNMR ($CDCl_3$, 400 MHz) δ: 7.51-7.19 (m, 5H), 6.89-6.65 (m, 6H), 5.96-5.99 (m, 0.5 H), 5.18-5.16 (d, *J* = 5.6 Hz, 0.5H), 4.88-4.84 (dd, *J* = 4.4 Hz, *J* = 12.4 Hz, 0.5H), 4.55-4.47 (m, 1H), 4.35-4.33 (m, 1H), 4.12-4.07 (m, 0.5 H), 3.98-3.89 (m, 2.5H), 3.80-3.62 (m, 1H), 3.27-3.09 (m, 1H), 2.93-2.68 (m,1.5 H), 1.39-1.35 (t, *J* = 6.8 Hz, 3H), 1.33-2.31 (d, 6H); ^{13}CNMR (100 MHz, $CDCl_3$) δ: 171.9, 171.2, 157.5, 156.9, 153.7, 153.5, 153.1, 152.7, 136.7, 135.7, 129.8, 129.6, 128.8, 128.5, 128.3, 127.7, 126.8, 125.6, 124.5, 116.1, 115.9, 115.6, 114.6, 114.3, 71.4, 70.3, 70.1, 64.2, 57.2, 51.8, 42.8, 35.4, 30.0, 28.7, 22.3, 22.2, 15.2; ; HRMS calcd. for $C_{28}H_{32}N_1O_4$, 446.23259 $[M + H]^+$; found 446.23242 $[M + H]^+$. Anal. ($C_{29}H_{32}N_1O_4$): C, H, N.

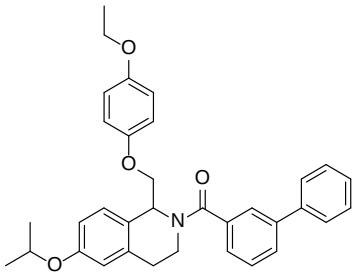

biphenyl-3-yl(1-((4-ethoxyphenoxy)methyl)-6-isopropoxy-3,4-dihydroisoquinolin-2(1H)-yl)methanone (1180-102): Tetrahydroisoquinoline **1180-102** was prepared via procedure XIV using

biphenyl-3-carboxylic acid (0.29 g, 1.5 mmol), N1-((ethylimino)methylene)-N3,N3-dimethylpropane-1,3-diamine (.25 g, 1.6 mmol), N,N-dimethylpyridin-4-amine (0.19 g, 1.6 mmol), and tetrahydroisoquinoline **28d** (0.46 g, 1.4 mmol). The crude residue was purified by silica gel chromatography (ISCO, Redisep 12 g column, 10 – 80% EtOAc/hexanes gradient) to afford the title compound as an off-white foam (0.10 g, 15 % mixture of two amide rotamers) TLC (EtOAc: hexanes, 1:1, v/v) Rf = 0.65 ^{1}HNMR ($CDCl_3$, 400 MHz) δ: 7.79-7.56 (m, 4H), 7.52-7.30 (m, 5H), 7.24-7.21 (m, 0.5 H), 6.91-6.66 (m, 6.5 H), 6.03-6.00 (t, *J* = 4.4 Hz, 0.5H), 5.25-5.21 (dd, *J* = 3.6 Hz, *J* = 9.2 Hz, 0.5H), 4.91-4.87 (dd, *J* = 5.6 Hz, *J* = 13.2 Hz, 0.5H), 4.55-4.49 (m, 1H), 4.41-4.34 (m, 1H), 4.17-4.12 (m, 0.5 H), 3.95-3.92 (m, 1.5 H), 3.89-3.65 (m, 1H), 3.28-3.14 (m, 1H), 2.95-2.69 (m, 2.5 H), 1.39-1.35 (t, *J* = 7.2 Hz, 3H), 1.33-1.32 (m, 6H);^{13}CNMR ($CDCl_3$,100 MHz) δ: 171.9, 171.1, 157.5, 156.9, 153.7, 153.45, 153.1, 152.6, 141.8, 141.5, 140.6, 140.5, 137.3, 137.1, 136.7, 135.7, 129.3, 129.1, 129.0, 128.9, 128.8, 128.5, 128.4, 127.9, 127.8, 127.4, 127.3, 126., 125.6, 125.5, 5124.6, 116.2, 115.9, 115.8, 115.6, 115.4, 114.3, 71.4, 70.4, 70.1, 64.2, 57.3, 51.9, 42.9, 35.5, 30.1, 28.6, 22.5, 22.3, 15.2; ; HRMS calcd. for $C_{45}H_{36}N_1O_4$, 522.26389 $[M + H]^+$; found 522.26390 $[M + H]^+$.

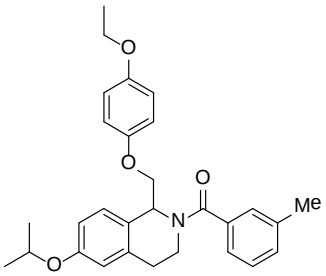

(1-((4-ethoxyphenoxy)methyl)-6-isopropoxy-3,4-dihydroisoquinolin-2(1H)-yl)(m-tolyl)methanone (1180-129): Tetrahydroisoquinoline **1180-129** was prepared via procedure XIII using tetrahydroisoquinoline **28d** (0.21 g, 0.62 mmol) and 3-methylbenzoyl chloride (0.11 mL, 0.74 mmol) in DCM (9.7 mL). The crude residue was purified by silica gel chromatography (ISCO, Redisep 12 g column, 10 – 80% EtOAc/hexanes gradient) to afford the title compound as an off-white foam (0.22 g, 78 % yield, mixture of two amide rotamers) TLC (EtOAc: hexanes, 1:1, v/v) Rf = 0.88; ^{1}HNMR ($CDCl_3$, 400 MHz) δ: 7.47-7.45 (m, 1H), 7.35-7.33 (m, 1H), 7.26-7.21 (m, 2H), 6.95-

6.71 (m, 1H), 6.02-6.01 (m, 0.5H), 5.27-5.25 (m, 0.5H), 4.90 (m, *J* = 4.4 Hz, *J* = 12.0 Hz, 0.5H), 4.61-5.54 (m, 1H), 4.39 (d, *J* = 5.2 Hz, 1H), 4.18-4.10 (m, 0.5H), 4.00 (q, *J* = 7.2 Hz, 2H), 3.89-3.67 (m, 1H), 3.31-3.13 (m, 1H), 2.98-2.72 (m, 2H), 2.41 (s, 3H), 1.42 (t, *J* = 6.4 Hz, 3H), 1.37 (d, *J* = 6.0 Hz, 6H); ^{13}C NMR ($CDCl_3$, 100 MHz) δ: 172.2, 171.4, 157.4, 156.9, 153.5, 153.1, 153.7, 138.7, 138.4, 136.7, 136.5, 135.8, 130.4, 128.8, 128.6, 128.3, 127.4, 125.6, 124.6, 123.6, 116.1, 115.9, 115.8, 115.6, 115.5, 114.5, 114.3, 71.4, 70.3, 70.0, 64.2, 57.1, 51.7, 42.8, 35.4, 30.1, 28.7, 22.3, 22.2, 21.6, 15.2; HRMS calcd. for $C_{29}H_{34}NO_4$, 460.24824 $[M + H]^+$; found, 460.24844 $[M + H]^+$; Anal. ($C_{29}H_{33}N_1O_4$): C, H, N.

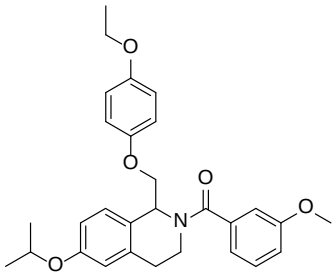

(1-((4-ethoxyphenoxy)methyl)-6-isopropoxy-3,4-dihydroisoquinolin-2(1H)-yl)(3-methoxyphenyl)methanone (1180-130): Tetrahydroisoquinoline **1180-130** was prepared via procedure XIII using tetrahydroisoquinoline **28d** (0.21 g, 0.62 mmol) and 3-methoxybenzoyl chloride (0.10 mL, 0.74 mmol) in DCM (9.7 mL). The crude residue was purified by silica gel chromatography (ISCO, Redisep 12 g column, 10 – 80% EtOAc/hexanes gradient) to afford the title compound as an off-white foam (0.20 g, 68 % yield, mixture of two amide rotamers) TLC (EtOAc: hexanes, 1:1, v/v) Rf = 0.69; ^{1}HNMR ($CDCl_3$, 400 MHz) δ: 7.35-7.22 (m, 1H), 7.09-7.07 (m, 1H), 6.97-6.68 (m, 9H), 5.99 (t, *J* = 4.8 Hz, 0.5H), 5.23-5.20 (m, *J* = 3.6 Hz, *J* = 8.8 Hz, 0.5H), 4.89-4.85 (m, *J* = 5.6 Hz, *J* = 12.8 Hz, 0.5H), 4.58-4.49 (m, 1H), 4.37-4.33 (m, 1H), 4.16-4.09 (m, 0.5H), 4.00-3.95 (q, *J* = 6.8 Hz, 2H), 3.82-3.79 (d, *J* = 11.2 Hz, 3H), 3.70-3.61 (m, 0.5H), 3.30-3.11 (m, 1H), 2.95-2.71 (m, 1.5H), 1.41-1.38 (t, *J* = 7.2 Hz, 3H), 1.35-1.34 (d, *J* = 6.0 Hz, 6H); ^{13}C NMR ($CDCl_3$, 100 MHz) δ: 171.7, 170.9, 159.9, 159.7, 156.9, 153.7, 153.5, 153.1, 152.7, 138.0, 137.8, 136.7, 135.8, 129.9, 129.6, 128.8, 128.3, 125.5, 124.6, 119.9, 118.8, 116.1, 115.9, 115.7, 115.6, 114.6, 114.3, 113.1, 112.0, 71.4, 70.4,

70.0, 64.2, 57.1, 55.6, 51.8, 42.8, 35.5, 30.0, 28.6, 22.7, 15.2; HRMS calcd. for $C_{29}H_{34}NO_5$, 476.24315 $[M + H]^+$; found, 476.24324 $[M + H]^+$.

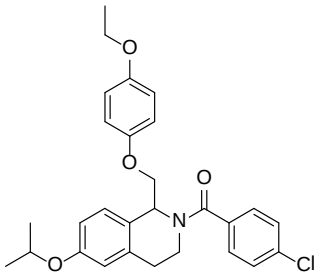

(4-chlorophenyl)(1-((4-ethoxyphenoxy)methyl)-6-isopropoxy-3,4-dihydroisoquinolin-2(1H)-yl)methanone (1180-132): Tetrahydroisoquinoline **1180-132** was prepared via procedure XIII using tetrahydroisoquinoline **28d** (0.21 g, 0.62 mmol) and 4-chlorobenzoyl chloride (0.095 mL, 0.74 mmol) in DCM (9.7 mL). The crude residue was purified by silica gel chromatography (ISCO, Redisep 12 g column, 10 – 80% EtOAc/hexanes gradient) to afford the title compound as an off-white foam (0.12 g, 40 % yield, mixture of two amide rotamers) TLC (EtOAc: hexanes, 1:1, v/v) Rf = 0.87; ^{1}HNMR ($CDCl_3$, 400 MHz) δ: 7.50-7.48 (m, 1H), 7.42-7.34 (m, 3H), 7.23-7.19 (m, 0.5H), 6.93-6.68 (m, 6.H), 5.99-5.97 (m, 0.5H), 5.16-5.14 (m, 0.5H), 4.89-4.83 (m, *J* = 4.8 Hz, *J* = 12.4 Hz, 0.5H), 4.57-4.51 (m, 1H), 4.36-4.34 (m, 1H), 4.14-4.08 (m, 0.5H), 3.97 (q, *J* = 6.8 Hz, 2H), 3.76-3.69 (m, 1H), 3.29-3.12 (m, 1H), 2.92-2.72 (m, 2H), 1.40 (t, *J* = 7.2 Hz, 3H), 1.34 (d, *J* = 5.6 Hz, 6H); ^{13}C NMR ($CDCl_3$, 100 MHz) δ: 170.9, 170.2, 157.5, 157.0, 153.8, 153.6, 153.0, 152.5, 136.6, 135.8, 135.7, 135.6, 135.1, 129.4, 129.1, 128.8, 128.4, 128.3, 125.3, 124.2, 116.2, 115.7, 115.6, 115.5, 114.7, 114.4, 71.3, 70.2, 70.1, 64.2, 57.3, 51.9, 42.9, 35.4, 29.9, 28.7, 22.3, 22.2, 15.2; HRMS calcd. for $C_{28}H_{31}NO_4Cl$, 480.19361 $[M + H]^+$; found, 480.19379 $[M + H]^+$; Anal. ($C_{28}H_{30}N_1O_4Cl$): C, H, N.

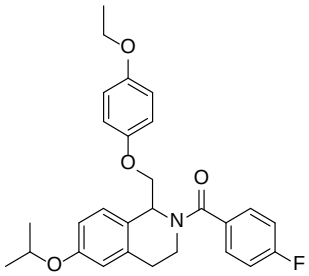

(1-((4-ethoxyphenoxy)methyl)-6-isopropoxy-3,4-dihydroisoquinolin-2(1H)-yl)(4-fluorophenyl)methanone (1180-133): Tetrahydroisoquinoline **1180-133** was prepared via procedure XIII using tetrahydroisoquinoline **28d** (0.21 g, 0.62 mmol) and 4-fluorobenzoyl chloride (0.089 mL, 0.74 mmol) in DCM (9.7 mL). The crude residue was purified by silica gel chromatography (ISCO, Redisep 12 g column, 10 – 80% EtOAc/hexanes gradient) to afford the title compound as an off-white foam (0.19 g, 65 % yield, mixture of two amide rotamers) TLC (EtOAc: hexanes, 1:1, v/v) Rf = 0.81; ^{1}HNMR ($CDCl_3$, 400 MHz) δ: 7.55-7.54 (m, 1H), 7.40-7.42 (m, 1H), 7.24-7.21 (m, 0.5H), 7.13-7.06 (m, 2H), 6.94-6.68 (m, 6.5H), 5.98-5.97 (m, 0.5H), 5.17-5.16 (m, 0.5H), 4.88-4.83 (m, *J* = 5.2 Hz, *J* = 12.4 Hz, 0.5H), 4.59-4.50 (m, 1H), 4.36 (s, 1H), 4.15-4.10 (m, 0.5H), 3.97 (q, *J* = 6.8 Hz, 2H), 3.79-3.67 (m, 1H), 3.29-3.11 (m, 1H), 2.91-2.73 (m, 2H), 1.39 (t, *J* = 7.2 Hz, 3H), 1.34 (d, *J* = 6.0 Hz, 6H); ^{13}C NMR ($CDCl_3$, 100 MHz) δ: 171.1, 170.3, 164.8, 162.3, 157.5, 156.9, 153.7, 153.0, 152.6, 136.7, 135.6, 132.7, 130.1, 129.1, 128.8, 128.3, 125.4, 124.3, 116.2, 115.9, 115.6, 114.7, 114.4, 71.3, 70.3, 70.0, 64.2, 57.4, 51.9, 42.9, 35.5, 29.9, 28.5, 22.3, 22.2, 15.1; HRMS calcd. for $C_{28}H_{31}NO_4F$, 464.22316 $[M + H]^+$; found, 464.22329 $[M + H]^+$.

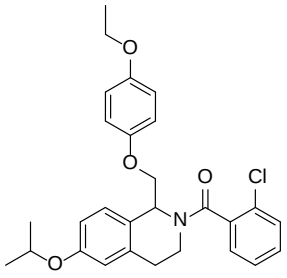

(2-chlorophenyl)(1-((4-ethoxyphenoxy)methyl)-6-isopropoxy-3,4-dihydroisoquinolin-2(1H)-yl)methanone (1180-148): Tetrahydroisoquinoline **1180-148** was prepared via procedure XIII using

tetrahydroisoquinoline **28d** (0.14 g, 0.41 mmol) and 2-chlorobenzoyl chloride (0.062 mL, 0.49 mmol) in DCM (6.3 mL). The crude residue was purified by silica gel chromatography (ISCO, Redisep 12 g column, 10 – 80% EtOAc/hexanes gradient) to afford the title compound as an yellow foam (0.090 g, 56 % yield, mixture of two amide rotamers). TLC (EtOAc: hexanes, 1:1, v/v) Rf = 0.86; ^{1}HNMR ($CDCl_3$, 400 MHz) δ: 7.59-7.21 (m, 4H), 6.96-6.67 (m, 7H), 6.06-6.00 (m, 0.5H), 4.99-4.95 (m, *J* = 4.8 Hz, *J* = 12.0 Hz, 0.5H), 4.88-4.84 (m, *J* = 4.0 Hz, *J* = 9.2 Hz, 0.5H), 4.59-4.50 (m, 1H), 4.41-4.31 (m, 1H), 4.09 (t, *J* = 9.6 Hz, 0.5H), 4.01-3.90 (m, 2H),3.91-3.75 (m, 0.5H), 3.64-3.49 (m, 1H), 3.30-3.04 (m, 1H), 2.89-2.72 (m, 1.5H), 1.41-1.34 (m, 9H); ^{13}C NMR ($CDCl_3$, 100 MHz) δ: 168.2, 167.8, 157.3, 157.0, 153.6, 153.5, 152.9, 152.6, 136.5, 136.1, 135.9, 135.7, 135.0, 130.8, 130.5, 130.3, 130.1, 129.9, 129.8, 129.3, 128.8, 128.7, 128.3, 128.1, 127.7, 127.5, 127.4, 127.1, 126.7, 125.4, 125.2, 124.5, 115.9, 115.8, 115.7, 115.6, 115.5, 115.4, 114.6, 114.3, 71.3, 70.4, 70.0, 64.2, 56.8, 51.7, 42.7, 42.3, 35.7, 29.9, 29.8, 28.8, 22.3, 15.2; HRMS calcd. for $C_{28}H_{31}N_1O_4Cl$, 480.19361 $[M + H]^+$; found, 480.19269 $[M + H]^+$. Anal. ($C_{28}H_{30}N_1O_4Cl$): C, H, N.

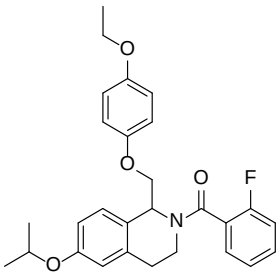

(1-((4-ethoxyphenoxy)methyl)-6-isopropoxy-3,4-dihydroisoquinolin-2(1H)-yl)(2-fluorophenyl)methanone (1180-147): Tetrahydroisoquinoline **1180-147** was prepared via procedure XIII using tetrahydroisoquinoline **28d** (0.14 g, 0.41 mmol) and 2-fluorobenzoyl chloride (0.049 mL, 0.41 mmol) in DCM (6.0 mL). The crude residue was purified by silica gel chromatography (ISCO, Redisep 12 g column, 10 – 80% EtOAc/hexanes gradient) to afford the title compound as an yellow foam (0.10 g, 53 % yield, mixture of two amide rotamers). TLC (EtOAc: hexanes, 1:1, v/v) Rf = 0.86; ^{1}HNMR ($CDCl_3$, 400 MHz) δ: 7.44-7.36 (m, 1H), 7.27-7.11 (m, 3H), 6.97-6.68 (m, 7H), 6.02 (t, *J* = 4.8 Hz, 0.5H), 5.02-4.92 (m, 0.5H), 4.57-4.51 (m, 1H), 4.39-4.31 (m, 1H), 4.14-4.06 (m, 0.5H),

4.00-3.90 (m, 2.5H), 3.75-3.67 (m, 1H), 3.31-3.09 (m, 1H), 2.93-2.73 (m, 1.5H), 1.39 (t, *J* = 7.2 Hz, 3H), 1.36-1.33 (m, 6H); ^{13}C NMR ($CDCl_3$, 100 MHz) δ: 166.7, 166.4, 157.4, 157.0, 153.5, 153.1, 152.6, 136.5, 132.9, 131.4, 128.8, 128.3, 125.3, 124.9, 124.2, 115.9, 115.7, 115.6, 115.4, 114.6, 114.4, 71.4, 70.3, 70.1, 64.2, 60.6, 51.9, 44.6, 42.5, 35.6, 29.9, 28.8, 22.3, 15.1; HRMS calcd. for $C_{28}H_{31}N_1O_4F$, 464.22316 $[M + H]^+$; found, 464.22228 $[M + H]^+$.

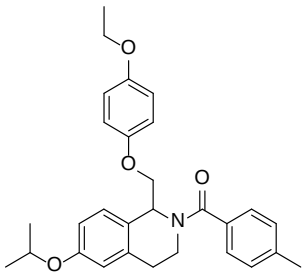

(1-((4-ethoxyphenoxy)methyl)-6-isopropoxy-3,4-dihydroisoquinolin-2(1H)-yl)(p-tolyl)methanone (1180-131): Tetrahydroisoquinoline **1180-131** was prepared via Procedure XIII using tetrahydroisoquinoline **28d** (0.21 g, 0.62 mmol) and 4-methylbenzoyl chloride (0.10 mL, 0.74 mmol) in DCM (9.7 mL). The crude residue was purified by silica gel chromatography (ISCO, Redisep 12 g column, 10 – 80% EtOAc/hexanes gradient) to afford the title compound as an off-white foam (0.18 g, 62 % yield, mixture of two amide rotamers) TLC (EtOAc: hexanes, 1:1, v/v) Rf = 0.72; ^{1}HNMR ($CDCl_3$, 400 MHz) δ: 7.34-7.17 (m, 4.5H), 6.93-6.68 (m, 6.5H), 6.01 (t, *J* = 4.4 Hz, 0.5H), 5.22-5.19 (m, *J* = 3.6 Hz, *J* = 8.8 Hz, 0.5H), 4.91-4.86 (m, *J* = 5.6 Hz, *J* = 13.2 Hz, 0.5H), 4.59-4.51 (m, 1H), 4.37 (d, *J* = 5.2 Hz, 1H), 4.16-4.06 (m, 0.5 H), 3.98 (q, *J* = 6.8 Hz, 2H), 3.84-3.63 (m, 1H), 3.31-3.11 (m, 1H), 2.95-2.70 (m, 2H), 2.37 (d, *J* = 9.2 Hz, 3H), 1.40 (t, *J* = 7.2 Hz, 3H), 1.35 (d, *J* = 6.4 Hz, 6H); ^{13}C NMR ($CDCl_3$, 100 MHz) δ: 172.2, 171.4, 157.4, 156.9, 153.5, 153.1, 152.7, 138.7, 138.4, 136.7, 136.5, 135.8, 130.4, 128.8, 128.6, 128.3, 127.4, 125.6, 124.6, 123.7, 116.1, 115.9, 115.8, 115.6, 115.5, 114.5, 114.3, 71.4, 70.4, 70.0, 64.2, 57.1, 51.7, 42.8, 35.4, 30.1, 28.7, 22.3, 22.2, 21.6, 15.2; HRMS calcd. for $C_{29}H_{34}NO_4$, 460.24824 $[M + H]^+$; found, 460.24829 $[M + H]^+$.

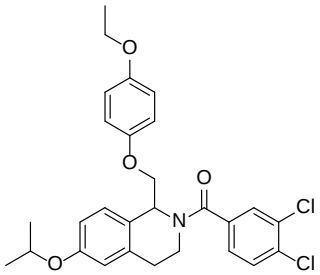

(3,4-dichlorophenyl)(1-((4-ethoxyphenoxy)methyl)-6-isopropoxy-3,4-dihydroisoquinolin-2(1H)-yl)methanone (1180-103): Tetrahydroisoquinoline **1180-103** was prepared via procedure XIII using tetrahydroisoquinoline **28d** (0.25 g, 0.73 mmol) and 3,4-dichlorobenzoyl chloride (0.18 g, 0.89 mmol) in DCM (12 mL). The crude residue was purified by silica gel chromatography (ISCO, Redisep 12 g column, 10 – 80% EtOAc/hexanes gradient) to afford the title compound as an off-white foam (0.16 g, 42 % mixture of two amide rotamers) TLC (EtOAc: hexanes, 1:1, v/v) Rf = 0.59 ^{1}HNMR ($CDCl_3$, 400 MHz) δ: 7.71-7.42 (m, 2H), 7.36-7.34 (m, 0.5 H), 7.22-7.15 (m, 1H), 6.92-6.89 (m, 0.5 H), 6.84-6.66 (m, 6H), 5.96-5.92 (m, 0.5 H), 5.11-5.08 (dd, *J* = 3.2 Hz, *J* = 9.2 Hz, 0.5H), 4.83-4.79 (dd, *J* = 4.8 Hz, *J* = 12.8 Hz, 0.5H), 4.56-4.48 (m, 1H), 4.36-4.29 (m, 1H), 4.15-4.09 (m, 0.5 H), 3.98-3.91 (m, 2.5 H), 3.71-3.67 (m, 1H), 3.27-3.08 (m, 1H), 2.91-2.72 (m, 1.5 H), 1.39-1.36 (t, *J* = 6.8 Hz, 3H), 1.33-1.32 (d, *J* = 1.6 Hz, 3H), 1.31-1.30 (d, *J* = 1.6 Hz, 3H); ^{13}CNMR ($CDCl_3$, 100 MHz) δ: 169.6, 168.8, 157.6, 157.1, 153.8, 153.6, 152.9, 152.3, 136.5, 136.4, 136.3, 135.4, 134.1, 133.9, 133.3, 132.8, 130.9, 130.6, 130.3, 129.1, 128.7, 128.3, 127.2, 126.2, 125.0, 123.9, 116.2, 115.8, 115.7, 115.6, 115.4, 115.2, 114.8, 114.5, 71.2, 70.1, 64.2, 57.4, 52.1, 42.8, 35.5, 29.9, 28.5, 22.3, 22.2, 15.2; HRMS calcd. for $C_{28}H_{30}Cl_2N_1O_4$, 514.15464 $[M + H]^+$; found 514.15456 $[M + H]^+$. Anal. ($C_{29}H_{32}N_1O_4$): C, H, N.

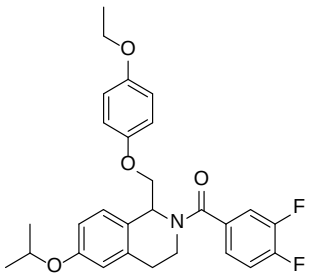

(3,4-difluorophenyl)(1-((4-ethoxyphenoxy)methyl)-6-isopropoxy-3,4-dihydroisoquinolin-2(1H)-yl)methanone (1180-134): Tetrahydroisoquinoline **1180-134** was prepared via procedure XIII using tetrahydroisoquinoline **28d** (0.21 g, 0.62 mmol) and 3,4-difluorobenzoyl chloride (0.094 mL, 0.74 mmol) in DCM (9.7 mL). The crude residue was purified by silica gel chromatography (ISCO, Redisep 12 g column, 10 – 80% EtOAc/hexanes gradient) to afford the title compound as an off-white foam (0.18 g, 62 % yield, mixture of two amide rotamers) TLC (EtOAc: hexanes, 1:1, v/v) Rf = 0.86; ^{1}HNMR ($CDCl_3$, 400 MHz) δ: 7.50-7.46 (m, 0.5H), 7.29-7.16 (m, 3H), 6.94-6.92 (m, 0.5H), 6.83-6.69 (m, 6H), 5.97 (bs, 0.5H), 5.16-5.15 (m, 0.5H), 4.84-4.82 (m, 0.5H), 4.59-4.51 (m, 1H), 4.35 (s, 1H), 4.15 (t, *J* = 10.4 Hz, 0.5H), 3.98 (q, *J* = 6.8 Hz, 2H), 3.76-3.71 (m, 0.5H), 3.29-3.14 (m, 1H), 2.90-2.75 (m, 2H), 1.40 (t, *J* = 6.8 Hz, 3H), 1.34 (d, *J* = 6.0 Hz, 6H); ^{13}C NMR ($CDCl_3$, 100 MHz) δ: 169.7, 168.9, 157.6, 157.1, 153.8, 153.6, 152.9, 152.4, 150.1, 149.9, 136.6, 135.4, 133.3, 128.7, 125.1, 124.5, 123.9, 117.9, 117.6, 117.4, 116.8, 116.2, 115.8, 115.5, 114.8, 114.5, 71.2, 70.1, 64.2, 57.4, 53.1, 42.9, 35.5, 29.9, 28.4, 22.3, 22.2, 15.1; HRMS calcd. for $C_{28}H_{30}NO_4F_2$, 482.21374 $[M + H]^+$; found, 482.21387 $[M + H]^+$; Anal. ($C_{28}H_{29}N_1O_4F_2$): C, H, N.

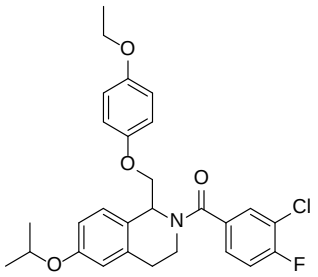

(3-chloro-4-fluorophenyl)(1-((4-ethoxyphenoxy)methyl)-6-isopropoxy-3,4-dihydroisoquinolin-2(1H)-yl)methanone (1180-144): Tetrahydroisoquinoline **1180-144** was prepared via procedure XIV using 3-chloro-4-fluorobenzoic acid (0.085 g, 0.49 mmol), N1-((ethylimino)methylene)-N3,N3-dimethylpropane-1,3-diamine (0.082 g, 0.53 mmol), N,N-dimethylpyridin-4-amine (0.055 g, 0.45 mmol), and tetrahydroisoquinoline **28d** (0.14 g, 0.41 mmol). The crude residue was purified by silica gel chromatography (ISCO, Redisep 12 g column, 10 – 80% EtOAc/hexanes gradient) to afford the title compound as an off-white foam (0.14 g, 69 % yield,

mixture of two amide rotamers). TLC (EtOAc: hexanes, 1:1, v/v) Rf = 0.32; ^{1}HNMR ($CDCl_3$, 400 MHz) δ: 7.74-7.72 (m, 0.5H), 7.45 (s, 1H), 7.29-7.13 (m, 2H), 6.97-6.93 (m, 0.5H), 6.82-6.69 (m, 5H), 5.98 (s, 0.5H), 5.15 (d, J = 6.4 Hz, 0.5H), 4.86-4.81 (m, *J* = 4.4 Hz, *J* = 12.0 Hz, 0.5H), 4.59-4.50 (m, 1H), 4.36 (m, 1H), 4.16 (t, *J* = 10.0 Hz, 0.5H), 4.01-3.96 (m, 2.5H), 3.75-3.68 (m, 1H), 3.30-3.15 (m, 1H), 2.93-2.75 (m, 1.5H), 1.40 (t, *J* = 6.8 Hz, 3H), 1.36-1.33 (m, 6H); ^{13}C NMR ($CDCl_3$, 100 MHz) δ: 169.8, 168.9, 160.2, 157.6, 157.1, 153.8, 153.6, 152.9, 152.4, 126.6, 135.4, 133.5, 130.9, 129.7, 128.7, 128.3, 128.1, 127.1, 125.1, 123.9, 121.5, 117.2, 116.8, 116.2, 115.8, 115.7, 115.6, 115.4, 114.8, 114.5, 71.2, 70.1, 64.2, 57.5, 52.2, 42.9, 35.6, 29.9, 28.4, 22.3, 22.2, 15.2; HRMS calcd. for $C_{28}H_{29}N_1O_4ClF$, 498.18419 $[M + H]^+$; found, 498.18419 $[M + H]^+$. Anal. ($C_{28}H_{29}N_1O_4ClF$): C, H, N.

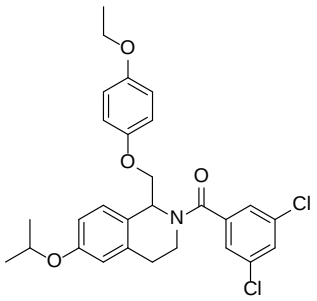

3,5-dichlorophenyl)(1-((4-ethoxyphenoxy)methyl)-6-isopropoxy-3,4-dihydroisoquinolin-2(1H)-yl)methanone (1180-101): Tetrahydroisoquinoline **1180-101** was prepared via procedure XIII using tetrahydroisoquinoline **28d** (0.20 g, 0.59 mmol) and 3,5-dischlorobenzoyl chloride (0.15 g, 0.70 mmol) in DCM (9.0 mL). The crude residue was purified by silica gel title compound as an off-white foam (0.070 g, 23 % mixture of two amide rotamers) TLC (EtOAc: hexanes, 1:1, v/v) Rf = 0.71 ^{1}HNMR ($CDCl_3$, 400 MHz) δ: 7.46-7.38 (m, 2H), 7.21-7.17 (m, 1H), 6.93-6.66 (m, 7H), 5.94-5.92 (m, 0.5 H), 5.08-5.50 (dd, *J* = 3.2 Hz, *J* = 9.6 Hz, 0.5H), 4.83-4.78 (dd, *J* = 5.2 Hz, *J* = 12.8 Hz, 0.5H), 4.56-4.48 (m, 1H), 4.33-4.28 (m, 1H), 4.17-4.14 (m, 0.5 H), 4.00-3.89 (m, 2.5 H), 3.68-3.67 (m, 1H), 3.28-3.07 (m, 1H), 2.93-2.72 (m, 1.5 H), 1.39-1.35 (t, *J* = 7.2 Hz, 3H), 1.33-1.32 (d, 6H); ^{13}CNMR ($CDCl_3$, 100 MHz) δ: 168.9, 168.2, 157.6, 157.2, 153.8, 152.9, 152.4, 139.4, 136.5, 135.7, 135.4, 129.8, 129.7, 128.7, 128.4, 126.5, 125.3, 124.9, 123.7, 116.2, 115.9, 115.7, 115.6, 115.3, 114.8, 114.5, 71.1,

70.1, 64.1, 57.4, 52.2, 42.8, 35.5, 29.9, 28.3, 22.3, 22.2, 15.1; HRMS calcd. for $C_{28}H_{30}Cl_2N_1O_4$, 514.15464 $[M + H]^+$; found 514.15456 $[M + H]^+$.

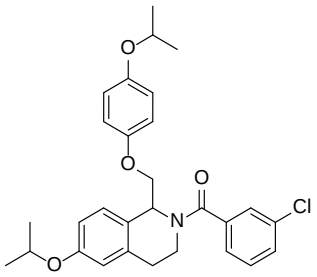

(3-chlorophenyl)(6-isopropoxy-1-((4-isopropoxyphenoxy)methyl)-3,4-dihydroisoquinolin-2(1H)-yl)methanone (1180-264): Tetrahydroisoquinoline **1180-264** was prepared via procedure XIII using tetrahydroisoquinoline **28e** (0.13 g, 0.36 mmol) and 3-chlorobenzoyl chloride (0.056 mL, 0.44 mmol) in dry DCM (5.8 mL). The crude residue was purified by silica gel chromatography (ISCO, Redisep 12 g column, 10 – 80% EtOAc/hexanes gradient) to afford the title compound as an off-white foam (0.048 g, 26 % mixture of two amide rotamers) TLC (EtOAc: hexanes, 1:3, v/v) Rf = 0.55; ^{1}HNMR ($CDCl_3$, 400 MHz) δ: 7.39-7.21 (m, 4H), 6.87-6.85 (m, 6H), 6.0-5.98 (m, 0.5H), 5.14-5.13 (m, 0.5H), 4.88-4.84 (m, J = 5.2 Hz, J = 12.0 Hz, 0.5), 4.60-4.53 (m, 1H), 4.46-4.40 (m, 1H), 4.36-4.32 (m, 1H), 4.17-4.06 (m, 0.5H), 3.95-3.92 (m, 0.5H), 3.74-3.66 (m, 1H), 3.30-2.73 (m, 2.5H), 1.35 (d, J = 6.4 Hz, 6H), 1.31 (d, J = 6.0 Hz, 6H); ^{13}CNMR (100 MHz, $CDCl_3$) δ: 157.3, 156.8, 152.9, 152.4, 152.3, 152.1, 138.2, 137.9, 136.4, 135.3, 134.6, 134.6, 129.9, 129.6, 129.5, 129.2, 128.5, 128.1, 127.9, 126.8, 125.6, 124.9, 124.6, 123.9, 117.5, 117.3, 117.2, 115.9, 115.6, 115.2, 115.1, 114.5, 114.2, 71.0, 70.8, 69.8, 57.1, 51.7, 42.6, 35.2, 29.7, 28.3, 22.1; HRMS calcd. for $C_{29}H_{33}ClN_1O_4$,494.20926 $[M + H]^+$; found 494.20919 $[M + H]^+$; mp: 103°C.

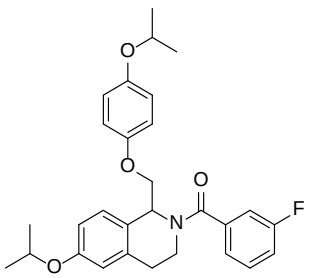

(3-fluorophenyl)(6-isopropoxy-1-((4-isopropoxyphenoxy)methyl)-3,4-dihydroisoquinolin-2(1H)-yl)methanone (1180-270): Tetrahydroisoquinoline **1180-270** was prepared via procedure XIII using tetrahydroisoquinoline **28e** (0.80 g, 0.23 mmol) and 3-fluorobenzoyl chloride (0.031 mL, 0.27 mmol) in dry DCM (3.5 mL). The crude residue was purified by silica gel chromatography (ISCO, Redisep 12 g column, 10 – 80% EtOAc/hexanes gradient) to afford the title compound as an off-white foam (0.074 g, 70 % mixture of two amide rotamers) TLC (EtOAc: hexanes, 1:3, v/v) Rf = 0.76; ^{1}HNMR ($CDCl_3$, 400 MHz) δ: 7.44-7.10 (m, 5H), 6.94-6.68 (m, 6H), 5.99 (t, J = 6.4 Hz, 0.5H), 5.18-5.13 (m, *J* = 5.6 Hz, *J* = 4.8 Hz, 0.5H), 4.89-4.48 (m, *J* = 5.6 Hz, *J* = 6.8 Hz, 0.5H), 4.58-4.48 (m, 1H), 4.47-4.36 (m, 1H), 4.39-4.31 (m, 1H), 4.17-4.10 (m, 0.5H), 3.97-3.92 (m, 0.5H), 3.76-3.64 (m, 1H), 3.32-3.09 (m, 1H), 2.96-2.72 (m, 1.5H), 1.36-1.29 (m, 12H); ^{13}CNMR (100 MHz, $CDCl_3$) δ: 170.5, 169.7, 164.0, 163.8, 161.6, 161.4, 157.6, 157.1, 153.1, 152.6, 152.5, 152.4, 138.7, 138.5, 136.6, 135.6, 130.7, 130.6, 130.3, 130.2, 130.1, 128.7, 128.3, 125.9, 125.2, 124.2, 123.4, 122.5, 120.5, 117.7, 117.6. 117.2. 116.9, 116.8, 116.7, 116.6, 116.2, 115.8, 115.4, 115.2, 114.7, 114.4, 114.3, 114.0, 71.3, 71.1, 71.0, 70.6, 70.2, 70.1, 60.6, 57.3, 53.7, 51.9, 42.8, 35.4, 31.8, 31.2, 29.9, 28.6, 22.9, 22.3, 22.2, 21.3, 14.4; HRMS calcd. for $C_{29}H_{33}FN_1O_4$, 478.23881 $[M + H]^+$; found 478.23858 $[M + H]^+$; Anal. ($C_{29}H_{32}FN_1O_4$): C, H, N

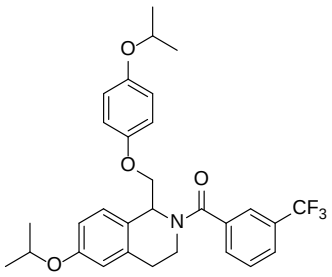

(6-isopropoxy-1-((4-isopropoxyphenoxy)methyl)-3,4-dihydroisoquinolin-2(1H)-yl)(3-(trifluoromethyl)phenyl)methanone (1180-271): Tetrahydroisoquinoline **1180-271** was prepared via procedure XIII using tetrahydroisoquinoline **28e** (0.80 g, 0.23 mmol) and 3-(trifluoromethyl)benzoyl chloride

chloride (0.041 mL, 0.27 mmol) in dry DCM (3.5 mL). The crude residue was purified by silica gel chromatography (ISCO, Redisep 12 g column, 10 – 80% EtOAc/hexanes gradient) to afford the title compound as an off-white foam (0.090 g, 77 % mixture of two amide rotamers) TLC (EtOAc: hexanes, 1:3, v/v) Rf = 0.83; ^{1}HNMR ($CDCl_3$, 400 MHz) δ: 7.91 (s, 0.5H), 7.69-7.49 (m, 3H), 7.25-7.22 (m, 0.5H), 6.92-6.69 (m, 8H), 5.99-6.00 (m, 0.5H), 5.10-5.08 (m, 0.5H), 4.90-4.86 (m, 0.5H), 4.59-4.48 (m, 1H), 4.47-4.38 (m, 2H), 4.18-4.12 (m, 0.5H), 3.95-3.92 (m, 0.5H), 3.73-3.71 (m, 1H), 3.33-3.12 (m, 1H), 2.94-2.74 (m, 1.5H), 1.36-1.29 (m, 12H); ^{13}CNMR (100 MHz, $CDCl_3$) δ: 170.5, 169.7, 157.6, 157.1, 153.1, 152.6, 152.5, 137.5, 137.3, 136.6, 135.5, 131.2, 130.2, 129.5, 129.3, 129.1, 128.7, 128.3, 126.5, 125.2, 123.9, 117.7, 117.6, 116.2, 115.9, 115.4, 114.8, 114.5, 71.3, 71.1, 70.1, 57.5, 53.7, 52., 42.9, 35.5, 29.9, 28.5, 22.3, 22.2; HRMS calcd. for $C_{30}H_{33}F_3N_1O_4$, 528.23562 $[M + H]^+$; found 528.23530 $[M + H]^+$.

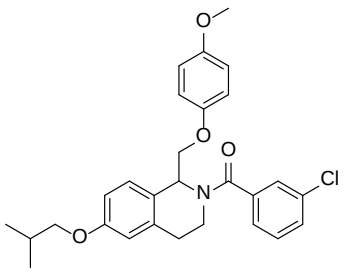

(3-chlorophenyl)(6-isobutoxy-1-((4-methoxyphenoxy)methyl)-3,4-dihydroisoquinolin-2(1H)-yl)methanone (1180-114): Dihydroisoquinoline **28f** was prepared via Procedure X using **15f** (1.1 g, 3.1 mmol) and phosphorous trichloride (1.9 mL, 3.1 mmol) in dry toluene (16 mL). The crude residue (0.82 g) was carried on without further purification. HRMS calcd. for $C_{21}H_{26}O_3N_1$, 340.19072 $[M + H]^+$; found 340.19061 $[M + H]^+$. Tetrahydroisoquinoline **28f** was prepared via Procedure XII using dihydroisoquinoline **27f** (0.82 g, 2.4 mmol) and sodium borohydride (0.27 g, 7.2 mmol) in dry MeOH (13 mL). The crude residue was purified by silica gel chromatography (ISCO, Redisep 20 g column, 0-20% MeOH/DCM gradient) to afford the title compound as a yellow solid (0.45 g, 55 %) in an impure form. The impurities were inseparable by chromatography. The product was visible by LCMS and was carried on without further purification. HRMS calcd. for $C_{21}H_{28}O_3N_1$, 342.20637 [M

+ H]$^+$; found 342.20630 [M + H]$^+$. Tetrahydroisoquinoline **1180-114** was prepared via Procedure XIII using tetrahydroisoquinoline **28f** (0.23 g, 0.66 mmol) and 3-chlorobenzoyl chloride (0.11 mL, 0.79 mmol) in DCM (10 mL). The crude residue was purified by silica gel chromatography (ISCO, Redisep 12 g column, 10 – 80% EtOAc/hexanes gradient) to afford the title compound as an off-white foam (0.087g, 27% yield, mixture of two amide rotamers) TLC (EtOAc: hexanes, 1:1, v/v) Rf = 0.68; ^{1}HNMR ($CDCl_3$, 400 MHz) δ: 7.58 (s, 0.5H), 7.39-7.19 (m, 4H), 6.92-6.67 (m, 6.5H), 5.97-5.96 (m, 0.5H), 5.12-5.11 (m, *J* = 3.2 Hz, *J* = 9.6 Hz, 0.5H), 4.37-4.30 (m, 1H), 4.13 (t, *J* =9.6 Hz, 0.5H), 3.93-3.89 (m, 1H), 3.72 (s, 3H), 3.69 (d, *J* = 6.4 Hz, 2H), 3.66-3.63 (m, 0.5H), 3.28-3.09 (m, 1H), 2.92-2.72 (m, 1.5H), 2.11-2.01 (m, 1H), 1.00 (d, *J* = 6.8 Hz, 6H); ^{13}C NMR ($CDCl_3$, 100 MHz) δ: 170.4, 169.7, 158.9, 158.4, 154.4, 154.3, 153.0, 153.6, 138.4, 138.2, 136.6, 135.5, 134.9, 134.5, 130.2, 129.9, 129.8, 128.7, 128.3, 128.2, 127.0, 125.8, 125.1, 124.9, 124.1, 115.9, 115.4, 114.9, 114.8, 114.4, 113.7, 113.5, 74.7, 71.3, 70.2, 57.3, 55.9, 51.9, 42.9, 35.5, 29.9, 28.5, 19.5, 19.4; HRMS calcd. for $C_{28}H_{31}NO_4{}^{35}Cl$, 480.19361 [M + H]$^+$; found, 480.19346 [M + H]$^+$; Anal. ($C_{28}H_{30}N_1O_4Cl$): C, H, N.

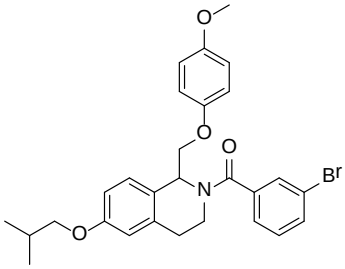

(3-bromophenyl)(6-isobutoxy-1-((4-methoxyphenoxy)methyl)-3,4-dihydroisoquinolin-2(1H)-yl)methanone (1180-115): Dihydroisoquinoline **27f** was prepared via Procedure X using **15f** (1.1 g, 3.1 mmol) and phosphorous trichloride (1.9 mL, 3.1 mmol) in dry toluene (16 mL). The crude residue (0.82 g) was carried on without further purification. HRMS calcd. for $C_{21}H_{26}O_3N_1$, 340.19072 [M + H]$^+$; found 340.19061 [M + H]$^+$. Tetrahydroisoquinoline **28f** was prepared via Procedure XII using dihydroisoquinoline **27f** (0.82 g, 2.4 mmol) and sodium borohydride (0.27 g, 7.2 mmol) in dry MeOH (13 mL). The crude residue was purified by silica gel chromatography (ISCO, Redisep 20 g column, 0-20% MeOH/DCM gradient) to afford the title compound as a yellow solid (0.45 g, 55 %)

in an impure form. The impurities were inseparable by chromatography. The product was visible by LCMS and was carried on without further purification. HRMS calcd. for $C_{21}H_{28}O_3N_1$, 342.20637 [M + H]$^+$; found 342.20630 [M + H]$^+$. Tetrahydroisoquinoline **1180-115** was prepared via Procedure XIII using tetrahydroisoquinoline **28f** (0.23 g, 0.66 mmol) and 3-chlorobenzoyl chloride (0.11 mL, 0.79 mmol) in DCM (10 mL). The crude residue was purified by silica gel chromatography (ISCO, Redisep 12 g column, 10 – 80% EtOAc/hexanes gradient) to afford the title compound as an off-white foam (0.087g, 27% yield, mixture of two amide rotamers) TLC (EtOAc: hexanes, 1:1, v/v) Rf = 0.71; ^{1}HNMR ($CDCl_3$, 400 MHz) δ: 7.73 (s, 0.5H), 7.54-7.5 (m, 1H), 7.42-7.39 (m, 0.5H), 7.29-7.19 (m, 2H), 6.92-6.67 (m, 7H), 5.95-5.96 (m, 0.5H), 5.12-5.10 (m, 0.5H), 4.86-4.81 (m, *J* = 5.2 Hz, *J* = 12.4 Hz, 0.5H), 4.33 (s, 1H), 4.12 (t, *J* = 9.6 Hz, 0.5H), 3.92-3.89 (m, 1H), 3.75 (s, 3H), 3.69 (d, *J* = 6.4 Hz, 2H), 3.66-3.63 (m, 0.5H), 3.27-3.11 (m, 1H), 2.90-2.72 (m, 1.5H), 2.11-2.01 (m, 1H), 1.00 (d, *J* = 6.8 Hz, 6H); ^{13}C NMR ($CDCl_3$, 100 MHz) δ: 170.3, 169.5, 160.3, 158.9, 158.4, 154.4, 154.3, 153.1, 152.6, 138.6, 136.6, 135.5, 132.9, 132.7, 131.0, 130.5, 130.1, 129.9, 128.7, 128.3, 126.2, 125.3, 125.1, 124.1, 122.9, 122.7, 115.9, 115.5, 114.9, 113.9, 114.4, 113.7, 113.5, 74.7, 71.3, 70.1, 57.3, 55.9, 51.9, 42.8, 40.4, 35.5, 29.9, 28.5, 19.5; HRMS calcd. for $C_{28}H_{31}NO_4{}^{79}Br$, 524.14310 [M + H]$^+$; found, 524.14301 [M + H]$^+$; Anal. ($C_{28}H_{30}N_1O_4Br$): C, H, N.

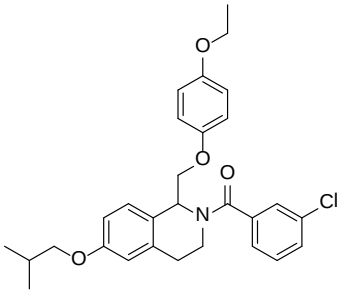

(3-chlorophenyl)(1-((4-ethoxyphenoxy)methyl)-6-isobutoxy-3,4-dihydroisoquinolin-2(1H)-yl)methanone (1180-124): Tetrahydroisoquinoline **1180-124** was prepared via Procedure XIII using tetrahydroisoquinoline **28g** (0.18 g, 0.50 mmol) and 3-chlorobenzoyl chloride (0.076 mL, 0.60 mmol) in DCM (7.7 mL). The crude residue was purified by silica gel chromatography (ISCO, Redisep 12 g column, 10 – 80% EtOAc/hexanes gradient) to afford the title compound as an off-white foam (0.80

g, 33 % yield, mixture of two amide rotamers) TLC (EtOAc: hexanes, 1:1, v/v) Rf = 0.67; ^{1}HNMR ($CDCl_3$, 400 MHz) δ: 7.59 (s, 0.5H), 7.42-7.21 (m, 4H), 6.94-6.92 (m, 0.5), 6.85-6.69 (m, 6H), 5.98 (t, *J* = 4.8 Hz, 0.5H), 5.15-5.12 (m, *J* = 3.6 Hz, *J* = 9.6 Hz, 0.5H), 4.89-4.84 (m, *J* = 5.2 Hz, *J* = 12.4 Hz, 0.5H), 4.39-4.32 (m, 1H), 4.14 (t, *J* = 10.4 Hz, 0.5H), 3.98 (q, *J* = 6.8 Hz, 2H), 3.94-3.92 (m, 0.5H), 3.79-3.75 (m, 0.5H), 3.71 (d, *J* = 6.4 Hz, 2H), 3.68-3.65 (m, 0.5H), 3.31-3.11 (m, 1H), 2.94-2.74 (m, 1.5H), 2.11-2.05 (m, 1H), 1.40 (t, *J* = 6.8 Hz, 3H), 1.03 (d, *J* = 6.8 Hz, 6H); ^{13}C NMR ($CDCl_3$, 100 MHz) δ: 170.5, 169.7, 158.9, 158.5, 153.7, 153.6, 153.0, 152.5, 138.4, 138.2, 136.6, 138.2, 136.6, 135.5, 134.9, 134.6, 130.3, 129.9, 128.7, 128.3, 128.2, 127.1, 125.9, 125.2, 124.9, 124.1, 115.9, 115.7, 115.6, 115.5, 114.9, 114.4, 113.7, 113.5, 74.7, 71.3, 70.2, 64.2, 57.3, 52.0, 42.9, 35.5, 29.9, 28.5, 19.5, 15.2; HRMS calcd. for $C_{29}H_{33}NO_4{}^{35}Cl$, 494.20926 $[M + H]^+$; found, 494.20919 $[M + H]^+$; mp: 75°C. Anal. ($C_{29}H_{32}N_1O_4Cl$): C, H, N

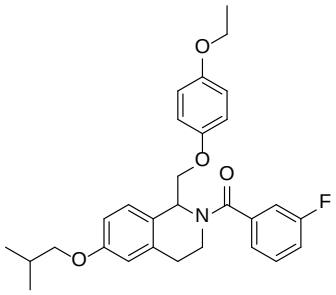

(1-((4-ethoxyphenoxy)methyl)-6-isobutoxy-3,4-dihydroisoquinolin-2(1H)-yl)(3-fluorophenyl)methanone (1180-126): Tetrahydroisoquinoline **1180-126** was prepared via Procedure XIII using tetrahydroisoquinoline **28g** (0.18 g, 0.50 mmol) and 3-fluorobenzoyl chloride (0.073 mL, 0.60 mmol) in DCM (7.7 mL). The crude residue was purified by silica gel chromatography (ISCO, Redisep 12 g column, 10 – 80% EtOAc/hexanes gradient) to afford the title compound as an off-white foam (0.61 g, 27 % yield, mixture of two amide rotamers). TLC (EtOAc: hexanes, 1:1, v/v) Rf = 0.83; ^{1}HNMR ($CDCl_3$, 400 MHz) δ: 7.47-7.09 (m, 5H), 6.94-6.92 (m, 0.5H), 6.87-6.74 (m, 5H),6.68-6.69 (m, 0.5H), 5.98 (t, *J* = 4.8 Hz, 0.5H), 5.16-5.14 (m, *J* = 6.4 Hz, *J* = 9.6 Hz, 0.5 H), 4.89-4.84 (m, *J* = 5.2 Hz, *J* = 12.8 Hz, 0.5H), 4.36-4.31 (m, 1H), 4.15-4.10 (m, 0.5H), 4.00-3.95 (q, *J* = 6.4 Hz, 2H), 3.93-3.91 (m, 0.5H), 3.79-3.74 (m, 0.5H), 3.71 (d, *J* = 6.4 Hz, 2H), 3.68-3.65 (m, 0.5H),

2.11-2.03 (m, 1H), 1.40 (t, J = 6.8 Hz, 3H), 1.03 (d, J = 6.8 Hz, 6H); ^{13}C NMR ($CDCl_3$, 100 MHz) δ: 170.6, 169.8, 164.0, 158.9, 158.4, 153.7, 153.6, 153.0, 152.5, 138.6, 136.6, 135.5, 130.7, 130.3, 128.7, 126.1, 125.2, 124.1, 123.4, 122.5, 120.7, 117.2, 116.8, 116.6, 115.8, 115.7, 115.6, 115.4, 115.2, 114.8, 114.4, 114.3, 114.1, 113.7, 113.4, 111.2, 74.6, 71.3, 70.2, 64.2, 57.3, 51.9, 42.8, 35.5, 29.9, 28.4, 19.5, 15.2; HRMS calcd. for $C_{29}H_{33}NO_4F$, 478.23881 $[M + H]^+$; found, 478.23887 $[M + H]^+$.

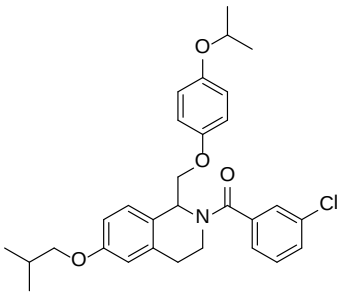

(3-chlorophenyl)(6-isobutoxy-1-((4-isopropoxyphenoxy)methyl)-3,4-dihydroisoquinolin-2(1H)-yl)methanone (1180-139): Tetrahydroisoquinoline **1180-139** was prepared via Procedure XIII using tetrahydroisoquinoline **28h** (0.12 g, 0.32 mmol) and 3-chlorobenzoyl chloride (0.049 mL, 0.38 mmol) in DCM (5.0 mL). The crude residue was purified by silica gel chromatography (ISCO, Redisep 12 g column, 10 – 80% EtOAc/hexanes gradient) to afford the title compound as an off-white foam (0.056 g, 34 % yield, mixture of two amide rotamers) TLC (EtOAc: hexanes, 1:1, v/v) Rf = 0.83; ^{1}HNMR ($CDCl_3$, 400 MHz) δ: 7.58-7.44 (m, 1H), 7.39-7.19 (m, 4H), 6.92-6.67 (m, 6H), 5.97 (t, J = 4.8 Hz, 0.5H), 5.13-5.10 (m, J = 3.2 Hz, J = 9.6 Hz, 0.5H), 4.87-4.82 (m, J = 5.6 Hz, J = 13.2 Hz, 0.5H), 4.45-4.37 (m, 1H), 4.36-4.29 (m, 1H), 4.14-4.09 (m, 0.5H), 3.92-3.89 (m, 0.5H), 3.79-3.72 (m, 1H), 3.69 (d, J = 6.4 Hz, 2H), 3.29-3.09 (m, 1H), 2.92-2.71 (m, 1.5H), 2.11-2.01 (m, 1H), 1.28 (d, J = 6.4 Hz, 6H), 1.00 (d, J = 6.8 Hz, 6H); ^{13}C NMR ($CDCl_3$, 100 MHz) δ: 170.1, 169.7, 158.9, 158.4, 153.1, 152.6, 152.4, 138.3, 138.1, 136.6, 135.5, 134.9, 134.7, 134.5, 133.6, 130.4, 130.3, 129.9, 128.6, 128.4, 128.3, 128.2, 127.0, 125.9, 124.9, 117.7, 117.6, 115.8, 115.4, 114.4, 113.7, 113.5, 74.7, 71.1, 70.1, 57.3, 52.0, 42.9, 35.5, 29.9, 22.3, 19.5; HRMS calcd. for $C_{30}H_{35}NO_3{}^{35}Cl$, 508.22491 $[M + H]^+$; found, 508.22516 $[M + H]^+$.

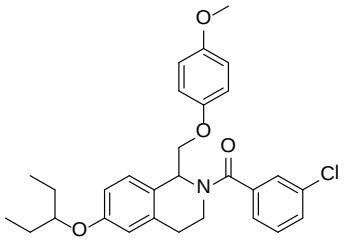

(3-chlorophenyl)(1-((4-methoxyphenoxy)methyl)-6-(pentan-3-yloxy)-3,4-dihydroisoquinolin-2(1H)-yl)methanone (1180-109): Tetrahydroisoquinoline **1180-109** was prepared via Procedure XIII using tetrahydroisoquinoline **28i** (0.16 g, 0.44 mmol) and 3-chlorobenzoyl chloride (0.069 mL, 0.52 mmol) in DCM (6.8 mL). The crude residue was purified by silica gel chromatography (ISCO, Redisep 12 g column, 10-80% EtOAc/hexanes gradient) to afford the title compound as a white foam (0.087 g, 41 % yield, mixture of two amide rotamers) TLC (EtOAc: hexanes, 1:1, v/v) Rf = 0.69; ^{1}HNMR ($CDCl_3$, 400 MHz) δ: 7.59 (s, 1H), 7.37-7.18 (m, 4H), 6.91-6.67 (m, 7H), 5.97 (t, *J* = 4.8 Hz, 0.5 H), 5.13-5.10 (m, *J* = 3.6 Hz, *J* = 10 Hz, 0.5 H), 4.86-4.82 (m, *J* = 5.6 Hz, *J* = 13.2 Hz, 0.5 H), 4.37-4.29 (m, 1H), 4.14-4.06 (m, 1.5 H), 3.92-3.89 (m, *J* = 3.2 Hz, *J* = 13.2 Hz, 0.5 H), 3.75 (s, 3H), 3.69-3.62 (m, 1H), 3.27-3.08 (m, 1H), 2.93-2.71 (m, 1.5H), 1.69-1.63 (m, 4H), 0.95 (t, *J* = 7.2 Hz, 6H); ^{13}CNMR ($CDCl_3$, 100 MHz) δ: 170.4, 169.6, 158.4, 157.9, 154.4, 154.2, 153.1, 152.6, 138.4, 138.3, 136.6, 135.5, 134.8, 134.5, 130.2, 129.9, 129.8, 128.7, 128.3, 128.2, 127.0, 125.9, 125.1, 124.9, 123.9, 116.3, 115.9, 115.4, 114.9, 114.8, 114.5, 80.3, 71.2, 70.1, 57.3, 55.9, 51.9, 42.8, 35.4, 29.9, 28.6, 26.4, 9.8; HRMS calcd. for $C_{29}H_{33}NO_4{}^{35}Cl$, 494.20962 $[M + H]^+$; found 494.21000 $[M + H]^+$; Anal. ($C_{29}H_{32}N_1O_4Cl$): C, H, N.

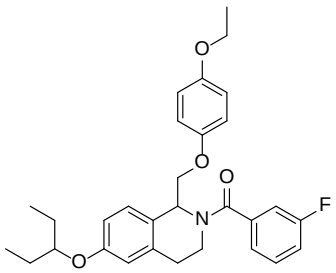

(1-((4-ethoxyphenoxy)methyl)-6-(pentan-3-yloxy)-3,4-dihydroisoquinolin-2(1H)-yl)(3-fluorophenyl)methanone (1180-125): Dihydroisoquinoline **27j** was prepared via Procedure XI

using **15o** (0.27 g, 0.69 mmol) and phosphorous trichloride (0.91 mL, 2.1 mmol) in dry toluene (3.5 mL). The crude residue (0.22 g) was carried on without further purification. HRMS calcd. for $C_{23}H_{30}O_3N_1$, 368.22202 $[M + H]^+$; found 368.22200 $[M + H]^+$. Tetrahydroisoquinoline **28j** was prepared via Procedure XII using dihydroisoquinoline **27j** (0.22 g, 0.61 mmol) and sodium borohydride (0.069 g, 1.8 mmol) in dry MeOH (3.0 mL). The crude residue was purified by silica gel chromatography (ISCO, Redisep 20 g column, 0-20% MeOH/DCM gradient) to afford the title compound as a yellow solid (0.15 g, 68 %) in an impure form. The impurities were inseparable by chromatography. The product was visible by LCMS and was carried on without further purification. HRMS calcd. for $C_{23}H_{31}O_3N_1$, 370.23767 $[M + H]^+$; found 370.23769 $[M + H]^+$. Tetrahydroisoquinoline **1180-125** was prepared via Procedure XIII using tetrahydroisoquinoline **28j** (0.15 g, 0.40 mmol) and 3-fluorobenzoyl chloride (0.049 mL, 0.60 mmol) in DCM (6.4 mL). The crude residue was purified by silica gel chromatography (ISCO, Redisep 12 g column, 10-80% EtOAc/hexanes gradient) to afford the title compound as a white foam (0.036 g, 17 % yield, mixture of two amide rotamers); TLC (EtOAc: hexanes, 1:1, v/v) Rf = 0.74; ^{1}HNMR ($CDCl_3$, 400 MHz) δ: 7.43-7.09 (m, 4.5H), 6.93-6.69 (m, 6.5H), 5.99-5.97 (m, 0.5H), 5.16-5.14 (m, J = 2.8 Hz, J = 9.2 Hz, 0.5H), 4.88-4.84 (m J = 5.2 Hz, J = 12.4 Hz, 0.5H), 4.36-4.32 (m, 1H), 4.16-4.08 (m, 1H), 4.00-3.96 (q, J = 6.8 Hz, 2H), 3.93-3.92 (m, 0.5H), 3.79-3.65 (m, 1H), 3.30-3.11 (m, 1H), 2.93-2.72 (m, 1.5H), 1.71-1.65 (m, 4H), 1.41-1.38 (t, J = 7.2 Hz, 3H), 0.99-0.95 (t, J = 7.2 Hz); ^{13}CNMR ($CDCl_3$, 100 MHz) δ: 170.5, 169.7, 162.8 (d, J = 247 Hz), 162.6 (d, J = 247 Hz), 158.4, 157.9, 153.7, 153.6, 153.0, 152.5, 138.8, 138.7, 138.6, 136.6, 135.5, 130.7, 130.7, 130.3, 130.2, 128.7, 128.3, 125.1, 124.0, 123.5, 122.5, 116.9, 116.8, 116.7, 116.6, 116.3, 115.9, 115.8, 115.7, 115.6, 115.4, 115.2, 114.7, 114.4, 114.3, 114.0, 80.4, 71.3, 70.2, 64.2, 57.3, 51.9, 42.7, 35.4, 29.9, 28.6, 26.2, 15.2, 9.8; HRMS calcd. for $C_{30}H_{53}NO_4F$, 492.25446 $[M + H]^+$; found 492.25426 $[M + H]^+$; Anal. ($C_{30}H_{35}N_1O_4Cl$): C, H, N.

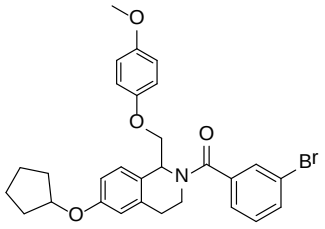

(3-bromophenyl)(6-(cyclopentyloxy)-1-((4-methoxyphenoxy)methyl)-3,4-dihydroisoquinolin-2(1H)-yl)methanone (1180-106): Tetrahydroisoquinoline **1180-106** was prepared via Procedure XIII using tetrahydroisoquinoline **28k** (0.092 g, 0.26 mmol) and 3-bromobenzoyl chloride (0.041 mL, 0.31 mmol) in DCM (4.1 mL). The crude residue was purified by silica gel chromatography (ISCO, Redisep12 g column, 10-80% EtOAc/hexanes gradient) to afford the title compound as a white foam (0.044 g, 32% yield, mixture of two amide rotamers) TLC (EtOAc: hexanes, 1:1, v/v) Rf = 0.44; ^{1}HNMR ($CDCl_3$, 400 MHz) δ: 8.20-7.69 (m, 1H), 7.53-7.41 (m, 2H), 7.34-7.17 (m, 1H), 6.90-6.64 (m, 7H), 5.97-5.95 (m, 0.5H), 5.11-5.10 (m, 0.5H), 4.86-4.81 (m, *J* = 5.2 Hz, *J* = 12.4 Hz, 0.5H), 4.73-4.72 (m, 1H), 4.33-4.32 (m, 1H), 4.12 (t, *J* = 10 Hz, 0.5H), 3.92-3.89 (dd, *J* = 3.6 Hz, *J* = 10 Hz, 0.5H), 3.75 (s, 3H), 3.70-3.65 (m, 1H), 3.27-3.09 (m, 1H), 2.89-2.70 (m, 1.5H), 1.88-1.73 (m, 6H), 1.66-1.56 (m, 2H); ^{13}CNMR ($CDCl_3$, 100 MHz) δ: 170.4, 169.6, 169.1, 157.8, 157.3, 154.4, 154.3, 153.1, 152.8, 138.6, 138.4, 136.6, 136.5, 135.4, 133.3, 132.9, 132.7, 131.0, 130.5, 130.3, 130.1, 129.8, 128.9, 128.6, 128.2, 126.3, 125.3, 124.8, 123.8, 122.9, 122.7, 122.6, 115.9, 115.5, 114.9, 114.8, 114.5, 79.5, 71.3, 70.2, 57.3, 55.9, 51.9, 42.8, 35.5, 33.0, 29.9, 28.5, 24.2; HRMS calcd. for $C_{29}H_{31}NO_4{}^{79}Br$, 536.14310 $[M + H]^+$; found 536.14408 $[M + H]^+$.

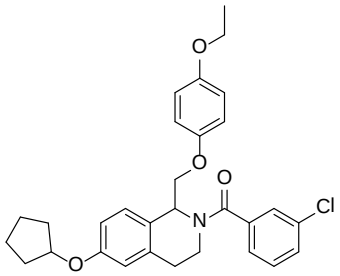

(3-chlorophenyl)(6-(cyclopentyloxy)-1-((4-ethoxyphenoxy)methyl)-3,4-dihydroisoquinolin-2(1H)-yl)methanone (1180-110): Tetrahydroisoquinoline **1180-110** was prepared via procedure XIII

using tetrahydroisoquinoline **28l** (0.18 g, 0.50 mmol) and 3-chlorobenzoyl chloride (0.080 mL, 0.60 mmol) in DCM (8.0 mL). The crude residue was purified by silica gel chromatography (ISCO, Redisep 12 g column, 10 – 80% EtOAc/hexanes gradient) to afford the title compound as an off-white foam (0.17 g, 68% yield, mixture of two amide rotamers) TLC (EtOAc: hexanes, 1:1, v/v) Rf = 0.69; ^{1}HNMR ($CDCl_3$, 400 MHz) δ: 8.04-7.94 (m, 0.5H), 7.55-7.53 (m, 0.5H), 7.40-7.25 (m, 3H), 7.20-7.17 (m, 0.5H), 6.90-6.75 (m, 5H), 6.70-6.64 (m, 1.5H), 5.98 (t, *J* = 5.2 Hz, 0.5H), 5.13-5.10 (m, *J* = 3.2 Hz, *J* = 9.6 Hz, 0.5H), 4.87-4.82 (m, *J* = 5.2 Hz, 12.8 Hz, 0.5H), 4.37-4.29 (m, 1H), 4.13 (t, *J* = 10.0 Hz, 0.5H), 3.96 (q, *J* = 7.2 Hz, 2H), 3.92-3.89 (m, 0.5H), 3.76-3.63 (m, 1H), 3.29-3.09 (m, 1H), 2.29-2.70 (m, 1.5H), 1.88-1.74 (m, 6H), 1.68-1.60 (m, 2H), 1.38 (t, *J* = 6.8 Hz); ^{13}C NMR ($CDCl_3$, 100 MHz) δ: 170.5, 169.8, 169.2, 157.8, 157.2, 153.7, 153.6, 152.9, 152.5, 138.3, 136.5, 135.4, 134.9, 134.8, 134.5, 133.7, 130.4, 130.2, 129.9, 129.8, 128.7, 128.2, 127.0, 125.9, 124.9, 123.8, 115.9, 115.7, 115.6, 115.5, 115.4, 114.5, 114.2, 79.5, 71.3, 70.1, 64.2, 57.3, 52.0, 42.8, 35.5, 33.1, 29.9, 28.6, 24.2, 15.2; HRMS calcd. for $C_{30}H_{33}NO_4{}^{35}Cl$, 506.20925 $[M + H]^+$; found, 506.20991 $[M + H]^+$.

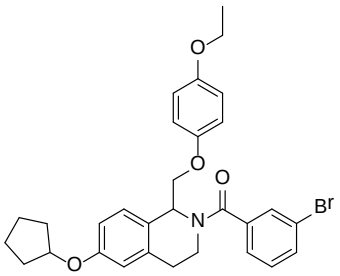

(3-bromophenyl)(6-(cyclopentyloxy)-1-((4-ethoxyphenoxy)methyl)-3,4-dihydroisoquinolin-2(1H)-yl)methanone (1180-111): Tetrahydroisoquinoline **1180-111** was prepared via Procedure XIII using tetrahydroisoquinoline **28l** (0.18 g, 0.50 mmol) and 3-bromobenzoyl chloride (0.080 mL, 0.60 mmol) in DCM (8.0 mL). The crude residue was purified by silica gel chromatography (ISCO, Redisep 12 g column, 10 – 80% EtOAc/hexanes gradient) to afford the title compound as an off-white foam (0.18 g, 64% yield, mixture of two amide rotamers) TLC (EtOAc: hexanes, 1:1, v/v) Rf = 0.69; ^{1}HNMR ($CDCl_3$, 400 MHz) δ: 8.19-7.67 (m, 1H), 7.55-7.51 (m, 1H), 7.42 (d, *J* = 7.6 Hz, 0.5H), 7.33-7.17 (m, 2H), 6.90-6.76 (m, 5H), 6.70-6.69 (m, 1H), 6.64 (s, 0.5H), 5.96 (t, *J* = 4.8 Hz, 0.5H),

5.13-5.10 (m, J = 3.4 Hz, 10.0 Hz, 0.5H), 4.86-4.81 (m, J = 5.6 Hz, J = 12.8 Hz, 0.5H), 4.74-4.70 (m, 1H), 4.36-4.29 (m, 1H), 4.12 (t, J = 10 Hz, 0.5H), 3.95 (q, J = 6.8 Hz, 2H), 3.92-3.89 (m, 0.5H), 3.76-3.63 (m, 1H), 3.28-3.08 (m, 1H), 2.90-2.71 (m, 1.5H), 1.88-1.76 (m, 6H), 1.68-1.60 (m, 2H), 1.37 (t, J = 6.8 Hz, 3H); ^{13}C NMR ($CDCl_3$, 100 MHz) δ: 170.3, 169.6, 157.8, 157.2, 153.7, 153.6, 152.9, 152.5, 138.6, 138.4, 136.5, 135.4, 1133.3, 132.9, 132.7, 131.0, 130.5, 130.2, 130.1, 129.8, 128.9, 128.6, 126.3, 125.3, 124.9, 123.8, 122.9, 122.7, 115.9, 115.6, 115.4, 114.3, 79.5, 71.3, 70.1, 64.2, 57.3, 51.9, 42.9, 35.8, 33.1, 29.9, 28.6, 24.2, 15.2; HRMS calcd. for $C_{30}H_{33}NO_4{}^{79}Br$, 550.15875 $[M + H]^+$; found, 550.15953 $[M + H]^+$.

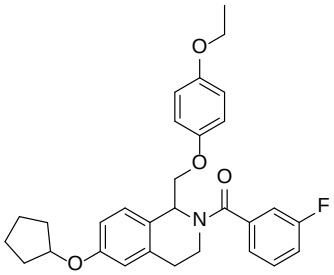

(6-(cyclopentyloxy)-1-((4-ethoxyphenoxy)methyl)-3,4-dihydroisoquinolin-2(1H)-yl)(3-fluorophenyl)methanone (1180-112): Tetrahydroisoquinoline **1180-112** was prepared via Procedure XIII using tetrahydroisoquinoline **28l** (0.18 g, 0.50 mmol) and 3-fluorobenzoyl chloride (0.073 mL, 0.60 mmol) in DCM (8.0 mL). The crude residue was purified by silica gel chromatography (ISCO, Redisep 12 g column, 10 – 80% EtOAc/hexanes gradient) to afford the title compound as an off-white foam (0.18 g, 64% yield, mixture of two amide rotamers) TLC (EtOAc: hexanes, 1:1, v/v) Rf = 0.69; ^{1}HNMR ($CDCl_3$, 400 MHz) δ: 7.85-7.71 (m, 0.5H), 7.43-7.09 (m, 4H), 6.90-6.74 (m, 5H), 6.69 (s, 1H), 6.64 (s, 0.5H), 5.97 (t, J = 4.4 Hz, J = 9.2 Hz, 0.5H), 5.15-5.11 (m, J = 2.8 Hz, J = 9.2 Hz, 0.5H), 4.87-4.82 (m, J = 5.6 Hz, J = 13.2 Hz, 0.5H), 4.74-4.71 (m, 1H), 4.37-4.29 (m, 1H), 4.11 (t, J = 10.4 Hz, 0.5H), 3.95 (q, J = 7.2 Hz, 2H), 3.91-3.89 (m, 0.5H), 3.76-3.63 (m, 1H), 3.28-3.08 (m, 1H), 2.93-2.70 (m, 1.5H), 1.88-1.76 (m, 6H), 1.68-1.60 (m, 2H), 1.37 (t, J = 6.8 Hz, 3H); ^{13}C NMR ($CDCl_3$, 100 MHz) δ: 170.6, 169.8, 164.0, 163.8, 161.6, 161.4, 157.8, 157.3, 153.7, 153.6, 153.0, 152.5, 138.7, 138.6, 138.5, 138.4, 136.5, 135.5, 130.7, 130.6, 130.3, 128.6, 128.2, 126.0, 124.9, 123.9, 123.5, 122.4,

120.4, 117.2, 116.9, 116.8, 116.7, 116.6, 115.9, 115.6, 115.5, 115.4, 115.2, 114.5, 114.3, 114.2, 114.0, 113.8, 106.2, 103.0, 94.5, 82.1, 79.5, 71.3, 70.2, 64.2, 57.3, 51.9, 42.8, 35.5, 33.1, 29.9, 28.6, 24.2, 15.2; HRMS calcd. for $C_{30}H_{33}NO_4F$, 490.23881 $[M + H]^+$; found, 490.23958 $[M + H]^+$.

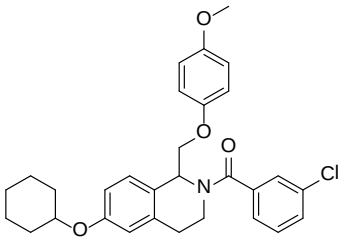

(3-chlorophenyl)(6-(cyclohexyloxy)-1-((4-methoxyphenoxy)methyl)-3,4-dihydroisoquinolin-2(1H)-yl)methanone (1180-107): Dihydroisoquinoline **27m** was prepared via Procedure XI using amide 15h (0.52 g, 1.4 mmol) and phosphorus trichloride (0.84 mL, 4.1 mmol) in dry toluene (7.6 mL). The crude solid was carried on without further purification. HRMS calcd. for $C_{23}H_{28}O_3N$, 366.20627 $[M + H]^+$; found 366.20615 $[M + H]^+$. Tetrahydroisoquinoline **28m** was prepared via Procedure XII using **27m** (0.58 g, 1.6 mmol) and sodium borohydride (0.18 g, 4.8 mmol) in dry MeOH (8.0 mL). The crude residue was subjected to flash column chromatography (ISCO, Redisep 24 g column, 0-10% MeOH/DCM gradient) to afford tetrahydroisoquinoline 8d (0.32 g, 55 %) in an impure form. The impurities were inseparable by chromatography. The product was visible by LCMS and was carried on without further purification. HRMS calcd. for $C_{23}H_{30}NO_3$, 368.22202 $[M + H]^+$; found, 368.22227 $[M + H]^+$. Tetrahydroisoquinoline **1180-107** was prepared via Procedure XIII using tetrahydroisoquinoline **28m** (0.16 g, 0.44 mmol) and 3-chlorobenzoyl chloride (0.071 mL, 0.53 mmol) in DCM (6.9 mL). The crude residue was purified by silica gel chromatography (ISCO, Redisep 12 g column, 10-80% EtOAc/hexanes gradient) to afford the title compound as a white foam (0.038 g, 17% yield, mixture of two amide rotamers) TLC (EtOAc: hexanes, 1:1, v/v) Rf = 0.72 ; ^{1}HNMR ($CDCl_3$, 400 MHz) δ: 7.57 (s, 0.5H), 7.39-7.17 (m, 3H), 7.25-7.23 (m, 1H), 7.19-7.17 (m, 0.5H), 6.90-6.66 (m, 6H), 5.96 (t, J = 4.8 Hz, 0.5H), 5.12-5.09 (m, 3.2 Hz, J = 9.2 Hz, 0.5H), 4.86-4.81 (m, J = 5.6 Hz, J = 12.8 Hz, 0.5H), 4.33-4.29 (m, 1H), 4.23-4.20 (m, 1H), 4.14-4.09 (m, 0.5H),

3.92-3.89 (m, 0.5H), 3.75 (s, 3H), 3.72-3.62 (m, 1H), 3.27-3.08 (m, 1H), 2.90-2.70 (m, 1.5H), 1.98-1.95 (m, 2H), 1.79-1.77 (m, 2H), 1.57-1.23 (m, 8H); ^{13}CNMR ($CDCl_3$, 100 MHz) δ: 170.4, 169.6, 167.2, 157.5, 156.9, 154.3, 153.1, 152.6, 138.4, 138.2, 136.6, 135.5, 134.8, 134.5, 132.0, 130.2, 129.8, 128.7, 128.3, 127.1, 125.8, 124.8, 124.1, 122.6, 117.7, 116.3, 116.0, 115.9, 115.4, 114.9, 114.8, 114.6, 71.3, 70.7, 70.2, 69.3, 66.6, 63.0, 59.0, 57.8, 57.3, 56.8, 55.9, 53.5, 51.9, 49.9, 48.0, 42.8, 37.5, 35.4, 31.9, 29.9, 28.5, 25.8, 23.9, 22.6; HRMS calcd. for $C_{30}H_{33}NO_4{}^{35}Cl$, 506.20926 $[M + H]^+$; found 506.20932 $[M + H]^+$; Anal. ($C_{30}H_{32}N_1O_4Cl$): C, H, N.

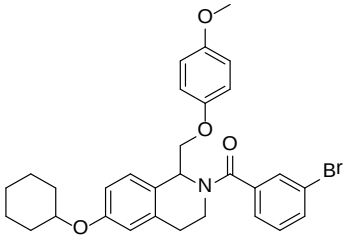

(3-bromophenyl)(6-(cyclohexyloxy)-1-((4-methoxyphenoxy)methyl)-3,4-dihydroisoquinolin-2(1H)-yl)methanone (1180-108): Dihydroisoquinoline **27m** was prepared via Procedure XI using amide **15h** (0.52 g, 1.4 mmol) and phosphorus trichloride (0.84 mL, 4.1 mmol) in dry toluene (7.6 mL). The crude solid was carried on without further purification. HRMS calcd. for $C_{23}H_{28}O_3N$, 366.20627 $[M + H]^+$; found 366.20615 $[M + H]^+$. Tetrahydroisoquinoline **28m** was prepared via Procedure XII using **27m** (0.58 g, 1.6 mmol) and sodium borohydride (0.18 g, 4.8 mmol) in dry MeOH (8.0 mL). The crude residue was subjected to flash column chromatography (ISCO, Redisep 24 g column, 0-10% MeOH/DCM gradient) to afford tetrahydroisoquinoline 8d (0.32 g, 55 %) in an impure form. The impurities were inseparable by chromatography. The product was visible by LCMS and was carried on without further purification. HRMS calcd. for $C_{23}H_{30}NO_3$, 368.22202 $[M + H]^+$; found, 368.22227 $[M + H]^+$. Tetrahydroisoquinoline **1180-108** was prepared via Procedure XIII using tetrahydroisoquinoline **28m** (0.16 g, 0.44 mmol) and 3-bromobenzoyl chloride (0.070 mL, 0.53 mmol) in DCM (6.9 mL). The crude residue was purified by silica gel chromatography (ISCO, Redisep 12 g column, 10-80% EtOAc/hexanes gradient) to afford the title compound as a white

foam (0.022 g, 9.0 % yield, mixture of two amide rotamers) TLC (EtOAc: hexanes, 1:1, v/v) Rf = 0.72; ^{1}HNMR ($CDCl_3$, 400 MHz) δ: 8.21-7.70 (m, 1H), 7.56-7.49 (m, 1H), 7.42-7.17 (m, 3H), 6.90-6.79 (m, 5H), 6.72-66. (m, 1H), 5.96 (t, *J* = 5.2 Hz, 0.5H), 5.11-5.09 (m, *J* = 6.0 Hz, *J* = 9.2 Hz, 0.5H), 4.85-4.81 (m, *J* = 6.0 Hz, *J* = 12.8 Hz, 0.5H), 4.33-4.29 (m, 1H), 4.23-4.18 (m, 1H), 4.13 (t, *J* = 10.4 Hz, 0.5H), 3.92-3.88 (m, 0.5H), 4.75 (s, 3H), 3.72-3.65 (m, 0.5H), 3.26-3.07 (m, 1H), 2.87-2.70 (m, 2H), 1.97-1.94 (m, 2H), 1.79-1.77 (m, 2H), 1.57-1.48 (m, 3H), 1.39-1.27 (m, 3H); ^{13}CNMR ($CDCl_3$, 100 MHz) δ: 170.3, 169.5, 157.5, 156.9, 154.4, 154.3, 153.1, 152.6, 138.6, 138.4, 136.7, 135.5, 133.4, 132.7, 131.0, 130.4, 130.3, 130.1, 129.8, 128.9, 128.7, 126.3, 125.3, 124.0, 122.9, 122.6, 116.3, 116.0, 115.9, 115.4, 114.9, 114.8, 114.6, 75.6, 71.3, 70.2, 57.3, 55.9, 51.9, 42.8, 35.5, 31.9, 29.9, 28.5, 23.9; HRMS calcd. for $C_{30}H_{33}NO_4{}^{79}Br$, 550.15875 $[M + H]^+$; found 550.15935 $[M + H]^+$.

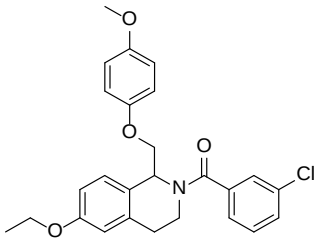

(6-(benzylthio)-1-((4-methoxyphenoxy)methyl)-3,4-dihydroisoquinolin-2(1H)-yl)(3-chlorophenyl)methanone (1180-152): Dihydroisoquinoline **28n** was prepared via procedure X using amide **15m** (0.67 g, 2.0 mmol) and phosphorous trichloride (1.3 mL, 6.1 mmol) in dry toluene (11 mL). The crude residue (0.84 g) was carried on without further purification. HRMS calcd. for $C_{19}H_{22}O_3N_1$, 312.15942 $[M + H]^+$; found 312.15912 $[M + H]^+$. Tetrahydroisoquinoline **28n** was prepared via procedure XII using dihydroisoquinoline **27n** (0.84 g, 2.7 mmol) and sodium borohydride (0.31 g, 8.1 mmol) in dry MeOH (14 mL). The crude residue was subjected to flash column chromatography (ISCO, Redisep 24 g column, 0-10% MeOH/DCM gradient) to afford tetrahydroisoquinoline 75 (0.21 g, 25 %) in an impure form. The impurities were inseparable by chromatography. The product was visible by LCMS and was carried on without further purification. Tetrahydroisoquinoline **1180-152** was prepared via procedure XIII using tetrahydroisoquinoline **28n**

(0.21 g, 0.68 mmol) and 3-chlorobenzoyl chloride (0.10 mL, 0.81 mmol) in DCM (11 mL). The crude residue was purified by silica gel chromatography (ISCO, Redisep 12 g column, 10-80% EtOAc/hexanes gradient) to afford the title compound as a white foam (0.059 g, 19 % yield, mixture of two amide rotamers) TLC (EtOAc: hexanes, 1:1, v/v) Rf = 0.71; ^{1}HNMR ($CDCl_3$, 400 MHz) δ: 7.61-7.56 (m, 0.5H), 7.42-7.22 (m, 4H), 6.95-6.69 (m, 6.5H), 5.98-6.01 (m, 0.5H), 5.16-5.13 (m, *J* = 3.2 Hz, *J* = 9.2 Hz, 0.5H), 4.89-4.85 (m, *J* = 5.2 Hz, *J* = 12.4 Hz, 0.5H), 4.37-4.32 (m, 1H), 4.15 (t, *J* = 10.4 Hz, 0.5H), 4.03 (q, *J* = 6.8 Hz, 2H), 3.96-3.92 (m, 0.5H), 3.77 (s, 3H), 3.73-3.67 (m, 1H), 3.31-3.12 (m, 1H), 2.95-2.74 (m, 1.5H), 1.42 (t, *J* = 6.8 Hz, 3H); ^{13}CNMR ($CDCl_3$, 100 MHz) δ: 170.5, 169.7, 158.6, 158.1, 154.3, 154.2, 153.1, 152.6, 141.4, 138.3, 138.2, 136.6, 135.6, 134.9, 134.6, 133.6, 131.7, 130.2, 129.9, 129.8, 128.7, 128.4, 128.3, 128.2, 127.0, 125.8, 125.2, 124.9, 124.2, 115.9, 115.5, 114.9, 114.4, 113.6, 113.4, 71.3, 70.2, 63.7, 57.3, 55.9, 51.9, 42.8, 35.5, 29.9, 28.5, 15.1, 14.1; HRMS calcd. for $C_{26}H_{27}NO_4{}^{35}Cl$, 452.16231 $[M + H]^+$; found 452.16203 $[M + H]^+$. Anal. ($C_{26}H_{26}N_1O_4Cl$): C, H, N.

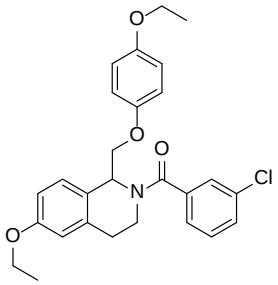

(3-chlorophenyl)(6-ethoxy-1-((4-ethoxyphenoxy)methyl)-3,4-dihydroisoquinolin-2(1H)-yl)methanone (1180-268): Dihydroisoquinoline **28o** was prepared via procedure X using amide **15l** (0.58 g, 1.7 mmol) and phosphorus trichloride (0.84 mL, 4.1 mmol) in dry toluene (8.4 mL). The crude solid was carried on without further purification. HRMS calcd. for $C_{20}H_{24}O_3N$, 326.17507 $[M + H]^+$; found 326.17457 $[M + H]^+$. Tetrahydroisoquinoline **28o** was prepared via procedure XII using **27o** (0.91 g, 2.8 mmol) and sodium borohydride (0.32 g, 8.4 mmol) in dry MeOH (14 mL). The crude residue was subjected to flash column chromatography (ISCO, Redisep 24 g column, 0-10% MeOH/DCM gradient) to afford tetrahydroisoquinoline 77 (0.12 g, 14 %) in an impure form. The

impurities were inseparable by chromatography. The product was visible by LCMS and was carried on without further purification. Tetrahydroisoquinoline **1180-268** was prepared via procedure XIII using tetrahydroisoquinoline **28o** (0.061 g, 0.19 mmol) and 3-chlorobenzoyl chloride (0.029 mL, 0.22 mmol) in DCM (2.9 mL). The crude residue was purified by silica gel chromatography (ISCO, Redisep 12 g column, 10-80% EtOAc/hexanes gradient) to afford the title compound as a white foam (0.039 g, 45 % yield, mixture of two amide rotamers) TLC (EtOAc: hexanes, 1:1, v/v) Rf = 0.70; ^{1}HNMR ($CDCl_3$, 400 MHz) δ: 7.6 (bs, 0.5H), 7.42-7.22 (m, 3.5H), 6.94-6.92 (m, 0.5H), 6.87-6.69 (m, 6.5H), 6.0-5.98 (m, 0.5H), 5.14-5.13 (m, 0.5H), 4.88-4.84 (m, 0.5H), 4.35-4.32 (m, 1H), 4.14 (t, J = 10 Hz, 0.5), 4.40 -3.92 (m, 4.5H), 3.79-3.66 (m, 1H), 3.31-3.11 (m, 1H), 2.98-2.74 (m 1.5H), 1.44-1.38 (m, 6H); ^{13}CNMR ($CDCl_3$, 100 MHz) δ: 170.4, 169.7, 158.7, 158.2, 153.8, 153.1, 152.6, 138.5, 138.3, 136.6, 135.6, 134.9, 134.6, 130.2, 129.9, 128.7, 128.3, 128.2, 127.1, 125.8, 125.4, 124.9, 124.4, 116.0, 115.8, 115.6, 114.9, 114.5, 113.7, 113.5, 71.4, 70.4, 64.3, 63.8, 57.4, 52.1, 42.9, 35.6, 30.0, 28.6, 15.2, 15.1; HRMS calcd. for $C_{27}H_{29}NO_4Cl$, 446.17796 $[M + H]^+$; found 446.17853 $[M + H]^+$.

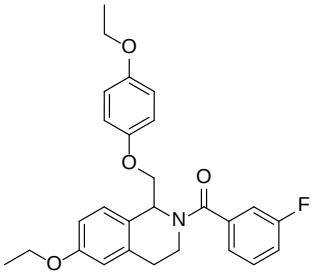

(6-ethoxy-1-((4-ethoxyphenoxy)methyl)-3,4-dihydroisoquinolin-2(1H)-yl)(3-fluorophenyl)methanone (1180-269): Dihydroisoquinoline **28o** was prepared via procedure X using amide **15l** (0.58 g, 1.7 mmol) and phosphorus trichloride (0.84 mL, 4.1 mmol) in dry toluene (8.4 mL). The crude solid was carried on without further purification. HRMS calcd. for $C_{20}H_{24}O_3N$, 326.17507 $[M + H]^+$; found 326.17457 $[M + H]^+$. Tetrahydroisoquinoline **28o** was prepared via procedure XII using **27o** (0.91 g, 2.8 mmol) and sodium borohydride (0.32 g, 8.4 mmol) in dry MeOH (14 mL). The crude residue was subjected to flash column chromatography (ISCO, Redisep 24 g column, 0-10% MeOH/DCM gradient) to afford tetrahydroisoquinoline 77 (0.12 g, 14 %) in an

impure form. The impurities were inseparable by chromatography. The product was visible by LCMS and was carried on without further purification. Tetrahydroisoquinoline **1180-269** was prepared via procedure XIII using tetrahydroisoquinoline **28o** (0.061 g, 0.19 mmol) and 3-fluorobenzoyl chloride (0.026 mL, 0.22 mmol) in DCM (2.9 mL). The crude residue was purified by silica gel chromatography (ISCO, Redisep 12 g column, 10-80% EtOAc/hexanes gradient) to afford the title compound as a white foam (0.025 g, 30 % yield, mixture of two amide rotamers) TLC (EtOAc: hexanes, 1:1, v/v) Rf = 0.70; ^{1}HNMR ($CDCl_3$, 400 MHz) δ: 7.43-7.09 (m, 4H), 6.94-6.91 (m, 0.5H), 6.86-6.73 (m, 6H), 6.68 (s, 0.5H), 6.0-5.98 (m, 0.5H), 5.16-5.14 (m, 0.5H), 4.88-4.84 (m, *J* = 5.6 Hz, *J* = 5.2 Hz, 0.5H), 4.36-4.32 (m, 1H), 4.12 (t, *J* = 10 Hz, 0.5H), 4.03-3.92 (m, 4.5H), 3.78-3.65 (m, 1H), 3.30-3.11 (m, 1H), 2.94-2.73 (m, 1.5H), 1.44-138 (m, 6H); ^{13}CNMR ($CDCl_3$, 100 MHz) δ: 170.6., 169.8, 162.8 (*J* = 247 Hz), 162.7 (*J* = 247 Hz), 158.6, 158.1, 153.8, 153.6, 153.0, 152.5, 138.8, 138.7, 138.6, 138.5, 136.6, 135.6, 130.7, 130.6, 130.4, 130.3, 128.7, 128.3, 125.3, 124.3, 123.4, 122.5, 116.9, 116.8, 116.7, 116.6, 115.9, 115.7, 115.6, 115.5, 115.4, 115.2, 114.9, 115.2, 114.9, 114.4, 114.3, 114.0, 113.6, 113.4, 71.4, 70.2, 64.2, 63.8, 63.7, 57.3, 51.9, 42.8, 35.4, 30.0, 28.6, 15.1, 15.0; HRMS calcd. for $C_{27}H_{29}NO_4F$, 450.20751 $[M + H]^+$; found 450.20805 $[M + H]^+$.

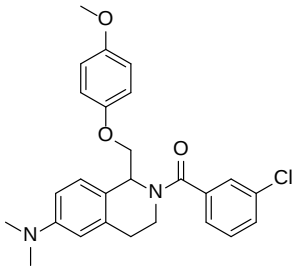

(3-chlorophenyl)(6-(dimethylamino)-1-((4-methoxyphenoxy)methyl)-3,4-dihydroisoquinolin-2(1H)-yl)methanone (1180-104): Tetrahydroisoquinoline **1180-104** was prepared via Procedure XIII using tetrahydroisoquinoline **28p** (0.26 g, 0.85 mmol) and 3-chlorobenzoyl chloride (0.14 mL, 1.0 mmol) in DCM (13 mL). The crude residue was purified by silica gel chromatography (ISCO, Redisep 12 g column, 10 – 80% EtOAc/hexanes gradient) to afford the title compound as a yellow foam (0.31 g, 81 % mixture of two amide rotamers) TLC (EtOAc: hexanes, 1:1, v/v) Rf = 0.43;

^{1}HNMR ($CDCl_3$, 400 MHz) δ: 7.59-7.16 (m, 4.5H), 6.89-6.76 (m, 4.5 H), 6.68-6.57 (m, 1H), 6.52-6.48 (m, 1H), 5.97-5.95 (t, *J* = 5.2 Hz, 0.5H), 5.12-5.09 (dd, *J* = 3.2 Hz, *J* = 9.2 Hz, 0.5H), 4.86-4.82 (dd, *J* = 5.2 Hz, *J* = 12.8 Hz, 0.5H), 4.33-4.31 (m, 1H), 4.14-4.09 (m, 0.5H), 3.92-3.88 (dd, *J* = 3.2 Hz, *J* = 6.8 Hz), 3.73 (s, 3H), 3.70-3.65 (m, 1H), 3.27-3.09 (m, 1H), 2.94 (s, 6H), 2.87-2.71 (m, 1.5 H); ^{13}CNMR (100 MHz, $CDCl_3$) δ: 170.4, 169.6, 154.3, 153.2, 152.7, 150.2, 138.6, 138.4, 136.1, 134.8, 134.5, 130.3, 130.2, 129.9, 129.8, 129.7, 128.3, 128.2, 127.9, 127.1, 125.8, 124.9, 115.9, 115.4, 114.9, 114.8, 112.7, 111.2, 71.2, 70.2, 57.3, 55.9, 51.8, 42.9, 40.7, 35.6, 30.2, 28.8; HRMS calcd. for $C_{26}H_{27}ClN_2O_3$, 451.17830 $[M + H]^+$; found 451.17929 $[M + H]^+$.

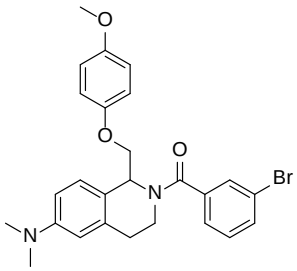

(3-bromophenyl)(6-(dimethylamino)-1-((4-methoxyphenoxy)methyl)-3,4-dihydroisoquinolin-2(1H)-yl)methanone (1180-105): Tetrahydroisoquinoline **1180-105** was prepared via Procedure XIII using tetrahydroisoquinoline **28p** (0.26 g, 0.85 mmol) and 3-bromobenzoyl chloride (0.14 mL, 1.0 mmol) in DCM (13 mL). The crude residue was purified by silica gel chromatography (ISCO, Redisep 12 g column, 10 – 80% EtOAc/hexanes gradient) to afford the title compound as a yellow foam (0.30 g, 76 % mixture of two amide rotamers) TLC (EtOAc: hexanes, 1:1, v/v) Rf = 0.43; ^{1}HNMR ($CDCl_3$, 400 MHz) δ: 7.75-7.41 (m, 2H), 7.31-7.15 (m, 2H), 6.89-6.85 (m, 2H), 6.82-6.77 (m, 3H), 6.67-6.57 (m, 1H), 6.52-6.47 (m, 1H), 5.97-5.94 (t, *J* = 5.2 Hz, 0.5H), 5.12-5.09 (dd, *J* = 3.6 Hz, *J* = 9.6 Hz, 0.5H), 4.86-4.82 (dd, *J* = 5.2 Hz, *J* = 12.8 Hz, 0.5H), 4.33-4.28 (m, 1H), 4.14-4.05 (m, 0.5 H), 3.92-3.88 (dd, *J* = 3.6 Hz, *J* = 10.0 Hz, 0.5H), 3.75 (s, 3H), 3.71-3.61 (m, 1H), 3.29-3.08 (m, 1H), 2.94 (s, 6H), 2.89-2.71 (m, 1.5H); ^{13}CNMR (100 MHz, $CDCl_3$) δ: 170.3, 169.5, 154.3, 154.2, 153.2, 152.6, 150.2, 149.8, 138.8, 138.6, 135.9, 134.9, 132.8, 132.7, 131.0, 130.4, 130.1, 129.8, 128.3, 127.9, 126.3, 125.3, 122.9, 122.6, 119.9, 115.9, 115.4, 114.8, 112.7, 112.4, 11.9, 111.2, 78.6, 71.2, 70.2, 57.3,

55.9, 51.9, 42.9, 40.8, 40.8, 35,7, 30.2, 28.8; HRMS calcd. for $C_{26}H_{27}BrN_2O_3$, 495.12778 $[M + H]^+$; found 495.12898 $[M + H]^+$.

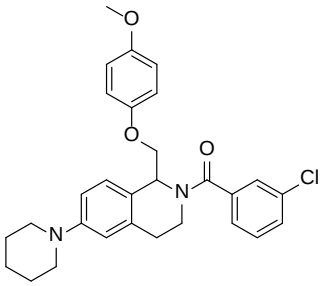

(3-chlorophenyl)(1-((4-methoxyphenoxy)methyl)-6-(piperidin-1-yl)-3,4-dihydroisoquinolin-2(1H)-yl)methanone (1180-116): Tetrahydroisoquinoline **1180-116** was prepared via Procedure XIII using tetrahydroisoquinoline **28q** (0.11 g, 0.32 mmol) and 3-chlorobenzoyl chloride (0.050 mL, 0.39 mmol) in DCM (5.0 mL). The crude residue was purified by silica gel chromatography (ISCO, Redisep 12 g column, 10 – 80% EtOAc/hexanes gradient) to afford the title compound as an off-white foam (0.11 g, 67 % yield, mixture of two amide rotamers) TLC (EtOAc: hexanes, 1:1, v/v) Rf = 0.48; ^{1}HNMR ($CDCl_3$, 400 MHz) δ: 7.58 (s, 0.5H), 7.37-7.23 (m, 3H), 7.18-7.16 (m, 0.5H), 6.89-6.7 (m, 7H), 5.96 (t, *J* = 4.8 Hz, 0.5H), 5.12-5.08 (m, *J* = 3.6 Hz, *J* = 3.6 Hz, 0.5H), 4.86-4.82 (m, *J* = 5.6 Hz, *J* = 13.2 Hz, 0.5H), 4.36-4.29 (m, 1H), 4.12 (t, *J* = 10.4 Hz, 0.5H), 3.92-3.89 (m, 0.5H), 3.75 (s, 3H), 3.72-3.62 (m, 0.5H), 3.28-3.32 (m, 1.5H), 3.15-3.08 (m, 4H), 2.91-2.69 (m, 1.5H), 1.76-1.66 (m, 4H), 1.58-1.57 (m, 2H); ^{13}C NMR ($CDCl_3$, 100 MHz) δ: 170.4, 169.6, 167.9, 153.3, 154.2, 153.1, 152.6, 151.7, 138.5, 138.3, 135.9, 134.9, 134.5, 133.1, 130.2, 129.8, 129.7, 128.8, 128.2, 127.9, 127.0, 125.9, 124.8, 122.4, 116.6, 115.9, 115.7, 115.4, 114.9, 114.8, 71.2, 70.1, 57.3, 55.9, 51.9, 50.6, 42.9, 35.6, 30.1, 29.9, 25.9, 24.4; HRMS calcd. for $C_{29}H_{32}N_2O_3{}^{35}Cl$, 491.20960 $[M + H]^+$; found, 491.20961 $[M + H]^+$.

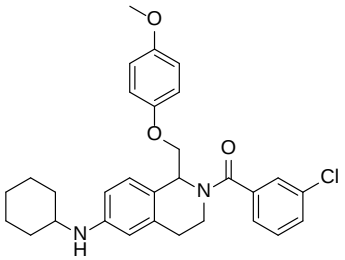

(3-chlorophenyl)(6-(cyclohexylamino)-1-((4-methoxyphenoxy)methyl)-3,4-dihydroisoquinolin-2(1H)-yl)methanone (1180-119): Tetrahydroisoquinoline **1180-119** was prepared via Procedure XIII using tetrahydroisoquinoline **28r** (0.17 g, 0.46 mmol) and 3-chlorobenzoyl chloride (0.059 mL, 0.46 mmol) in DCM (7.1 mL). The crude residue was purified by silica gel chromatography (ISCO, Redisep 12 g column, 10 – 80% EtOAc/hexanes gradient) to afford the title compound as an off-white foam (0.087 g, 37 % yield, mixture of two amide rotamers) TLC (EtOAc: hexanes, 1:1, v/v) Rf = 0.73; ^{1}HNMR ($CDCl_3$, 400 MHz) δ: 7.58 (s, 0.5H), 7.39-7.23 (m, 3H), 7.08-7.06 (m, 0.5H), 6.68-6.76 (m, 5H), 6.52-6.35 (m, 2H), 5.92 (t, *J* = 4.8, 0.5H), 5.07-5.04 (m, *J* = 3.6 Hz, *J* = 9.6 Hz, 0.5H), 4.83-4.79 (m, *J* = 5.6 Hz, *J* = 12.8 Hz, 0.5H), 4.30-4.26 (m, 1H), 4.12-4.07 (m, 0.5H), 3.89-3.85 (m, 0.5H), 3.76 (s, 3H), 3.68-3.56 (m, 1.5H), 3.24-3.18 (m, 1H), 3.12-3.04 (m, 0.5H), 2.87-2.64 (m, 1.5H), 2.06-2.01 (m, 2H), 1.76-1.73 (m, 2H), 1.65-1.62 (m, 1H), 1.39-1.31 (m, 2H), 1.26-1.09 (m, 4H); ^{13}C NMR ($CDCl_3$, 100 MHz) δ: 170.5, 169.6, 162.3, 160.7, 154.3, 153.2, 152.7, 138.5, 138.3, 136.3, 135.2, 134.8, 134.5, 132.8, 130.2, 129.8, 129.7, 128.6, 128.2, 127., 125.9, 124.9, 120.5, 115.9, 114.9, 114.8, 113.2, 112.1, 71.8, 71.2, 70.2, 61.7, 58.7, 57.3, 55.9, 53.8, 52.5, 51.9, 42.8, 35.6, 33.5, 29.9, 28.6, 26.0, 25.2; HRMS calcd. for $C_{30}H_{34}N_2O_3{}^{35}Cl$, 505.22525 $[M + H]^+$; found, 505.22541 $[M + H]^+$.

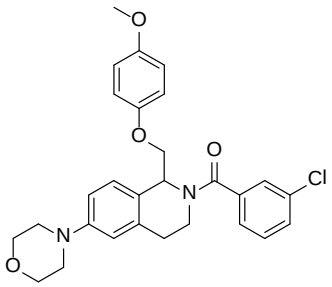

(3-chlorophenyl)(1-((4-methoxyphenoxy)methyl)-6-morpholino-3,4-dihydroisoquinolin-2(1H)-yl)methanone (1180-120): Tetrahydroisoquinoline **1180-120** was prepared via Procedure XIII using tetrahydroisoquinoline **28s** (0.23 g, 0.67 mmol) and 3-chlorobenzoyl chloride (0.10 mL, 0.80 mmol) in DCM (11 mL). The crude residue was purified by silica gel chromatography (ISCO, Redisep 12 g column, 10 – 80% EtOAc/hexanes gradient) to afford the title compound as an off-white foam (0.18 g, 55 % yield, mixture of two amide rotamers) TLC (EtOAc: hexanes, 1:1, v/v) Rf = 0.74; ^{1}HNMR ($CDCl_3$, 400 MHz) δ: 7.57 (s, 0.5H), 7.39-7.19 (m, 4H), 6.93-6.65 (m, 6.5H), 5.96 (t, *J* = 5.2 Hz, 0.5H), 5.12-5.09 (m, *J* = 3.6 Hz, *J* = 9.2 Hz, 0.5H), 4.86-4.81 (m, *J* = 5.2 Hz, *J* = 12.8 Hz, 0.5H), 4.36-4.29 (m, 1H), 4.14-4.09 (m, 0.5H), 3.92-3.89 (m, 0.5H), 3.83 (t, *J* = 4.8 Hz, 4H), 3.78 (s, 3H), 3.69-3.62 (m, 1.5H), 3.28-3.20 (m, 0.5H), 3.17-3.13 (m, 4H), 2.92-2.70 (m, 1.5H); ^{13}C NMR ($CDCl_3$, 100 MHz) δ: 170.4, 169.7, 154.4, 154.2, 153.1, 152.6, 150.9, 150.4, 138.9, 138.2, 136.1, 135.11, 134.8, 134.5, 130.3, 129.9, 129.8, 128.4, 128.2, 128.1, 127.0, 125.8, 124.9, 124.6, 123.4, 115.9, 115.4, 114.9, 114.8, 114.2, 71.2, 70.1, 67.0, 57.3, 55.9, 51.9, 49.4, 49.2, 42.9, 35.6, 30.1, 28.7, 21.3; HRMS calcd. for $C_{28}H_{30}N_2O_4{}^{35}Cl$, 493.18886 $[M + H]^+$; found, 493.18900 $[M + H]^+$; mp: 108°C.

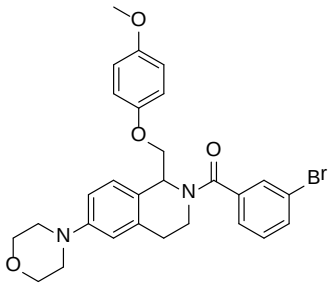

(3-bromophenyl)(1-((4-methoxyphenoxy)methyl)-6-morpholino-3,4-dihydroisoquinolin-2(1H)-yl)methanone (1180-121): Tetrahydroisoquinoline **1180-121** was prepared via Procedure XIII using tetrahydroisoquinoline **28s** (0.23 g, 0.67 mmol) and 3-bromobenzoyl chloride (0.11 mL, 0.80 mmol) in DCM (11 mL). The crude residue was purified by silica gel chromatography (ISCO, Redisep 12 g column, 10 – 80% EtOAc/hexanes gradient) to afford the title compound as an off-white foam (0.16 g, 46 % yield, mixture of two amide rotamers) TLC (EtOAc: hexanes, 1:1, v/v) Rf = 0.72; ^{1}HNMR ($CDCl_3$, 400 MHz) δ: 7.72 (s, 0.5H), 7.55-7.49 (m, 1.5H), 7.41-7.19 (m, 2H), 6.93-

6.91 (m, 0.5H), 6.86-6.65 (m, 6.5H), 5.95 (t, *J* = 4.8 Hz, 0.5H), 5.12-5.09 (m, *J* = 3.2 Hz, *J* = 9.6 Hz, 0.5H), 4.86-4.82 (m, *J* = 5.2 Hz, *J* = 12.0 Hz, 0.5H), 4.39-4.29 (m, 1H), 4.12 (t, *J* = 10.4 Hz, 0.5H), 3.92-3.89 (m, 0.5H), 3.84 (t, *J* = 4.8 Hz, 4H), 3.74 (s, 3H), 3.69-3.56 (m, 1.5H), 3.27-3.20 (m, 0.5H), 3.13 (s, 4H), 2.91-2.70 (m, 1.5H); ^{13}C NMR ($CDCl_3$, 100 MHz) δ: 170.3, 169.5, 154.4, 154.2, 153.1, 152.6, 150.9, 150.5, 138.6, 138.5, 137.2, 135.1, 132.8, 130.9, 130.5, 130.2, 129.9, 128.4, 128.1, 126.3, 125.3, 124.6, 123.4, 122.9, 122.6, 116.1, 115.9, 115.5, 114.9, 114.8, 114.2, 71.2, 70.1, 67.0, 62.2, 57.3, 55.9, 51.9, 49.4, 49.2, 42.9, 35.6, 30.1, 28.7; HRMS calcd. for $C_{28}H_{30}N_2O_4{}^{79}Br$, 537.13835 $[M + H]^+$; found, 537.13859 $[M + H]^+$; Anal. ($C_{28}H_{29}N_2O_4Br$): C, H, N.

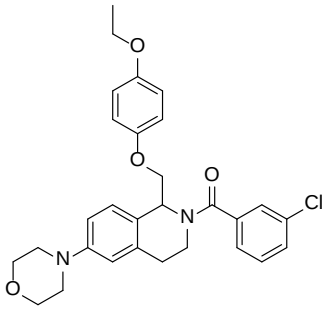

(3-chlorophenyl)(1-((4-ethoxyphenoxy)methyl)-6-morpholino-3,4-dihydroisoquinolin-2(1H)-yl)methanone (1180-127): Tetrahydroisoquinoline **1180-127** was prepared via Procedure XIII using tetrahydroisoquinoline **28t** (0.21 g, 0.57 mmol) and 3-chlorobenzoyl chloride (0.086 mL, 0.67 mmol) in DCM (8.8 mL). The crude residue was purified by silica gel chromatography (ISCO, Redisep 12 g column, 10 – 80% EtOAc/hexanes gradient) to afford the title compound as an off-white foam (0.11 g, 38 % yield, mixture of two amide rotamers) TLC (EtOAc: hexanes, 1:1, v/v) Rf = 0.32; ^{1}HNMR ($CDCl_3$, 400 MHz) δ: 7.57 (s, 0.5H), 7.37-7.19 (m, 4H), 6.93-6.91 (m, 0.5H),6.82-6.77 (m, 5H), 6.71-6.65 (m, 1H), 5.97-5.95 (m, 0.5H), 5.12-5.09 (m, *J* = 5.2 Hz, *J* = 9.2 Hz, 0.5H), 4.33-4.29 (m, 1H), 4.14-4.09 (m, 0.5H), 3.95 (q, *J* = 7.2 Hz, 2H), 3.84 (t, *J* = 4.4 Hz, 4H), 3.73-3.64 (m, 1H), 3.28-3.14 (m, 5H), 2.90-2.70 (m, 2H), 1.37 (t, *J* = 6.8 Hz, 3H); ^{13}C NMR ($CDCl_3$, 100 MHz) δ: 170.4, 169.6, 154.2, 153.7, 153.6, 153.0, 152.5, 150.9, 150.5, 138.4, 138.2, 136.2, 135.1, 134.9, 134.5, 133.4, 130.2, 129.9, 128.5, 128.1, 127.0, 125.8, 124.7, 123.5, 115.8, 115.7, 115.6, 115.4, 114.8, 114.2, 71.2, 70.1,

67.1, 64.2, 57.3, 55.9, 51.9, 49.4, 49.2, 42.9, 40.0, 35.6, 30.1, 28.7, 26.3, 15.2; HRMS calcd. for $C_{29}H_{32}N_2O_4{}^{35}Cl$, 507.20451 $[M + H]^+$; found, 507.20466 $[M + H]^+$.

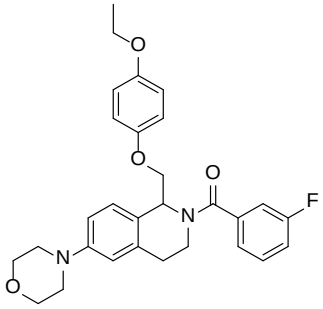

(1-((4-ethoxyphenoxy)methyl)-6-morpholino-3,4-dihydroisoquinolin-2(1H)-yl)(3-fluorophenyl)methanone (1180-128): Tetrahydroisoquinoline **1180-128** was prepared via Procedure XIII using tetrahydroisoquinoline **28t** (0.21 g, 0.57 mmol) and 3-fluorobenzoyl chloride (0.082 mL, 0.67 mmol) in DCM (8.8 mL). The crude residue was purified by silica gel chromatography (ISCO, Redisep 12 g column, 10 – 80% EtOAc/hexanes gradient) to afford the title compound as an off-white foam (0.11 g, 38 % yield, mixture of two amide rotamers) TLC (EtOAc: hexanes, 1:1, v/v) Rf = 0.28; ^{1}HNMR ($CDCl_3$, 400 MHz) δ: 7.41-7.07 (m, 4.5H), 6.93-6.91 (m, 0.5H), 6.82-6.65 (m, 6H), 5.96-5.94 (m, 0.5H), 5.14-5.11 (m, 0.5H), 4.88-4.82 (m, *J* = 4.8 Hz, *J* = 12.8 Hz, 0.5H), 4.33-4.31 (m, 1H), 4.11 (t, *J* =10.0 Hz, 0.5H), 3.95 (q, *J* = 7.2 Hz, 2H), 3.91-3.90 (m, 0.5H), 3.85 (t, *J* = 4.4 Hz, 4H), 3.78-3.63 (m, 1H), 3.28-3.14 (m, 5H), 2.91-2.70 (m, 1.5H), 1.37 (t, *J* = 6.8 Hz, 3H); ^{13}C NMR ($CDCl_3$, 100 MHz) δ: 170.5, 169.7, 153.7, 153.6, 153.0, 152.5, 138.6, 136.2, 130.6, 130.3, 128.4, 128.1, 123.4, 122.5, 116.9, 116.7, 115.8, 115.6, 115.5, 115.4, 115.1, 114.2, 71.2, 70.1, 67.0, 64.2, 57.2, 51.9, 49.3, 42.9, 35.6, 30.1, 28.7, 15.2; HRMS calcd. for $C_{29}H_{32}N_2O_4F$, 491.23406 $[M + H]^+$; found, 491.23406 $[M + H]^+$.

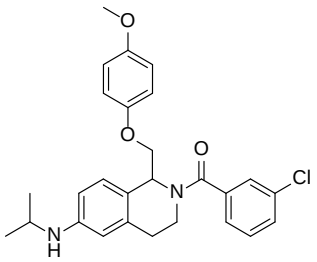

(3-chlorophenyl)(6-(isopropylamino)-1-((4-methoxyphenoxy)methyl)-3,4-dihydroisoquinolin-2(1H)-yl)methanone (1180-150): Tetrahydroisoquinoline **1180-150** was prepared via procedure XIII using tetrahydroisoquinoline **28u** (0.039 g, 0.12 mmol) and 3-chlorobenzoyl chloride (0.015 mL, 0.12 mmol) in DCM (1.8 mL). The crude residue was purified by silica gel chromatography (ISCO, Redisep 12 g column, 10 – 80% EtOAc/hexanes gradient) to afford the title compound as a yellow foam (0.024 g, 42 % yield, mixture of two amide rotamers). TLC (EtOAc: hexanes, 1:1, v/v) Rf = 0.59; ^{1}HNMR ($CDCl_3$, 400 MHz) δ: 7.60-7.25 (m, 4H), 6.89-6.78 (m, 5H), 6.52-6.36 (m, 2H), 5.95 (t, *J* = 5.2 Hz, 0.5H), 5.10-5.07 (m, *J* = 2.8 Hz, *J* = 9.2 Hz, 0.5H), 4.86-4.81 (m, *J* = 5.6 Hz, *J* = 13.2 Hz, 0.5H), 4.33-4.29 (m, 1H), 4.15-4.06 (m, 0.5H), 3.92-3.88 (dd, *J* = 3.6 Hz, *J* = 10.0 Hz, 0.5H), 3.77 (s, 3H), 3.71-3.67 (m, 1H), 3.65-3.57 (m, 1H), 3.28-3.06 (m, 1.5H), 2.89-2.67 (m, 2H), 1.23-1.21 (m, 6H); ^{13}C NMR ($CDCl_3$, 100 MHz) δ: 170.4, 169.6, 154.3, 153.1, 152.6, 138.5, 138.4, 136.4, 135.4, 134.9, 134.5, 130.2, 129.8, 129.7, 128.6, 128.2, 127.0, 125.9, 124.9, 115.9, 115.4, 114.9, 114.8, 114.1, 113.3, 71.2, 70.2, 57.3, 55.9, 51.9, 42.8, 35.5, 29.9, 28.6, 22.9, 22.7; HRMS calcd. for $C_{27}H_{30}N_2O_3Cl$, 465.19395 $[M + H]^+$; found, 465.19225 $[M + H]^+$; mp: 108°C.

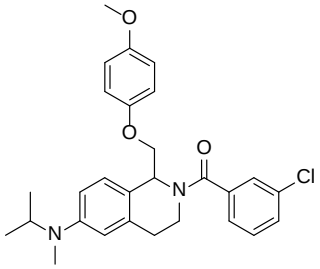

(3-chlorophenyl)(6-(isopropyl(methyl)amino)-1-((4-methoxyphenoxy)methyl)-3,4-dihydroisoquinolin-2(1H)-yl)methanone (1180-146): Tetrahydroisoquinoline 1180-146 was prepared via procedure XIII using tetrahydroisoquinoline **28v** (0.13 g, 0.39 mmol) and 3-chlorobenzoyl chloride (0.050 mL, 0.39 mmol) in DCM (6.2 mL). The crude residue was purified by silica gel chromatography (ISCO, Redisep 12 g column, 10 – 80% EtOAc/hexanes gradient) to afford the title compound as a yellow foam (0.098 g, 52 % yield, mixture of two amide rotamers). TLC (EtOAc: hexanes, 1:1, v/v) Rf = 0.72; ^{1}HNMR ($CDCl_3$, 400 MHz) δ: 7.42-7.17 (m, 4H), 6.91-

6.80 (m, 5H), 6.75-6.54 (m, 2H), 5.99 (t, *J* = 5.2 Hz, 0.5H), 5.14-5.11 (m, *J* = 3.2 Hz, *J* = 9.6 Hz, 0.5H), 4.89-4.85 (m, *J* = 5.2 Hz, *J* = 12.4 Hz, 0.5H), 4.36-4.29 (m, 0.5H), 4.18-4.07 (m, 1.5H), 3.96-3.91 (m, 0.5H), 3.78-3.60 (m, 4H), 3.31-3.12 (m, 1H), 2.94-2.74 (m, 5H), 1.20-1.18 (m, 6H); ^{13}C NMR ($CDCl_3$, 100 MHz) δ: 170.4, 169.6, 154.3, 153.2, 152.7, 149.7, 149.4, 138.6, 138.4, 136.1, 134.9, 134.5, 130.2, 129.8, 129.7, 128.4, 128.2, 128.0, 127.0, 125.9, 124.9, 120.8, 119.5, 115.9, 115.4, 114.8, 114.6, 114.4, 112.9, 112.7, 112.3, 111.4, 71.2, 70.2, 57.2, 55.9, 51.8, 48.9, 48.8, 42.9, 35.7, 30.3, 30.0, 28.9, 19.7; HRMS calcd. for $C_{28}H_{32}N_2O_3Cl$, 479.20960 $[M + H]^+$; found, 479.20975 $[M + H]^+$; Anal. ($C_{28}H_{31}N_2O_3Cl$): C, H, N.

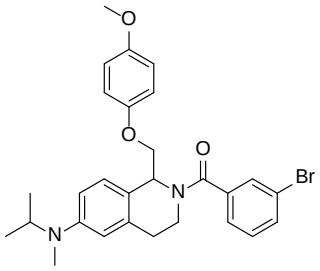

(3-bromophenyl)(6-(isopropyl(methyl)amino)-1-((4-methoxyphenoxy)methyl)-3,4-dihydroisoquinolin-2(1H)-yl)methanone (1180-145): Tetrahydroisoquinoline **1180-145** was prepared via Procedure XIII using tetrahydroisoquinoline **28v** (0.13 g, 0.39 mmol) and 3-chlorobenzoyl chloride (0.050 mL, 0.39 mmol) in DCM (6.2 mL). The crude residue was purified by silica gel chromatography (ISCO, Redisep 12 g column, 10 – 80% EtOAc/hexanes gradient) to afford the title compound as a yellow foam (0.051 g, 25 % yield, mixture of two amide rotamers). TLC (EtOAc: hexanes, 1:1, v/v) Rf = 0.71; ^{1}HNMR ($CDCl_3$, 400 MHz) δ: 8.23-8.00 (m, 0.5H), 7.78-7.70 (m, 0.5H), 7.57-7.44 (m, 2H), 7.36-7.16 (m, 2H), 6.90-6.80 (m, 4H), 6.75-6.64 (m, 1H), 6.59-6.55 (m, 1H), 5.98 (t, *J* = 5.6 Hz, 0.5H), 5.14-5.11 (m, *J* = 3.2 Hz, *J* = 10.0 Hz, 0.5H), 4.89-4.84 (m, *J* = 5.2 Hz, *J* = 12.4 Hz, 0.5H), 4.35-4.29 (m, 1H), 4.17-4.06 (m, 1.5H), 3.95-3.91 (m, 0.5H), 3.78 (s, 3H), 3.73-3.58 (m, 1H), 3.31-3.12 (m, 1H), 2.94-2.68 (4.5H), 1.19-1.17 (m, 6H); ^{13}C NMR ($CDCl_3$, 100 MHz) δ: 170.4, 169.5, 154.3, 153.2, 152.7, 149.7, 138.6, 136.4, 136.0, 134.9, 133.3, 132.8, 132.7, 131.0, 130.4, 130.2, 130.1, 129.8, 129.8, 128.9, 128.4, 128.0, 126.4, 125.3, 122.6, 119.6, 115.9, 115.4, 114.9,

114.8, 113.1, 112.5, 111.6, 71.2, 70.2, 57.3, 55.9, 51.9, 49.2, 48.9, 42.9, 35.7, 30.1, 28.8, 19.6, 19.5; HRMS calcd. for $C_{28}H_{32}N_2O_3Br$, 523.15908 $[M + H]^+$; found, 523.15922 $[M + H]^+$.

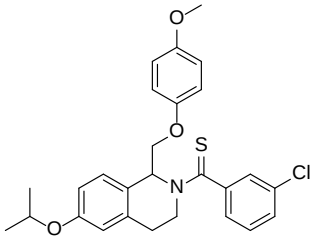

(3-chlorophenyl)(6-isopropoxy-1-((4-methoxyphenoxy)methyl)-3,4-dihydroisoquinolin-2(1H)-yl)methanethione (1180-163): Tetrahydroisoquinoline **1180-163** was prepared via procedure XV using tetrahydroisoquinoline **1180-55** (0.045 g, 0.97 mmol) and 2,4-bis(4-methoxyphenyl)-1,3,2,4-dithiadiphosphetane 2,4-disulfide (0.039 g, 0.97 mmol) in toluene (5.0 mL). The crude residue was purified by silica gel chromatography (ISCO, Redisep 12 g column, 0-80% EtOAc/hexanes gradient) to afford the title compound as a yellow foam (0.032 g, 68%, mixture of two thioamide rotamers); TLC (EtOAc:hexanes, 1:1, v/v) Rf = 0.80; ^{1}H NMR ($CDCl_3$, 400 MHz) δ: 7.32-7.25 (m, 3.5H), 7.14-7.13 (m, 0.5H), 6.87-6.70 (m, 7H), 5.75-5.70 (m, *J* = 5.2 Hz, *J* = 5.2 Hz, 0.5H), 5.14-5.38 (m, *J* = 4.0 Hz, *J* = 3.6 Hz, 0.5H), 4.70-4.69 (doublet of doublet, *J* = 4.0 Hz, *J* = 4.0 Hz, 0.5H), 4.58-4.52 (m, 1H), 4.50-4.46 (doublet of doublet, *J* = 4.4 Hz, *J* = 4.0 Hz, 0.5H), 4.20-4.15 (m, 0.5H), 4.05-3.87 (m, 2H), 3.77 (s, 3H), 3.72-3.64 (m, 0.5H), 3.36-3.28 (m, 0.5H), 2.98-2.90 (m, 1H), 2.83-2.79 (m, 0.5H), 1.36-1.34 (m, 6H); ^{13}C NMR (100 MHz, $CDCl_3$) δ: 200.4, 198.9, 157.9, 158.1, 154.5, 154.4, 152.9, 152.4, 145.0, 144.7, 134.9, 134.7, 130.2, 128.8, 128.6, 128.5, 128.1, 124.9, 123.5, 116.0, 115.9, 115.7, 115.1, 114.9, 114.8, 114.7, 70.8, 70.2, 61.5, 58.4, 55.9, 48.1, 30.1, 28.1, 22.3, 22.2; HRMS calcd. for $C_{27}H_{28}ClNO_3S$, 482.15512 $[M + H]^+$; 488.15514 $[M + H]^+$ found; mp: 80°C.

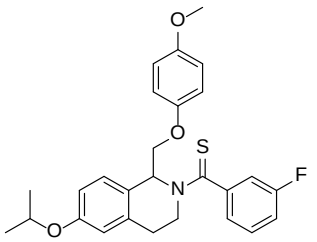

(3-fluorophenyl)(6-isopropoxy-1-((4-methoxyphenoxy)methyl)-3,4-dihydroisoquinolin-2(1H)-yl)methanethione (1180-166): Tetrahydroisoquinoline **1180-166** was prepared via procedure XV using tetrahydroisoquinoline **1180-140** (0.028 g, 0.61 mmol) and 2,4-bis(4-methoxyphenyl)-1,3,2,4-dithiadiphosphetane 2,4-disulfide (0.025 g, 0.61 mmol) in toluene (4.0 mL). The crude residue was purified by silica gel chromatography (ISCO, Redisep 12 g column, 0-80% EtOAc/hexanes gradient) to afford the title compound as a yellow foam (0.19 g, 65%, mixture of two thioamide rotamers); TLC (EtOAc:hexanes, 1:1, v/v) Rf = 0.83; ^{1}H NMR ($CDCl_3$, 400 MHz) δ: 7.34-7.25 (m, 1H), 7.08-6.97 (m, 2H), 6.88-6.69 (m, 8H), 5.75-5.70 (m, *J* = 4.4 Hz, *J* = 4.8 Hz, 0.5H), 5.42-5.39 (m, *J* = 4.0 Hz, *J* = 4.4 Hz, 0.5H), 4.71-4.67 (doublet of doublet, *J* = 4.4 Hz, *J* = 4.4 Hz, 0.5H), 4.56-4.52 (m, 1H), 4.50-4.46 (m, *J* = 4.4 Hz, *J* = 4.4 Hz, 0.5H), 4.21-4.16 (t, *J* = 9.6 Hz, 0.5H), 4.05-3.87 (m, 1.5H), 3.77-3.59 (m, 3H), 3.36-3.27 (m, 0.5H), 2.99-2.91 (m, 1H), 2.83-2.78 (m, 0.5H), 1.36-1.34 (m, 6H); ^{13}C NMR (100 MHz, $CDCl_3$) δ: 200.5, 199.1, 164.4, 161.1, 157.9, 157.1, 154.6, 154.4, 152.9, 152.4, 154.4, 145.3, 136.2, 134.9, 130.7, 130.6, 130.1, 128.5, 128.1, 124.9, 123.5, 116.0, 115.9, 115.8, 115.7, 115.6, 115.4, 115.1, 114.9, 114.8, 114.6, 70.9, 70.3, 70.2, 70.1, 61.4, 58.4, 55.9, 40.1, 42.7, 30.1, 28.1, 22.3; HRMS calcd. for $C_{27}H_{38}FNO_3SNa$, 488.16661 $[M + H]^+$; 488.16668 $[M + H]^+$ found.

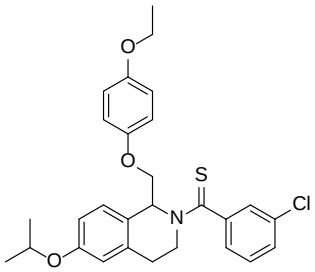

(3-chlorophenyl)(1-((4-ethoxyphenoxy)methyl)-6-isopropoxy-3,4-dihydroisoquinolin-2(1H)-yl)methanethione (1180-149): Tetrahydroisoquinoline **1180-149** was prepared via procedure XV using tetrahydroisoquinoline **1180-83** (0.067 g, 0.14 mmol) and 2,4-bis(4-methoxyphenyl)-1,3,2,4-dithiadiphosphetane 2,4-disulfide (0.029 g, 0.071 mmol) in toluene (5.0 mL). The crude residue was purified by silica gel chromatography (ISCO, Redisep 12 g column, 0-80% EtOAc/hexanes gradient) to afford the title compound as a yellow foam (0.024 g, 33%, mixture of two thioamide rotamers)

TLC (EtOAc:hexanes, 1:5, v/v) Rf = 0.58; ^{1}H NMR ($CDCl_3$, 400 MHz) δ: 7.32-7.22 (m, 3H), 7.14-7.13 (m, 1H), 6.86-6.70 (m, 7H), 5.75-5.70 (m, *J* = 5.2 Hz, *J* = 12.8 Hz, 0.5H), 5.41-5.38 (m, *J* = 4.0 Hz, *J* = 9.6 Hz, 0.5H), 4.70-4.67 (m, *J* = 4.0 Hz, *J* = 10.0 Hz, 0.5H), 4.60-4.52 (m, 1H), 4.49-4.46 (m, *J* = 4.8 Hz, *J* = 10.4 Hz, 0.5H), 4.23-4.13 (m, 1H), 4.08-3.87 (m, 3.5H), 3.71-3.63 (m, 0.5H), 3.36-3.27 (m, 0.5H), 2.98-2.79 (m, 1.5H), 1.42-1.33 (m, 9H); ^{13}C NMR (75 MHz, $CDCl_3$) δ: 200.4, 198.9, 157.8, 157.1, 153.9, 152.7, 152.9, 152.3, 145.0, 144.8, 136.2, 134.9, 134.8, 130.2, 129.7, 128.8, 128.6, 128.5, 128.2, 124.9, 123.5, 116.0, 115.9, 115.7, 115.6, 115.5, 115.1, 114.8, 70.8, 70.2, 70.1, 64.2, 61.5, 58.4, 48.1, 42.7, 30.1, 28.1, 22.3, 15.1; HRMS calcd. for $C_{28}H_{31}NO_3ClS$, 496.17077 $[M + H]^+$; 496.17044 $[M + H]^+$ found.

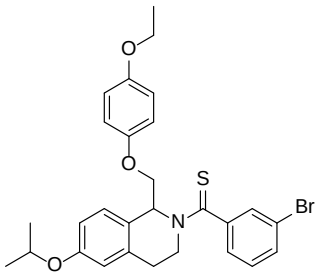

(3-bromophenyl)(1-((4-ethoxyphenoxy)methyl)-6-isopropoxy-3,4-dihydroisoquinolin-2(1H)-yl)methanethione (1180-156): Tetrahydroisoquinoline **1180-156** was prepared via procedure XV using tetrahydroisoquinoline **1180-86** (0.033 g, 0.081 mmol) and 2,4-bis(4-methoxyphenyl)-1,3,2,4-dithiadiphosphetane 2,4-disulfide (0.043 g, 0.081 mmol) in toluene (3.0 mL). The crude residue was purified by silica gel chromatography (ISCO, Redisep 12 g column, 0-80% EtOAc/hexanes gradient) to afford the title compound as a yellow foam (0.030 g, 68%, mixture of two thioamide rotamers); TLC (EtOAc:hexanes, 1:1, v/v) Rf = 0.80; ^{1}H NMR ($CDCl_3$, 400 MHz) δ: 7.50-7.40 (m, 1.5H), 7.25-7.17 (m, 1.5H), 6.88-6.69 (m, 8H), 5.74-5.70 (m, *J* = 4.8 Hz, *J* = 12.0 Hz, 0.5H), 5.41-5.38 (m, *J* = 4.0 Hz, *J* = 9.6 Hz, 0.5H), 4.70-4.66 (m, *J* = 4.0 Hz, *J* = 5.6 Hz, 0.5H), 4.59-4.52 (m, 1H), 4.49-4.45 (m, *J* = 4.8 Hz, *J* = 10.4 Hz, 0.5H), 4.20-4.12 (m, 0.5H), 4.04-3.87 (m, 4H), 3.71-3.63 (m, 0.5H), 3.36-3.27 (m, 0.5H), 2.98-2.90 (m, 1H), 2.83-2.79 (m, 0.5H), 1.42-1.33 (m, 9H); ^{13}C NMR (100 MHz, $CDCl_3$) δ: 200.2, 198.8, 157.9, 157.1, 153.8, 153.7, 152.8, 152.3, 145.3, 144.9, 136.2, 131.7, 131.5, 130.4, 128.5,

128.1, 125.9, 123.5, 122.8, 116.0, 115.9, 115.7, 115.6, 115.5, 115.1, 114.6, 70.8, 70.1, 64.2, 61.5, 58.4, 48.1, 42.7, 30.1, 29.9, 28.1, 22.3, 22.2, 15.1; HRMS calcd. for $C_{28}H_{30}BrNO_3S$, 540.12025 $[M + H]^+$; 540.12060 $[M + H]^+$ found. Anal. ($C_{28}H_{30}N_1O_3SBr$): C, H, N.

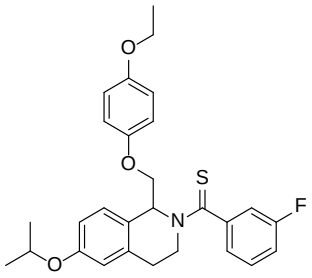

(1-((4-ethoxyphenoxy)methyl)-6-isopropoxy-3,4-dihydroisoquinolin-2(1H)-yl)(3-fluorophenyl)methanethione (1180-154): Tetrahydroisoquinoline **1180-154** was prepared via procedure XV using tetrahydroisoquinoline **1180-87** (0.10 g, 0.22 mmol) and 2,4-bis(4-methoxyphenyl)-1,3,2,4-dithiadiphosphetane 2,4-disulfide (0.045 g, 0.11 mmol) in toluene (8.0 mL). The crude residue was purified by silica gel chromatography (ISCO, Redisep 12 g column, 0-80% EtOAc/hexanes gradient) to afford the title compound as a yellow foam (0.035 g, 35%, mixture of two thioamide rotamers) TLC (EtOAc:hexanes, 1:1, v/v) Rf =0.69; ^{1}HNMR ($CDCl_3$, 400 MHz) δ: 7.34-7.33 (m, 1H), 7.07-6.97 (m, 2.5H), 6.88-6.69 (m, 7.5H), 5.75-5.70 (m, 5.2 Hz, 4.8 Hz, 0.5H), 5.42-5.38 (m, 3.6 Hz, 4.0 Hz, 0.5H), 4.70-4.67 (doublet of doublet, J = 4.4 Hz, J = 10.0 Hz, 0.5H), 4.59-4.52 (m, 1H), 4.49-4.46 (doublet of doublet, J = 4.8 Hz, J = 10.0 Hz, 0.5H), 4.21-4.13 (m, 0.5H), 4.05-3.86 (m, 2H), 3.77 (s, 3H), 3.71-3.64 (m, 0.5H), 3.36-3.27 (m, 0.5H), 2.99-2.90 (m, 1H), 2.83-2.77 (m, 0.5H), 1.42-1.33 (m, 9H); ^{13}C NMR (100 MHz, $CDCl_3$) δ: 199.2, 161.5, 157.9, 157.1, 153.9, 153.8, 152.9, 145.4, 136.2, 134.9, 130.7, 130.6, 128.5, 128.2, 124.9, 123.6, 116.0, 115.9, 115.8, 115.7, 115.6, 115.5, 115.4, 115.1, 114.7, 70.9, 64.3, 61.5, 58.4, 48.1, 42.8, 30.2, 29.9, 28.1, 22.4, 22.3, 15.2; HRMS calcd. for $C_{28}H_{31}NO_3FS$, 480.20032 $[M + H]^+$; 480.19774 $[M + H]^+$ found; mp: 75°C; Anal. ($C_{28}H_{30}N_1O_3SF$): C, H, N.

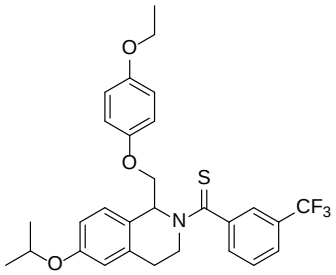

(1-((4-ethoxyphenoxy)methyl)-6-isopropoxy-3,4-dihydroisoquinolin-2(1H)-yl)(3-(trifluoromethyl)phenyl)methanethione (1180-168): Tetrahydroisoquinoline **1180-168** was prepared via procedure XV using tetrahydroisoquinoline **1180-92** (0.084 g, 0.16 mmol) and 2,4-bis(4-methoxyphenyl)-1,3,2,4-dithiadiphosphetane 2,4-disulfide (0.066 g, 0.16 mmol) in toluene (8.2 mL). After stirring for 8 hours, the reaction was worked up. The crude residue was purified by silica gel chromatography (ISCO, Redisep 12 g column, 0-80% EtOAc/hexanes gradient) to afford the title compound as a yellow foam (0.021 g, 56%, mixture of two thioamide rotamers) TLC (EtOAc:hexanes, 1:1, v/v) Rf =0.85; ^{1}HNMR ($CDCl_3$, 300 MHz) δ: 7.63-7.43 (m, 3H), 7.28-7.25 (m, 1H), 6.89-6.70 (m, 7H), 5.75-5.73 (m, 0.5H), 5.37-5.33 (m, J = 4.2 Hz, J = 3.6 Hz, 0.5H), 4.73-4.68 (m, 0.5H), 4.59-4.47 (m, 1.5H), 4.23-4.16 (m, 0.5H), 4.01-3.87 (m, 4H), 3.75-3.65 (m, 0.5H), 3.40-3.29 (m, 0.5H), 2.98-2.76 (m, 1.5H), 1.42-1.34 (9H); ^{13}C NMR (100 MHz, $CDCl_3$) δ: 200.3, 198.9, 157.9, 157.2, 153.9, 153.7, 152.8, 152.2, 144.2, 143.9, 136.2, 134.8, 129.5, 128.9, 128.5, 128.1, 125.4, 124.9, 123.3, 116.0, 115.9, 115.8, 115.6, 115.2, 114.7, 70.9, 70.2, 64.2, 61.6, 58.6, 48.2, 42.7, 30.0, 28.1, 22.2, 15.1; HRMS calcd. for $C_{29}H_{31}NO_3F_3S$, 530.19822 $[M + H]^+$; 530.19888 $[M + H]^+$ found; mp: 93°C.

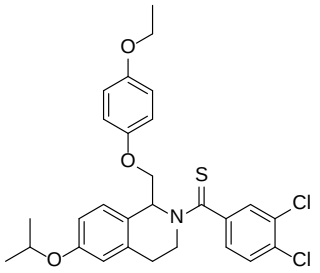

(3,4-dichlorophenyl)(1-((4-ethoxyphenoxy)methyl)-6-isopropoxy-3,4-dihydroisoquinolin-2(1H)-yl)methanethione (1180-155): Tetrahydroisoquinoline **1180-155** was prepared via procedure

XV using tetrahydroisoquinoline **1180-103** (0.045 g, 0.087 mmol) and 2,4-bis(4-methoxyphenyl)-1,3,2,4-dithiadiphosphetane 2,4-disulfide (0.035 g, 0.087 mmol) in toluene (3.0 mL). The crude residue was purified by silica gel chromatography (ISCO, Redisep 12 g column, 0-80% EtOAc/hexanes gradient) to afford the title compound as a yellow foam (0.020 g, 43%, mixture of two thioamide rotamers); TLC (EtOAc:hexanes, 1:5, v/v) Rf = 0.35; ^{1}H NMR ($CDCl_3$, 400 MHz) δ: 7.46-7.34 (m, 1H), 7.26-7.24 (m, 0.5H), 7.11-7.08 (dd, *J* = 2.0 Hz, *J* = 8.4 Hz, 0.5H), 6.90-6.70 (m, 7H), 5.72-5.67 (m, *J* = 5.2 Hz, *J* = 13.2 Hz, 0.5H), 5.40-5.37 (m, 4.0 Hz, *J* = 10.0 Hz, 0.5H), 4.69-4.67 (dd, *J* = 4.0 Hz, *J* = 10.0 Hz, 0.5H), 4.59-4.50 (m, 1H), 4.48-4.45 (dd, *J* = 4.4 Hz, *J* = 10.0 Hz, 0.5H), 4.22-4.13 (m, 0.5H), 4.04-3.89 (m, 4H), 3.70-3.62 (m, 0.5H), 3.35-3.27 (m, 0.5H), 2.95-2.80 (m, 1.5H), 1.42-1.33 (m, 9H); ^{13}C NMR (100 MHz, $CDCl_3$) δ: 199.2, 197.8, 157.9, 157.2, 153.9, 153.7, 152.8, 152.2, 143.1, 142.8, 136.2, 134.8, 133.1, 132.9, 132.7, 130.8, 128.4, 128.1, 124.8, 123.3, 116.1, 115.8, 115.7, 115.6, 115.5, 115.2, 114.7, 70.8, 70.2, 64.2, 61.6, 58.5, 53.6, 48.2, 42.6, 30.1, 29.9, 28.0, 22.3, 22.2, 15.1; HRMS calcd. for $C_{28}H_{29}Cl_2NO_3S$, 530.13180 $[M + H]^+$; 530.13173 $[M + H]^+$ found. Anal. ($C_{28}H_{29}N_1O_3SCl_2$): C, H, N.

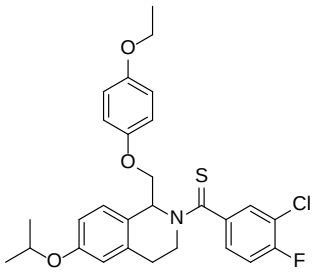

(3-chloro-4-fluorophenyl)(1-((4-ethoxyphenoxy)methyl)-6-isopropoxy-3,4-dihydroisoquinolin-2(1H)-yl)methanethione (1180-165): Tetrahydroisoquinoline **1180-165** was prepared via procedure XV using tetrahydroisoquinoline **1180-144** (0.072 g, 0.14 mmol) and 2,4-bis(4-methoxyphenyl)-1,3,2,4-dithiadiphosphetane 2,4-disulfide (0.058 g, 0.14 mmol) in toluene (7.2 mL). The crude residue was purified by silica gel chromatography (ISCO, Redisep 12 g column, 0-80% EtOAc/hexanes gradient) to afford the title compound as a yellow foam (0.026 g, 35%, mixture of two thioamide rotamers); TLC (EtOAc:hexanes, 1:1, v/v) Rf = 0.95; ^{1}H NMR ($CDCl_3$, 400 MHz)

δ: 7.32-7.24 (m, 1H), 7.15-7.14 (m, 1H), 6.89-6.70 (m, 8H), 5.73-5.68 (m, *J* = 6.0 Hz, *J* = 5.6 Hz, 0.5H), 5.14-5.38 (m, *J* = 4.0 Hz, *J* = 3.6 Hz, 0.5H), 4.70-4.66 (m, *J* = 4.0 Hz, *J* = 4.0 Hz, 0.5H), 4.58-4.51 (m, 1H), 4.49-4.45 (m, *J* = 4.4 Hz, *J* = 4.4 Hz, 0.5H), 4.23-4.14 (m, 0.5H), 4.01-3.89 (m, 4H), 3.70-3.63 (m, 0.5H), 3.37-3.29 (m, 0.5H), 2.98-2.81 (m, 1.5H), 1.42-1.34 (m, 9H); ^{13}C NMR (100 MHz, $CDCl_3$) δ: 199.6, 198.1, 159.4, 158.6, 157.9, 157.2, 157.1, 156.9, 153.9, 153.8, 152.8, 152.2, 140.5, 140.2, 136.2, 134.8, 128.5, 128.1, 124.8, 123.4, 116.9, 116.1, 115.9, 115.7, 115.6, 115.5, 115.4, 114.7, 70.8, 70.2, 70.1, 64.2, 64.1, 61.6, 58.6, 48.2, 42.7, 30.1, 27.9, 22.3, 22.2, 15.2; HRMS calcd. for $C_{28}H_{30}ClFNO_3S$, 514.16135 $[M + H]^+$; 514.16130 $[M + H]^+$ found.

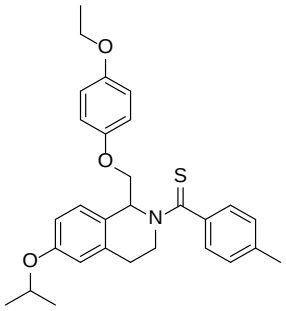

(1-((4-ethoxyphenoxy)methyl)-6-isopropoxy-3,4-dihydroisoquinolin-2(1H)-yl)(p-tolyl)methanethione (1180-304): Tetrahydroisoquinoline **1180-304** was prepared via procedure XVI using tetrahydroisoquinoline **1180-131** (0.106 g, 0.221 mmol) and 2,4-bis(4-methoxyphenyl)-1,3,2,4-dithiadiphosphetane 2,4-disulfide (0.089 g, 0.221 mmol) in toluene (8.2 mL). The crude residue was purified by silica gel chromatography (ISCO, Redisep 12 g column, 0-50% EtOAc/hexanes gradient) to afford the title compound as a yellow foam (0.053 g, 50%, mixture of two thioamide rotamers); TLC (EtOAc:hexanes, 1:3, v/v) Rf = 0.65; ^{1}H NMR ($CDCl_3$, 400 MHz) δ:7.37-7.35 (m, 1H), 7.25-7.22 (m, 1H), 6.99-6.78 (m, 9H), 5.86-5.81 (m, *J* = 4.4 Hz, *J* = 3.6 Hz, 0.5H), 5.62-5.87 (m, *J* = 4.8 Hz, *J* = 4.4 Hz, 0.5H), 4.80-4.77 (m, 0.5H), 4.67-4.57 (m, 2H), 4.28-4.20 (m, 1H), 4.07 (q, *J* = 6.8 Hz, 2H), 4.01-3.95 (m, 1H), 3.82-3.74 (m, 0.5H), 3.45-3.39 (m, 0.5H), 3.09-3.00 (m, 1H), 2.89-2.85 (m, 1H), 2.46 (d, *J* =6.0 Hz, 3H), 1.51-1.43 (m, 9H); ^{13}NMR ($CDCl_3$, 100 MHz) δ: 202.7, 201.3, 157.5, 156.8, 153.5, 153.4, 152.7, 152.2, 140.7, 140.5, 138.5, 138.3, 136.1, 134.9, 129.1, 128.6, 128.3, 127.9,

125.1, 123.8, 115.7, 115.4, 115.3, 115.2, 115.1, 114.7, 114.3, 70.8, 70.2, 69.9, 63.9, 60.9, 58.2, 47.8, 42.8, 29.9, 27.9, 22.1, 22.0, 21.3, 14.9; HRMS calcd. for $C_{29}H_{34}N_1O_2S$, 476.22539 $[M + H]^+$; found 466.22524 $[M + H]^+$.

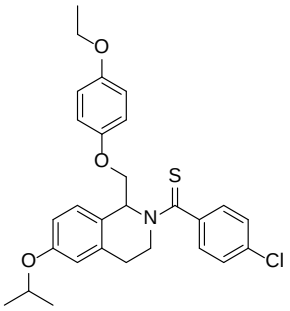

(4-chlorophenyl)(1-((4-ethoxyphenoxy)methyl)-6-isopropoxy-3,4-dihydroisoquinolin-2(1H)-yl)methanethione (1180-305): Tetrahydroisoquinoline **1180-305** was prepared via procedure XVI using tetrahydroisoquinoline **1180-132** (0.054 g, 0.105 mmol) and 2,4-bis(4-methoxyphenyl)-1,3,2,4-dithiadiphosphetane 2,4-disulfide (0.042 g, 0.105 mmol) in toluene (3.9 mL). The crude residue was purified by silica gel chromatography (ISCO, Redisep 12 g column, 0-50% EtOAc/hexanes gradient) to afford the title compound as a yellow foam (0.037 g, 70%, mixture of two thioamide rotamers); TLC (EtOAc:hexanes, 1:3, v/v) Rf = 0.70; ^{1}H NMR ($CDCl_3$, 400 MHz) δ:7.37-7.35 (m, 1H), 7.29-7.20 (m, 3H), 6.89-6.69 (m, 7H), 5.75-5.70 (m, J = 5.2 Hz, J = 6.4 Hz, 0.5H), 5.44-5.40 (m, J = 4.4 Hz, 0.5H), 4.71-4.58 (m, 0.5H), 4.57-4.52 (m, 1H), 4.49-4.46 (m, 0.5H), 4.19-4.14 (m, 0.5H), 4.07-3.88 (4H), 3.71-3.64 (m, 0.5H), 3.35-3.27 (m, 0.5H), 2.98-2.90 (m, 1H), 2.82-2.78 (m, 0.5H), 1.42-1.34 (m, 9H); ^{13}NMR (CDCl3, 100 MHz) δ: 200.9, 199.5, 157.6, 156.9, 153.5, 152.6, 152.1, 141.7, 141.5, 135.9, 134.7, 134.4, 134.2, 128.8, 128.2, 127.8, 124.8, 123.4, 115.8, 115.7, 115.4, 115.3, 114.8, 114.4, 70.7, 70.1, 69.9, 63.9, 61.1, 58.2, 47.8, 42.6, 29.8, 27.8, 21.9, 14.8; HRMS calcd. for $C_{28}H_{30}N_1O_3SCl$, 496.17077 $[M + H]^+$; found 496.17131 $[M + H]^+$.

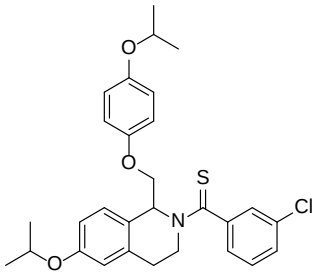

(3-chlorophenyl)(6-isopropoxy-1-((4-isopropoxyphenoxy)methyl)-3,4-dihydroisoquinolin-2(1H)-yl)methanethione (1180-265): Tetrahydroisoquinoline **1180-265** was prepared via procedure XVI using tetrahydroisoquinoline **1180-264** (0.026 g, 0.053 mmol) and 2,4-bis(4-methoxyphenyl)-1,3,2,4-dithiadiphosphetane 2,4-disulfide (0.032 g, 0.080 mmol) in toluene (0.53 mL). The crude residue was purified by silica gel chromatography (ISCO, Redisep 12 g column, 0-80% EtOAc/hexanes gradient) to afford the title compound as a yellow foam (0.014 g, 51%, mixture of two thioamide rotamers); TLC (EtOAc:hexanes, 1:3, v/v) Rf = 0.76; ^{1}H NMR ($CDCl_3$, 400 MHz) δ: 7.33-7.25 (m, 3.5 H), 7.14-7.13 (m, 0.5H), 6.88-6.69 (m, 7H), 5.75-5.71 (m, J = 5.6 Hz, J = 4.0 Hz, 0.5H), 5.41-5.37 (m, J = 4.0 Hz, J = 4.4 Hz, 0.5H), 4.69-4.68 (m, 0.5H), 4.58-4.52 (m, 1H),4.49-4.40 (m, 1.5), 4.22-4.12 (m, 0.5H), 4.04-3.88 (m, 2H), 3.71-3.64 (m, 0.5), 3.36-3.28 (m, 0.5H), 2.98-2.90 (m, 1H), 2.83-2.79 (m, 0.5H), 1.36-1.34 (m, 6H), 1.32-1.29 (m, 6H); ^{13}C NMR (100 MHz, $CDCl_3$) δ: 200.1, 198.7, 157.6, 156.9, 152.7, 152.4, 152.3, 152.2, 144.8, 144.5, 135.9, 134.7, 134.6, 129.9, 128.6, 128.4, 128.3, 127.9, 124.7, 123.3, 117.5, 117.3, 115.8, 115.6, 115.4, 115.3, 115.1, 114.9, 70.9, 70.6, 69.9, 61.3, 58.2, 47.9, 42.5, 29.8, 29.7, 27.8, 22.1, 22.0; HRMS calcd. for $C_{29}H_{33}ClNO_3S$, 510.18642 $[M + H]^+$; 510.18687 $[M + H]^+$ found.

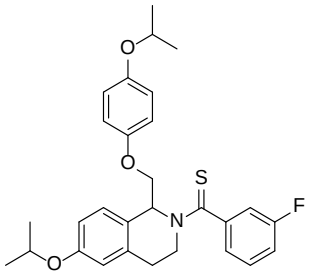

(3-fluorophenyl)(6-isopropoxy-1-((4-isopropoxyphenoxy)methyl)-3,4-dihydroisoquinolin-2(1H)-yl)methanone (1180-272): Tetrahydroisoquinoline **1180-272** was prepared via procedure XVI using tetrahydroisoquinoline **1180-270** (0.043 g, 0.090 mmol) and 2,4-bis(4-methoxyphenyl)-1,3,2,4-dithiadiphosphetane 2,4-disulfide (0.073 g, 0.18 mmol) in toluene (0.902 mL). The crude residue was purified by silica gel chromatography (ISCO, Redisep 12 g column, 10 – 80% EtOAc/hexanes gradient) to afford the title compound as an off-white foam (0.030 g, 67 % mixture of two amide rotamers) TLC (EtOAc: hexanes, 1:3, v/v) Rf = 0.89; ^{1}HNMR ($CDCl_3$, 400 MHz) δ: 7.38-7.32 (m, 0.8H), 7.25 (s, 0.2H), 7.07-6.97 (m, 2H), 6.88-6.80 (m, 5H), 6.78-6.72 (m, 2.5H), 6.70-6.69 (m, 0.5H), 5.75-5.70 (m, J = 4.8 Hz, J = 5.2 Hz, 0.5H), 5.42-5.38 (m, J = 4.0 Hz, J = 4.4 Hz, 0.5H), 4.71-4.67 (m, 0.5H), 4.58-4.52 (m, 1H), 4.49-4.39 (m, 2H), 4.19 (t, J = 10 Hz, 0.5H), 5.06-3.87 (m, 1.5H), 3.72-3.64 (m, 0.5H), 3.36-3.27 (m, 0.5H), 2.99-2.91 (m, 1H), 2.83-2.78 (m, 0.5H), 1.36-134 (m, 6H), 1.32-1.30 (m, 6H); ^{13}C NMR (100 MHz, $CDCl_3$) δ: 200.4, 199.0, 162.6 (J = 247 Hz), 157.8, 157.0, 152.9, 152.6, 152.5, 152.3, 145.3, 145.2, 136.1, 134.9, 130.6, 130.5, 128.4, 128.0, 124.9, 123.5, 117.6, 117.5, 115.9, 115.8, 115.7, 115.6, 115.5, 115.4, 115.3, 115.0, 114.6, 71.1, 71.0, 70.7, 70.2, 70.1, 70.0, 61.4, 58.3, 48.0, 42.7, 30.0, 28.0, 22.3, 22.2; HRMS calcd. for $C_{29}H_{33}FNSO_3$, 429.21597 $[M + H]^+$; found 429.21623 $[M + H]^+$

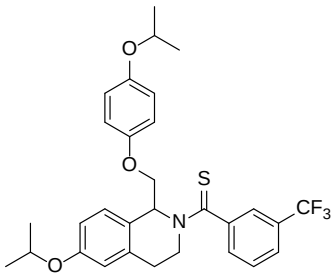

(6-isopropoxy-1-((4-isopropoxyphenoxy)methyl)-3,4-dihydroisoquinolin-2(1H)-yl)(3-(trifluoromethyl)phenyl)methanethione (1180-273): Tetrahydroisoquinoline **1180-273** was prepared via procedure XVI using tetrahydroisoquinoline **1180-271** (0.043 g, 0.093 mmol) and 2,4-bis(4-methoxyphenyl)-1,3,2,4-dithiadiphosphetane 2,4-disulfide (0.075 g, 0.18 mmol in toluene (0.93 mL). The crude residue was purified by silica gel chromatography (ISCO, Redisep 12 g column, 10 –

80% EtOAc/hexanes gradient) to afford the title compound as an off-white foam (0.035 g, 69 % mixture of two amide rotamers) TLC (EtOAc: hexanes, 1:3, v/v) Rf = 0.62; ^{1}HNMR ($CDCl_3$, 400 MHz) δ: 7.63-7.44 (m, 3H), 6.88-6.80 (m, 5H), 6.78-6.70 (m, 3H), 5.73 (bs, 0.5H), 5.36-5.33 (m, *J* = 4.0 Hz, *J* = 4.4 Hz, 0.5H), 4.73-4.58 (m, 0.5H), 5.57-4.40 (m, 3H), 4.19 (t, *J* = 10 Hz, 0.5H), 3.99-3.89 (m, 1.5H), 3.73-3.66 (m, 0.5H), 3.38-3.30 (m, 0.5H), 2.97-2.91 (m, 1H), 2.85-2.79 (m, 0.5H), 1.36-1.34 (m, 6H), 1.32-1.30 (m, 6H); ^{13}C NMR (100 MHz, $CDCl_3$) δ: 200.1, 198.7, 157.7, 156.9, 152.7, 152.5, 152.3, 152.1, 143.9, 143.6, 134.6, 129.2, 128.8, 128.3, 127.8, 125.2, 125.1, 125.1, 124.6, 123.1, 117.4, 117.3, 115.9, 115.8, 115.6, 115.4, 114.1, 114., 115.6, 114.4, 70.8, 70.6, 70.0, 69.9, 69.8, 61.3, 58.3, 47.9, 29.8, 27.8, 22.0, 21.9; HRMS calcd. for $C_{30}H_{33}F_3N_1O_3S$, 544.21278 $[M + H]^+$; found 544.21250 $[M + H]^+$.

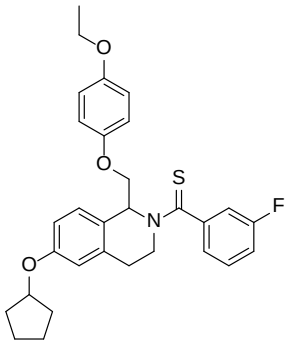

(6-(cyclopentyloxy)-1-((4-ethoxyphenoxy)methyl)-3,4-dihydroisoquinolin-2(1H)-yl)(3-fluorophenyl)methanethione (1180-162): Tetrahydroisoquinoline **1180-162** was prepared via General Procedure XV using tetrahydroisoquinoline **1180-112** (0.074 g, 0.18 mmol) and 2,4-bis(4-methoxyphenyl)-1,3,2,4-dithiadiphosphetane 2,4-disulfide (0.089 g, 0.18 mmol) in toluene (9.0 mL). The crude residue was purified by silica gel chromatography (ISCO, Redisep 12 g column, 0-80% EtOAc/hexanes gradient) to afford the title compound as a yellow foam (0.037 g, 40%); TLC (EtOAc:hexanes, 1:1, v/v) Rf = 0.90; ^{1}H NMR ($CDCl_3$, 400 MHz) δ: 7.38-7.33 (m, 1H), 7.07-6.97 (m, 2H), 6.87-6.68 (m, 8H), 5.75-5.70 (m, *J* = 4.4 Hz, *J* = 5.2 Hz, 0.5H), 5.42-5.38 (m, *J* = 4.0 Hz, *J* = 4. 4 Hz, 0.5H), 4.77-4.74 (m, 1H), 4.70-4.67 (dd, *J* = 4.4 Hz, *J* = 4.0 Hz, 0.5H), 4.49-4.46 (dd, *J* = 4.4 Hz, *J* = 4.8 Hz, 0.5H), 4.21-4.16 (m ,0.5H), 4.05-3.87 (m, 4H), 3.72-3.64 (m, 0.5H), 3.60-3.27 (m,

0.5H), 2.98-2.91 (m, 1H), 2.83-2.78 (m, 0.5H),1.93-1.76 (m, 6H), 1.65-1.60 (m, 2H), 1.42-1.38 (m, 3H); ^{13}C NMR (100 MHz, $CDCl_3$) δ: 200.4, 1990, 158.1, 157.3, 153.9, 152.9, 152.3, 145.4, 145.1, 136.1, 134.8, 120.6, 128.4, 127.9, 124.7, 123.3, 118.7, 115.9, 1155.7, 115.6, 115.3, 114.9, 114.5, 79.5, 70.8, 70.3, 64.2, 61.4, 58.4, 48.1, 42.8, 33.0, 30.1, 28.1, 24.2, 15.1; HRMS calcd. for $C_{30}H_{33}FNO_3S$, 506.21597 $[M + H]^+$; 506.21516 $[M + H]^+$ found. Anal. ($C_{30}H_{32}N_1O_3SF$): C, H, N.

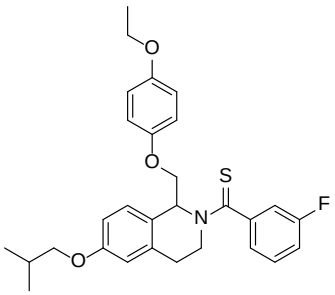

(1-((4-ethoxyphenoxy)methyl)-6-isobutoxy-3,4-dihydroisoquinolin-2(1H)-yl)(3-fluorophenyl)methanethione (1180-169): Tetrahydroisoquinoline **1180-169** was prepared via General Procedure XI using tetrahydroisoquinoline **1180-126** (0.029 g, 0.061 mmol) and 2,4-bis(4-methoxyphenyl)-1,3,2,4-dithiadiphosphetane 2,4-disulfide (0.024 g, 0.061 mmol) in toluene (3.0 mL). The crude residue was purified by silica gel chromatography (ISCO, Redisep 12 g column, 0-80% EtOAc/hexanes gradient) to afford the title compound as a yellow foam (0.018 g, 59%); TLC (EtOAc:hexanes, 1:6, v/v) Rf = 0.58; ^{1}H NMR ($CDCl_3$, 300 MHz) δ: 7.39-7.25 (m, 2H), 7.08-6.97 (m, 2H), 6.89-6.70 (m, 7H), 5.75-5.70 (m, *J* = 4.2 Hz, *J* = 5.1 Hz, 0.5H), 5.43-5.38 (m, *J* = 3.9 Hz, *J* = 3.9 Hz, 0.5H), 4.71-4.67 (dd, *J* = 3.9 Hz, *J* = 6.0 Hz, 0.5H), 4.50-4.45 (dd, *J* = 4.8 Hz, *J* = 5.7 Hz, 0.5H), 4.21-4.15 (m, 0.5H), 4.06-3.86 (m, 3.5H), 3.73-3.63 (m, 3H), 3.38-3.27 (m, 0.5H), 3.00-2.78 (m, 1.5H), 2.13-2.04 (m, 1H), 1.42-1.37 (m, 3H), 1.04-1.02 (d, *J* = 6.9 Hz, 6H); ^{13}C NMR (75 MHz, $CDCl_3$) δ: 200.5, 199.1, 164.4, 161.1, 159.2, 158.5, 153.9, 153.7, 152.9, 152.3, 145.4, 145.3, 145.1, 145.0, 136.2, 134.9, 130.7, 130.6, 128.4, 128.1, 124.9, 123.6, 115.9, 115.8, 115.7, 115.6, 115.5, 115.4, 114.7, 114.2, 114.0, 113.7, 74.7, 70.9, 70.3, 64.2, 61.4, 58.4, 48.1, 42.7, 30.1, 28.5, 28.1, 19.6, 19.4, 15.1; HRMS calcd. for $C_{29}H_{33}FNO_3S$, 494.21707 $[M + H]^+$; 494.21639 $[M + H]^+$ found.

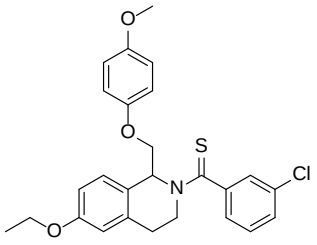

(3-chlorophenyl)(6-ethoxy-1-((4-methoxyphenoxy)methyl)-3,4-dihydroisoquinolin-2(1H)-yl)methanethione (1180-170): Tetrahydroisoquinoline **1180-170** was prepared via General Procedure XI using tetrahydroisoquinoline **1180-268** (0.14 g, 0.31 mmol) and 2,4-bis(4-methoxyphenyl)-1,3,2,4-dithiadiphosphetane 2,4-disulfide (0.13 g, 0.31 mmol) in toluene (12 mL). The crude residue was purified by silica gel chromatography (ISCO, Redisep 12 g column, 0-80% EtOAc/hexanes gradient) to afford the title compound as a yellow foam (0.017 g, 12 %); TLC (EtOAc:hexanes, 1:1, v/v) Rf = 0.85; ^{1}H NMR ($CDCl_3$, 300 MHz) δ: 7.33-7.12 (m, 4H), 6.90-6.70 (m, 7H), 5.76-5.70 (m, *J* = 4.8 Hz, *J* = 4.8 Hz, 0.5H), 5.42-5.38 (m, *J* = 3.9 Hz, *J* = 3.6 Hz, 0.5H), 4.72-4.67 (dd, *J* = 4.2 Hz, *J* = 3.9 Hz, 0.5H), 4.50-4.45 (dd, *J* = 4.8 Hz, *J* = 4.2 Hz, 0.5H), 4.22-3.86 (m, 4H), 3.78 (m, 3H), 3.73-3.63 (m, 1H), 3.38-3.27 (m, 0.5H), 3.00-2.78 (m, 1.5H), 1.45-1.40 (t, *J* = 6.9 Hz, 3H); ^{13}C NMR (100 MHz, $CDCl_3$) δ: 200.4, 199.0, 158.9, 158.2, 154.6, 152.9, 152.4, 145.1, 144.7, 136.2, 134.9, 134.8, 130.2, 129.7,l 129.2, 128.8, 128.7, 128.5. 128.1, 124.9, 123.6, 115.9, 115.6, 114.9, 114.8, 114.7, 114.6, 114.2, 114.0, 113.7, 70.9, 70.2, 63.8, 63.7, 61.5, 58.4, 55.9, 48.2, 42.7, 42.4, 30.1, 28.1, 15.1; HRMS calcd. for $C_{26}H_{27}ClNO_3S$, 468.14057 $[M + H]^+$; 468.13993 $[M + H]^+$ found.

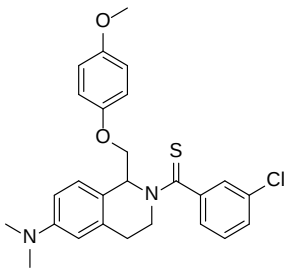

(3-chlorophenyl)(6-(dimethylamino)-1-((4-methoxyphenoxy)methyl)-3,4-dihydroisoquinolin-2(1H)-yl)methanethione (1180-167): Tetrahydroisoquinoline **1180-167** was prepared via General Procedure XI using tetrahydroisoquinoline **1180-104** (0.050 g, 0.11 mmol) and 2,4-bis(4-

methoxyphenyl)-1,3,2,4-dithiadiphosphetane 2,4-disulfide (0.045 g, 0.11 mmol) in toluene (5.5 mL). The crude residue was purified by silica gel chromatography (ISCO, Redisep 12 g column, 0-80% EtOAc/hexanes gradient) to afford the title compound as a yellow foam (0.25 g, 45%); TLC (EtOAc:hexanes, 1:1, v/v) Rf = 0.85; ^{1}H NMR ($CDCl_3$, 400 MHz) δ: 7.32-7.22 (m, 3.5H), 7.13-7.12 (m, 0.5H), 6.87-6.82 (m, 5H), 6.75-6.73 (m, 0.5H), 6.62-6.55 (m, 1.5H), 5.74-5.70 (m, *J* = 4.8 Hz, *J* = 4.4 Hz, 0.5H), 5.39-5.37 (m, *J* = 4.0 Hz, *J* = 4.0 Hz, 0.5H), 4.69-4.65 (m, *J* = 4.0 Hz, *J* = 3.6 Hz, 0.5H), 4.92-4.46 (m, *J* = 4.8 Hz, *J* = 4.8 Hz, 0.5H), 4.19-3.79 (m, 2H), 3.77 (m, 3H), 3.72-3.64 (m, 1H), 3.35-3.28 (m, 0.5H), 2.98-2.92 (7H), 2.84-2.79 (m, 0.5H); ^{13}C NMR (75 MHz, $CDCl_3$) δ: 120.2, 198.9, 154.5, 154.4, 153.0, 152.4, 150.2, 149.1, 145.1, 144.8, 135.7, 134.8, 134.6, 130.2, 129.7, 128.7, 128.6, 128.3, 127.8, 123.8, 119.8, 115.9, 115.5, 114.9, 114.8, 113.1, 112.8, 111.6, 70.7, 70.2, 61.5, 58.4, 55.9, 48.3, 42.9, 41.5, 40.9, 30.3, 28.4; HRMS calcd. for $C_{26}H_{28}ClN_2O_2S$, 467.15545 $[M + H]^+$; 467.15551 $[M + H]^+$ found.

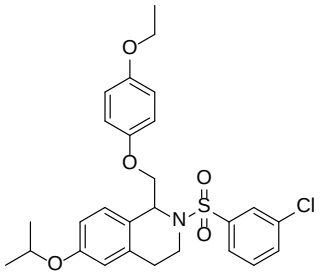

2-((3-chlorophenyl)sulfonyl)-1-((4-ethoxyphenoxy)methyl)-6-isopropoxy-1,2,3,4-tetrahydroisoquinoline (1180-199): To a solution of tetrahydroisoquinoline **28d** (.063 g, 0.19 mmol) in dry DCM (0.56 mL), triethylamine (0.028 mL, 0.20 mmol) was added followed by 3-chlorobenzene-1-sulfonyl chloride (0.024 ml, 0.17 mmol). After stirring for 5 hours, the reaction was quenched with water and diluted with DCM. The organic layer was washed with water (3x) and brine (3x), dried with $MgSO_4$, filtered, and concentrated in vacuo. The crude material was purified by silica gel chromatography (ISCO, Redisep 12 g column, 0-60% EtOAc/hexanes gradient) to afford the title compound as an off-white foam (0.055 g, 63%) TLC (EtOAc:hexanes, 2:1, v/v) Rf = 0.63; ^{1}H NMR ($CDCl_3$, 300 MHz) δ: 7.88 (s, 1H), 7.73 (d, *J* = 7.6 Hz, 1H), 7.46-7.44 (m, 1H), 7.34 (t, *J* = 7.6

Hz, 1H), 7.10 (d, *J* = 8.8 Hz, 1H), 6.81-6.72 (m, 5H), 6.59 (s, 1H), 5.30 (t, *J* = 5.6 Hz, 1H), 4.53-4.48 (m, 1H), 4.22-4.17 (m, 1H), 4.09-4.05 (m, 1H), 3.97 (q, *J* = 6.8 Hz, 2H), 3.82-3.76 (m, 1H), 3.63-3.36 (m, 1H), 2.89-2.81 (m, 1H), 2.75-2.69 (m, 1H), 1.39 (t, *J* = 7.2 Hz, 3H), 1.33-1.31 (m, 6H); ^{13}C NMR (100 MHz, $CDCl_3$) δ: 157.0, 153.3, 152.3, 142.2, 135.3, 134.9, 132.5, 130.1, 128.5, 127.3, 125.2, 124.2, 115.5, 115.3, 114.2, 71.7, 69.7, 63.9, 55.1, 40.2, 28.0, 22.0, 14.9; HRMS calcd. for $C_{27}H_{31}NO_5SCl$, 538.14254 $[M + H]^+$; 538.14196 $[M + H]^+$ found.

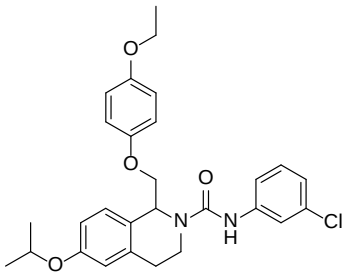

N-(3-chlorophenyl)-1-((4-ethoxyphenoxy)methyl)-6-isopropoxy-3,4-dihydroisoquinoline-2(1H)-carboxamide (1180-224): To a solution of tetrahydroisoquinoline **28d** (0.055 g, 0.16 mmol) in dry THF (1.5 mL) and 1-chloro-3-isocyanatobenzene (0.023 g, 0.15 mmol) was added slowly. The reaction was monitored by LCMS for depletion of starting material. After stirring for 2 hours, the reaction appeared to be complete. The reaction was allowed to stir for 2 hours before the solvent was removed *in vacuo* and the resulting mixture was purified by silica gel chromatography (ISCO, Redisep 12 g column, 0-80% EtOAc/hexanes gradient) to afford the title compound as an off-white foam (0.011 g, 15%) TLC (EtOAc:hexanes, 1:1, v/v) Rf = 0.83; ^{1}H NMR ($CDCl_3$, 300 MHz) δ: 7.92 (bs, 1H), 7.48-7.47 (m, 1H), 7.21-7.19 (m, 2H), 7.12 (d, J = 8.4 Hz, 1H), 6.99-6.97 (m, 1H), 6.90-6.85 (m, 4H), 6.81-6.78 (doublet of doublets, *J* = 2.4 Hz, *J* = 8.4 Hz, 1H), 6.73-6.72 (m, 1H), 5.31-5.29 (m, 1H), 4.59-4.53 (m, 1H), 4.35-4.29 (m, 2H), 4.17 (t, *J* = 9.6 Hz, 1H), 4.00 (q, *J* = 7.2 Hz, 2H), 3.28-3.21 (m, 1H), 3.07-2.99 (m, 1H), 2.82-2.77 (m, 1H), 1.41 (t, *J* = 6.8 Hz, 3H), 1.36-1.34 (m, 6H); ^{13}C NMR (100 MHz, $CDCl_3$) δ: 157.1, 155.9, 154.1, 151.7, 140.9, 137.3, 129.9, 128.2, 123.6, 122.3, 119.1, 116.9, 115.8, 115.6, 115.5, 114.5, 72.9, 69.9, 56.1, 37.8, 28.7, 22.0, 18.8; HRMS calcd. for $C_{28}H_{31}N_2O_4ClNa$, 517.18646 $[M + H]^+$; 517.18617$[M + H]^+$ found.

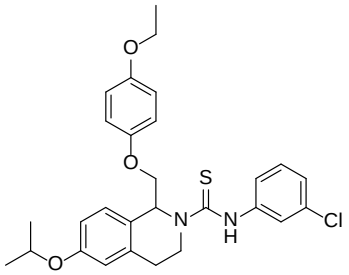

N-(3-chlorophenyl)-1-((4-ethoxyphenoxy)methyl)-6-isopropoxy-3,4-dihydroisoquinoline-2(1H)-carbothioamide (1180-210): To a solution of tetrahydroisoquinoline **28d** (0.040 g, 0.12 mmol) in THF (0.78 mL) was slowly added 1-chloro-3-isothiocyanatobenzene (0.015 ml, 0.11 mmol) dissolved in THF (0.34 mL). The reaction was allowed to stir for 1 hour before the solvent was removed *in vacuo* and the resulting mixture was purified by silica gel chromatography (ISCO, Redisep 12 g column, 0-80% EtOAc/hexanes gradient) to afford the title compound as an off-white foam (0.034 g, 64%) TLC (EtOAc:hexanes, 1:1, v/v) Rf = 0.86; ^{1}H NMR ($CDCl_3$, 300 MHz) δ: 8.85 (bs, 1H), 7.45 (s, 1H), 7.28-7.21 (m, 2H), 7.10-7.06 (m, 2H), 6.91-6.84 (m, 4H), 6.79-6.76 (m, 1H), 6.75-6.67 (m, 1H), 5.68-5.66 (m, 1H), 5.09 (bs, 1H), 4.57-4.51 (m, 1H), 4.37-4.34 (m, 1H), 4.28-4.23 (m, 1H), 4.00-3.96 (q, J = 6.8 Hz, 2H), 3.50-3.43 (m, 1H), 3.23-3.15 (m, 1H), 2.82-2.78 (m, 1H), 1.39 (t, J = 7.2 Hz, 3H), 1.33-1.31 (m, 6H); ^{13}C NMR (100 MHz, $CDCl_3$) δ: 184.0, 157.3, 154.3, 151.3, 141.4, 137.3, 134.1, 129.6, 128.1, 124.7, 123.9, 122.9, 121.8, 115.7, 114.7, 72.9, 69.9, 63.9, 59.7, 43.6, 28.2, 21.9, 14.8; HRMS calcd. for $C_{28}H_{32}N_2O_3SCl$, 511.18167 $[M + H]^+$; 511.18088 $[M + H]^+$ found.

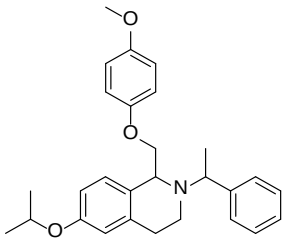

6-isopropoxy-1-((4-methoxyphenoxy)methyl)-2-(1-phenylethyl)-1,2,3,4-tetrahydroisoquinoline (31): Compound **28a** (0.073 g, 0.40 mmol) was added to a solution of diisopropylethylamine (0.094 ml, 0.54 mmol) and tetrahydroisoquinoline 8r (0.10 g, 0.31 mmol) dissolved in dry acetonitrile (0.36 ml). The reaction was allowed to stir at room temperature for 24

hours and then at 40°C for an additional 24 hours. The volatiles were concentrated and the crude residue was purified by silica gel chromatography (7:1 hexanes:EtOAc with 2.8% NEt_3) to afford the title compound as clear oil (0.033 g, 25%, 1:1 mixture of racemic diastereomers).

Upper Rf: TLC (EtOAc: hexanes, 1:7, 2.8% NEt_3, v/v) Rf = 0.60; ^{1}HNMR ($CDCl_3$, 400 MHz) δ: 7.41-7.39 (m, 2H), 7.34-7.23 (m, 4H), 7.14-7.12 (m, 1H), 6.89-6.82 (m, 3H), 6.77-6.70 (m, 1H), 6.63-6.62 (m, 1H), 4.55-4.49 (m, 1H), 4.35 (t, *J* = 5.6 Hz, 1H), 4.27-4.23 (m, 1H), 4.01-3.96 (m, 2H), 3.78 (s, 3H), 3.13-3.06 (m, 1H), 2.90-2.82 (m, 1H), 2.79-2.74 (m, 1H), 2.48-2.42 (dt, *J* = 3.6 Hz, *J* = 16.4 Hz, 1H), 1.39 (d, *J* = 6.0 Hz, 3H), 1.34 (d, *J* = 6.0 Hz, 6H).

Lower Rf: TLC (EtOAc: hexanes, 1:7, 2.8% NEt_3, v/v) Rf = 0.45; ^{1}HNMR ($CDCl_3$, 400 MHz) δ: 7.43-7.41 (m, 2H), 7.33-7.23 (m, 3H), 7.02 (d, *J* = 8.4 Hz, 1H), 6.79-6.66 (m, 6H), 4.56-4.50 (m, 1H), 4.24-4.20 (m, 1H), 4.11 (t, *J* = 6.0 Hz, 1H), 3.97-3.92 (m, 1H), 3.89-3.86 (m, 1H), 3.76 (s, 3H), 3.21-3.17 (m, 2H), 2.96-2.88 (m, 1H), 2.56-2.50 (dt, *J* = 3.6 Hz, *J* = 16.8 Hz, 1H), 1.44 (d, *J* = 6.8 Hz, 3H), 1.34 (d, *J* = 5.6 Hz, 6H).

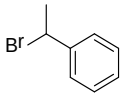

(1-bromoethyl)benzene (32): (*R*)-1-phenylethanol (0.72 ml, 6.6 mmol) and perbromomethane (3.3 g, 9.8 mmol) were dissolved in dry DCM (22 ml) and brought to 0 °C using an ice bath. Triphenylphosphine (3.4 g, 13 mmol) was added and the reaction was allowed to warm to room temperature. After stirring for 2 hours, TLC indicated complete conversion. After evaporation of the volatiles, hexane was added and the precipitated white solid was filtered. The filtrate was concentrated *in vacuo*. The crude residue was purified by silica gel chromatography (ISCO, Redisep 12 g column, 0 – 60 % EtOAc/hexanes gradient) to afford the title compound as a clear liquid (0.32 g, 28 % yield, mixture of enantiomers) TLC (EtOAc: hexanes, 1:1, v/v) Rf = 0.89; ^{1}HNMR ($CDCl_3$, 400 MHz) δ: 7.47-7.44 (m, 2H), 7.38-7.27 (m, 3H), 5.24 (q, *J* = 7.2 Hz, 1H), 2.07 (d, *J* = 6.4 Hz, 3H); ^{13}C NMR ($CDCl_3$, 100 MHz) δ: 128.9, 128.6, 127.0, 49.8, 27.0.

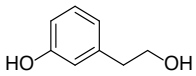

3-(2-hydroxyethyl)phenol (36): 2-(3-hydroxyphenyl)acetic acid (2.6 g, 17 mmol) was dissolved in dry THF (50. ml) and brought to 0 °C using an ice bath. Borane dimethyl sulfide (17 ml, 34 mmol) was added dropwise. The ice bath was removed and the reaction was slowly heated to 75°C using an oil bath and allowed to reflux overnight. The reaction was quenched with a dropwise addition of MeOH and the volatiles were removed *in vacuo*. The crude residue was purified by silica gel chromatography (ISCO, Redisep 40 g column, 0-80% EtOAc/hexanes gradient) to afford the title compound as a clear oil (2.1 g, 91 %) TLC (EtOAc:hexanes, 1:1, v/v) Rf = 0.27; ^{1}H NMR ($CDCl_3$, 400 MHz) δ: 7.21-7.17 (m, 1H), 6.81-6.79 (m, 1H), 6.72-6.71 (m, 2H), 3.87 (t, *J* = 6.4 Hz, 2H), 2.83 (t, *J* = 6.4 Hz, 2H); ^{13}C NMR (100 MHz, $CDCl_3$) δ: 156.2, 140.4, 130.1, 121.3, 116.3, 113.9, 63.7, 38.9; HRMS calcd. for $C_8H_{11}O_2$, 139.07536 $[M + H]^+$; 139.07506 $[M + H]^+$ found.

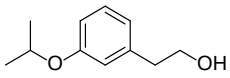

2-(3-isopropoxyphenyl)ethanol (37): Compound **36** (7.8 g, 57 mmol) was dissolved in dry Acetonitrile (171 ml) and cesium carbonate (56 g, 170 mmol) was added. The reaction was allowed to stir at room temp for 1 hour before 2-iodopropane (6.8 ml, 68 mmol) was added. The reaction was then heated to 60 °C and allowed to stir overnight. The reaction was quenched with saturated ammonium chloride and was extracted into EtOAc. The organic layer was washed with water (3x) and brine (3x), dried with $MgSO_4$, filtered, and concentrated *in vacuo*. The crude residue was purified by silica gel chromatography (ISCO, Redisep 40 g column, 0-90% EtOAc/hexanes gradient) to afford the title compound as a clear oil (6.6 g, 65 %) TLC (EtOAc:hexanes, 1:1, v/v) Rf = 0.60; ^{1}H NMR ($CDCl_3$, 400 MHz) δ: 7.24-7.20 (m, 1H), 6.81-6.76 (m, 3H), 4.59-4.53 (m, 1H), 3.86-3.82 (m, 2H), 2.81 (t, J = 6.4 Hz, 2H), 1.35 (d, J = 6.4 Hz, 6H); ^{13}C NMR (100 MHz, $CDCl_3$) δ: 158.3, 140.3, 129.8, 121.4, 116.9, 113.7, 69.9, 63.8, 39.4, 22.3; HRMS calcd. for $C_{11}H_{17}O_2$, 181.12231 $[M + H]^+$; 181.12231 $[M + H]^+$ found.

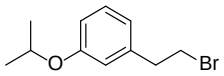

1-(2-bromoethyl)-3-isopropoxybenzene (38): Compound **37** (6.0g, 34 mmol) was dissolved in DCM (69 ml) and perbromomethane (13 g, 39 mmol) was added. Triphenylphosphine (11 g, 40. mmol) was added slowly over a period of 30 minutes and then the reaction was allowed to stir overnight at room temperature. After stirring for 24 hours, the volatiles were removed *in vacuo* and 1:1 hexanes:Et_2O mixture was added to the residue. A white solid crashed out of solution. The reaction was filtered, and the filtrate was concentrated *in vacuo* to afford the crude residue. The crude residue was purified by silica gel chromatography (ISCO, Redisep 40 g column, 0-60% EtOAc/hexanes gradient) to afford the title compound as a yellow liquid (7.5 g, 92 %) TLC (EtOAc:hexanes, 1:3, v/v) Rf = 0.86; ^{1}H NMR ($CDCl_3$, 400 MHz) δ: 7.25 (t, *J* = 8.0 Hz, 1H), 6.85-6.78 (m, 3H), 4.61-4.55 (m, 1H), 3.59 (t, *J* = 8.0 Hz, 2H), 3.16 (t, *J* = 7.6 Hz, 7.6 Hz, 2H), 1.38 (d, *J* = 6.0 Hz, 6H); ^{13}C NMR (100 MHz, $CDCl_3$) δ: 158.3, 140.6, 129.8, 120.9, 116.6, 114.2, 69.9, 39.7, 33.1, 22.3; HRMS calcd. for $C_{11}H_{16}BrO$, 243.03790 $[M + H]^+$; 243.03796 $[M + H]^+$ found.

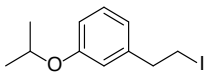

1-(2-iodoethyl)-3-isopropoxybenzene (39): Compound **38** (2.0 g, 8.2 mmol) was dissolved in acetone (33 ml) and sodium iodide (3.7 g, 25 mmol) was added. The reaction was brought to 45 °C and allowed to reflux overnight. After 20 hours, the volatiles were removed *in vacuo* and the residue was taken up into DCM. Et_2O was added and a white solid crashed out of solution. The reaction was filtered and the filtrate was concentrated *in vacuo* to afford the crude residue. The crude residue was purified by silica gel chromatography (ISCO, Redisep 40 g column, 0-60% EtOAc/hexanes gradient) to afford the title compound as a yellow oil (1.2 g, 53 %) TLC (EtOAc:hexanes, 1:3, v/v) Rf = 0.80; ^{1}H NMR ($CDCl_3$, 400 MHz) δ: 7.23 (t, *J* = 7.6 Hz, 1H), 6.83-6.74 (m, 3H), 4.60-4.54 (m, 1H), 3.36 (t, *J* = 7.6 Hz, 2H), 3.16 (t, *J* = 7.6 Hz, 2H), 1.36 (d, *J* = 6.0 Hz, 6H); ^{13}C NMR (100 MHz, $CDCl_3$) δ:

158.3, 142.4, 129.8, 120.7, 116.2, 114.2, 69.9, 40.7, 22.3, 5.7; HRMS calcd. for $C_{11}H_{16}IO$, 291.02403 $[M + H]^+$; 291.02424 $[M + H]^+$ found.

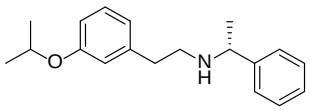

(*R*)-N-(3-isopropoxyphenethyl)-1-phenylethanamine ((*R*)-41): Compound **39** (5.1 g, 17 mmol) was dissolved in dry THF (87 ml) and (*R*)-1-phenylethanamine (2.8 g, 23 mmol) was added followed by *N*-ethyl-*N*-isopropylpropan-2-amine (4.6 ml, 26 mmol). The reaction was then heated to 60 °C and allowed to stir overnight. After stirring overnight, the volatiles were removed *in vacuo* and the reaction was taken up into DCM and washed with water (3x) and brine (3x), dried with $MgSO_4$, filtered, and concentrated *in vacuo*. The crude residue was purified by silica gel chromatography (ISCO, Redisep 40 g column, 0-90% EtOAc/hexanes gradient) to afford the title compound as a yellow oil (1.6 g, 33 %) TLC (EtOAc:hexanes, 1:1, v/v) Rf = 0.28; ^{1}H NMR ($CDCl_3$, 400 MHz) δ: 7.33-7.15 (m, 5H), 7.17 (t, *J* = 8.0 Hz, 1H), 6.74-6.70 (m, 3H), 4.55-4.49 (m, 1H), 3.78 (q, *J* = 6.8 Hz, 1H), 2.96-2.69 (m, 2H), 1.34-1.32 (m, 9H); ^{13}C NMR (100 MHz, $CDCl_3$) δ: 158.2, 145.8, 141.9, 129.6, 128.6, 127.1, 126.7, 121.1, 116.6, 113.5, 69.8, 58.4, 49.0, 36.6, 24.5, 22.3; HRMS calcd. for $C_{19}H_{26}NO$, 284.20089 $[M + H]^+$; 284.20034 $[M + H]^+$ found; $[\alpha]_D^{20}$ = +43.8 (*c* 1.0, dry $CHCl_3$).

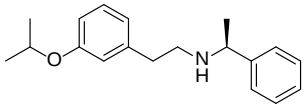

(*S*)-N-(3-isopropoxyphenethyl)-1-phenylethanamine ((*S*)-41): Compound **39** (3.2 g, 11 mmol) was dissolved in dry THF (42 ml) and (*S*)-1-phenylethanamine (1.7 g, 14 mmol) was added followed by *N*-ethyl-*N*-isopropylpropan-2-amine (2.1 ml, 16 mmol). The reaction was then heated to 60 °C and allowed to stir overnight. After stirring overnight, the volatiles were removed *in vacuo* and the reaction was taken up into DCM and washed with water (3x) and brine (3x), dried with $MgSO_4$, filtered, and concentrated *in vacuo*. The crude residue was purified by silica gel chromatography (ISCO, Redisep 40 g column, 0-90% EtOAc/hexanes gradient) to afford the title compound as a

yellow oil (1.6 g, 33 %) TLC (EtOAc:hexanes, 1:1, v/v) Rf = 0.25; ^{1}H NMR ($CDCl_3$, 400 MHz) δ: 7.33-7.23 (m, 5H), 7.17 (t, *J* = 8.0 Hz, 1H), 6.75-6.71 (m, 3H), 4.55-4.49 (m, 1H), 3.77 (q, *J* = 6.8 Hz, 1H), 2.80-2.69 (m, 4H), 1.34-1.32 (m, 9H); ^{13}C NMR (100 MHz, $CDCl_3$) δ: 158.2, 145.9, 141.9, 129.6, 128.7, 127.1, 126.8, 121.1, 116.6, 113.5, 69.8, 58.4, 49.1, 36.7, 24.6, 22.3; HRMS calcd. for $C_{19}H_{26}NO$, 284.20089 $[M + H]^+$; 284.20087 $[M + H]^+$ found; $[\alpha]_D^{20}$ = -43.3 (*c* 1.0, dry $CHCl_3$).

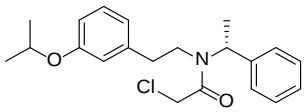

(*R*)-2-chloro-N-(3-isopropoxyphenethyl)-N-(1-phenylethyl)acetamide ((*R*)-42): Compound **(*R*)-41** (1.6 g, 5.7 mmol) was dissolved in dry DCM (25 ml) and brought to 0 °C using an ice bath. Triethylamine (1.6 ml, 11 mmol) was added followed by 2-chloroacetyl chloride (0.55 ml, 6.9 mmol). After stirring for 4 hours the reaction was quenched with 1M HCl and extracted into DCM, washed with water (3x), brine (3x), dried with $MgSO_4$, filtered, and concentrated *in vacuo*. The crude residue was purified by silica gel chromatography (ISCO, Redisep 40 g column, 0-70% EtOAc/hexanes gradient) to afford the title compound as a yellow solid (1.7 g, 87 %, a mixture of rotamers) TLC (EtOAc:hexanes, 1:1, v/v) Rf = 0.80; ^{1}H NMR ($CDCl_3$, 400 MHz) δ: 7.40-7.33 (m, 5H), 7.18-7.10 (m, 1H), 6.74-6.69 (m, 1H), 6.60-6.58 (m, 1H), 6.52-6.46 (m, 1H), 6.00 (q, *J* = 6.4 Hz, 0.5H), 5.72 (q, *J* = 6.8 Hz, 0.5H), 4.53-4.47 (m, 1H), 4.29-4.21 (m, 1H), 4.05 (s, 1H), 3.39-3.29 (m, 1.5H) 3.26-3.16 (m, 0.5H), 2.79-2.72 (m, 0.5H), 2.61-2.53 (m, 0.5H), 2.48-2.41 (m, 0.5H), 2.31-2.23 (m, 0.5H), 1.68-1.60 (m, 3H), 1.33-1.30 (m, 6H); ^{13}C NMR (100 MHz, $CDCl_3$) δ: 166.9, 166.6, 158.3, 158.1, 141.0, 140.2, 139.7, 130.0, 129.6, 129.0, 128.9, 128.3, 128.2, 127.2, 121.1, 120.7, 116.6, 116.4, 113.8, 69.9, 69.8, 56.2, 52.5, 46.1, 45.9, 42.0, 41.8, 37.5, 34.8, 22.3, 18.4, 16.8; HRMS calcd. for $C_{21}H_{26}ClNO_2Na$, 382.15443 $[M + H]^+$; 382.15435 $[M + H]^+$ found; $[\alpha]_D^{20}$ = +54.6 (*c* 1.0, dry $CHCl_3$).

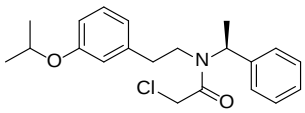

(*S*)-2-chloro-N-(3-isopropoxyphenethyl)-N-(1-phenylethyl)acetamide ((*S*)-42): Compound **(*S*)-41** (1.4 g, 4.8 mmol) was dissolved in dry DCM (21 ml) and brought to 0 °C using an ice bath. Triethylamine (1.3 ml, 9.6 mmol) was added followed by 2-chloroacetyl chloride (0.46 ml, 5.7 mmol). After stirring for 4 hours the reaction was quenched with 1M HCl and extracted into DCM, washed with water (3x), brine (3x), dried with $MgSO_4$, filtered, and concentrated *in vacuo*. The crude residue was purified by silica gel chromatography (ISCO, Redisep 40 g column, 0-70% EtOAc/hexanes gradient) to afford the title compound as a yellow solid (1.7 g, 87 %, a mixture of rotamers) TLC (EtOAc:hexanes, 1:1, v/v) Rf = 0.88; ^{1}H NMR ($CDCl_3$, 400 MHz) δ: 7.41-7.33 (m, 5H), 7.18-7.11 (m, 1H), 6.74-6.69 (m, 1H), 6.60-6.58 (m, 1H), 6.52-6.46 (m, 1H), 6.00 (q, *J* = 6.8 Hz, 0.5H), 5.17 (q, *J* = 6.8 Hz, 0.5H), 4.53-4.47 (m, 1H), 4.29-4.21 (m, 1H), 4.05 (s, 1H), 3.39-3.29 (m, 1.5H), 3.24-3.16 (m, 0.5H), 2.80-2.72 (m, 0.5H), 2.61-2.53 (m, 0.5H), 2.48-2.41 (m, 0.5H), 2.31-2.23 (m, 0.5H), 1.66-1.60 (m, 3H), 1.34-1.30 (m, 6H); ^{13}C NMR (100 MHz, $CDCl_3$) δ: 166.9, 166.6, 158.3, 158.1, 141.0, 140.2, 139.7, 130.0, 129.6, 129.0, 128.9, 128.3, 128.2, 127.2, 121.1, 120.7, 116.6, 116.4, 113.8, 69.9, 69.8, 56.2, 52.5, 46.1, 45.9, 42.1, 41.7, 37.5, 24.8, 22.3, 18.4, 16.8; HRMS calcd. for $C_{21}H_{27}ClNO_2$, 360.17248 $[M + H]^+$; 360.17287 $[M + H]^+$ found; $[\alpha]_D^{20}$ = -54.9 (*c* 1.0, dry $CHCl_3$).

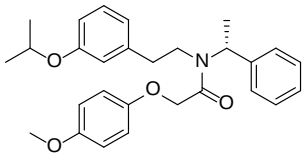

(*R*)-N-(3-isopropoxyphenethyl)-2-(4-methoxyphenoxy)-N-(1-phenylethyl)acetamide ((*R*)-34): 4-methoxyphenol (0.74 g, 5.9 mmol) was dissolved in dry Acetonitrile (7.5 ml) and cesium carbonate (4.9 g, 15 mmol) was added. The reaction was allowed to stir for 2 hours before **(*R*)-42** (1.8 g, 4.9 mmol) dissolved in dry Acetonitrile (7.5 ml) was added. The reaction was then allowed to stir at room temperature overnight. After stirring for 24 hours, the reaction was quenched with saturated ammonium chloride and extracted into EtOAc. The organic layer was washed with water and brine, dried with $MgSO_4$, filtered, and concentrated *in vacuo*. The crude residue was purified by

silica gel chromatography (ISCO, Redisep 40 g column, 0-80% EtOAc/hexanes gradient) to afford the title compound as a yellow oil (2.0 g, 88 %, a mixture of rotamers) TLC (EtOAc:hexanes, 1:1, v/v) Rf = 0.83; ^{1}H NMR ($CDCl_3$, 400 MHz) δ: 7.40-7.31 (m, 4H), 7.16-7.08 (m, 1H), 6.95-6.82 (m, 4H), 6.79 (s, 1H), 6.72-6.67 (m, 1H), 6.57-6.60 (m, 1H), 6.00 (q, *J* = 7.2 Hz, 0.5H), 5.35 (q, *J* = 6.4 Hz, 0.5H), 4.86-4.78 (dd, *J* = 13.2 Hz, *J* = 8.4 Hz, 1H), 4.67 (s, 1H), 4.52-4.43 (m, 1H), 3.79-3.77 (m, 3H), 3.39-3.31 (m, 1.5H), 3.22-3.24 (m, 0.5H), 2.77-2.69 (m, 0.5H), 2.65-2.57 (m, 0.5H), 2.46-2.39 (m, 0.5H), 2.32--2.24 (m, 0.5H), 1.61 (d, *J* = 6.4 Hz, 3H), 1.29 (d, *J* = 6.4 Hz, 6H); ^{13}C NMR (100 MHz, $CDCl_3$) δ: 168.6, 168.3, 158.3, 158.1, 154.6, 153.5, 152.3, 150.5, 141.2, 140.4, 140.0, 129.9, 129.6, 128.9, 128.8, 128.2, 128.1, 127.4, 121.2, 120.8, 116.4, 116.3, 116.0, 115.8, 115.0, 114.9, 113.9, 69.8, 69.1, 68.5, 60.7, 60.0, 55.9, 55.2, 52.4, 45.7, 37.3, 34.9, 22.3, 18.3, 16.9; HRMS calcd. for $C_{28}H_{34}NO_4$, 448.24824 $[M + H]^+$; 448.24786 $[M + H]^+$ found; $[\alpha]_D^{20}$ = +48.0 (*c* 1.0, dry $CHCl_3$).

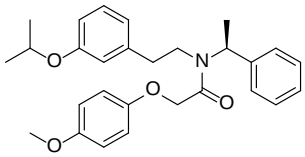

(*S*)-N-(3-isopropoxyphenethyl)-2-(4-methoxyphenoxy)-N-(1-phenylethyl)acetamide ((*S*)-34): 4-methoxyphenol (0.55 g, 4.4 mmol) was dissolved in dry acetonitrile (5.6 ml) and cesium carbonate (2.4 g, 7.4 mmol) was added. The reaction was allowed to stir for 2 hours before **(*S*)-42** (1.3 g, 3.7 mmol) dissolved in dry Acetonitrile (5.6 ml) was added. The reaction was then allowed to stir at room temperature overnight. After stirring for 24 hours, the reaction was quenched with saturated ammonium chloride and extracted into EtOAc. The organic layer was washed with water and brine, dried with $MgSO_4$, filtered, and concentrated *in vacuo*. The crude residue was purified by silica gel chromatography (ISCO, Redisep 40 g column, 0-80% EtOAc/hexanes gradient) to afford the title compound as a yellow oil (1.4 g, 89 %, a mixture of rotamers) TLC (EtOAc:hexanes, 1:1, v/v) Rf = 0.85; ^{1}H NMR ($CDCl_3$, 400 MHz) δ: 7.40-7.27 (m, 5H), 7.17-7.09 (m, 1H), 6.96-6.79 (m, 5H), 6.73-6.68 (m, 1H), 6.58-6.56 (m, 1H), 6.05-6.01 (m, 0.5H), 5.37-5.32 (m, 0.5H), 4.87-4.78 (dd, *J* = 13.2 Hz,

J = 8.0 Hz, 1H), 4.67 (m, 1H), 4.52-4.44 (m, 1H), 3.79-3.76 (m, 3H), 3.40-3.30 (m, 1.5H), 3.23-3.15 (m, 0.5H), 2.77-2.70 (m, 0.5H), 2.65-2.58 (m, 0.5H), 2.47-2.40 (m, 0.5H), 2.32-2.26 (m, 0.5H), 1.63-1.61 (m, 3H), 1.30 (d, *J* = 6.0 Hz, 6H); ^{13}C NMR (100 MHz, $CDCl_3$) δ: 168.6, 168.3, 158.3, 158.1, 154.6, 153.6, 152.4, 152.3, 150.3, 141.2, 140.4, 140.1, 129.9, 129.6, 128.6, 128.8, 128.2, 128.0, 127.3, 121.2, 120.8, 116.4, 116.3, 115.9, 115.8, 114.9, 113.8, 69.8, 69.1, 68.5, 60.0, 55.9, 55.2, 45.7, 37.3, 34.9, 22.3, 18.3, 16.9; HRMS calcd. for $C_{28}H_{34}NO_4$, 448.24824 $[M + H]^+$; 448.24809 $[M + H]^+$ found; $[\alpha]_D^{20}$ = -47.6 (*c* 1.0, dry $CHCl_3$).

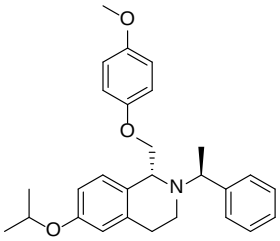

(*R*)-6-isopropoxy-1-((4-methoxyphenoxy)methyl)-2-((*S*)-1-phenylethyl)-1,2,3,4-tetrahydroisoquinoline ((*R, S*)-31): Dihydroisoquinoline **(*S*)-43** was prepared via Procedure XI using **(*S*)-34** (1.9 g, 4.4 mmol) and phosphorous trichloride (2.7 mL, 13 mmol) in dry toluene (67 mL). The crude residue (2.5 g) was carried on without further purification. Tetrahydroisoquinoline **(*R, S*)-31** was prepared via Procedure XII using dihydroisoquinoline **(*S*)-43** (2.5 g, 5.8 mmol) and sodium borohydride (0.44 g, 12 mmol) in dry MeOH (29 mL). The crude residue was purified by silica gel chromatography (7:1 hexanes:EtOAc with 2.8% NEt_3) to afford the title compound as clear oil (0.37 g, 15%, d.r. 9:1); TLC (EtOAc:hexanes, 1:7 with 2.8 NEt_3, v/v) Rf = 0.43; ^{1}H NMR ($CDCl_3$, 400 MHz) δ: 7.43-7.41 (m, 2H), 7.33-7.23 (m, 4H), 7.02 (d, *J* = 8.0 Hz, 1H), 6.79-6.65 (m, 5H), 4.55-4.50 (m, 1H), 4.24-4.20 (m, 1H), 4.12-4.09 (m, 1H), 3.96-3.92 (m, 1H), 3.89-3.85 (m, 1H), 3.77 (s, 3H), 3.21-3.17 (m, 2H), 2.96-2.88 (m, 1H), 2.55-2.50 (doublet of triplets, *J* = 3.6 Hz, *J* = 16.8 Hz, 1H), 1.44 (d, *J* = 6.8 Hz, 3H), 1.33 (d, *J* = 6.0 Hz, 6H); ^{13}C NMR (100 MHz, $CDCl_3$) δ: 156.6, 153.7, 153.4, 146.3, 137.3, 130.1, 128.5, 127.8, 127.3, 127.0, 115.5, 114.7, 113.9, 72.4, 69.9, 59.6, 5.7, 55.9,

40.6, 25.4, 22.4, 22.3, 21.2; HRMS calcd. for $C_{28}H_{34}NO_3$, 432.25332 $[M + H]^+$; 432.25289 $[M + H]^+$ found.

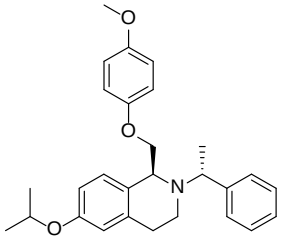

(*S*)-6-isopropoxy-1-((4-methoxyphenoxy)methyl)-2-((*R*)-1-phenylethyl)-1,2,3,4-tetrahydroisoquinoline ((*S, R*)-31): Dihydroisoquinoline **(*R*)-43** was prepared via Procedure XI using **(*R*)-34** (0.88 g, 1.9 mmol) and phosphorous trichloride (1.2 mL, 1.9 mmol) in dry toluene (18 mL). The crude residue (1.5 g) was carried on without further purification. Tetrahydroisoquinoline (***S, R*)-31** was prepared via Procedure XII using dihydroisoquinoline **(*R*)-43** (1.5g, 3.6 mmol) and sodium borohydride (0.27 g, 7.2 mmol) in dry MeOH (18 mL). The crude residue was purified by silica gel chromatography (7:1 hexanes:EtOAc with 2.8% NEt_3) to afford the title compound as clear oil (0.23 g, 15 %, d.r. 85:15); TLC (EtOAc:hexanes, 1:7 with 2.8 NEt_3, v/v) Rf = 0.43; ^{1}H NMR ($CDCl_3$, 400 MHz) δ: 7.43-7.41 (m, 2H), 7.33-7.23 (m, 4H), 7.02 (d, *J* = 8.0 Hz, 1H), 6.79-6.66 (m, 5H), 4.56 - 4.50 (m, 1H), 4.24-4.20 (m, 1H), 4.12-4.09 (m, 1H), 3.95 (q, *J* = 8.0 Hz, 1H), 3.89-3.86 (m, 1H), 3.76 (s, 3H), 3.20-3.14 (m, 2H), 2.96-2.88 (m, 1H), 2.56-2.51 (doublet of triplets, *J* = 3.6 Hz, *J* = 16.8 Hz, 1H), 1.45 (d, *J* = 6.8 Hz, 3H), 1.34 (d, *J* = 6.0 Hz, 6H); ^{13}C NMR (100 MHz, $CDCl_3$) δ:156.6, 153.8, 153.4, 146.3, 137.3, 130.1, 128.5, 127.8, 127.4, 127.0, 115.6, 114.7, 113.9, 72.4, 69.9, 59.6, 57.7, 55.9, 40.6, 25.5, 22.4, 21.2; HRMS calcd. for $C_{28}H_{34}NO_3$, 432.25332 $[M + H]^+$; 432.25457 $[M + H]^+$ found.

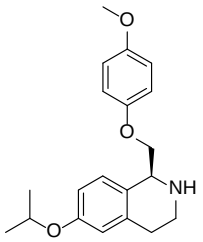

(*S*)-6-isopropoxy-1-((4-methoxyphenoxy)methyl)-1,2,3,4-tetrahydroisoquinoline ((*S*)-28a): Tetrahydroisoquinoline **(*S, R*)-31** (0.37 g, 0.87 mmol) was dissolved in 2-propanol (8.7 ml) and THF (8.7 ml). Palladium on carbon (0.19 g, 0.18 mmol) was added and the reaction was hydrogenated at room temperature using a balloon overnight. After stirring for 24 hours, the reaction was filtered thru celite washing with MeOH and EtOAc and the residue was concentrated *in vacuo*. The crude residue was purified by silica gel chromatography (ISCO, Redisep 24 g column, 0-20% MeOH/DCM gradient) to afford the title compound as clear oil (0.15 g, 51%); TLC (DCM:MeOH, 10:1, v/v) Rf = 0.78; ^{1}H NMR ($CDCl_3$, 400 MHz) δ: 7.08 (d, J = 8.4 Hz, 1H), 6.91-6.82 (m, 4H), 6.75-6.71 (m, 1H), 6.68-6.67 (m, 1H), 4.56-4.50 (m, 1H), 4.38-4.35 (dd, J = 3.6 Hz, J = 8.8 Hz, 1H), 4.16-4.05 (m, 2H), 3.78 (s, 3H), 3.26-3.20 (m, 1H), 3.07-3.00 (m, 1H), 2.85-2.81 (m, 2H), 1.33 (d, J = 6.0 Hz, 6H); ^{13}C NMR (100 MHz, $CDCl_3$) δ: 156.7, 154.2, 137.4, 127.7, 126.7, 116.3, 115.8, 114.9, 114.0, 71.4, 69.9, 55.9, 54.8, 39.8, 30.2, 22.3; HRMS calcd. for $C_{20}H_{26}NO_3$, 328.19072 $[M + H]^+$; 328.19039 $[M + H]^+$ found; $[\alpha]_D^{20}$ = +14.2 (*c* 1.0, dry $CHCl_3$).

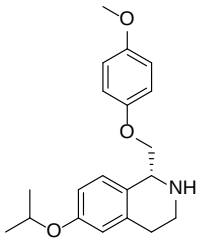

(*R*)-6-isopropoxy-1-((4-methoxyphenoxy)methyl)-1,2,3,4-tetrahydroisoquinoline ((*R*)-28a): Tetrahydroisoquinoline **(*R,S)*-31** (0.23 g, 0.53 mmol) was dissolved in 2-propanol (5.3 ml) and THF (5.3 ml). Palladium on carbon (0.11 g, 0.11 mmol) was added and the reaction was hydrogenated at room temperature using a balloon overnight. After stirring for 24 hours, the reaction was filtered thru celite washing with MeOH and EtOAc and the residue was concentrated *in vacuo*. The crude residue was purified by silica gel chromatography (ISCO, Redisep 24 g column, 0-20% MeOH/DCM gradient) to afford the title compound as clear oil (0.11 g, 64%); TLC (DCM:MeOH, 10:1, v/v) Rf = 0.61; ^{1}H NMR ($CDCl_3$, 400 MHz) δ: 7.08 (d, J = 8.8 Hz, 1H), 6.90-6.83 (m, 4H), 6.74-6.71 (m, 1H),

6.67-6.66 (m, 1H), 4.56-4.50 (m, 1H), 4.38-4.35 (dd, *J* = 3.6 Hz, *J* = 8.8 Hz, 1H), 4.16-4.05 (m, 2H), 3.78 (s, 3H), 3.26-3.20 (m, 1H), 3.06-3.00 (m, 1H), 2.88-2.80 (m, 2H), 1.33 (d, *J* = 5.6 Hz, 6H); ^{13}C NMR (100 MHz, $CDCl_3$) δ: 157.2, 154.4, 152.6, 136.0, 127.6, 123.9, 116.1, 115.9, 114.8, 114.7, 70.4, 70.0, 55.9, 54.6, 39.9, 28.4, 22.3; HRMS calcd. for $C_{20}H_{26}NO_3$, 328.19072 $[M + H]^+$; 328.19120 $[M + H]^+$ found; $[\alpha]_D^{20}$ = -15.9 (*c* 1.0, dry $CHCl_3$).

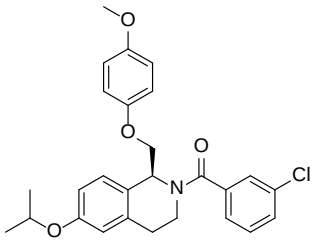

(*S*)-(3-chlorophenyl)(6-isopropoxy-1-((4-methoxyphenoxy)methyl)-3,4-dihydroisoquinolin-2(1H)-yl)methanone ((*S*)-1180-55): Tetrahydroisoquinoline **(*S*)-1180-55** was prepared via procedure XIII using **(*S*)-28a** (.15 g, 0.45 mmol) and 3-chlorobenzoyl chloride (0.069 ml, 0.54 mmol) in DCM (7.0 mL). The crude residue was purified by silica gel chromatography (ISCO, Redisep 12 g column, 10-80% EtOAc/hexanes gradient) to afford the title compound as an off-white solid (0.12 g, 57%, a mixture of rotamers) TLC (EtOAc:hexanes, 1:1, v/v) Rf = 0.61; ^{1}H NMR ($CDCl_3$, 400 MHz) δ: 7.40-7.21 (m, 4H), 6.94-6.69 (m, 7H), 5.99 (t, *J* = 5.2 Hz, 0.5H), 5.16-5.13 (m, *J* = 3.6 Hz, *J* = 9.2 Hz, 0.5H), 4.89-4.84 (m, *J* = 5.2 Hz, *J* = 12.4 Hz, 0.5H), 4.59-4.50 (m, 1H), 4.40-4.32 (m, 1H), 4.17-4.12 (m, 0.5H), 3.95-3.92 (m, 0.5H), 3.77 (s, H), 3.76-3.59 (m, 1H), 3.31-3.11 (m, 1H), 2.94-2.37 (m, 1.5H), 1.35 (d, *J* = 6.0 Hz, 6H); ^{13}C NMR (100 MHz, $CDCl_3$) δ: 170.4, 169.6, 157.6, 157.0, 154.4, 154.3, 153.1, 153.6, 138.4, 138.2, 136.6, 135.6, 134.9, 134.5, 130.2, 129.9, 128.7, 128.3, 128.2, 127.0, 125.9, 125.2, 124.9, 124.1, 116.2, 115.9, 115.5, 114.9, 114.8, 114.7, 114.4, 71.2, 70.1, 57.3, 55.9, 51.9, 42.8, 35.4, 29.9, 28.5, 22.3, 22.2; HRMS calcd. for $C_{27}H_{29}ClNO_4$, 466.17796 $[M + H]^+$; 466.17840$[M + H]^+$ found; $[\alpha]_D^{20}$ = -92.4 (*c* 1.0, dry $CHCl_3$); The enantiomeric excess was determined to be 100% ee using an Agilent pump on a ChiralPak OD-RH column (4.6 mm x 150 mm, 5 μm) with the

following conditions: 65% MeCN/35% water plus 0.1% formic acid isocratic over 70 min, 0.20 mL per min flow rate, read at 254 nm, t_{R1} = 59.15 min, t_{R2} = 61.49 min.

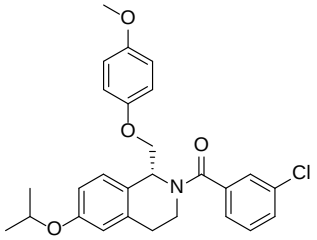

(*R*)-(3-chlorophenyl)(6-isopropoxy-1-((4-methoxyphenoxy)methyl)-3,4-dihydroisoquinolin-2(1H)-yl)methanone ((*R*)-1180-55): Tetrahydroisoquinoline **(*R*)-1180-55** was prepared via procedure XIII using **(*R*)-28a** (0.064 g, 0.19 mmol) and 3-chlorobenzoyl chloride (0.052 ml, 0.38 mmol) in DCM (3.0 mL). The crude residue was purified by silica gel chromatography (ISCO, Redisep 12 g column, 10-80% EtOAc/hexanes gradient) to afford the title compound as an off-white solid (0.064 g, 74%, a mixture of rotamers) TLC (EtOAc:hexanes, 1:1, v/v) Rf = 0.65; ^{1}H NMR ($CDCl_3$, 400 MHz) δ: 7.40-7.21 (m, 4H), 6.94-6.69 (m, 7H), 6.00 (t, *J* = 5.2 Hz, 0.5H), 5.16-5.13 (m, *J* = 3.2 Hz, *J* = 9.2 Hz, 0.5H), 4.89-4.85 (m, *J* = 5.2 Hz, *J* = 12.4 Hz, 0.5H), 4.58-4.51 (m, 1H), 4.39-4.32 (m, 1H), 4.15 (t, *J* = 10.4 Hz, 0.5H), 3.96-3.92 (m, 0.5H), 3.77 (s, 3H), 3.72-3.59 (m, 1H), 3.31-3.11 (m, 1H), 2.95-2.73 (m, 1.5H), 1.34 (d, *J* = 6.0 Hz, 6H); ^{13}C NMR (100 MHz, $CDCl_3$) δ: 170.5, 169.7, 168.5, 157.6, 157.1, 154.4, 154.3, 153.1, 125.5, 138.3, 138.2, 136.6, 135.6, 134.8, 134.6, 133.5, 130.2, 129.8, 128.7, 128.4, 128.2, 127.0, 125.8, 125.2, 124.9, 124.1, 116.2, 115.9, 114.9, 114.8, 114.7, 114.5, 71.3, 70.1, 57.3, 55.9, 51.9, 42.8, 35.5, 29.9, 28.6, 22.3, 22.2; HRMS calcd. for $C_{27}H_{28}ClNO_4Na$, 488.15991 $[M + H]^+$; 488.15943 $[M + H]^+$ found; $[\alpha]_D^{20}$ = +90.7 (*c* 1.0, dry $CHCl_3$); The enantiomeric excess was determined to be 92% ee using an Agilent pump on a ChiralPak OD-RH column (4.6 mm x 150 mm, 5 μm) with the following conditions: 65% MeCN/35% water plus 0.1% formic acid isocratic over 90 min, 0.20 mL per min flow rate, read at 254 nm, t_{R1} = 59.15 min, t_{R2} = 61.49 min.

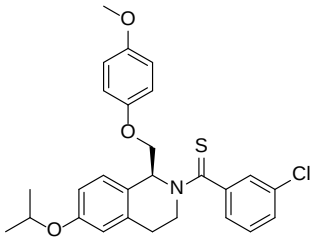

(*S*)-(3-chlorophenyl)(6-isopropoxy-1-((4-methoxyphenoxy)methyl)-3,4-dihydroisoquinolin-2(1H)-yl)methanethione ((*S*)-1180-163): Tetrahydroisoquinoline **(*S*)-1180-163** was prepared via procedure XV using tetrahydroisoquinoline **(*S*)-1180-55** (0.033 g, 0.071 mmol) and 2,4-bis(4-methoxyphenyl)-1,3,2,4-dithiadiphosphetane 2,4-disulfide (0.029 g, 0.071 mmol) in toluene (3.5 mL). The crude residue was purified by silica gel chromatography (ISCO, Redisep 4 g column, 0-80% EtOAc/hexanes gradient) to afford the title compound as a yellow foam (0.022 g, 65%, a mixture of rotamers) TLC (EtOAc:hexanes, 1:1, v/v) Rf = 0.80; ^{1}H NMR ($CDCl_3$, 300 MHz): 7.33-7.25 (m, 3.5H), 7.14-7.13 (m, 0.5H), 6.86-6.70 (m, 7H), 5.75-5.70 (m, J = 5.2 Hz, J = 13.2 Hz, 0.5H), 5.41-5.38 (m, J = 4.0 Hz, J = 9.6 Hz, 0.5H), 4.70-4.67 (double of doublets, J = 4.4 Hz, J = 10.4 Hz, 0.5H), 4.58-4.52 (m, 1H), 4.50-4.46 (doublet of doublet, J = 4.8 Hz, J = 10.0 Hz, 0.5H), 4.20-4.17 (m, 0.5H), 4.04-3.87 (m, 2H), 3.77 (s, 3H), 3.71-3.63 (m, 0.5H), 3.36-3.28 (m, 0.5H), 2.99-2.92 (m, 1H), 2.83-2.79 (m, 0.5H), 1.36-1.34 (m, 6H); ^{13}C NMR (100 MHz, $CDCl_3$) δ: 200. 4, 199.0, 157.8, 157.1, 154.5, 154.4, 152.9, 152.4, 145.0, 144.8, 136.2, 134.9, 130.2, 129.7, 128.7, 128.6, 128.5, 128.1, 124.9, 123.5, 115.9, 115.7, 115.5, 115.1, 114.9, 114.8, 114.7, 70.9, 70.1, 70.1, 61.5, 58.4, 55.9, 48.1, 42.7, 30.1, 28.1, 22.3; HRMS calcd. for $C_{27}H_{28}ClNO_3SNa$, 482.15512 $[M + H]^+$; 482.15515 $[M + H]^+$ found; $[\alpha]_D^{20}$ = -142.0 (*c* 0.10, dry $CHCl_3$); The enantiomeric excess was determined to be 96% ee using an Agilent pump on a ChiralPak AD-H column (4.6 mm x 150 mm, 5 μm) with the following conditions: 10% IPA/90% hexanes over 40 min, 1.0 mL per min flow rate, read at 254 nm, t_{R1} = 24.18 min, t_{R2} = 32.19.

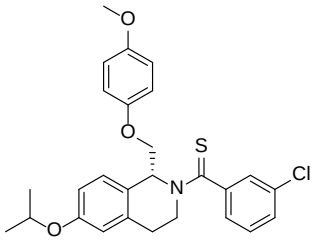

(*R*)-(3-chlorophenyl)(6-isopropoxy-1-((4-methoxyphenoxy)methyl)-3,4-dihydroisoquinolin-2(1H)-yl)methanethione ((*R*)-1180-163): Tetrahydroisoquinoline **(*R*)-1180-163** was prepared via procedure XV using tetrahydroisoquinoline **(*R*)-1180-55** (0.022 g, 0.048 mmol) and 2,4-bis(4-methoxyphenyl)-1,3,2,4-dithiadiphosphetane 2,4-disulfide (0.019 g, 0.048 mmol) in toluene (2.7 mL). The crude residue was purified by silica gel chromatography (ISCO, Redisep 4 g column, 0-80% EtOAc/hexanes gradient) to afford the title compound as a yellow foam (0.011 g, 49%, a mixture of rotamers) TLC (EtOAc:hexanes, 1:1, v/v) Rf = 0.79 ; ^{1}H NMR ($CDCl_3$, 300 MHz): 7.33-7.25 (m, 3.5H), 7.14-7.13 (m, 0.5H), 6.86-6.70 (m, 7H), 5.75-5.70 (m, *J* = 5.2 Hz, *J* = 13.2 Hz, 0.5H), 5.41-5.38 (m, *J* = 4.0 Hz, *J* = 9.6 Hz, 0.5H), 4.70-4.67 (dd, *J* = 4.4 Hz, *J* = 10.4 Hz, 0.5H), 4.58-4.52 (m, 1H), 4.50-4.46 (dd, *J* = 4.8 Hz, *J* = 10.0 Hz, 0.5H), 4.20-4.17 (m, 0.5H), 4.04-3.87 (m, 2H), 3.77 (s, 3H), 3.71-3.63 (m, 0.5H), 3.36-3.28 (m, 0.5H), 2.99-2.92 (m, 1H), 2.83-2.79 (m, 0.5H), 1.36-1.34 (m, 6H) HRMS calcd. for $C_{27}H_{28}ClNO_3SNa$, 482.15512 $[M + H]^+$; 482.15516 $[M + H]^+$ found; $[\alpha]_D^{20}$ = +114.0 (*c* 0.10, dry $CHCl_3$); The enantiomeric excess (ee) was determined to be 100% ee using an Agilent pump on a ChiralPak AD-H column (4.6 mm x 150 mm, 5 μm) with the following conditions: 10% IPA/90% hexanes over 40 min, 1.0 mL per min flow rate, read at 254 nm, t_{R1} = 24.18 min, t_{R2} = 32.19.

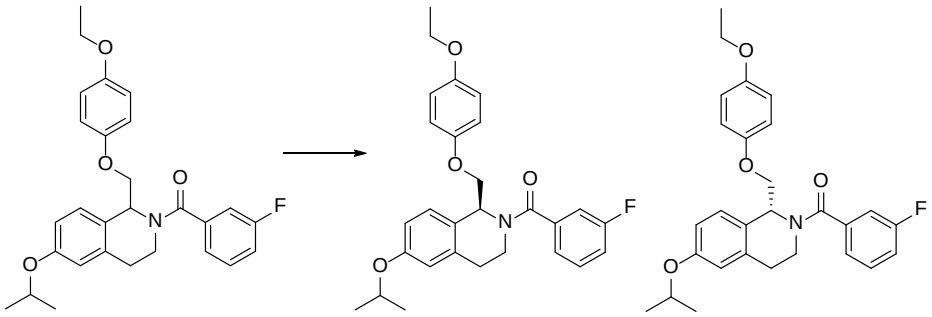

Separation of 1180-87 enantiomers: Semi-preparative separation of **1180-87** enantiomers from racemic **1180-87** (0.14 g) was done using a ChiralPak AD-H (30 mm x 250 mm) with the following conditions: 20 mL/min flow rate, 8 mL injection volume (2 mg / 1 mL), 70% hexanes / 30% IPA over 45 minutes to afford ***(S)*-(-)-1180-87** (0.055 g): t_R: 25.2; ***(R)*-(+)-1180-87** (0.056 g): t_R: 46.1 minutes. The enantiomeric excess (ee) was determined using an Agilent pump on a ChiralPak AD-H column (4.6 mm x 150 mm, 5 μm) with the following conditions: 1 mL/min flow rate, 10 μL injection volume, 80% hexanes / 20% IPA; ***S*-(-)-1180-87**: t_R: 18.1 minutes, 100% ee, $[\alpha]_D^{20}$ = -102 (*c* 0.1, dry $CHCl_3$), ***R*-(+)-1180-87**: t_R: 33.4 minutes, 100% ee, $[\alpha]_D^{20}$ = +103 (*c* 1.0, dry $CHCl_3$). The proton spectrum for each enantiomer was identical to that of the racemic mixture.

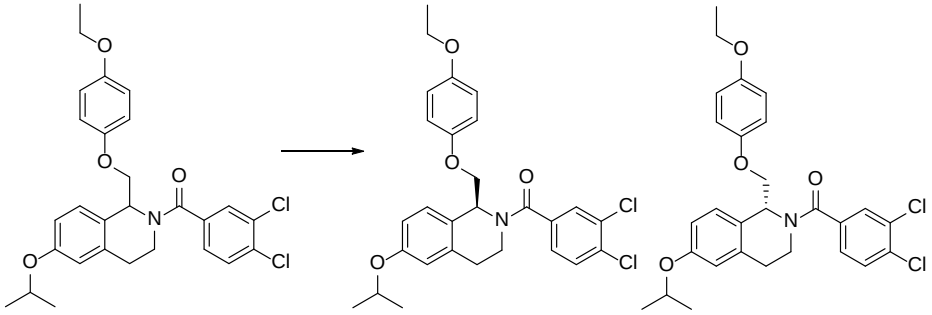

Separation of 1180-103 enantiomers: Separation of **1180-103** enantiomers from racemic **1180-103** (0.043 g) was done using a ChiralPak AD-H (30 mm x 250 mm) with the following conditions: 20 mL/min flow rate, 8 mL injection volume (2 mg / 1 mL), 70% hexanes / 30% IPA over 45 minutes to affods ***S*-(-)-1180-103** (0.020 g): t_R: 48.6; ***(R)*-(+)-1180-103** (0.020 g): t_R: 72.3 minutes. The enantiomeric excess (ee) was determined using an Agilent pump on a ChiralPak AD-H column (4.6 mm x 150 mm, 5 μm) with the following conditions: 1 mL/min flow rate, 10 μL injection volume, 75% hexanes / 25% IPA; ***S*-(-)-1180-103**: t_R: 27.3 minutes, 100% ee, $[\alpha]_D^{20}$ = -88.0 (*c* 0.1, dry $CHCl_3$), ***R*-(+)-1180-103**: t_R: 40.0 minutes, 100% ee, $[\alpha]_D^{20}$ = +121 (*c* 1.0, dry $CHCl_3$). The proton spectrum for each enantiomer was identical to that of the racemic mixture.

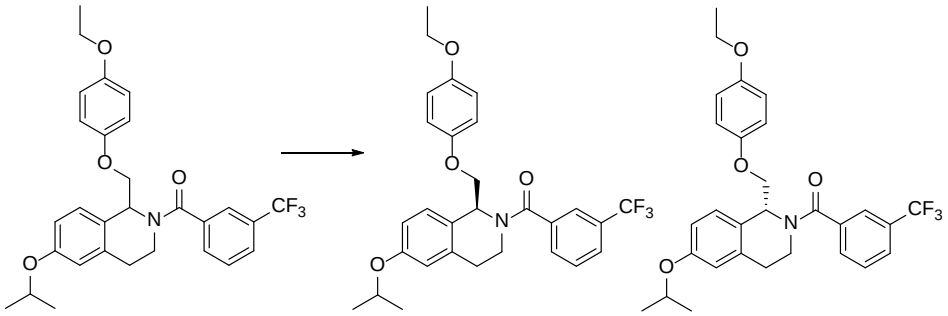

Separation of 1180-92 enantiomers: Separation of **1180-92** enantiomers from racemic **1180-92** (0.13 g) was done using a ChiralPak AD-H (30 mm x 250 mm) with the following conditions: 20 mL/min flow rate, 8 mL injection volume (2 mg / 1 mL), 80% hexanes / 20% IPA over 60 minutes to afford **(*S*)-(-)-1180-92** (0.049 g): t_R: 27.5; **(*R*)-(+)-1180-92** (0.055 g): t_R: 41.6 minutes. The enantiomeric excess (ee) was determined using an Agilent pump on a ChiralPak AD-H column (4.6 mm x 150 mm, 5 μm) with the following conditions: 1 mL/min flow rate, 10 μL injection volume, 80% hexanes / 20% IPA; **(*S*)-(-)-1180-92**: t_R: 11.7 minutes, 100% ee, $[\alpha]_D^{20}$ = -103 (*c* 0.1, dry $CHCl_3$), **(*R*)-(+)-1180-92**: t_R: 17.4 minutes, 100% ee, $[\alpha]_D^{20}$ = +100 (*c* 1.0, dry $CHCl_3$). The proton spectrum for each enantiomer was identical to that of the racemic mixture.

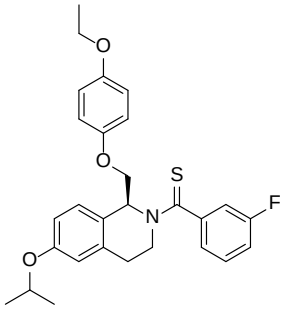

(*S*)-(1-((4-ethoxyphenoxy)methyl)-6-isopropoxy-3,4-dihydroisoquinolin-2(1H)-yl)(3-fluorophenyl)methanethione (*S*-(-)-1180-154): Tetrahydroisoquinoline ***S*-(-)-1180-154** was prepared via procedure XVI using tetrahydroisoquinoline ***S*-(-)-1180-87** (0.047 g, 0.096 mmol) and 2,4-bis(4-methoxyphenyl)-1,3,2,4-dithiadiphosphetane 2,4-disulfide (0.039 g, 0.096 mmol) in toluene (3.6 mL). The crude residue was purified by silica gel chromatography (ISCO, Redisep 12 g column, 0-80% EtOAc/hexanes gradient) to afford the title compound as a yellow foam (0.026 g, 56%,

mixture of two thioamide rotamers); TLC (EtOAc:hexanes, 1:3, v/v) Rf = 0.70; $[\alpha]_D^{20}$ = -121.0 (*c* 0.10, dry $CHCl_3$); Following recrystallization with DCM/hexanes, the enantiomeric excess was determined to be 100% ee using an Agilent pump on a ChiralPak AD-H column (4.6 mm x 150 mm, 5 μm) with the following conditions: 10% IPA/90% hexanes over 100 min, 0.025 mL per min flow rate, read at 254 nm, t_{R1} = 73.9 min, t_{R2} = 78.7 min. The proton spectrum was identical to that of racemic **1180-87**.

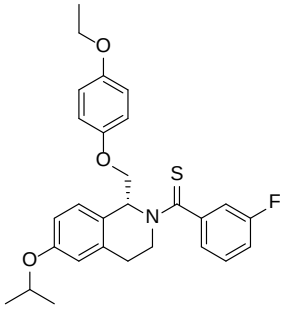

(*R*)-(1-((4-ethoxyphenoxy)methyl)-6-isopropoxy-3,4-dihydroisoquinolin-2(1H)-yl)(3-fluorophenyl)methanethione (*R*-(+)-1180-154): Tetrahydroisoquinoline ***R*-(+)-1180-154** was prepared via procedure XVI using tetrahydroisoquinoline ***R*-(+)-1180-87** (0.046 g, 0.096 mmol) and 2,4-bis(4-methoxyphenyl)-1,3,2,4-dithiadiphosphetane 2,4-disulfide (0.040 g, 0.096 mmol) in toluene (3.6 mL). The crude residue was purified by silica gel chromatography (ISCO, Redisep 12 g column, 0-50% EtOAc/hexanes gradient) to afford the title compound as a yellow foam (0.031 g, 65%, mixture of two thioamide rotamers); TLC (EtOAc:hexanes, 1:3, v/v) Rf = 0.70; $[\alpha]_D^{20}$ = +129.0 (*c* 0.10, dry $CHCl_3$); Following recrystallization with DCM/hexanes, the enantiomeric excess was determined to be 100% ee using an Agilent pump on a ChiralPak AD-H column (4.6 mm x 150 mm, 5 μm) with the following conditions: 10% IPA/90% hexanes over 100 min, 0.025 mL per min flow rate, read at 254 nm, t_{R1} = 73.9 min, t_{R2} = 78.7 min. The proton spectrum was identical to that of racemic **1180-87**.

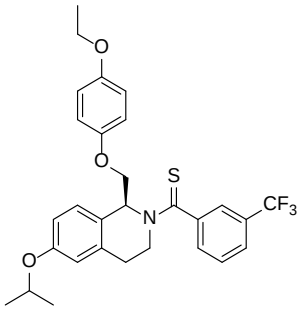

(*S*)-(-)-(1-((4-ethoxyphenoxy)methyl)-6-isopropoxy-3,4-dihydroisoquinolin-2(1H)-yl)(3-(trifluoromethyl)phenyl)methanethione ((*S*)-(-)-1180-168): Tetrahydroisoquinoline **(*S*)-(-)-1180-168** was prepared via procedure XVI using tetrahydroisoquinoline **(*S*)-(-)-1180-92** (0.037 g, 0.073 mmol) and 2,4-bis(4-methoxyphenyl)-1,3,2,4-dithiadiphosphetane 2,4-disulfide (0.027 g, 0.073 mmol) in toluene (2.7 mL). The crude residue was purified by silica gel chromatography (ISCO, Redisep 12 g column, 0-50% EtOAc/hexanes gradient) to afford the title compound as a yellow foam (0.019 g, 50%, mixture of two thioamide rotamers); $[\alpha]_D^{20}$ = -162.0 (*c* 0.10, dry $CHCl_3$); The enantiomeric excess (ee) was determined using an Agilent pump on a ChiralPak AD-H column (4.6 mm x 150 mm, 5 μm) with the following conditions: 15% IPA/85% hexanes over 30 min, 1.0 mL per min flow rate, read at 254 nm, t_{R1} = 11.58, t_{R2} = 13.15 min. The proton spectrum was identical to that of racemic **1180-92**.

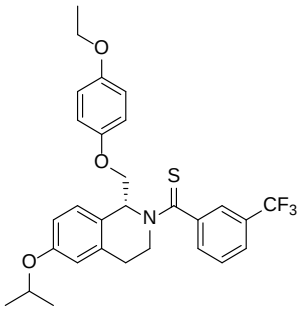

(*R*)-(+)-(1-((4-ethoxyphenoxy)methyl)-6-isopropoxy-3,4-dihydroisoquinolin-2(1H)-yl)(3-(trifluoromethyl)phenyl)methanethione (*R*)-(+)-1180-168): Tetrahydroisoquinoline **(R)-(+)-1180-168** was prepared via procedure XVI using tetrahydroisoquinoline **(*R*)-(+)-1180-92** (0.042 g, 0.82 mmol) and 2,4-bis(4-methoxyphenyl)-1,3,2,4-dithiadiphosphetane 2,4-disulfide (0.030 g, 0.082

mmol) in toluene (3.1 mL). The crude residue was purified by silica gel chromatography (ISCO, Redisep 12 g column, 0-50% EtOAc/hexanes gradient) to afford the title compound as a yellow foam (0.021 g, 48%, mixture of two thioamide rotamers); $[\alpha]_D^{20}$ = +136.0 (*c* 0.10, dry $CHCl_3$); The enantiomeric excess (ee) was determined using an Agilent pump on a ChiralPak AD-H column (4.6 mm x 150 mm, 5 μm)with the following conditions: 15% IPA/85% hexanes over 30 min, 1.0 mL per min flow rate, read at 254 nm, t_{R1} = 11.58, t_{R2} = 13.15 min. The proton spectrum was identical to that of racemic **1180-92.**

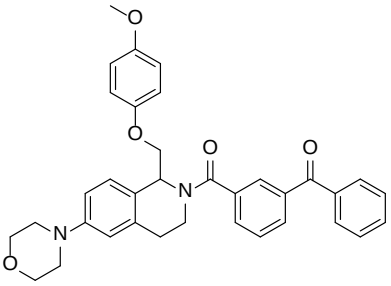

(3-benzoylphenyl)(1-((4-methoxyphenoxy)methyl)-6-morpholino-3,4-dihydroisoquinolin-2(1H)-yl)methanone (1180-135): 3-benzoylbenzoic acid (0.79 g, 3.5 mmol) was dissolved in dry DCM (6.6 ml) and dry DMF (2.0 mL), and brought to 0 °C using an ice bath. N1-((ethylimino)methylene)-N3,N3-dimethylpropane-1,3-diamine (0.59 g, 3.8 mmol) and N,N-dimethylpyridin-4-amine (0.47 g, 3.8 mmol) were added and the reaction was allowed to stir for 2 hours before tetrahydroisoquinoline **28s** (1.1 g, 3.2 mmol) dissolved in dry DCM (6.6 ml) was added. The reaction was allowed to stir overnight and warm to room temperature. The reaction was quenched with DI water, extracted into DCM, washed with water (3x) and brine (3x), dried with $MgSO_4$, filtered, and concentrated *in vacuo*. The crude residue was purified by silica gel chromatography (ISCO, Redisep 12 g column, 10 – 80% EtOAc/hexanes gradient) to afford the title compound as a yellow foam (0.20 g, 12 % yield, mixture of two amide rotamers) TLC (EtOAc: hexanes, 1:1, v/v) Rf = 0.33; ^{1}HNMR ($CDCl_3$, 400 MHz) δ: 8.04 (s, 0.5H), 7.89-7.72 (m, 4H), 7.64-7.44 (m, 5H), 7.25-7.23 (m, 0.5H), 6.93-6.92 (m, 0.5H), 6.84-6.73 (m, 5H), 6.67-6.61 (m, 1.5H), 6.00-5.98 (m, 0.5H), 5.14-5.12 (m, 0.5H), 4.91-4.86 (m, *J* = 4.8 Hz, *J* = 12.4 Hz, 0.5H), 4.38-4.36 (m, 1H),

4.14-4.08 (m, 0.5H), 3.93-3.90 (m, 1H), 3.86 (t, J = 4.0 Hz, 4H), 3.76 (s, 3H), 3.71-3.69 (m, 1.5H), 3.29-3.16 (m, 5H), 2.91-2.73 (m, 1H); ^{13}C NMR ($CDCl_3$, 100 MHz) δ: 196.3, 196.2, 170.9, 170.2, 154.3, 153.1, 152.5, 150.9, 150.5, 138.2, 137.9, 137.3, 136.9, 136.7, 136.1, 135.1, 133.1, 132.9, 131.7, 131.2, 130.7, 130.4, 129.3, 129.0, 128.8, 128.7, 128.5, 129.0, 124.8, 123.5, 115.9, 115.3, 114.8, 114.2, 71.3, 69.9, 67.0, 57.3, 55.9, 51.9, 49.4, 49.2, 43.1, 35.5, 30.1, 28.7; HRMS calcd. for $C_{35}H_{35}N_2O_5$, 563.25405 $[M + H]^+$; found, 563.25392 $[M + H]^+$.

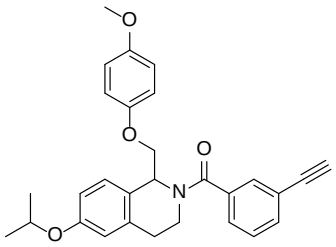

(3-ethynylphenyl)(6-isopropoxy-1-((4-methoxyphenoxy)methyl)-3,4-dihydroisoquinolin-2(1H)-yl)methanone (1180-282): A sealed vial was charged with copper(I) iodide (2.6 mg, 0.014 mmol), bis(triphenylphosphine)palladium(II) dichloride (1.7 mg, 0.0070 mmol), and tetrahydroisoquinoline **1180-153**. The vial was sealed, evacuated, and purged with argon twice before THF (0.67 ml) was added followed by triethylamine (0.59 ml, 4.3 mmol) and ethynyltrimethylsilane (0.025 ml, 0.18 mmol). The reaction was allowed to stir at room temperature overnight before the reaction vessel was quenched with a saturated solution of NH_4Cl. The organic layer was diluted with DCM, washed with a saturated solution of NH_4Cl (3x), dried with $MgSO_4$, and concentrated *in vacuo*. The crude residue was purified by silica gel chromatography (ISCO, Redisep 12 g column, 10-80% EtOAc/hexanes gradient) to afford tetrahydroisoquinoline **44** as a white solid (0.038 g, 54%). ^{1}H NMR ($CDCl_3$, 400 MHz) δ: 8.13 (bs, 1H), 7.93-7.85 (m, 2H), 7.78-7.70 (m, 1.5H), 7.63-7.61 (m, 0.5H), 7.33-7.19 (m, 5H), 7.13-7.08 (m, 1.5H), 6.39 (t, J = 5.2 Hz, 0.5H), 5.53 (m, J = 3.2 Hz, J = 3.2 Hz, 0.5H), 5.26 (m, J = 5.2 Hz, J = 5.2 Hz, 0.5H), 4.98-4.91 (m, 1H), 4.76-4.72 (m, 1H), 4.56 (t, J = 10.4 Hz, 0.5H), 4.33-4.31 (m, 0.5H), 4.17 (m, 3H), 4.14-4.05 (m, 1H), 3.67-3.51 (m, 1H), 3.38-3.11 (m, 1.5H), 1.74 (d, J = 6.4 Hz, 6H), 0.66-0.60 (m, 9H). Tetrahydroisoquinonline **57** was dissolved in

DCM (0.60 mL) and potassium carbonate (0.033 g, 0.24 mol) was added followed by MeOH (0.60 mL). The reaction was allowed to stir for 2 hours at room temperature before the reaction was quenched with water and extracted into DCM. The organic layer was dried with $MgSO_4$, filtered, and concentrated *in vacuo*. The crude residue was purified by silica gel chromatography (ISCO, Redisep 12 g column, 10-60% EtOAc/hexanes gradient) to afford tetrahydroisoquinoline **1180-282** as a white solid (0.038 g, 54%). ^{1}H NMR ($CDCl_3$, 400 MHz) δ: 7.55 (m, 2H), 7.42-7.32 (m, 2H), 6.93-6.80 (m, 6H), 6.73-6.68 (m, 2H), 5.99 (t, *J* = 4.8 Hz, 0.5H), 5.14-5.13 (m, 0.5H), 4.90-4.85 (m, 0.5H),4.56-4.51 (m, 1H), 4.36-4.32 (m, 1H), 4.14 (t, *J* = 10.0 Hz, 0.5H), 3.95-3.91 (m, 0.5H), 3.77 (s, 3H), 3.29-3.12 (m, 2H), 2.90-2.72 (m, 2H), 1.34 (d, *J* = 6.0 Hz, 6H); ^{13}C NMR ($CDCl_3$, 100 MHz) δ: 170.9, 170.1, 157.5, 157.0, 154.3, 154.2, 153.0, 152.8, 136.9, 136.8, 136.6, 135.6, 133.3, 133.2, 131.4, 130.3, 128.9, 128.7, 128.5, 128.3, 128.1, 127.1, 125.2, 124.2, 122.8, 122.5, 116.1, 115.9. 115.8, 115.4, 114.8, 114.7, 114.6, 114.3, 83.1, 82.9, 78.4, 78.2, 71.3, 70.2, 70.0, 57.2, 55.9, 51.8, 42.7, 35.4, 29.9, 28.5, 22.2, 22.1; HRMS calcd. for $C_{29}H_{30}O_4N$, 456.21693 $[M + H]^+$; found, 456.21632 $[M + H]^+$

2.6.2 Computational analysis

1000-steps (100 steps per rotatable bond) of Monte Carlo Macro Model (MCMM) and Mixed torsional/Low-Mode (MTLM) sampling were performed on molecules the OPLS2005 force field within the MacroModel module of Maestro. The GBSA/H2O solvation model was used along with a relaxed 5 kcal/mol energy cut-off. To ensure complete energy convergence the resulting structures were subjected to 50 steps of FMNR minimization with a gradient of 0.5.

2.6.3 Crystal structure data and experimental

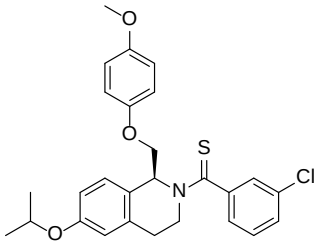

Single crystals of $C_{27}H_{28}ClNO_3S$ (**(*S*)-(-)-1180-163**) were recrystallised from a mixture of DCM and hexane by slow evaporation. A suitable crystal (0.764×0.484×0.154 mm3) was selected and mounted on a loop paratone oil on a Apex II Cu diffractometer. The crystal was kept at 173(2) K during data collection. Using Olex2[64], the structure was solved with the Superflip[65] structure solution program, using the Charge Flipping solution method. The model was refined with the ShelXL[66] refinement package using Least Squares minimisation. Crystal data: M = 482.01, monoclinic, P21 (No. 4, a = 5.7587 Å, b = 16.3557 Å, c = 13.105 Å, β = 91.808°, α = γ = 90°,V = 1233.71(10) Å3, T = 173(2) K, Z = 2, μ (Mo Kα) = 2.390, 9144 reflections measured, 4191 unique (Rint = 0.0635) which were used in all calculations. The final wR2 was 0.3083 (all data) and R1 was 0.1020 (I > 2(I)). Crystals grown and data collected and analyzed by John Bacsa, PhD at the Emory X-crystallography core facility. Crystallographic data is summarized in **Table 37**.

Table 37. Crystal data and structure refinement for (*S*)-(-)-1180-163

Formula	$C_{27}H_{28}ClNO_3S$
$D_{calc.}$/ g cm^{-3}	1.298
μ/mm^{-1}	2.390
Formula Weight	482.01
Colour	colourless
Shape	plate
Max Size/mm	0.76
Mid Size/mm	0.48
Min Size/mm	0.15
T/K	173(2)
Crystal System	monoclinic
Flack Parameter	0.05(4)
Hooft Parameter	0.027(12)
Space Group	$P2_1$
a/Å	5.7587(3)
b/Å	16.3557(8)
c/Å	13.1050(6)
α/°	90
β/°	91.808(3)
γ/°	90
V/Å^3	1233.71(10)
Z	2
Z'	1
Θ_{min}/°	2.702
Θ_{max}/°	68.050

Measured Refl.	9144
Independent Refl.	4191
$I > 2\sigma(I)$	3383
R_{int}	0.0635
Parameters	302
Restraints	195
Largest Peak	0.932
Deepest Hole	-0.566
GooF	1.314
wR_2 (all data)	0.3083
wR_2	0.2798
R_1 (all data)	0.1243
R_1	0.1020

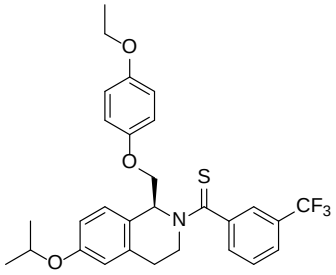

Single colorless needle-shaped crystals of (**KLS-5-36**) were recrystallised from a mixture of hexane and DCM by slow evaporation. A suitable crystal (0.74×0.18×0.06 mm) was selected and mounted on a loop with paratone oil on a Bruker APEXII diffractometer. The crystal was cooled to T = 100(2) K during the data collection. The structure was solved with the **XT**[67] structure solution program, using combined Patterson and dual-space recycling methods and by using **Olex2**[64] as the graphical interface. The model was refined with version 2014/7 of **ShelXL**[66] using Least Squares minimization. Crystal Data: Mr = 529.61, triclinic, P1 (No. 1), a = 5.7575(13) Å, b = 14.972(4) Å, c = 16.491(4) Å, α = 109.214(4)°, β = 90.080(3)°, γ = 94.123(3)°, V = 1338.4(6) Å3, T = 100(2) K, Z =

2, Z' = 2, μ(MoKα) = 0.173, 9735 reflections measured, 9735 unique which were used in all calculations. The final *wR2* was 0.3656 (all data) and *R1* was 0.1277 (I > 2σ(I)). The Flack parameter was 0.04. Crystals grown and data collected and analyzed by John Bacsa, PhD at the Emory X-crystallography core facility. Crystallographic data is summarized in **Table 38**.

Table 38. Crystal data and structure refinement for (*S*)-(-)-1180-168

Compound	**KLS-5-36**
Formula	C29H30F3NO3S
Dcalc./ g cm-3	1.314
μ/mm-1	0.173
Formula Weight	529.61
Colour	Colorless
Shape	Needle
Max Size/mm	0.74
Mid Size/mm	0.18
Min Size/mm	0.06
T/K	100(2)
Crystal System	Triclinic
Flack Parameter	0.04(17)
Hooft Parameter	0.01(9)
Space Group	P1
a/Å	5.7575(13)
b/Å	14.972(4)
c/Å	16.491(4)
α/°	109.214(4)
β/°	90.080(3)

γ/°	94.123(3)
V/Å3	1338.4(6)
Z	2
Z'	2
Θmin/°	1.308
Θmax/°	25.349
Measured Refl.	9735
Independent Refl.	9735
Reflections I > 2sigma(I)	6429
Rint	.
Parameters	689
Restraints	583
Largest Peak	1.344
Deepest Hole	-0.769
GooF	1.212
wR2 (all data)	0.3656
wR2	0.3146
R1 (all data)	0.1950
R1	0.1277

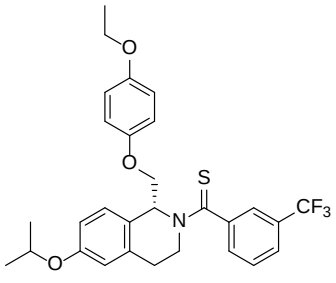

Single colorless needle-shaped crystals of (**KLS-5-37**) were recrystallised from a mixture of hexane and DCM by vapor diffusion. A suitable crystal (1.59×0.24×0.20 mm) was selected and mounted on a loop with paratone oil on a Bruker APEX-II CCD diffractometer. The crystal was cooled to T = 100(2) K during the data collection. The structure was solved with the **XT**[67]structure solution program, using combined Patterson and dual-space recycling methods and by using **Olex2**[64] as the graphical interface. The structure was refined with version 2014/7 of **ShelXL**[66] using Least Squares minimisation. Crystal Data: Mr = 529.60, triclinic, P1 (No. 1), a = 5.7506(17) Å, b = 14.940(4) Å, c = 16.445(5) Å, α = 109.164(4)°, β = 90.044(4)°, γ = 94.177(4)°, V = 1330.6(7) Å3, T = 100(2) K, Z = 2, Z' = 2, μ(MoKα) = 0.174, 20124 reflections measured, 13381 unique ($Rint$ = 0.0498) which were used in all calculations. The final $wR2$ was 0.2236 (all data) and $R1$ was 0.0822 (I > 2σ(I)). The Flack parameter was 0.03. Crystals grown and data collected and analyzed by John Bacsa, PhD at the Emory X-crystallography core facility. Crystallographic data is summarized in **Table 39**.

Table 39. Crystal data and structure refinement for (*R*)-(+)-1180-168

Compound	**KLS-5-37**
Formula	C29H30F3NO3S
Dcalc./ g cm-3	1.322
μ/mm-1	0.174
Formula Weight	529.60
Colour	Colorless
Shape	Needle
Max Size/mm	1.59
Mid Size/mm	0.24
Min Size/mm	0.20
T/K	100(2)
Crystal System	triclinic
Flack Parameter	0.03(5)

Hooft Parameter	0.03(5)
Space Group	P1
a/*Å*	5.7506(17)
b/*Å*	14.940(4)
c/*Å*	16.445(5)
α/°	109.164(4)
β/°	90.044(4)
γ/°	94.177(4)
V/Å3	1330.6(7)
Z	2
Z'	2
Θmin/°	2.545
Θmax/°	29.154
Measured Refl.	20124
Independent Refl.	13381
Reflections I > 2σ(I)	10982
Rint	0.0498
Parameters	713
Restraints	136
Largest Peak	1.342
Deepest Hole	-0.554
GooF	1.073
wR2 (all data)	0.2236
wR2	0.2014
R1 (all data)	0.0991

R1	0.0822

2.6.4 In vitro analysis of 1180-55 series analogs

All protocols utilizing *Xenopus laevis* were approved by Emory University Institutional Animal Care and Use Committee. Two-electrode voltage-clamp recordings were performed on *Xenopus laevis* oocytes were injected with mRNA to express recombinant rat GluN1/GluN2A-, GluN1/GluN2B-, GluN1/GluN2C-, GluN1/GluN2D-, GluA1-, or GluK2-containing receptors. cDNAs for rat GluN1-1a (GenBank accession numbers U11418 and U08261; hereafter GluN1), GluN2A (D13211), GluN2B (U11419), GluN2C (M91563), GluN2D (L31611), GluA1 (X17184), GluK (Z11548) were provided by D. S. Heinermann from the Salk Institute, S. Nakanishi from Kyoto University, and P. Seeburg from University of Heidelberg. Oocyte isolation, cRNA synthesis and cRNA were performed as previously described[68]. For the two-electrode voltage clamp recordings, oocytes were situated in a perfusion chamber and continually washed with the recording solution that contained 90 mM NaCl, 1.0 mM KCl, 0.5 mM BaCl2, 0.005 mM EDTA, and 10 mM HEPES at a pH of 7.4 and a temperature of 23°C. The glass electrodes with a tip resistance of 0.5 – 2.5 MΩ were pulled from thin-walled glass capillary tubes and filled with 0.3-3.0 M KCl. The membrane potential of the oocytes was held at -40 mV by an OC-725C amplifier (Warner Instrument Co). All compounds were made as 20 mM stock solutions in DMSO and diluted to reach the desired final concentration in recording solution containing 100 μM glutamate and 30 μM glycine; final DMSO content was 0.05-0.5% (vol/vol). Oocytes expressing GluK2 receptors were pretreated with concanavalin A (10 μM) for 10 minutes. Recombinant GluNA1 and GluK2 receptors were activated by 100 μM glutamate. A gradual increase in current response over the course of the experiment is common with oocytes expressing GluN1/GluNA, but to prevent this, oocytes expressing GluN1/GluN2A were either pretreated with 50 μM BAPTA-AM (1,2-bis(oaminophenoxy)ethane-N,N,N',N'-tetraacetic acid tetraacetoxymethyl ester) for 10 min or injected with 50 nl of 2 mM K-

BAPTA (potassium 1,2-bis(o-aminophenoxy)ethane-N,N,N',N'-tetraacetic acid). All compounds that had a modest effect on GluN1/GluN2A expressing oocytes were not studied further.

Every test compound was recorded at 5-7 concentrations in a least 4 oocytes from at least 2 different frogs. The potentiation of the test compounds at a concentration of 30 μM was averaged and reported as $I_{30\mu M}$ / $I_{control}$ (mean ± SEM, %), where I equals current. A few compounds were reported as $I_{10\mu M}$ / $I_{control}$ (mean ± SEM, %). For test compounds with potentiation that exceeded 120% at 30 μM, an EC_{50} value (the half-maximal effective concentration of potentiator) was determined by fitting the following equation

$$Response = (100 - maximum) / (1 + ([concentration] / EC_{50})^{N}) + maximum$$

to the mean composite composition-response data normalized to the current in the absence of the potentiator (100%) where N equals the Hill slope and maximum is the maximal response predicted for saturating concentration of potentiator.

To compare both the EC_{50} values and maximum potentiation of two compounds at the same subunit, an unpaired t-test was run. Compounds were only denoted as being stastically different if the p value was less than 0.05.

Reference:

(1) Santangelo Freel, R. M.; Ogden, K. K.; Strong, K. L.; Khatri, A.; Chepiga, K. M.; Jensen, H. S.; Traynelis, S. F.; Liotta, D. C. Synthesis and Structure Activity Relationship of Tetrahydroisoquinoline-Based Potentiators of GluN2C and GluN2D Containing N-Methyl-D-Aspartate Receptors. *J. Med. Chem.* **2013**, *56* (13), 5351–5381.

(2) Mullasseril, P.; Hansen, K. B.; Vance, K. M.; Ogden, K. K.; Yuan, H.; Kurtkaya, N. L.; Santangelo, R.; Orr, A. G.; Le, P.; Vellano, K. M.; Liotta, D. C.; Traynelis, S. F. A Subunit-Selective Potentiator of NR2C- and NR2D-Containing NMDA Receptors. *Nat. Commun.* **2010**, *1*, 90.

(3) Ogden, K. K.; Traynelis, S. F. Contribution of the M1 Transmembrane Helix and Pre-M1 Region to Positive Allosteric Modulation and Gating of N-Methyl-D-Aspartate Receptors. *Mol. Pharmacol.* **2013**, *83* (5), 1045–1056.

(4) Baddeley, A. Working Memory. *Science* **1992**, *255* (5044), 556–559.

(5) Baddeley, A. Working Memory: Theories, Models, and Controversies. *Annu. Rev. Psychol.* **2012**, *63* (1), 1–29.

(6) Goldman-Rakic, P. S. Cellular Basis of Working Memory. *Neuron* **1995**, *14* (3), 477–485.

(7) Granon, S.; Vidal, C.; Thinus-Blanc, C.; Changeux, J.-P.; Poucet, B. Working Memory, Response Selection, and Effortful Processing in Rats with Medial Prefrontal Lesions. *Behav. Neurosci.* **1994**, *108* (5), 883–891.

(8) Lehohla, M.; Kellaway, L.; Russell, V. A. NMDA Receptor Function in the Prefrontal Cortex of a Rat Model for Attention-Deficit Hyperactivity Disorder. *Metab. Brain Dis.* **2004**, *19* (1-2), 35–42.

(9) Sheng, M.; Cummings, J.; Roldan, L. A.; Jan, Y. N.; Jan, L. Y. Changing Subunit Composition of Heteromeric NMDA Receptors during Development of Rat Cortex. *Nature* **1994**, *368* (6467), 144–147.
(10) Monaco, S. A.; Gulchina, Y.; Gao, W.-J. NR2B Subunit in the Prefrontal Cortex: A Double-Edged Sword for Working Memory Function and Psychiatric Disorders. *Neurosci. Biobehav. Rev.* **2015**, *56*, 127–138.
(11) Yihui Cui; Jing Jin; Xuliang Zhang; Hao Xu; Liguo Yang; Dan Du; Qingwen Zeng; Joe Z. Tsien; Huiting Yu; Xiaohua Cao. Forebrain NR2B Overexpression Facilitating the Prefrontal Cortex Long-Term Potentiation and Enhancing Working Memory Function in Mice. *PLoS ONE* **2011**, *6* (5), 1–10.
(12) Tang, Y.-P.; Shimizu, E.; Dube, G. R.; Rampon, C.; Kerchner, G. A.; Zhuo, M.; Liu, G.; Tsien, J. Z. Genetic Enhancement of Learning and Memory in Mice. *Nature* **1999**, *401* (6748), 63–69.
(13) Cao, X.; Cui, Z.; Feng, R.; Tang, Y.-P.; Qin, Z.; Mei, B.; Tsien, J. Z. Maintenance of Superior Learning and Memory Function in NR2B Transgenic Mice during Ageing. *Eur. J. Neurosci.* **2007**, *25* (6), 1815–1822.
(14) Jacobs, S. A.; Tsien, J. Z. Genetic Overexpression of NR2B Subunit Enhances Social Recognition Memory for Different Strains and Species. *PLoS ONE* **2012**, *7* (4), e36387.
(15) White, T. L.; Youngentob, S. L. The Effect of NMDA-NR2B Receptor Subunit over-Expression on Olfactory Memory Task Performance in the Mouse. *Brain Res.* **2004**, *1021* (1), 1–7.
(16) Paoletti, P.; Bellone, C.; Zhou, Q. NMDA Receptor Subunit Diversity: Impact on Receptor Properties, Synaptic Plasticity and Disease. *Nat. Rev. Neurosci.* **2013**, *14* (6), 383–400.
(17) Wang, X.-J. Synaptic Basis of Cortical Persistent Activity: The Importance of NMDA Receptors to Working Memory. *J. Neurosci.* **1999**, *19* (21), 9587–9603.
(18) Wang, X. J. Synaptic Reverberation Underlying Mnemonic Persistent Activity. *Trends Neurosci.* **2001**, *24* (8), 455–463.
(19) Okabe, S.; Collin, C.; Auerbach, J. M.; Meiri, N.; Bengzon, J.; Kennedy, M. B.; Segal, M.; McKay, R. D. G. Hippocampal Synaptic Plasticity in Mice Overexpressing an Embryonic Subunit of the NMDA Receptor. *J. Neurosci.* **1998**, *18* (11), 4177–4188.
(20) Wenk, G. L.; Barnes, C. A. Regional Changes in the Hippocampal Density of AMPA and NMDA Receptors across the Lifespan of the Rat. *Brain Res.* **2000**, *885* (1), 1–5.
(21) Clayton, D. A.; Mesches, M. H.; Alvarez, E.; Bickford, P. C.; Browning, M. D. A Hippocampal NR2B Deficit Can Mimic Age-Related Changes in Long-Term Potentiation and Spatial Learning in the Fischer 344 Rat. *J. Neurosci.* **2002**, *22* (9), 3628–3637.
(22) Bai, L.; Hof, P. R.; Standaert, D. G.; Xing, Y.; Nelson, S. E.; Young, A. B.; Magnusson, K. R. Changes in the Expression of the NR2B Subunit during Aging in Macaque Monkeys. *Neurobiol. Aging* **2004**, *25* (2), 201–208.
(23) Magnusson, K. R.; Brim, B. L.; Das, S. R.; Magnusson, K. R.; Brim, B. L.; Das, S. R. Selective Vulnerabilities of N-Methyl-D-Aspartate (NMDA) Receptors during Brain Aging. *Front. Aging Neurosci.* **2010**, *2*, 11.
(24) Brim, B. L.; Haskell, R.; Awedikian, R.; Ellinwood, N. M.; Jin, L.; Kumar, A.; Foster, T. C.; Magnusson, K. R. Memory in Aged Mice Is Rescued by Enhanced Expression of the GluN2B Subunit of the NMDA Receptor. *Behav. Brain Res.* **2013**, *238*, 211–226.
(25) Traynelis, S. F.; Hartley, M.; Heinemann, S. F. Control of Proton Sensitivity of the NMDA Receptor by RNA Splicing and Polyamines. *Science* **1995**, *268* (5212), 873–876.
(26) Williams, K.; Zappia, A. M.; Pritchett, D. B.; Shen, Y. M.; Molinoff, P. B. Sensitivity of the N-Methyl-D-Aspartate Receptor to Polyamines Is Controlled by NR2 Subunits. *Mol. Pharmacol.* **1994**, *45* (5), 803–809.
(27) Malayev, A.; Gibbs, T. T.; Farb, D. H. Inhibition of the NMDA Response by Pregnenolone Sulphate Reveals Subtype Selective Modulation of NMDA Receptors by Sulphated Steroids. *Br. J. Pharmacol.* **2002**, *135* (4), 901–909.
(28) Masuko, T.; Kuno, T.; Kashiwagi, K.; Kusama, T.; Williams, K.; Igarashi, K. Stimulatory and

Inhibitory Properties of Aminoglycoside Antibiotics at N-Methyl-D-Aspartate Receptors. *J. Pharmacol. Exp. Ther.* **1999**, *290* (3), 1026–1033.
(29) Geurink, P. P.; Prely, L. M.; van der Marel, G. A.; Bischoff, R.; Overkleeft, H. S. Photoaffinity Labeling in Activity-Based Protein Profiling. *Top. Curr. Chem.* **2012**, *324*, 85–113.
(30) Kotzyba-Hibert, F.; Kapfer, I.; Goeldner, M. Recent Trends in Photoaffinity Labeling. *Angew. Chem. Int. Ed. Engl.* **1995**, *34* (12), 1296–1312.
(31) Prestwich, G. D.; Dormán, G.; Elliott, J. T.; Marecak, D. M.; Chaudhary, A. Benzophenone Photoprobes for Phosphoinositides, Peptides and Drugs. *Photochem. Photobiol.* **1997**, *65* (2), 222–234.
(32) Li, Y. Z.; Kirby, J. P.; George, M. W.; Poliakoff, M.; Schuster, G. B. 1,2-Didehydroazepines from the Photolysis of Substituted Aryl Azides: Analysis of Their Chemical and Physical Properties by Time-Resolved Spectroscopic Methods. *J. Am. Chem. Soc.* **1988**, *110* (24), 8092–8098.
(33) Rostovtsev, V. V.; Green, L. G.; Fokin, V. V.; Sharpless, K. B. A Stepwise Huisgen Cycloaddition Process: copper(I)-Catalyzed Regioselective "Ligation" of Azides and Terminal Alkynes. *Angew. Chem. Int. Ed Engl.* **2002**, *41* (14), 2596–2599.
(34) Speers, A. E.; Adam, G. C.; Cravatt, B. F. Activity-Based Protein Profiling in Vivo Using a Copper(I)-Catalyzed Azide-Alkyne [3 + 2] Cycloaddition. *J. Am. Chem. Soc.* **2003**, *125* (16), 4686–4687.
(35) Himo, F.; Lovell, T.; Hilgraf, R.; Rostovtsev, V. V.; Noodleman, L.; Sharpless, K. B.; Fokin, V. V. Copper(I)-Catalyzed Synthesis of Azoles. DFT Study Predicts Unprecedented Reactivity and Intermediates. *J. Am. Chem. Soc.* **2005**, *127* (1), 210–216.
(36) Salisbury, C. M.; Cravatt, B. F. Optimization of Activity-Based Probes for Proteomic Profiling of Histone Deacetylase Complexes. *J. Am. Chem. Soc.* **2008**, *130* (7), 2184–2194.
(37) Dalpiaz, A.; Cacciari, B.; Mezzena, M.; Strada, M.; Scalia, S. Solid Lipid Microparticles for the Stability Enhancement of a Dopamine Prodrug. *J. Pharm. Sci.* **2010**, *99* (11), 4730–4737.
(38) Manivel, P.; Rai, N. P.; Jayashankara, V. P.; Arunachalam, P. N. Base Catalyzed Mitsunobu Reactions as a Tool for the Synthesis of Aryl Sec-Alkyl Ethers. *Tetrahedron Lett.* **2007**, *48* (15), 2701–2705.
(39) Klapars, A.; Buchwald, S. L. Copper-Catalyzed Halogen Exchange in Aryl Halides: An Aromatic Finkelstein Reaction. *J. Am. Chem. Soc.* **2002**, *124* (50), 14844–14845.
(40) Wolter, M.; Nordmann, G.; Job, G. E.; Buchwald, S. L. Copper-Catalyzed Coupling of Aryl Iodides with Aliphatic Alcohols. *Org. Lett.* **2002**, *4* (6), 973–976.
(41) Fagan, P. J.; Hauptman, E.; Shapiro, R.; Casalnuovo, A. Using Intelligent/Random Library Screening To Design Focused Libraries for the Optimization of Homogeneous Catalysts: Ullmann Ether Formation. *J. Am. Chem. Soc.* **2000**, *122* (21), 5043–5051.
(42) Altman, R. A.; Shafir, A.; Choi, A.; Lichtor, P. A.; Buchwald, S. L. An Improved Cu-Based Catalyst System for the Reactions of Alcohols with Aryl Halides. *J. Org. Chem.* **2008**, *73* (1), 284–286.
(43) Zhang, H.; Ma, D.; Cao, W. N,N-Dimethylglycine-Promoted Ullmann-Type Coupling Reactions of Aryl Iodides with Aliphatic Alcohols. *Synlett* **2007**, *2007* (2), 0243–0246.
(44) Ono, M.; Watanabe, R.; Kawashima, H.; Kawai, T.; Watanabe, H.; Haratake, M.; Saji, H.; Nakayama, M. 18F-Labeled Flavones for in Vivo Imaging of β-Amyloid Plaques in Alzheimer's Brains. *Bioorg. Med. Chem.* **2009**, *17* (5), 2069–2076.
(45) Ma, D.; Cai, Q.; Zhang, H. Mild Method for Ullmann Coupling Reaction of Amines and Aryl Halides. *Org. Lett.* **2003**, *5* (14), 2453–2455.
(46) Xu, H.; Wolf, C. Efficient Copper-Catalyzed Coupling of Aryl Chlorides, Bromides and Iodides with Aqueous Ammonia. *Chem. Commun.* **2009**, No. 21, 3035–3037.
(47) Minor, D. L.; Wyrick, S. D.; Charifson, P. S.; Watts, V. J.; Nichols, D. E.; Mailman, R. B. Synthesis and Molecular Modeling of 1-Phenyl-1,2,3,4-Tetrahydroisoquinolines and Related 5,6,8,9-Tetrahydro-13bH-Dibenzo[a,h]quinolizines as D1 Dopamine Antagonists. *J. Med. Chem.* **1994**, *37* (25), 4317–4328.
(48) Coppola, G. M.; Kukkola, P. J.; Stanton, J. L.; Neubert, A. D.; Marcopulos, N.; Bilci, N. A.;

Wang, H.; Tomaselli, H. C.; Tan, J.; Aicher, T. D.; Knorr, D. C.; Jeng, A. Y.; Dardik, B.; Chatelain, R. E. Perhydroquinolylbenzamides as Novel Inhibitors of 11β-Hydroxysteroid Dehydrogenase Type 1. *J. Med. Chem.* **2005**, *48* (21), 6696–6712.
(49) Santangelo Freel, R. M.; Ogden, K. K.; Strong, K. L.; Khatri, A.; Chepiga, K. M.; Jensen, H. S.; Traynelis, S. F.; Liotta, D. C. Correction to Synthesis and Structure Activity Relationship of Tetrahydroisoquinoline-Based Potentiators of GluN2C and GluN2D Containing N-Methyl-D-Aspartate Receptors. *J. Med. Chem.* **2014**, *57* (11), 4975–4975.
(50) Louafi, F.; Hurvois, J.-P.; Chibani, A.; Roisnel, T. Synthesis of Tetrahydroisoquinoline Alkaloids via Anodic Cyanation as the Key Step. *J. Org. Chem.* **2010**, *75* (16), 5721–5724.
(51) Dabbagh, A. H.; Faghihi, K. Isotope Effect and Kinetic Studies of the Reaction of Tertiary Alcohols with Triphenylphosphine–Carbon Tetrachloride: Ion Pair or Concerted? *Tetrahedron* **2000**, *56* (22), 3611–3617.
(52) Weiss, R. G.; Snyder, E. I. Conversion of Some Bicycloheptanols to Chlorides Using Triphenylphosphine-Carbon Tetrachloride. Stereochemistry and Mechanistic Implications. *J. Org. Chem.* **1970**, *35* (5), 1627–1632.
(53) Jones, L. A.; Sumner, C. E.; Franzus, B.; Huang, T. T. S.; Snyder, E. I. The Intermediate from the Triphenylphosphine-Tetrachloromethane-Alcohol Reaction: Relative Rates of Intermediate Formation, Kinetics, and Mechanism of Intermediate Decomposition. *J. Org. Chem.* **1978**, *43* (14), 2821–2827.
(54) Dabbagh, A. H.; Faghihi, K. Isotope Effect and Kinetic Studies of the Reaction of Tertiary Alcohols with Triphenylphosphine–Carbon Tetrachloride: Ion Pair or Concerted? *Tetrahedron* **2000**, *56* (22), 3611–3617.
(55) Polniaszek, R. P.; McKee, J. A. Stereoselective Reductions of Chiral Iminium Ions. *Tetrahedron Lett.* **1987**, *28* (39), 4511–4514.
(56) Youte, J.-J.; Barbier, D.; Al-Mourabit, A.; Gnecco, D.; Marazano, C. An Enantioselective Access to 1-Alkyl-1,2,3,4-Tetrahydroisoquinolines. Application to a New Synthesis of (−)-Argemonine†. *J. Org. Chem.* **2004**, *69* (8), 2737–2740.
(57) Kunitomo, J.; Komori, K.; Takaba, K. Asymmetric Synthesis of (R)-(+)-Noranicanine. *HETEROCYCLES* **1996**, *43* (8), 1681.
(58) Andersen, J.; Madsen, U.; Björkling, F.; Liang, X. Rapid Synthesis of Aryl Azides from Aryl Halides under Mild Conditions. *Synlett* **2005**, No. 14, 2209–2213.
(59) Cheng, H.; Wan, J.; Lin, M.-I.; Liu, Y.; Lu, X.; Liu, J.; Xu, Y.; Chen, J.; Tu, Z.; Cheng, Y.-S. E.; Ding, K. Design, Synthesis, and in Vitro Biological Evaluation of 1H-1,2,3-Triazole-4-Carboxamide Derivatives as New Anti-Influenza A Agents Targeting Virus Nucleoprotein. *J. Med. Chem.* **2012**, *55* (5), 2144–2153.
(60) Price Jr., D. W.; Dirk, S. M.; Maya, F.; Tour, J. M. Improved and New Syntheses of Potential Molecular Electronics Devices. *Tetrahedron* **2003**, *59* (14), 2497–2518.
(61) Wiberg, K. B.; Rablen, P. R. Why Does Thioformamide Have a Larger Rotational Barrier Than Formamide? *J. Am. Chem. Soc.* **1995**, *117* (8), 2201–2209.
(62) Wiberg, K. B.; Rush, D. J. Solvent Effects on the Thioamide Rotational Barrier: An Experimental and Theoretical Study. *J. Am. Chem. Soc.* **2001**, *123* (9), 2038–2046.
(63) Perola, E.; Charifson, P. S. Conformational Analysis of Drug-Like Molecules Bound to Proteins: An Extensive Study of Ligand Reorganization upon Binding. *J. Med. Chem.* **2004**, *47* (10), 2499–2510.
(64) Oleg V. Dolomanov, L. J. B. OLEX2: A Complete Structure Solution, Refinement and Analysis Program. *J Appl Cryst J Appl Cryst* **2009**, *42* (42), 339–341.
(65) Palatinus, L.; Chapuis, G. *SUPERFLIP* – a Computer Program for the Solution of Crystal Structures by Charge Flipping in Arbitrary Dimensions. *J. Appl. Crystallogr.* **2007**, *40* (4), 786–790.
(66) Sheldrick, G. M. A Short History of *SHELX*. *Acta Crystallogr. A* **2008**, *64* (1), 112–122.
(67) Sheldrick, G. M. *SHELXT* – Integrated Space-Group and Crystal-Structure Determination.

Acta Crystallogr. Sect. Found. Adv. **2015**, *71* (1), 3–8.
(68) Dravid, S. M.; Erreger, K.; Yuan, H.; Nicholson, K.; Le, P.; Lyuboslavsky, P.; Almonte, A.; Murray, E.; Mosley, C.; Barber, J.; French, A.; Balster, R.; Murray, T. F.; Traynelis, S. F. Subunit-Specific Mechanisms and Proton Sensitivity of NMDA Receptor Channel Block. *J. Physiol.* **2007**, *581* (1), 107–128.

Chapter 3: CIQ and 1180-55 represent divergent class of compounds in terms of SAR, pharmacology, and molecular determinants for potentiation.

3.1 The significance of a modulator for GluN2B-containing NMDA receptors

The GluN2 subunit composition of the NMDA receptor determines important pharmacological properties, such as receptor open probability[1], deactivation time course[2], and expression location in the brain[3,4]. For this reason, the select inhibition or potentiation of only one GluN2-containing NMDA receptor has been explored, but the literature is lacking in terms of potent and efficacious small molecule, drug-like subunit selective modulators. Ifenprodil, which is an inhibitor selective for the GluN2B subunit, was the first molecule identified that was selective for one GluN2 subunit over the others[5,6]. The compound is 400-fold more selective for inhibition at the GluN2B subunit over the other GluN2 subunits, and for this reason, ifenprodil has been used in a number of therapeutic studies[7–9]. Other subunit-selective inhibitors include TCN-201 for the GluN2A subunit[10] and the GluN2C/GluN2D-selective inhibitor DQP-1105[11]. Inhibitors for all four GluN2 NMDA receptors exist, but only GluN2C and GluN2D subunit-selective potentiators for the NMDA are identified in the literature; PYD is a GluN2C selective potentiator[12] and CIQ is selective for GluN2C and GluN2D-containing NMDA receptors[13].

A GluN2B potentiator for the NMDA receptor does not exist in the literature, and a GluN2B potentiator could act as a probe to study cognitive enhancement for the aging population[14–18] and potentially schizophrenia[19]. Importantly, the work that is currently done to study enhancement of the GluN2B NMDA receptor is done with mice that have been genetically engineered, a resource and time consuming endeavor[20–22].

Although many of the compounds mentioned above were discovered in high-throughput screens to find modulators of the NMDA receptors, we identified a GluN2B potentiator (**1180-55**) for the NMDA receptor by developing a SAR around CIQ, the tetrahydroisoquinoline compound selective for GluN2C and GluN2D subunits. This less conventional method of identification is advantageous because it has already been established that the CIQ series is tolerated in mice[23] and can cross the

blood-barrier following intravenous (IV) and intraperitoneal (IP) injection[23], meaning that this scaffold is amenable for use as a therapeutic and clinical tool. Throughout this thesis, a number of ways that **1180-55** and CIQ differ have been discussed, and the findings are summarized below. This work shows that the tetrahydroisoquinoline scaffold, once regarded as a GluN2C and GluN2D subunit selective modulator, can also be utilized as a GluN2B potentiator. A modulator for the GluN2B subunit could allow for unprecedented studies on the positive and negative effects of the enhancement of GluN2B-containing NMDA receptors.

3.2 CIQ and 1180-55 are divergent regarding SAR

Compound **1180-55** was discovered by changing the dimethoxy groups on the C-ring to a single isopropoxy, a change that led to GluN2B-containing receptor potentiation. After extensive modifications to all three rings of **1180-55**, differences in SAR have emerged between the two classes. These differences are mainly highlighted by dissimilarities at the B-ring, the C-ring, and the A-ring linker (**Table 36**). The C-ring is important for GluN2B activity, as no other part of the molecule alone has been able to induce GluN2B activity on the CIQ scaffold; no functionality on the A-ring or the B-ring caused GluN2B-activity on a C-ring dimethoxy-containing compound. A branched or cyclic ether on the C-ring is an important pharmacophore for the GluN2B-active tetrahydroisoquinoline scaffolds. The B-ring is also important for GluN2B-selectivity, as increasing the B-ring functionality by one carbon atom when moving from a methoxy group (**1180-55**) to an ethoxy (**1180-83**), led to GluN2B/GluN2C-selective compounds. Additionally, the isopropoxy functionality on the B-ring led to GluN2B/GluN2C activity over GluN2D. This is in contrast to CIQ where an ethoxy group on the B-ring (**1180-53**, not shown) completely eliminated activity. Although GluN2B activity is highly dependent on C-ring functionality, the B-ring also plays an important role in subunit selectivity, and the ethoxy- and isopropoxy functionality on the B-ring is a second important pharmacophore of the GluN2B-active tetrahydroisoquinoline compounds. The most striking difference between the two scaffolds though is the thioamide linker, which is completely inactive on CIQ and any CIQ-like scaffold (**Chapter 1.4.3**), but increases the potency

significantly on **1180-55** scaffolds. Of all the compounds that were synthesized in the CIQ series and the **1180-55** series, any compound that was GluN2C/D-selective as the amide was inactive as the thioamide, but all amide containing compounds that potentiated GluN2B-, GluN2C-, and GluN2D-containing receptors exhibited activity as the thioamide. These results suggest that the thioamide A-ring linker is an important part of the pharmacophore for GluN2B-active compounds.

Table 36. Comparison of CIQ and 1180-55 scaffolds

	CIQ	**1180-55**
	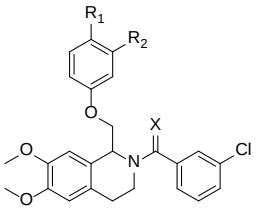	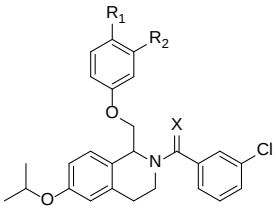
R_1 = OEt, R_2 = H	**No activity at any subunits**	**GluN2B/C**
X = S	**No activity at any subunits**	**GluN2B/GluN2C/GluN2D**
R_1 = H, R_2 = OMe	**No activity at any subunits**	**GluN2C/GluN2D**
Thiourea linker	**No activity at any subunits**	**Glu2C/GluN2D**

Two specific changes to the **1180-55** scaffold that also induced different effects on NMDA potentiation than the same changes to the CIQ scaffold were a methoxy group in the *meta*-position of the B-ring and thiourea linker between the core and the A-ring. While these two functional groups were inactive on the CIQ scaffold, they caused GluN2C/D activity on the **1180-55** scaffold, which means that in these two cases, the isopropoxy on the C-ring was able to revive GluN2C/D activity that had been eliminated. Although this was not further explored, compounds **1180-82** with a methoxy group on the B-ring (**Table 19**) and **1180-149** with a thiourea linker (**Table 28**) could become starting points to develop potent GluN2C/D-selective compounds or even GluN2C-selective compounds. These four examples in **Table 29** highlight that in addition to having differences in pharmacological properties and different structural determinants (**Chapter 2.2.4**), CIQ and **1180-55** also have unique SARs and pharmacophores.

3.3 CIQ and 1180-55 are divergent regarding structural determinants for potentiation

Pharmacological experiments revealed that **1180-55** enhanced the glutamate and glycine potency for all NMDA receptors regardless of GluN2 composition (**Chapter 2.2.4**). This is in contrast to CIQ, which has no impact on agonist potency at any subunits. **1180-55** slows down the deactivation time course of the receptor following the removal of glutamate at all NMDA receptors, which is a feature that is absent with studies conducted with CIQ[13]. Perhaps the most significant difference though is work that has shown that CIQ and **1180-55** have different structural determinants for potentiation. It is well established that the pre M1 and the M1 helix of the GluN2D subunit is important for CIQ-mediated potentiation on GluN1/GluN2D NMDA receptors; point mutations made to the pre M1 and M1 helix of the GluN2D subunit significantly influenced CIQ potentiation[24], although point mutations made to the pre M1 and the M1 helix of the GluN1 subunit had minimal impact on CIQ activity (**Figure 20, Chapter 2**). This suggests that the GluN2C and GluN2D potentiation of CIQ compounds is a result of interaction with the pre M1 and M1 helix of the GluN2 subunits of the NMDA receptor.

Interestingly when these same point mutations were made to the pre M1 and M1 helix of the GluN2B subunit to elucidate the structural determinants of **1180-55** mediated potentiation, GluN2B pre M1 and M1 helix point mutations had a minimal effect (**Figure 1**, right) suggesting that the GluN2B potentiation of **1180-55** is not a result of interaction with the GluN2B subunit. Instead, when GluN1/GluN2B NMDA receptors were studied, it was the pre M1 and M1 helix point mutations to the GluN1 subunit that impacted **1180-55** activity (**Figure 21**, **Chapter 2**). When GluN1/GluN2D NMDA were studied however, point mutations to the pre M1 and M1 helix of the GluN2D subunit did influence **1180-55** activity (**Figure 1**, left). This suggests that the GluN2B potentiation of **1180-55** may be due to an interaction with the pre M1 and M1 helix of the GluN1 subunit, but the GluN2C/D potentiation of **1180-55** is a result of interaction with the GluN2 subunit. While CIQ only has structural determinants residing in the GluN2 subunit, **1180-55** has structural determinants that residue on both the GluN1 and GluN2 subunits.

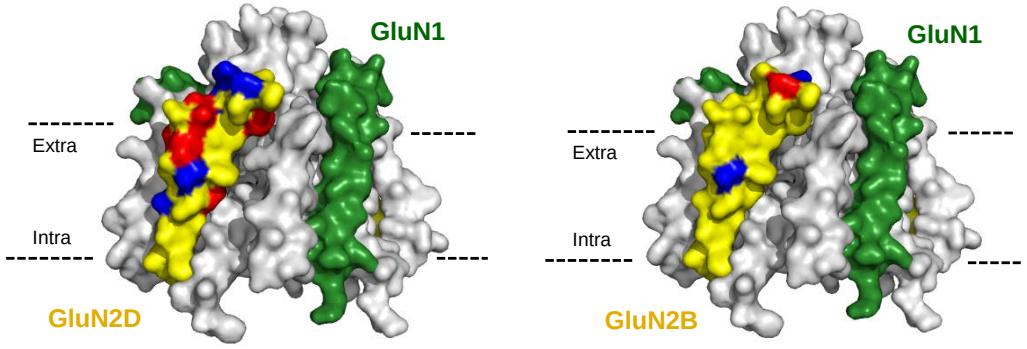

Figure 1. Point mutations on the GluN2D (left) and GluN2B (right) pre M1 and M1 helix that influence 1180-55 activity. Mutations in red decrease 1180-55 activity, while mutations in blue increase activity.

The SAR around **1180-55** and the separation of a number of potent compounds has revealed that the GluN2B potentiation of compounds that exhibit pan potentiation is typically exclusive to only one enantiomer; that is, one enantiomer is active at GluN2B/GluN2C/GluN2D or GluN2B/GluN2C, while the other enantiomer is selective for GluN2C/GluN2D. The only exception to this is the **1180-55** scaffold where the both enantiomers are active at all three subunits (**Table 31**, **Chapter 2**). Based on the biological data from a number of enantiomer pairs, we believe that the (*R*)- and (*S*)-enantiomers are interacting with different subunits of the NMDA receptor. In all cases, with two exceptions, the (*S*)-(-)-enantiomer is active at the GluN2B subunit, while the (*R*)-enantiomer is either GluN2C/GluN2D selective or completely inactive. The two exceptions include **1180-55** in which both enantiomers are active at all three subunits and **1180-168** where the (*R*)-enantiomer is the active enantiomer, while the (S)-enantiomer is inactive. For these reasons, we believe that the (*S*)-enantiomer (or the (*R*)-enantiomer in the case of **1180-168**) is interacting with GluN1 subunit (**Figure 2**). Since the GluN1 subunit is an obligatory subunit of the receptor, it stands to reason that this explains why many of the compounds are pan-potentiators; the GluN1 subunit will exist in every NMDA receptor regardless of GluN2 subunit composition.

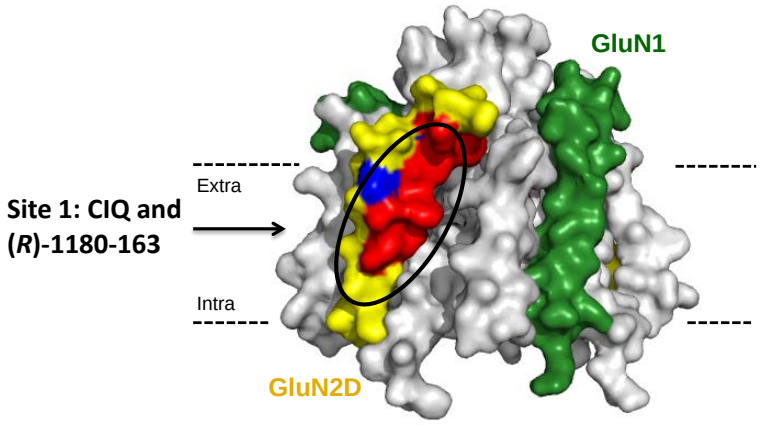

Figure 2. Site on the GluN2D subunit that is responsible for GluN2C/GluN2D selective potentiation. Our work suggests that (R)-(+)-1180-163, a GluN2C/GluN2D selective compound, is similar to CIQ due to similar structural determinants.

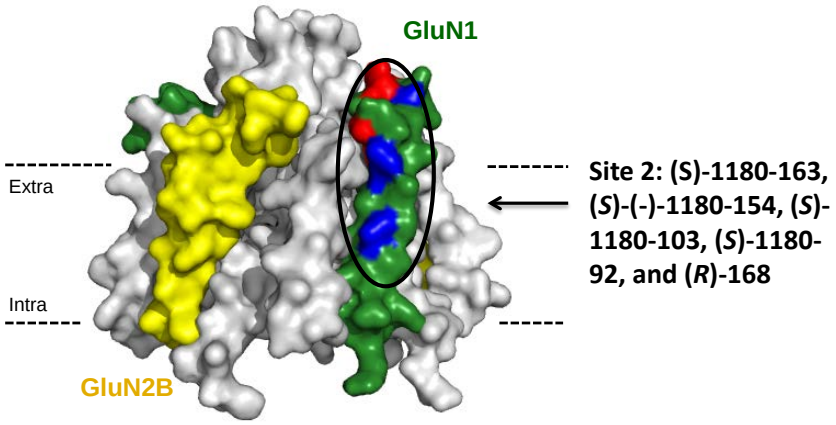

Figure 3. Site on the GluN1 subunit that is responsible for GluN2BGluN2C/GluN2D potentiation. Our work suggests that the compounds listed are exclusively interacting with the GluN1 subunit. Note that both enantiomers are interacting with the NMDA receptor in the case of 1180-163 only.

While (*S*)-(-)-**1180-163** is a pan potentiation and is most likely interacting with the GluN1 subunit, the (*R*)-(+)-enantiomer is CIQ-like and selective for GluN2C/GluN2 subunits. This suggests that the (*R*)-(+)-**1180-163** is interacting with the GluN2C and GluN2D subunits (**Figure 3**). When the other enantiomers discussed in **Chapter 2** were separated however, only the (S)-(-)-enantiomer was active, while the (R)-enantiomer was inactive – not selective at GluN2C and GluN2D. (In the case of **1180-168**, this is reversed and the (R)-(+)-enantiomer holds all activity, while the (S)-(-)-enantiomer is inactive). This suggests that these enantiomers are not interacting with the GluN2 subunit at all, and

by synthesizing these compounds, we have developed compounds that exclusively interact with the GluN1 subunit. Structural determinants on the GluN1 pre M1 and M1 helix represent a new location of allosteric modulation and could represent a new binding site that has not previously been explored. Selectivity for this class can be defined in two different ways and a number of compounds have explored both definitions. First, a number of compounds are selective in terms of potentiation over **1180-55**. These compounds either induce GluN2B/GluN2C potentiation over GluN2D, or in the case of **1180-87**, are selective for GluN2B potentiation over GluN2C/GluN2D potentiation. Secondly, selectivity for this class can also refer to the structural determinants for activity. Initial point mutations made to the pre M1 and M1 helix revealed that **1180-55** is interacting with both the GluN1 and GluN2D pre M1 and M1 helices. The synthesis of a number of compounds and the separation of key enantiomers has led to the hypothesis that a number of compounds are exclusively interacting with the GluN1 subunit. This structural determinant work, in combination with the SAR and pharmacological studies, shows that **1180-55** is a completely distinct class from CIQ, and the tetrahydroisoquinoline scaffold is no longer limited to GluN2C/D selective potentiation and interaction with the GluN2 pre M1 and M1 helix.

References:

(1) Erreger, K.; Dravid, S. M.; Banke, T. G.; Wyllie, D. J. A.; Traynelis, S. F. Subunit-Specific Gating Controls Rat NR1/NR2A and NR1/NR2B NMDA Channel Kinetics and Synaptic Signalling Profiles. *J. Physiol.* **2005**, *563* (2), 345–358.

(2) Vicini, S.; Wang, J. F.; Li, J. H.; Zhu, W. J.; Wang, Y. H.; Luo, J. H.; Wolfe, B. B.; Grayson, D. R. Functional and Pharmacological Differences Between RecombinantN-Methyl-D-Aspartate Receptors. *J. Neurophysiol.* **1998**, *79* (2), 555–566.

(3) Monyer, H.; Burnashev, N.; Laurie, D. J.; Sakmann, B.; Seeburg, P. H. Developmental and Regional Expression in the Rat Brain and Functional Properties of Four NMDA Receptors. *Neuron* **1994**, *12* (3), 529–540.

(4) Akazawa, C.; Shigemoto, R.; Bessho, Y.; Nakanishi, S.; Mizuno, N. Differential Expression of Five N-Methyl-D-Aspartate Receptor Subunit mRNAs in the Cerebellum of Developing and Adult Rats. *J. Comp. Neurol.* **1994**, *347* (1), 150–160.

(5) Williams, K. Ifenprodil Discriminates Subtypes of the N-Methyl-D-Aspartate Receptor: Selectivity and Mechanisms at Recombinant Heteromeric Receptors. *Mol. Pharmacol.* **1993**, *44* (4), 851–859.

(6) Chenard, B. L.; Bordner, J.; Butler, T. W.; Chambers, L. K.; Collins, M. A.; De Costa, D. L.; Ducat, M. F.; Dumont, M. L.; Fox, C. B. (1S,2S)-1-(4-Hydroxyphenyl)-2-(4-Hydroxy-4-Phenylpiperidino)-1-Propanol: A Potent New Neuroprotectant Which Blocks N-Methyl-D-Aspartate Responses. *J. Med. Chem.* **1995**, *38* (16), 3138–3145.

(7) Gotti, B.; Duverger, D.; Bertin, J.; Carter, C.; Dupont, R.; Frost, J.; Gaudilliere, B.; MacKenzie, E. T.; Rousseau, J.; Scatton, B. Ifenprodil and SL 82.0715 as Cerebral Anti-Ischemic Agents. I. Evidence for Efficacy in Models of Focal Cerebral Ischemia. *J. Pharmacol. Exp. Ther.* **1988**, *247* (3), 1211–1221.

(8) Taniguchi, K.; Shinjo, K.; Mizutani, M.; Shimada, K.; Ishikawa, T.; Menniti, F. S.; Nagahisa, A. Antinociceptive Activity of CP-101,606, an NMDA Receptor NR2B Subunit Antagonist. *Br. J. Pharmacol.* **1997**, *122* (5), 809–812.

(9) Boyce, S.; Wyatt, A.; Webb, J. K.; O'Donnell, R.; Mason, G.; Rigby, M.; Sirinathsinghji, D.; Hill, R. G.; Rupniak, N. M. J. Selective NMDA NR2B Antagonists Induce Antinociception without Motor Dysfunction: Correlation with Restricted Localisation of NR2B Subunit in Dorsal Horn. *Neuropharmacology* **1999**, *38* (5), 611–623.

(10) Bettini, E.; Sava, A.; Griffante, C.; Carignani, C.; Buson, A.; Capelli, A. M.; Negri, M.; Andreetta, F.; Senar-Sancho, S. A.; Guiral, L.; Cardullo, F. Identification and Characterization of Novel NMDA Receptor Antagonists Selective for NR2A- over NR2B-Containing Receptors. *J. Pharmacol. Exp. Ther.* **2010**, *335* (3), 636–644.

(11) Hansen, K. B.; Traynelis, S. F. Structural and Mechanistic Determinants of a Novel Site for Noncompetitive Inhibition of GluN2D-Containing NMDA Receptors. *J. Neurosci.* **2011**, *31* (10), 3650–3661.

(12) Zimmerman, S. S.; Khatri, A.; Garnier-Amblard, E. C.; Mullasseril, P.; Kurtkaya, N. L.; Gyoneva, S.; Hansen, K. B.; Traynelis, S. F.; Liotta, D. C. Design, Synthesis, and Structure–Activity Relationship of a Novel Series of GluN2C-Selective Potentiators. *J. Med. Chem.* **2014**, *57* (6), 2334–2356.

(13) Mullasseril, P.; Hansen, K. B.; Vance, K. M.; Ogden, K. K.; Yuan, H.; Kurtkaya, N. L.; Santangelo, R.; Orr, A. G.; Le, P.; Vellano, K. M.; Liotta, D. C.; Traynelis, S. F. A Subunit-Selective Potentiator of NR2C- and NR2D-Containing NMDA Receptors. *Nat. Commun.* **2010**, *1*, 90.

(14) Cui, Y.; Jin, J.; Zhang, X.; Xu, H.; Yang, L.; Du, D.; Zeng, Q.; Tsien, J. Z.; Yu, H.; Cao, X. Forebrain NR2B Overexpression Facilitating the Prefrontal Cortex Long-Term Potentiation and Enhancing Working Memory Function in Mice. *PLoS ONE* **2011**, *6* (5), e20312.

(15) Tang, Y.-P.; Shimizu, E.; Dube, G. R.; Rampon, C.; Kerchner, G. A.; Zhuo, M.; Liu, G.; Tsien, J. Z. Genetic Enhancement of Learning and Memory in Mice. *Nature* **1999**, *401* (6748), 63–69.

(16) Cao, X.; Cui, Z.; Feng, R.; Tang, Y.-P.; Qin, Z.; Mei, B.; Tsien, J. Z. Maintenance of Superior Learning and Memory Function in NR2B Transgenic Mice during Ageing. *Eur. J. Neurosci.* **2007**, *25* (6), 1815–1822.

(17) Wenk, G. L.; Barnes, C. A. Regional Changes in the Hippocampal Density of AMPA and NMDA Receptors across the Lifespan of the Rat. *Brain Res.* **2000**, *885* (1), 1–5.

(18) Clayton, D. A.; Mesches, M. H.; Alvarez, E.; Bickford, P. C.; Browning, M. D. A Hippocampal NR2B Deficit Can Mimic Age-Related Changes in Long-Term Potentiation and Spatial Learning in the Fischer 344 Rat. *J. Neurosci.* **2002**, *22* (9), 3628–3637.

(19) Weickert, C. S.; Fung, S. J.; Catts, V. S.; Schofield, P. R.; Allen, K. M.; Moore, L. T.; Newell, K. A.; Pellen, D.; Huang, X.-F.; Catts, S. V.; Weickert, T. W. Molecular Evidence of N-Methyl-D-Aspartate Receptor Hypofunction in Schizophrenia. *Mol. Psychiatry* **2013**, *18* (11), 1185–1192.

(20) Jacobs, S. A.; Tsien, J. Z. Genetic Overexpression of NR2B Subunit Enhances Social Recognition Memory for Different Strains and Species. *PLoS ONE* **2012**, *7* (4), e36387.

(21) White, T. L.; Youngentob, S. L. The Effect of NMDA-NR2B Receptor Subunit over-Expression on Olfactory Memory Task Performance in the Mouse. *Brain Res.* **2004**, *1021* (1), 1–7.

(22) Okabe, S.; Collin, C.; Auerbach, J. M.; Meiri, N.; Bengzon, J.; Kennedy, M. B.; Segal, M.; McKay, R. D. G. Hippocampal Synaptic Plasticity in Mice Overexpressing an Embryonic Subunit of the NMDA Receptor. *J. Neurosci.* **1998**, *18* (11), 4177–4188.

(23) Ogden, K. K.; Khatri, A.; Traynelis, S. F.; Heldt, S. A. Potentiation of GluN2C/D NMDA Receptor Subtypes in the Amygdala Facilitates the Retention of Fear and Extinction Learning in Mice. *Neuropsychopharmacology* **2014**, *39* (3), 625–637.
(24) Ogden, K. K.; Traynelis, S. F. Contribution of the M1 Transmembrane Helix and Pre-M1 Region to Positive Allosteric Modulation and Gating of N-Methyl-D-Aspartate Receptors. *Mol. Pharmacol.* **2013**, *83* (5), 1045–1056.